frontiers | Research Topics

Secondary metabolites and metabolism in tea plants

Edited by
Zhaoliang Zhang, Vagner A. Benedito, Chuankui Song, Jian Zhao, Enhua Xia, Weiwei Wen and Lanting Zeng

Published in
Frontiers in Plant Science

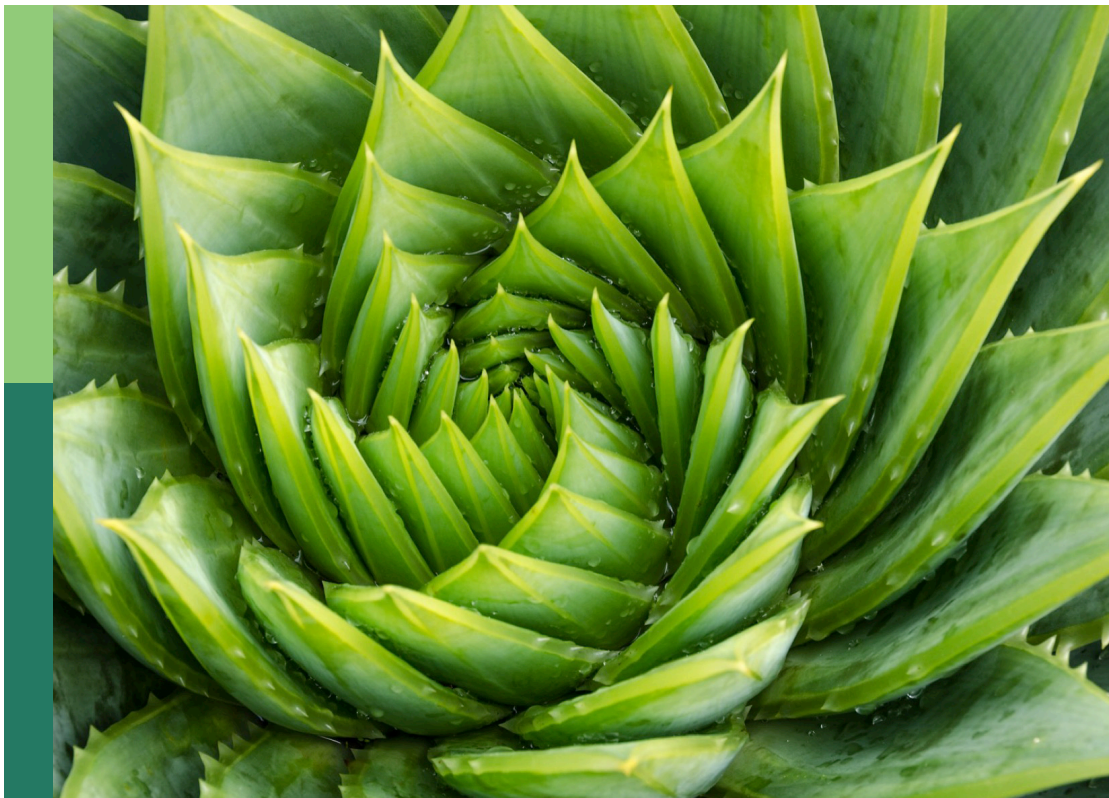

ISSN 1664-8714
ISBN 978-2-83251-784-0
DOI 10.3389/978-2-83251-784-0

About Frontiers

Frontiers is more than just an open access publisher of scholarly articles: it is a pioneering approach to the world of academia, radically improving the way scholarly research is managed. The grand vision of Frontiers is a world where all people have an equal opportunity to seek, share and generate knowledge. Frontiers provides immediate and permanent online open access to all its publications, but this alone is not enough to realize our grand goals.

Frontiers journal series

The Frontiers journal series is a multi-tier and interdisciplinary set of open-access, online journals, promising a paradigm shift from the current review, selection and dissemination processes in academic publishing. All Frontiers journals are driven by researchers for researchers; therefore, they constitute a service to the scholarly community. At the same time, the *Frontiers journal series* operates on a revolutionary invention, the tiered publishing system, initially addressing specific communities of scholars, and gradually climbing up to broader public understanding, thus serving the interests of the lay society, too.

Dedication to quality

Each Frontiers article is a landmark of the highest quality, thanks to genuinely collaborative interactions between authors and review editors, who include some of the world's best academicians. Research must be certified by peers before entering a stream of knowledge that may eventually reach the public - and shape society; therefore, Frontiers only applies the most rigorous and unbiased reviews. Frontiers revolutionizes research publishing by freely delivering the most outstanding research, evaluated with no bias from both the academic and social point of view. By applying the most advanced information technologies, Frontiers is catapulting scholarly publishing into a new generation.

What are Frontiers Research Topics?

Frontiers Research Topics are very popular trademarks of the *Frontiers journals series*: they are collections of at least ten articles, all centered on a particular subject. With their unique mix of varied contributions from Original Research to Review Articles, Frontiers Research Topics unify the most influential researchers, the latest key findings and historical advances in a hot research area.

Find out more on how to host your own Frontiers Research Topic or contribute to one as an author by contacting the Frontiers editorial office: frontiersin.org/about/contact

Secondary metabolites and metabolism in tea plants

Topic editors

Zhaoliang Zhang — Anhui Agriculture University, China
Vagner A. Benedito — West Virginia University, United States
Chuankui Song — Anhui Agriculture University, China
Jian Zhao — Hunan Agricultural University, China
Enhua Xia — Anhui Agriculture University, China
Weiwei Wen — Huazhong Agricultural University, China
Lanting Zeng — South China Botanical Garden, Chinese Academy of Sciences (CAS), China

Citation

Zhang, Z., Benedito, V. A., Song, C., Zhao, J., Xia, E., Wen, W., Zeng, L., eds. (2023). *Secondary metabolites and metabolism in tea plants*. Lausanne: Frontiers Media SA. doi: 10.3389/978-2-83251-784-0

Table of contents

05 Editorial: Secondary metabolites and metabolism in tea plants
Zhaoliang Zhang, Chuankui Song, Jian Zhao, Enhua Xia, Weiwei Wen, Lanting Zeng and Vagner A. Benedito

08 Functional Analyses of Flavonol Synthase Genes From *Camellia sinensis* Reveal Their Roles in Anther Development
Yufeng Shi, Xiaolan Jiang, Linbo Chen, Wei-Wei Li, Sanyan Lai, Zhouping Fu, Yajun Liu, Yumei Qian, Liping Gao and Tao Xia

19 Non-Volatile Metabolic Profiling and Regulatory Network Analysis in Fresh Shoots of Tea Plant and Its Wild Relatives
Chen-Kai Jiang, Zhi-Long Liu, Xuan-Ye Li, Sezai Ercisli, Jian-Qiang Ma and Liang Chen

31 The Tea Plant Leaf Cuticle: From Plant Protection to Tea Quality
Mingjie Chen

44 Theanine Improves Salt Stress Tolerance *via* Modulating Redox Homeostasis in Tea Plants (*Camellia sinensis* L.)
Ziping Chen, Shijia Lin, Juan Li, Tingting Chen, Quan Gu, Tianyuan Yang and Zhaoliang Zhang

57 Transcriptome-Wide Analysis and Functional Verification of RING-Type Ubiquitin Ligase Involved in Tea Plant Stress Resistance
Dawei Xing, Tongtong Li, Guoliang Ma, Haixiang Ruan, Liping Gao and Tao Xia

68 Metabolic Flow of C6 Volatile Compounds From LOX-HPL Pathway Based on Airflow During the Post-harvest Process of Oolong Tea
Zi-wei Zhou, Qing-yang Wu, Zi-xin Ni, Qing-cai Hu, Yun Yang, Yu-cheng Zheng, Wan-jun Bi, Hui-li Deng, Zhen-zhang Liu, Nai-xin Ye, Zhong-xiong Lai and Yun Sun

79 Mechanism Underlying the Shading-Induced Chlorophyll Accumulation in Tea Leaves
Jiaming Chen, Shuhua Wu, Fang Dong, Jianlong Li, Lanting Zeng, Jinchi Tang and Dachuan Gu

93 Tonoplast-Localized Theanine Transporter CsCAT2 May Mediate Theanine Storage in the Root of Tea Plants (*Camellia sinensis* L.)
Lin Feng, Yongchao Yu, Shijia Lin, Tianyuan Yang, Qi Chen, Linlin Liu, Jun Sun, Pengcheng Zheng, Zhaoliang Zhang and Xiaochun Wan

103 Systematic Analysis of the R2R3-MYB Family in *Camellia sinensis*: Evidence for Galloylated Catechins Biosynthesis Regulation
Jingyi Li, Shaoqun Liu, Peifen Chen, Jiarong Cai, Song Tang, Wei Yang, Fanrong Cao, Peng Zheng and Binmei Sun

116 Exogenous Application of Gallic Acid Induces the Direct Defense of Tea Plant Against *Ectropis obliqua* Caterpillars
Xin Zhang, Wei Ran, Xiwang Li, Jin Zhang, Meng Ye, Songbo Lin, Miaomiao Liu and Xiaoling Sun

124 Carbon and Nitrogen Metabolism Are Jointly Regulated During Shading in Roots and Leaves of *Camellia Sinensis*
Chenyu Shao, Haizhen Jiao, Jiahao Chen, Chenyu Zhang, Jie Liu, Jianjiao Chen, Yunfei Li, Jing Huang, Biao Yang, Zhonghua Liu and Chengwen Shen

144 Cytosolic *Nudix Hydrolase 1* Is Involved in Geranyl β-Primeveroside Production in Tea
Hanchen Zhou, Shijie Wang, Hao-Fen Xie, Guofeng Liu, Lubobi Ferdinand Shamala, Jingyi Pang, Zhengzhu Zhang, Tie-Jun Ling and Shu Wei

156 An Integrated Metabolome and Transcriptome Analysis Reveal the Regulation Mechanisms of Flavonoid Biosynthesis in a Purple Tea Plant Cultivar
SaSa Song, Yu Tao, LongHan Gao, HuiLing Liang, DeSong Tang, Jie Lin, YuChun Wang, Frederick G. Gmitter Jr. and ChunFang Li

168 Identification and Expression Analysis of *CAMTA* Genes in Tea Plant Reveal Their Complex Regulatory Role in Stress Responses
Qiying Zhou, Mingwei Zhao, Feng Xing, Guangzhi Mao, Yijia Wang, Yafeng Dai, Minghui Niu and Hongyu Yuan

182 Effects of Different Shading Treatments on the Biomass and Transcriptome Profiles of Tea Leaves (*Camellia sinensis* L.) and the Regulatory Effect on Phytohormone Biosynthesis
Zhou-Tao Fang, Jing Jin, Ying Ye, Wei-Zhong He, Zai-Fa Shu, Jing-Na Shao, Zhu-Sheng Fu, Jian-Liang Lu and Jian-Hui Ye

193 Differences in transcriptomic and metabolomic analyses of metabolites of shoots on tea plants of different ages and relevant regulatory network
Meng Yuan Li, Yun Zhi Zhang, Zi You Zhang, Yan Hui Zhang, Qian Qian Ren and Shan Jin

frontiers | Frontiers in Plant Science

TYPE Editorial
PUBLISHED 14 February 2023
DOI 10.3389/fpls.2023.1143022

OPEN ACCESS

EDITED AND REVIEWED BY
Sumit Ghosh,
Council of Scientific and Industrial Research (CSIR), India

*CORRESPONDENCE
Vagner A. Benedito
Vagner.benedito@mail.wvu.edu

SPECIALTY SECTION
This article was submitted to Plant Metabolism and Chemodiversity, a section of the journal Frontiers in Plant Science

RECEIVED 12 January 2023
ACCEPTED 30 January 2023
PUBLISHED 14 February 2023

CITATION
Zhang Z, Song C, Zhao J, Xia E, Wen W, Zeng L and Benedito VA (2023) Editorial: Secondary metabolites and metabolism in tea plants.
Front. Plant Sci. 14:1143022.
doi: 10.3389/fpls.2023.1143022

Editorial: Secondary metabolites and metabolism in tea plants

Zhaoliang Zhang [1], Chuankui Song [1], Jian Zhao [2], Enhua Xia [1], Weiwei Wen [3], Lanting Zeng [4] and Vagner A. Benedito [5]*

[1]State Key Laboratory of Tea Plant Biology and Utilization, School of Tea and Food Science and Technology, Anhui Agriculture University, Anhui, China, [2]Key Laboratory of Tea Science of Ministry of Education, College of Horticulture, Hunan Agricultural University, Changsha, China, [3]Key Laboratory of Horticultural Plant Biology (MOE), College of Horticulture and Forestry Sciences, Huazhong Agricultural University, Wuhan, China, [4]South China Botanical Garden, Chinese Academy of Sciences (CAS), Guangzhou, China, [5]School of Agriculture and Food, Davis College of Agriculture, Natural Resources and Design, West Virginia University, Morgantown, WV, United States

KEYWORDS

***Camellia sinensis*, specialized metabolism of plants, tea quality, plant biochemistry, natural products**

Editorial on the Research Topic
Secondary metabolites and metabolism in tea plants

Tea is the world's most popular prepared beverage. It is prepared from the delicate shoots of the tea plant (*Camellia sinensis*, Theaceae). It is one of the most important cash crops in the world, with 60% of tea produced by smallholders in low-income nations (FAO, 2022). The sustainability of tea production is currently challenged by climate change and the excessive use of chemical fertilizers, herbicides, and pesticides. Tea plants synthesize secondary metabolites to survive under various stresses such as extreme temperature, UV radiation, drought, nutrient deficiency, pathogen infection, and herbivore feeding. Moreover, the complex flavor and aroma and the health-promoting properties of tea are provided by the large amounts and abundant types of secondary metabolites in tea leaves, which are the reason for the popularity of teas. Catechins, theanine, caffeine, volatiles, and their derivatives are the most critical and prominent secondary metabolites for tea quality.

Secondary metabolites accumulate due to dynamic biosynthesis, storage, transport, and decomposition. Secondary metabolism, as in other plant species, is developmentally and environmentally controlled, but there is still much to learn about its regulatory mechanisms in tea. Knowing more about them will allow us to use them to manage secondary metabolism in tea and develop better cultivation tactics for improved beverage quality. This special issue is an important contribution to the field by reporting on substantial advances in understanding the molecular basis of secondary metabolism in tea plants. This special issue has 16 papers, 15 of which are original research reports on various aspects of tea metabolite storage, transport, signal transduction, and metabolic control.

After the tea leaves are picked, they undergo a series of processes to become the final product. Post-harvest processing varies depending on the variety of tea produced. For example, black tea and oolong tea are made from leaves that have been withered or partially dried before the oxidation step. During oxidation, enzymes in the leaves react with oxygen in the air, changing the color and flavor of the leaves. The leaves are then dried to halt the oxidation process. Indeed, oolong tea gets its characteristic floral aroma from fatty acid-derived volatiles formed during post-harvest processing. Zhou et al. investigated changes in

alcohol dehydrogenase activity, gene expression, and the fatty acid metabolome in oolong tea leaves during processing. The data showed that oxygen supply during processing coordinates the metabolic flow of C6 aldehydes of the LOX-HPL pathway and that an oxidative micro-environment leads to enzymatic reactions forming distinctive acids and derivative esters of this tea type.

Phenylpropanoids encompass a broad family of secondary metabolites found in plants, whose primary precursor is phenylalanine and, to a lesser extent, tyrosine. This class consists of five chemical groups (flavonoids, lignin, phenolic acids, stilbenes, and coumarins), some of which have antioxidant and anti-inflammatory features that benefit human health. Tea contains a high concentration of phenylpropanoids, including galloylated catechins and the bioactive flavonoid epigallocatechin gallate. On the other hand, the biosynthesis of galloylated catechins is poorly known. Li et al. investigated 118 R2R3-MYB transcription factor genes in the tea genome. They discovered nine genes whose expression levels were enriched in buds and growing leaves, which contain the most galloylated catechins. Three of these genes were discovered to be connected to key biosynthetic genes for epigallocatechin gallate and galloylated catechins, making them excellent candidates for further functional studies.

Aside from their health benefits, flavonoids contribute significantly to the astringent tea flavor. Flavonols are flavonoids with a unique B-ring structure (3-hydroxyflavone). Shi et al. investigated the metabolic features of phenolic chemicals throughout flower development using metabolomic and transcriptome studies. Their studies demonstrated that the flavonol content of flowers increased with development, with petals and stamens being the primary locations of flavone and flavonol accumulation. Moreover, the expression of *CsFLSb* was considerably different in fertile and sterile flowers. This suggests that flavonols influence fertility. The study also identified three *CsFLS* genes with diverse roles in vegetative and reproductive organs. This research underscores the importance of balancing vegetative and reproductive growth in tea plants.

Purple tea has a distinctive color, flavor, and enhanced health value due to high levels of flavonoids and anthocyanins. Song et al. discovered that a reduction in flavonoids and anthocyanin concentrations caused leaves of a purple variety to turn green. Although the mechanisms of flavonoid and anthocyanin synthesis have been studied in several purple tea cultivars, the molecular regulation of these activities during leaf growth and color variation remains unclear. The authors discovered regulatory genes and networks involved in flavonoid production in purple tea plants using an integrated transcriptome and metabolome study, indicating that the purple color is due to the co-pigmentation of quercetin and kaempferol derivatives. They also discovered many genes that could be involved in flavonoid and anthocyanin accumulation in purple leaves. This study adds to our understanding of the metabolic and molecular mechanisms behind the formation of flavonoids and anthocyanins in tea plants.

Gallic acid is a polyphenolic molecule present in tea with antioxidant and anti-inflammatory effects. According to Zhang et al., spraying gallic acid on tea plants activated defense mechanisms against caterpillars by stimulating jasmonic acid signaling and the synthesis of various phenylpropanoid compounds. These results suggest that gallic acid is an effective inducer of direct defense responses in tea plants against caterpillars. This study will help us better understand the relationship between plants and herbivore insects and aid in developing cultivation protection strategies.

Color plays a critical role in tea quality. Shading is a common technique used in the cultivation of tea plants to improve the quality of the tea leaves. Shading is typically achieved using netting or other materials that block some sunlight from reaching the tea plants. Increased chlorophyll content *via* shading improves tea leaf color *via* unknown mechanisms. Additionally, Chen et al. explored the effect of shading on the expression of genes involved in chlorophyll synthesis in tea plants. They found that decreased light intensity induces gene expression of a protochlorophyllide oxidoreductase (CsPOR), leading to increased chlorophyll content. The study also identified three transcription factors as possible regulators of this process and some key interactions. The content of other metabolites is also affected by shading. Shao et al. employed non-targeted metabolomics to examine the metabolic pathways in the shoots and roots of two tea cultivars under shade and relighting conditions over the summer. The amino acid synthase genes *CsGS1.1* and *CsTSI* were induced in the leaves and roots of both cultivars. These findings reveal the effects of shading on carbon and nitrogen metabolism in both leaves and roots and that root metabolism influences leaf metabolism to increase tea quality.

Fang et al. investigated how phytohormone and transcriptome profiles of tea leaves changed when black, blue, and red net shading was used. They discovered that blue net shading enhanced bud density, fresh weight of 100 buds, and yield much more than black net shading while having an equivalent effect on flavonoid content. The different shading treatments affected phenylpropanoid biosynthesis, MAPK signaling, and hormone signal transduction, as revealed by the transcriptome profiles. The levels of salicylic acid and melatonin correlated with light signal perception and signaling genes, and several genes had stronger interactions with phytohormone biosynthetic genes. These results suggest that different shading affects the development and physiology of tea plants through the regulation of phytohormone levels.

Zhou et al. found five calmodulin-binding transcription activator (CAMTA) genes in the tea genome and categorized them into three classes. They were detected in several organs under various stress treatments. Co-expressed genes were identified in cold and dry conditions, forming five distinct co-expression networks centered on CAMTA genes. Cold treatment boosted hormone regulation, transcriptional control, and protein processing-related pathways, whereas drought increased hormone, lipid, and carbon metabolism. Their protein interaction network study showed that CAMTAs bind to distinct cis-elements in target gene promoters and control their transcription. These findings pave the way for further studies into the involvement of CAMTA genes in stress responses in tea plants.

Jiang et al. used an untargeted metabolomics method to investigate relationships between genes and metabolites in fresh shoots of 68 tea accessions. Their findings highlight the intricate interactions between non-volatile metabolite content and gene expression levels. This work will contribute to a better understanding of the genetic control of metabolites in fresh tea shoots.

Geraniol is a volatile monoterpene alcohol that contributes to the aroma of tea. According to Zhou et al., it is present in tea leaves as

geranyl-primeveroside. Geranyl-primeveroside levels vary in tea leaves depending on age and tissue color, with younger, greener leaves having higher levels than older, darker leaves. The study also identified and described two geraniol synthase genes and two Nudix hydrolase genes in the tea genome and found that CsNUDX1-cyto is more efficient at converting geranyl-pyrophosphate to geranyl-monophosphate *in vitro* than CsNUDX1-chlo.

According to Shan et al., the older the tea plant, the better the scent and taste of the tea it produces, becoming more nuanced and sweeter with less astringency. They reported that gene expression and metabolite levels differed among the leaves of younger and older plants. These findings imply that secondary metabolic pathways, such as flavonoid biosynthesis, may play a role in the variations in tea quality across plants of different ages.

Non-proteogenic amino acids play important roles in plant development and stress response. Theanine is a prominent glutamine analog in green tea that may have antidepressant and soothing qualities. It influences tea quality and price by adding an umami flavor to the beverage. Its physiological role is not well understood. Feng et al. identified and characterized CsCAT2, a theanine transporter localized to the tonoplast that is involved in the transport and storage of theanine in the roots throughout the winter when theanine is stored. Its expression decreases in the spring during theanine transfer from roots to shoots. Chen et al. reported that salt stress increased the levels of theanine and other amino acids in new shoots. This increase was associated with the upregulation of genes involved in theanine biosynthesis. When applied to new shoots, theanine increased tolerance to salt stress in tea plants and Arabidopsis and increased antioxidant activity in shoots under salt stress. These findings suggest that theanine plays a role in salt stress tolerance in tea plants *via* a redox homeostasis pathway.

E3 ubiquitin ligases were studied in the tea genome by Xing et al.. They discovered 335 genes encoding RING finger proteins, with 53 responding to stress. When one of them (*CsMIEL1*) was overexpressed in Arabidopsis, it decreased tolerance to methyl jasmonate and reduced anthocyanin accumulation in response to cold.

Finally, Chen reviewed the role of the leaf cuticle in tea quality. Given its role in preventing water loss in the plant, as opposed to the withering procedure used to reduce water loss after processing, the cuticle's influence on tea quality is undefined. This review delves into numerous elements of cuticle structure and composition, as well as knowledge gaps and open questions that could be future study topics.

The seven topic editors of this special issue would like to express their heartfelt gratitude to the 125 authors and many peer reviewers who contributed to this special issue. We are indebted to the many peer reviewers who generously provided their expertise and time to read and provide feedback on the manuscripts. We are confident that this volume will serve to advance tea research by shedding light on the mechanisms contributing to the production of the rich aroma and complex secondary metabolite profile of this popular beverage consumed daily by billions of people worldwide.

Author contributions

All authors listed have made a substantial, direct, and intellectual contribution to the work and approved it for publication.

Funding

This work is supported by grants from the National Natural Science Foundation of China (32072624) and the National Key R&D Program of China (2021YFD1601101).

Acknowledgments

The editorial team is thankful to all authors who submitted their manuscripts to this Research Topic and the peer reviewers, who dedicated expert time to assess and provide feedback to improve the quality of the publications.

Conflict of interest

The authors declare that the research was conducted in the absence of any commercial or financial relationships that could be construed as a potential conflict of interest.

Publisher's note

Reference

FAO (2022) *International tea market: Market situation, prospectus and emerging issues*. Available at: https://www.fao.org/3/cc0238en/cc0238en.pdf.

frontiers in Plant Science

ORIGINAL RESEARCH
published: 01 October 2021
doi: 10.3389/fpls.2021.753131

Functional Analyses of Flavonol Synthase Genes From *Camellia sinensis* Reveal Their Roles in Anther Development

Yufeng Shi[1], Xiaolan Jiang[1], Linbo Chen[2], Wei-Wei Li[1], Sanyan Lai[1], Zhouping Fu[1], Yajun Liu[3], Yumei Qian[4], Liping Gao[3] and Tao Xia[1]**

[1] State Key Laboratory of Tea Plant Biology and Utilization, Anhui Agricultural University, Hefei, China, [2] Tea Research Institute, Yunnan Academy of Agricultural Sciences, Yunnan Engineering Research Center of Tea Germplasm Innovation and Matching Cultivation, Menghai, China, [3] School of Life Sciences, Anhui Agricultural University, Hefei, China, [4] School of Biological and Food Engineering, Suzhou University, Suzhou, China

OPEN ACCESS

Edited by:
Lanting Zeng, South China Botanical Garden, Chinese Academy of Sciences (CAS), China

Reviewed by:
Xiaomin Yu, Fujian Agriculture and Forestry University, China
Xin Li, Tea Research Institute, Chinese Academy of Agricultural Sciences (CAAS), China

***Correspondence:**
Liping Gao
gaolp62@126.com
Tao Xia
xiatao62@126.com

Specialty section:
This article was submitted to Plant Metabolism and Chemodiversity, a section of the journal Frontiers in Plant Science

Received: *04 August 2021*
Accepted: *13 September 2021*
Published: *01 October 2021*

Citation:
Shi Y, Jiang X, Chen L, Li W-W, Lai S, Fu Z, Liu Y, Qian Y, Gao L and Xia T (2021) Functional Analyses of Flavonol Synthase Genes From Camellia sinensis Reveal Their Roles in Anther Development. Front. Plant Sci. 12:753131. doi: 10.3389/fpls.2021.753131

Flavonoids, including flavonol derivatives, are the main astringent compounds of tea and are beneficial to human health. Many researches have been conducted to comprehensively identify and characterize the phenolic compounds in the tea plant. However, the biological function of tea flavonoids is not yet understood, especially those accumulated in floral organs. In this study, the metabolic characteristics of phenolic compounds in different developmental stages of flower buds and various parts of the tea flower were investigated by using metabolomic and transcriptomic analyses. Targeted metabolomic analysis revealed varying accumulation patterns of different phenolic polyphenol compounds during flowering; moreover, the content of flavonol compounds gradually increased as the flowers opened. Petals and stamens were the main sites of flavone and flavonol accumulation. Compared with those of fertile flowers, the content of certain flavonols, such as kaempferol derivatives, in anthers of hybrid sterile flowers was significantly low. Transcriptomic analysis revealed different expression patterns of genes in the same gene family in tea flowers. The *CsFLSb* gene was significantly increased during flowering and was highly expressed in anthers. Compared with fertile flowers, *CsFLSb* was significantly downregulated in sterile flowers. Further functional verification of the three *CsFLS* genes indicated that *CsFLSb* caused an increase in flavonol content in transgenic tobacco flowers and that *CsFLSa* acted in leaves. Taken together, this study highlighted the metabolic properties of phenolic compounds in tea flowers and determined how the three *CsFLS* genes have different functions in the vegetative and reproductive organs of tea plants. Furthermore, *CsFLSb* could regulated flavonol biosynthesis in tea flowers, thus influencing fertility. This research is of great significance for balancing the reproductive growth and vegetative growth of tea plants.

Keywords: *Camellia sinensis*, flower development, flower sterility, flavonols, flavonol synthase

INTRODUCTION

Tea plant is a highly popular beverage crop cultivated in tropical and temperate regions around the world (Valduga et al., 2019). Tea plants are rich in polyphenols, caffeine, and amino acids, which are beneficial for human health, including antibacterial and anti-inflammatory properties, cancer prevention, and brain dysfunction suppression (Tang et al., 2019; Xing et al., 2019). Tea polyphenols include phenolic acids, catechins, anthocyanins, flavones, and flavonol and are synthesized through the shikimate, phenylpropanoid, and flavonoid pathways (Jiang et al., 2013; **Figure 1**). Polyphenols in help plants to resist biotic and abiotic stresses. For example, under drought conditions, the metabolic flux to the synthetic pathway of secondary metabolites, such as flavanols and anthocyanins, is upregulated (Jiang et al., 2017; Zahedi et al., 2019). In *Arabidopsis thaliana* and tobacco, the accumulation of anthocyanins is regulated, which yields improved tolerance to low temperature, drought, and salt stress (Li et al., 2017; Naing et al., 2018). Given their antioxidant effects, flavonols can help plants deal with stress by, for example, maintaining the steady state of reactive oxygen species (ROS) and thus protecting pollen from temperature stress (Muhlemann et al., 2018).

Flavonols, such as kaempferol (K) and quercetin (Q), can act as endogenous negative regulators of auxin transport, thereby affecting plant development (Jacobs and Rubery, 1988; Brown et al., 2001). These flavonoids can block the binding ability of the indole-3-acetic acid (IAA) polar transport inhibitor N-1-naphthylphthalamic acid and inhibit auxin movement in hypocotyl segments (Jacobs and Rubery, 1988; Wasson et al., 2006). The polar transport of auxin regulates the polar growth of plant tips, such as the root tip, the stem tip, filaments, and the pollen tube (Tansengco et al., 2004). Compared with wild-type strains, Arabidopsis mutants lacking flavonoids have fewer root hairs, shorter root hairs, and pollen tubes that exhibit abnormal growth (Schiefelbein et al., 1993). Knocking out the chalcone synthase (*CHS*) gene in petunias and silencing the expression of the flavonol synthase (*FLS*) gene in tobacco both reduce flavonol content, leading to blocked pollen tube germination and male sterility (Napoli et al., 1999; Mahajan et al., 2011). The addition of a low concentration of flavonols to the germination medium promotes pollen germination and pollen tube growth (Ylstra et al., 1992; Pollak et al., 1995).

The physiological significance of polyphenols in the tea plant is unclear. Exploration of the relationship between phenolic compounds and reproduction has practical significance. Tea plants have a long reproductive growth period, requiring 2 years from flowering to seed maturity. A competitive relationship exists between their reproductive and vegetative growth (Liu et al., 2020). Tea leaves are the raw material for making the beverage, however, flowering and seed production consume a large amount of nutrients contained in the leaf, thereby reducing the economic value of the tea plant. Therefore, flowers are regarded as industrial waste by tea farmers. However, for breeders, flowering is an essential physiological process of tea plants. Thus, determining the balance between the reproductive growth and vegetative growth of tea plants is a known challenge in the tea industry. To ensure the quality of tea beverage products in the following year, tea farmers usually take measures such as artificial pruning and spraying plant growth regulators to inhibit reproduction (Liu et al., 2019). Understanding the relationship between the development of flowers and secondary metabolites (such as polyphenols) in tea plants will provide new ideas for effectively controlling the reproductive growth of tea plants.

Although the tea flower is bisexual, it is self-incompatible (Seth et al., 2019); thus, cross-pollination is the main propagation method of tea plants. Although tea plants bloom numerous each year, the fruit-setting rate is only 2–14.13% (Dong, 2001). Changes in the levels of plant hormones, including ABA, IAA, and ethylene etc., are involved in regulating pollen–pistil interactions (Baker et al., 1997). As a second messenger, $Ca2^{+}$ plays a key role in self-incompatibility (Wheeler et al., 2009). Many genes are involved in self-incompatibility, such as the *S* locus (S-locus) with multiple alleles (Takayama et al., 2000), *S-RNase* gene (Sun et al., 2018), *HT* gene, other modified genes (Kondo et al., 2002; Goldraij et al., 2006; Puerta et al., 2009), and *S-Locus F-box* (*SLF*) gene (Sun et al., 2015), which is involved in ubiquitin-mediated protein degradation (Hua and Kao, 2006).

It remains unclear how the phenolic compounds in flower buds change during flowering and whether they are involved in regulating the development of stamens and pistils. In this study, we used targeted metabolomic and transcriptomic analyses to evaluate the metabolism differences of phenolic compounds in buds at different developmental stages and in various parts of the tea flower. The key compounds and genes related to flower bud development was analyzed. These compounds and genes were then verified in fertile and hybrid sterile flower buds and transgenic tobacco.

MATERIALS AND METHODS

Plant Materials

Cultivars of the tea plant "Shuchazao" were grown in an experimental tea field at Anhui Agricultural University, Hefei, China (East longitude 117.27, North latitude 31.86). The tea plant "Fudingbaicha" cultivars were grown in the Tea Plant Cultivar and Germplasm Resource Garden in Guohe Town, Anhui Agricultural University. The sterile flowers were obtained from the Tea Research Institute, Yunnan Academy of Agricultural Sciences/Yunnan Engineering Research Center of Tea Germplasm Innovation and Matching Cultivation, Menghai, China. For the convenience of comparison, the developmental stage of the flower was artificially divided into six stages (S1–S6) with significant differences in shape and size. The flower bud in stage 1 is extremely small, only 3.0–3.5 mm in diameter. The floral organ primordia have been previously initiated and differentiated (Zhang, 2012; Zhou et al., 2017). According to the cross-sectional view of the flower bud, in stage 3 of the flower bud, its petals begin to appear white and its anthers become bright yellow due to pigment accumulation. Second leaves and flowers at different developmental stages and different parts of the flower were collected and frozen immediately in liquid nitrogen and stored at −80°C. Live branches with flowers were kept fresh

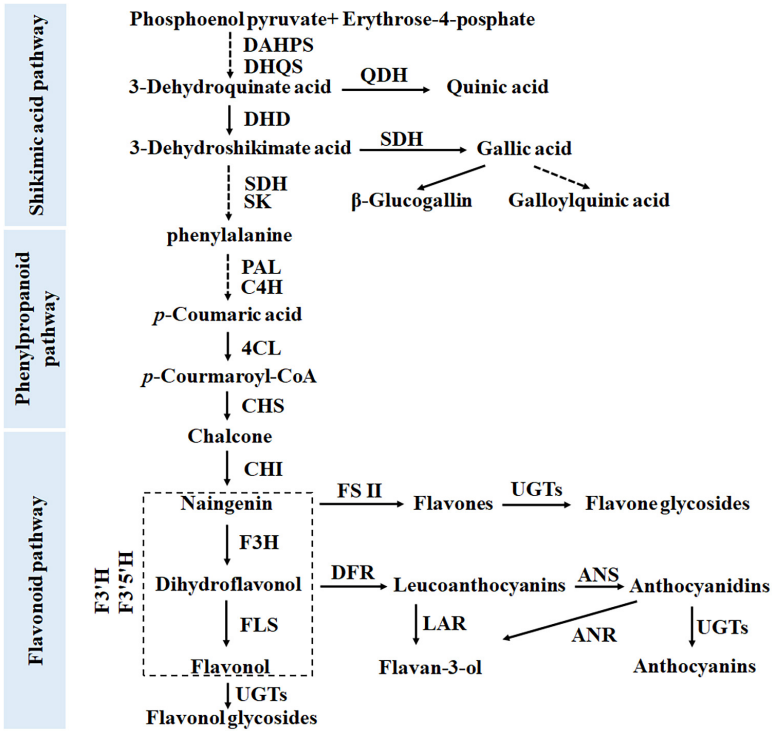

FIGURE 1 | Biosynthetic pathway of phenolic compounds in tea plants, including the shikimate, phenylpropanoid, and flavonoid pathways.

in absorbent sponge for subsequent experiments. Tobacco G28 (*Nicotiana tabacum* cv. G28) and transgenic tobacco were grown in a growth chamber at a constant temperature of 24 ± 3°C and 12/12 h light/dark cycle (Jiang et al., 2020).

Metabolic Analysis of Phenolic Compounds in Tea and Tobacco Flowers

The total polyphenol content of the tea samples was extracted and identified as described by Jiang et al. (2013) and Zhuang et al. (2020) with some modifications: 50 mg (dry weight) of samples was extracted with 2 mL of 80% methanol solution. The parameters of fragmentor voltage and collision energy were optimized by Zhuang et al. (2020). The quantitative detection of the compounds was performed using the MRM mode of the Agilent 6460 QQQ-MS/MS LC system (Agilent Technologies, Palo Alto, CA, United States). The flavonol glycosides were extracted from tobacco flowers and quantified as proposed by Jiang et al. (2018, 2020).

Transcriptome Analysis

The tissue samples used for transcriptome analysis were as follows: different developmental periods (stages 1, 3, and 5) of tea flowers of *Camellia sinensis cv. Shuchazao*. All samples were immediately frozen in liquid nitrogen and stored at −80°C. Each tissue had three biological repeats. On the basis of tea plants genome data, transcriptome sequencing and data analysis of tea flowers at stages 1, 3, and 5 were performed by BGI Gene Tech (Shenzhen, China) using the BGISEQ-500 platform.

Transcriptome data of different parts of flowers were obtained from the Tea Plant Information Archive (TPIA[1]). The data of *CsFLSb* expression in sterile and fertile flowers were obtained from transcriptomic data of the Yunnan Academy of Agricultural Sciences and Yunnan Engineering Research Center of Tea Germplasm Innovation and Matching Cultivation.

Quantitative Real-Time PCR of Flavonoid Pathway Genes

Total RNA was isolated, and RNA quality and quantity were determined according to the method of Wang et al. (2018). First-strand cDNA synthesis was performed using PrimeScript RT Master Mix (Takara, DaLian, China). Two-Step real-time PCR assays were performed as described by Wang et al. (2018). The primer sequences used in this study are listed in **Supplementary Table 3**; they were selected following Wang et al. (2018). The data were expressed as the mean of three replicates.

Genetic Transformation of *CsFLSs*

Tobacco genetic transformation was performed using the pCB2004-*Agrobacterium tumefaciens* expression system. The specific transgenic methods for tobacco were described by Jiang et al. (2020), and genetically modified materials were also obtained from Jiang et al. (2020).

[1]http://tpia.teaplant.org

Statistical Analysis

Mass spectrometry samples were assessed at least three times independently, and all data are represented as the mean ± SD. The peak area data were preprocessed using the area normalization method, and the processed data were used for the subsequent statistical analyses. After standardization, the data fell into a specific interval [0, 1]. The heat map of gene analysis was generated using Microsoft Office Excel (Microsoft, Redmond, WA, United States).

RESULTS

Metabolic Analysis of Phenolic Compounds and Expression Analysis of Related Biosynthetic Genes in Flower Buds at Different Developmental Stages

To investigate the metabolism characteristics of phenolic compounds in flower buds during the flowering process (**Figure 2A**), we collected flower buds at different developmental stages and used UPLC-MRM-MS system to detect differences in the types and contents of phenolic compounds among them. Given that the flower is a metamorphic branch and that the phenolic compounds in the leaves on the branch are already well understood (Jiang et al., 2013), the types and contents of phenolic compounds in the second leaf were used as references for the UPLC-MRM-MS analysis. The results revealed no significant difference in the types of phenolic compounds between tea leaves and flowers (**Supplementary Table 1** and **Figure 2C**). Similar to leaves, flowers have the following main types of phenolic compounds: phenolic acids, catechins (flavan-3-ols), proanthocyanins (PAs), flavanols, and flavonol glycosides (FGs). Their biosynthesis involves the shikimate pathway and its subsequent phenylpropanoid and flavonoid pathways (Wang et al., 2018). Several typical derivatization reactions, such as galloylation and condensation of flavan-3-ols, glycosylation of flavone and flavonol, and hydroxylation reactions of flavonoids, enrich these compounds (Zhuang et al., 2020).

Catechins, especially galloyl type EGCG and ECG, are the main phenolic compounds in tea leaves and flowers. Because proanthocyanins are the condensation products of catechins monomers, proanthocyanin and catechin monomers share the same synthesis pathway. Heat map analysis revealed that, in addition to EC and ECG, these catechins and PAs compounds exhibit similar patterns of change in flower development—their content gradually decreases as the flower develops (**Figure 2B**). In addition, the proanthocyanin content of the flowers in both S1 and S6 was significantly higher than that in the second leaf, but the content of the main catechin EGCG exhibited the opposite trend. This means that the condensation reaction rate in flowers is higher than that in leaves, whereas galloylation exhibited the opposite trend.

The derivatives of gallic acid (GA) and quinic acid (QA), the main phenolic acid derivatives, are derived from different branches of the shikimic acid (SA) pathway. They exhibited completely different trends in flower development: the content of GA derivatives gradually increased with the development of the flower, whereas that of QA derivatives reached the highest level in stage 1 (**Figure 2B**). In the second leaves, the content of GA derivatives was greatly increased. For example, the β-glucogallin (βG) content was 46.06 times higher in the flower bud at stage 6 than in the second leaf. Given that the content of hydrolyzed tannins in flowers is high, flower buds are a suitable substitute for studying the biosynthesis of hydrolyzed tannins in tea plants.

Based on the difference in the number of hydroxyl groups in the B-ring, flavonols can be divided into monohydroxy, dihydroxy, and trihydroxy compounds. Their representative glycosides are kaempferol (K), quercetin (Q), and myricetin (M), respectively. M glucosides with trihydroxy in the B-ring display a different trend from K and Q glucosides during flower development. During flower development, the contents of K and Q glucosides display an increasing trend, especially when their content exceeds that in the second leaf in the flower bud at S6.

In summary, the increase in the content of flavonol and GA derivatives is a significant metabolic feature during flower bud development. Compared with that in the second leaf, the content of QA derivatives, M derivatives, and the main catechin EGCG in the flower bud is lower.

To further understand the differences in gene expression related to phenol metabolism during flower development, we implemented a transcriptome sequencing project by using the BGISEQ-500 platform and the flower buds at stages 1, 3, and 5 as materials and focused on the differential expression of structural genes and transcription factor genes related to the shikimate, phenylpropanoid, and flavonoid pathways. RNAseq raw data has been submitted to Sequence Read Archive (SRA,[2]), and the accession number is PRJNA760230.

The results revealed that different members of the five gene families, such as *DHD/SDH* and Phospho-2-dehydro-3-deoxyheptonate aldolase (*DAHPS*) gene families, belonging to the shikimate pathway exhibit a differential expression pattern during flower development. The functions of 39 transcripts of 13 gene families belonging to the phenylpropanoid and flavonoid pathways have been verified (Wang et al., 2018). Our results indicated that most members of the 13 gene families were highly expressed in the flower buds at stage 1 (**Figure 2D**). A few genes were highly expressed in flowers at stage 3 or 5, such as *PALc* and *PALe*, *C4Hc*, *FLSb*, *FLSc*, and *DFRb3*. This was also evident in the differential expression analysis of transcription factors including MYB, bHLH, and the glycosylation-related UDP-glycosyltransferase gene family (**Supplementary Table 2**). Notably, the gene expressions of *FLSb* and *FLSc*, which are involved in flavonol synthesis, were significantly upregulated at stage 3, which was probably related to flavonol accumulation at the different developmental stages of tea flowers. Real-time quantitative PCR was performed to verify the reliability of the transcriptometric sequencing results, and the results were consistent with the transcriptometric sequencing results (**Supplementary Figure 1**).

[2]https://www.ncbi.nlm.nih.gov/sra/?term=PRJNA760230

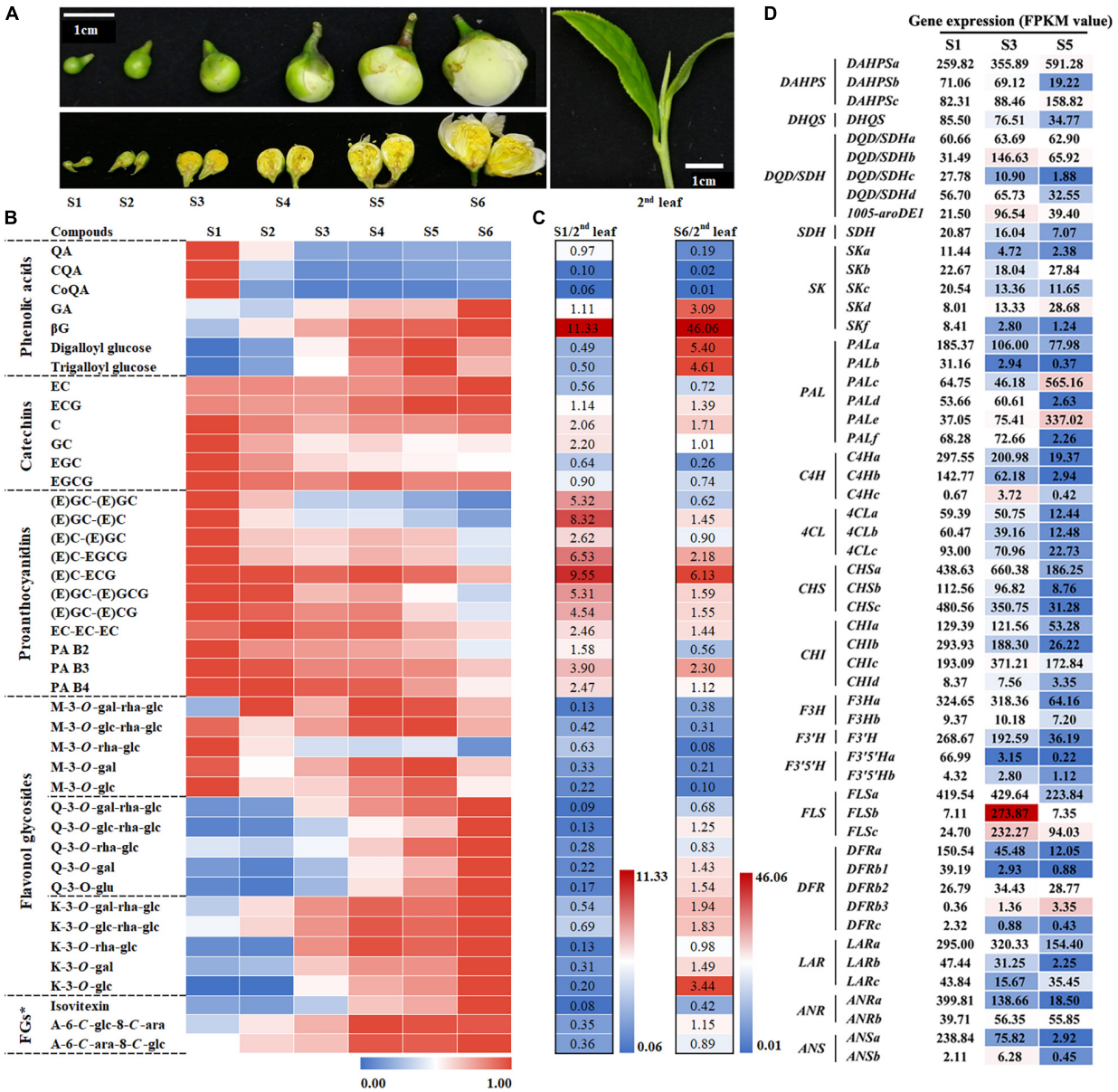

FIGURE 2 | Metabolic analysis of phenolic compounds and expression analysis of related biosynthetic genes at different flower bud developmental stages. **(A)** Phenotypes of different stages of flower buds and the second leaf. S1–S6 represent developmental stages 1–6, respectively. **(B)** Characteristics of phenolic compound accumulation in different flower developmental stages. The peak area data were processed and fall into an interval of 0–1 according to the ratio. FGs*, Flavone glycosides. **(C)** Comparison of the phenolic compound accumulation between S1 or S6 and the second leaf. **(D)** Expression analysis of genes in the shikimate, phenylpropanoid, and flavonoid pathways at different flower development stages. The value represents the FPKM value. The S1 FPKM value of each gene transcript was defined as numerical value 1, and the stage 3 and S5 FPKM values were converted proportionally.

Metabolic Analysis of Phenolic Compounds and Expression Analysis of Related Biosynthetic Genes in Various Parts of Tea Flowers

The tea flower can be divided into petal, stamen (anther and filament), pistil (stigma and style), and calyx (**Figure 3A**). Among them, Petals, anther and filament are the main components of flowers, accounting for 36, 34, and 25% respectively. UPLC-MRM-MS analysis was used to detect and analyze the metabolism of polyphenols in these parts. The results indicated that the polyphenol content of various parts of the flower bud varied greatly (**Figure 3B**). The contents of flavonol and flavone glycosides in petals and anthers were significantly higher than that in other parts of the flower bud, and their contents were the highest in petals. Thus, petals and anthers were determined to be the main sources of flavonols in tea flowers at stage 6. Moreover, filaments were the main source of GA derivatives in

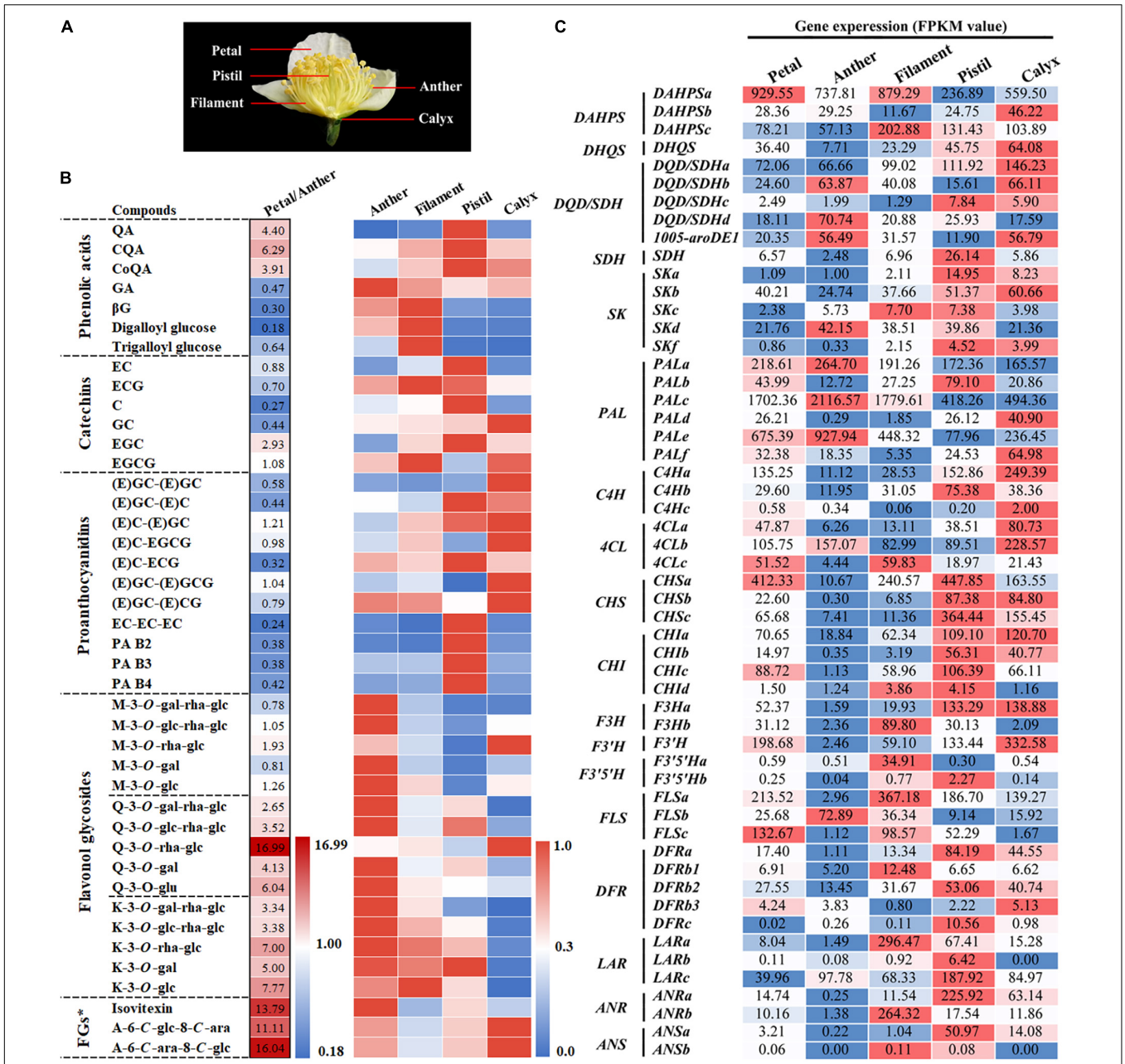

FIGURE 3 | Metabolic analysis of phenolic compounds and expression analysis of related biosynthetic genes in different parts of tea flowers. **(A)** Phenotypes of different parts of the flower. **(B)** Metabolic analysis of the main phenolic compounds in different parts of tea flowers. The petal/anther data were relative peak area comparisons of the petal to the anther. The peak area data of anthers, filaments, pistils, and calyxes were processed and fell into the interval [0, 1] according to the ratio. FGs*, Flavone glycosides. **(C)** Expression analysis of genes in the shikimate, phenylpropanoid, and flavonoid pathways in different parts of the tea flower. The value represents the FPKM value.

tea flowers at stage 6. Because the content of GA derivatives and gallic acylated catechins, including EGCG and ECG, was higher in filaments than in other flower bud parts, we speculate that the galloylation catalyzed by the SCPL enzyme in filaments was higher than that in other parts.

The content of B-ring dihydroxycatechins and their polymer was higher in the pistil than in other flower bud parts. However, the contents of monomers and polymers of B-ring trihydroxy compounds such as EGC, GC, and EGCG and M glycoside compounds were lower in pistils than in the other parts. This means that the predominant F3′5′H-catalyzed B-ring trihydroxylation reaction in tea leaves was weaker in pistils. Catechin accumulation characteristics in the calyx were opposite to in the pistil. Similar to leaves, the calyx was observed to accumulate more B-ring trihydroxy catechin monomers and their polymers.

In conclusion, as a specialized or metamorphic branch, the accumulation of phenolic compounds in various parts of the tea flower exhibits differing characteristics, which also means that the flower is a good material for studying the different branches of biosynthesis of phenolic compounds of tea plants.

To further understand the differences in gene expression related to phenol metabolism in different parts of the flower bud, we analyzed the transcriptome information of various parts of flower buds. According to the transcriptomic analysis of different developmental stages of tea flowers, we analyzed the genes related to the shikimate, phenylpropanoid, and flavonoid pathways. The results are illustrated in **Figure 3C**. *DFR*s, *LAR*s, *ANR*s, and other genes were highly expressed in the pistil and calyx; such expression was related to the accumulation of catechins, proanthocyanins, and other substances in the pistil and calyx. *F3H*, *FLS*s, and other genes related to the synthesis of flavonol were highly expressed in anthers and filaments; this was related to the accumulation of flavonol in flower petals, anthers, and filaments. Notably, *FLSb* exhibited a particularly high expression pattern in anthers, suggesting that *FLSb* may be closely related to anther development.

Correlation Between Flavonols and Tea Flower Fertility

The results described in the previous section suggest that the anther has a high flavonol content. This raises the question of whether flavonols are closely related to the development of anthers. To answer this question, we compared phenolic content between fertile flowers and hybrid sterile flowers without pollen (**Figures 4A,B**). In addition to some K and Q glycosides, UPLC-MRM-MS analysis revealed that the contents of most phenolic compounds, including catechins, proanthocyanins, phenolic acids, flavone glycosides, and M derivatives in sterile flowers, were higher than those in fertile flowers. For example, the contents of Kaempferol-3-*O*-glucoside (K-3-*O*-glc) and Kaempferol-3-*O*-rutinoside (K-3-*O*-rha-glc) in sterile flowers are only 45.2 and 29.0% of the contents in fertile flowers, respectively. This result suggests that K and Q glycosides are probably related to the development of the anther. Moreover, compared with fertile flowers, *CsFLSb* expression in sterile flowers was extremely low.

Functional Differences Between *CsFLSa*, *CsFLSb*, and *CsFLSc*

Three flavonol synthase genes—*CsFLSa*, *CsFLSb*, and *CsFLSc*—were analyzed to determine their function in flavonol synthesis. The enzymatic properties of the recombinant protein of these three genes have been investigated (Jiang et al., 2020). However, the differences in their function in plants have not been thoroughly studied. By using the pCB2004-*Agrobacterium tumefaciens* expression system, we expressed *CsFLSa*, *CsFLSb*, and *CsFLSc* in tobacco and obtained stable transgenic tobacco plants. The growth status of these transgenic plants was consistent with that of the control transgenic plants (CK; **Figure 5A**). Compared with CK tobacco flowers, the flowers of the three transgenic tobacco plants heterologously expressing *CsFLSb* and *CsFLSc* exhibited changes in their characteristics (**Figure 5C**). Compared with the pink CK tobacco flower, the color of *CsFLSb*-OE and *CsFLSc*-OE tobacco flowers was lighter—almost white, whereas that of *CsFLSa* transgenic tobacco flower remained seemingly unchanged (**Figure 5C**).

The accumulation of flavonols in CK and three transgenic tobacco flowers and the first and second leaves was detected with UPLC-MRM-MS. The characteristics of flavonol accumulation in transgenic tobacco leaves and flowers differed (**Figure 5B**). Compared with CK, the flavonol content increased in the leaves of *CsFLSa*-OE plants and decreased in those of *CsFLSb*-OE and *CsFLSc*-OE plants. However, the flavonol content of the *CsFLSa* tobacco flower exhibited no distinct change, whereas that of *CsFLSb*-OE and *CsFLSc*-OE tobacco flower flavonol content, especially K flavonol glycosides, increased significantly; and Q flavonol glycoside content decreased in *CsFLSc*-OE tobacco flowers (**Figure 5D**).

In summary, *CsFLSa*, *CsFLSb*, and *CsFLSc* regulate flavonol accumulation in transgenic tobacco in different parts. Accordingly, we speculate that these genes have different functions in tea plants.

DISCUSSION

Flavan-3-ols with a C6-C3-C6 structure are the main compounds accumulated in leaves of tea plants, accounting for 70% of the total polyphenols (4). Second only to that of flavan-3-ols, flavonol glycoside content in tea leaves can reach >2% (Wu et al., 2016). Both flavan-3-ols and flavonol glycosides are directly related to the bitterness and astringency of tea beverages (Zhuang et al., 2020). Therefore, their biosynthesis has attracted much attention from scientists. The main pathways of favan-3-ols and flavonol glycosides synthesis are the same as those in Arabidopsis and other model plants. They all come from the shikimate pathway and its downstream phenylpropanoid and flavonoid synthesis pathways (Jiang et al., 2013; **Figure 1**).

Each step in the shikimate, phenylpropanoid, and flavonoid synthesis pathways is controlled by multiple gene families (Wang et al., 2018). This means that these pathways have network regulation characteristics. Phenolic acids, including SA and GA derivatives, mainly come from the SA pathway located upstream of the phenylpropanoid pathway (**Figure 1**). Huang et al. (2019) reported that four 3-dehydroquinate dehydratase/shikimate dehydrogenase (*DQD/SDH*) genes in tea plants are responsible for the synthesis of SA and GA, respectively. In particular, the SDH enzyme, a bifunctional enzyme, controls the synthetic metabolic flow of GA, QA, and SA in plants. The results presented in **Figure 2** show that the accumulations of QA and GA derivatives exhibit very different trends, a finding which may be attributable to the differential expression of these gene family members.

The biosynthesis of flavan-3-ols or flavonol glycosides in various organs of tea plants can be controlled by different homologous genes of the same gene family. Because the types of phenolic compounds accumulated in different parts of the tea flower are highly different (**Figure 2**), floral organs may be

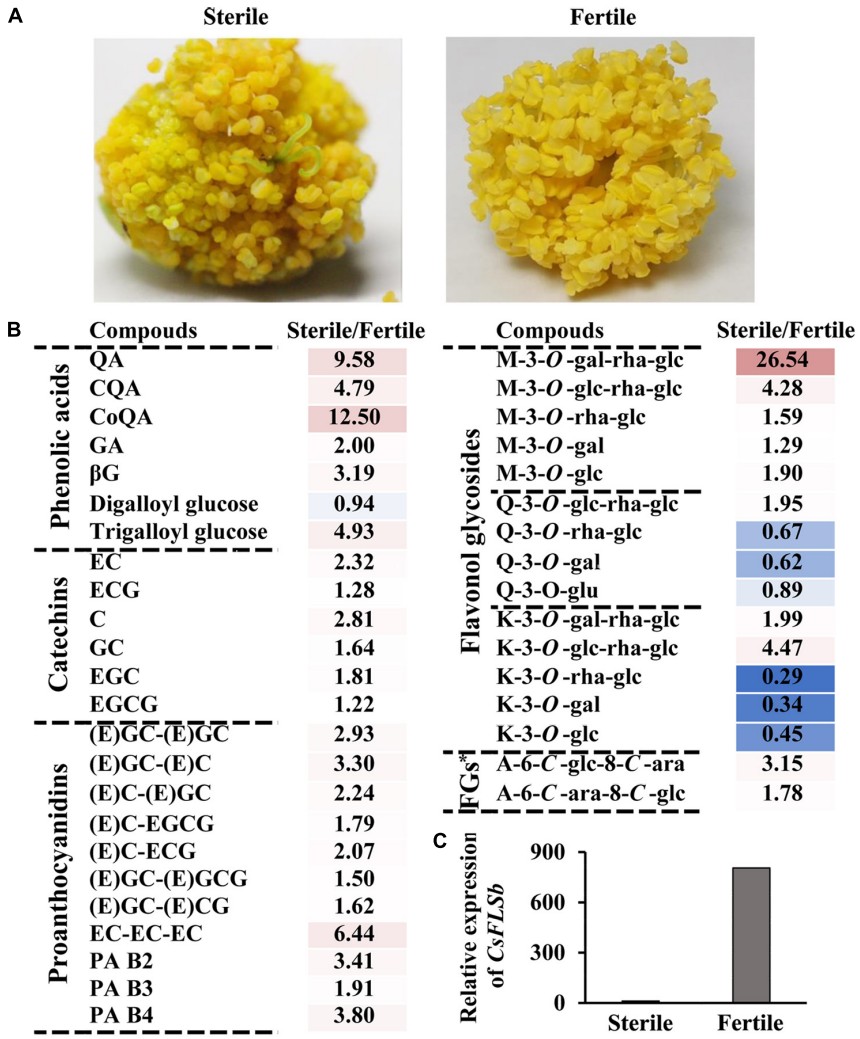

FIGURE 4 | Characteristics of phenolic compound accumulation in the anthers of hybrid sterile and fertile tea flowers and *CsFLSb* gene expression in hybrid sterile and fertile flowers. **(A)** Anther phenotypes of the hybrid sterile flower with no pollen and fertile flowers. **(B)** Metabolic analysis of phenolic compounds between hybrid sterile anther and fertile anther. FGs*, Flavone glycosides. **(C)** *CsFLSb* expression in hybrid sterile and fertile flowers; the histogram shows the FPKM values.

good materials for studying the network regulation of phenolic compound biosynthesis.

Many studies have attempted to identify flavonols and their biosynthesis regulation in tea plants (Wu et al., 2016; Jiang et al., 2020). However, their physiological significance in tea plants remains unclear. Given the antioxidant function of phenolic compounds *in vitro* (Jiménez-Zamora et al., 2016; Zeng et al., 2017), it is speculated that phenolic compounds in plants can also participate in the plant's antiepidemic response through their antioxidant capacity. In many model plants, phenolic compounds, including anthocyanins, phenolic acids, lignin, flavonols, and proanthocyanins, participate in the physiological processes of plant growth, flowering and fruiting, and resistance to biotic and abiotic stresses (Muro-Villanueva et al., 2019; Shi et al., 2019; Su et al., 2020). This article found that not only the leaves, but also the flowers of tea plants accumulate high levels of phenolic compounds (**Figure 2**). So, is the so highly accumulated phenolic compounds in tea flowers related to its development or resistance?

Flavonols are involved in the development of floral organs and flower fertility (Mo et al., 1992; Napoli et al., 1999). *CHS* gene knockout in petunias and *FLS* gene silencing in tobacco can suppress the whitening of anthers, induce male sterility, and influence other traits (Napoli et al., 1999; Mahajan et al., 2011). Compared with wild-type *A. thaliana*, that with low flavonol accumulation significantly inhibits pollen tube growth (Schiefelbein et al., 1993). The pollen germination and pollen tube elongation can be restored by adding low-concentration flavonol to the germination medium (Ylstra et al., 1992; Pollak et al., 1995). In this study, we also found a correlation between flavonols and anther growth (**Figure 4**). During flower development, the content of flavonol K and Q glycosides gradually increased (**Figure 2**). Mass spectrometry detection of materials in different

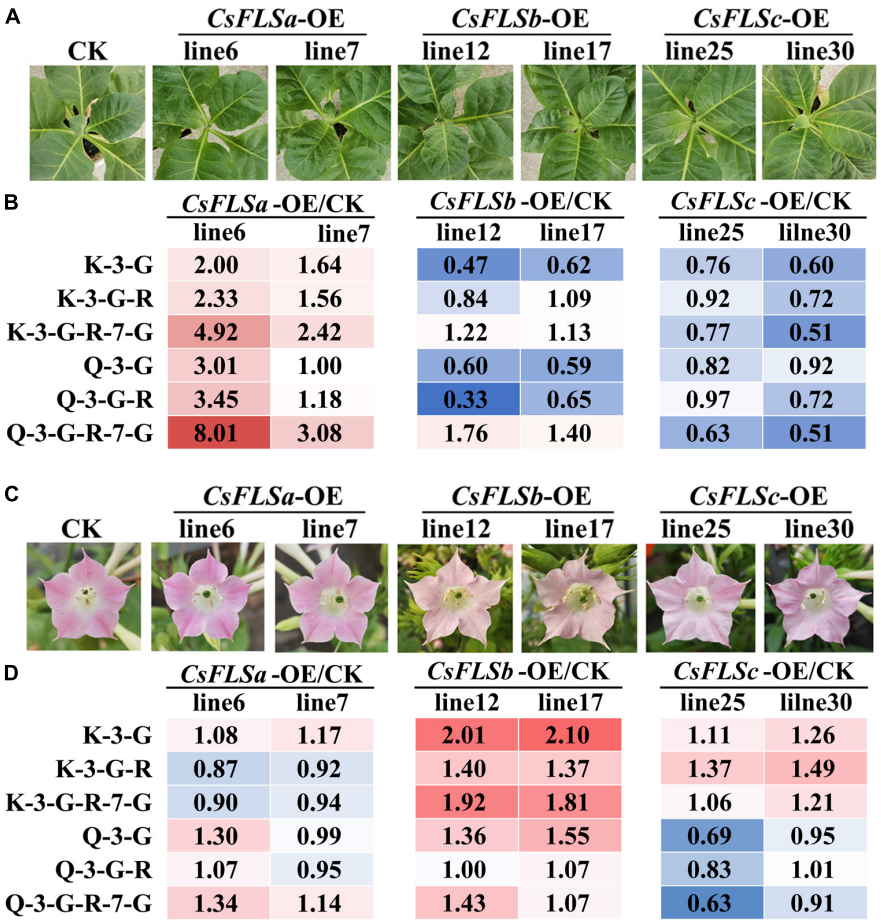

FIGURE 5 | Flavonol accumulation characteristics in *CsFLS*s transgenic tobacco leaf and flower. **(A)** Phenotypes of CK and *CsFLSa*, *CsFLSb*, and *CsFLSc* transgenic tobacco leaves. **(B)** Relative accumulation of kaempferol and quercetin glycoside extracts from CK and *CsFLS*s tobacco leaves. **(C)** Phenotypes of CK and *CsFLSa*, *CsFLSb*, and *CsFLSc* tobacco flowers. **(D)** Relative accumulation of kaempferol and quercetin glycosides of CK and *CsFLS*s tobacco flowers. CK, empty vector control.

parts of the flower revealed that most flavonol glycosides mainly accumulated in petals and anthers (**Figure 3**). The content of K and Q glycosides in sterile flower anthers was lower than that in fertile flower anthers (**Figure 4**). Our transcriptomic analysis (**Figures 2–4**) and the previous studies (Chen et al., 2019) screened out flavonol pathway genes related to flower development and fertility. *CsFLSb* changed significantly during flowering, and its expression was high in anthers in fertile flowers and extremely low in sterile flowers. These results indicate that *CsFLSb* played an essential role in the regulation of anther development by affecting flavonol synthesis during flower development. Our study findings on phenol accumulation, together with transcriptomic analysis, help to reveal the mechanism of sterility in tea plants. However, molecular data are limited for tea plants. Future studies should attempt to elucidate the other aspects mechanisms. Our metabolome and transcriptome analysis results help to reveal the mechanism of tea flower sterility. However, these landscape data alone are not enough, and further mechanism studies are needed in the future.

Flavonol synthases are key genes in flavonol synthesis. Notably, in the leaves of tea plants, the expression of *FLSa* is considerably high and that of *FLSb* and *FLSc* is relatively low (Wang et al., 2018). However, *FLSb* and *FLSc* expression in the flowers in stage 3 was 38.5 times and 9.4 times higher, respectively, than that in S1 (**Figure 2**). The function of *CsFLS* genes has been studied using enzymology and transgenic tobacco methods. An enzymological analysis revealed three recombinant *CsFLS* proteins that can catalyze dihydroflavonols to form flavonols (Jiang et al., 2020). In this study, we observed that tobacco overexpressed with *CsFLSa*, *CsFLSb*, and *CsFLSc* showed the opposite trend of accumulating flavonol (**Figure 5**). This result further proved that *CsFLSb* and *CsFLSc* rather than *CsFLSa* are responsible for the synthesis of flavonol glycosides in the flowers of tea plants.

DATA AVAILABILITY STATEMENT

The data presented in the study are deposited in the Sequence Read Archive repository, accession number PRJNA760230.

AUTHOR CONTRIBUTIONS

LG and TX conceived and designed the study. YS, XJ, LG, and TX drafted the manuscript. YS performed the experiments. YS and XJ analyzed the data. LC provided some plant materials and transcriptomic data. ZF, W-WL, SL, and YQ assisted with experiments, materials, and analytical tools. YL reviewed and edited the manuscript. All authors read and approved the final version of the manuscript.

FUNDING

This work was financially supported by the National Key Research and Development Program of China (2018YFD1000601), Youth Science and Technology Talents Support Program (2020) by Anhui Association for Science and Technology (RCTJ202010), the National Natural Science Foundation of China (31902069, 31870676 and 31870677), and the Natural Science Foundation of Anhui Province, China (1908085MC100).

SUPPLEMENTARY MATERIAL

The Supplementary Material for this article can be found online at: https://www.frontiersin.org/articles/10.3389/fpls.2021.753131/full#supplementary-material

Supplementary Figure 1 | Verification of the relative expression levels of genes by qRT-PCR. Expression patterns of parts of structural genes in S1, S3, S5 flowers involved in phenylpropanoid and flavonoid pathways by qRT-PCR, including **(A)** C4Ha, **(B)** 4CLb, **(C)** CHIc, **(D)** F3Ha, **(E)** F3′H, **(F)** FLSb, **(G)** LARc, **(H)** ANRa, and **(I)** ANRb.

REFERENCES

Baker, R. P., Hasenstein, K. H., and Zavada, M. S. (1997). Hormonal changes after compatible and incompatible pollination in *Theobroma cacao* L. *HortScience* 32, 1231–1234. doi: 10.21273/hortsci.32.7.1231

Brown, D. E., Rashotte, A. M., Murphy, A. S., Normanly, J., Tague, B. W., Peer, W. A., et al. (2001). Flavonoids act as negative regulators of auxin transport in vivo in *Arabidopsis*. *Plant Physiol.* 126, 524–535. doi: 10.1104/pp.126.2.524

Chen, L., Qu, H., Xia, L., Liu, Y., Jiang, H., Sun, Y., et al. (2019). Transcriptome profiling of the fertile parent and sterile hybrid in tea plant flower buds. *Hereditas* 156:12. doi: 10.1186/s41065-019-0090-z

Dong, L. (2001). Progressin the field of tea cross-breeding research. *Tea Sci.* 21, 7–10. doi: 10.3969/j.issn.1000-369X.2001.01.003

Goldraij, A., Kondo, K., Lee, C. B., Hancock, C. N., Sivaguru, M., Vazquez-Santana, S., et al. (2006). Compartmentalization of S-RNase and HT-B degradation in self-incompatible Nicotiana. *Nature* 439, 805–810. doi: 10.1038/nature04491

Hua, Z., and Kao, T. H. (2006). Identification and characterization of components of a putative petunia S-locus F-box-containing E3 ligase complex involved in S-RNase-based self-incompatibility. *Plant Cell* 18, 2531–2553. doi: 10.1105/tpc.106.041061

Huang, K., Li, M., Liu, Y., Zhu, M., Zhao, G., Zhou, Y., et al. (2019). Functional analysis of 3-Dehydroquinate dehydratase/shikimate dehydrogenases involved in shikimate pathway in *Camellia sinensis*. *Front. Plant Sci.* 10:1268. doi: 10.3389/fpls.2019.01268

Jacobs, M., and Rubery, P. H. (1988). Naturally occurring auxin transport regulators. *Science* 241, 346–349. doi: 10.1126/science.241.4863.346

Jiang, X., Hua, H., Shuxiang, Z., Yajun, L., Haiyan, W., Wei-Wei, D., et al. (2017). Comparison of phenolic compound accumulation profiles in eight evergreen woody core eudicots indicating the diverse ecological adaptability of *Camellia sinensis*. *Sci. Horticulturae* 219, 200–206. doi: 10.1016/j.scienta.2017.03.018

Jiang, X., Huang, K., Zheng, G., Hou, H., Wang, P., Jiang, H., et al. (2018). CsMYB5a and CsMYB5e from *Camellia sinensis* differentially regulate anthocyanin and proanthocyanidin biosynthesis. *Plant Sci.* 270, 209–220. doi: 10.1016/j.plantsci.2018.02.009

Jiang, X., Liu, Y., Li, W., Zhao, L., Meng, F., Wang, Y., et al. (2013). Tissue-specific, development-dependent phenolic compounds accumulation profile and gene expression pattern in tea plant [*Camellia sinensis*]. *PLoS One* 8:e62315. doi: 10.1371/journal.pone.0062315

Jiang, X., Shi, Y., Fu, Z., Li, W. W., Lai, S., Wu, Y., et al. (2020). Functional characterization of three flavonol synthase genes from *Camellia sinensis*: roles in flavonol accumulation. *Plant Sci.* 300:110632. doi: 10.1016/j.plantsci.2020.110632

Jiménez-Zamora, A., Delgado-Andrade, C., and Rufián-Henares, J. A. (2016). Antioxidant capacity, total phenols and color profile during the storage of selected plants used for infusion. *Food Chem.* 199, 339–346. doi: 10.1016/j.foodchem.2015.12.019

Kondo, K., Yamamoto, M., Matton, D. P., Sato, T., Hirai, M., Norioka, S., et al. (2002). Cultivated tomato has defects in both S-RNase and HT genes required for stylar function of self-incompatibility. *Plant J.* 29, 627–636. doi: 10.1046/j.0960-7412.2001.01245.x

Li, P., Li, Y. J., Zhang, F. J., Zhang, G. Z., Jiang, X. Y., Yu, H. M., et al. (2017). The Arabidopsis UDP-glycosyltransferases UGT79B2 and UGT79B3, contribute to cold, salt and drought stress tolerance via modulating anthocyanin accumulation. *Plant J.* 89, 85–103. doi: 10.1111/tpj.13324

Liu, H. Y., Xu, J. H., Lu, L., and Yan, C. J. (2019). Analysis and measures of flowering factors of Baiye No.1 tea plant in Zhenjiang area. *South China Agriculture* 013, 33–35.

Liu, Y., Hao, X., Lu, Q., Zhang, W., Zhang, H., Wang, L., et al. (2020). Genome-wide identification and expression analysis of flowering-related genes reveal putative floral induction and differentiation mechanisms in tea plant (*Camellia sinensis*). *Genomics* 112, 2318–2326. doi: 10.1016/j.ygeno.2020.01.003

Mahajan, M., Ahuja, P. S., and Yadav, S. K. (2011). Post-transcriptional silencing of flavonol synthase mRNA in tobacco leads to fruits with arrested seed set. *PLoS One* 6:e28315. doi: 10.1371/journal.pone.0028315

Mo, Y., Nagel, C., and Taylor, L. P. (1992). Biochemical complementation of chalcone synthase mutants defines a role for flavonols in functional pollen. *Proc. Natl. Acad. Sci. U S A.* 89, 7213–7217. doi: 10.1073/pnas.89.15.7213

Muhlemann, J. K., Younts, T. L. B., and Muday, G. K. (2018). Flavonols control pollen tube growth and integrity by regulating ROS homeostasis during high-temperature stress. *Proc. Natl. Acad. Sci. U S A.* 115, E11188–E11197. doi: 10.1073/pnas.1811492115

Muro-Villanueva, F., Mao, X., and Chapple, C. (2019). Linking phenylpropanoid metabolism, lignin deposition, and plant growth inhibition. *Curr. Opin. Biotechnol.* 56, 202–208. doi: 10.1016/j.copbio.2018.12.008

Naing, A. H., Ai, T. N., Lim, K. B., Lee, I. J., and Kim, C. K. (2018). Overexpression of rosea1 from snapdragon enhances anthocyanin accumulation and abiotic stress tolerance in transgenic tobacco. *Front. Plant Sci.* 9:1070. doi: 10.3389/fpls.2018.01070

Napoli, C. A., Fahy, D., Wang, H. Y., and Taylor, L. P. (1999). white anther: a petunia mutant that abolishes pollen flavonol accumulation, induces male sterility, and is complemented by a chalcone synthase transgene. *Plant Physiol.* 120, 615–622. doi: 10.1104/pp.120.2.615

Pollak, P. E., Hansen, K., Astwood, J. D., and Taylor, L. P. (1995). Conditional male fertility in maize. *Sexual Plant Reprod.* 8, 231–241.

Puerta, A. R., Ushijima, K., Koba, T., and Sassa, H. (2009). Identification and functional analysis of pistil self-incompatibility factor HT-B of Petunia. *J. Exp. Bot.* 60, 1309–1318. doi: 10.1093/jxb/erp005

Schiefelbein, J., Galway, M., Masucci, J., and Ford, S. (1993). Pollen tube and root-hair tip growth is disrupted in a mutant of *Arabidopsis thaliana*. *Plant Physiol.* 103, 979–985. doi: 10.1104/pp.103.3.979

Seth, R., Bhandawat, A., Parmar, R., Singh, P., Kumar, S., and Sharma, R. K. (2019). *Camellia sinensis* global transcriptional insights of pollen-pistil interactions commencing self-incompatibility and fertilization in tea [(L.) *O. Kuntze*]. *Int. J. Mol. Sci.* 20:539. doi: 10.3390/ijms20030539

Shi, M., Huang, F., Deng, C., Wang, Y., and Kai, G. (2019). Bioactivities, biosynthesis and biotechnological production of phenolic acids in *Salvia miltiorrhiza*. *Crit. Rev. Food Sci. Nutr.* 59, 953–964. doi: 10.1080/10408398.2018.1474170

Su, W., Tao, R., Liu, W., Yu, C., Yue, Z., He, S., et al. (2020). Characterization of four polymorphic genes controlling red leaf colour in lettuce that have undergone disruptive selection since domestication. *Plant Biotechnol. J.* 18, 479–490. doi: 10.1111/pbi.13213

Sun, L., Williams, J. S., Li, S., Wu, L., Khatri, W. A., Stone, P. G., et al. (2018). S-Locus F-Box proteins are solely responsible for S-RNase-Based self-incompatibility of petunia pollen. *Plant Cell* 30, 2959–2972. doi: 10.1105/tpc.18.00615

Sun, P., Li, S., Lu, D., Williams, J. S., and Kao, T. H. (2015). Pollen S-locus F-box proteins of Petunia involved in S-RNase-based self-incompatibility are themselves subject to ubiquitin-mediated degradation. *Plant J. Cell Mol. Biol.* 83, 213–223. doi: 10.1111/tpj.12880

Takayama, S., Shiba, H., Iwano, M., Shimosato, H., Che, F. S., Kai, N., et al. (2000). The pollen determinant of self-incompatibility in *Brassica campestris*. *Proc. Natl. Acad. Sci. U S A.* 97, 1920–1925. doi: 10.1073/pnas.040556397

Tang, G. Y., Meng, X., Gan, R. Y., Zhao, C. N., Liu, Q., Feng, Y. B., et al. (2019). Health functions and related molecular mechanisms of tea components: an update review. *Int. J. Mol. Sci.* 20:6196. doi: 10.3390/ijms20246196

Tansengco, M. L., Imaizumi-Anraku, H., Yoshikawa, M., Takagi, S., Kawaguchi, M., Hayashi, M., et al. (2004). Pollen development and tube growth are affected in the symbiotic mutant of Lotus japonicus, crinkle. *Plant Cell Physiol.* 45, 511–520. doi: 10.1093/pcp/pch076

Valduga, A. T., Gonçalves, I. L., Magri, E., and Delalibera Finzer, J. R. (2019). Chemistry, pharmacology and new trends in traditional functional and medicinal beverages. *Food Res. Int.* 120, 478–503. doi: 10.1016/j.foodres.2018.10.091

Wang, W., Zhou, Y., Wu, Y., Dai, X., Liu, Y., Qian, Y., et al. (2018). Insight into catechins metabolic pathways of camellia sinensis based on genome and transcriptome analysis. *J. Agric. Food Chem.* 66, 4281–4293. doi: 10.1021/acs.jafc.8b00946

Wasson, A. P., Pellerone, F. I., and Mathesius, U. (2006). Silencing the flavonoid pathway in Medicago truncatula inhibits root nodule formation and prevents auxin transport regulation by rhizobia. *Plant Cell* 18, 1617–1629. doi: 10.1105/tpc.105.038232

Wheeler, M. J., de Graaf, B. H., Hadjiosif, N., Perry, R. M., Poulter, N. S., Osman, K., et al. (2009). Identification of the pollen self-incompatibility determinant in *Papaver rhoeas*. *Nature* 459, 992–995. doi: 10.1038/nature08027

Wu, Y., Jiang, X., Zhang, S., Dai, X., Liu, Y., Tan, H., et al. (2016). Quantification of flavonol glycosides in *Camellia sinensis* by MRM mode of UPLC-QQQ-MS/MS. *J. Chromatogr. B Analyt. Technol. Biomed. Life Sci.* 101, 10–17. doi: 10.1016/j.jchromb.2016.01.064

Xing, L., Zhang, H., Qi, R., Tsao, R., and Mine, Y. (2019). Recent advances in the understanding of the health benefits and molecular mechanisms associated with green tea polyphenols. *J. Agric. Food Chem.* 67, 1029–1043. doi: 10.1021/acs.jafc.8b06146

Ylstra, B., Touraev, A., Moreno, R. M., Stöger, E., van Tunen, A. J., Vicente, O., et al. (1992). Flavonols stimulate development, germination, and tube growth of tobacco pollen. *Plant Physiol.* 100, 902–907. doi: 10.1104/pp.100.2.902

Zahedi, S. M., Karimi, M., and Venditti, A. (2019). Plants adapted to arid areas: specialized metabolites. *Nat. Prod. Res.* doi: 10.1080/14786419.2019.1689500 Online ahead of print.

Zeng, L., Luo, L., Li, H., and Liu, R. (2017). Phytochemical profiles and antioxidant activity of 27 cultivars of tea. *Int. J. Food Sci. Nutr.* 68, 525–537. doi: 10.1080/09637486.2016.1263834

Zhang, Y. (2012). *Morphological Study on Flower Bud Differentiation and Floral Organ Development of Tea Plant*. Master thesis, China: Shaanxi Normal University.

Zhou, X., Li, J., Zhu, Y., Ni, S., Chen, J., Feng, X., et al. (2017). De novo assembly of the *Camellia nitidissima* transcriptome reveals key genes of flower pigment biosynthesis. *Front. Plant Sci.* 8:1545. doi: 10.3389/fpls.2017.01545

Zhuang, J., Dai, X., Zhu, M., Zhang, S., Dai, Q., Jiang, X., et al. (2020). Evaluation of astringent taste of green tea through mass spectrometry-based targeted metabolic profiling of polyphenols. *Food Chem.* 305:125507. doi: 10.1016/j.foodchem.2019.125507

Conflict of Interest: The authors declare that the research was conducted in the absence of any commercial or financial relationships that could be construed as a potential conflict of interest.

Publisher's Note: All claims expressed in this article are solely those of the authors and do not necessarily represent those of their affiliated organizations, or those of the publisher, the editors and the reviewers. Any product that may be evaluated in this article, or claim that may be made by its manufacturer, is not guaranteed or endorsed by the publisher.

frontiers in Plant Science

ORIGINAL RESEARCH
published: 01 October 2021
doi: 10.3389/fpls.2021.746972

Non-Volatile Metabolic Profiling and Regulatory Network Analysis in Fresh Shoots of Tea Plant and Its Wild Relatives

Chen-Kai Jiang[1,2†], Zhi-Long Liu[3†], Xuan-Ye Li[1], Sezai Ercisli[4], Jian-Qiang Ma[1] and Liang Chen[1*]*

[1] Key Laboratory of Tea Biology and Resources Utilization, Ministry of Agriculture and Rural Affairs, Tea Research Institute of the Chinese Academy of Agricultural Sciences, Hangzhou, China, [2] State Key Laboratory for Quality and Safety of Agro-Products, Zhejiang Academy of Agricultural Sciences, Hangzhou, China, [3] Lishui Academy of Agricultural and Forestry Sciences, Lishui, China, [4] Department of Horticulture, Faculty of Agriculture, Ataturk University, Erzurum, Turkey

OPEN ACCESS

Edited by:
Chuankui Song,
Anhui Agriculture University, China

Reviewed by:
Ziyin Yang,
South China Botanical Garden, Chinese Academy of Sciences, China
Xingtan Zhang,
Chinese Academy of Agricultural Sciences (CAAS), China

***Correspondence:**
Jian-Qiang Ma
majianqiang@tricaas.com
Liang Chen
liangchen@tricaas.com;
chenliang@caas.cn

† These authors have contributed equally to this work

Specialty section:
This article was submitted to Plant Metabolism and Chemodiversity, a section of the journal Frontiers in Plant Science

Received: *25 July 2021*
Accepted: *31 August 2021*
Published: *01 October 2021*

Citation:
Jiang C-K, Liu Z-L, Li X-Y, Ercisli S, Ma J-Q and Chen L (2021) Non-Volatile Metabolic Profiling and Regulatory Network Analysis in Fresh Shoots of Tea Plant and Its Wild Relatives. Front. Plant Sci. 12:746972. doi: 10.3389/fpls.2021.746972

There are numerous non-volatile metabolites in the fresh shoots of tea plants. However, we know little about the complex relationship between the content of these metabolites and their gene expression levels. In investigating this, this study involved non-volatile metabolites from 68 accessions of tea plants that were detected and identified using untargeted metabolomics. The tea accessions were divided into three groups from the results of a principal component analysis based on the relative content of the metabolites. There were differences in variability between the primary and secondary metabolites. Furthermore, correlations among genes, gene metabolites, and metabolites were conducted based on Pearson's correlation coefficient (PCC) values. This study offered several significant insights into the co-current network of genes and metabolites in the global genetic background. Thus, the study is useful for providing insights into the regulatory relationship of the genetic basis for predominant metabolites in fresh tea shoots.

Keywords: correlation, fresh shoots, network, non-volatile metabolites, tea plant

INTRODUCTION

Tea plants have a long history of cultivation, processing, and consumption worldwide because they contain special metabolites, specifically secondary metabolites. The metabolites in tea plants play a role in abiotic and biotic stresses during their growth and development. Furthermore, these metabolites are retention substances or precursors that transform other quality compounds in tea. Therefore, metabolites in the fresh shoots of tea plants, as substance bases, contribute to the flavor and health-enhancing functions of drinkable tea. Many studies have been conducted to explore the phytochemical compounds in the leaves of tea plants. These metabolites can be divided into volatile and non-volatile compounds based on their boiling points. Non-volatile compounds account for 99.97–99.99% of the total dry tea weight (Kim et al., 2016), among which flavonoids, theanine, and caffeine have attracted extensive attention during the last few decades. It is important to improve our understanding of the regulatory network of metabolites. Firstly, it is helpful in altering the expression of key genes and the content of metabolites through cultivation measures. Secondly, it forecasts the quality and yield of plants based on metabolite traits that are easy

to test. Thirdly, it allows the control of metabolic flow by improving or inhibiting the activity of major enzymes in metabolic engineering. However, most previous studies have focused on the relationships between genes and metabolites. Therefore, the relationship between metabolites remains unclear and requires further probing to understand the regulatory mechanism underlying their relationship.

Previous studies have investigated the effects of an ambient environment, including light, temperature, elevation, and cultivation measures, on the metabolites of tea (Kfoury et al., 2018; Liu et al., 2018). For example, high elevation teas contain statistically sweeter, floral, honey-like compounds as opposed to low elevation tea, which contains statistically greener, herbal, hay-like, bitter compounds (Kfoury et al., 2018). The reduction in flavonols and catechins in shading tea plants was mainly modulated through the downregulation of biosynthetic genes and transcription factors associated with flavonoid biosynthesis caused by reduced UV-B radiation (Liu et al., 2018). Other studies have focused on the regulation of compound biosynthesis by certain genes or metabolic differences in certain varieties (Cao et al., 2020; Li et al., 2021; Zheng et al., 2021). For instance, 13 metabolites were associated with the zigzag-shaped morphology of tea plants (Cao et al., 2020). Five miRNAs may play important roles in regulating the biosynthesis of flavor compounds, including linalool, geraniol, and 2-phenylethanol, in the different tissues of tea plants (Li et al., 2021). A large number of metabolites related to light protection were found to significantly accumulate in the albino tea cultivar, including flavones, anthocyanins, flavonols, flavanones, vitamins and their derivatives, and polyphenols and phenolamides (Zheng et al., 2021). Furthermore, untargeted metabolomic analyses detected 129 and 199 annotated metabolites that were differentially accumulated in different tea groups, and signature metabolites were identified (Yu et al., 2020). However, few studies have investigated the metabolic variations of tea plants in terms of their global genetic background and elucidated the relationship among metabolites. The compound biosynthesis in tea plants is tightly regulated by internal regulatory factors and environmental cues. Genes and metabolites are two internal factors that regulate the expression levels of downstream genes and the content of downstream metabolites. Thus, it is necessary to investigate the regulatory networks among gene–gene, gene–metabolite, and metabolite–metabolite.

Over the past decades, metabolomics has been widely applied in the identification and quantification of metabolites in plants. Ultra-performance liquid chromatography (UPLC) coupled with mass spectrometry (MS) is a powerful tool for simultaneously detecting 100s of non-volatile compounds in tea. In this study, one bud and two leaves (two and a bud) were harvested from tea plants in the first flush of spring in Hangzhou, China. By using untargeted metabolomics integrated with transcriptomics, we performed comprehensive metabolic profiling and verified the co-current network of genes and metabolites associated with the predominant components in fresh tea shoots. Our results provided insights into the genetic basis of important secondary metabolites, such as catechins, caffeine, and theanine, and will be helpful in accelerating genetic improvement and tea breeding in the future.

Abbreviations: C, catechin; EC, epicatechin; GC, gallocatechin; EGC, epigallocatechin; CG, catechin-3-gallate; ECG epicatechin-3-gallate; GCG, gallocatechin-3-gallate; GA, gallic acid; EGCG, epigallocatechin-3-gallate; QC, quality control; RT, retention time; PCA, principal component analysis; FDR, false discovery rate; DAM, different accumulated metabolite; PCC, Pearson correlation coefficient; MR, mutual rank.

MATERIALS AND METHODS

Plant Materials

The samples were collected from 68 accessions of tea plants in the section *Thea* (L.) Dyer, genus *Camellia* L., namely, 42 accessions of *C. sinensis* (L.) O. Kuntze var. *sinensis*; 17 accessions of *C. sinensis* var. *assamica* (Masters) Kitamura; 6 accessions of *C. sinensis* var. *pubilimba* Chang; 1 accession each of *C. tachangensis* F. C. Zhang, *C. taliensis* (W. W. Smith) Melchior, and *Camellia* sp. (**Supplementary Table 1**). Standard two and a bud in the first round were harvested from at least 10 individual tea plants from March 16 to April 30, 2019. The growth vigor of all the tea plants was similar under the same cultivation conditions and agricultural practices planted in the China National Germplasm Hangzhou Tea Repository at the Tea Research Institute, Chinese Academy of Agricultural Sciences in Hangzhou, China. Samples were treated with liquid nitrogen (LN) immediately after collection from the tea plants and were stored at −80°C until they were freeze-dried.

Sample Extraction

We added 10 ml of 70% methanol with an internal standard (0.025 mg/ml of sulfacetamide and 0.075 mg/ml of tolbutamide) to 200 mg (±0.1 mg) of tea powder. The mixture was extracted in an ultrasonic unit (Branson 5510, Branson Ultrasonics Co., Ltd., USA) at 40 for 30 min at 80 W. The supernatants were filtered through a 0.22-μm filter membrane after stewing at 4°C in the dark for 2 h. The extracts were stored at −80°C until injection. Quality control (QC) was prepared by pooling 100 μl of the extract from all samples.

Liquid Chromatography–Mass Spectrometry Conditions

Standards and metabolites were detected using a UPLC (Thermo Scientific Dionex Ultimate 3000, Thermo Fisher Scientific, Waltham, MA, USA)-Q-Orbitrap (Thermo Scientific Q Exactive, Thermo Fisher Scientific, Waltham, MA, USA) with an Agilent SB-AQ C18 column (1.8 μm, 2.1 mm × 100 mm, Agilent Technologies, Santa Clara, CA, USA). Solvents A and B were water containing 0.1% formic acid and acetonitrile. The injection was 2 μl. The flow rate was 0.3 ml/min. The column temperature was set to 40°C. The gradient evolution program was as follows: 0–6 min, 5–20% B; 6–10 min, 2,095% B; 10–11.5 min, 95% B; and 11.5–15 min, 95–5% B. The MS operation parameters were as follows: an ion source, electrospray ionization; source temperature, 550°C; normalized collision energy, 15, 30, and 60; isolation window, 4 m/z (mass-to-charge ratio); loop count, 10; dynamic exclusion, 10.0 s; positive and negative modes with

electron spray ionization at capillary voltages of 3.5 and 3.2 kV, respectively; and the temperatures of drying gas and aux gas were 320 and 350°C, respectively. The mass range was set from 70 to 1,000 at a resolution of 70,000, and the top 10 peak areas were selected. Samples in the same year were run in the same experiment, and several technical replicates of a QC were distributed across every 10 samples to reduce the influence of intensity drifts.

Metabolic Data Processing

The m/z, retention time (RT), characterized fragments, and peak intensity were extracted using Xcalibur (Thermo Fisher Scientific, USA). The local database of authentic standards was obtained from mzVault based on the information of the raw files. Raw metabolome data pretreatment, including peak alignment, peak extraction, and compound identification, was performed using Xcalibur Compound Discoverer 2. The dominant parameters of the database alignment were as follows: mass tolerance of 5 ppm; threshold of signal–noise ratio 1.5; and precursor selection MS. Retention time and MS2 spectra were used for local database alignment. The MS2 spectrum was also aligned with online mass databases, including the Human Metabolome Database (HMDB) (http://www.hmdb.ca/), Kyoto Encyclopedia of Genes and Genomes (KEGG) (https://www.kegg.jp/), and PlantCyc (https://www.plantcyc.org/).

RNA Sequencing

Total RNA was isolated using the RNAprep Pure Plant Kit (Tiangen Biotech Co., Ltd., Beijing, China) according to the protocol of the manufacturer. The degradation and purity of the RNA were examined by 1% agarose gel electrophoresis and a NanoPhotometer® spectrophotometer (Implen, Westlake Village, CA, USA). Ribonucleic acid integrity was assessed using the RNA Nano 6000 Assay Kit of the Bioanalyzer 2100 system (Agilent Technologies, Santa Clara, CA, USA). The high-quality RNA samples from the tea plants were prepared using an Illumina TruSeq RNA Sample Prep Kit (Illumina, Inc., San Diego, CA, USA), and cDNA libraries were constructed using an Ultra™ RNA Library Prep Kit for Illumina® (New England Biolabs, Inc., Ipswich, MA, USA). The complementary DNAs were purified using Beckman AMPure XP beads (Beckman Coulter, Brea, CA, USA) and subsequently moved to an Agilent High Sensitivity DNA Kit (Agilent 2100, USA) for the detection of inserted cDNA fragments. Afterward, the cDNA libraries were quantified with a Bio-Rad KIT iQ SYBR Green kit (Bio-Rad CFX 96, Bio-Rad Laboratories, Inc., Hercules, CA, USA), and cDNA libraries were subsequently sequenced using a TruSeq SBS Kit v3 (Illumina HiSeq2500, USA). The clean reads were subsequently aligned to the reference genome (http://pcsb.ahau.edu.cn:8080/CSS/). An index of the reference genome was built using HISAT2 v2.0.5, and paired-end clean reads were aligned to the reference genome. A database of splice junctions was generated using HISAT2 based on gene model annotation for an optimized mapping result. Then, the expected number of fragments per kilobase of transcript sequence per million base pairs of each gene was calculated based on the length of the gene and the reads count mapped to the corresponding gene.

Quantitative Reverse-Transcription PCR Analyses

Nine genes responsible for flavonoids were randomly selected for the validation of gene expression using a quantitative reverse-transcription PCR (qRT-PCR). This information has been described in our previous study including 12 genes (Jiang et al., 2021). The qRT-PCR reactions were conducted using the following parameters: 95°C for 10 min, 45 cycles at 94°C for 10 s, and 58°C for 15 s. Three independent biological replicates and three technical replicates of each reaction were performed using glyceraldehyde 3-phosphate dehydrogenase (GAPDH) as a reference gene. Fluorescence intensity was measured using a LightCycler 480 machine (Roche, Sussex, UK), and the relative expression values of genes were subsequently calculated using the $2^{-\Delta\Delta Ct}$ method.

Data Analysis

Principal component analysis (PCA) based on metabolites was conducted and visualized using the package ggplot2. The samples were divided into several groups based on the PCA. Fold changes in the relative content of metabolites were calculated according to the formula: variability = maximum/minimum. The metabolites in every two groups with a fold change >2 and a false discovery rate (FDR) <0.05, using the DESeq package, were regarded as different accumulated metabolites (DAMs). Volcano plots were plotted using the package ggplot2. Pearson's correlation coefficient (PCC) values of metabolite–metabolite pairs, gene–gene pairs, or metabolite–gene pairs were calculated using R 3.6.3. The ranks for every pair were obtained based on PCC values from high to low. Then, the mutual rank (MR) was calculated using the formula: $\sqrt{rank(AB) \times rank(BA)}$. Mutual rank was converted into network edge weight using the decay function $e^{-(MR-1)/100} \geq 0.01$. The compounds were selected based on an FDR < 0.05 and PCC > 0.8 to construct metabolite correlation networks. The clean reads were aligned to the genome of 'Shuchazao' (Wei et al., 2018; Xia et al., 2020) and 'Longjing 43' (Wang P. et al., 2020) and then annotated for flavonoid, theanine, and caffeine metabolisms using the Basic Local Alignment Search Tool (National Library of Medicine, USA). The compounds and genes were selected based on an FDR < 0.05 and PCC > 0.4 to construct the gene–metabolite correlation networks. The network was visualized using the Cytoscape software (1991, 1999 Free Software Foundation, Inc.).

RESULTS

Overview of Metabolites in Fresh Tea Shoots

In the process of sample detection, QC samples were interred every 10 injections to monitor the stability of the detection system. The Pearson correlation coefficient between every two QC samples ranged from 0.99 to 1 (**Supplementary Figure 1**), indicating that the system was stable. A total of 3,775 features were detected using UPLC-Q-Orbitrap, 251 of which were

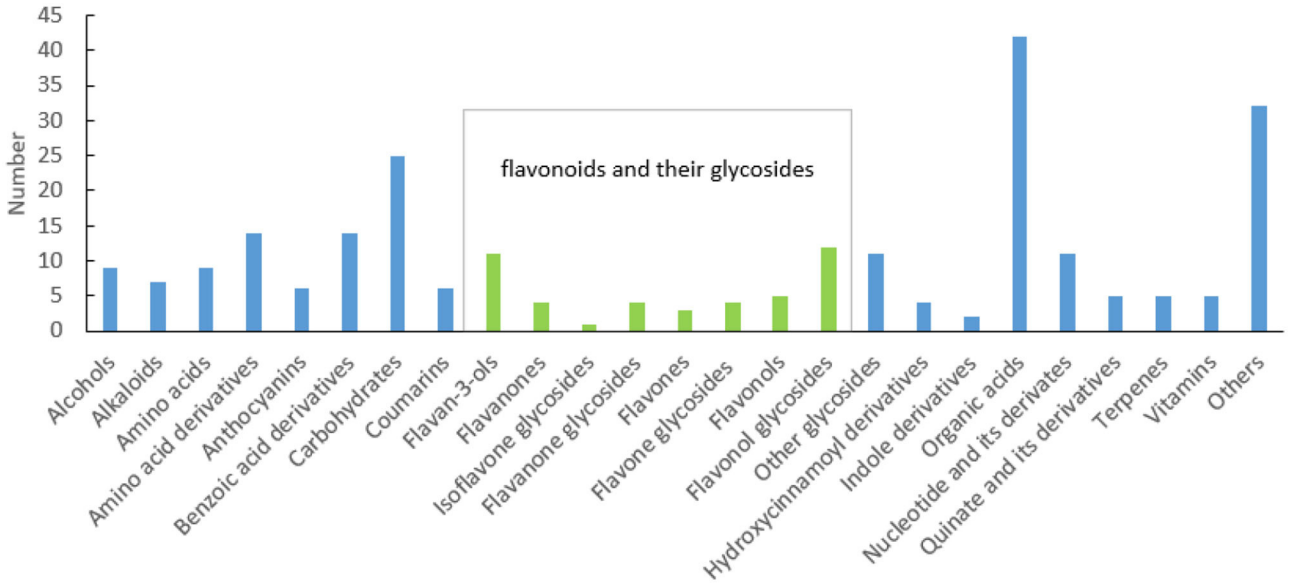

FIGURE 1 | Classification of metabolites in fresh tea shoots.

identified (**Supplementary Table 2**). Among them, 84 (aa001–aa084) were identified by aligning to the standards, 13 (bb001–bb013) were identified according to the structural information of scientific articles, and the rest (cc001–cc154) were identified through alignment to the public databases. These metabolites can be classified into 25 categories. As described in **Figure 1**, flavonoids and their glycosides, organic acids, and carbohydrates are the top three classifications. Anthocyanins, flavan-3-ols, flavanones, isoflavone glycosides, flavanone glycosides, flavones, flavone glycosides, flavonols, flavonol glycosides, quinate and its derivatives, and some benzoic acid derivatives are polyphenols. A total of 61 polyphenols were identified. This suggested that there are various polyphenols present in fresh tea shoots. Among them, 29 flavonoid polymers, including flavonoids, sugars, and gallic acids, were identified in fresh tea shoots (**Supplementary Table 2**). Most of these compounds are catechin polymers and flavonoid glycosides. Procyanidins, ubiquitous and widely secondary metabolites in plants, are condensed flavonoid forms with more than two units of flavanols, corresponding to brown or non-visible-colored pigments (Saigo et al., 2020). Procyanidin B1, procyanidin B3, procyanidin B4, procyanidin C1, and GC-GCG are dimers of catechins, suggesting that a large part of procyanidin is a dimer of catechins. Moreover, glucose and rhamnose are the main glycosides that combine with flavonoids. In addition to the abovementioned compounds, metabolites with galactosylation, rutinosylation, and primeverosylation were also detected in processed tea (Dai et al., 2016). Solubility, molecular stability, and subcellular transport ability increased after glycosylation. Furthermore, flavonols were the majority of aglycones, whose glycosides were glucose and rhamnose, among others. These flavonols were luteolin, myricetin, quercetin, kaempferol, and taxifolin.

Afterward, we applied the unsupervised PCA to all samples (**Figure 2A**). The QC samples were distributed at the center of the score graph. In addition to the QC samples, the samples were divided into three groups (**Supplementary Table 1**). PC1 and PC2 accounted for 41 and 15.4 % of the variation rate, respectively. DMS (different metabolites) [(FDR $<$ 0.05) and |log2(fold change)| $>$ 1] between every two groups were investigated (**Figures 2B–D**). The contents of nicotinamide, neochlorogenic acid, mascaroside, and propofol were higher in group 1 than those in group 2 (**Figure 2B**). The contents of L-theanine, caffeine, quercitrin, cynarine, silandrin, and kolaflavanone were higher in group 1 than those in group 3 (**Figure 2C**). *C. sinensis* var. *sinensis*, *C. sinensis* var. *assamica,* and *C. sinensis* var. *pubilimba* were distributed in groups 1 and 2. *C. taliensis* and *C. tachangensis* were present in the first group. Group 3 included two tea resources: 'Jinping 1', *C. sinensis* var. *assamica,* and 'Kekecha' belong to *C. sinensis* var. *pubilimba*, indicating that they were unique. Furthermore, the contents of gallocatechin, theobromine, 3,4-dihydroxybenzaldehyde, procyanidin B1, GC-GCG, diGC-GA, gly-lys, 2-methylcitric acid, nifurquinazo, aspirin, 1-*O*-vanilloyl-β-D-glucose, and cynarine were higher in group 3 than those in the other two groups. The contents of theobromine and GC-GCG were much higher in 'Kekecha' than in the other accessions. The common DAM in three pairs, namely, 1,2-Di-*O*-galloyl-HHDP-glucose, was significantly higher in group 3 than in the other two groups. Yang et al. (2008) believed that 1,2-di-*O*-galloyl-HHDP-glucose only exists in *C. taliensis*. However,

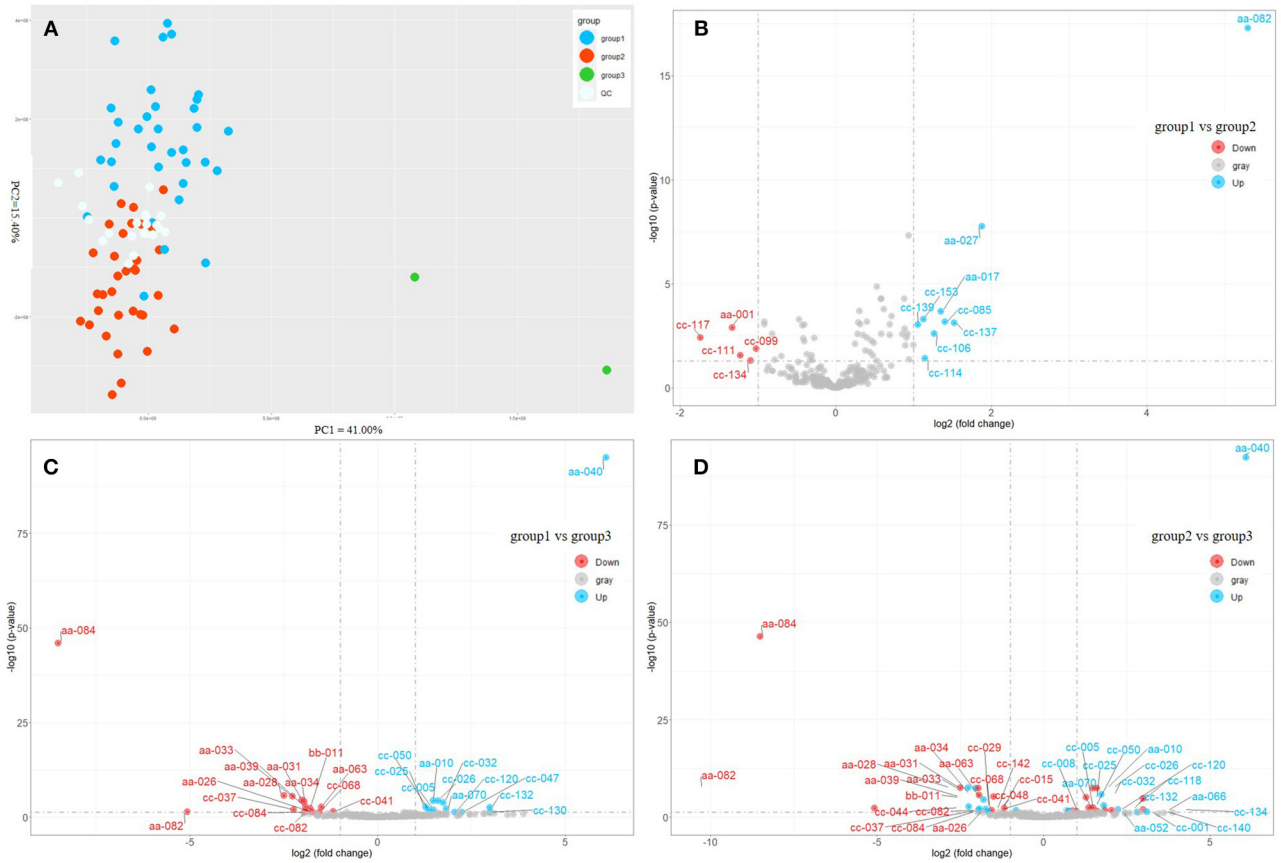

FIGURE 2 | Comparison of metabolic profiles of different tea accessions. **(A)** Principal component analysis of different tea accessions based on the content of metabolites. **(B)** Volcano plot of differentially accumulated metabolites (DAMs) between Group 1 and Group 2. **(C)** Volcano plot of DAMs between Group 1 and Group 3. **(D)** Volcano plot of DAMs between Group 2 and Group 3. aa-001, L-Arginine; aa-010, L-Theanine; aa-017, Nicotinamide; aa-026, Gallocatechin; aa-027, Neochlorogenic acid; aa-028, Theobromine; aa-031, 3,4-Dihydroxybenzaldehyde; aa-033, Procyanidin B3; aa-034, Catechin; aa-039, 4-Hydroxybenzaldehyde; aa-040, Caffeine; aa-063, Procyanidin B1; aa-066, Vitexin-2"-O-rhamnoside; aa-070, Quercitrin; aa082, 1,2-di-O-galloyl-hhdp-glucose; aa-084, GC-GCG; bb-011, diGC-GA; cc-001, Agmatine; cc-005, 4-Amino-4-deoxypentopyranose; cc-015, 2-Acetamido-2-deoxyglucose; cc-025, 4-piperidinecarboxamide; cc-026, Ethanal tetramer; aa-052, Quercetin 3-O-alpha-D-xylopyranoside; cc-008, (2S,4S)-4-Amino-2-hydroxy-2-methylpentanedioic acid; cc-047, N-phenyl-beta-D-glucopyranosylamine; cc-050, Tert-butyl 3-amino-1-methyl-2,3-dioxopropylcarbamate; cc-085, Benzyl 6-O-beta-D-xylopyranosyl-beta-d-glucopyranoside; cc-099, 4,7,8-trihydroxy-3-(4-hydroxyphenyl)dibenzo[b,d]furan-1,2-diyl diacetate ; cc-114, Gallocatechin-(4alpha->8)-epigallocatechin; cc-142, 1,4-anhydro-6-O-dodecanoyl-2,3-bis-O-(2-hydroxyethyl)-D-glucitol; cc-029, 5'-Xanthylic acid; cc-032, Streptamine 4-phosphate; cc-037, Gly-lys; cc-041, 2-Methylcitric acid; cc-044, Hymexazol O-glucoside; cc-048, N-acetyl-l-2-aminoadipic acid; cc-068, Nifurquinazol; cc-082, Aspirin; cc-084, 1-O-vanilloyl-beta-D-glucose; cc-106, Mascaroside; cc-111, Astilbin; cc-117, Tiliroside; cc-118, Olsalazine; cc-120, Cynarine; cc-130, Silandrin; cc-132, Kolaflavanone; cc-134, Lamifiban; cc-137, Methyl 3,4,5-trimethoxycinnamate; cc-139, Propofol; cc-140, 7-Dehydrocholesterol benzoate; cc-153, Beta-D-ethyl glucuronide.

it has also been observed in *C. sinensis* and *C. tachangensis*. Interestingly, the relative content of 1,2-di-*O*-galloyl-HHDP-glucose was much higher (45.32 times) in 'Kekecha', which belongs to *C. sinensis* var. *pubilimba*, compared with *C. taliensis*. Accordingly, 1,2-di-*O*-galloyl-HHDP-glucose was not unique to *C. taliensis*.

Variability of Metabolites

To explore the variability of metabolites in the fresh shoots of 69 tea accessions, the fold changes in the relative contents of metabolites were calculated according to the formula: variability = maximum/minimum. As shown in **Figure 3**, the variability of the nine metabolites was less than three. The metabolites with low variability include four organic acids, two catechins, one amino acid derivative, one glycoside, and one nucleotide. These metabolites were conserved, indicating that they play important roles during the normal growth and development of tea plants. In addition to epigallocatechin-3-gallate (EGCG) and gallocatechin-3-gallate (ECG), the remaining were primary metabolites. The content and proportion of catechins are indices for processing suitability. Interestingly, the contents of EGCG and ECG showed low variation among the different varieties. Thus, the variability of other catechins and their derivatives was explored, as presented in **Table 1**. The variability of catechin-3-gallat (CG), epicatechin (EC), epigallocatechin (EGC), gallocatechin (GC), and C ranged from 5.73 to 16.84, demonstrating their moderate

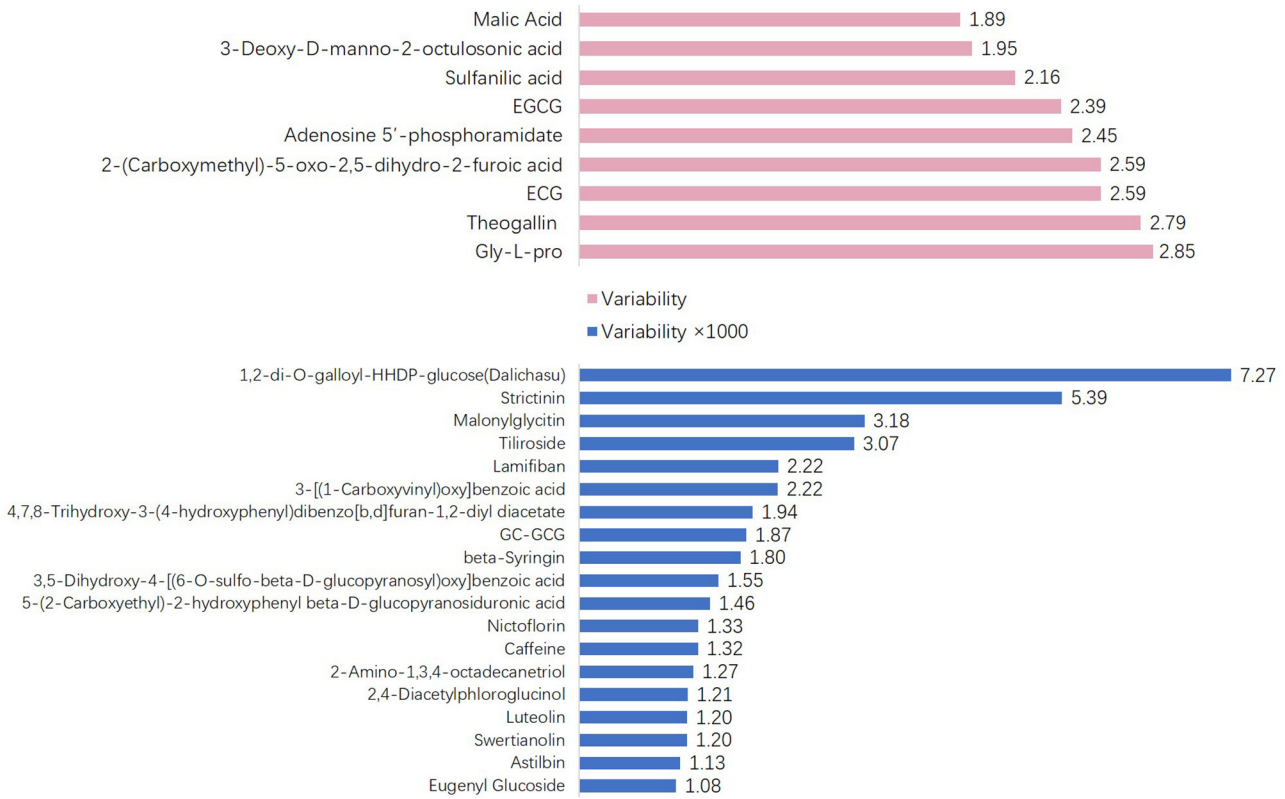

FIGURE 3 | The metabolites whose variability was >5- or more than 1,000-fold.

variation, while the variability of the downstream metabolites of catechins [GC-EGC, EGCG3"Me, EGCG4"Me, GC-diGA, GC-gallocatechin-3-gallate (GCG)] was high, ranging between 320.52 and 1865.35. These results suggest that most catechins have significant variations in tea plants, especially catechin polymers. The variability in the 19 cases was more than 1,000 (**Figure 3**). Dalichasu, strictinin, malonylglycitin, and tiliroside were the top four compounds with a variability of more than 3,000. The first two are alkaloids, and the rest are flavonoid glycosides. This implied that secondary metabolites, especially the downstream metabolites, were more influenced by genetic background.

Correlation Among Important Metabolites

The correlation among metabolites could present the associations between metabolic content, which helps improve metabolic networks and discover new metabolic pathways. Therefore, PCC was calculated between every two relative contents of the identified metabolites. A total of 49 pairs of metabolites were highly correlated (**Figure 4A**), as their absolute PCC values were >0.8. Moreover, all the correlations were positive. Among them, the PCC of 29 pairs was >0.9 (**Figure 4B**). Seven metabolites in one network were further discussed (**Figure 4C**). They were procyanidin B1, procyanidin B2, procyanidin C1, catechin, 4-hydroxybenzaldehyde, 3,4-dihydroxybenzaldehyde, and theobromine. Procyanidin B1, procyanidin B2, procyanidin C1, and catechin are involved in the flavonoid biosynthesis pathway. 4-hydroxybenzaldehyde, 3,4-dihydroxybenzaldehyde, and theobromine were involved in the biosynthesis of alkaloids derived from the shikimate and caffeine metabolism pathways. Tea plants with high flavonoid content also have high caffeine content, indicating that flavonoids may be closely related to caffeine metabolism.

Network of Metabolites and Genes Responsible for Flavonoids, Theanine, and Caffeine

To validate the gene expression level calculated using transcriptomic data, nine genes responsible for flavonoid biosynthesis were randomly selected for a qRT-PCR. The results of the qRT-PCR are consistent with those of RNA sequencing (Jiang et al., 2021). Metabolites are the comprehensive outcomes of gene expression regulated by internal and external factors. A combined analysis of gene expression level and metabolite content was performed to elucidate the transcriptional regulation mechanism underlying the flavonoid, theanine, and caffeine metabolisms. Firstly, the genes in the flavonoid, theanine, and caffeine biosynthesis pathways were screened after being aligned to the reference genomes of 'Shuchazao' and 'Longjing43'. Afterward, PCC was calculated between the gene expression levels and metabolite contents. Finally, the gene-metabolite

TABLE 1 | Variability of catechins and their derivatives.

Name	Variability folds
EGCG	2.39
ECG	2.59
Procyanidin B4	4.46
CG	5.73
EC	7.66
Procyanidin C1	7.71
Procyanidin B1	10.92
EGC	11.20
GC	14.63
C	16.84
Procyanidin B3	24.00
GC-EGC	320.52
EGCG3"Me	366.68
EGCG4"Me	800.58
GC-diGA	834.36
GC-GCG	1865.35

network was visualized (PCC $>$ 0.4, FDR $<$ 0.05). As shown in **Figure 5A**, 22 genes play a role in flavonoid metabolism. The genes TEA013315 and novel 0.7909 were highly correlated with epicatechin gallate (aa068), myricetin (aa056), dihydromyricetin (aa065), and catechin (aa034). As presented in **Figure 5B**, three genes could be divided into three groups based on their regulated metabolites. Among them, TEA28914 was isolated from the center of pantothenic acid (aa023), 1,3,7-trimethyluric acid (aa032), kaempferitrin (aa049), cymaroside (aa054), and theacrine (aa081). The genes TEA032217 and TEA032123 were linked to malic acid (aa011) and dihydromyricetin (aa065). Compared with the genes regulating the flavonoid and theanine metabolisms, five genes in the caffeine biosynthesis pathway were distributed in one group (**Figure 5C**). In addition, TEA015791 contained 25 metabolites, suggesting its essential role in caffeine metabolism, which deserves further investigation.

DISCUSSION

The samples from the 68 accessions of tea plants were divided into three groups based on the composition and content of the metabolites (**Supplementary Table 1**). According to the results of the compound identification, there were abundant tea polyphenols in fresh tea leaves (**Figure 1**), as the essential signature of tea, both for its higher amount and wider variation compared with other plants. Commercial tea is also rich in various polyphenols, including esterified and non-esterified flavan-3-ols, flavonols, flavone glycosides, phenolic acid ester derivatives, proanthocyanidins, and hydrolysable tannins (Zhuang et al., 2020). Therefore, it was demonstrated that tea polyphenols undergo a series of complex transformations in the manufacturing process. All tea plants were divided into three groups based on the PCA (**Figure 2A**). *C. taliensis* and *C. tachangensis*, which are important wild relatives of cultivated tea, only existed in the first group. *C. sinensis* var. *sinensis*, *C. sinensis* var. *assamica*, and *C. sinensis* var. *pubilimba* were distributed in the first and second groups. *C. taliensis* can grow on Mengku Snow Mountain, China, at an altitude of 2,750 m, implying its strong stress resistance (Zhang et al., 2015). Thus, it may harbor abundant gene resources that have strong cold resistance, which can enhance the genetic improvement of cultivated tea. The molecular phylogenetic tree showed that *C. tachangensis*, *C. gymnogyna*, and *C. taliensis* were clustered into a group based on chloroplast genomes. Additionally, *C. sinensis* var. *sinensis*, *C. sinensis* var. *assamica*, and *C. sinensis* var. *pubilimba* were clustered into another group (Hao et al., 2019). This result was partially in accordance with chloroplast research. In this study, some *C. sinensis* tea plants were also included in the first group. This suggests that the cultivated tea plants in the first group were closer to the wild ones than those in the second group. 'Kekecha', also named cocoa tea, is a natural, low-caffeine, theobromine-rich tea plant that was discovered by Professor Chang Hung-ta in the 1980s (Chang et al., 1988). The variability of 19 metabolites in different tea resources was more than 1,000-fold. Dalichasu, strictinin, malonylglycitin, and tiliroside were the top four compounds, with a variability of more than 3,000-fold. Dalichasu is a polyphenol that is the signature component of *C. taliensis* (Yang et al., 2008). Strictinin was responsible for the anti-influenza activity of Yunnan bitter tea (Kucha), traditionally used for the treatment of the common cold (Lin et al., 2020). Malonylglycitin and tiliroside are isoflavone glycosides and flavonol glycosides, respectively. These compounds were dramatically altered in different tea resources, indicating their peculiar character for distinguishing accessions. Most of the compounds with relatively low variability were the primary metabolites. The conservatism of primary metabolite content is significant for maintaining a stable physiological status. In general, the variation of secondary metabolites was greater than the primary metabolites, demonstrating that the former was more characteristic in different tea accessions. Catechins and their derivatives have high variability as essential secondary metabolites in tea plants. Catechins in tea leaves include four free types, including C, EC, GC, and EGC, and four gallate types, including CG, ECG, GCG, and EGCG. In this study, GCG was not determined because its content was lower than the detection limit. The polymers of GCG and GC-GCG were detected instead. The polymeric forms of flavonoids occur naturally in plants and primarily consist of oligomeric and dimeric catechins. Condensed catechins are proanthocyanidins (Malgorzata and Anna, 2019). Polymerization stabilized flavonoids and caused changes in their specific properties. A polymeric complex catechin compound showed better thermal stability than catechin (Malgorzata and Anna, 2020).

In addition to the physiological functions of tea plants, catechins and their derivatives contribute to the medicinal properties and sensation characteristics of tea infusions for humans. The effect of 'Benifuki' tea on human hypertension is mainly the result of the strong inhibitory effect of EGCG3"Me on angiotensin I-converting enzyme activity (Kurita et al., 2010). The effects of EGCG3"Me and EGCG4"Me on reducing blood pressure, anti-anaphylaxis, and anti-inflammation were more

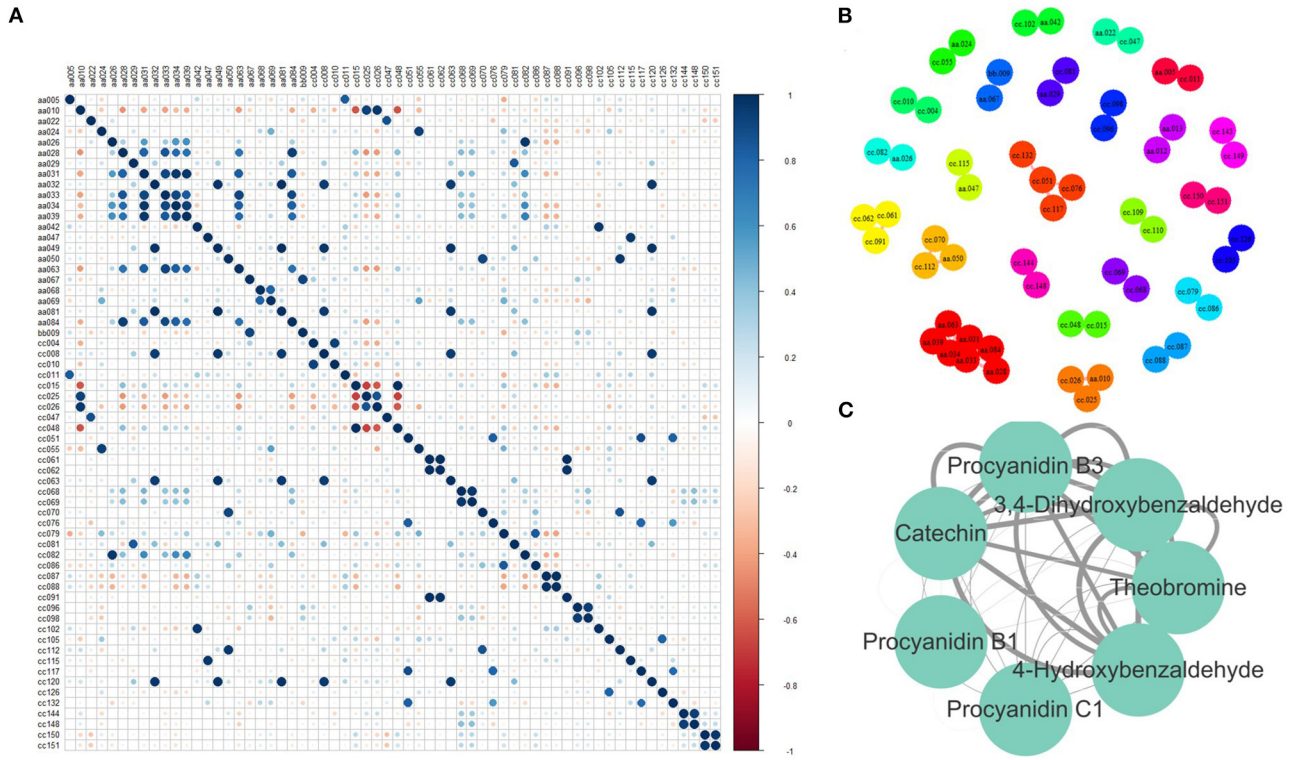

FIGURE 4 | Correlation between metabolites. **(A)** Pearson correlation coefficient (PCC) between every two metabolites. **(B)** Metabolite pairs with a PCC > 0.8. **(C)** Metabolite pairs with a PCC > 0.9 (The width of the edge represents the absolute value of PCC). aa005, Sucrose; aa010, L-Theanine; aa022, Gallic acid; aa024, Theogallin; aa026, GC; aa028, Theobromine; aa029, Methyl gallate; aa031, 3, 4-Dihydroxybenzaldehyde; aa032, 1, 3, 7-Trimethyluric acid; aa033, Procyanidin B3; aa034, C; aa039, 4-Hydroxybenzaldehyde; aa042, TriGA-glucose; aa047, Isoquercetin; aa049, Kaempferitrin; aa050, EGCG4"Me; aa063, Procyanidin B1; aa067, Vitexin; aa068, ECG; aa069, CG; aa081, Theacrine; aa084, GC-GCG; bb009, Eriodictyol C-hexoside; cc010, Glycerophosphoglycerol; cc015, 2-Acetamido-2-deoxyglucose; cc025, 4-Piperidinecarboxamide; cc026, Ethanal tetramer; cc047, N-Phenyl-beta-D-glucopyranosylamine; cc004, 1-Deoxy-D-altro-heptulose 7-phosphate; cc008, (2S, 4S)-4-Amino-2-hydroxy-2-methylpentanedioic acid; cc011, 7-Hydroxy-6-methyl-8-(1-D-ribityl)lumazine; cc051, 2-(3, 4, 5-Trihydroxyphenyl)-3, 4, 5, 7-chromanetetrol; cc070, 5-(2-Carboxyethyl)-2-hydroxyphenyl beta-D-glucopyranosiduronic acid; cc081, 5-Hydroxy-6-methoxy-3-(4-methoxyphenyl)-4-oxo-4H-chromen-7-yl beta-D-glucopyranosiduronic acid; cc144, 2-Linoleoyl-sn-glycero-3-phosphoethanolamine; cc148, 1-Linoleoyl-sn-glycero-3-phosphocholine; cc048, N-Acetyl-L-2-aminoadipic acid; cc055, Adenosine 5′-phosphoramidate; cc061, 3-[(1-Carboxyvinyl)oxy]benzoic acid; cc062, Malonylglycitin; cc063, Histidylglycine; cc068, Nifurquinazol; cc069, beta-D-glucose pentaacetate; cc076, (-)-L-Chicoric acid; cc079, Phenylacetaldehyde; cc082, Aspirin; cc086, 1, 3-Propane sultone; cc087, 7-Ethoxycoumarin; cc088, Sinapaldehyde glucoside; cc091, 2, 4-Diacetylphloroglucinol; cc096, Gentiopicrin; cc098, Sweroside; cc102, 1, 6-bis-O-galloyl-beta-D-glucose; cc105, 4-Carboxy nevirapine; cc112, Malonylgenistin; cc115, N-Adenylylanthranilic acid; cc117, Tiliroside; cc120, Cynarine; cc126, Picrotin; cc132, Kolaflavanone; cc150, Allylcyclohexane; cc151, p-Menth-3-ene.

significant than those of EGCG. Catechins and epicatechins are absorbed from the human intestinal tract after transforming into *O*-methylated derivatives (Suzuki et al., 2000). Therefore, methylated catechins are more easily absorbed than catechins. Caffeoyl-CoA 3-*O*-methyltransferase (CCoAOMT) has been reported to directly catalyze the synthesis of EGCG3″Me. On the other hand, *CsbHLH62*, *CsWRKY31*, and *CsWRKY48* might negatively regulate the biosynthesis of EGCG3"Me by trans-repressing its expression of the downstream genes *CCoAOMT*, *CsLAR*, and *CsDFR* of the EGCG3"Me biosynthetic pathway (Luo et al., 2018, 2019). A tandem mass spectrum analysis characterized EGCG4"Me as resulting from epicatechin carbocation and the methyl group of methanol (Wang X. et al., 2020). Most catechin polymers are GC derivatives. Our previous research suggested that GC accounts for a small amount of the total catechin content (Jiang et al., 2020). It is likely that GC formed polymers with EGC, GCG, and gallic acid (GA) as one of the factors for its low absolute content in tea leaves. In this study, the contents of GC-GCG and theobromine were extremely higher in 'Kekecha' than in other accessions, which is consistent with the results of previous studies (Peng et al., 2019). The monomeric units of procyanidins were linked through a C4–C8 or C4–C6 bond (B-type), which can coexist with an additional C2–O–C7 or less abundant C2–O–C5 bond (A-type). Procyanidins were detected and were all B-type (procyanidins B1, B3, and B4) (**Table 1**). It was also revealed that the bonds of catechin C1 are most commonly C-4 to C-8 (Li et al., 2013).

In addition to polymerization, glycosylation is one of the most popular methods for improving stability using various enzymes that possess transglycosylation activity (Cho

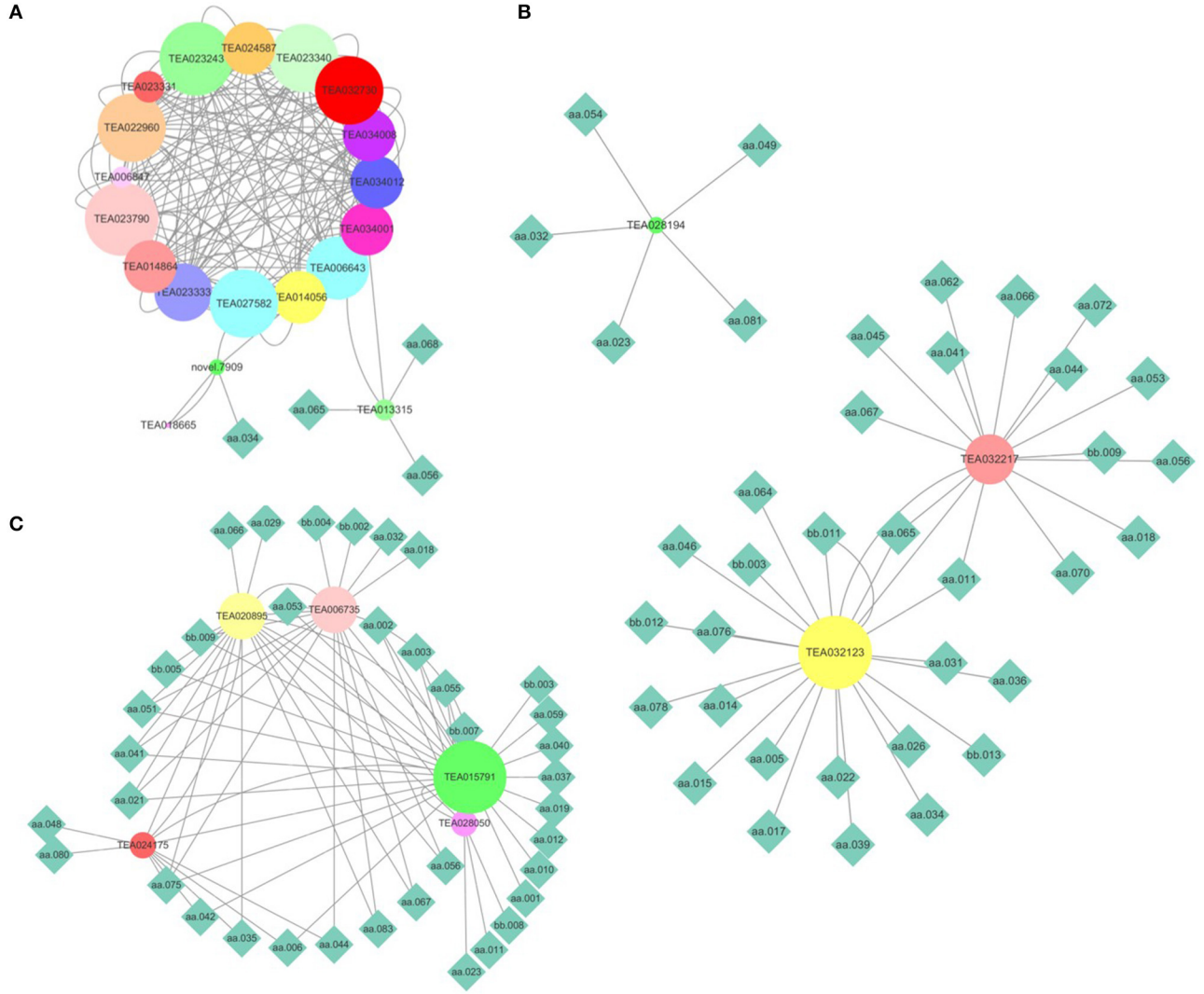

FIGURE 5 | Combined analysis of gene expression levels and metabolite contents. **(A)** Flavonoid metabolism; **(B)** theanine metabolism; **(C)** caffeine metabolism. (The node size reflects the degree value. Nodes were colored based on the hub-gene group). aa001, L-Arginine; aa002, L-Alanine; aa003, L-Aspartic acid; aa005, Sucrose; aa006, L-Proline; aa010, L-Theanine; aa011, Malic Acid; aa012, L-Isoleucine; aa014, Citric acid; aa015, Adenine; aa017, Nicotinamide; aa018, GA-glucose; aa019, L-Phenylalanine; aa021, EGCG3"Me; aa023, Pantothenic acid; aa026, GC; aa029, Methyl gallate; aa031, 3, 4-Dihydroxybenzaldehyde; aa032, 1, 3, 7-Trimethyluric acid; aa034, C; aa035, Strictinin; aa036, Chlorogenic acid; aa037, Procyanidin B4; aa039, 4-Hydroxybenzaldehyde; aa040, Caffeine; aa041, EGCG; aa042, TriGA-glucose; aa044, Schaftoside; aa045, Myricetin 3-O-galactoside; aa046, Rutin; aa048, Ellagic acid; aa049, Kaempferitrin; aa051, Naringin; aa053, Prunin; aa054, Cynaroside; aa055, 2-Hydroxy cinnamic acid; aa056, Myricetin; aa059, Baicalin; aa062, Kaempferol; aa064, Procyanidin C1; aa065, Dihydromyricetin; aa066, Vitexin-2"-O-rhamnoside; aa067, Vitexin; aa068, Epicatechin gallate (ECG); aa070, Quercitrin; aa075, L-Glutathione oxidized; aa076, Guanine; aa078, Esculin; aa080, Shikimic acid; aa081, Theacrine; aa083, GC-diGA; bb002, Glutaric acid; bb003, 2, 5-Dihydroxy benzoic acid O-hexside; bb004, Ellagic acid glucoside; bb005, Protocatechuic acid O-glucoside; bb007, diGA-glucose; bb008, 3-O-p-Coumaroyl quinic acid; bb009, Eriodictyol C-hexoside; bb011, diGC-GA; bb012, Nictoflorin; bb013, 4', 7-Dihydroxyflavanone.

et al., 2011). Phenolic acid, flavonol, flavone, and isoflavone are catalyzed into glycosylated compounds by the flavonoid UDP-glycosyltransferase, which transfers glycosyl groups from activated glycosyl donors to flavonoids (Achnine et al., 2005). In green and black tea, flavonol glycosides cover subclasses of quercetin *O*-glycosides, kaempferol *O*-glycosides, and myricetin *O*-glycosides (Li et al., 2020). In Pu'er tea, quercetin, myricetin, and kaempferol are the main aglycones of tea flavonols (Jiang et al., 2018). This indicated that these flavonol glycosides are the flavor components of tea and the substances possessing anti-stress functions in fresh tea leaves. Glycosides, an important substrate of glucosidase during tea fermentation, contribute to the nutrition and flavor of tea. The glycosylation of flavonol aglycones is the last step in flavonol biosynthesis, catalyzed by uridine diphospho-glycosyltransferases (Xie et al., 2020). The main factors that lead to low or no detection of glycosides were

as follows: (1) β-primeverosides were the aroma precursors in fresh tea leaves. The content of glycosides in fresh tea shoots was relatively lower than that in processed tea, as a number of these compounds are formed during tea processing (Zhou et al., 2017). (2) We did not use a specific method to explore glycosylated compounds. Presently, a very small portion of MS features can be structurally annotated (Da Silva et al., 2015; Nash and Dunn, 2019). For instance, only 6.65% of the features were identified in this study. From the deamination and decarboxylation reaction of theanine, *N*-ethyl-pyrrolidone may combine with C6 or C8 of the A ring of catechins to produce a catechin–theanine complex (Li et al., 2018). In addition, catechin–theanine complexes were not detected in this study, wherein their presence at levels below the detection limit is one possible reason.

To investigate the gene regulatory network of flavonoids, theanine, and caffeine syntheses in tea plants, a gene–metabolite network was constructed according to the PCC value. Only four metabolites were closely associated with the 22 genes responsible for flavonoid biosynthesis. The relationship between genes was closer than that between genes and metabolites. In contrast, more metabolites, rather than genes, were in the network of theanine and caffeine. Flavonoid biosynthesis may be regulated in a more complicated manner than theanine or caffeine biosynthesis. According to current knowledge, there are 12 structural genes (excluding alleles) in the flavonoid metabolism pathway. Five and four structural genes (excluding alleles) are in the theanine and caffeine metabolism pathways, respectively (Wei et al., 2018; Zhu et al., 2019). Theacrine, 1,3,7,9-tetramethyluric acid, showed an effect similar to that of caffeine that enhanced locomotor activation through dopaminergic and adenosinergic systems while exhibiting superior toxicity to caffeine (Ashburn et al., 2019). It is the major purine alkaloid in the leaves of a special Chinese tea, *C. assamica* var. *kucha* Hung T. Chang and H.S.Wang, a variety of *Theaceae* (Zheng et al., 2002). Morphologically, *kucha* is not significantly different from *sinensis*, so it is usually classified as *C. sinensis*. It was also the dominant purine alkaloid detected in *C. sinensis* var. *pusanensis* Kurihara (Li et al., 2017). However, theacrine content was not related to tea varieties. More interestingly, it was highly correlated with the theanine metabolism, similar to the gene–metabolite (theanine) network. The network of metabolites and genes revealed that candidate genes regulated the related metabolites.

CONCLUSIONS AND FUTURE PROSPECTS

The non-volatile metabolic profiling of fresh shoots from 68 tea accessions was performed based on the results of non-targeted metabolomics. First, 251 metabolites were identified by aligning to the standards, structural information of scientific articles, or public databases. All tea samples could be classified into three groups. Varieties of *C. sinensis*, involving var. *sinensis*, var. *assamica*, and var. *pubilimba*, were distributed in the first and second groups. The wild tea plants, including *C. taliensis* and *C. tachangensis*, only existed in the first group. 'Jinping 1' belonged to *C. sinensis* var. *assamica* and 'Kekecha' belonged to *C. sinensis* var. *pubilimba* in the third group. Second, the variabilities of the metabolites were counted. Compared with the primary metabolites, the secondary metabolites, especially the downstream metabolites, were more influenced by genetic background. Third, flavonoid polymers had attracted increasing attention for their importance in tea growth and development. Catechins were commonly formed in their dimers, called procyanidin. Glucose and rhamnose were the main glycosides that combine with flavonoids. Fourth, correlations among metabolites were conducted based on PCC. The contents of flavonoids and caffeine were likely positively correlated in most circumstances. Finally, a network of metabolites and genes responsible for flavonoids, theanine, and caffeine was constructed. Results showed that TEA013315 and novel 0.7909 were highly correlated with epicatechin gallate. The gene TEA28914 was isolated from the center of pantothenic acid, 1,3,7-trimethyluric acid, kaempferitrin, cymaroside, and theacrine. The genes TEA032217 and TEA032123 were linked to malic acid and dihydromyricetin. The regulatory mechanisms underlying these genes and metabolites require further study.

DATA AVAILABILITY STATEMENT

The data presented in the study are deposited in the NCBI repository, accession number PRJNA760638. The raw data were published on https://www.ncbi.nlm.nih.gov/bioproject/760638.

AUTHOR CONTRIBUTIONS

LC, J-QM, and C-KJ designed the experiments. C-KJ, Z-LL, and X-YL conducted the experiments. C-KJ analyzed and wrote the manuscript. LC and SE polished the manuscript. All authors contributed to the article and approved the submitted version.

FUNDING

This work was supported by the National Natural Science Foundation of China (32072631, U19A2030), the China Agriculture Research System of MOF and MARA, and the Chinese Academy of Agricultural Sciences through the Agricultural Science and Technology Innovation Program (CAAS-ASTIP-2017-TRICAAS).

SUPPLEMENTARY MATERIAL

The Supplementary Material for this article can be found online at: https://www.frontiersin.org/articles/10.3389/fpls.2021.746972/full#supplementary-material

REFERENCES

Achnine, L., Huhman, D. V., Farag, M. A., Sumner, L. W., Blount, J. W., and Dixon, R. A. (2005). Genomics-based selection and functional characterization of triterpene glycosyltransferases from the model legume *Medicago truncatula*. *Plant J.* 41, 875–888. doi: 10.1111/j.1365-313X.2005.02344.x

Ashburn, B. O., Le, D. J., and Nishimura, C. K. (2019). Computational analysis of theacrine, a purported nootropic and energy-enhancing nutritional supplement. *Comput. Chem.* 7, 27–37. doi: 10.4236/cc.2019.71002

Cao, H. L., Wang, F. Q., Lin, H. Z., Ye, Y. J., Zheng, Y. C., Li, J. M., et al. (2020). Transcriptome and metabolite analyses provide insights into zigzag-shaped stem formation in tea plants (*Camellia sinensis*). *BMC Plant Biol.* 20:98. doi: 10.1186/s12870-020-2311-z

Chang, H. T., Ye, C. X., and Zhang, A. M. (1988). A discovery of new tea resource—cocoa tea tree containing theobromine from China. *Food Research International (Ottawa, Ont.)* 3, 131–133.

Cho, H., Kim, H., Seo, D., Jung, J., Park, J., Baek, N., et al. (2011). Biosynthesis of (+)-catechin glycosides using recombinant amylosucrase from Deinococcus geothermalis DSM 11300. *Enzyme Microb. Technol.* 49, 246–253. doi: 10.1016/j.enzmictec.2011.05.007

Da Silva, R. R., Dorrestein, P. C. P. U., and Quinn, R. A. (2015). Illuminating the dark matter in metabolomics. *Proc. Nat. Acad. Sci. U. S. Am.* 112, 12549–12550. doi: 10.1073/pnas.1516878112

Dai, W. D., Tan, J. F., Lu, M. L., Xie, D. C., Li, P. L., Lv, H. P., et al. (2016). Nontargeted modification-specific metabolomics investigation of glycosylated secondary metabolites in tea (*Camellia sinensis* L.) based on liquid chromatography-high resolution mass spectrometry. *J. Agric. Food Chem.* 64, 6783–6790. doi: 10.1021/acs.jafc.6b02411

Hao, W. J., Ma, J. Q., Ma, C. L., Jin, J. Q., and Chen, L. (2019). The complete chloroplast genome sequence of *Camellia tachangensis* F. *C.* Zhang (Theaceae). *Mitochondr. DNA Part B* 4, 3344–3345. doi: 10.1080/23802359.2019.1673247

Jiang, C.,k., Zeng, Z., Huang, Y. H., and Zhang, X. (2018). Chemical compositions of Pu'er tea fermented by *Eurotium Cristatum* and their lipid-lowering activity. *LWT Food Sci. Technol.* 98, 204–211. doi: 10.1016/j.lwt.2018.08.007

Jiang, C. K., Ma, J. Q., Liu, Y. F., Chen, J. D., Ni, D. J., and Chen, L. (2020). Identification and distribution of a single nucleotide polymorphism responsible for the catechin content in tea plants. *Horticult. Res.* 7:24. doi: 10.1038/s41438-020-0247-y

Jiang, C. K., Ni, D. J., Yao, M. Z., Ma, J. Q., and Chen, L. (2021). Metabolic and transcriptome analysis reveals metabolite variation and flavonoid regulatory networks in fresh shoots of tea (Camellia sinensis) over three seasons. *Front. Agric. Sci. Eng.* 8, 215–230. doi: 10.15302/JFASE-2021382

Kfoury, N., Morimoto, J., Kern, A., Scott, E. R., Orians, C. M., Ahmed, S., et al. (2018). Striking changes in tea metabolites due to elevational effects. *Food Chem.* 264, 334–341. doi: 10.1016/j.foodchem.2018.05.040

Kim, Y., Lee, K., and Kim, M. K. (2016). Volatile and non-volatile compounds in green tea affected in harvesting time and their correlation to consumer preference. *J. Food Sci. Technol.* 53, 3735–3743. doi: 10.1007/s13197-016-2349-y

Kurita, I., Maeda-Yamamoto, M., Tachibana, H., and Kamei, M. (2010). Antihypertensive Effect of Benifuuki Tea Containing O-Methylated EGCG. *J. Agric. Food Chem.* 58, 1903–1908. doi: 10.1021/jf904335g

Li, C. F., Ma, J. Q., and Huang, D. J. (2018). Comprehensive dissection of metabolic changes in albino and green tea cultivars. *J. Agric. Food Chem.* 58, 2040–2048. doi: 10.1021/acs.jafc.7b05623

Li, H., Lin, Q. Q., Yan, M. L., Wang, M. L., Wang, P., Zhao, H., et al. (2021). Relationship between secondary metabolism and miRNA for important flavor compounds in different tissues of tea plant (*Camellia sinensis*) as revealed by genome-wide miRNA analysis. *J. Agric. Food Chem.* 69:7440. doi: 10.1021/acs.jafc.0c07440

Li, J., Wang, J. Q., Yao, Y. F., Hua, J. J., Zhou, Q. H., Jiang, Y. W., et al. (2020). Phytochemical comparison of different tea (*Camellia sinensis*) cultivars and its association with sensory quality of finished tea. *LWT Food Sci. Technol.* 117:108595. doi: 10.1016/j.lwt.2019.108595

Li, S. Y., Sui, Y., Xiao, J., Wu, Q., Hu, B., Xie, B. J., et al. (2013). Absorption and urinary excretion of A-type procyanidin oligomers from Litchi chinensis pericarp in rats by selected ion monitoring liquid chromatography-mass spectrometry. *Food Chem.* 138, 1536–1542. doi: 10.1016/j.foodchem.2012.09.120

Li, Y. F., Ouyang, S. H., Chang, Y. Q., Wang, T. M., Li, W. X., Tian, H. Y., et al. (2017). A comparative analysis of chemical compositions in *Camellia sinensis* var. puanensis Kurihara, a novel Chinese tea, by HPLC and UFLC-Q-TOF-MS/MS. *Food Chem.* 216, 282–288. doi: 10.1016/j.foodchem.2016.08.017

Lin, P. R., Kuo, P. C., Li, Y. C., Jhuo, C. F., Hsu, W. L., and Tzen, J. T. C. (2020). Theacrine and strictinin, two major ingredients for the anti-influenza activity of Yunnan Kucha tea. *J. Ethnopharmacol.* 262:113190. doi: 10.1016/j.jep.2020.113190

Liu, L. L., Li, Y. G., She, G. B., Zhang, X. C., Jordan, B., Chen, Q., et al. (2018). Metabolite profiling and transcriptomic analyses reveal an essential role of UVR8-mediated signal transduction pathway in regulating flavonoid biosynthesis in tea plants (*Camellia sinensis*) in response to shading. *BMC Plant Biol.* 18, 1–18. doi: 10.1186/s12870-018-1440-0

Luo, Y., Yu, S. S., Li, J., Li, Q., Wang, K. B., Huang, J. N., et al. (2018). Molecular characterization of WRKY transcription factors that act as negative regulators of O-methylated catechin biosynthesis in tea plants (*Camellia sinensis* L.). *J. Agric. Food Chem.* 66, 11234–11243. doi: 10.1021/acs.jafc.8b02175

Luo, Y., Yu, S. S., Li, J., Li, Q., Wang, K. B., Huang, J. N., et al. (2019). Characterization of the transcriptional regulator *CsbHLH62* that negatively regulates EGCG3"Me biosynthesis in *Camellia sinensis*. *Gene* 699, 8–15. doi: 10.1016/j.gene.2019.03.002

Malgorzata, L. B., and Anna, M. (2019). Structure-activity relationships analysis of monomeric and polymeric polyphenols (quercetin, rutin and catechin) obtained by various polymerization methods. *Chem. Biodiv.* 16:e1900426. doi: 10.1002/cbdv.201900426

Malgorzata, L. B., and Anna, M. (2020). Natural polymeric compound based on high thermal stability catechin from green tea. *Biomolecules* 10:E1191. doi: 10.3390/biom10081191

Nash, W. J., and Dunn, W. B. (2019). From mass to metabolite in human untargeted metabolomics: Recent advances in annotation of metabolites applying liquid chromatography-mass spectrometry data. *Trends Anal. Chem.* 120:115324. doi: 10.1016/j.trac.2018.11.022

Peng, J., Jia, Y., Hu, T., Du, J., Wang, Y., Cheng, B., et al. (2019). GC-(4→ 8)-GCG, A proanthocyanidin dimer from *Camellia ptilophylla*, modulates obesity and adipose tissue inflammation in high-fat diet induced obese mice. *Mol. Nutri. Food Res.* 63:82. doi: 10.1002/mnfr.201900082

Saigo, T., Wang, T., Watanabe, M., and Tohge, T. (2020). Diversity of anthocyanin and proanthocyanin biosynthesis in land plants. *Curr. Opin. Plant Biol.* 55, 93–99. doi: 10.1016/j.pbi.2020.04.001

Suzuki, M., Yoshino, K., Maeda-Yamamoto, M., Miyase, T., and Sano, M. (2000). Inhibitory effects of tea catechins and O-methylated derivatives of (-)-epigallocatechin-3-O-gallate on mouse type IV allergy. *J. Agric. Food Chem.* 48, 5649–5653. doi: 10.1021/jf000313d

Wang, P. Q., Liu, Y. J., Zhang, L. J., Wang, W. Z., Hou, H., Zhao, Y., et al. (2020). Functional demonstration of plant flavonoid carbocations proposed to be involved in the biosynthesis of proanthocyanidins. *Plant J.* 101, 18–36. doi: 10.1111/tpj.14515

Wang, X. C., Feng, H., Chang, Y. X., Ma, C. L., Wang, L. Y., Hao, X. Y., et al. (2020). Population sequencing enhances understanding of tea plant evolution. *Nat. Commun.* 11:4447. doi: 10.1101/2020.03.19.998393

Wei, C. L., Yang, H., Wang, S. B., Zhao, J., Liu, C., Gao, L. P., et al. (2018). Draft genome sequence of *Camellia sinensis* var. sinensis provides insights into the evolution of the tea genome and tea quality. *Proceed. Nat. Acad. Sci. USA* 115, E4151–E4158. doi: 10.1073/pnas.1719622115

Xia, E. H., Tong, W., Hou, Y., An, Y. L., Chen, L. B., Wu, Q., et al. (2020). The reference genome of tea plant and resequencing of 81 diverse accessions provide insights into its genome evolution and adaptation. *Mol. Plant* 13, 1013–1026. doi: 10.1016/j.molp.2020.04.010

Xie, L. F., Cao, Y. L., Zhao, Z. K., Ren, C. H., Xing, M. Y., Wu, B. P., et al. (2020). Involvement of MdUGT75B1 and MdUGT71B1 in flavonol galactoside/glucoside biosynthesis in apple fruit. *Food Chem.* 312:126124. doi: 10.1016/j.foodchem.2019.126124

Yang, C. R., Zhang, Y. J., Gao, D. F., Gao, K. K., and Jiang, H. J. (2008). Evaluation of *Camellia taliensis* (W.W.Smith) Melchior germplasms and the origin of large leave tea. *Tea Sci. Technol.* 3, 1–4.

Yu, X. M., Xia, J. J., Chen, S., Yu, Y., Ma, J. Q., Lin, Y. Z., et al. (2020). Metabolite signatures of diverse *Camellia sinensis* tea populations. *Nat. Commun.* 11:5586. doi: 10.1038/s41467-020-19441-1

Zhang, H. B., Xia, E. H., Huang, H., Jiang, J. J., Liu, B. Y., and Gao, L. Z. (2015). De novo transcriptome assembly of the wild relative of tea tree (*Camellia taliensis*) and comparative analysis with tea transcriptome identified putative genes associated with tea quality and stress response. *BMC Genom.* 16:298. doi: 10.1186/s12864-015-1494-4

Zheng, X. Q., Ye, C. X., Kato, M., Crozier, A., and Ashihara, H. (2002). Theacrine (1,3,7,9-tetramethyluric acid) synthesis in leaves of a Chinese tea, kucha (*Camellia assamica* var. *kucha). Phytochemistry* 60, 129–134. doi: 10.1016/S0031-9422(02)00086-9

Zheng, Y. C., Wang, P. J., Chen, X. J., Yue, C., Guo, Y. C., Yang, J. F., et al. (2021). Integrated transcriptomics and metabolomics provide novel insight into changes in specialized metabolites in an albino tea cultivar (*Camellia sinensis* (L.) O. Kuntz). *Plant Physiol. Biochem.* 160, 27–36. doi: 10.1016/j.plaphy.2020.12.029

Zhou, Y., Zeng, L. T., Gui, J. D., Liao, Y. Y., Li, J. L., Tang, J. C., et al. (2017). Functional characterizations of β-glucosidases involved in aroma compound formation in tea (*Camellia sinensis*). *Food Res. Int.* 96, 206–214. doi: 10.1016/j.foodres.2017.03.049

Zhu, B. Y., Chen, L. B., Lu, M. Q., Zhang, J., Han, J. Y., Deng, W. W., et al. (2019). Caffeine content and related gene expression: novel insight into caffeine metabolism in *Camellia* plants containing low, normal, and high caffeine concentrations. *J. Agric. Food Chem.* 67, 3400–3411. doi: 10.1021/acs.jafc.9b00240

Zhuang, J. H., Dai, X. L., Zhu, M. Q., Zhang, S. X., Dai, Q. Y., Jiang, X. L., et al. (2020). Evaluation of astringent taste of green tea through mass spectrometry -based targeted metabolic profiling of polyphenols. *Food Chem.* 305:125507. doi: 10.1016/j.foodchem.2019.125507

Conflict of Interest: The authors declare that the research was conducted in the absence of any commercial or financial relationships that could be construed as a potential conflict of interest.

Publisher's Note: All claims expressed in this article are solely those of the authors and do not necessarily represent those of their affiliated organizations, or those of the publisher, the editors and the reviewers. Any product that may be evaluated in this article, or claim that may be made by its manufacturer, is not guaranteed or endorsed by the publisher.

frontiers in Plant Science

REVIEW
published: 01 October 2021
doi: 10.3389/fpls.2021.751547

The Tea Plant Leaf Cuticle: From Plant Protection to Tea Quality

*Mingjie Chen**

College of Life Sciences, Henan Provincial Key Laboratory of Tea Plant Biology, Xinyang Normal University, Xinyang, China

Camellia sinensis (tea tree) is a perennial evergreen woody crop that has been planted in more than 50 countries worldwide; its leaves are harvested to make tea, which is one of the most popular nonalcoholic beverages. The cuticle is the major transpiration barrier to restrict nonstomatal water loss and it affects the drought tolerance of tea plants. The cuticle may also provide molecular cues for the interaction with herbivores and pathogens. The tea-making process almost always includes a postharvest withering treatment to reduce leaf water content, and many studies have demonstrated that withering treatment-induced metabolite transformation is essential to shape the quality of the tea made. Tea leaf cuticle is expected to affect its withering properties and the dynamics of postharvest metabolome remodeling. In addition, it has long been speculated that the cuticle may contribute to the aroma quality of tea. However, concrete experimental evidence is lacking to prove or refute this hypothesis. Even though its relevance to the abiotic and biotic stress tolerance and postharvest processing properties of tea tree, tea cuticle has long been neglected. Recently, there are several studies on the tea cuticle regarding its structure, wax composition, transpiration barrier organization, environmental stresses-induced wax modification, and structure–function relations. This review is devoted to tea cuticle, the recent research progresses were summarized and unresolved questions and future research directions were also discussed.

Keywords: *Camellia sinensis*, cuticle, wax, transpiration rate, transpiration barrier, correlation analysis, structure–function relation

OPEN ACCESS

Edited by:
Jian Zhao,
Anhui Agricultural University, China

Reviewed by:
Ziyin Yang,
South China Botanical Garden, Chinese Academy of Sciences, China
Jing Zhuang,
Nanjing Agricultural University, China

***Correspondence:**
Mingjie Chen
mjchen@xynu.edu.cn

Specialty section:
This article was submitted to Plant Metabolism and Chemodiversity, a section of the journal Frontiers in Plant Science

Received: *01 August 2021*
Accepted: *30 August 2021*
Published: *01 October 2021*

Citation:
Chen M (2021) The Tea Plant Leaf Cuticle: From Plant Protection to Tea Quality. Front. Plant Sci. 12:751547. doi: 10.3389/fpls.2021.751547

INTRODUCTION

The cuticle is a hydrophobic coating on the aerial surface of all plants and serves as the interacting interface with the surrounding environment. Recently, a cuticle was also found from the surface of the root cap and lateral roots (Berhin et al., 2019). Plant cuticle protects the plant from dehydration or uncontrolled water absorption (Eigenbrode and Espelie, 1995), pathogen infection (Barthlott and Neinhuis, 1997), insect attack (Eigenbrode and Espelie, 1995), UV radiation (Reicosky and Hanover, 1978; Solovchenko and Merzlyak, 2003), and organ fusion (Weng et al., 2010; Ingram and Nawrath, 2017). The cuticle is a composite structure of polyester and waxes. The polymer matrix is constituted by cutin, cutan, and polysaccharides which form the cuticle backbone (Nawrath, 2006; Domínguez, et al., 2011a; Philippe et al., 2020a). Cutin consists of C16 and C18 hydroxy and epoxy–hydroxy fatty acids, and glycerol monomers (Kolattukudy, 2001; Nawrath, 2006; Pollard et al., 2008). Polysaccharides are found within the cuticular layer or throughout the cuticle (Guzmán et al., 2014a,b; Philippe et al., 2020b). The waxes are either overlaid on the outer surface of cutin matrix as epicuticular waxes (EWs) or embedded inside a cutin polyster network as intracuticular waxes

(IWs; Jetter and Riederer, 2016). So far, the well-characterized wax components include very-long-chain fatty acids (VLCFAs) and their derivatives (alcohols, aldehydes, alkanes, ketones, and wax esters), flavonoids, and alicyclic compounds (triterpenoids, sterols, and tocopherols) (Post-Beittenmiller, 1996; Jenks and Ashworth, 2003; Kunst and Samuels, 2003; Samuels et al., 2008).

There are multiple excellent reviews on plant cuticle in existing literature (Eigenbrode and Espelie, 1995; Kerstiens, 1996a,b; Kunst and Samuels, 2003; Buchholz, 2006; Nawrath, 2006; Shepherd and Griffiths, 2006; Bird, 2008; Pollard et al., 2008; Samuels et al., 2008; Reina-Pinto and Yephremov, 2009; Bernard and Joubès, 2013; Lee and Suh, 2013; Hen-Avivi et al., 2014; Domínguez, et al., 2015; Fernandez et al., 2016; Fich et al., 2016; Ingram and Nawrath, 2017; Philippe et al., 2020a; Skrzydeł et al., 2021), and readers may consult them for further information. The scope of this review is to focus on recent research progresses in tea cuticle. The tea tree possesses several advantages as a model system for cuticle research. They are as follows: (1) it is well adapted to growth chamber or green house conditions; (2) it is a perennial evergreen shrub or tree, and new twigs can emerge year around which make research material readily available; (3) it can be clonally propagated to warrant material with same genetic background, which removes the effect of genetic variance on research results; (4) it has two different types of cuticles during leaf developments, which makes it unique to study cuticle development and evolution; (5) it is self-incompatible, with large genetic variations accrued during its evolutionary history through natural and artificial selection. Thousands of germplasms have been systemically collected, which provide a rich genetic resource to study cuticle structural–functional relationship as well as to discover new pathways for wax lipid biosynthesis. In the following pages, the recent progress in tea leaf cuticle research was first summarized, and then unresolved questions and future research directions were discussed.

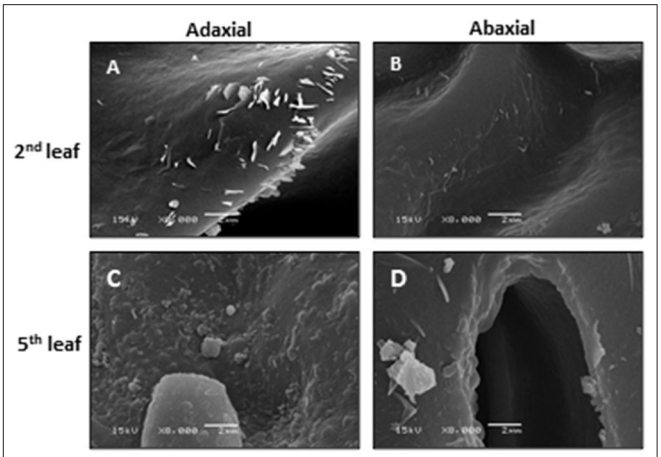

FIGURE 1 | The scanning electron microscopy of the adaxial and abaxial surfaces of the second leaf and the fifth leaf. Bar = 2 μm. Modified from Chen et al. (2020). Scientific Reports 10: 6696.

TEA CUTICLE SURFACE STRUCTURE

Observed by scanning electron microscopy (SEM), the microcrystalline structure from the tea EWs shows three major shapes: rods, papilla, and plates. With tea leaf maturation, the sizes and shapes of wax crystals change accordingly. On tea buds, the wax crystals mainly show a papilla-like structure. The tender second leaf is dominated by rod-like crystals, whereas the mature fifth leaf is dominated by papilla- and plate-like wax crystals (**Figure 1**). Regardless of leaf position or maturity, more wax crystals are present on the adaxial surface compared with its abaxial surface. Koch and Ensikat (2008) demonstrated that crystal shapes are closely associated with wax compositions. Thus, the observed wax crystal changes during tea leaf maturation could reflect their wax chemical changes. The growth conditions also significantly affect the shape and density of the wax crystal. Water deprivation treatment significantly increases the density of the leaf wax crystal (Chen et al., 2020).

The cuticle thickness can be measured by SEM or transmission electric microscope (TEM). For the SEM method, the cuticle membrane needs to be isolated in advance. Jetter and Riederer (2016) applied this method and measured cuticle thickness from eight different plant species and found that the average cuticle thickness is in the range of 1–7 μm. Zhu et al. (2018) applied the TEM method to measure tea leaf cuticle thickness. Under the TEM image, the epidermal cell wall shows a layered configuration based on the staining patterns in an osmium tetroxide-uranyl acetate combination. Right under the cuticle, the cell wall is densely stained. In contrast, the epidermal cell wall facing the cytoplasm is only lightly stained. These differential staining patterns could reflect the compositional difference of the epidermal cell wall. Jeffree (2006) suggested that these densely stained layers are rich in pectin, and the constituent galacturonic acid moieties have free carboxyl groups which provide potential sites for ester linkages with cutin. Since the cuticle is just lightly stained by dyes like osmium tetroxide-uranyl acetate, there is a good contrast between the cuticle and cell wall, which makes the cuticle easily differentiated from cell wall in TEM imaging (**Figure 2**). Another advantage of the TEM method is that the cuticle thickness on the adaxial and the abaxial surface can be measured simultaneously. Zhang et al. (2021) applied the TEM method and measured the cuticle thickness of the fifth leaf from eight different tea germplasms, and the data were summarized in **Table 1**. The average thickness of the adaxial cuticle is in the range of 2.12–2.99 μm and the abaxial cuticle thickness is in the range of 1.24–1.46 μm. For individual tea germplasm, the adaxial cuticle generally is thicker than that of its abaxial counterpart.

The TEM method also enables measuring the thickness of the EW layer and the IW layer. Zhu et al. (2018) follow up on the changes of cuticle thickness during tea leaf maturation. In the rapidly growing tea twig, the closer to the apical bud, the more tender the leaf is. Thus, the authors use the leaf position as a proxy for leaf maturity. The cellular characteristics also demonstrated that the second leaf from the apical bud is immature, and the fifth leaf becomes fully mature. In *Camellia sinensis cv Fuyun 6*, the adaxial cuticle thickness of the second leaf was 1.15 μm, and the

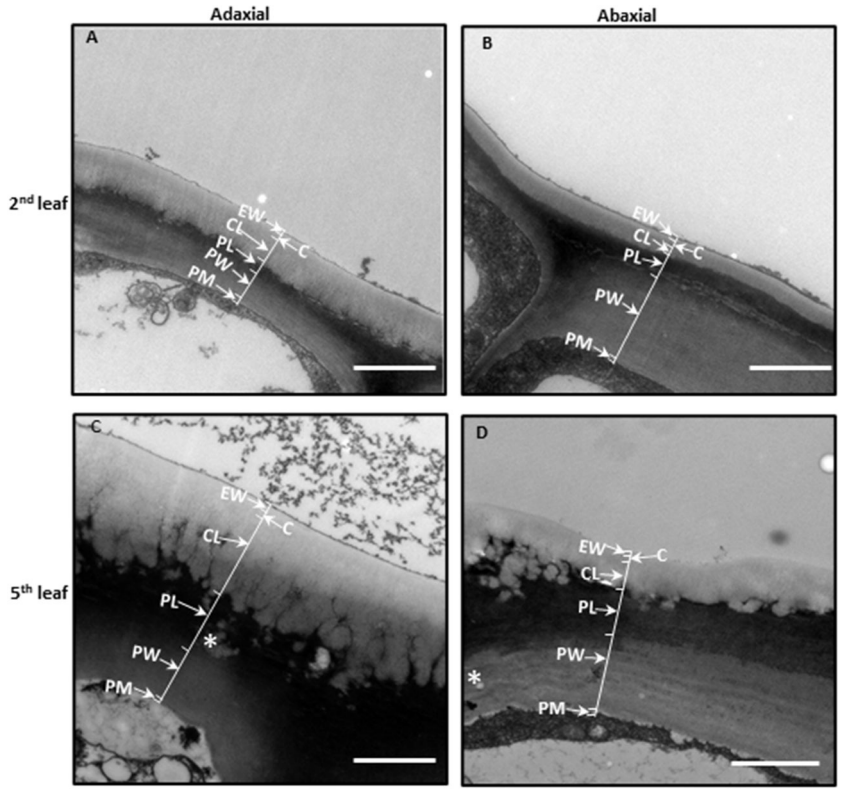

FIGURE 2 | The leaf cuticle structure of *Camellia sinensis cv Fuyun 6.* **(A)** The adaxial side of the second leaf. **(B)** The abaxial side of the second leaf. **(C)** The adaxial side of the fifth leaf. **(D)** The abaxial side of the fifth leaf. Epicuticular waxes (EWs) cover the cuticle proper **(C)**, which is cutin embedded with intracuticular waxes (IWs). The cuticular layer (CL) seem also to contain intracuticular wax. Pectinaceous layer (PL), primary cell walls (PWs), and the plasma membrane (PM). Bar = 2 μm. The thickness of the cuticle was indicated by arrows. Cited from Zhu et al. (2018). Scientific Reports 8: 14944.

average thickness of the EW layer and the IW layer was 0.19 and 0.97 μm, respectively; the average abaxial cuticle thickness was 0.47 μm, and the EW layer and the IW layer account for 0.13 and 0.34 μm, respectively. Although the total cuticle thickness of the fifth is doubled, the EW layer is only slightly increased, suggesting that the majority of the increase in cuticle thickness is attributed to the IW layer (Zhu et al., 2018).

The morphology of each cuticular layer also shows differential changes. The epicuticular layer facing the outer surface maintains a straight outline during leaf maturation; however, the IW layer facing the cell wall shows dramatic morphological changes with leaf maturation. The initial straight lines disappeared and were substituted by many small ridges, between ridges channels also are visible. During leaf maturation, the adaxial cuticle showed more pronounced structural changes compared with the abaxial cuticle (**Figure 2**).

TEA LEAF CUTICULAR WAX COMPOSITION AND DISTRIBUTION PATTERNS

Chemical analysis demonstrates that tea leaf cuticular waxes are constituted by 14 chemical classes, including acids, 1-alkanols, aldehydes, alkanes, 1-alkanol esters, glycol esters, benzyl esters, phenethyl esters, phthalate esters, glycols, tocopherols, triterpenoids, sterols, and caffeine (Zhu et al., 2018; Zhang et al., 2020). It is well documented that the amounts and composition of cuticular waxes vary greatly among plant species, organs, tissues, or even developmental stages (Barthlott and Neinhuis, 1997; Jetter et al., 2007; Kosma et al., 2010; Buschhaus and Jetter, 2011; Bernard and Joubès, 2013). To offer a more detailed overview about wax distribution patterns, Zhang et al. (2020) isolated the EWs and the IWs from the adaxial and the abaxial surface, and then quantified the wax coverage and compositions. The wax coverages from the adaxial and the abaxial surfaces do not correlate with their respective cuticle thickness. Although the adaxial cuticle is thicker than that of the abaxial cuticle, its wax coverage is similar to the abaxial surface. On the adaxial surface, the waxes are almost equally distributed between EWs and IWs; however, on the abaxial surface, the IWs coverage is about 1.45–3.33 times higher than that of the EWs. For individual germplasms, the coverage of the adaxial EWs generally was higher than that of the abaxial EWs. Among the four cuticular compartments, the coverage of the abaxial IWs ranked as the highest among all the tea germplasms studied. By combining the cuticle thickness and the wax coverage data, the wax density from the adaxial and the abaxial surface is obtained. The EW density from the adaxial and the abaxial surfaces are 17.4 ± 1.0 and 19.7 ± 1.4 mg cm^{-3}, respectively; the IW density from the adaxial

TABLE 1 | Cuticle thickness (μm) from the adaxial and the abaxial leaf surface of the eight tea germplasms.

	Jinguanyin	0316B	Wuniuzao	0306A	0306H	Fuyun20	0202-10	Hongyafoshou
Adaxial	2.99±0.11^{a}	2.42±0.07^{c}	2.12±0.07^{d}	2.77±0.15^{ab}	2.77±0.04^{ab}	2.56±0.06^{bc}	2.78±0.08^{ab}	2.65±0.12^{bc}
Abaxial	1.46±0.04^{a}	1.33±0.05^{ab}	1.37±0.02^{ab}	1.37±0.06^{ab}	1.24±0.02^{b}	1.45±0.05^{a}	1.36±0.05^{ab}	1.31±0.02^{b}

Different lower-case letters represent statistically significant ($p < 0.05$). Data are expressed as mean ± SE ($n = 6$).

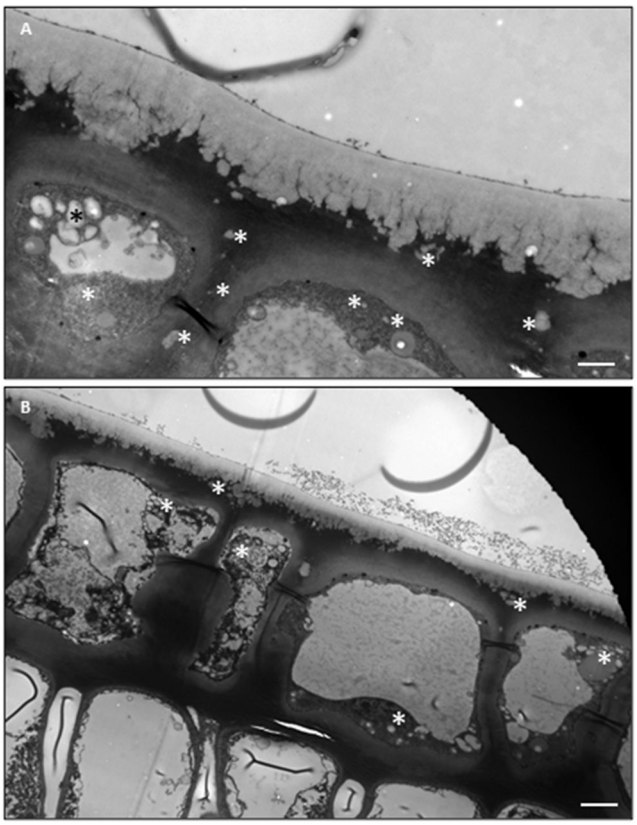

FIGURE 3 | TEM imagines of the adaxial and the abaxial epidermal cells and the underlying palisiad cells. **(A)** The adaxial surface. **(B)** The abaxial surface. Bar = 2 μm.

and the abaxial surface are 3.9 ± 0.1 and 7.8 ± 0.2 mg cm^{-3}, respectively. Overall, the wax density from the adaxial surface is lower than that of the abaxial surface.

Compared to the abaxial EWs, the adaxial EWs showed higher coverage of aldehydes, 1-alkanols, alkanes, and β-tocopherol. Compared to the abaxial IWs, the adaxial IWs showed higher coverage of 1-alkanols, alkanes, and β-tocopherol, but lower coverage of triterpenoids, steroids, and caffeine (Chen et al., 2021). Due to these unsymmetrical distributions of individual wax components on both leaf surfaces, the adaxial coverages of 1-alkanols, alkanes, and β-tocopherol are higher than that of the abaxial surface; in contrast, the adaxial coverage of triterpenoids, steroids, and caffeine are lower than that of the abaxial surface. The unsymmetrical deposition of cuticular wax into the adaxial and the abaxial surfaces may have ecophysiological implications for these two leaf surfaces. However, the underlying mechanisms to shape such wax distribution patterns remain unclear.

CUTICULAR WAX TRANSPORT

All the wax components are synthesized in the endoplasmic reticulum (ER) of epidermal cells (Li-Beisson et al., 2010). After synthesis in the ER, waxes need to be transported to the plasma membrane (PM) for export. It is widely accepted that there are three possible routes for wax transportation from ER to PM: (1) Golgi and trans-Golgi network-mediated vesicle trafficking (Kunst and Samuels, 2003); (2) transport by cytosolic carrier proteins such as acyl-CoA binding proteins (Leung et al., 2006; Xiao and Chye, 2009; Xue et al., 2014); and (3) direct transfer through ER–PM membrane contact sites (Levine, 2004; Bernard and Joubès, 2013).

For the translocation of cuticular waxes from the PM to the apoplast, ATP-binding cassette transporter family proteins including ABCG1, 2, 6, 11, 12, 13, 20, and 32, play important roles (Vishwanath et al., 2015; Fich et al., 2016; Shanmugarajah et al., 2019). ABCG11 forms heterodimer with ABCG12 and is required for ABCG12 trafficking to the PM (Pighin et al., 2004; Bird et al., 2007; Luo et al., 2007; Panikashvili et al., 2007; Ukitsu et al., 2007; McFarlane et al., 2010). Since the ABCG11 and ABCG12 double mutants still retain ∼50% surface wax (Bird et al., 2007), the other ABCG transporters are expected to be involved in wax secretion.

Lipid transfer proteins have been suggested to be involved in the transport of hydrophobic cuticular lipids from the PM through the hydrophilic cell wall and to the cuticle (Somerville et al., 2000). One member of this family, glycosylphosphatidylinositol-anchored lipid transfer protein (LTPG), is localized to the exterior face of the PM and may be involved in wax transport (Sterk et al., 1991; Thomas et al., 1993; Kunst and Samuels, 2003; DeBono et al., 2009; Lee et al., 2009). Since LTPG has a glycosylphosphatidylinositol (GPI) anchor to move across the cell wall with wax cargo, the GPI anchor needs to be cleaved first; alternatively, LTPG could have a different function in wax export.

Under the observation of TEM, the epidermal cells are filled with 1–2 μm whitish drops, which are not observed in the underlying palisade cells (**Figures 3A,B**). These drops are suggested to be lipid inclusion bodies of oleophilic droplets (Hoffmann-Benning et al., 1994). Similar size of inclusion bodies is also observed within the periclinal pectin layer of the cell wall as well as the anticlinal pectin layer which is formed by two neighboring epidermal cells (**Figures 3A,B**). These observations raise the possibility that cuticular wax could be transported from ER to PM in the form of inclusion bodies. Once reaching PM

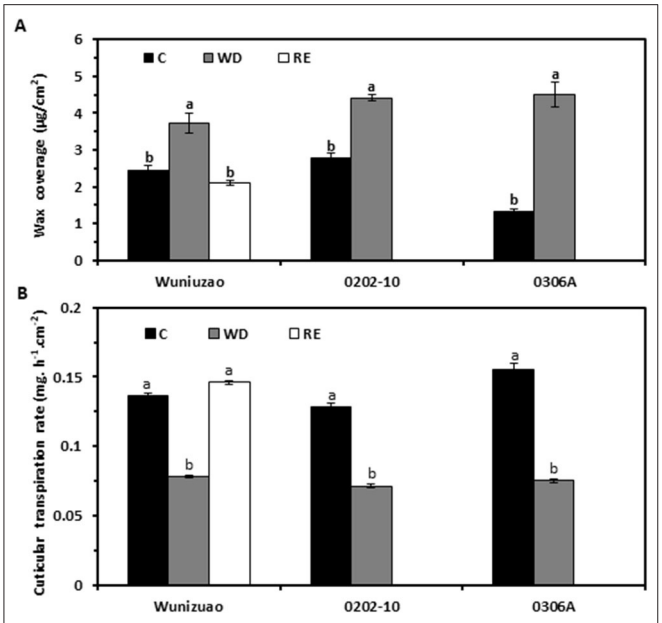

FIGURE 4 | The water deprivation and rehydration treatments alter wax coverage and cuticular transpiration rate dynamically in three tea germplasms. **(A)** Wax coverage changes under different growth conditions. **(B)** Cuticular transpiration rate changes under different growth conditions. C: control; WD: water deprivation; RE: rehydration. Statistically significant changes within the same germplasm under different treatments were indicated by different letters. Modified from Zhang et al. (2021). Frontiers in Plant Science 11: 600069.

these inclusion bodies could be exported into the apoplast by exocytic vesicles and then diffuse through the pectin layer of the cell wall, until they reach and superimpose into the existing cuticle facing the protoplast surface. In deep-water rice and sorghum, osmiophilic vesicles near to or fusing with the PM have been reported before (Hoffmann-Benning et al., 1994; Jenks et al., 1994; Jeffree, 2006; Pollard et al., 2008), suggesting that such wax transportation mechanisms could exist in multiple plants. However, the structure and chemical composition of these inclusion bodies in tea and other plants remain unresolved.

DEVELOPMENTAL AND ENVIRONMENTAL MODIFICATION OF TEA CUTICLE AND CUTICULAR WAX

Based on the presence and percentage of triterpenoids, plant cuticle can be divided into two types: the cuticle mainly is composed of VLCFAs and their derivatives, and the cuticle contains a high percentage of triterpenoids besides VLCFAs (Jetter and Riederer, 2016). Zhu et al. (2018) and Chen et al. (2020) found that the cuticular waxes from the juvenile (tender) leaf are mainly constituted by VLCFAs and their derivatives; in contrast, the mature leaf cuticle contains high levels of triterpenoids in addition to VLCFAs. Similar observation was recently reported in *Sorghum bicolor* (Busta et al., 2021). By now, it still remains unclear when the leaf cuticle makes such a transition and what are the underlying mechanisms. The analysis of cuticular waxes from each leaf position of a growing twig would clarify this issue. It has been reported that in other plant species, oxidosqualene cyclase (OSC) genes control the accumulation of cuticular triterpenoids (Thimmappa et al., 2014). The cuticular wax chemistry transition during tea leaf maturation could also be associated with *CsOSCs* expression. It will be interesting to investigate how many isoforms of *CsOSCs* are present in the tea genome, and how they are activated in epidermal cells during tea leaf maturation and contribute to triterpenoid accumulation in the leaf cuticle.

Cuticle structure and wax composition can also be affected by environmental factors such as drought (Chen et al., 2020; Zhang et al., 2021). Even though the tender leaves and the mature leaves have profound differences in cuticular wax chemistry, drought stress induces both types of leaves with some common compositional changes in cuticular waxes. For example, the wax coverage, cuticle thickness, and osmiophilicity of the tender leaf and mature leaf are increased, and some new wax species are synthesized and existing wax profiles are commonly modified (Chen et al., 2020).

The life span of tea leaf is around 1 year; it is expected that tea leaves will experience annual rain season and dry season. Since the cuticle is generally regarded as a nonliving tissue, the question is whether the cuticle modification is reversible once the stress conditions (such as drought) have disappeared. Zhang et al. (2021) reported that wax coverage and cuticular transpiration barriers indeed are reinforced by drought, but can be reversed following rehydration treatment (**Figures 4A,B**). There are multiple potential nonexclusive mechanisms working together to regulate cuticular wax deposition, including *in vivo* wax synthesis or transport in epidermal cells, dynamic phase separation between the EWs and the IWs, *in vitro* polymerization (Spencer et al., 1988), and retro transportation into epidermal cell wall or cytoplasm for further transformation (**Figure 5**; Zhang et al., 2021).

TEA LEAF CUTICULAR TRANSPIRATION RATE MEASUREMENT

The principal function of the cuticle is to serve as a water transpiration barrier. The cuticular transpiration measurement provides essential information regarding its barrier properties. Several different methods have been developed in the past, including microbalance (Schönherr and Lendzian, 1981), ^{14}C-epoxiconazole tracer permeability assay (Ballmann et al., 2011), and specially designed transpiration chamber (Becker et al., 1986). Different detection technologies were also developed, including the electrolysis cell (Keidel, 1959), moisture sensor, and ^{3}H-labeled water in combination with a scintillation counter (Schreiber et al., 2001). Cuticular membrane isolation method, based on enzyme digestion, was also developed (Schönherr and Riederer, 1986). These technical advances facilitate the cuticular transpiration measurement (Becker et al., 1986). A common limitation of these methods is that only isolated cuticular membrane can be applied; in addition, the isolated cuticular membrane must be stomata-free. To overcome these

limitations, Zhang et al. (2020) developed a new method that can measure the cuticular transpiration rates from the excised intact leaf; in addition, the transpiration from the adaxial and the abaxial surface can be obtained simultaneously. To make this measurement method robust and reproducible, several pretreatments are required: (1) Water equilibration: To minimize the influence of leaf water content variations on transpiration rate measurement, the excised twigs are equilibrated in water overnight to make leaf water contents even. (2) Close stomata: The stomata have a large influence on the cuticular transpiration rate measurement and it is desirable to make the stomata closed fully. For this purpose, three different treatments are applied: (1) the water equilibration be performed under the dark condition to promote stomata closure; (2) before leaf excision for transpiration measurement the ABA is applied to promote stomata closure. The data demonstrated that for the fully equilibrated leaf these combined treatments still cannot make stomata close fully. However, dehydration treatment for 4–5 h following leaf excision can effectively make stomata close, thus a constant minimal transpiration rate can be reached (Burghardt and Riederer, 2003; Zhang et al., 2020). Based on this phenomenon, the residual stomata transpiration can be estimated by using the total leaf transpiration difference between 0 and 5 h after leaf excision. The minimal transpiration (T) can be obtained from the leaf drying curve after the stomata became fully closed. (3) Vaseline application. Vaseline can be applied onto leaf abaxial surface to block stomata transpiration.

The total leaf transpiration rate (T) of control can be expressed as: (I) $T = T_{Ad} + T_{Ab,}$ where T_{Ad} and T_{Ab} represent the adaxial and the abaxial leaf transpiration rates, respectively. The adaxial transpiration rate can be regarded as equivalent to the adaxial cuticular transpiration rate. Due to the presence of stomata, the abaxial transpiration rate (T_{Ab}) is the sum of the abaxial cuticular transpiration rate (T_{Ab_c}) and the residual stomatal transpiration rate (T_{Ab_s}). A mathematical relationship can be expressed as: (II) $T_{Ab} = T_{Ab\_c} + T_{Ab\_s}$.

Using vaseline to seal the leaf surface can effectively reduce water transpiration. When both leaf surfaces are sealed with vaseline, the observed leaf transpiration rate ($T_{Ad/Vas::Ab/Vas}$) is equivalent to total leaf transpiration rate (T) multiplied by a vaseline diffusion coefficient factor k: (III) $T_{Ad/Vas::Ab/Vas} = k \times T$. Since $T_{Ad/Vas::Ab/Vas}$ and T can be experimentally measured from the control and the Vaseline-treatment group, the k value can be calculated. Theoretically, k is a parameter related to the applied vaseline film and affected by the film thickness and evenness; Thus it should be a constant once a stable vaseline film is established. However, after leaf excision, the observed total transpiration rate T of the control gradually decreased whereas the observed total transpiration rate from vaseline-sealed group kept fairly stable, which resulted in the k value increasing gradually. The decrease in the total transpiration rate of the control plants likely results from the gradual stomata closure induced by leaf dehydration following excision. A stable k can be obtained after stomata closure fully, which takes about 4–5 h following tea leaf excision.

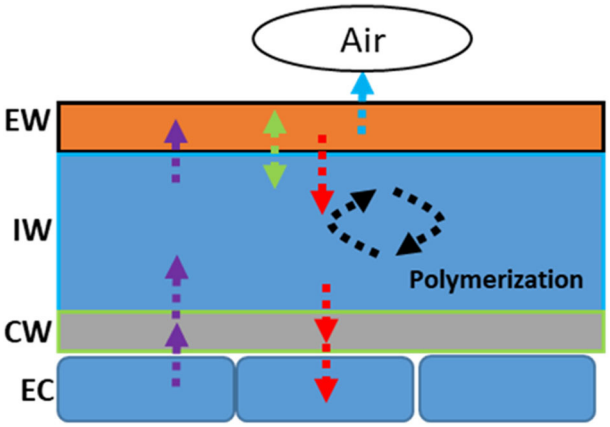

FIGURE 5 | Schematic representation of the modification modes of the cuticular wax in response to drought stress. EW: epicuticular waxes; IW: intracuticular waxes; CW: cell wall; EC: epidermal cell.

When the adaxial surface is sealed with vaseline (Ad/Vas), the observed total transpiration rate ($T_{Ad/Vas}$) is given by the formula: (IV) $T_{Ad/Vas} = k \times T_{Ad} + T_{Ab.}$

Similarly, when the abaxial surface is sealed with vaseline (Ab/Vas), the observed total transpiration rate ($T_{Ab/Vas}$) is given by the formula: (V) $T_{Ab/Vas} = T_{Ad} + k \times T_{Ab.}$

Based on the observed value for T, $T_{Ad/Vas::Ab/Vas,}$ $T_{Ad/Vas,}$ $T_{Ab/Vas,}$ the mathematical formula I–V, the cuticular transpiration rates from the adaxial, and the abaxial leaf surface can be calculated. Zhang et al. (2020) found that the abaxial cuticular transpiration rate is about 1-fold higher than that of the adaxial cuticular transpiration rate in *C. sinensis cv Fuyun 6*. To test if this is a common or just a germplasm-specific phenomenon, Chen et al. (2021) measured the cuticular transpiration rates from other eight tea germplasms and found that the abaxial cuticular transpiration rates showed much larger variations among these tea germplasms and was about 1.8–3.3 folds higher than that of the adaxial surface; in contrast, the adaxial cuticular transpiration rates showed much smaller variations across diverse germplasms (**Figure 6**). These results demonstrated the unsymmetrical distribution of the cuticular transpiration barrier between the adaxial and the abaxial surfaces.

CUTICULAR TRANSPIRATION BARRIER ORGANIZATIONS ON THE ADAXIAL AND THE ABAXIAL LEAF SURFACES

It has been demonstrated that cuticular waxes rather than cutin matrix make significant contributions to the cuticular transpiration barrier (Schönherr, 1976; Vogg et al., 2004; Jetter and Riederer, 2016; Sadler et al., 2016). Since cuticular waxes can be divided into EWs and IWs (Jetter and Riederer, 2016), the question is which one, the EWs, the IWs, or both contribute to the cuticular transpiration barrier? To answer this question, a simple way is to selectively remove EWs and then measure the

leaf transpiration changes. If EWs removal significantly increases the leaf transpiration rate, then this would suggest that these EWs play an important role in shaping the surface transpiration barrier. If EWs removal does not affect the transpiration rate, this would suggest that these EWs do not contribute much to the transpiration barrier. Previous work has shown that gum Arabic can selectively and efficiently strip off EWs without affecting IWs (Jetter and Schäffer, 2001; Jetter and Riederer, 2016; Zeisler and Schreiber, 2016). Zeisler and Schreiber (2016) and Zeisler et al. (2018) studied 10 different plant species including the tea tree, and the authors concluded that the adaxial EWs are not the main cuticular transpiration barrier, instead, the adaxial IWs constitute the main cuticular transpiration barrier. This conclusion is independently confirmed by Zhang et al. (2020) who applied a different measurement method. However, the transpiration barrier organization for the abaxial cuticle remains largely unresolved due to the technical hurdles. The established new method by Zhang et al. (2020) paved the way to measure the abaxial cuticular transpiration rate. The data demonstrated that the abaxial EWs constitute a major cuticular transpiration barrier, whereas the abaxial IWs do not (**Figure 7**). Correlation analysis from the adaxial and the abaxial surface suggest that the differential distribution of VLCFAs, 1-alkanol esters, and glycols may contribute to the unsymmetrical cuticular transpiration barrier on both leaf surfaces (Zhang et al., 2020). By now, it still remains unclear what the ecobiological implications for the differential organization of cuticular transpiration barrier on the two surfaces of the leaves are. We speculate that the adaxial surface is optimized to restrict water loss, whereas the abaxial surface could be evolved to cope with other environmental stresses, which compromise its potency as an efficient water transpiration barrier. Since the adaxial and the abaxial cuticles are independently synthesized by the adaxial and the abaxial epidermal cells, respectively, and the adaxial epidermal cells and the abaxial epidermal cells have different niches (such as light irradiance), differential regulations of wax synthesis or transport from the adaxial and the abaxial epidermal cells may occur, and this would eventually affect wax composition on the EWs and the IWs of the adaxial and the abaxial cuticle.

CUTICULAR WAXES THAT AFFECT CUTICULAR TRANSPIRATION RATE OR RESISTANCE UNDER NORMAL AND STRESS CONDITIONS

Cuticular waxes from individual cuticular compartments can be isolated and their coverage and composition is measured by GC-MS and GC-FID. Cuticular transpiration rates or resistance can also be determined from individual cuticular compartments. The correlation analysis between wax chemistry and cuticular transpiration offers a powerful tool to identify contributing wax components to cuticular transpiration barrier properties. This brings up two questions: (1) Are the contributing waxes for the transpiration barrier affected by plant growth conditions? (2) Does the wax subcompartment localization affect its contribution to the transpiration barrier property? To address these questions,

TABLE 2 | Correlations (Pearson's R^2 values) between cuticular transpiration rate and a different compound class of cuticular waxes.

	Adaxial surface		Abaxial surface	
	EW	IW	EW	IW
Acides	−0.51	−0.25	−0.07	−0.54
Aldehydes	−0.68*	−0.59*	−0.14	+0.03
1-Alkanols	−0.39	−0.32	−0.07	−0.93*
Alkanes	−0.13	+0.06	−0.01	+0.01
1-Alkanol esters	−0.59*	+0.09	−0.08	+0.08
Glycol esters	−0.52	−0.00	−0.33	−0.12
Phthalate esters	−0.39	+0.15	−0.39	+0.26
Glycols	−0.00	+0.42	−0.01	−0.03
β-Tocopherol	−0.37	−0.04	−0.07	−0.01
Triterpenoids	−0.53	−0.71*	+0.01	−0.88*
Steroids	−0.00	−0.07	+0.07	−0.74*
Caffeine	−0.50	+0.00	−0.36	+0.00
Subtotal coverage	−0.51	−0.78*	−0.11	−0.97*

Plus (+) and minus (–) represent positive and negative correlation with minimum transpiration rate. Values labeled with asterisk are significant at $P < 0.05$. EW, epicuticular wax; IW, intracuticular wax.
Cited from Zhang et al. (2021).

Zhang et al. (2020) grew three tea germplasms in a greenhouse. Water was withheld for a certain period to induce drought stress, and then water was resumed for the recovery of plants. The EWs and the IWs from the adaxial and the abaxial surfaces of the fifth leaf were isolated and quantified, whereas the cuticular transpiration rates were measured from leaf drying curves. The data showed that the cuticular transpiration barriers were enhanced by drought stress, and the initial weak cuticular transpiration barriers were preferentially reinforced, an effect known as "make up for shortcomings," and rehydration treatment lessened the cuticular transpiration barrier. Thus, the cuticular transpiration barrier can be reversibly modified depending on the growth conditions of plants. Correlation analysis demonstrated that the modification of the cuticular transpiration barrier does not require an overhaul of all wax components, instead targeted deposition of some specific wax compounds into individual cuticular compartments is sufficient to alter the cuticular transpiration barrier properties (**Table 2**).

In literature, it has been controversial regarding alicyclic compounds (triterpenoids and steroids) for their contributions to the cuticular transpiration rate. The triterpenoids were reported to be positively correlated with cuticular transpiration rates. Thus they were not regarded as contributors to the cuticular transpiration barrier (Vogg et al., 2004; Buschhaus and Jetter, 2012; Jetter and Riederer, 2016), whereas in other reports they were identified as a contributor to the cuticular transpiration barrier (Schuster et al., 2016; Zeisler and Schreiber, 2016; Romero and Rose, 2019). Zhang et al. (2021) found that under drought stress the triterpenoids and steroids from IWs were negatively and significantly correlated with cuticular transcription rate, suggesting that they contribute to the cuticular transpiration barrier under drought conditions. Under the

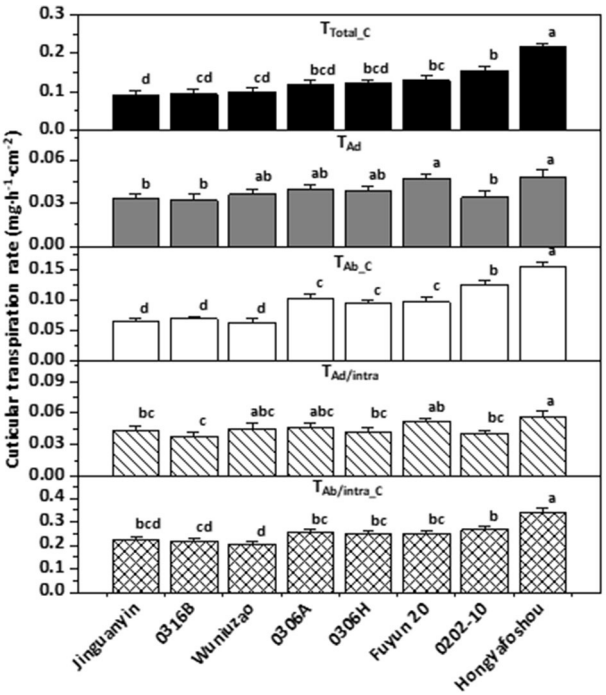

FIGURE 6 | The cuticular transpiration rates of the eight tea germplasms. Different lower-case letters represent statistically significant (P $P < 0.05$). TTotal_C: the total cuticular transpiration rate; TAd: the adaxial cuticular transpiration rate; TAb_C: the abaxial cuticular transpiration rate; TAd/intra: the adaxial intracuticular transpiration rate; TAb/intra_C: the abaxial intracuticular transpiration rate. Modified from Chen et al. (2021). Frontiers in Plant Science 12: 655799.

described experimental conditions, tea plants were also subjected to high temperature and high light radiation stresses besides dehydration stress (Zhang et al., 2021). To cope with these multiple stresses, alicyclic compounds could serve as cuticle nanofiller to increase cuticle stiffness and breaking stress and decrease its maximum strain. Consistent with this notion, under normal growth conditions, triterpenoids and steroids were not found to be correlated with cuticular transpiration rate (Chen et al., 2021). Recently, Busta et al. (2021) compared the leaf wax divergence between sorghum and maize, and they identified an OSC gene (Sobic.008G142400.1) which is involved in generating the majority of sorghum leaf surface triterpenoids. These triterpenoids are major components of the IW layer on both sides of the leaf. They could act as strengthening nanofillers (Tsubaki et al., 2013) and contribute to the performance of the leaf cuticle at elevated temperatures (Schuster et al., 2016). These findings collectively support the notion that cuticle triterpenoids play important roles under stress conditions rather than normal growth conditions (Chen et al., 2021). It remains an open question whether triterpenoids play other critical functions (such as defense) under normal growth conditions. Considering that such a large quantity of triterpenoid accumulation in the cuticle requires considerable carbon and energy input from the plants, they must contribute to the health or fitness of tea plants to be retained during the evolutionary history of tea.

THE ROLES OF TEA LEAF CUTICLE IN BIOTIC STRESSES

Cuticular wax synthesis gene was induced by pathogen attack (Bourdenx et al., 2011; Zhao et al., 2020), raising the possibility that cuticle is involved in insects and pathogen defense. Recently, caffeine was detected from the tea leaf cuticle (Zhang et al., 2020, 2021; Chen et al., 2021), raising an interesting question that cuticular caffeine may be involved in insects or pathogens resistance. Due to its dual hydrophilic and lipophilic character, caffeine can freely penetrate cell-, tissue-, and organ-related barriers (Gundlach et al., 1992). In *Coffea* caffeine accumulation is boosted by insect- and pathogen-infestation (Filho and Mazzafera, 2000). In tomato, cabbage, and orchid exogenous application of caffeine can enhance their resistance to insects and pathogens (Hollingsworth et al., 2002; Ashihara et al., 2008). Transgenic tobacco plants producing caffeine showed enhanced pathogen resistance (Kim and Sano, 2008). The caffeine content in *Coffea arabica* showed a positive correlation with their resistance to *Colletotrichum coffeanum*-induced coffee berry disease (Biratu et al., 1996). These data demonstrated that caffeine indeed participates in herbivore or pathogen resistance. However, the underlying molecular mechanisms remain elusive. Wang et al. (2016) reported that tea caffeine level was increased by the infection of *Colletotrichum fructicola*, caffeine strongly inhibited mycelial growth *in vitro* by affecting mycelial cell wall integrity and PM permeability. Li et al. (2016) found that foliar application of exogenous caffeine in tea tree can enhance lipoxygenase activity and endogenous jasmonic acid content, and decrease *C. gloeosporioides*-induced necrotic lesions. These findings provide novel insights into the molecular mechanisms of caffeine in plant defense response. The tea cuticular caffeine could serve as the first line of defense in efficiently repelling pests and pathogens (Uefuji et al., 2005; Kim and Sano, 2008).

Besides caffeine, triterpenoids are mostly considered to have roles in plant protection and defense from pathogens or herbivores due to their inherent antimicrobial, antifungal, antiparasitic, insecticidal, and anti-feedant properties (Augustin et al., 2011; Osbourn et al., 2011). Zhu et al. (2018) found that the cuticle from the mature tea leaves is dominated by triterpenoids and sterols which are absent from that of the tender tea leaves. Zhou et al. (2019) also reported that triterpenoid ester content increased with leaf maturation. It is worth noting that the triterpenoid distribution pattern is in sharp contrast with caffeine, which is higher from the tender leaves than that of mature leaves (Ashihara et al., 2008). The differential distribution patterns might suggest that caffeine plays larger defense roles in the tender tea leaves, whereas triterpenoids are the major defense compounds in mature tea leaves. The cuticular triterpenoids, like its counterpart of cuticular caffeine, could also serve as molecular signatures during the initial phase of the interaction between pathogens, herbivores, and their plant host. Under this scenario, the chemical defense imposed by the tea host may force insects

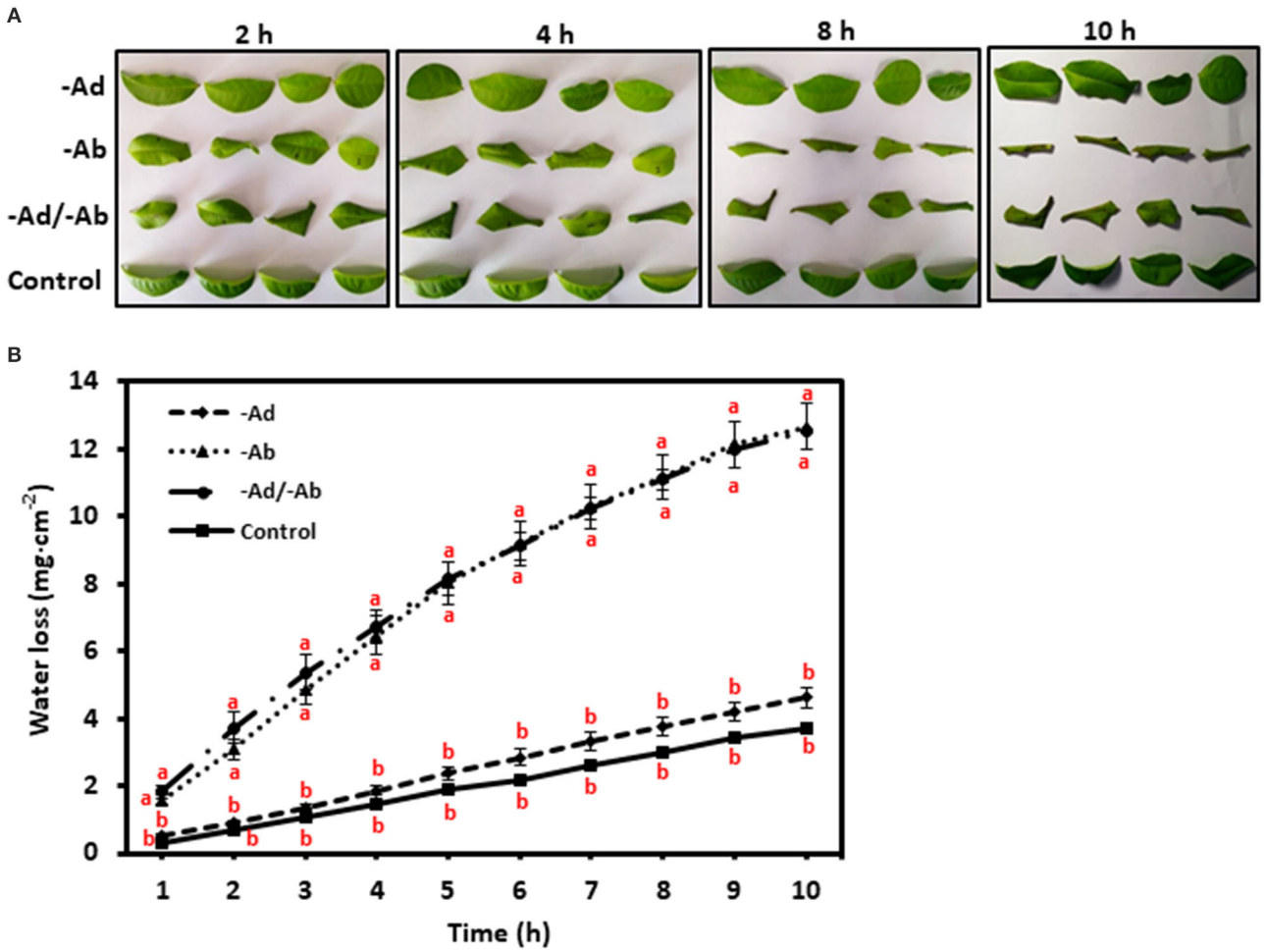

FIGURE 7 | (A,B) Adaxial and abaxial epicuticular waxes (EWs) had different contributions to the leaf transpiration barrier. –Ad, adaxial EW waxes were removed by gum Arabic; –Ab, abaxial EW waxes were removed by gum Arabic; –Ad/–Ab, EW waxes from both surfaces were removed by gum arabic. Data are expressed as means ± standard error ($n = 5$). Statistical analysis was performed among different treatments at same time point, and different letters at the same time point indicate statistically significant ($p<0.05$). Cited from Zhang et al. (2020). Frontiers in Plant Science 11: 420.

or pathogens to apply avoidance or adaption strategies. In tea green leafhopper [*Empoasca (Matsumurasca) onukii Matsuda*], a polyphagous phloem feeding specialist pest of tea plants in Asian tea growing regions (Qin et al., 2015), the nymphs and adults suck phloem sap of tender leaves rather than mature leaves and the female adults lay eggs within the stem of tender shoots. *Ectropis oblique hypulina Wehrli*, a chewing tea insect, only feeds on the tender tea leaves. These observations suggest that caffeine may play minor roles against green leafhopper and *E. oblique* infestation. To support this note, it has been reported that tea caffeine levels are not affected by green leafhopper (Zhao et al., 2020). It requires further clarification if these feeding preferences are related to triterpenoid avoidance. In contrast, anthracnose is only found on mature leaves but not tender leaves of tea plants (Wang et al., 2016). Since a reduced endogenous caffeine content is positively correlated with increased susceptibility of tea to *C. gloeosporioides*, and the mature leaves show lower caffeine contents compared with that of tender leaves (Ashihara et al., 2008), the data suggest that caffeine, rather than triterpenoids, play major roles in the defense of this fungal pathogen. Overall, these data suggest that different insects and pathogens could develop different tolerance to caffeine or triterpenoids during their coevolution history.

THE CONTRIBUTIONS OF LEAF CUTICLE FOR TEA QUALITY

Tea leaf cuticle could affect tea quality in several ways: (1) Cuticle can affect the processing properties of tea leaves. Generally, the thicker the cuticle, the more brittle it is. This not only affects the processing properties of tea leaves but also the appearance of the processed tea which is an important quality factor; (2) postharvest withering treatment reduces leaf water content, thus, facilitating metabolite transformation. It is an essential step to shape the quality of made tea. As an efficient transpiration barrier,

FIGURE 8 | The stem from a growing twig of *Camellia sinensis*.

tea leaf cuticle affects the postharvest withering dynamic and thus could affect postharvest metabolome remodeling and tea quality. Interestingly, the cuticular transpiration rates show large variations among different tea germplasm (**Figure 6**; Chen et al., 2021). It remains poorly understood how the withering dynamic changes affect metabolite transformation and tea quality. (3) It has long been speculated that tea leaf cuticle contributes to the aroma quality of made tea. The wax chemical characterization provides two pieces of evidence to support this speculation (Zhu et al., 2018). Firstly, aromatic precursors are found in the tea cuticle in the form of esters, including benzyl alcohol, phenethyl alcohol, 1-butanol, isobutanol, and 2-ethyl-1-hexanol; secondly, benzyl esters and phenethyl esters are only found in the tender leaf which is used to make tea, and absent in the mature tea leaf. During postharvest tea processing, the tea leaves could be disintegrated, which results in the release of hydrolase, lipase, or esterase onto the leaf surface; the ester bond could be cleaved; and the cuticle aroma precursors be released, thus contributing to the aroma quality of made tea. The black tea shows a richer aroma than that of green tea. The black tea processing includes a rolling step which leads to complete leaf disintegration, and this would facilitate aroma precursor release from tea cuticle. (4) As a hydrophobic layer, the cuticle could slow down the release of tea-soluble contents into infusion during tea brewing. An unintended effect of tea processing might be to break the integrity of the cuticle to facilitate metabolite release. White tea, the less processed tea which only includes two steps, namely withering and drying, could better preserve the cuticle integrity in the processed tea. Interestingly, white tea is well-known to be more resistant to brewing than other types of tea. This correlation may provide indirect indication of the roles of the tea cuticle for tea brewing.

CONCLUDING REMARKS AND FUTURE PERSPECTIVE

In the past several years, significant progresses have been made to understand the tea leaf cuticle. The tea cuticular waxes are constituted by 14 chemical classes including acids, 1-alkanols, aldehydes, alkanes, 1-alkanol esters, glycol esters, benzyl esters, phenethyl esters, phthalate esters, glycols, tocopherols, triterpenoids, sterols, and caffeine. The cuticular waxes from the tender leaf are constituted by VLCFAs; in contrast, the cuticular waxes from the mature leaves are dominated by a high percentage of triterpenoids and steroids. In response to environmental stresses, the tender leaf and the mature leaf show some common and distinct patterns for cuticle modification including *in vivo* wax synthesis or transport in epidermal cells, dynamic phase separation between the EWs and the IWs, *in vitro* polymerization, and retro transportation into epidermal cell wall or cytoplasm for further transformation. The adaxial and the abaxial leaf surfaces showed different transpiration barrier organizations; the adaxial IWs were the major transpiration barrier, whereas the abaxial EWs constitute another major leaf transpiration barrier. Cuticular transpiration barrier modification does not require the overhaul of all wax components. Instead, targeted deposition of specific wax compounds into individual cuticular compartments is sufficient to alter cuticular transpiration barrier properties. Tea cuticle may contain molecular signatures for the initial interactions with some pathogens and herbivores, which could determine the susceptibility or resistance of tea to these biological stresses; in addition, the tea cuticle may contribute to the quality of tea made through several different mechanisms.

Even though these progresses were made in the past several years, there are many unresolved questions that should be addressed in the future. Below, the author would like to briefly discuss some of them:

1. From the mature tea leaf cuticle, ∼43% of the wax mass detected by GC was not chemically identified (Zhu et al., 2018) due to their spectra being not in the National Bureau of Standards Mass Spectral Library. In the future, other analytical methods should be applied to resolve their chemical identity which is critical to understand structure–function relationships of the tea cuticle.
2. After the waxes are removed from the tea cuticle, the remaining polymer matrix still can maintain structural integrity. Generally, the polymer matrix of cuticle includes cutin, cutan, and polysaccharides (Nawrath, 2006; Domínguez, et al., 2011b). So far, the chemical composition of tea cuticle polyester has not been characterized, and in the future, this question should be addressed to have a holistic understanding of the mechanical characteristics of the cuticle.
3. What are the molecular mechanisms to regulate triterpenoid synthesis in epidermal cells during leaf development? In grape, Myb5b regulates triterpenoid synthesis, but the downstream targets are waiting to be identified. It still remains unclear whether a tea homolog of Myb5b would play similar roles as grape to activate triterpenoid synthesis.
4. How are triterpenoids transported across PM and cell walls? Are VLCFAs and triterpenoids transported through similar or distinct mechanisms?
5. Although the epidermis may contain detectable amount of chlorophyll (Suh et al., 2005), such low levels hardly make the epidermis trophic-independent. The cuticle synthesis in the

epidermal cells represents huge carbon and energy investment for the plants. Thus, the epidermal cells are expected to rely on the underlying palisade cells or mesophyll cells for carbon and energy supply, either through the symplast pathway or apoplast pathway. One would expect that there should be active transport of photoassimilates between epidermal cells and the underlying palisade cells or mesophyll cells. Currently, it remains largely unknown what metabolites are transported into epidermal cells and how they are transported.

6. Besides tea leaves, the growing tender stems also are covered by a layer of cuticle. Initially, these stems showed a green color, then gradually became lignified and lost their green color. At this stage, the stem cuticle was replaced by a suberin layer (**Figure 8**). Currently, little information is available regarding wax composition, synthesis, and regulation from the tender tea stem. The developmental gradient of the tea stem cuticle could offer a useful system to study wax and suberin biosynthesis and regulation.

AUTHOR CONTRIBUTIONS

The author confirms being the sole contributor of this work and has approved it for publication.

FUNDING

This work was supported by the Key-Area Research and Development Program of Guangdong Province (Grant No. 2020B020220004), the Guangdong Key Laboratory of Tea Plant Resources Innovation and Utilization/Tea Research Institute, the Guangdong Academy of Agricultural Sciences (Grant No. 2020KF06), the National Science Foundation of China (Grant No. 31870803), and the startup fund from Xinyang Normal University to MC.

ACKNOWLEDGMENTS

The author thanks Zijian Chen (Hitachi ABB Power Grids Co., Jefferson City, Missouri, USA) for English language editing, and Luming Yao and Caiming Wu (Electron microscopy core in the State Key Laboratory of Cellular Stress Biology, School of Life Sciences, Xiamen University) for TEM and SEM sample preparation, the electron microscopy core from the Institute of Quality Standard and Testing Technology for Agro-Products, and the Fujian Academy of Agricultural Sciences for TEM and SEM observation.

REFERENCES

Ashihara, H., Sano, H., and Crozier, A. (2008). Caffeine and related purine alkaloids: biosynthesis, catabolism, function and genetic engineering. *Phytochem.* 69, 841–856. doi: 10.1016/j.phytochem.2007.10.029

Augustin, J. M., Kuzina, V., Andersen, S. B., and Bak, S. (2011). Molecular activities, biosynthesis and evolution of triterpenoid saponins. *Phytochemistry* 72, 435–457. doi: 10.1002/chin.201128264

Ballmann, C., De Oliveira, S., Gutenberger, A., Waßmann, F., and Schreiber, L. (2011). A radioactive assay allowing the quantitative measurement of cuticular permeability of intact *Arabidopsis thaliana* leaves. *Planta* 234, 9–20. doi: 10.1007/s00425-011-138-4

Barthlott, W., and Neinhuis, C. (1997). Purity of the sacred lotus, or escape from contamination in biological surfaces. *Planta* 202, 1–8. doi: 10.1007/s004250050096

Becker, M., Kerstiens, G., and Schönherr, J. (1986). Water permeability of plant cuticles: permeance, diffusion and partition coefficients. *Trees* 1, 54–60. doi: 10.1007/bf00197025

Berhin, A., de Bellis, D., Franke, R. B., Buono, R. A., Nowack, M. K., and Nawrath, C. (2019). The root cap cuticle: a cell wall structure for seedling establishment and lateral root formation. *Cell* 176, 1–12. doi: 10.1016/j.cell.2019.01.005

Bernard, A., and Joubès, J. (2013). *Arabidopsis* cuticular waxes: advances in synthesis, export and regulation. *Prog. Lipid Res.* 52, 110–129. doi: 10.1016/j.plipres.2012.10.002

Biratu, T., Omondi, C., and Hindorf, H. (1996). Caffeine content in relation to resistance of Coffea arabica L. to coffee berry disease (Colletotrichum coffeanum Noack). *Z. Pflanzenkr. Pflanzenschutz* 103, 15–19.

Bird, D., Beisson, F., Brigham, A., Shin, J., Greer, S., Jetter, R., et al. (2007). Characterization of *Arabidopsis* ABCG11/WBC11, an ATP binding cassette (ABC) transporter that is required for cuticular lipid secretion. *Plant J.* 52, 485–498. doi: 10.1111/j.1365-313X.2007.03252.x

Bird, D. A. (2008). The role of ABC transporters in cuticular lipid secretion. *Plant Sci.* 174, 563–569. doi: 10.1016/j.plantsci.2008.03.016

Bourdenx, B., Bernard, A., Domergue, F., Pascal, S., Leger, A., Roby, D., et al. (2011). Overexpression of Arabidopsis ECERIFERUM1 promotes wax very long-chain alkane biosynthesis and influences plant response to biotic and abiotic stresses. *Plant Physiol.* 156, 29–45. doi: 10.1104/pp.111.172320

Buchholz, A. (2006). Characterization of the diffusion of non-electrolytes across plant cuticles: properties of the lipophilic pathway. *J. Exp. Bot.* 57, 2501–2513. doi: 10.1093/jxb/erl023

Burghardt, M., and Riederer, M. (2003). Ecophysiological relevance of cuticular transpiration of deciduous and evergreen plants in relation to stomatal closure and leaf water potential. *J. Exp. Bot.* 54, 1941–1949. doi: 10.1093/jxb/erg195

Buschhaus, C., and Jetter, R. (2011). Composition differences between epicuticular and intracuticular wax substructures: how do plants seal their epidermal surfaces? *J. Exp. Bot.* 62, 841–853. doi: 10.1093/jxb/erq366

Buschhaus, C., and Jetter, R. (2012). Composition and physiological function of the wax layers coating arabidopsis leaves: β-amyrin negatively affects the intracuticular water barrier. *Plant Physiol.* 160, 1120–1129. doi: 10.1104/pp.112.198473

Busta, L., Schmitz, E., Kosma, D. K., Schnable, J. C., and Cahoon, E. B. (2021). A co-opted steroid synthesis gene, maintained in sorghum but not maize, is associated with a divergence in leaf wax chemistry. *PNAS* 118:e2022982118. doi: 10.1073/pnas.2022982118

Chen, M. J., Zhang, Y., Kong, X. R., Du, Z. H., Zhou, H. W., Yu, Z. X., et al. (2021). Leaf cuticular transpiration barrier organization in tea tree under normal growth conditions. *Front. Plant Sci.* 12:655799. doi: 10.3389/fpls.2021.655799

Chen, M. J., Zhu, X. F., Zhang, Y., Du, Z. H., Chen, X. B., Kong, X. R., et al. (2020). Drought stress modify cuticle of tender tea leaf and mature leaf for transpiration barrier enhancement through common and distinct modes. *Sci. Rep.* 10:6696. doi: 10.1038/s41598-020-63683-4

DeBono, A., Yeats, T. H., Rose, J. K. C., Bird, D., Jetter, R., Kunst, L., et al. (2009). *Arabidopsis* LTPG is a glycosylphosphatidylinositol-anchored lipid transfer protein required for export of lipids to the plant surface. *Plant Cell* 21, 1230–1238. doi: 10.1105/tpc.108.064451

Domínguez, E., Cuartero, J., and Heredia, A. (2011a). An overview on plant cuticle biomechanics. *Plant Sci.* 181, 77–84. doi: 10.1016/j.plantsci.2011.04.016

Domínguez, E., Heredia-guerreo, J. A., and Heredia, A. (2015). Plant cutin genesis: unanswered questions. *Trends Plant Sci.* 20, 551–558. doi: 10.1016/j.tplants.2015.05.009

Domínguez, E., Heredia-Guerrero, J. A., and Heredia, A. (2011b). The biophysical design of plant cuticles: an overview. *New Phytol.* 189, 938–949. doi: 10.1111/j.1469-8137.2010.03553.x

Eigenbrode, S. D., and Espelie, K. E. (1995). Effects of plant epicuticular lipids on insect herbivores. *Annu. Rev. Entomol.* 40, 171–194. doi: 10.1146/annurev.en.40.010195.001131

Fernandez, V., Guzman-Delgado, P., Graca, J., Santos, S., and Gil, L. (2016). Cuticle structure in relation to chemical composition: reassessing the prevailing model. *Front. Plant Sci.* 7:427. doi: 10.3389/fpls.2016.00427

Fich, E. A., Segerson, N. A., and Rose, J. K. C. (2016). The plant polyester cutin: biosynthesis, structure, and biological roles. *Annu. Rev. Plant Biol.* 67, 207–233. doi: 10.1146/annurev-arplant-043015-111929

Filho, O., and Mazzafera, P. (2000). Caffeine does not protect coffee against the leaf miner *Perileucoptera coffeella*. *J. Chem. Ecol.* 26, 1447–1464. doi: 10.1023/A:1005587725704

Gundlach, H., Miiller, M. J., Kutchan, T. M., and Zenk, M. H. (1992). Jasmonic acid is a signal transducer in elicitor-induced plant cell cultures. *PNAS* 89, 2389–2393. doi: 10.1073/pnas.89.6.2389

Guzmán, P., Fernández, V., García, M. L., Khayet, M., Fernández, A., and Gil, L. (2014a). Localization of polysaccharides in isolated and intact cuticles of eucalypt, poplar and pear leaves by enzyme-gold labelling. *Plant Physiol. Biochem.* 76, 1–6. doi: 10.1016/j.plaphy.2013.12.023

Guzmán, P., Fernández, V., Graca, J., Cabral, V., Kayali, N., Khayet, M., et al. (2014b). Chemical and structural analysis of *Eucalyptus globulus* and *E. camaldulensis* leaf cuticles: a lipidized cell wall region. *Front. Plant Sci.* 5:481. doi: 10.3389/fpls.2014.00481

Hen-Avivi, S., Lashbrooke, J., Costa, F., and Aharoni, A. (2014). Scratching the surface: genetic regulation of cuticle assembly in fleshy fruit. *J. Exp. Bot.* 65, 4653–4664. doi: 10.1093/jxb/eru225

Hoffmann-Benning, S., Klomparens, K. L., and Kende, H. (1994). Characterization of growth-related osmiophilic particles in corn coleoptiles and deepwater rice internodes. *Ann. Bot.* 74, 563–572. doi: 10.1006/anbo.1994.1156

Hollingsworth, R. G., Armstrong, J. W., and Campbell, E. (2002). Pest control: caffeine as a repellent for slugs and snails. *Nature* 417, 915–916. doi: 10.1038/417915a

Ingram, G., and Nawrath, C. (2017). The roles of the cuticle in plant development: organ adhesions and beyond. *J. of Exp. Bot.* 68, 5307–5321. doi: 10.1093/jxb/erx313

Jeffree, C. E. (2006). "The fine structure of the plant cuticle," in *Biology of the Plant Cuticle*, eds M. Riederer and C. Muller (London: Blackwell), 11–125.

Jenks, M. A., and Ashworth, E. N. (2003). Plant epicuticular waxes: function, production, and genetics. *Horticult. Rev.* 23, 1–68. doi: 10.1002/9780470650752.ch1

Jenks, M. A., Rich, P. J., and Ashworth, E. N. (1994). Involvement of cork cells in the secretion of epicuticular wax filaments on *Sorghum bicolor (L) Moench*. *Int. J. Plant Sci.* 155, 506–518. doi: 10.1086/297190

Jetter, R., Kunst, L., and Samuels, A. L. (2007). "Composition of plant cuticular waxes," in *Biology of the Plant Cuticle, Vol. 23*, eds M. Riederer and C. Muller (Oxford: Blackwell), 145–181.

Jetter, R., and Riederer, M. (2016). Localization of the transpiration barrier in the epi- and intracuticular waxes of eight plant species: water transport resistances are associated with fatty acyl rather than alicyclic components. *Plant Physiol.* 170, 921–934. doi: 10.1104/pp.15.01699

Jetter, R., and Schäffer, S. (2001). Chemical composition of the *Prunus laurocerasus* leaf surface: dynamic changes of the epicuticular wax film during leaf development. *Plant Physiol.* 126, 1725–1737. doi: 10.1104/pp.126.4.1725

Keidel, F. A. (1959). Determination of water by direct amperometric measurement. *Anal. Chem.* 31, 2043–2048. doi: 10.1021/ac60156a050

Kerstiens, G. (1996a). Cuticular water permeability and its physiological significance. *J. Exp. Bot.* 47, 1813–1832. doi: 10.1093/jxb/47.12.1813

Kerstiens, G. (1996b). Signaling across the divide: a wider perspective of cuticular structure-function relationships. *Trends Plant Sci.* 1, 125–129. doi: 10.1016/S1360-1385(96)90007-2

Kim, Y. S., and Sano, H. (2008). Pathogen resistance of transgenic tobacco plants producing caffeine. *Phytochemistry* 69, 882–888. doi: 10.1016/j.phytochem.2007.10.021

Koch, K., and Ensikat, H. J. (2008). The hydrophobic coatings of plant surfaces: epicuticular wax crystals and their morphologies, crystallinity and molecular self-assembly. *Micron* 39, 759–772. doi: 10.1016/j.micron.2007.11.010

Kolattukudy, P. E. (2001). "Polyesters in higher plants," in *Advances in Biochemical Engineering Biotechnology: Biopolyesters*, eds W. Babel and A. Steinbuechel (Berlin: Springer-Verlag), 1–49.

Kosma, D. K., Parsons, E. P., Isaacson, T., Lü, S., Rose, J. K. C., and Jenks, M. A. (2010). Fruit cuticle lipid composition during development in tomato ripening mutants. *Physiol. Plant* 139, 107–117. doi: 10.1111/j.1399-3054.2009.01342.x

Kunst, L., and Samuels, A. L. (2003). Biosynthesis and secretion of plant cuticular wax. *Prog. Lipid Res.* 42, 51–80. doi: 10.1016/s0163-7827(02)00045-0

Lee, S. B., Go, Y. S., Bae, H. J., Park, J. H., Cho, S. H., Cho, H. J., et al. (2009). Disruption of glycosylphosphatidylinositol-anchored lipid transfer protein gene altered cuticular lipid composition, increased plastoglobules, and enhanced susceptibility to infection by the fungal pathogen *Alternaria brassicicola*. *Plant Physiol.* 150, 42–54. doi: 10.1104/pp.109.137745

Lee, S. B., and Suh, M. C. (2013). Recent advances in cuticular wax biosynthesis and its regulation in *Arabidopsis*. *Mol. Plant* 6, 246–249. doi: 10.1093/mp/sss159

Leung, K. C., Li, H. Y., Xiao, S., Tse, M. H., and Chye, M. L. (2006). *Arabidopsis* ACBP3 is an extracellularly targeted acyl-CoA-binding protein. *Planta* 223, 871–881. doi: 10.1007/s00425-005-0139-2

Levine, T. (2004). Short-range intracellular trafficking of small molecules across endoplasmic reticulum junctions. *Trends Cell Biol.* 14, 483–490. doi: 10.1016/j.tcb.2004.07.017

Li, X., Ahammed, G. J., Li, Z. X., Tang, M. J., Yan, P., and Han, W. Y. (2016). Decreased biosynthesis of jasmonic acid via lipoxygenase pathway compromised caffeine-induced resistance to *Colletotrichum gloeosporioides* under elevated CO_2 in tea seedlings. *Phytopathology* 106, 1270–1277. doi: 10.1094/PHYTO-12-15-0336-R

Li-Beisson, Y., Shorrosh, B., Beisson, F., Andersson, M. X., Arondel, V., Bates, P. D., et al. (2010). (2010). Acyl-lipid metabolism. *The arabidopsis book.* 8:e0133. doi: 10.1199/tab.0133

Luo, B., Xue, X. Y., Hu, W. L., Wang, L. J., and Chen, X. Y. (2007). An ABC transporter gene of *Arabidopsis thaliana*, AtWBC11, is involved in cuticle development and prevention of organ fusion. *Plant Cell Physiol.* 48, 1790–1802. doi: 10.1128/IAI.00733-06

McFarlane, H. E., Shin, J. J., Bird, D. A., and Samuels, A. L. (2010). *Arabidopsis* ABCG transporters, which are required for export of diverse cuticular lipids, dimerize in different combinations. *Plant Cell* 22, 3066–3075. doi: 10.1105/tpc.110.077974

Nawrath, C. (2006). Unraveling the complex network of cuticular structure and function. *Curr. Opin. Plant Biol.* 9, 281–287. doi: 10.1016/j.pbi.2006.03.001

Osbourn, A., Goss, R. J., and Field, R. A. (2011). The saponins: polar isoprenoids with important and diverse biological activities. *Nat. Prod. Rep.* 28, 1261–1268. doi: 10.1039/c1np00015b

Panikashvili, D., Savaldi-Goldstein, S., Mandel, T., Yifhar, T., Franke, R. B., Hofer, R., et al. (2007). The *Arabidopsis* DESPERADO/AtWBC11 transporter is required for cutin and wax secretion. *Plant Physiol.* 145, 1345–1360. doi: 10.1104/pp.107.105676

Philippe, G., Geneix, N., Petit, J., Guillon, F., Sandt, C., Rothan, C., et al. (2020a). Assembly of tomato fruit cuticles: a cross-talk between the cutin polyester and cell wall polysaccharides. *New Phyt.* 226, 809–822. doi: 10.1111/nph.16402

Philippe, G., Sorensen, I., Jiao, C., Sun, X., Fei, Z., Domozych, D. S., et al. (2020b). Cutin and suberin: assembly and origins of specialized lipidic cell wall scaffolds. *Curr. Opin. Plant Biol.* 55, 11–20. doi: 10.1016/j.pbi.2020.01.008

Pighin, J. A., Zheng, H. Q., Balakshin, L. J., Goodman, I. P., Western, T. L., Jetter, R., et al. (2004). Plant cuticular lipid export requires an ABC transporter. *Science* 306, 702–704. doi: 10.1126/science.1102331

Pollard, M., Beisson, F., Li, Y., and Ohlrogge, J. B. (2008). Building lipid barriers: biosynthesis of cutin and suberin. *Trends Plant Sci.* 13, 236–246. doi: 10.1016/j.tplants.2008.03.003

Post-Beittenmiller, D. (1996). Biochemistry and molecular biology of wax production in plants. *Annu. Rev. Plant Physiol. Plant Mol. Biol.* 47, 405–430. doi: 10.1146/annurev.arplant.47.1.405

Qin, D., Zhang, L., Xiao, Q., Dietrich, C., and Matsumura, M. (2015). Clarification of the identity of the tea green leafhopper based on morphological comparison between Chinese and Japanese specimens. *PLoS ONE* 10:e0139202. doi: 10.1371/journal.pone.0139202

Reicosky, D. A., and Hanover, J. W. (1978). Physiological effects of surface waxes: I. Light reflectance for glaucous and nonglaucous Picea pungens. *Plant Physiol.* 62, 101–104. doi: 10.1104/pp.62.1.101

Reina-Pinto, J. J., and Yephremov, A. (2009). Surface lipids and plant defenses. *Plant Physio. Biochem*. 47, 540–549. doi: 10.1016/j.plaphy.2009.01.004

Romero, P., and Rose, J. K. C. (2019). A relationship between tomato fruit softening, cuticle properties and water availability. *Food Chem.* 295, 300–310. doi: 10.1016/j.foodchem.2019.05.118

Sadler, C., Schroll, B., Zeisler, V., Waßmann, F., Franke, R., and Schreiber, L. (2016). Wax and cutin mutants of *Arabidopsis*: quantitative characterization of the cuticular transport barrier in relation to chemical composition. *Biochim. Biophys. Acta* 1861, 1336–1344. doi: 10.1016/j.bbalip.2016.03.002

Samuels, L., Kunst, L., and Jetter, R. (2008). Sealing plant surfaces: cuticular wax formation by epidermal cells. *Annu. Rev. Plant Biol.* 59, 683–707. doi: 10.1146/annurev.arplant.59.103006.093219

Schönherr, J. (1976). Water permeability of isolated cuticular membranes: the effect of cuticular waxes on diffusion of water. *Planta* 131, 159–164. doi: 10.1007/BF00389989

Schönherr, J., and Lendzian, K. (1981). A simple and inexpensive method of measuring water permeability of isolated plant cuticular membranes. *Z. Pflanzenphysiol* 102, 321–327. doi: 10.1016/S0044-328X(81)80203-6

Schönherr, J., and Riederer, M. (1986). Plant cuticles sorb lipophilic compounds during enzymatic isolation. *Plant Cell Environ.* 9, 459–466. doi: 10.1111/j.1365-3040.1986.tb01761.x

Schreiber, L., Skrabs, M., Hartmann, K., Diamantopoulos, P., Simanova, E., and Santrucek, J. (2001). Effect of humidity on cuticular water permeability of isolated cuticular membranes and leaf disks. *Planta* 214, 274–282. doi: 10.2307/23386529

Schuster, A., Burghardt, M., Alfarhan, A., Bueno, A., Hedrich, R., Leide, J., et al. (2016). Effectiveness of cuticular transpiration barriers in a desert plant at controlling water loss at high temperatures. *AoB Plants* 8:plw027. doi: 10.1093/aobpla/plw027

Shanmugarajah, K., Linka, N., Grafe, K., Smits, S. H. J., Weber, A. P. M., Zeier, J., et al. (2019). ABCG1 contributes to suberin formation in *Arabidopsis thaliana* roots. *Sci. Rep.* 9:11381. doi: 10.1038/s41598-019-47916-9

Shepherd, T., and Griffiths, D. W. (2006). The effects of stress on plant cuticular waxes. *New Phyt.*171, 469–499. doi: 10.1111/j.1469-8137.2006.01826.x

Skrzydeł, J., Borowska-Wykret, D., and Kwiatkowska, D. (2021). Structure, assembly and function of cuticle from mechanical perspective with special focus on perianth. *Int. J. Mol. Sci.* 22:4160. doi: 10.3390/ijms22084160

Solovchenko, A., and Merzlyak, M. (2003). Optical properties and contribution of cuticle to UV protection in plants: experiments with apple fruit. *Photochem. Photobiol. Sci.* 2, 861–866. doi: 10.1039/b302478d

Somerville, C. R., Browse, J., Jaworski, J., and Ohlrogge, J. (2000). "Lipids," in *Biochemistry and Molecular Biology of Plants*, eds B. B. Buchanan, W. Gruissem, and R. L. Jones (Rockville, MD: American Society of Plant Physiologists), Chap 10, 456–526.

Spencer, C. M., Cai, Y., Martin, R., Gaffney, S. H., Goulding, E. N., Magnolato, D., et al. (1988). Polyphenol complexation –Some thoughts and observations. *Phytochemistry* 27, 2397–2409. doi: 10.1016/0031-9422(88)87004-3

Sterk, P., Booij, H., Schellekens, G. A., Van Kammen, A., and De Vries, S. C. (1991). Cell-specific expression of the carrot EP2 lipid transfer protein gene. *Plant Cell* 3, 907–921. doi: 10.1105/tpc.3.9.907

Suh, M. C., Samuels, A. L., Jetter, R., Kunst, L., Pollard, M., Ohlrogge, J., et al. (2005). Cuticular lipid composition, surface structure, and gene expression in *Arabidopsis* stem epidermis. *Plant Physiol.* 139, 1649–1665. doi: 10.1104/pp.105.070805

Thimmappa, R., Geisler, K., Louveau, T., O'Maille, P., and Osbourn, A. (2014). Triterpene biosynthesis in plants. *Annu. Rev. Plant Biol.* 65, 225–257. doi: 10.1146/annurev-arplant-050312-120229

Thomas, S., Kanekom, Y., and Somerville, C. (1993). A nonspecific lipid transfer protein from *Arabidopsis* is a cell-wall protein. *Plant J.* 3, 427–436. doi: 10.1046/j.1365-313X.1993.t01-25-00999.x

Tsubaki, S., Sugimura, K., Teramoto, Y., Yonemori, K., and Azuma, J. (2013). Cuticular membrane of Fuyu persimmon fruit is strengthened by triterpenoid nano-fillers. *PLoS ONE* 8:e75275. doi: 10.1371/journal.pone.0075275

Uefuji, H., Tatsumi, Y., Morimoto, M., Kaothien-Nakayama, P., Ogita, S., and Sano, H. (2005). Caffeine production in tobacco plants by simultaneous expression of three coffee N-methyltransferases and its potential as a pest repellant. *Plant Mol. Biol.* 59, 221–227. doi: 10.1007/s11103-005-8520-x

Ukitsu, H., Kuromori, T., Toyooka, K., Goto, Y., Matsuoka, K., Sakuradani, E., et al. (2007). Cytological and biochemical analysis of *COF1*, an *Arabidopsis* mutant of an ABC transporter gene. *Plant Cell Physiol.* 48, 1524–1533. doi: 10.1093/pcp/pcm139

Vishwanath, S. J., Delude, C., Domergue, F., and Rowland, O. (2015). Suberin: biosynthesis, regulation, and polymer assembly of a protective extracellular barrier. *Plant Cell Rep.* 34, 573–586. doi: 10.1007/s00299-014-1727-z

Vogg, G., Fischer, S., Leide, J., Emmanuel, E., Jetter, R., Levy, A. A., et al. (2004). Tomato fruit cuticular waxes and their effects on transpiration barrier properties: functional characterization of a mutant deficient in a very-long chain fatty acid β-ketoacyl-CoA synthase. *J. Exp. Bot.* 55, 1401–1410. doi: 10.1093/jxb/erh149

Wang, Y. C., Qian, W. J., Li, N. N., Hao, X. Y., Wang, L., Xiao, B., et al. (2016). Metabolic changes of caffeine in tea plant (*Camellia sinensis L.* O. Kuntze) as defense response to *Colletotrichum fructicola*. *J. Agric. Food Chem.* 64, 6685–6693. doi: 10.1021/acs.jafc.6b02044

Weng, H., Molina, I., Shockey, J., and Browse, J. (2010). Organ fusion and defective cuticle function in a *lacs1 lacs2* double mutant of *Arabidopsis*. *Planta* 231, 1089–1100. doi: 10.1007/s00425-010-1110-4

Xiao, S., and Chye, M. L. (2009). An *Arabidopsis* family of six acyl-CoA binding proteins has three cytosolic members. *Plant Physiol. Biochem.* 47, 479–484. doi: 10.1016/j.plaphy.2008.12.002

Xue, Y., Xiao, S., Kim, J., Lung, S. C., Chen, L., Tanner, J. A., et al. (2014). *Arabidopsis* membrane-associated acyl-CoA-binding protein ACBP1 is involved in stem cuticle formation. *J. Exp. Bot.* 65, 5473–5483. doi: 10.1093/jxb/eru304

Zeisler, V., Müller, Y., and Schreiber, L. (2018). Epicuticular wax on leaf cuticles does not establish the transpiration barrier, which is essentially formed by intracuticular wax. *J. Plant Physiol.* 227, 66–74. doi: 10.1016/j.jplph.2018.03.018

Zeisler, V., and Schreiber, L. (2016). Epicuticular wax on cherry laurel (*Prunus laurocerasus*) leaves does not constitute the cuticular transpiration barrier. *Planta* 243, 65–81. doi: 10.1007/s00425-015-2397-y

Zhang, Y., Che, X. B., Du, Z. H., Zhang, W. J., Devkota, A. R., Chen, Z. J., et al. (2020). A proposed method for simultaneous measurement of cuticular transpiration from different leaf surfaces in *Camellia sinensis*. *Front. Plant Sci.* 11:420. doi: 10.3389/fpls.2020.00420

Zhang, Y., Du, Z. H., Han, Y. T., Chen, X. B., Kong, X. R., Sun, W. J., et al. (2021). Plasticity of the cuticular transpiration barrier in response to water shortage and resupply in *Camellia sinensis*: a role of cuticular waxes. *Front. Plant Sci.* 11:600069. doi: 10.3389/fpls.2020.600069

Zhao, X., Chen, S., Wang, S., Shan, W., Wang, X., Lin, Y., et al. (2020). Defensive responses of tea plants (*Camellia sinensis*) against tea green leafhopper attack: a multi-omics study. *Front. Plant Sci.* 10:1705. doi: 10.3389/fpls.2019.01705

Zhou, X., Chen, X., Du, Z., Zhang, Y., Zhang, W., Kong, X., et al. (2019). Terpenoid esters are the major constituents from leaf lipid droplets of *Camellia sinensis*. *Front. Plant Sci.* 10:179. doi: 10.3389/fpls.2019.00179

Zhu, X. F., Zhang, Y., Du, Z. H., Chen, X. B., Zhou, X., Kong, X. R., et al. (2018). Tender leaf and fully-expanded leaf exhibited distinct cuticle structure and wax lipid composition in *Camellia sinensis cv Fuyun 6*. *Sci. Rep.* 8:14944. doi: 10.1038/s41598-018-33344-8

Conflict of Interest: The author declares that the research was conducted in the absence of any commercial or financial relationships that could be construed as a potential conflict of interest.

Publisher's Note: All claims expressed in this article are solely those of the authors and do not necessarily represent those of their affiliated organizations, or those of the publisher, the editors and the reviewers. Any product that may be evaluated in this article, or claim that may be made by its manufacturer, is not guaranteed or endorsed by the publisher.

frontiers in Plant Science

ORIGINAL RESEARCH
published: 15 October 2021
doi: 10.3389/fpls.2021.770398

Theanine Improves Salt Stress Tolerance *via* Modulating Redox Homeostasis in Tea Plants (*Camellia sinensis* L.)

Ziping Chen[1†], Shijia Lin[1†], Juan Li[2†], Tingting Chen[1], Quan Gu[3], Tianyuan Yang[1] and Zhaoliang Zhang[1]*

[1] State Key Laboratory of Tea Plant Biology and Utilization, Anhui Agricultural University, Hefei, China, [2] Biotechnology Center, Anhui Agricultural University, Hefei, China, [3] School of Biology, Food and Environment, Hefei University, Hefei, China

Theanine, a unique non-proteinogenic amino acid, is one of the most abundant secondary metabolites in tea. Its content largely determines green tea quality and price. However, its physiological roles in tea plants remain largely unknown. Here, we showed that salt stress significantly increased the accumulation of glutamate, glutamine, alanine, proline, and γ-aminobutyric acid, as well as theanine, in the new shoots of tea plants. We further found that salt stress induced the expression of theanine biosynthetic genes, including *CsGOGATs*, *CsAlaDC*, and *CsTSI*, suggested that salt stress induced theanine biosynthesis. Importantly, applying theanine to the new shoots significantly enhanced the salt stress tolerance. Similar effects were also found in a model plant Arabidopsis. Notably, exogenous theanine application increased the antioxidant activity of the shoots under salt stress, suggested by reduced the reactive oxygen species accumulation and lipid peroxidation, as well as by the increased SOD, CAT, and APX activities and expression of the corresponding genes. Finally, genetic evidence supported that catalase-mediated antioxidant scavenging pathway is required for theanine-induced salt stress tolerance. Taken together, this study suggested that salt stress induces theanine biosynthesize in tea plants to enhance the salt stress tolerance through a CAT-dependent redox homeostasis pathway.

Keywords: ***Camellia sinensis*** **L., salt stress, theanine biosynthesis, ROS scavenging enzymes, catalases**

OPEN ACCESS

Edited by:
Deyu Xie,
North Carolina State University, United States

Reviewed by:
Jay Prakash Awasthi,
Assam University, India
Mingjie Chen,
Xinyang Normal University, China

***Correspondence:**
Zhaoliang Zhang
zhlzhang@ahau.edu.cn

† These authors have contributed equally to this work

Specialty section:
This article was submitted to Plant Metabolism and Chemodiversity, a section of the journal Frontiers in Plant Science

Received: *03 September 2021*
Accepted: *27 September 2021*
Published: *15 October 2021*

Citation:
Chen Z, Lin S, Li J, Chen T, Gu Q, Yang T and Zhang Z (2021) Theanine Improves Salt Stress Tolerance via Modulating Redox Homeostasis in Tea Plants (Camellia sinensis L.). Front. Plant Sci. 12:770398. doi: 10.3389/fpls.2021.770398

INTRODUCTION

The tea plant (*Camellia sinensis* L.) is an important economic woody crop, and widely cultivated in the world (Chen et al., 2007). It contains numerous secondary metabolites, including theanine (γ-glutamylethylamide), flavonoids and caffeine. As a unique non-proteinogenic amino acid in tea plants, theanine is the component conferring the particular "umami" tastes, anti-depression and neuroprotection benefits of green tea infusion (Ashihara, 2015). Theanine is the most abundant free amino acid in tea plants, however, its physiological roles in tea plants remains unknown.

It is synthesized from glutamate and ethylamine *via* theanine synthatase (CsTS). In recent study, the TS gene (*CsTSI*) was identified in tea plants (Wei et al., 2018). CsTSI is highly homologous to glutamine synthetases (GSs) which also can catalyze theanine synthesis (Cheng et al., 2017;

Wei et al., 2018). Glutamate Synthases (GOGATs) catalyze glutamate biosynthesis in tea plants, while ethylamine is synthesized by alanine decarboxylase (CsAlaDC; Takeo, 1979; Bai et al., 2019). Genes involved in theanine metabolism have been systemically identified along with the completion of the genome sequencing in tea plants (Xia et al., 2019). Theanine metabolism is regulated by many environment factors, especially high salinity, heat, drought, nutrient levels and light intensity (Deng et al., 2012; Wang et al., 2016; Li et al., 2018a; Yang et al., 2020, 2021). However, theanine, as a species-specific secondary metabolite, its roles in the adaption to these abiotic stresses for tea plants need to be explored.

Excessive irrigation and fertilization increase salt contents in soils, which imposes salt stress to crops, including tea plants (Causapé et al., 2004). Salt stress reduces the yield and quality of tea and greatly diminishes the widespread of tea plants (Upadhyaya and Panda, 2013). High soil salinity has become one of the major adverse environmental stresses in global agricultural production. Salt stress usually reduces efficiency of photosynthetic apparatus including PSII and the electron transport chain, and elicits the accumulation of reactive oxygen species (ROS), and ultimately leads to cell damage and oxidative stress (Wang et al., 2007; Considine and Foyer, 2021).

Plants have evolved a complex antioxidant defense system to balance the ROS levels in response to salt stress (Bose et al., 2013). Generally, the superoxide (O_2^-) is converted into hydrogen peroxide (H_2O_2) through superoxide dismutase (SOD). Then, that H_2O_2 is converted into H_2O and oxygen by ascorbate peroxidases (APXs), catalases (CATs), as well as other free radical scavengers (Bose et al., 2013). ROS imbalance is harmful to plants; however, H_2O_2 is also involved in the chloroplast-to-nucleus retrograde signaling which is critical for salt stress response in plants (Park and Seo, 2021; Zhuang et al., 2021).

Recent studies have reported that salt stress affects nitrogen (N) and amino acid metabolism in plants (Silveira et al., 2003; Dluzniewska et al., 2007). Ammonium is assimilated first into the glutamine by GSs, and then is assimilated into glutamate by GOGATs in plants (Groat and Vance, 1981; Miflin and Habash, 2002). Glutamate is further used to synthesize other amino acids like proline, γ-aminobutyric acid (GABA) and asparagine, etc. (Yang et al., 2020). Salt stress induces the accumulation of proline and GABA which act as compatible osmolyte or signaling molecule involved in mitigating high salinity stress (Szabados and Savouré, 2010; Hayat et al., 2012; Bao et al., 2015).

In animals, theanine is involved in various physiological functions, such as improvement of sleep quality, relaxation, neuroprotection, and Parkinson's disease, etc. (Narukawa et al., 2008; Sharma et al., 2018; Deb et al., 2019). Impressively, theanine alleviates Cd-induced oxidative damage through reducing malondialdehyde (MDA) and ROS levels in the brain of mouse (Ben et al., 2016). It was reported that salt stress induces theanine biosynthesis in tea plants (Deng et al., 2012). In addition, exogenous supply of glutamate alleviated the salinity stress-induced inhibition of seed germination and radicle growth of buck wheat and cucumber (Chang et al., 2010; Yang, 2014). Given that theanine is a natural analog of glutamate, we hypothesize that theanine improves salt stress tolerance *via* modulating ROS homeostasis in tea plants.

In this study, we observed that salt stress induced theanine biosynthesis in the new shoots of tea plants, and exogenous theanine application enhanced the resistance to salt stress in the new shoots. We explored the underlying mechanism, with particular emphasis on the reestablishment of redox homeostasis by theanine. The study provided novel insights into the physiological roles of theanine in tea plants.

MATERIALS AND METHODS

Plant Materials and Treatments

New shoots were collected from tea plants (*Camellia sinensis* var. *sinensis cv.* "Shuchazao") grown in the tea plantation of Anhui Agricultural University in Hefei, China. For salt stress treatment, new shoots were exposed to nutrient solution containing 0, 100, 150, or 200 mM NaCl. To study the function of theanine, new shoots were exposed to nutrient solution containing 150 mM NaCl (NaCl), 10 mM theanine (Thea), 150 mM NaCl and 10 mM Thea (NaCl + Thea). Control samples (Con) were exposed to normal nutrient solution. The composition of the nutrient solution used was as follows: 0.54 mM $(NH_4)_2SO_4$, 0.18 mM $Ca(NO_3)_2$, 0.1 mM, KH_2PO_4, 0.41 mM K_2SO_4, 0.39 mM $CaCl_2$, 1.03 mM $MgSO_4$, 6.27 μM $C_{10}H_{12}FeN_2NaO_8$, 9.25 μM H_3BO_3, 3.9 μM $CuSO_4$, 18.2 μM $MnSO_4$, 0.4 mM $Al_2(SO_4)_3{\cdot}18H_2O$, 0.53 μM Na_2MoO_4, and 1.53 μM $ZnSO_4$, and the pH of the nutrient solution was adjusted to 4.5–5.0 (Konishi et al., 1985).

Arabidopsis seeds of *cat2cat3* and *cat1cat2cat3* mutants were generous gifts from Professor Changle Ma in Shandong Normal University, China. Arabidopsis seeds were surface-sterilized by sodium hypochlorite and rinsed four times with sterile water, and then cultured on the solid Murashige and Skoog (MS) medium (pH 5.8) containing 1% (w/v) agar and 1% (w/v) sucrose. Seeds were stratified at 4°C for 2 days, and then transferred into the growth chamber with day/night cycle of 16 h/8 h, 150 μmol m^{-2} s^{-1} irradiance, 23/18°C, and 70% relative humidity. Arabidopsis wild-type (WT) and mutants were grown on MS medium containing 0 or 100 mM NaCl with or without 1 mM theanine. The time points of treatments were illustrated in the corresponding legends. After treatments, seedlings were imaged using a Canon IXUS 130 camera. Meanwhile, all tissues were sampled according to the demands of each experiment, and immediately frozen in liquid nitrogen and stored at −80°C until utilization.

Determination of Fv/Fm

After treatments, the new shoots of tea plants were dark adapted for 30 min before measurement of chlorophyll fluorescence. Maximum photochemical efficiency of photosystem II (Fv/Fm) was measured in the 2nd leaves by an imaging-PAM chlorophyll fluorimeter fitted with a computer-operated PAM-control unit (IMAG-MAXI; Heinz Walz, Effeltrich, Germany) as described previously (Li et al., 2018b).

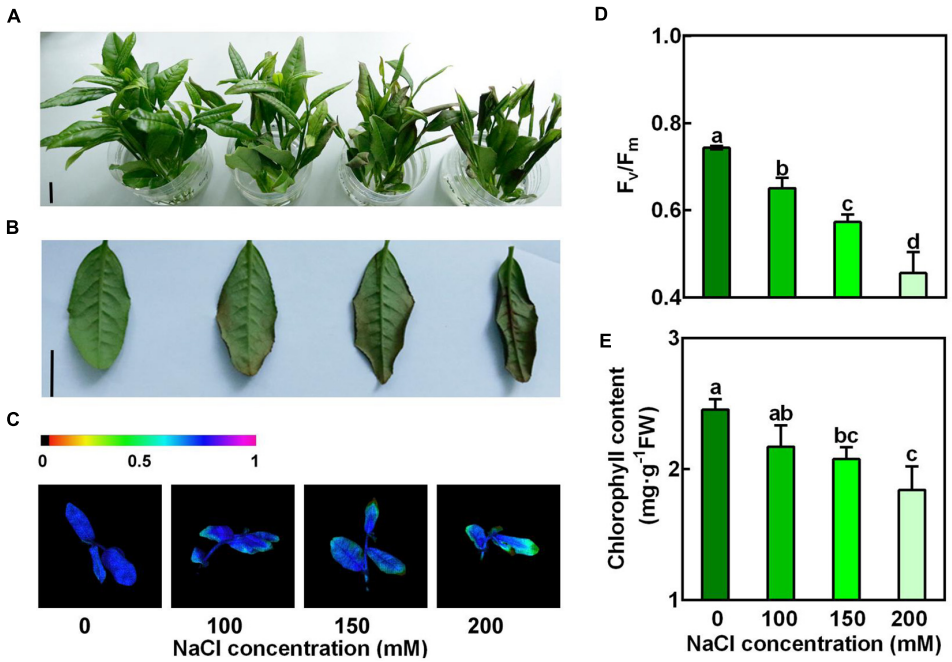

FIGURE 1 | Concentration-dependent effects of NaCl on the new shoots of tea plants. Tea new shoots of tea plants were treated in nutrient solution containing 0, 100, 150, or 200 mM NaCl. **(A,B)** Phenotypes of the new shoots and the 2nd leaves exposed to 0, 100, 150, or 200 mM NaCl treatments. Photographs were taken 3 days after treatment. Bar = 2 cm. **(C,D)** Pseudo-color image and statistical analysis of Fv/Fm of the 2nd leaves 2 days after treatment. The Pseudo-color gradient shows the degree of damage: 1, no damage; 0, strong damage. **(E)** Chlorophyll contents of the 2nd leaves. The contents were determined 3 days after treatment. Data are means ± SE of at least three biological replicates. Bars with different letters are significantly different at $P < 0.05$ according to Duncan's multiple range test.

Determination of Chlorophyll Content

Total chlorophyll in seedlings leaves was extracted using 95% (v/v) ethanol for 48 h in darkness, and the content was then calculated by examining the absorbance at 649, 665, and 470 nm as previously described (Lichtenthaler, 1987).

Measurement of Free Amino Acids

Amino acids in tea leaves were detected by the method previously described (Lu et al., 2019). Briefly, amino acids were extracted from 0.1 g samples with 2 ml of 4% (w/v) sulfosalicylic acid. After ultrasound extraction for 30 min at 50°C, and centrifuged at 12,000 *g* for 30 min, supernatants were filtered through a 0.22 μm filter for the amino acid content assay. Amino acids were separated by the High-Speed Amino Acid Analyzer system used a mobile phase involving lithium citrate and UV–Vis detection at 570 and 440 nm. The amounts of amino acids were determined according to the calibration curve of amino acid standard.

Determination of Theanine Content

Theanine was extracted with distilled water as previously described, with some modifications (Tsushida and Takeo, 1984). About 100 mg of freeze-dried sample powder were dissolved in 3 ml distilled water and heated in a water bath at 100°C for 30 min. After centrifugation at 13,000 rpm for 20 min, the supernatant was filtered with 0.22 μm filter for subsequent HPLC-based analysis of theanine content.

The detection conditions of HPLC analysis were as previously described (Dong et al., 2020). Theanine content was detected using the HPLC analysis (Waters e2695 system consisting a 2489 ultraviolet (UV)-visible detector, Waters Corporation, Milford, MA, United States), equipped with a C18 column (5 μm, 250 mm × 4.6 mm) at 28°C. The mobile phase comprised water **(A)**, acetonitrile **(B)**, and the gradient elution was performed as follows: B 0% (v/v) to 100% at 40 min, to 100% at 45 min and to 0% at 60 min. The amount of theanine was determined according to a calibration curve of theanine standard. L-Theanine standard and acetonitrile were purchased from Sigma-Aldrich (St Louis, MO, United States).

Determination of Reactive Oxygen Species

H_2O_2 and superoxide anion ($O_2^{-\bullet}$) levels were detected by histochemical staining methods (Xie et al., 2012). For H_2O_2 detection, leaves were incubated in 1 mg ml^{-1} solution of 3, 3′-diaminobenzidine (DAB) in 50 mM Tris-acetate buffer (pH 6.5) for 24 h in darkness at room temperature. For $O_2^{-\bullet}$ detection, leaves were immersed in a 0.1% solution of nitroblue tetrazolium (NBT) in K-phosphate buffer (pH 6.5) in darkness for 12 h at room temperature. Afterward, the chlorophyll of leaves was removed with 95% ethanol. All samples were observed using a Canon IXUS 130 camera.

Content of thiobarbituric acid-reactive substance (TBARS; an indicator of lipid peroxidation) was measured by the method

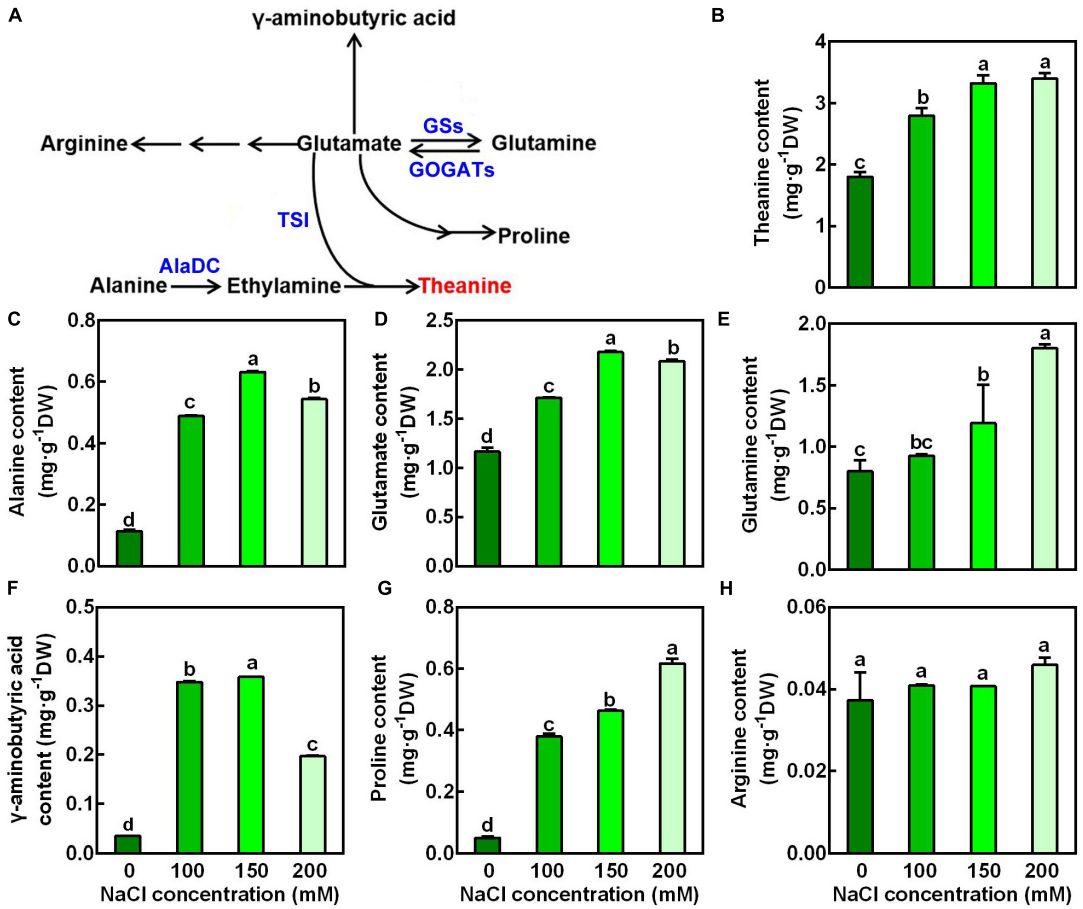

FIGURE 2 | Effects of NaCl treatments on the accumulation of glutamate-pathway and theanine-related amino acids in the 2nd leaves of the new shoots. **(A)** Biosynthetic pathways of glutamate-pathway and theanine-related amino acids. GS, GOGAT, AlaDC, and TSI represent genes encoding glutamine synthetase, glutamate synthase, alanine decarboxylase, and theanine synthatase, respectively. **(B–H)** Amino acid contents in the 2nd leaves of new shoots. The new shoots were treated in nutrient solution containing 0, 100, 150, or 200 mM NaCl for 3 days before the leaves were collected for amino acid content measurement. Theanine **(B)**, alanine **(C)**, glutamate **(D)**, glutamine **(E)**, γ-aminobutyric acid **(F)**, proline **(G)**, arginine **(H)** were detected by the High-Speed Amino Acid Analyzer system. Data are means ± SE of three biological replicates. Bars with different letters are significantly different at $P < 0.05$ according to Duncan's multiple range test.

previously described (Buege and Aust, 1978). 0.5 g fresh tissue was ground with 3 ml 5% trichloroacetic acid (TCA) using a mortar and pestle, then added with 3 ml 0.5% 2-thiobarbituric acid (TBA) in 5% TCA. After incubation in 100°C water bath for 30 min, centrifuged at 12,000*g* for 15 min, then determined by examining the absorbance at 450, 532, and 600 nm. The concentration of lipid peroxides, together with oxidation modified proteins, was quantified in terms of TBARS amount using an extinction coefficient of 155 mM^{-1} cm^{-1} and expressed as nmol g^{-1} fresh weight (FW).

Determination of Antioxidant Enzyme

About 0.1 g the 2nd leaf sample was homogenized with 1 ml of 50 mM phosphate buffer (pH 7.8), or together with 1 mM ascorbic acid (ASC; in the case of ascorbate peroxidase activity determination), then centrifuged at 12,000*g* (4°C) for 15 min. Then, supernatants were used for determination of protein concentrations and the enzyme activity assays.

Superoxide dismutase activity was determined by the capacity of inhibiting the photochemical reduction of NBT at A_{560} (Beauchamp and Fridovich, 1971). Catalase (CAT) activity was measured by the absorbance decrease at 240 nm due to the H_2O_2 decomposition (extinction coefficient of 40 M^{-1} cm^{-1}) (Cui et al., 2013). Ascorbate peroxidase (APX) activity was measured by monitoring the decrease at A_{290} as reduced ascorbic acid was oxidized (extinction coefficient of 2.8 mM^{-1} cm^{-1}) (Xie et al., 2008). Protein was determined by the method of Bradford (1976).

RNA Extraction and Quantitative Real-Time RT-PCR

Total RNA was extracted using an RNAprep Pure kit (Tiangen, Beijing, China), according to the manufacturer's instructions. RNA concentration and quality were detected by the NanoDrop 2000 (Thermo Fisher Scientific, Wilmington, DE, United States). cDNAs were synthesized from 1 μg of total RNA using an

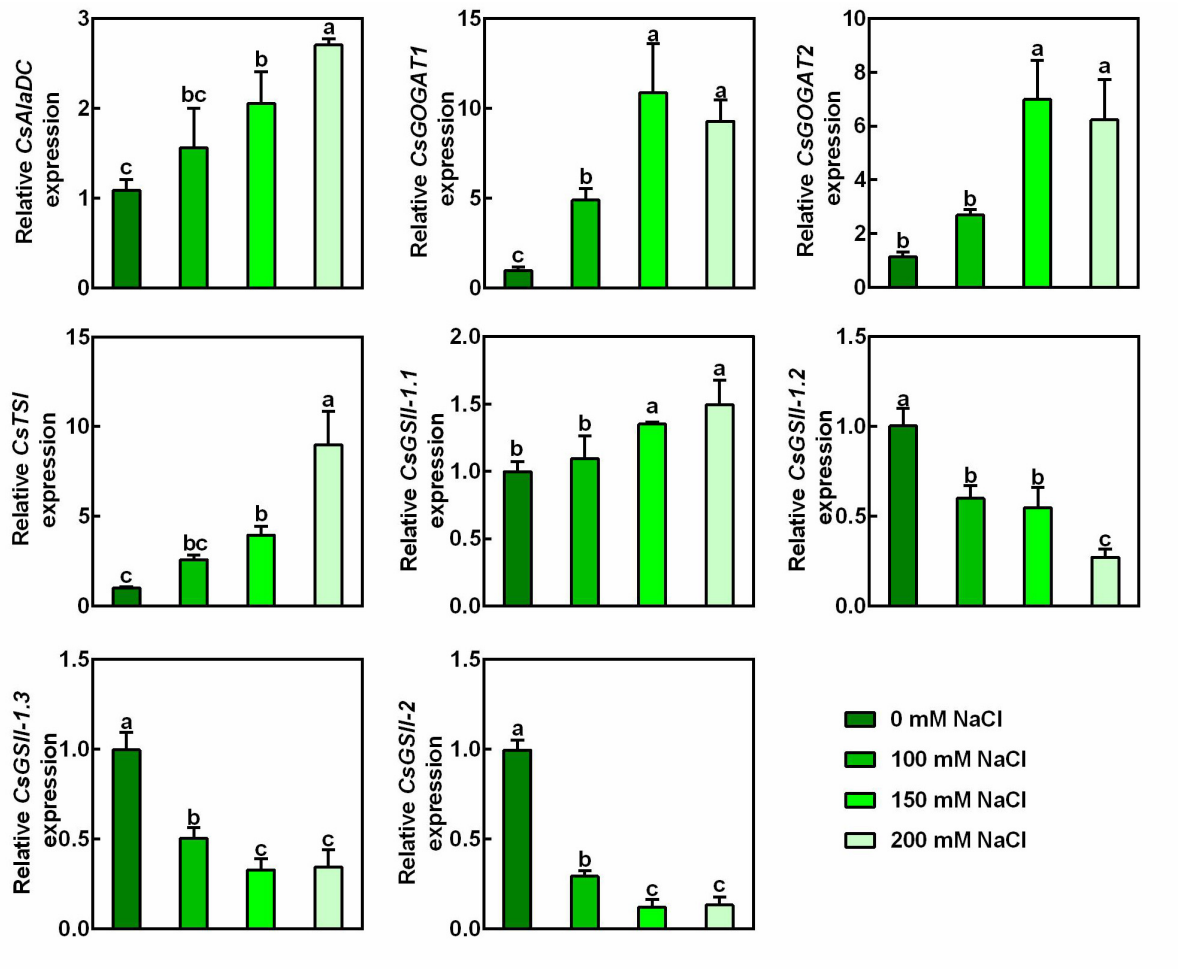

FIGURE 3 | Effects of NaCl treatments on expression of theanine biosynthetic genes in the 2nd leaves of the new shoots. The new shoots of tea plants were treated in nutrient solution containing 0, 100, 150, or 200 mM NaCl. The expression of *CsAlaDC* (TEA005658), *CsGOGAT1* (TEA003892), *CsGOGAT2* (TEA026779), *CsTSI* (TEA015198), *CsGSII-1.1* (TEA015580), *CsGSII-1.2* (TEA032123), *CsGSII-1.3* (TEA032217), and *CsGSII-2* (TEA028194) in the 2nd leaves 2 days after treatment was analyzed by qRT-PCR. Expression levels were presented as values relative to control samples, after normalization to the internal control gene *CsGAPDH* (TEA025584). Data are means ± SE of three biological replicates. Bars with different letters are significantly different at $P < 0.05$ according to Duncan's multiple range test.

oligo(dT) primer and an EasyScript All-in-One First-Strand cDNA Synthesis SuperMix (One-Step gDNA Removal) Synthesis (TransGen Biotech, Beijing, China). Real-time quantitative reverse-transcription (RT) PCR was conducted using a QuantStudio 6 Flex System (Thermo Lifetech, United States) with TransStart® Green qPCR SuperMix (TransGen Biotech, Beijing, China) by the gene-specific primers (**Supplementary Table 1**). The expression levels of genes were normalized to *CsGAPDH* transcript level, and presented as values relative to corresponding control samples.

Statistical Analysis

Statistical analysis was performed using SPSS 18.0 software. Data were means ± SE of at least three biological replicates. The asterisks indicate significant differences by Student's *t*-test (*$P < 0.05$). For statistical analysis, data was analyzed by one-way analysis of variance (ANOVA) followed by Duncan's multiple range test, and $P < 0.05$ were considered statistically significant.

RESULTS

New Shoots of Tea Plants Were Sensitive to Salt Stress

To examine the sensitivity of new shoots of tea plants to salt stress, the new shoots sampled from tea plantation were incubated in solutions containing 0, 100, 150, and 200 mM NaCl for 3 days (**Figures 1A,B**). We observed that 100, 150, and 200 mM NaCl severely damaged these new shoots. The effects of salt stress on the representative physiological characters, such as maximum photochemical efficiency of photosystem II (Fv/Fm) and loss of chlorophyll, were investigated. In our

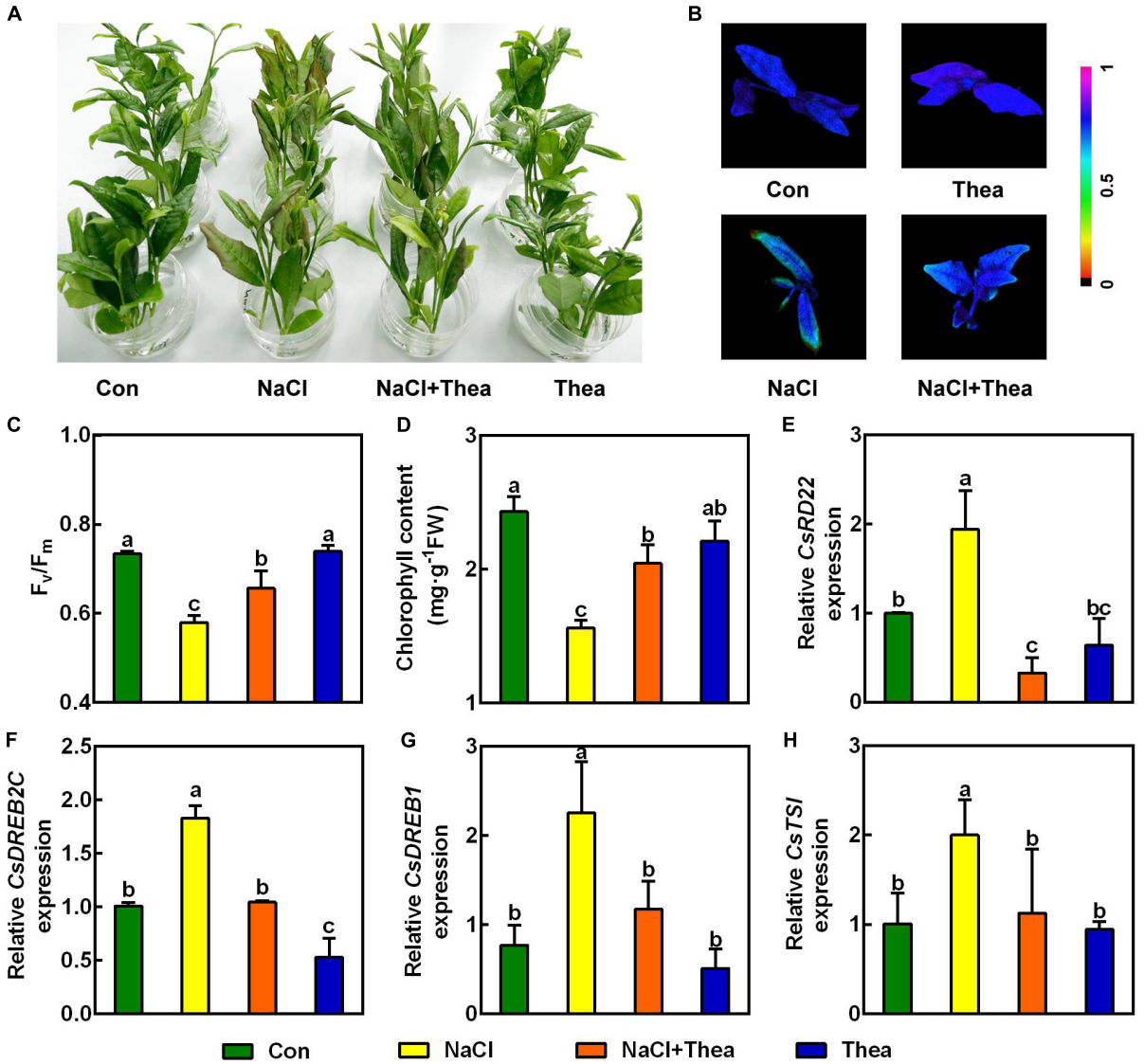

FIGURE 4 | Exogenous theanine alleviated salt stress to the new shoots of tea plants. The new shoots of tea plants were treated in nutrient solution containing 150 mM NaCl (NaCl), 10 mM theanine (Thea), 150 mM NaCl and 10 mM Thea (NaCl + Thea), with normal nutrient solution as control (Con). **(A)** Phenotypes of the new shoots. Photographs were taken 3 days after treatment. **(B,C)** Pseudo-color image and statistical analysis of Fv/Fm of the 2nd leaves 2 days after treatment. The Pseudo-color gradient shows the degree of damage: 1, no damage; 0, strong damage. **(D)** Chlorophyll contents in the 2nd leaves. The contents were determined 3 days after treatment. **(E–H)** The expression of *CsRD22* (TEA005584), *CsDREB2C* (TEA000861), *CsDREB1* (TEA010806), and *CsTSI* (TEA015198) in 2nd leaves. The expression was analyzed 2 days after treatment by qRT-PCR. Expression levels were presented as values relative to Con samples, after normalization to the internal control gene *CsGAPDH* (TEA025584). Data are means ± SE of three biological replicates. Bars with different letters are significantly different at $P < 0.05$ according to Duncan's multiple range test.

experimental conditions, salt stress significantly lowered the Fv/Fm in the 2nd leaves of the new shoots, in proportion to the NaCl concentrations (**Figures 1C,D**). Compared to the control, chlorophyll contents were also significantly decreased in high salinity-stressed leaves (**Figure 1E**). When subjected to 150 and 200 mM NaCl, chlorophyll contents were reduced by 15.5% and 24.9%, respectively. These results indicated high salinity imposed significant damage to the new shoots of tea plants.

Salt Stress Increased the Accumulation of Glutamate, Glutamine, Proline, γ-Aminobutyric Acid, Alanine and Theanine in the New Shoots

To examine the changes of amino acid accumulation in the new shoots in response to salt stress, the 2nd leaves were sampled 3 days after treatment and were used for amino acid measurement by High-Speed Amino Acid Analyzer system. The glutamate

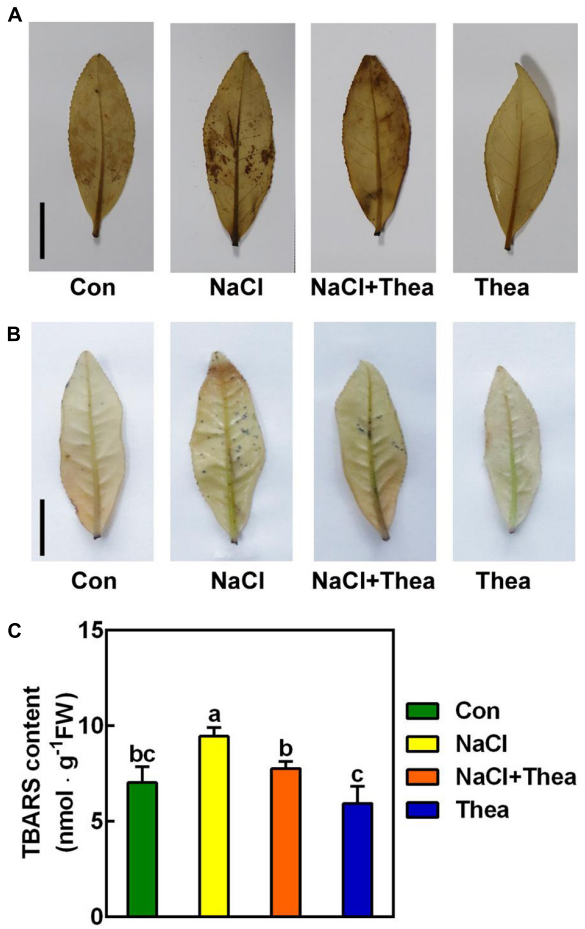

FIGURE 5 | The effects of exogenous theanine on reactive oxygen species (ROS) accumulation in the leaves of new shoot exposed to salt stress. The new shoots of tea plants were treated in nutrient solution containing 150 mM NaCl (NaCl), 10 mM theanine (Thea), 150 mM NaCl, and 10 mM Thea (NaCl + Thea), with normal nutrient solution as control (Con). **(A,B)** H_2O_2 **(A)** and $O_2^{-\bullet}$ **(B)** accumulation in the 2nd leaves of new shoots exposed to Con, NaCl, NaCl + Thea, and Thea. Three days after treatment, the leaves were stained with DAB and NBT, respectively, and were immediately photographed. Scale bar = 2 cm. **(C)** Thiobarbituric acid-reactive substances (TBARS; an indicator of lipid peroxidation) contents in the 2nd leaves. The contents were measured 3 days after treatment. At least three individual samples were analyzed. Data are means ± SE of at least three bilogical replicates. Bars with different letters are significantly different at $P < 0.05$ according to Duncan's multiple range test.

pathway amino acids (glutamine, proline, GABA, arginine, and theanine) were then analyzed (**Figure 2A**). Alanine, which provides ethylamine for theanine synthesis, was also analyzed. As shown in **Figure 2B**, NaCl treatments significant increased the accumulation of theanine in the new shoots. For example, it was increased by 0.84-fold after 3 days exposure to 150 mM NaCl compared to the control (0 mM NaCl). Besides, it was evident that NaCl treatments markedly increased the accumulation of alanine, glutamate, glutamine, GABA and proline (**Figures 2C–G**). Glutamate and alanine were increased 0.87- and 4.73-fold by 150 mM NaCl, respectively. In contrast, arginine content was not significantly changed by salt stress (**Figure 2H**). These results indicated that glutamate pathway amino acids were induced by salt stress, and implied a role of these amino acids in tolerance to salt stress.

To ascertain the effect of salt stress on the theanine biosynthesis, transcript levels of genes encoding theanine synthatase (TS), alanine decarboxylase (AlaDC), glutamine synthetase (GS), and glutamate synthase (GOGAT) (**Figure 2A**) were analyzed by real-time RT-PCR. Interestingly, compared to the control condition, the expression of theanine biosynthetic pathway genes, including *CsAlaDC*, *CsGOGAT1*, *CsGOGAT2,* and *CsTSI* was significantly induced by salt stress in a concentration-dependent manner (**Figure 3**). The expression of *CsGSII-1.1* was also slightly induced; however, the expression of *CsGSII-1.2*, *CsGSII-1.2,* and *CsGSII-2* was largely repressed by salt stress. These results implied salt stress increased theanine accumulation was probably through induced theanine biosynthesis in the new shoots of tea plants.

Given that 150 mM NaCl significantly inhibited Fv/Fm and chlorophyll accumulation, and induced theanine biosynthesis, this concentration of NaCl was chosen for the further experiments.

Exogenous Theanine Application Alleviated Salt Stress Damage to the New Shoots of Tea Plants

Previously studies showed salt stress-induced proline and GABA improve tolerance to salt stress in plants (Moukhtari et al., 2020; Wu et al., 2020). To examine whether theanine plays a role in enhancing salt stress tolerance in the new shoots of tea plants, the effects of 10 mM exogenous theanine on the salt stress sensitivity, Fv/Fm, and chlorophyll level in the absence and presence of 150 mM NaCl treatment were investigated. Under salt stress treatment, exogenous theanine application significantly alleviated the damage of salt stress to the new shoots. This is evidenced by that exogenous theanine improved the performance, Fv/Fm and chlorophyll content of the new shoots in response to salt stress (**Figures 4A–D**). In the molecular level, the expression of salt stress-responsive genes, such as *CsRD22*, *CsDREB2C*, *CsDREB1*, and *CsTSI*, was reduced to the control level by theanine (**Figures 4 E–H**). In addition, application of 1 mM theanine to the model plant Arabidopsis also improved the salt stress tolerance of the seedlings (**Supplementary Figure 1**). It is noteworthy that exogenous theanine application under normal condition did not showed obvious effects on the new shoots of tea plants and Arabidopsis seedlings (**Figures 4A–H** and **Supplementary Figure 1**). These results indicated that theanine improved salt stress tolerance of the new shoots of tea plants.

Exogenous Theanine Reduced Reactive Oxygen Species Accumulation in the Salt Stressed Leaves

Reactive oxygen species are induced by salt stress, which leads to growth stunt and even cell death (Considine and Foyer, 2021). To explore the mechanism underlying the improved salt stress tolerance by theanine, we examined

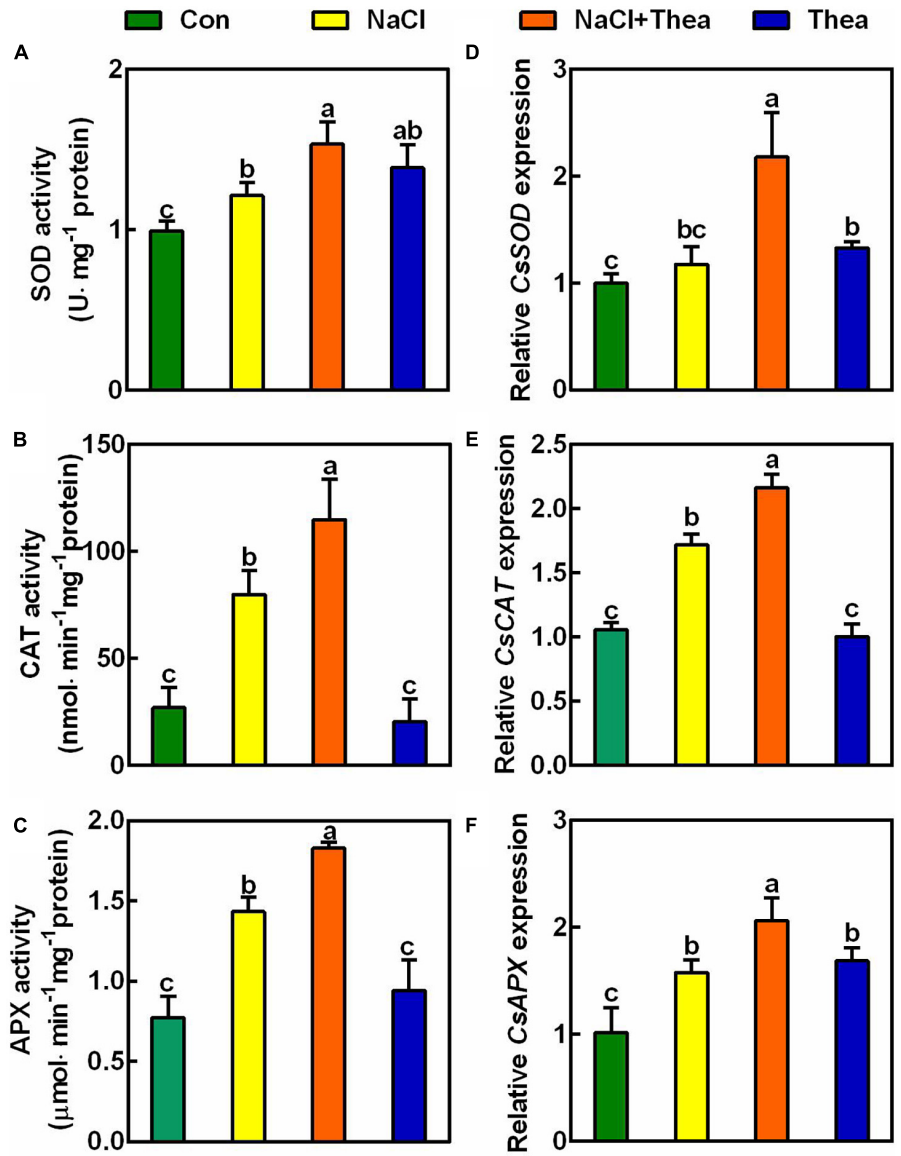

FIGURE 6 | The effects of exogenous theanine on the activities of ROS scavenging enzymes and the expression of genes encoding the enzymes. The new shoots of tea plants were treated for 3 days in nutrient solution containing 150 mM NaCl (NaCl), 10 mM theanine (Thea), 150 mM NaCl and 10 mM Thea (NaCl + Thea), with normal nutrient solution as control (Con). **(A–C)** The activities of SOD, CAT, and APX in the 2nd leaves of the new shoots. **(D–F)** The expression of *CsSOD* (TEA00629), *CsCAT* (TEA002986), and *CsAPX* (TEA000543) in the 2nd leaves. The expression was analyzed 2 days after treatment by qRT-PCR. Expression levels were presented as values relative to Con samples, after normalization to the internal control gene *CsGAPDH* (TEA025584). Data are means ± SE of three biological replicates. Bars with different letters are significantly different at $P < 0.05$ according to Duncan's multiple range test.

the effects of theanine on ROS levels. By histochemical staining with diaminobenzidine (DAB) and nitroblue tetrazolium (NBT) staining, the accumulation of H_2O_2 and $O_2^{-\bullet}$ in the 2nd leaves were, respectively, analyzed. As expected, compared to the shoots under control condition, NaCl-treated leaves accumulated more H_2O_2 and $O_2^{-\bullet}$, while NaCl and theanine co-treatment greatly reduced H_2O_2 and $O_2^{-\bullet}$ accumulation (**Figures 5A,B**). Consistently, theaine also reduced thiobarbituric acid-reactive substances (TBARS; an indicator of lipid peroxidation) accumulation in the salt stressed leaves (**Figure 5C**). These results suggested that theanine alleviated salt stress-induced oxidative damage to new shoots of tea plants.

To explore how exogenous theanine reduced ROS accumulation, we examined the activities of ROS scavenging enzymes, including SOD, CAT, and APX. The results showed that salt stress increased SOD, CAT, and APX activities, and exogenous theanine further improved the activities of these enzymes (**Figures 6A–C**). At the level of gene expression, salt stress also significantly induced the expression of *CsCAT* and *CsAPX*, and exogenous theanine further significantly induced

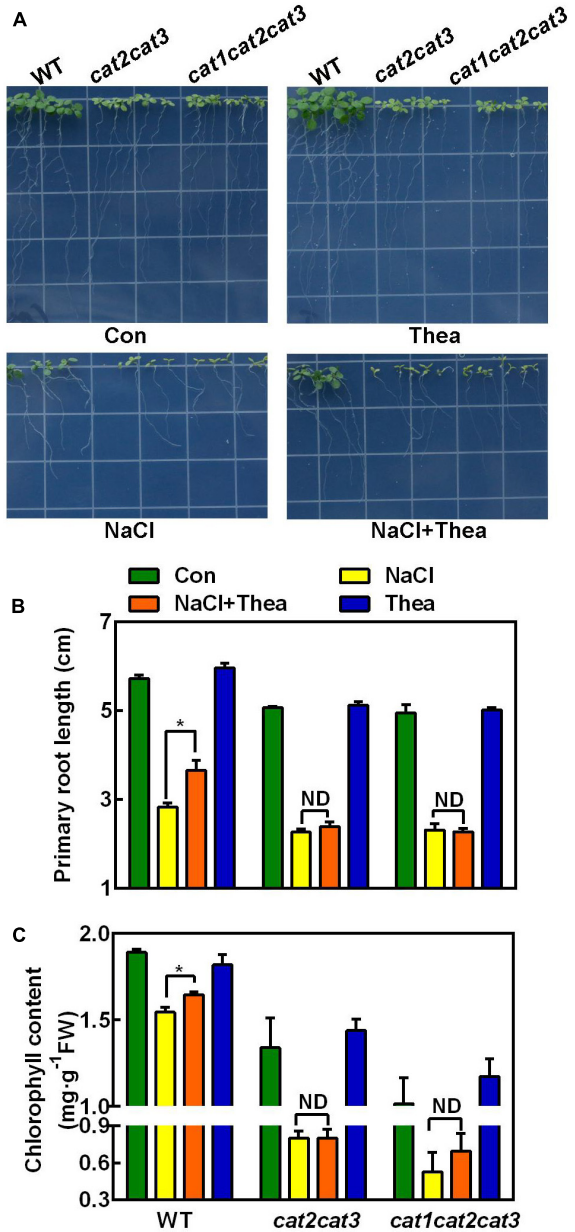

FIGURE 7 | The effects of exogenous theanine on the salt stress tolerance of *Arabidopsis* wild-type (WT), *cat2cat3* and *cat1cat2cat3* mutants. **(A)** Phenotypes of WT *Arabidopsis* and *cat2cat3* and *cat1cat2cat3* mutants grown on MS medium containing 100 mM NaCl (NaCl), 100 mM NaCl and 1 mM theanine (NaCl + Thea), 1 mM theanine (Thea) for 10 days. The medium without NaCl and theanine was the control (Con). **(B,C)** Primary root length and total chlorophyll content in leaves of WT, *cat2cat3* and *cat1cat2cat3* mutants grown under the indicated conditions. Data are means ± SE of three biological replicates. Asterisks indicate significant differences from WT under NaCl treatment based on Student's *t*-test (*$P < 0.05$). ND, no significant difference.

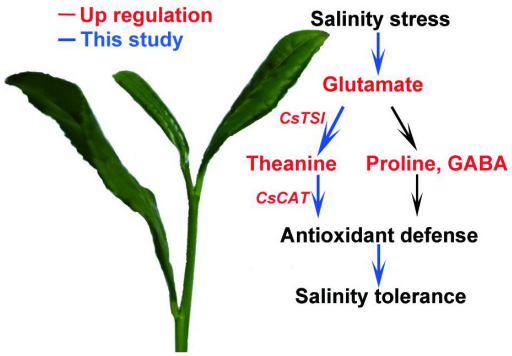

FIGURE 8 | A proposed model of theanine-mediated tolerance to salt stress in tea plants. Salt stress increases glutamate accumulation and the expression of theanine biosynthetic genes to promote theanine biosynthesis. Theanine enhances plant high-salinity tolerance through a CAT-dependent ROS scavenging pathway.

the expression of *CsSOD*, *CsCAT*, and *CsAPX* (**Figures 6D–F**). Therefore, exogenous theanine induced the expression of genes encoding ROS scavenging enzymes and increased the activities of these enzymes, under salt stress condition. These results supported the notion that salt stress-induced theanine contributes to salt stress tolerance *via* (at least partially) ROS scavenging pathway.

Genetic Evidence Revealed That Catalase Is Required for Theanine-Induced Salinity Tolerance

Catalases are highly responsive to stresses and are critical for scavenging H_2O_2 in plants (Mhamdi et al., 2012; Su et al., 2018). There are three genes *CAT1*, *CAT2*, and *CAT3* encoding catalases in Arabidopsis. *cat2cat3* double mutant and *cat1cat2cat3* triple mutant were obtained in Arabidopsis (Su et al., 2018). To investigate the role of ROS scavenging pathway in theanine-induced salt stress tolerance, we used these double and triple mutants for further study, given that we cannot knock down or overexpress the *CsCATs* in tea plants. Similar to the wild-type (WT), *cat2cat3* and *cat1cat2cat3* mutants also exhibited hypersensitivity to NaCl treatment (**Figure 7**). However, unlike WT, theanine did not improve salt stress tolerance of *cat2cat3* and *cat1cat2cat3* mutants, in terms of primary root growth and chlorophyll content (**Figures 7A–C**). These results indicated that catalase-mediated H_2O_2 scavenging pathway is required for theanine-induced salt stress tolerance in Arabidopsis, and implied that salt stress-induced theanine improves salt stress tolerance by modulating H_2O_2 scavenging in tea plants.

DISCUSSION

Theanine has favorable physiological effects on human health, including antioxidant and immune-regulation properties (Deng et al., 2016; Gong et al., 2019). A positive correlation exists between theanine and antioxidative activity, suggesting that theanine plays a role in modulating redox homeostasis in animals (Li et al., 2012; Deng et al., 2016; Zeng et al., 2020).

Previous results showed that theanine contents in tea plants were influenced by abiotic stress, such as salinity, drought, and heat stress (Deng et al., 2012; Wang et al., 2016; Li et al., 2018a). It is known that these abiotic stresses, especially salt stress, elicits the accumulation of ROS and results in redox imbalance (Bose et al., 2013; Considine and Foyer, 2021).

Under our experimental conditions, theanine accumulation was obviously induced by salt stress in the new shoots of tea plants (**Figure 2B**). Besides, salt stress improved the glutamate accumulation, a direct substrate for theanine biosynthesis, as well as the alanine, a precursor of ethylamine in tea plants (**Figures 2C,D**; Sasaoka and Kito, 1964; Takeo, 1974). These findings are consistent with the former result (Deng et al., 2012). We further showed that the induced expression of theanine biosynthetic genes *CsAlaDC*, *CsGOGAT1*, *CsGOGAT2*, and *CsTSI* could be responsible for the increased theanine biosynthesis and accumulation.

Salt stress significantly inhibits electron transport at the oxidizing side of photosystem II (PSII) and decreases the PSII activity, which leads to reduced photosynthesis (Xia et al., 2004). A decline in chlorophyll content can also decrease the photosynthesis in plant during salinity stress (Heuer and Plaut, 1989). Thereby, the growth and productivity of plants were severely affected by salt stress (Jamil et al., 2014). Interestingly, in this study, we found the application of theanine was able to relieve high salinity-induced damage to the new shoots, the reduction of maximum quantum efficiency of photosystem II (Fv/Fm) and chlorophyll content (**Figures 4A–D**). Additionally, the induction of salt stress-responsive genes including *CsRD22*, *CsDREB2C*, *CsDREB1*, and *CsTSI* was also significantly recovered by theanine (**Figures 4E–H**). Combined with the protective effect of theanine in model plant Arabidopsis wild-type seedlings against salt stress (**Supplementary Figure 1**), and the high abundance of theanine in tea plants, we speculate that theanine is a key regulator of salt stress resistance in tea plants.

Redox imbalance, such as the overproduction of ROS and lipid peroxidation, was induced by salt stress (Miller et al., 2010; Considine and Foyer, 2021). ROS, in turn, inhibit protein synthesis and damage the protein subunits and pigments of PSII (Murata et al., 2007). Previous studies strongly revealed that an efficient antioxidant system contributes to salt stress tolerance in plants (Miller et al., 2010). The health benefits of theanine in animals are associated with its antioxidant actions (Williams et al., 2019). The present study demonstrated that theanine counteracted NaCl-induced H_2O_2, $O_2^{-\bullet}$ and TBARS accumulation in the leaves of new shoots (**Figure 5**), and also increased the activities of SOD, CAT, and APX and the expression of the corresponding genes (**Figures 6A–F**). These results were consistent with the observations in animals. For example, theanine prevented ethanol-triggered ROS and MDA generation *via* restoring the antioxidant capability of hepatocytes (Li et al., 2012). The anti-inflammatory and antioxidative actions triggered by theanine were further confirmed in *Escherichia coli*-infected and D-galactose-induced liver dysfunction (Deng et al., 2016; Zeng et al., 2020). Together, our results suggested that theanine modulates oxidative damage in tea plants under salt stress condition.

Among the antioxidant enzymes, catalase is an important respiratory enzyme in plants, and its activity is closely related to plant resistance (Mhamdi et al., 2012). Chinese cabbage plants overexpressing maize catalase (ZmCAT) showed enhanced tolerance to high salinity (Tseng et al., 2007). Silencing *GhWRKY46* in cotton by virus-induced gene silencing reduced the catalase activity, and resulted in hypersensitivity to salt stress (Li et al., 2021). It was also found that Arabidopsis *cat2-1* mutant exhibited increased sensitivity to salt stress (Bueso et al., 2007). In the present study, we also found Arabidopsis *cat2cat3* double mutant and *cat1cat2cat3* triple mutant were hypersensitive to salt stress, and theanine could not enhance the salt stress tolerance of these mutants (**Figure 7**). This result provided genetic evidence that CAT-mediated redox homeostasis is required for theanine-induced salt stress tolerance.

Production of ROS was accelerated by over-reduced ferredoxin during photosynthetic electron transfer in the chloroplasts, impaired electron transport processes in the mitochondria and photorespiration in peroxisomes in plants (Ahmed et al., 2009). The nucleus-encoding ROS scavenging enzymes are responsible for maintaining the redox homeostasis in these organelles. In the present study, we showed that theanine application induced the expression of genes encoding SOD, APX, and CAT (**Figures 6E–F**). However, it is unclear how theanine induced the expression of these genes. Recently, the retrograde signaling from chloroplast to nucleus was reported to be critical for salt stress tolerance in plants (Park and Seo, 2021; Zhuang et al., 2021). This retrograde signaling is required for the induction of ROS scavenging pathway genes such as *CSD2* (Zhuang et al., 2021). Interestingly, theanine is mainly distributed in cytosol and chloroplast in the new shoots of tea plants (Fu et al., 2021). It will be interesting to investigate whether theanine regulates the expression of *SOD*, *APX*, and CAT *via* chloroplast to nucleus retrograde signaling pathway.

Many studies have reported that proline or GABA improve salt stress tolerance in plants (Moukhtari et al., 2020; Wu et al., 2020). In this study, we showed that salt stress induces theanine biosynthesis, and the induced theanine is associated with enhanced salt stress tolerance in the new shoots of tea plants. Theanine-induced salt stress tolerance is probably *via* modulating ROS homeostasis in a CAT-dependent ROS scavenging pathway (**Figure 8**). To our knowledge, this is the first report to link theanine with salt stress tolerance and ROS homeostasis in tea plants. This study provided new insights into the physiological role of theanine in tea plants.

DATA AVAILABILITY STATEMENT

The original contributions presented in the study are included in the article/**Supplementary Material**, further inquiries can be directed to the corresponding author/s.

AUTHOR CONTRIBUTIONS

ZZ and ZC conceived the study and designed the experiments. ZC, SL, JL, and TC performed the experiments. QG and TY participated in the preparation of plant materials. ZC wrote the manuscript. ZZ revised and finalized the manuscript. All authors read and approved the final version of the manuscript.

FUNDING

This work was supported by grants from the National Natural Science Foundation of China (3207624 and 3177073), Collaborative Innovation Project of Universities in Anhui Province (GXXT-2020-080), the Base of Introducing Talents for Tea Plant Biology and Quality Chemistry (D20026), and the Talent Research Fund Project of Hefei University (No. 18-19RC13).

ACKNOWLEDGMENTS

We thank Changle Ma in College of Life Sciences, Shandong Normal University, China for kindly providing the *cat2cat3* and *cat1cat2cat3* mutants.

SUPPLEMENTARY MATERIAL

The Supplementary Material for this article can be found online at: https://www.frontiersin.org/articles/10.3389/fpls.2021.770398/full#supplementary-material

REFERENCES

Ahmed, P., Jaleel, C. A., Azooz, M. M., and Nabi, G. (2009). Generation of ROS and non-enzymatic antioxidants during abiotic stress in plants. *Bot. Res. Intl.* 2, 11–20.

Ashihara, H. (2015). Occurrence, biosynthesis and metabolism of theanine (γ-Glutamyl-L-ethylamide) in plants: a comprehensive review. *Nat. Prod. Commun.* 10, 803–810. doi: 10.1177/1934578X1501000525

Bai, P., Wei, K., Wang, L., Zhang, F., Ruan, L., Li, H., et al. (2019). Identification of a novel gene encoding the specialized alanine decarboxylase in tea (*Camellia sinensis*) plants. *Molecules* 24:540. doi: 10.3390/molecules24030540

Bao, H., Chen, X., Lv, S., Jiang, P., Feng, J., Fan, P., et al. (2015). Virus-induced gene silencing reveals control of reactive oxygen species accumulation and salt tolerance in tomato by γ-aminobutyric acid metabolic pathway. *Plant Cell Environ.* 38, 600–613. doi: 10.1111/pce.12419

Beauchamp, C., and Fridovich, I. (1971). Superoxide dismutase: improved assays and an assay applicable to acrylamide gels. *Anal. Biochem.* 44, 276–287. doi: 10.1016/0003-2697(71)90370-8

Ben, P., Zhang, Z., Zhu, Y., Xiong, A., Gao, Y., Mu, J., et al. (2016). L-Theanine attenuates cadmium-induced neurotoxicity through the inhibition of oxidative damage and tau hyperphosphorylation. *Neurotoxicology* 57, 95–103. doi: 10.1016/j.neuro.2016.09.010

Bose, J., Rodrigo-Moreno, A., and Shabala, S. (2013). ROS homeostasis in halophytes in the context of salinity stress tolerance. *J. Exp. Bot.* 65, 1241–1257. doi: 10.1093/jxb/ert430

Bradford, M. M. (1976). A rapid and sensitive method for the quantitation of microgram quantities of protein utilizing the principle of protein-dye binding. *Anal. Biochem.* 72, 248–254. doi: 10.1016/0003-2697(76)90527-3

Buege, J. A., and Aust, S. D. (1978). Microsomal lipid peroxidation. *Methods Enzymol.* 52, 302–310. doi: 10.1016/S0076-6879(78)52032-6

Bueso, E., Alejandro, S., Carbonell, P., Perez-Amador, M. A., and Serrano, R. (2007). The lithium tolerance of the Arabidopsis *cat2* mutant reveals a cross-talk between oxidative stress and ethylene. *Plant J.* 52, 1052–1065. doi: 10.1111/j.1365-313X.2007.03305.x

Causapé, J., Quílez, D., and Aragüés, R. (2004). Assessment of irrigation and environmental quality at the hydrological basin level: ii. Salt and nitrate loads in irrigation return flows. *Agr. Water Manage.* 70, 211–228. doi: 10.1016/j.agwat.2004.06.006

Chang, C., Wang, B., Shi, L., Li, Y., Duo, L., and Zhang, W. (2010). Alleviation of salt stress-induced inhibition of seed germination in cucumber (*Cucumis sativus* L.) by ethylene and glutamate. *J. Plant Physiol.* 167, 1152–1156. doi: 10.1016/j.jplph.2010.03.018

Chen, L., Zhou, Z. X., and Yang, Y. J. (2007). Genetic improvement and breeding of tea plant (*Camellia sinensis*) in China: from individual selection to hybridization and molecular breeding. *Euphytica* 154, 239–248. doi: 10.1007/s10681-006-9292-3

Cheng, S., Fu, X., Wang, X., Liao, Y., Zeng, L., Dong, F., et al. (2017). Studies on biochemical formation pathway of the amino acid L-theanine in tea (*Camellia sinensis*) and other plants. *J. Agric. Food Chem.* 65, 7210–7216. doi: 10.1021/acs.jafc.7b02437

Considine, M. J., and Foyer, C. H. (2021). Stress effects on the reactive oxygen species (ROS)-dependent regulation of plant growth and development. *J. Exp. Bot.* 72, 5795–5806. doi: 10.1093/jxb/erab265

Cui, W., Zhang, J., Xuan, W., and Xie, Y. (2013). Up-regulation of heme oxygenase-1 contributes to the amelioration of aluminum-induced oxidative stress in *Medicago sativa*. *J. Plant Physiol.* 170, 1328–1336. doi: 10.1016/j.jplph.2013.05.014

Deb, S., Dutta, A., Phukan, B. C., Manivasagam, T., Justin Thenmozhi, A., Bhattacharya, P., et al. (2019). Neuroprotective attributes of L-theanine, a bioactive amino acid of tea, and its potential role in Parkinson's disease therapeutics. *Neurochem. Int.* 129:104478. doi: 10.1016/j.neuint.2019.104478

Deng, W. W., Wang, S., Chen, Q., Zhang, Z. Z., and Hu, X. Y. (2012). Effect of salt treatment on theanine biosynthesis in *Camellia sinensis* seedlings. *Plant Physiol. Biochem.* 56, 35–40. doi: 10.1016/j.plaphy.2012.04.003

Deng, Y., Xiao, W., Chen, L., Liu, Q., Liu, Z., and Gong, Z. (2016). In vivo antioxidative effects of L-theanine in the presence or absence of *Escherichia coli*-induced oxidative stress. *J. Funct. Foods* 24, 527–536. doi: 10.1016/j.jff.2016.04.029

Dluzniewska, P., Gessler, A., Dietrich, H., Schnitzler, J. P., Teuber, M., and Rennenberg, H. (2007). Nitrogen uptake and metabolism in *Populus*×*canescens* as affected by salinity. *New Phytol.* 173, 279–293. doi: 10.1111/j.1469-8137.2006.01908.x

Dong, C., Li, F., Yang, T., Feng, L., Zhang, S., Li, F., et al. (2020). Theanine transporters identified in tea plants (*Camellia sinensis* L.). *Plant J.* 101, 57–70. doi: 10.1111/tpj.14517

Fu, X., Liao, Y., Cheng, S., Xu, X., Grierson, D., and Yang, Z. (2021). Nonaqueous fractionation and overexpression of fluorescent-tagged enzymes reveals the subcellular sites of L-theanine biosynthesis in tea. *Plant Biotechnol. J.* 19, 98–108. doi: 10.1111/pbi.13445

Gong, Z., Lin, L., Liu, Z., Zhang, S., Liu, A., Chen, L., et al. (2019). Immune-modulatory effects and mechanism of action of L-theanine on ETEC-induced immune-stressed mice via nucleotide-binding oligomerization domain-like receptor signaling pathway. *J. Funct. Foods* 54, 32–40. doi: 10.1016/j.jff.2019.01.011

Groat, R. G., and Vance, C. P. (1981). Root nodule enzymes of ammonia assimilation in Alfalfa (*Medicago sativa* L.): development patterns and response to applied nitrogen. *Plant Physiol.* 67, 1198–1203. doi: 10.1104/pp.67.6.1198

Hayat, S., Hayat, Q., Alyemeni, M. N., Wani, A. S., Pichtel, J., and Ahmad, A. (2012). Role of proline under changing environments: a review. *Plant Signal. Behav.* 7, 1456–1466. doi: 10.4161/psb.21949

Heuer, B., and Plaut, Z. (1989). Photosynthesis and osmotic adjustment of two sugarbeet cultivars grown under saline conditions. *J. Exp. Bot.* 4, 437–440. doi: 10.1093/jxb/40.4.437

Jamil, M., Rehman, S. U., and Rha, E. S. (2014). Response of growth, PSII photochemistry and chlorophyll content to salt stress in four *Brassica species*. *Life Sci. J.* 11, 139–145.

Konishi, S., Miyamoto, S., and Taki, T. (1985). Stimulatory effects of aluminum on tea plants growth under low and high phosphorus supply. *Soil Sci. Plant Nutr.* 31, 361–368. doi: 10.1080/00380768.1985.10557443

Li, G., Ye, Y., Kang, J., Yao, X., Zhang, Y., Jiang, W., et al. (2012). L-Theanine prevents alcoholic liver injury through enhancing the antioxidant capability of hepatocytes. *Food Chem. Toxicol.* 50, 363–372. doi: 10.1016/j.fct.2011.10.036

Li, X., Wei, J. P., Ahammed, G. J., Zhang, L., Li, Y., Yan, P., et al. (2018a). Brassinosteroids attenuate moderate high temperature-caused decline in tea quality by enhancing theanine biosynthesis in *Camellia sinensis* L. *Front. Plant Sci.* 9:1016. doi: 10.3389/fpls.2018.01016

Li, X., Wei, J. P., Scott, E. R., Liu, J. W., Shuai, G., Li, Y., et al. (2018b). Exogenous melatonin alleviates cold stress by promoting antioxidant defense and redox homeostasis in *Camellia sinensis* L. *Molecules* 23:65. doi: 10.3390/molecules23010165

Li, Y., Chen, H., Li, S., Yang, C., and Wang, D. J. (2021). GhWRKY46 from upland cotton positively regulates the drought and salt stress responses in plant. *Environ. Exp. Bot.* 186:104438. doi: 10.1016/j.envexpbot.2021.104438

Lichtenthaler, H. K. (1987). Chlorophylls and carotenoids: pigments of photosynthetic biomembranes. *Methods Enzymol.* 148, 350–382. doi: 10.1016/0076-6879(87)48036-1

Lu, M., Han, J., Zhu, B., Jia, H., Yang, T., Wang, R., et al. (2019). Significantly increased amino acid accumulation in a novel albino branch of the tea plant (*Camellia sinensis*). *Planta* 249, 363–376. doi: 10.1007/s00425-018-3007-6

Mhamdi, A., Noctor, G., and Baker, A. (2012). Plant catalases: peroxisomal redox guardians. *Arch. Biochem. Biophys.* 525, 181–194. doi: 10.1016/j.abb.2012.04.015

Miflin, B. J., and Habash, D. Z. (2002). The role of glutamine synthetase and glutamate dehydrogenase in nitrogen assimilation and possibilities for improvement in the nitrogen utilization of crops. *J. Exp. Bot.* 53, 979–987. doi: 10.1093/jexbot/53.370.979

Miller, G., Suzuki, N., Ciftci-Yilmaz, S., and Mittler, R. J. P. (2010). Reactive oxygen species homeostasis and signalling during drought and salinity stresses. *Plant Cell Environ.* 33, 453–467. doi: 10.1111/j.1365-3040.2009.02041.x

Moukhtari, A. E., Cabassa-Hourton, C., Farissi, M., and Savouré, A. (2020). How does proline treatment promote salt stress tolerance during crop plant development. *Front. Plant Sci.* 11:1127. doi: 10.3389/fpls.2020.01127

Murata, N., Takahashi, S., Nishiyama, Y., and Allakhverdiev, S. I. (2007). Photoinhibition of photosystem II under environmental stress. *Biochim. Biophys. Acta* 1767, 414–421. doi: 10.1016/j.bbabio.2006.11.019

Narukawa, M., Morita, K., and Hayashi, Y. (2008). L-theanine elicits an umami taste with inosine 5′-monophosphate. *Biosci. Biotechnol. Biochem.* 72, 3015–3017. doi: 10.1271/bbb.80328

Park, K. Y., and Seo, S. Y. (2021). Translocation of chloroplast NPR1 to the nucleus in retrograde signaling for adaptive response to salt stress in tobacco. *bioRxiv* [Preprint] doi: 10.1101/2021.03.24.436779

Sasaoka, K., and Kito, M. (1964). Synthesis of theanine by tea seedling homogenate. *Agric Biol Chem.* 28, 313–317. doi: 10.1080/00021369.1964.10858238

Sharma, E., Joshi, R., and Gulati, A. (2018). L-Theanine: an astounding sui generis integrant in tea. *Food Chem.* 242, 601–610. doi: 10.1016/j.foodchem.2017.09.046

Silveira, J. A. G., de Almeida Viégas, R., da Rocha, I. M. A., de Oliveira Monteiro-Moreira, A. C., de Azevedo Moreira, R., and Oliveira, J. T. A. (2003). Proline accumulation and glutamine synthetase activity are increased by salt-induced proteolysis in cashew leaves. *J. Plant Physiol.* 160, 115–123. doi: 10.1078/0176-1617-00890

Su, T., Wang, P., Li, H., Zhao, Y., Lu, Y., Dai, P., et al. (2018). The *Arabidopsis* catalase triple mutant reveals important roles of catalases and peroxisome-derived signaling in plant development. *J. Integr. Plant Biol.* 60, 65–81. doi: 10.1111/jipb.12649

Szabados, L., and Savouré, A. (2010). Proline: a multifunctional amino acid. *Trends Plant Sci.* 15, 89–97. doi: 10.1016/j.tplants.2009.11.009

Takeo, T. (1974). L-alanine as a precursor of ethylamine in *Camellia sinensis*. *Phytochemistry* 13, 1401–1406. doi: 10.1016/0031-9422(74)80299-2

Takeo, T. (1979). Formation of amino acids induced by ammonia application and seasonal level fluctuation of amino acids contents in tea plant. *Chagyo Kenkyu* 56:70.

Tseng, M. J., Liu, C. W., and Yiu, J. C. (2007). Enhanced tolerance to sulfur dioxide and salt stress of transgenic Chinese cabbage plants expressing both superoxide dismutase and catalase in chloroplasts. *Plant Physiol. Biochem.* 45, 822–833. doi: 10.1016/j.plaphy.2007.07.011

Tsushida, T., and Takeo, T. (1984). Ethylamine content of fresh tea shoots and made tea determined by high performance liquid chromatography. *J. Agric. Food Chem.* 35, 77–83. doi: 10.1002/jsfa.2740350113

Upadhyaya, H., and Panda, S. K. (2013). Abiotic stress response in tea [*Camellia sinensis* L (O) Kuntze]: an overview. *Rev. Agr. Sci.* 1, 1–10. doi: 10.7831/ras.1.1

Wang, R., Chen, S., Deng, L., Fritz, E., Hüttermann, A., and Polle, A. (2007). Leaf photosynthesis, fluorescence response to salinity and the relevance to chloroplast salt compartmentation and anti-oxidative stress in two poplars. *Trees* 21, 581–591. doi: 10.1007/s00468-007-0154-y

Wang, W., Xin, H., Wang, M., Ma, Q., Wang, L., Kaleri, N. A., et al. (2016). Transcriptomic analysis reveals the molecular mechanisms of drought-stress-induced decreases in *Camellia sinensis* leaf quality. *Front. Plant Sci.* 7:385. doi: 10.3389/fpls.2016.00385

Wei, C., Yang, H., Wang, S., Zhao, J., Liu, C., Gao, L., et al. (2018). Draft genome sequence of *Camellia sinensis* var. sinensis provides insights into the evolution of the tea genome and tea quality. *Proc. Natl. Acad. Sci. U. S. A.* 115, E4151–E4158. doi: 10.1073/pnas.1719622115

Williams, J., Sergi, D., McKune, A. J., Georgousopoulou, E. N., Mellor, D. D., and Naumovski, N. (2019). The beneficial health effects of green tea amino acid L-theanine in animal models: promises and prospects for human trials. *Phytother. Res.* 33, 571–583. doi: 10.1002/ptr.6277

Wu, X., Jia, Q., Ji, S., Gong, B., Li, J., Lv, G., et al. (2020). Gamma-aminobutyric acid (GABA) alleviates salt damage in tomato by modulating Na^+ uptake, the GAD gene, amino acid synthesis and reactive oxygen species metabolism. *BMC Plant Biol.* 20:465. doi: 10.1186/s12870-020-02669-w

Xia, E. H., Li, F. D., Tong, W., Li, P. H., Wu, Q., Zhao, H. J., et al. (2019). Tea plant information archive: a comprehensive genomics and bioinformatics platform for tea plant. *Plant Biotechnol. J.* 17, 1938–1953. doi: 10.1111/pbi.13111

Xia, J., Li, Y., and Zou, D. (2004). Effects of salinity stress on PSII in *Ulva lactuca* as probed by chlorophyll fluorescence measurements. *Aquat. Bot.* 80, 129–137. doi: 10.1016/j.aquabot.2004.07.006

Xie, Y., Ling, T., Han, Y., Liu, K., Zheng, Q., Huang, L., et al. (2008). Carbon monoxide enhances salt tolerance by nitric oxide-mediated maintenance of ion homeostasis and up-regulation of antioxidant defence in wheat seedling roots. *Plant Cell Environ.* 31, 1864–1881. doi: 10.1111/j.1365-3040.2008.01888.x

Xie, Y., Mao, Y., Lai, D., Wei, Z., and Shen, W. (2012). H_2 enhances *Arabidopsis* salt tolerance by manipulating *ZAT10/12*-mediated antioxidant defence and controlling sodium exclusion. *PLoS One* 7:e49800. doi: 10.1371/journal.pone.0049800

Yang, H. (2014). Effects of amino acid on seed germination and seedling growth of buckwheat under salt stress. *Guizhou Agr. Sci.* 42, 30–33.

Yang, T., Li, H., Tai, Y., Dong, C., Cheng, X., Xia, E., et al. (2020). Transcriptional regulation of amino acid metabolism in response to nitrogen deficiency and nitrogen forms in tea plant root (*Camellia sinensis* L.). *Sci. Rep.* 10:6868. doi: 10.1038/s41598-020-63835-6

Yang, T., Xie, Y., Lu, X., Yan, X., Wang, Y., Ma, J., et al. (2021). Shading promoted theanine biosynthesis in the roots and allocation in the shoots of the tea plant (*Camellia sinensis* L.) cultivar Shuchazao. *J. Agric. Food Chem.* 69, 4795–4803. doi: 10.1021/acs.jafc.1c00641

Zeng, L., Lin, L., Peng, Y., Yuan, D., Zhang, S., Gong, Z., et al. (2020). L-theanine attenuates liver aging by inhibiting advanced glycation end products in D-galactose-induced rats and reversing an imbalance of oxidative stress and inflammation. *Exp. Gerontol.* 131:110823. doi: 10.1016/j.exger.2019.110823

Zhuang, Y., Wei, M., Ling, C., Liu, Y., Amin, A. K., Li, P., et al. (2021). EGY3 mediates chloroplastic ROS homeostasis and promotes retrograde signaling in response to salt stress in Arabidopsis. *Cell Rep*. 36:109384. doi: 10.1016/j.celrep

Conflict of Interest: The authors declare that the research was conducted in the absence of any commercial or financial relationships that could be construed as a potential conflict of interest.

Publisher's Note: All claims expressed in this article are solely those of the authors and do not necessarily represent those of their affiliated organizations, or those of the publisher, the editors and the reviewers. Any product that may be evaluated in this article, or claim that may be made by its manufacturer, is not guaranteed or endorsed by the publisher.

frontiers in Plant Science

ORIGINAL RESEARCH
published: 21 October 2021
doi: 10.3389/fpls.2021.733287

Transcriptome-Wide Analysis and Functional Verification of RING-Type Ubiquitin Ligase Involved in Tea Plant Stress Resistance

Dawei Xing[1], Tongtong Li[1], Guoliang Ma[2], Haixiang Ruan[2], Liping Gao[2] and Tao Xia[1]**

[1] State Key Laboratory of Tea Plant Biology and Utilization, Anhui Agricultural University, Hefei, China, [2] School of Life Sciences, Anhui Agricultural University, Hefei, China

OPEN ACCESS

Edited by:
Vagner A. Benedito, West Virginia University, United States

Reviewed by:
Dudy Bar-Zvi, Ben-Gurion University of the Negev, Israel
Sandeep Chapagain, Louisiana State University, United States
Yuling Lin, Fujian Agriculture and Forestry University, China
Sung Chul Lee, Chung-Ang University, South Korea

***Correspondence:**
Liping Gao
gaolp62@126.com
Tao Xia
xiatao62@126.com

Specialty section:
This article was submitted to Plant Metabolism and Chemodiversity, a section of the journal Frontiers in Plant Science

Received: *30 June 2021*
Accepted: *29 September 2021*
Published: *21 October 2021*

Citation:
Xing D, Li T, Ma G, Ruan H, Gao L and Xia T (2021) Transcriptome-Wide Analysis and Functional Verification of RING-Type Ubiquitin Ligase Involved in Tea Plant Stress Resistance. Front. Plant Sci. 12:733287. doi: 10.3389/fpls.2021.733287

The ubiquitin/26S proteasome pathway is a critical protein-degradation pathway in plant growth and development as well as in nearly all biological and abiotic stress processes. Although as a member of the ubiquitin/26S proteasome pathway, the E3 ubiquitin ligase family has been shown to be essential for the selective degradation of downstream target proteins, it has been rarely reported in tea plants (*Camellia sinensis*). In this study, through database searches and extensive manual deduplication, 335 RING finger family proteins were selected from the Tea Plant Information Archive. These proteins were divided into six categories by the difference of RING finger domain: RING-H2, RING-HCa, RING-HCb, RING-C2, RING-v, and RING-G. Stress-induced differential gene expression analysis showed that 53 proteins in RING finger family can respond to selected exogenous stress. *In vitro* ubiquitination assays indicated that TEA031033, which was named CsMIEL1, exhibited the activity of E3 ubiquitin ligases. *CsMIEL1-overexpressing* transgenic *Arabidopsis thaliana* seedlings were resistant to some exogenous abiotic stresses, such as salt and drought stress but sensitive to exogenous methyl jasmonate treatment. Furthermore, CsMIEL1 reduced the accumulation of anthocyanin in transgenic plants in response to low temperature treatment. The results of this article provide basic date for studying the role of ubiquitin/26S proteasome pathway in tea plants response to stresses.

Keywords: *Camellia sinensis*, RING-containing proteins, E3 ubiquitin ligase, MIEL1, biological and abiotic stress

INTRODUCTION

Tea plant [*Camellia sinensis* (L.) O. Kuntze], a perennial evergreen woody plant, encounters various abiotic (drought, heat, cold, and salt) and biological stresses (pests, viruses, and herbivore foraging). Under these stresses, plants undergo various degrees of damage. For example, under high salt stress, an imbalance of Na^+/K^+ inside and outside the cell restricts plant growth and accumulates excessive reactive oxygen species, which causes osmotic and even oxidative stresses (Munns and Tester, 2008). Through long-term natural selection, plants have evolved various physiological and biochemical defense mechanisms to deal with stresses (Hou et al., 2009), such as antioxidant defense mechanisms (Dai and Mumper, 2010), apoptosis (Jones, 2001), and autophagy (Avin-Wittenberg, 2019). Plants can tolerate a harsh environment and maintain normal growth, in recent years, more

and more researches have begun to pay attention to how the ubiquitination process of plants works under various stresses.

The 26s-proteasome-mediated ubiquitination degradation pathway (ubiquitin/26s proteasome) is central to apoptosis (Kurepa et al., 2012). The ubiquitination of substrate proteins requires the participation of E1-ubiquitin-activating, E2-ubiquitin-conjugating enzymes, and E3-ubiquitin ligases. First, the cysteine residue (Cys) on the active site of E1 is covalently bound to the terminal glycine of the ubiquitin molecule through a high-energy thioester bond, and Adenosine 5′-triphosphate (ATP) is consumed to activate the ubiquitin (Stone, 2014). Second, the ubiquitin is transferred to the Cys residue of E2 to form an E2-Ub thioester complex. Finally, E3 transfers the ubiquitin from E2 to the substrate protein (Downes et al., 2003). After that, the 26S proteasome degrades the ubiquitinated-modified substrate protein, and the deubiquitinating enzyme hydrolyzes and releases the ubiquitin, which triggers the ubiquitination modification process.

As a key of the ubiquitin-proteasome pathway, E3 ligases are critical in the recognition of target substrates. Because of the importance of E3 ligase, the genes encoding E3 are the most numerous in the same plant genome. For example, in the *Arabidopsis thaliana* genome, approximately 6% of the genes are related to the ubiquitin/26s proteasome pathway (Fu et al., 1999; Yan et al., 2000; Bachmair et al., 2001; Gagne et al., 2002; Kosarev et al., 2002). Two genes encode E1 and are the least numerous. At least 37 genes encode E2 and E2-like proteins, but more than 1,400 genes encode E3 (Smalle and Vierstra, 2004; Mazzucotelli et al., 2006; Vierstra, 2009). E3 ubiquitin ligases can be divided into HECT, Ubox, and RING types, but RING-type ligases can be additionally divided into complex and simple types (Vierstra, 2003). The Cys-rich RING protein was originally named the "*Really Interesting New Gene*" based on its unique domain (Freemont, 1993), the structure of the RING finger domain that binds a pair of zinc atoms is conserved (Yang et al., 2019), and eight conserved docking sites in the domain exist for binding the ubiquitin-E2 intermediate during ubiquitin transfer (Barlow et al., 1994; Borden et al., 1995; Zheng et al., 2000). The RING finger domain is similar to the well-known Zinc-finger domain in structure; however, the Zinc-finger domain functions in the form of DNA-protein binding, whereas the RING-finger domain functions in the form of a protein–protein interaction (Nardelli et al., 1991).

In previous studies, it has been shown that more than 70% of RING-containing proteins in *Arabidopsis thaliana* act as an E3 ubiquitin ligase (Stone et al., 2005). For example, AtATL78 is a RING-type E3 ubiquitin ligase located in the plasma membrane, which promotes ABA-dependent plant stomata closure, and also can participate in cold and drought stress responses. In a study of cold stress response, it was found that compared with the wild-type plants, the transcription levels of cold-stress-induced genes *RD29A*, *RD29B*, *RD20,* and *P5CS1* were significantly upregulated in *atl78* mutants, and lower H_2O_2 accumulation was detected, which indicated that AtATL78 was a negative factor in cold stress regulation (Suh et al., 2016). Research has also investigated the RING-H2 type protein MYB30-INTERACTING E3 LIGASE 1 (MIEL1). In *Arabidopsis*, MIEL1 mediates the degradation of the transcription factor MYB30, which acts as a positive regulator of the hypersensitive cell death program in plants, and it can interact with AtMIEL1 (Marino et al., 2019), the interaction between MIEL1 and MYB30 affected the formation of the plant's waxy layer, weakens the plant's defense ability (Lee et al., 2017), and MIEL1 also negatively regulates ABA signaling by promoting MYB96 turnover (Lee and Seo, 2016). In apples, MdMYB308L is a known target gene identified to interact with MIEL1, it positively regulates cold tolerance and anthocyanin accumulation by interacting with MdbHLH33 and enhancing its binding to MdCBF2 and MdDFR promoters. When MIEL1 interacts with MYB308L, MdMIEL1 directly degrades MdMYB308L through the 26S-proteasome-mediated ubiquitination degradation pathway, thereby reducing the cold tolerance and anthocyanin accumulation promoted by MdMYB308L (An et al., 2017).

Although numerous studies have concluded that RING domain–containing proteins have multiple regulatory roles in plant growth and development, few studies have investigated the function of RING finger family proteins in tea plants. In this study, RING-containing proteins in tea plants were selected from the Tea Plant Information Archive (TPIA), and the predicted responses of RING domain proteins to abiotic and biotic stresses were explored. One of them was proven to have a ubiquitination function and likely contributing to the resistance of *A. thaliana* to abiotic stress.

MATERIALS AND METHODS

Identification of RING Domain-Containing Proteins in the Tea Plant

We downloaded the sequence of 477 RING-containing proteins that have been reported to be present in *Arabidopsis* (Stone et al., 2005) from The Arabidopsis Information Resource (TAIR)[1] and constructed their domains in Pfam[2]. Six different Hidden Markov model (HMM) motifs were collected. HMM-Blast was applied to the protein sequences in the database downloaded from TPIA[3] with HMMer[4] (Mistry et al., 2013). For the prediction and analysis of the domains of these proteins, we used InterPro[5] for the initial appraisal. Pfam (see text footnote 2) and SMART[6] for a secondary verification and determination of redundant domains.

Expression Analysis of RING Finger Family Genes in the Tea Plant

We downloaded the expression levels of these RING family genes under different stresses from TPIA (**Supplementary Table 1**). The gradient of cold treatment was CA1-6h (10°C for 6 h), CA1-7d (4–10°C for 7 days), CA2-7d (0–4°C for 7 days), and

[1]https://www.arabidopsis.org
[2]http://pfam.xfam.org
[3]http://tpia.teaplant.org/
[4]http://www.hmmer.org/
[5]http://www.ebi.ac.uk/interpro/
[6]http://smart.embl.de/

DA-7d [recovery afterward at room temperature (20–25°C) for 7 days] (Wang et al., 2013). Salt and drought treatments were conducted for 24, 48, and 72 h (Zhang et al., 2017). MeJA treatment was applied in gradients of 12, 24, and 48 h (Shi et al., 2015). We calculated the relative ratio of these expression levels to the control, which was normalized by log2 (**Supplementary Figure 1**). When the expression of H2-type genes under stress at any time is upregulated or down-regulated twice as much as the control (**Supplementary Figure 2**), we selected and collected it for Venn diagram analysis (**Figure 2**).

Four Exogenous Hormone Treatments on Branches of the Tea Plant

Tea plants (*Camellia sinensis* var. Sinensis cv. Shuchazao) were collected from the Tea Plant Cultivar and Germplasm Resource Garden in Guohe Town, Anhui Agricultural University. Tea branches having the same growth conditions and divided into four groups, after which they were placed in erlenmeyer flasks containing the same amount of water. After 24 h of adaptation, the water was replaced with 200 mM NaCl solution for Group 1 and with 25% PEG4000 solution for Group 2. Group 3 was treated by smearing 0.25% MeJA on each leaf. Group 4 was treated at 10°C, respectively. The 2nd leaves tissues were collected at seven time points: 0, 6, 12, 24, 36, 42, and 60 h for Group 1; 0, 4, 8, 16, 24, and 36 h for Group 2; at 0, 6, 12, 24, and 36 h for Group 3; 0, 6, 12, 24, 36, 72, and 96 h for Group 4. At each time point, three repeats were performed. Samples were immediately frozen in liquid nitrogen and kept at −80°C for RNA extraction.

Quantitative Real-Time RT-PCR Analysis

Total RNA was extracted using the FastPure Plant Total RNA Isolation Kit (polysaccharides and polyphenolics-Rich) (Vazyme Cat. RC401-01) according to the manufacturer recommendations. The cDNA were synthesized using PrimeScript RT Reagent Kit Perfect Real Time (TaKaRa, Dalian, China; Code: DRR037A) and stored at −20°C for later use. Verifying PCR product-amplification specificity was determined using the fusion curve (55–95°C). The housekeeping gene was glyceraldehyde-3-phosphate dehydrogenase. The RT-qPCR mixture consisted of 10 μL of CHAMQ SYBR qPCR mixture (Vazyme), 7.4 μL of ddH2O, 0.8 μL of upstream and downstream primers, and 1 μl of cDNA. RT-qPCR reacted in the 96-well optical reaction plates at 95°C for 30 s, followed by 40 cycles at 95°C for 5 s and reaction at 60°C for 30 s PCR product amplification specificity was determined using the melting curve (55–95°C). Three biological replicates and three experimental replicates were applied for each sample. The relative expression values were calculated using the $2^{-\Delta\Delta Ct}$ method. In each group, untreated branches were used as control. All primers used for RT-qPCR analysis were recorded in **Supplementary Table 4**.

Subcellular Location Analysis

The steps of subcellular localization analysis were referred to Yoo et al. (2007), and some modifications were made. *CsMIEL1* was constructed on pUC19-GFP vector and transformed into *Arabidopsis* protoplasts of leaves.

In vitro Ubiquitination Assays

The entire *CsMIEL* and *CsMIEL1-C192S* open reading frame was cloned into the pEGX vector and expressed in *Escherichia coli*, the primers are displayed in **Supplementary Table 5**. The *in vitro* ubiquitination assays were performed as described elsewhere (Zhao et al., 2012). For the E3 ubiquitin ligase activity assay, recombinant wheat (*Triticum aestivum*) E1 (GI: 136632), human E2 (UBCH5B; 100 ng), and purified *Arabidopsis* ubiquitin with HIS-tag (UBQ14, AT4G02890; 500 ng) were mixed and used for the assay. The mixture was incubated at 30°C for 2 h, boiled at 100°C for 5 min, and frozen at −20°C until the SDS-PAGE analysis. After Western blotting, the reactants isolated by SDS-PAGE were incubated with GST antibody (1:10,000) and observed using ECL chromogenic solution.

Sequence Alignment and Phylogenetic Analysis

Multiple sequence alignments of the full-length RING proteins were performed by DNAMAN (Version 6.0; Lynnon Corporation, Quebec City, QC, Canada) with default parameters. The phylogenetic tree was constructed with molecular evolutionary genetics analysis (MEGA) software (Version 6.0)[7] (Tamura et al., 2013), using the neighbor-joining (NJ), minimal evolution (ME), and maximum parsimony (MP) methods and the bootstrap test carried out with 1,000 iterations to test the significance of the nodes.

Generation of the Overexpressing Transgenic *Arabidopsis thaliana*

Arabidopsis ecotype *Columbia (Col-0)* plants were grown in Murashige and Skoog (MS) media at 22°C in long day conditions (16 h of light and 8 h of darkness) and used as wild types and for genetic transformation and other analyses. The *Agrobacterium tumefaciens GV3101* strain was grown in LB media supplemented with 50 μg/mL kanamycin and 20 μg/mL rifampicin. The *CsMIEL1-MYC* and *CsMIEL1-C192S-MYC* construct consisted of the coding sequence under the control of a 35S promoter. Transgenic *Arabidopsis thaliana* organisms were generated using floral-dip transformation (Clough and Bent, 1998). All T0 generation seeds were sown on MS medium containing 15 μg/mL glyphosate for selection. RNA was extracted and reverse transcribed into cDNA for semi-quantitative PCR, and finally four *CsMIEL1-MYC* transgenic lines and *CsMIEL1-C192S-MYC* transgenic lines were obtained. Among them, Line 2, 4, and 6 of CsMIEL1 have high expression level, and Line 8 is low. Line 2, 3, and 4 of *C192S* are high, and Line 1 has low expression level (**Supplementary Figure 3**). Through the glyphosate selecting of each generation until the T3 generation, PCR verification assays have confirmed that the overexpressing line is homozygous.

Stress Induction in *Arabidopsis thaliana* Seedlings

Wild-type, *CsMIEL1-MYC*, and *CsMIEL1-C192S-MYC* overexpressing *Arabidopsis thaliana* were sown simultaneously

[7]http://www.megasoftware.net/

in Petri dishes containing the same volume of MS medium under common growth conditions. After 10 days of pre-culture, the seedling of the same size was selected and treated on the MS medium with 100 mM NaCl (Zhang et al., 2008; Kuki et al., 2020), 200 mM mannitol (Malefo et al., 2020), 100 μm of MeJA (Leon-Reyes et al., 2010), and 10°C (Zhang et al., 2008) for another 10 days. Plants were grown for 10 days under normal conditions after pre-culture as controls (Mock). In all biological replicates, at least 50 plants were used for each treatment, and the error bars represent the standard deviation of replicates.

Extraction of Anthocyanin Content

Extraction of anthocyanin was extracted according to Jiang et al. (2017) with some modifications. In total, 0.2 g of plant tissue was quick-frozen in liquid nitrogen for preparation for subsequent experiments. During extraction, plant tissues were fully ground with a ball mill and extracted four times through the addition of a 500 μL extraction buffer. The ratio of the buffer was 80% methanol, 1% hydrochloric acid, and 19% water. After each extraction, the homogenate was centrifuged at 12,000 rpm for 10 min and combined. The absorbance values were measured at 530 nm, and each genotype was repeated at least three times.

Measurement of Plants Growth Index

The plants were stripped from the MS medium, and various growth indicators were measured manually. We recorded the data of all biological replicates for calculating the average and standard deviation. The measurement was all done by one person to control the error.

Statistical Analysis

For statistical analyses, IBM SPSS Statistics version 19 were use. The Tukey's and least significant difference (LSD) multiple comparison tests were used to analyze significant differences between pairs. Differences were considered statistically significant when $^{*}P < 0.05$ and $^{**}P < 0.01$. All the results were based on the average of three parallel experiments.

RESULTS

Classification of RING Protein in *Camellia sinensis*

We downloaded the sequence of the RING family in *Arabidopsis* for analysis of this huge family in the tea plant. After deduplication and comparison, 335 RING-contain proteins were identified. On the basis of the differences in amino acid sequences at these binding sites and the number of amino acids between each site, these 335 domain in tea plant were divided into six categories: RING-H2, RING-HCa, RING-HCb, RING-C2, RING-v, and RING-G. In all types, the amino acid residues at positions 1, 2, 3, 6, 7, and 8 were conserved and consisted of Cys, whereas the amino acid residues 4 and 5 were not conserved. According to the aforementioned classifications, 64% (214) of the RING domain in tea plant were distributed into the RING-H2 group. The metal-ligand positions 4 and 5 are two His residues, which accounted for the name of the RING-H2 group. According to the characteristics of the amino acid residues of metal ligands 4 and 5, the remaining RING types were classified into RING-HCa, HCb, C2, V, and G groups. The differences between HCa and HCb groups corresponded to the number of amino acids between positions 7 and 8. Between metal ligands 7 and 8, the HCa group comprised two and four amino acids, respectively. Few members belonged to the HCb and G groups (only three members and one member, respectively). Similar to *Arabidopsis,* most proteins were the H2 type followed by the HCa type. In contrast to *Arabidopsis thaliana*, among the 477 RING proteins in *Arabidopsis thaliana*, 41 (8.6%) HCb-type proteins were present, whereas only 3 HCbs were present in the tea plants. We downloaded data from the Grape Genome Browser[8] database and performed the same manual search and identification of the RING domain in grapes to compare the RING-containing protein classifications of different species (**Supplementary Table 2**). Apple's data in the table comes from previous reports (Zhang et al., 2008). Among the four species, the distribution of RING domains was consistent; the H2-type domains were the most numerous followed by the HCa-type domains. The number of V-type and C2-type domains in each species was nearly identical, but the number of HCb-type domains differed substantially. Research has speculated that the RING-D domain may only exists in *Arabidopsis thaliana* (Stone et al., 2005). Accordingly, in our search of tea plants and grapes, we did not identify this type of RING domain. But in Apple, a D-type RING domain was found (Zhang et al., 2008). However, no C2-type grape RING domains were found in this selection. Perhaps due to the problem of genome assembly and annotation, the identification in tea plant did not involve S/T-Type, D-type, mH2-type and mHC-type, and the structure of these types was not explained in detail (**Figure 1**).

We predict other motifs of RING finger proteins in tea plants. The results indicated that 235 members exhibited no other motifs and contained only the RING finger domain. An additional 17 domains were identified in the remaining RING-containing proteins, such as the WD40 domain, IBR domain, and other motifs with unknown functions (**Supplementary Table 3**). The WD40 domain is cited as a binding module for pSer/Thr. Additionally, when present in ubiquitin ligase, the WD40 domain may also be related to the phosphorylation of the relevant substrate (Deshaies, 1999; Koepp et al., 1999; Nakayama et al., 2000). The IBR domain is a common Cys-rich region located between two RING domains, but its function is unknown (van der Reijden et al., 1999). The identification of numerous domains suggests that the RING-containing proteins in tea plants may have multiple regulation or regulated mechanisms and perform diverse functions.

Selection of RING-Containing Proteins Involved in Stress Resistance

To figure out the RING finger genes related to stress responses in tea plants, we analyzed the induced expression difference data of 335 genes provided by TPIA under different stresses. Abiotic stresses included cold, salt, and drought treatments. Responses

[8]https://www.genoscope.cns.fr/externe/GenomeBrowser/Vitis/

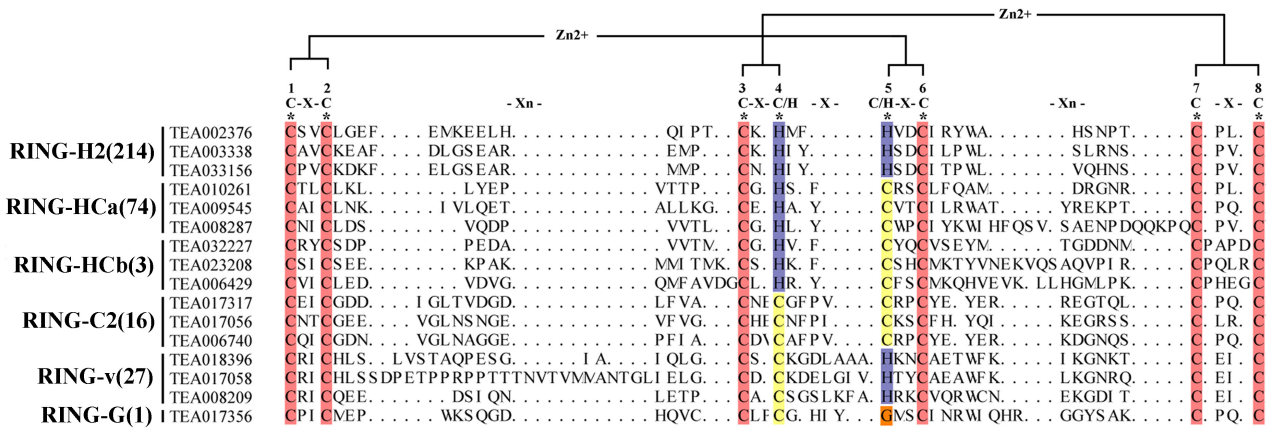

FIGURE 1 | Structural analysis of RING finger domains. Bracketed numbers represent the amount in each RING domain. *Eight conserved docking sites. Red represents amino acid conserved sites, other colors represent different residues.

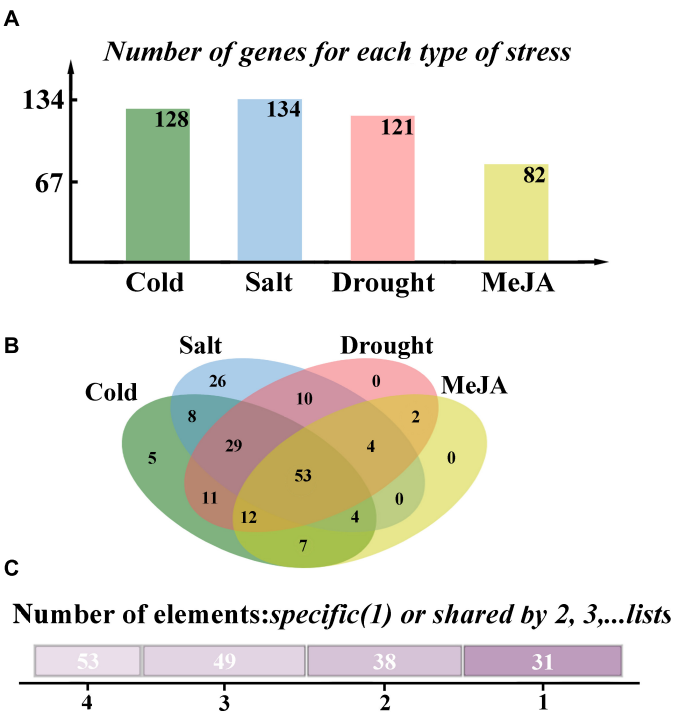

D

Names	Total	Genes
Respond to all stresses	53	TEA014374、TEA021740、TEA005436、TEA008163、TEA015849、TEA021476、TEA016910、TEA005449、TEA024404、TEA028518、TEA003799、TEA027131、TEA007355、TEA005672、TEA004205、TEA030268、TEA022988、TEA025633、TEA003950、TEA022172、TEA003760、TEA002444、TEA021873、TEA033737、TEA007023、TEA021039、TEA026272、TEA003023、TEA030881、TEA004728、TEA024051、TEA000957、
Only respond to cold stress	5	TEA020403、TEA009806、TEA001776、TEA017845、TEA003928
Only respond to salt stress	26	TEA025991、TEA030586、TEA018396、TEA032227、TEA003400、TEA018320、TEA000134、TEA003897、TEA019597、TEA015571、TEA002123、TEA024791、TEA021622、TEA023147、TEA026792、TEA016278、TEA032680、TEA030713、TEA025141、TEA027349、TEA032257、TEA022529、TEA015630、TEA026041、TEA012016、TEA010971

FIGURE 2 | Selection of RING-containing proteins in response to stresses in tea plants. **(A)** Number of genes responding to various types of stresses. **(B)** Venn diagram of genes responding to different stresses. **(C)** The number of genes responding to stresses at the same time. **(D)** List of genes responding to different stresses.

to biological stress were simulated by detecting the response of plants to exogenous methyl jasmonate (MeJA). Differentially expressed H2-type RING genes were individually compared and analyzed, and the results are presents in **Supplementary Figure 2**. **Figure 2A** reports the number of genes responding to various stresses. In total, 128, 134, 121, and 82 genes responded to cold stress, salt stress, drought stress, and exogenous MeJA treatment, respectively. A Venn diagram indicates that 53 genes responded to all stresses (cold stress, drought stress, salt stress, and MeJA treatment), and 31 genes respond to only one form of stress. A total of 26 genes responded only to salt stress, and five responded only to cold stress. However, no gene responded only to drought stress or MeJA treatment (**Figures 2B,C**). These findings are reported in **Figure 2D**.

To verify the response of these genes to stress, we treated the branches of tea plants with a low degree of lignification with

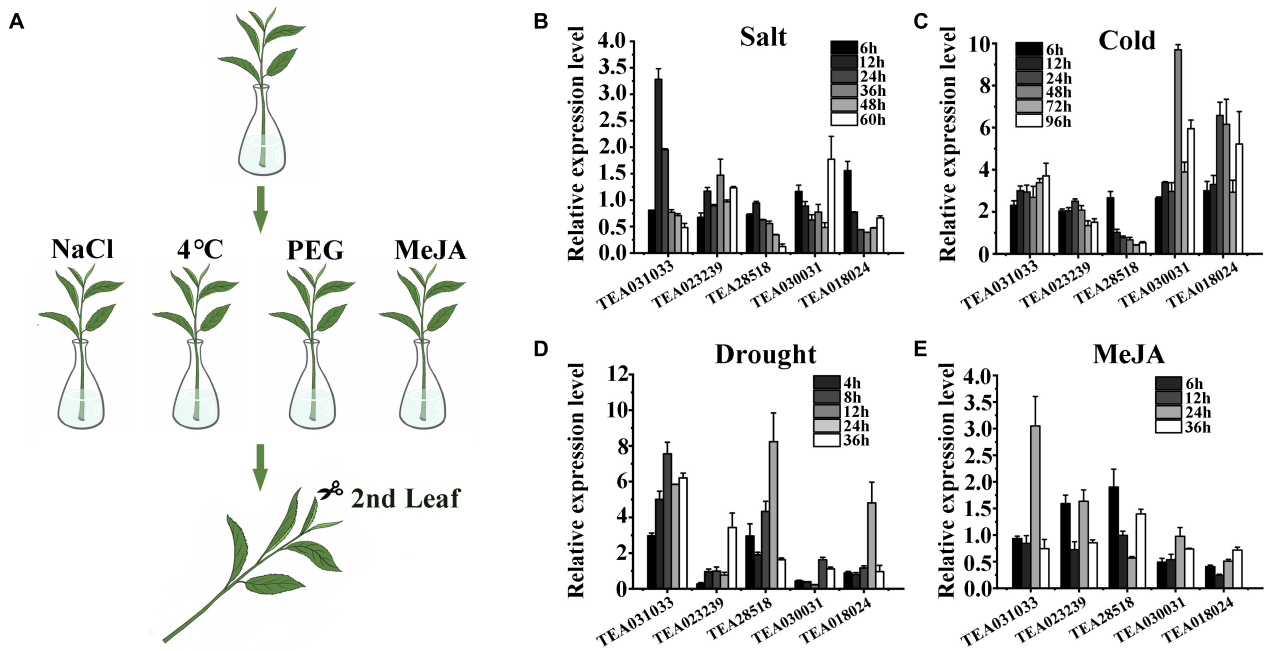

FIGURE 3 | Validation of transcriptomic data by quantitative real-time analysis. **(A)** Schematic of four stress treatments on branches of the tea plant. **(B–E)** Quantitative real-time analysis data of five selected genes subjected to four stresses.

NaCl, PEG4000, a low-temperature condition, and exogenous MeJA to simulate the four selected stresses. After the treatments were completed, RNA was extracted from the second leaf and reverse transcribed into cDNA for Quantitative real-time RT–PCR analysis (RT-qPCR) (**Figure 3A**). In the process of designing and RT-qPCR primers, we found that for many genes, the target fragments could not be cloned, or the amplified products were not specific, and most genes could not design primers with an efficiency of 90–110%. This may be caused by genome assembly and annotation issues. Therefore, we selected five genes that met the requirements of amplification efficiency for RT-qPCR: TEA031033, TEA023239, TEA28518, TEA030031, and TEA018024. The results of the RT-qPCR analysis indicated that gene responses to salt and MeJA were relatively low (**Figures 3B,E**), but responses to drought and cold were more substantial (**Figures 3C,D**). Among the selected genes, TEA031033 had the strongest response when treated with NaCl for 12 h: the response was 3.28 times that of the control (**Figure 3B**). After 24 h of MeJA treatment, the expression level of TEA031033 was approximately three times that of the control (**Figure 3E**), which also represented the most considerable gene response to exogenous MeJA. TEA030031 and TEA018024 responded significantly to cold stress; their strongest response to cold stress were 9.6 and 6.6 times that of the control, respectively (**Figure 3C**), but TEA030031 had a weak response to salt, drought, and MeJA treatment. Under drought stress, the strongest response values of TEA28518, TEA031033, and TEA018024 were 8.23, 7.55, and 4.8 times that of the control, respectively. These five genes exhibited different levels of response to biotic and abiotic stresses, but TEA031033 had a relatively high level of response to all four types of stress. Therefore, we conducted an in-depth investigation on this gene to identify its specific function in tea plants.

CsMIEL1 as an E3 Ubiquitin Ligase

We cloned TEA031033 and compared its sequence with that of other species. Our results indicated that TEA031033 has a RING finger domain at the C-terminus and a Zinc-finger domain at the N-terminus (**Figure 4A**). The phylogenetic analysis results indicated that AtMIEL1 had the highest homology with TEA031033 (**Figure 4B**). Consequently, TEA031033 was named CsMIEL1. Subcellular localization results show that *CsMIEL1* is localized in the nucleus (**Supplementary Figure 4**).

First, to verify the specific function of CsMIEL1 in tea plants, we investigated the potential presence of E3 ubiquitin ligase activity, an *in vitro* ubiquitination assay was conducted. We cloned the open reading frame of the *CsMIEL1* and C192S site-directed mutagenesis, the 192th residue of C192S was changed from Cys to Ser (**Figure 5A**). Polyubiquitinated CsMIEL1 were found in the presence of ATP, ubiquitin, E1, E2, and CsMIEL1-GST fused proteins using an anti-GST antibody, an absence of any factor had cause CsMIEL1 to not be ubiquitinated. However, even in the presence of all the auxiliary factors, no polyubiquitin CsMIEL1-C192S was detected in assays (**Figure 5B**). As a result, we concluded that the RING finger family protein CsMIEL1 exhibited E3 ubiquitin ligase activity and that this ubiquitination activity was lost after mutation at position 192. Moreover, we concluded that the complete RING domain is

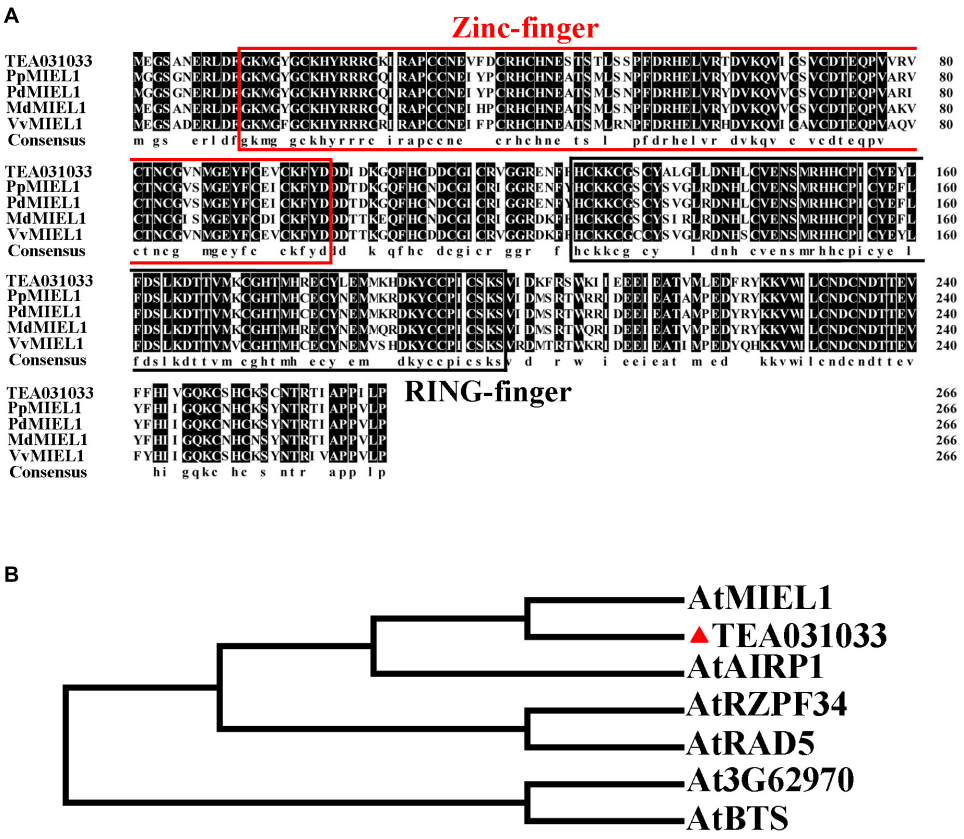

FIGURE 4 | Bioinformatics analysis of CsMIEL1. **(A)** Amino acid sequence alignment of MIEL1 in different species. **(B)** Phylogenetic analysis of TEA031033 and RING-containing proteins in *Arabidopsis*.

necessary to preserve the E3 ubiquitin ligase activity of the RING finger protein.

Overexpression of *CsMIEL1* Alters Root Development Under Various Stresses

To investigate the functions of CsMIEL1, we obtained *35S: CsMIEL1-MYC* and *35S: CsMIEL1-C192S-MYC* overexpressing *Arabidopsis* plants. The four selected stress treatments were performed on the wild-type, *CsMIEL1-MYC*, and *CsMIEL1-C192S-MYC*, respectively (**Figure 6A**). For the transgenic plant seedlings and wild-type seedlings grown at room temperature for 10 days without any exogenous hormones, no significant differences existed across the growth indicators, including leaf length (LL) and width (WL), hypocotyl length (LH), and root number and length (**Figure 6B**).

Under salt stress conditions, the growth of both transgenic plant seedlings and wild-type (WT) seedlings was inhibited. The growth of *CsMIEL1-MYC* transgenic plants was less pronounced than that of wild-type and *CsMIEL1-C192S-MYC* plants, which was reflected in the significantly longer length of the petiole (LP) and primary root (LPR) compared with the control (**Figure 6C**). Similarly, under drought stress, the growth of the transgenic plant and wild-type seedlings was also inhibited, but the length of the primary root (LPR) and hypocotyl (LH) and the number of lateral roots (NL) of *CsMIEL1-MYC* transgenic plants were significantly greater than those of the control and *CsMIEL1-C192S-MYC* (**Figure 6D**).

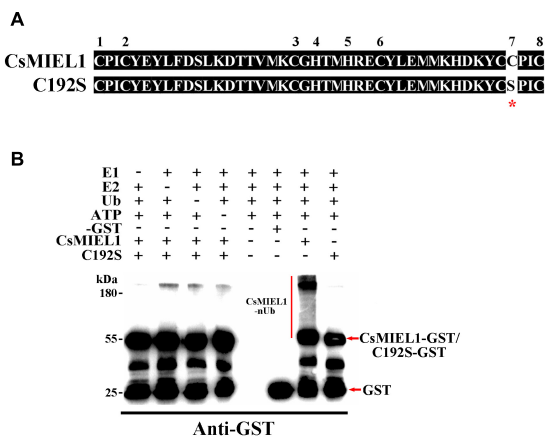

FIGURE 5 | Verification of the activity of CsMIEL1. **(A)** Comparison of the amino acid sequence of CsMIEL1 and CsMIEL1-C192S. **(B)** *In vitro* ubiquitination analysis of CsMIEL1 and CsMIEL1-C192S. *Sited-directed mutagenesis position.

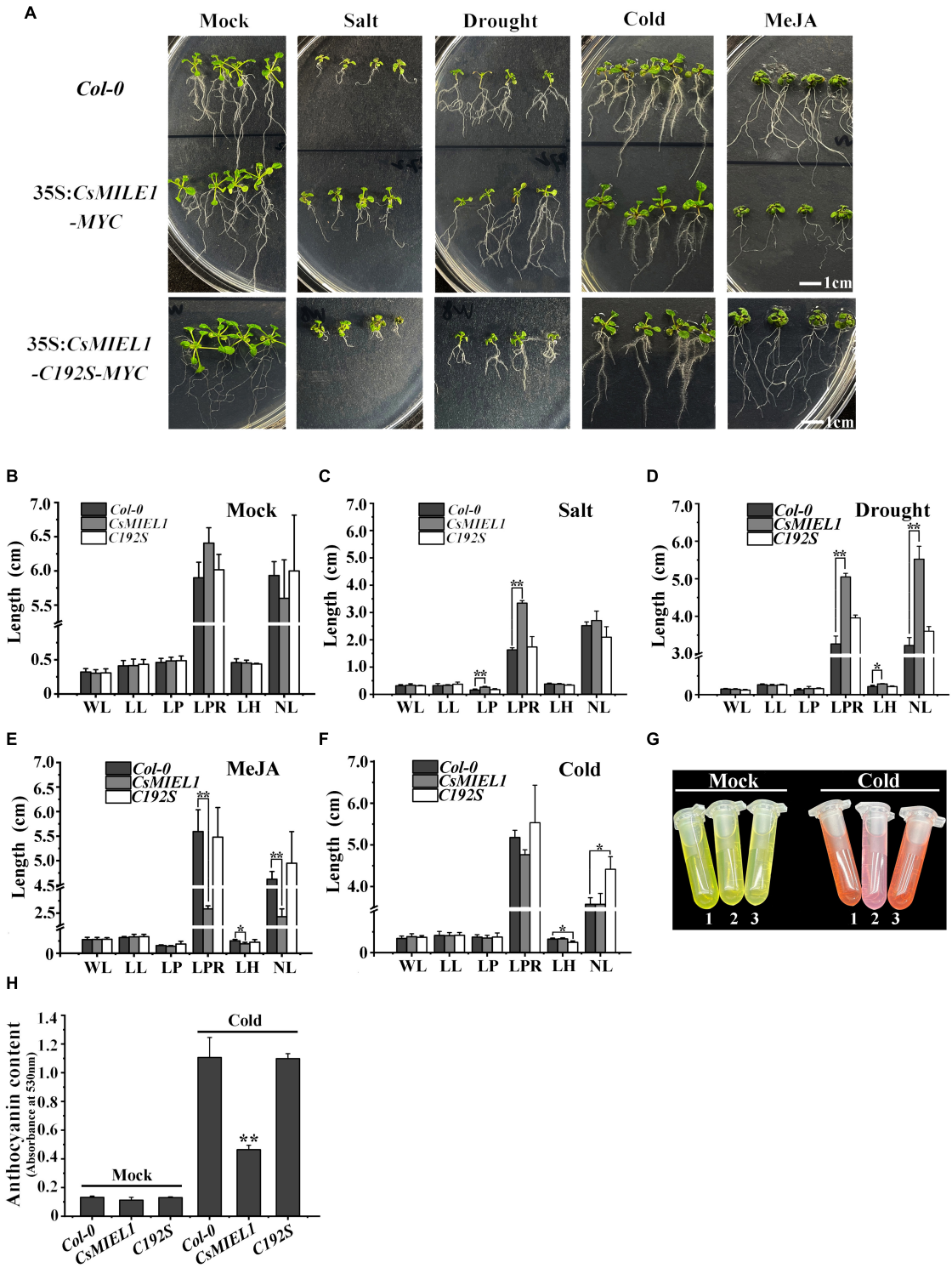

FIGURE 6 | Resistance experiment of transgenic *Arabidopsis* plants to four stresses. **(A)** Four stress treatments for wild-type (*Col-0*), *CsMIEL1*, and *CsMIEL1-C192S* overexpressing *Arabidopsis thaliana* seedlings. **(B–F)** Data on each index of the three types of seedlings under the four stress treatments. Mock, Seedlings without stress treatment; WL, Width of leaf; LL, Length of leaf; LP, Length of petiole; LPR, Length of primary root; LH, Length of hypocotyl; NL, Number of lateral roots. **(G,H)** Anthocyanin concentration of three *Arabidopsis* genotype under cold stress and normal conditions. In all biological replicates, at least 50 plants were used for each treatment, and the error bars represent the standard deviation of replicates. The asterisks indicate the significance level (*$P < 0.05$, **$P < 0.01$) based on the LSD's honestly significant difference test.

The effect of cold treatment on the growth of all seedlings was not particularly notable. The difference in growth indicators between *CsMIEL1-MYC* transgenic plants and WT did not reach a significant level, although its primary root length (LPT) was lower than these of wild-type and *CsMIEL1-C192S-MYC* transgenic plants (**Figure 6F**). Under low-temperature conditions, the anthocyanin levels of *CsMIEL1-MYC* transgenic plants were significantly lower than these in the control and *CsMIEL1-C192S-MYC* transgenic plants (**Figures 6G,H**).

The result in **Figure 6E** showed that *CsMIEL1*-overexpressing plants were hypersensitive to MeJA and that the growth of the root system of the *CsMIEL1-MYC* transgenic plant was significantly inhibited. Additionally, after these three genotypes were treated with exogenous MeJA, the primary root length (LPT), hypocotyl length (LH), and lateral root number (NL) of the *CsMIEL1*-overexpressing plants were shorter than those of the wild-type and *CsMIEL1-C192S-MYC* transgenic plants.

DISCUSSION

RING finger proteins are vital in plant growth, development, and stress resistance (Deshaies and Joazeiro, 2009). Researchers have thoroughly investigated the RING finger family in *Arabidopsis*; at least 477 RING proteins have been identified (Stone et al., 2005; Yang et al., 2016), and many genes encoding RING domain proteins have been proven to be involved in cold stress (Dong et al., 2006; Suh et al., 2016), heat stress (Lim et al., 2013; Liu et al., 2016), drought stress (Lee et al., 2009; Ryu et al., 2010), salt stress (Qin et al., 2008; Fang et al., 2015), sugar treatment (Huang et al., 2010), and defense responses (Huang et al., 2010; Marino et al., 2019). Although RING proteins have been reported in many species, few studies have explored RING finger family proteins in tea plants. In this study, we could at least find 335 genes encoding RING proteins from tea plants genome. It can be seen that RING finger proteins is a superfamily in the plant kingdom.

In order to understand the role of RING finger proteins in the resistance of tea plants, we used the transcriptome sequencing data provided by the TPIA to select the RING finger genes involved in the resistance of tea plants to biotic and abiotic stresses. By comparing their gene expression differences, a total of 53 H2-type genes encoding RING proteins were found to respond to cold stress, drought stress, salt stress, and MeJA treatments. This also shows that the RING finger proteins family may be widely involved in the anti-stress effects of tea plants. Among them, TEA031033 was selected for function confirmation in this paper, due to its relatively high level of response to all four types of stress.

The protein cloned from TEA031033 is highly conserved with the MIEL proteins reported in other species (Lee and Seo, 2016; An et al., 2017), and named as CsMIEL1. CsMIEL1 contains a Zinc-finger domain at the N-terminus and a RING finger domain at the C-terminus, with 79.78% sequence identity with AtMIEL1 and 83% sequence identity with MdMIEL1. *In vitro* ubiquitination analysis has confirmed that CsMIEL1 has ubiquitin ligase activity, and its 192th amino acid Cys is closely related to its ubiquitination activity. Under exogenous hormones treatments, overexpressing *CsMIEL1* transgenic plants showed a certain degree of resistance to salt stress and drought stress and were hypersensitive to exogenous MeJA. But *C192S* transgenic plants did not show the same response to these stresses as *CsMIEL1*, and most were no different from wild-type.

The lack of understanding of the targets of MIEL1 limits our understanding of the diversity of their responses to stress. E3 ubiquitin ligases often function by interacting with their target proteins. AtMYB30, acts as a positive regulator of the hypersensitive cell death program in plants, and it can interact with AtMIEL1 (Marino et al., 2019). Besides, AtMIEL1 can also change the response to ABA by interacting with AtMYB96 (Lee and Seo, 2016). MdMYB308L is a known target gene identified to interact with MIEL1. It positively regulates cold tolerance and anthocyanin accumulation by interacting with MdbHLH33 and enhancing its binding to MdCBF2 and MdDFR promoters, while apple RING E3 ubiquitin ligase MdMIEL1 decreases the cold tolerance and anthocyanin accumulation promoted by MdMYB308L and directly degrade MdMYB308L (An et al., 2017). The response of *CsMIEL1* overexpressing plants to various stresses indicates the diversity of downstream target proteins. Consequently, the selection of CsMIEL1-interacting proteins is particularly critical for future research. In the previous studies, MIEL1 has a negative regulatory effect on both salt and drought stress, which is contrary to our results, while CsMIEL1's regulation of cold stress was similar to MIEL1 in apples. Because E3s have a high selectivity for downstream proteins, we speculate that the downstream target protein of CsMIEL1 may not be homologous to the target protein reported in previous studies. We also need a variety of other methods (such as yeast library screening) to screen and identify the target protein.

DATA AVAILABILITY STATEMENT

The datasets presented in this study can be found in online repositories. The names of the repository/repositories and accession number(s) can be found in the article/**Supplementary Material**.

AUTHOR CONTRIBUTIONS

HR and GM were responsible for using the HMMer search sequence. TL was mainly responsible for the classification and deduplication of sequences. DX was responsible for the remaining work and writing of the manuscript. LG and TX conceived and designed the study. LG drafted the manuscript. All authors contributed to the article and approved the submitted version.

FUNDING

We thank the National Natural Science Foundation of China (31870677, 31870676, 32072621, and 31902069), National Key Research and Development Program of China

(2018YFD1000601), and Natural Science Foundation of Anhui Province, China (1908085MC100).

ACKNOWLEDGMENTS

Thanks to Yang (China Agricultural University, Beijing, China) for providing E1, E2, and ubiquitin fusion proteins for *in vitro* ubiquitination assay. Thanks to Zheng (Anhui Agricultural University, Hefei, China) for supporting my work and accompanying me in daily life.

SUPPLEMENTARY MATERIAL

The Supplementary Material for this article can be found online at: https://www.frontiersin.org/articles/10.3389/fpls.2021.733287/full#supplementary-material

REFERENCES

An, J. P., Liu, X., Li, H. H., You, C. X., Wang, X. F., and Hao, Y. J. (2017). Apple RING E3 ligase MdMIEL1 inhibits anthocyanin accumulation by ubiquitinating and degrading MdMYB1 protein. *Plant Cell Physiol.* 58, 1953–1962. doi: 10.1093/pcp/pcx129

Avin-Wittenberg, T. (2019). Autophagy and its role in plant abiotic stress management. *Plant Cell Environ.* 42, 1045–1053. doi: 10.1111/pce.13404

Bachmair, A., Novatchkova, M., Potuschak, T., and Eisenhaber, F. (2001). Ubiquitylation in plants: a post-genomic look at a post-translational modification. *Trends Plant Sci.* 6, 463–470. doi: 10.1016/S1360-1385(01)02080-5

Barlow, P. N., Luisi, B., Milner, A., Elliott, M., and Everett, R. (1994). Structure of the C3HC4 Domain by 1H-nuclear magnetic resonance spectroscopy: A new structural class of zinc-finger. *J. Mol. Biol.* 237, 201–211. doi: 10.1006/jmbi.1994.1222

Borden, K. L., Boddy, M. N., Lally, J., O'Reilly, N. J., Martin, S., Howe, K., et al. (1995). The solution structure of the RING finger domain from the acute promyelocytic leukaemia proto-oncoprotein PML. *EMBO J.* 14, 1532–1541. doi: 10.1002/j.1460-2075.1995.tb07139.x

Clough, S. J., and Bent, A. F. (1998). Floral dip a simplified method for Agrobacterium -mediated transformation of Arabidopsis thaliana.pdf. *Plant J.* 16, 735–743. doi: 10.1046/j.1365-313x.1998.00343.x

Dai, J., and Mumper, R. J. (2010). Plant phenolics: extraction, analysis and their antioxidant and anticancer properties. *Molecules* 15, 7313–7352. doi: 10.3390/molecules15107313

Deshaies, R. J. (1999). SCF and Cullin/Ring H2-based ubiquitin ligases. *Annu. Rev. Cell. Dev. Biol.* 15, 435–467. doi: 10.1146/annurev.cellbio.15.1.435

Deshaies, R. J., and Joazeiro, C. A. (2009). RING domain E3 ubiquitin ligases. *Annu. Rev. Biochem.* 78, 399–434. doi: 10.1146/annurev.biochem.78.101807.093809

Dong, C. H., Agarwa, M., Zhang, Y., Xie, Q., and Zhu, J. K. (2006). The negative regulator of plant cold responses, HOS1, is a RING E3 ligase that mediates the ubiquitination and degradation of ICE1. *Proc. Natl. Acad. Sci. U S A* 103, 8281–8286. doi: 10.1073/pnas.0602874103

Downes, B. P., Stupar, R. M., Gingerich, D. J., and Vierstra, R. D. (2003). The HECT ubiquitin-protein ligase (UPL) family in Arabidopsis: UPL3 has a specific role in trichome development. *Plant J.* 35, 729–742. doi: 10.1046/j.1365-313X.2003.01844.x

Fang, H., Meng, Q., Xu, J., Tang, H., Tang, S., Zhang, H., et al. (2015). Knock-down of stress inducible OsSRFP1 encoding an E3 ubiquitin ligase with transcriptional activation activity confers abiotic stress tolerance through enhancing antioxidant protection in rice. *Plant Mol. Biol.* 87, 441–458. doi: 10.1007/s11103-015-0294-1

Freemont, P. S. (1993). The RING finger. A novel protein sequence motif related to the zinc finger. *Ann. N. Y. Acad. Sci.* 684, 174–192. doi: 10.1111/j.1749-6632.1993.tb32280.x

Fu, H., Girod, P. A., Doelling, J. H., van Nocker, S., Hochstrasser, M., Finley, D., et al. (1999). Structure and functional analysis of the 26S proteasome subunits from plants. *Mol. Biol. Rep.* 26, 137–146. doi: 10.1023/A:1006926322501

Gagne, J. M., Downes, B. P., Shiu, S. H., Durski, A. M., and Vierstra, R. D. (2002). The F-box subunit of the SCF E3 complex is encoded by a diverse superfamily of genes in Arabidopsis. *Proc. Natl. Acad. Sci. U S A* 99, 11519–11524. doi: 10.1073/pnas.162339999

Hou, X., Xie, K., Yao, J., Qi, Z., and Xiong, L. (2009). A homolog of human ski-interacting protein in rice positively regulates cell viability and stress tolerance. *Proc. Natl. Acad. Sci. U S A* 106, 6410–6415. doi: 10.1073/pnas.0901940106

Huang, Y., Li, C. Y., Pattison, D. L., Gray, W. M., Park, S., and Gibson, S. I. (2010). SUGAR-INSENSITIVE3, a RING E3 ligase, is a new player in plant sugar response. *Plant Physiol.* 152, 1889–1900. doi: 10.1104/pp.109.150573

Jiang, X., Hou, H., Zhang, S., Liu, Y., Wang, H., Deng, W.-W., et al. (2017). Comparison of phenolic compound accumulation profiles in eight evergreen woody core eudicots indicating the diverse ecological adaptability of *Camellia sinensis*. *Sci. Horticult.* 219, 200–206. doi: 10.1016/j.scienta.2017.03.018

Jones, A. M. (2001). Programmed cell death in development and defense. *Plant Physiol.* 125, 94–97. doi: 10.1104/pp.125.1.94

Koepp, D. M., Harper, J. W., and Elledge, S. J. (1999). How the cyclin became a cyclin regulated proteolysis in the cell cycle. *Cell* 97, 431–434. doi: 10.1016/S0092-8674(00)80753-9

Kosarev, P., Mayer, K. F., and Hardtke, C. S. (2002). Evaluation and classification of RING-finger domains encoded by the Arabidopsis genome. *Genome Biol.* 3:RESEARCH0016. doi: 10.1186/gb-2002-3-4-research0016

Kuki, Y., Ohno, R., Yoshida, K., and Takumi, S. (2020). Heterologous expression of wheat WRKY transcription factor genes transcriptionally activated in hybrid necrosis strains alters abiotic and biotic stress tolerance in transgenic *Arabidopsis*. *Plant Physiol. Biochem.* 150, 71–79. doi: 10.1016/j.plaphy.2020.02.029

Kurepa, J., Wang, S., and Smalle, J. (2012). The role of 26S proteasome-dependent proteolysis in the formation and restructuring of microtubule networks. *Plant Signal. Behav.* 7, 1289–1295. doi: 10.4161/psb.21543

Lee, H. G., Kim, J., Suh, M. C., and Seo, P. J. (2017). The MIEL1 E3 ubiquitin ligase negatively regulates cuticular wax biosynthesis in arabidopsis stems. *Plant Cell Physiol.* 58, 1249–1259. doi: 10.1093/pcp/pcx065

Lee, H. G., and Seo, P. J. (2016). The Arabidopsis MIEL1 E3 ligase negatively regulates ABA signalling by promoting protein turnover of MYB96. *Nat. Commun.* 7:12525. doi: 10.1038/ncomms12525

Lee, H. K., Cho, S. K., Son, O., Xu, Z., Hwang, I., and Kim, W. T. (2009). Drought stress-induced Rma1H1, a RING membrane-anchor E3 ubiquitin ligase homolog, regulates aquaporin levels via ubiquitination in transgenic Arabidopsis plants. *Plant Cell* 21, 622–641. doi: 10.1105/tpc.108.061994

Leon-Reyes, A., Van der Does, D., De Lange, E. S., Delker, C., Wasternack, C., Van Wees, S. C., et al. (2010). Salicylate-mediated suppression of jasmonate-responsive gene expression in *Arabidopsis* is targeted downstream of the jasmonate biosynthesis pathway. *Planta* 232, 1423–1432. doi: 10.1007/s00425-010-1265-z

Lim, S. D., Cho, H. Y., Park, Y. C., Ham, D. J., Lee, J. K., and Jang, C. S. (2013). The rice RING finger E3 ligase, OsHCI1, drives nuclear export of multiple substrate proteins and its heterogeneous overexpression enhances acquired thermotolerance. *J. Exp. Bot.* 64, 2899–2914. doi: 10.1093/jxb/ert143

Liu, J., Zhang, C., Wei, C., Liu, X., Wang, M., Yu, F., et al. (2016). The RING finger ubiquitin E3 Ligase OsHTAS enhances heat tolerance by promoting H2O2-induced stomatal closure in rice. *Plant Physiol.* 170, 429–443. doi: 10.1104/pp.15.00879

Malefo, M. B., Mathibela, E. O., Crampton, B. G., and Makgopa, M. E. (2020). Investigating the role of Bowman-Birk serine protease inhibitor in *Arabidopsis* plants under drought stress. *Plant Physiol. Biochem.* 149, 286–293. doi: 10.1016/j.plaphy.2020.02.007

Marino, D., Froidure, S., Canonne, J., Khaled, S. B., Khafif, M., Pouzet, C., et al. (2019). Addendum: Arabidopsis ubiquitin ligase MIEL1 mediates degradation of the transcription factor MYB30 weakening plant defence. *Nat. Commun.* 10:1475. doi: 10.1038/s41467-019-09341-4

Mazzucotelli, E., Belloni, S., Marone, D., De Leonardis, A. M., Guerra, D., Di Fonzo, N., et al. (2006). The E3 ubiquitin ligase gene family in plants_ regulation by degradation. *Curr. Genom.* 7, 509–522. doi: 10.2174/138920206779315728

Mistry, J., Finn, R. D., Eddy, S. R., Bateman, A., and Punta, M. (2013). Challenges in homology search: HMMER3 and convergent evolution of coiled-coil regions. *Nucleic Acids Res.* 41:e121. doi: 10.1093/nar/gkt263

Munns, R., and Tester, M. (2008). Mechanisms of salinity tolerance. *Annu. Rev. Plant Biol.* 59, 651–681. doi: 10.1146/annurev.arplant.59.032607.092911

Nakayama, K., Nagahama, H., Minamishima, Y. A., Matsumoto, M., Nakamichi, I., Kitagawa, K., et al. (2000). Targeted disruption of Skp2 results in accumulation of cyclin E and p27Kip1, polyploidy and centrosome overduplication. *EMBO J.* 19, 2069–2081. doi: 10.1093/emboj/19.9.2069

Nardelli, J., Gibson, T. J., Vesque, C., and Charnay, P. (1991). Base sequence discrimination by zinc-finger DNA-binding domains. *Nature* 349, 175–178. doi: 10.1038/349175a0

Qin, F., Sakuma, Y., Tran, L. S., Maruyama, K., Kidokoro, S., Fujita, Y., et al. (2008). Arabidopsis DREB2A-interacting proteins function as RING E3 ligases and negatively regulate plant drought stress-responsive gene expression. *Plant Cell* 20, 1693–1707. doi: 10.1105/tpc.107.057380

Ryu, M. Y., Cho, S. K., and Kim, W. T. (2010). The Arabidopsis C3H2C3-type RING E3 ubiquitin ligase AtAIRP1 is a positive regulator of an abscisic acid-dependent response to drought stress. *Plant Physiol.* 154, 1983–1997. doi: 10.1104/pp.110.164749

Shi, J., Ma, C., Qi, D., Lv, H., Yang, T., Peng, Q., et al. (2015). Transcriptional responses and flavor volatiles biosynthesis in methyl jasmonate-treated tea leaves. *BMC Plant Biol.* 15:233. doi: 10.1186/s12870-015-0609-z

Smalle, J., and Vierstra, R. D. (2004). The ubiquitin 26S proteasome proteolytic pathway. *Annu. Rev. Plant Biol.* 55, 555–590. doi: 10.1146/annurev.arplant.55.031903.141801

Stone, S. L. (2014). The role of ubiquitin and the 26S proteasome in plant abiotic stress signaling. *Front. Plant Sci.* 5:135. doi: 10.3389/fpls.2014.00135

Stone, S. L., Hauksdottir, H., Troy, A., Herschleb, J., Kraft, E., and Callis, J. (2005). Functional analysis of the RING-type ubiquitin ligase family of Arabidopsis. *Plant Physiol.* 137, 13–30. doi: 10.1104/pp.104.052423

Suh, J. Y., Kim, S. J., Oh, T. R., Cho, S. K., Yang, S. W., and Kim, W. T. (2016). Arabidopsis Toxicos en Levadura 78 (AtATL78) mediates ABA-dependent ROS signaling in response to drought stress. *Biochem. Biophys. Res. Commun.* 469, 8–14. doi: 10.1016/j.bbrc.2015.11.061

Tamura, K., Stecher, G., Peterson, D., Filipski, A., and Kumar, S. (2013). MEGA6: molecular evolutionary genetics analysis version 6.0. *Mol. Biol. Evol.* 30, 2725–2729. doi: 10.1093/molbev/mst197

van der Reijden, B. A., Erpelinck-Verschueren, C. A., Löwenberg, B., and Jansen, J. H. (1999). TRIADs: A new class of proteins with a novel cysteine-rich signature. *Protein Sci.* 8, 1557–1561. doi: 10.1110/ps.8.7.1557

Vierstra, R. (2003). The ubiquitin/26S proteasome pathway, the complex last chapter in the life of many plant proteins. *Trends Plant Sci.* 8, 135–142. doi: 10.1016/S1360-1385(03)00014-1

Vierstra, R. D. (2009). The ubiquitin-26S proteasome system at the nexus of plant biology. *Nat. Rev. Mol. Cell. Biol.* 10, 385–397. doi: 10.1038/nrm2688

Wang, X. C., Zhao, Q. Y., Ma, C. L., Zhang, Z. H., Cao, H. L., Kong, Y. M., et al. (2013). Global transcriptome profiles of Camellia sinensis during cold acclimation. *BMC Genom.* 14:415. doi: 10.1186/1471-2164-14-415

Yan, N., Yan, N., Doelling, J. H., Falbel, T. G., Durski, A. M., Vierstra, R. D., et al. (2000). The ubiquitin-specific protease family from arabidopsis.AtUBP1 and 2 are required for the resistance to the amino acid analog canavanine. *Plant Physiol.* 12, 1828–1843. doi: 10.1104/pp.124.4.1828

Yang, L., Liu, Q., Liu, Z., Yang, H., Wang, J., Li, X., et al. (2016). Arabidopsis C3HC4-RING finger E3 ubiquitin ligase AtAIRP4 positively regulates stress-responsive abscisic acid signaling. *J. Integr. Plant Biol.* 58, 67–80. doi: 10.1111/jipb.12364

Yang, L., Miao, M., Lyu, H., Cao, X., Li, J., Li, Y., et al. (2019). Genome-wide identification, evolution, and expression analysis of RING finger gene family in solanum lycopersicum. *Int. J. Mol. Sci.* 20:4864. doi: 10.3390/ijms20194864

Yoo, S. D., Cho, Y. H., and Sheen, J. (2007). Arabidopsis mesophyll protoplasts: a versatile cell system for transient gene expression analysis. *Nat. Protoc.* 2, 1565–1572. doi: 10.1038/nprot.2007.199

Zhang, Q., Cai, M., Yu, X., Wang, L., Guo, C., Ming, R., et al. (2017). Transcriptome dynamics of *Camellia* sinensis in response to continuous salinity and drought stress. *Tree Genet. Genom.* 13:78. doi: 10.1007/s11295-017-1161-9

Zhang, X., Liu, S., and Takano, T. (2008). Two cysteine proteinase inhibitors from Arabidopsis thaliana, AtCYSa and AtCYSb, increasing the salt, drought, oxidation and cold tolerance. *Plant Mol. Biol.* 68, 131–143. doi: 10.1007/s11103-008-9357-x

Zhao, Q., Liu, L., and Xie, Q. (2012). In vitro protein ubiquitination assay. *Methods Mol. Biol.* 876, 163–172. doi: 10.1007/978-1-61779-809-2_13

Zheng, N., Wang, P., Jeffrey, P. D., and Pavletich, N. P. (2000). Structure of a c-Cbl-UbcH7 complex_ RING domain function in ubiquitin-protein ligases. *Cell* 102, 533–539. doi: 10.1016/S0092-8674(00)00057-X

Conflict of Interest: The authors declare that the research was conducted in the absence of any commercial or financial relationships that could be construed as a potential conflict of interest.

Publisher's Note: All claims expressed in this article are solely those of the authors and do not necessarily represent those of their affiliated organizations, or those of the publisher, the editors and the reviewers. Any product that may be evaluated in this article, or claim that may be made by its manufacturer, is not guaranteed or endorsed by the publisher.

frontiers in Plant Science

ORIGINAL RESEARCH
published: 22 October 2021
doi: 10.3389/fpls.2021.738445

Metabolic Flow of C6 Volatile Compounds From LOX-HPL Pathway Based on Airflow During the Post-harvest Process of Oolong Tea

Zi-wei Zhou[1,2,3], *Qing-yang Wu*[2,3], *Zi-xin Ni*[2,3], *Qing-cai Hu*[2,3], *Yun Yang*[2,3], *Yu-cheng Zheng*[2], *Wan-jun Bi*[2,3], *Hui-li Deng*[2,3], *Zhen-zhang Liu*[2], *Nai-xin Ye*[2], *Zhong-xiong Lai*[3] *and Yun Sun*[2]*

[1] College of Life Science, Ningde Normal University, Ningde, China, [2] Key Laboratory of Tea Science in Fujian Province, College of Horticulture, Fujian Agriculture and Forestry University, Fuzhou, China, [3] Institute of Horticultural Biotechnology, Fujian Agriculture and Forestry University, Fuzhou, China

OPEN ACCESS

Edited by:
Lanting Zeng,
South China Botanical Garden,
Chinese Academy of Sciences (CAS), China

Reviewed by:
Jason Tzen,
National Chung Hsing University, Taiwan
Jianlong Li,
Guangdong Academy of Agricultural Sciences (GDAAS), China

***Correspondence:**
Yun Sun
sunyun1125@126.com

Specialty section:
This article was submitted to Plant Metabolism and Chemodiversity, a section of the journal Frontiers in Plant Science

Received: 08 July 2021
Accepted: 20 September 2021
Published: 22 October 2021

Citation:
Zhou Z-w, Wu Q-y, Ni Z-x, Hu Q-c, Yang Y, Zheng Y-c, Bi W-j, Deng H-l, Liu Z-z, Ye N-x, Lai Z-x and Sun Y (2021) Metabolic Flow of C6 Volatile Compounds From LOX-HPL Pathway Based on Airflow During the Post-harvest Process of Oolong Tea. Front. Plant Sci. 12:738445. doi: 10.3389/fpls.2021.738445

Aroma is an essential quality indicator of oolong tea, a tea derived from the *Camellia sinensis* L. plant. Carboxylic 6 (C6) acids and their derivative esters are important components of fatty acid (FA)-derived volatiles in oolong tea. However, the formation and regulation mechanism of C6 acid during postharvest processing of oolong tea remains unclear. To gain better insight into the molecular and biochemical mechanisms of C6 compounds in oolong tea, a combined analysis of alcohol dehydrogenase (ADH) activity, *CsADH2* key gene expression, and the FA-derived metabolome during postharvest processing of oolong tea was performed for the first time, complemented by *CsHIP* (hypoxia-induced protein conserved region) gene expression analysis. Volatile fatty acid derivative (VFAD)-targeted metabolomics analysis using headspace solid-phase microextraction–gas chromatography time-of-flight mass spectrometry (HS-SPEM-GC-TOF-MS) showed that the (*Z*)-3-hexen-1-ol content increased after each turnover, while the hexanoic acid content showed the opposite trend. The results further showed that both the ADH activity and *CsADH* gene expression level in oxygen-deficit-turnover tea leaves (ODT) were higher than those of oxygen-turnover tea leaves (OT). The C6-alcohol-derived ester content of OT was significantly higher than that of ODT, while C6-acid-derived ester content showed the opposite trend. Furthermore, the HIP gene family was screened and analyzed, showing that ODT treatment significantly promoted the upregulation of *CsHIG4* and *CsHIG6* gene expression. These results showed that the formation mechanism of oolong tea aroma quality is mediated by airflow in the lipoxygenase–hydroperoxide lyase (LOX-HPL) pathway, which provided a theoretical reference for future quality control in the postharvest processing of oolong tea.

Keywords: oolong tea, C6 compounds, ADH, turn over, hypoxia

INTRODUCTION

Oolong tea, which is derived from the *Camellia sinensis* L. plant, is a well-known traditional Chinese tea. It is favored by consumers owing to its health benefits and pleasant flavor, especially its floral aroma (Ng et al., 2017). Aroma formation in oolong tea mainly results from complicated manufacturing processes (Liu et al., 2018), including solar-withering, turnover, panning, rolling, and drying. To date, about 80 types of volatile aroma compounds have been identified in fresh tea leaves, while more than 300 have been found in oolong tea (Yang et al., 2013). Volatile compounds that constitute oolong aroma are divided into four classes based on their origin, namely, fatty acid derivatives, phenylpropanoids/benzenoids, terpenoids, and norisoprenoids (Fu et al., 2017). Fatty acid (FA) derivatives of carboxylic 6 (C6) volatile compounds are considerably accumulated and transformed during the postharvest processing of oolong tea (Zhou et al., 2020). Postharvest processing imparts the oolong tea with a rich and varied natural floral and fruity aroma. Volatile fatty acid derivatives (VFADs) of C6 compounds, such as hexanal, (*Z*)-3-hexen-1-ol, and hexanoic acid, are not only favorable indicators for tea technicians during oolong tea processing but also precursors of dispersive fruit esters and boiling-point aroma substances.

Polyunsaturated fatty acids (PUFAs), α-linolenic acid, and linoleic acid are oxidatively cleaved by the lipoxygenase–hydroperoxide lyase (LOX-HPL) enzyme system under stress to form C6 aldehydes, which have been shown to undergo enzymatic reduction to form C6 alcohols under the control of alcohol dehydrogenase (ADH) aided by NAD+ (Matsui et al., 1991; Qian et al., 2016). However, based on the aroma metabolism profile of pan-fired green tea (Kawakami and Yamanishi, 1999), An'xi Tieguanyin oolong tea (Guo et al., 2021), and flowery black tea (Shi et al., 2018) the metabolic flow of C6 aldehydes relies on the oxygen supply in the upstream of LOX-HPL pathway. Under hypoxic conditions, C6 aldehydes can be reduced to C6 alcohols, which are then esterified, while under normoxic conditions, C6 aldehydes can be oxidized to C6 acids, which are then esterified (**Figure 1**) (Hao et al., 2016; Qian et al., 2016). Therefore, we speculated that C6 acids, in a competitive relationship with C6 alcohols, accumulate during the postharvest processing of oolong tea.

Presently, there are few reports on the transformation of short-chain aliphatic aldehydes, alcohols, and acids in the plant kingdom. In this study, to verify our prediction and explore the metabolic flow of C6 aldehydes during postharvest processing of oolong tea, normoxic and hypoxic turnover tea leaves were used as research materials with fresh leaves as the control. The dynamics of C6 volatile compounds in manufactured tea leaves, both before and after turnover treatment conducted three times, were compared and analyzed. Furthermore, the response of ADH and its related genes to oxygen in the LOX-HPL pathway was evaluated using an artificial airflow difference. Finally, the transcript levels of hypoxia-induced protein genes were verified. This study aimed to explore the influence of FA metabolism of oolong tea on the formation of aroma quality mediated by airflow factors. The results provided new insights for future research on quality regulation in oolong tea processing.

MATERIALS AND METHODS

Plant Materials and Treatments

Tea process leaves were collected from *C. sinensis* cv. Huangdan at the educational practicing base of Fujian Agriculture and Forestry University (Fuzhou, China) in July 2018. The plucking standard was "one bud and three leaves," referring to one bud and three leaves on the same branch, which is usually used throughout oolong tea manufacture in China. The fresh tea leaves (F) were withered under gentle sunlight (26°C, 150,000 lux) during the late evening for 20 min. Afterward, half of the withered leaves (1,000 g) were shaken three times for 5 min, hourly (T1–T3) until fixation. The sampling points were before and after each turnover. The solar-withered leaves (W) were regarded as leaves before the first turnover (bT1), and the tea leaves before the second and third turnover were regarded as bT2 and bT3, respectively. Similarly, the leaves turned over for the first time were regarded as leaves after the first turnover (aT1), and the tea leaves after the second and third turnover were regarded as aT2 and aT3 (**Figure 2**).

The remaining withered leaves were subjected to both treatment schemes. The first scheme was an oxygen deficiency treatment. The withered leaves were shaken three times on one side of the turnover machine covered in black plastic film (oxygen-deficit-turnover tea leaves, ODT), while the other side served as a positive control (oxygen-turnover tea leaves, OT), and F acted as a negative control (**Figure 3**).

Sampling for each treatment above was repeated at least three times. All other samples above were wrapped in tin foil, fixed using the liquid nitrogen sample-fixing method, and stored in an ultra-low temperature refrigerator at −70°C.

GC-TOF-MS-Based FA-Derived Volatiles

Aroma components were analyzed in accordance with previous studies (Chen et al., 2020), with minor modifications. Processed leaf samples were freeze-dried and ground with a mortar and pestle. The resulting powder (2 g) was transferred to a 20-ml solid-phase microextraction (SPME) bottle and the cap was immediately closed. A 65-μm polydimethylsiloxane/divinylbenzene SPME syringe fiber (Supelco Bel-lefonte, PA, USA) was used for all headspace (HS)-SPME extractions, with an incubation temperature of 80°C, a pre-extraction incubation time of 31 min, and HS-SPME extraction time of 60 min. The aroma components were detected using an Agilent 7890B gas chromatograph (Agilent Co., Santa Clara, CA, USA) coupled with a Pegasus HT time-of-flight mass spectrometer (LECO Co., Saint Joseph, MI, USA) (GC-TOF MS). A capillary column [Rxi-5sil MS, Restek, USA; 30 m × 0.25 mm × 0.25 μm (film thickness)] was employed using high purity helium as the carrier gas at a flow rate of 1 ml/min. Injections were performed in splitless mode using an injection port temperature of 250°C. The transfer line temperature was set to 275°C. The GC oven temperature program was initially held at 50°C for 5 min, followed by a temperature ramp of

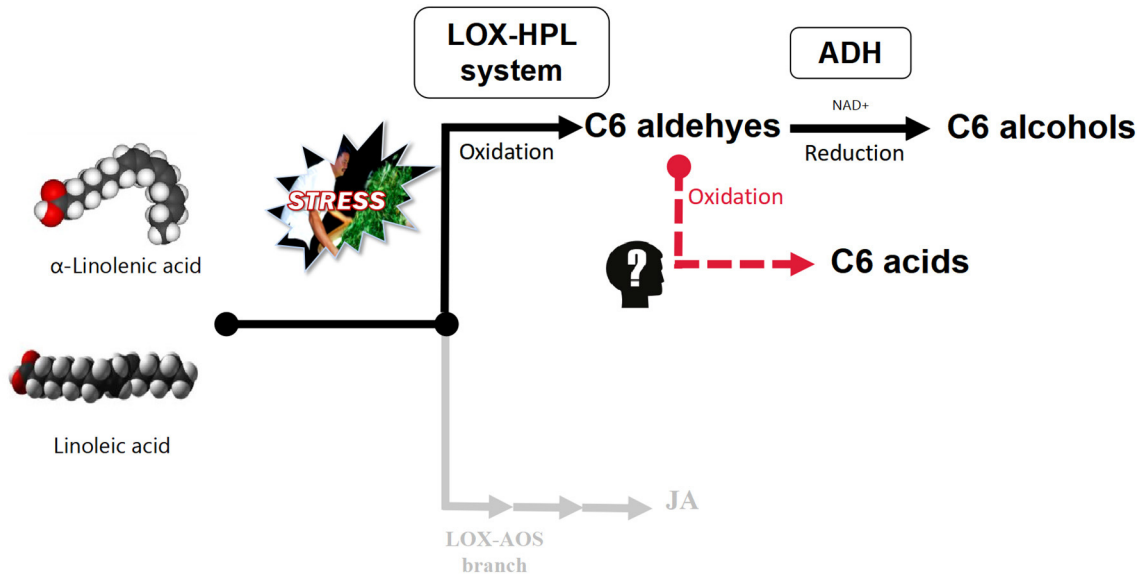

FIGURE 1 | LOX-HPL pathway for C6 compounds derived from long-chain unsaturated fatty acids. Long-chain unsaturated fatty acids (such as α-linolenic acid and linoleic acid) are the precursors of metabolic pathways. The enzyme system composed of LOX (lipoxygenase, EC1.13.11.12) and HPL (hydroperoxide lyase, EC4.1.2.-) oxidatively cleaved long-chain unsaturated fatty acids to form C6 aldehydes, while ADH (alcohol dehydrogenase, EC1.1.1.1) reduced C6 aldehydes to C6 alcohols. However, it was not clear whether C6 aldehydes could form C6 acids through nonenzymatic reactions.

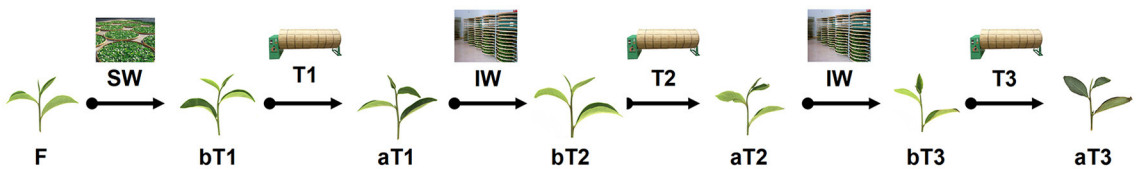

FIGURE 2 | Schematic diagram of sampling points before and after each turnover treatment. F, fresh tea leaves. bT1–bT3, process tea samples before each turnover treatment. aT1–aT3, process tea samples after each turnover treatment. Indoor withering was performed for 30 min between each turnover treatment.

3°C/min to 210°C with a 3-min hold, and a final temperature ramp of 15°C/min to 230°C. The MS operating parameters were as follows: ionization potential, −70 eV; ion source temperature, 250°C; acquisition voltage, 1,530 V; mass range, 30–500 amu; and 10 spectra/s.

ADH Activity Analysis

Alcohol dehydrogenase activity was monitored using an ultraviolet-visible spectrophotometer (Perkin-Elmer, Waltham, MA, USA). Enzyme activity measurements were performed using an ADH activity detection kit following the instructions of the manufacturer (Beijing Solarbio Science & Technology Co., Ltd., China). The ADH activity was calculated using the mass of the original sample, as reported previously (Zhou et al., 2020).

Source of Omics Data

The target gene sequence and functional annotation were based on reference tea plant genome sequences downloaded from the Tea Plant Information Archive (TPIA; http://tpia.teaplant.org/) (Xia et al., 2020). Fragments per kilobase of transcript per million mapped reads (FPKM) values and primer design were based on transcriptome sequencing data previously generated in our laboratory (pending submission). The protein annotation sequence (CSSChrLev20200506PEP) of the chromosome-level genome of *C. sinensis* cv. Shuchazao was downloaded from TPIA, the Stockholm file of the Hidden Markov Model (HMM) of the HIG_1_N domain was obtained from the Pfam database (http://pfam.xfam.org/), and then a seed file of PF04588 was generated. The "hmmbuild" program in the hmmer-3.0-window software package (Eddy and Pearson, 2011) (http://eddylab.org/software/hmmer3/3.0/) was used to build and complete the establishment of the HMM file of HIG. The "hmmsearch" program in the same software package was run to obtain eight candidate *CsHIG* genes, which were denoted *CsHIG1–CsHIG8*.

Gene Expression Analysis

Lyophilized process samples (0.1 g) were ground to powder in liquid nitrogen. Total RNA was extracted from the frozen powder using the RNAprep Pure Plant Kit (Tiangen Biotech Co. Ltd.,

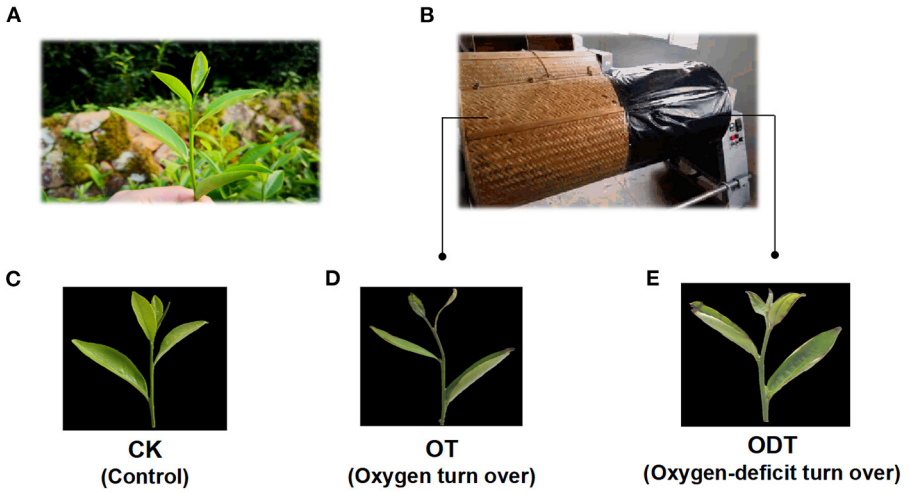

FIGURE 3 | Sampling schematic diagram of oxygen deficiency and normal turnover treatment. **(A)** Fresh leaves were sampled from a tea plant (*Camellia sinensis* cv. Huangdan) in the tea garden. **(B)** *In situ* photographs were taken at the turnover test site. **(C–E)** Apparent imaging of control (CK), oxygen-turnover tea leaves (OT), and oxygen-deficit-turnover tea leaves (ODT).

Beijing, China). cDNA was generated with the PrimeScript RT Reagent Kit with a gDNA Eraser (TaKaRa Biotech Co., Ltd., Dalian, China). Quantitative real-time PCR (qRT-PCR) was performed as previously described using a LightCycler 480 Real-Time PCR System (Roche Molecular Systems, Alameda, CA, USA) (Zhou et al., 2020). The reaction mixture had a total volume of 20 μL, comprising cDNA (1 μL), 2 × TB Green Premix Ex Taq II (TaKaRa; 10 μL), 10 μM forward primer (0.8 μL), 10 μM reverse primer (0.8 μL), and double-distilled water (ddH_2O, 7.4 μL). Amplification reactions were conducted as follows: denaturation for 10 s at 95°C, 40 cycles of 5 s at 95°C, and 20 s between 55 and 60°C using the Tm function of the primers. Fluorescent detection was performed after each extension step. Amplification reactions were conducted as follows: denaturation for 10 s at 95°C, 40 cycles of 5 s at 95°C, and 20 s between 55 and 60°C using the Tm function of the primers. Fluorescent detection was performed after each extension step. The relative expression values were calculated using the comparative CT ($2^{-\Delta\Delta CT}$) method (Livak and Schmittgen, 2001). *CsGAPDH* (NCBI accession number: JKA295375.1) was used as a reference gene. Primer sequences of selected genes were designed by DNAMAN version 7 (Lynnon Biosoft, Vaudreuil, Canada) and are listed in **Supplementary Table 1**, including CSA019598, *CsADH*, CL822.Contig4, CsHIF4, and CsHIF6. Primer synthesis was performed by TSINGKE Co., Ltd (Beijing, China).

Statistical Analysis

All experimental results are provided as mean ± standard error of the mean (SEM). Statistical analysis was conducted using SPSS (PASW Statistics Base 18, IBM, Chicago, IL, USA) to determine significance. Statistical differences between measurements were assessed using Tukey's test ($^*P < 0.05$, $^{**}P < 0.01$) after analysis of variance. All figures were generated using Prism (GraphPad, Version 6.01, GraphPad Software Inc, San Diego, CA, USA).

RESULTS AND DISCUSSION

Changes in C6 Volatile Compounds in LOX-HPL Pathway During Turnover and Indoor-Withering Process

Turnover plays a critical role in the formation of the natural floral and fruity aroma of oolong tea (Zeng et al., 2016). A large number of C6 volatile compounds represented by GLVs (green leaf volatiles) are formed and transformed during the turnover process (Ono et al., 2016). GLVs can be transformed into terpenoid volatiles and provide signaling substances generated by abiotic stress (Hu et al., 2018). Targeted detection of C6 acids and C6 alcohols during the postharvest processing of oolong tea showed that three types of C6 alcohol were detected, namely, hexanol (CAS: 111-27-3), (*Z*)-3-hexen-1-ol (CAS: 928-96-1), and (*E*)-2-hexen-1-ol (CAS: 928-95-0), with hexanoic acid (CAS: 142-62-1) as the only C6 acid detected. Both the C6 acid and C6 alcohols showed an overall increasing trend during the postharvest processing of oolong tea. Among them, the C6 alcohol contents had increased significantly after the third turnover, while hexanoic acid showed the opposite trend. Notably, the turnover stage is conducive to increasing the C6 alcohol content, while the spreading stage promotes C6 acid accumulation. Peak areas representing the total abundance of (*Z*)-3-hexen-1-ol and hexanoic acid showed an increasing trend during the postharvest processing of oolong tea (**Figures 4A–D**), benefiting from sufficient C6 aldehydes from the oxidation and cleavage of PUFAs by the LOX-HPL enzyme system. Correlations were statistically assessed using Spearman's test. A highly significant negative correlation was noted between the peak areas representing the abundances of (*Z*)-3-hexen-1-ol and hexanoic acid ($r = -0.881$, $p < 0.01$) (**Figure 4E**). Therefore, a competitive relationship might exist between C6 alcohols and C6 acids during the postharvest process of oolong tea. In previous studies, C_6 volatile compounds and

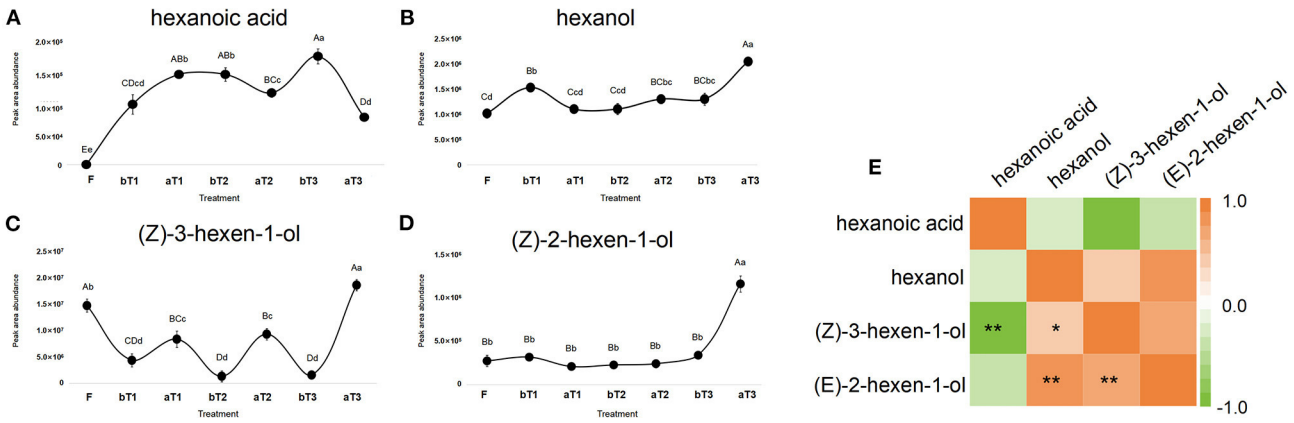

FIGURE 4 | Dynamic changes in C6 acid and C6 alcohols peak area abundance and correlation heat map during postharvest processing of oolong tea. **(A–D)** Dynamic changes of **(A)** hexanoic acid, **(B)** hexanol, **(C)** (*Z*)-3-hexen-1-ol, and **(D)** (*Z*)-2-hexen-1-ol. **(E)** Analysis of correlation heat map between C6 acid and C6 alcohols. F, fresh tea leaves; bT1–bT3, tea leaves before the three turnover treatments; aT1–aT3, tea leaves after the three turnover treatments. Different capital letters (A–D) and lowercase letters (a–d) represent significant differences at the $p < 0.01$ and $p < 0.05$ levels using Tukey's test, respectively. One or two asterisks denote a statistically significant difference (*$P < 0.05$; **$P < 0.01$) in relative amount between C6 acid and C6 alcohols during the turnover process of oolong tea.

their derivatives exhibited disparate changing trends under turnover and indoor-withering treatment (Chen et al., 2018). Furthermore, the activity of LOX, a rate-limiting enzyme in the LOX pathway localized in the chloroplast, can respond to turnover (Liu et al., 2018; Chen et al., 2021). Our research group has reported that C6 volatiles and the structural genes of the LOX pathway can respond to mechanical force during a turnover to form aliphatic aromas in oolong tea (Zhou et al., 2019a,b). However, the nature of the difference between (*Z*)-3-hexen-1-ol and hexanoic acid is relatively unusual and needs to be further explored.

Analysis of ADH and *CsADH* Gene Expression Patterns Under Hypoxic Turnover Conditions

ADH (alcohol dehydrogenase, EC 1.1.1.1), a zinc-containing enzyme involved in short-chain alcohol metabolism in the biological kingdom, reduces C6 aldehydes to C6 alcohols under biotic and abiotic stress in the LOX-HPL pathway (Cirilli et al., 2012). However, C6 aldehydes might be further oxidized to form C6 acids under normoxic conditions. Therefore, the reduction of C6 aldehydes to C6 alcohols by ADH seems to require hypoxic conditions. Changes in external airflow factors can create normoxic or hypoxic conditions during turnover, which might mediate *CsADH* gene transcription levels and ADH activity, affecting the formation of, and changes in, fatty acid aroma components during postharvest processing of oolong tea. The ADH activity and expression levels of three *CsADH* genes in CK, OT, and ODT were measured. The ADH activity was the highest in ODT (0.16 μmol/min/mL), followed by OT (0.09 μmol/min/mL), and lowest in CK (0.03 μmol/min/mL). The ADH activity in ODT was significantly higher than those in CK and OT ($P < 0.01$) (**Figure 5A**). CK, ODT, and OT showed transcription levels of the *CsADH* genes. Three ADH regulatory genes were selected based on previous studies, designated as CSA019598, *CsADH*, and CL822.Contig4 (Zhou et al., 2020). The CL822.Contig4 expression level of ODT was significantly higher than those of CK ($P < 0.01$) and OT ($P < 0.05$), which was significantly positively correlated with the change in ADH activity (**Figure 5B**). However, a different expression pattern was observed for CSA019598 and *CsADH*. These two genes showed the highest expression levels in CK. In OT and ODT, the *CsADH* gene expression level decreased to similar levels (**Figures 5C,D**). However, the CSA019598 expression level decreased significantly and extremely significantly in ODT (0.773) and OT (0.383), respectively. As indicated above, turnover under hypoxic conditions might stimulate ADH activity. CL822.Contig4 might be a key regulatory gene during the postharvest processing of oolong tea. In a previous study, *CsADH* gene expression levels firstly increased and then decreased as the manufacturing process progressed (Hu et al., 2018). However, the potential candidate gene (CSA019598), previously acquired by our research group (Zhou et al., 2020), showed no significant correlation with changes in ADH activity. This might be attributed to the process mode, processing room environment, or even the tea growing season (Sekiya et al., 1984). Based on the comparison of the tea tree genome (CSS, CSA), we found that the gene did not belong to the ADH family, but the 2-alkenal reductase (AER) family. Both AER and ADH genes belonged to the alcohol dehydrogenase (MDR) superfamily. These two amino acid sequences have high similarities (Persson et al., 2008). CsADH gene was one of the members of the AER gene family (Xia et al., 2020). This may be the main reason for the opposite trend of this gene and CSA019598.

Analysis of FA-Derived Volatiles in Oolong tea Under Hypoxic Turnover Conditions

VFAD-targeted analysis of oolong tea manufactured under normoxic and hypoxic conditions (**Figure 6**) showed that

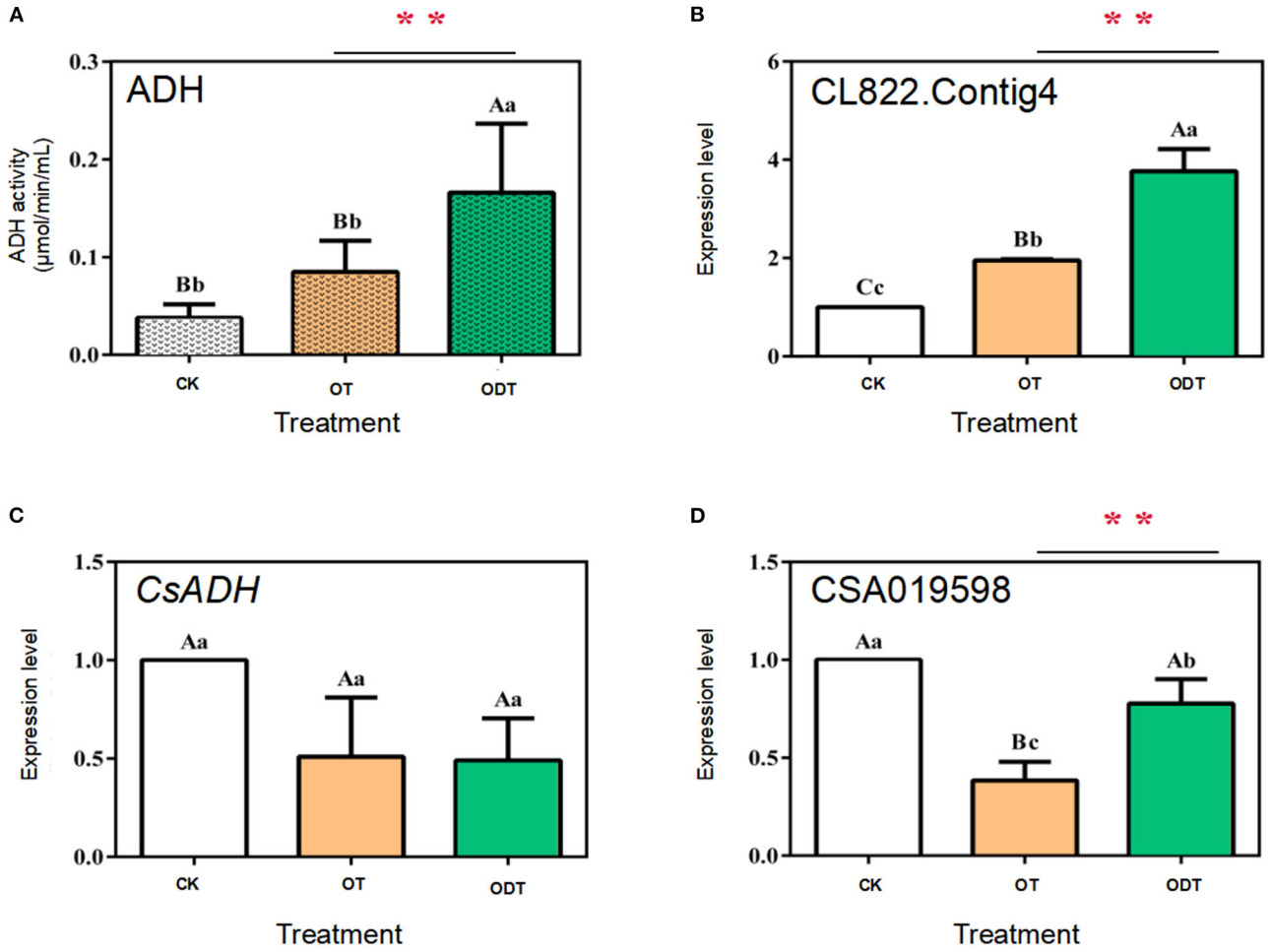

FIGURE 5 | ADH enzyme activity and relative expression levels of three *CsADH* genes under normoxic and hypoxic conditions during the turnover process of oolong tea. **(A)** Enzyme activity of ADH (EC 1.1.1.1); **(B–D)** expression levels of **(B)** CSA019598, **(C)** CSA019598 of *CsADH* (GenBank accession no. HM440157.1), and **(D)** CL822.Contig4. Data are expressed as means ± standard errors of the mean of six independent experiments. Different uppercase letters ($P < 0.01$) and lowercase letters ($P < 0.05$) indicate significant differences among different treatments from Tukey's test. CK (control group) represents fresh tea leaves without any treatment. ODT (oxygen-deficient leaves) represents fresh tea leaves turned over under hypoxic conditions. OT (normal leaves) represents fresh tea leaves turned over under normoxic conditions. Two asterisks denote a statistically significant difference (**$P < 0.01$) in relative amount between ODT and OT during the postharvest processing of oolong tea.

hexanal was detected among C6 aldehydes, with the content (2.31×10^5) in OD being significantly higher than that in ODT (1.66×10^5). Hexanal is the oxidative product of PUFAs in the LOX-HPL enzyme system. This system is beneficial to the oxidative cleavage of substrates under normoxic conditions, thus promoting hexanal accumulation. Hexanoic acid and hexanol were not detected in the manufactured oolong tea and might have been transformed or lost during the fixation, rolling, and drying processes. However, esters derived from hexanoic acid and hexanol indirectly reflected the metabolic flow of hexanal in ODT and OT. Hexanoic acid esters (HAEs) detected were (*E*)-2-hexenyl hexanoate (CAS: 53398-86-0), 4-hexenyl hexanoate (CAS: 31501-11-8), and hexyl hexanoate (CAS: 123-66-0). The contents of these three esters in OT were higher than those in ODT. Among them, the contents of (*E*)-2-hexenyl hexanoate, (7.03×10^4) and hexyl hexanoate (9.1×10^5) in OT were extremely significantly ($P < 0.01$) and significantly ($P < 0.05$) higher than those in ODT (5.59×10^4 and 8.41×10^5, respectively). In contrast, hexanol-derived esters (HAEs) measured included (*Z*)-3-hexen-1-yl benzoate (CAS: 25152-85-6), (*Z*)-3-hexen-1-yl propanoate (CAS: 33467-74-2), (*Z*)-3-hexenyl butanoate (CAS: 16491-36-4), and (*Z*)-3-hexenyl hexanoate (CAS: 31501-11-8). Notably, the contents of these four compounds in OT were lower than those in ODT. Except for (*Z*)-3-hexenyl hexanoate, compounds (*Z*)-3-hexen-1-yl benzoate (3.38×10^5), (*Z*)-3-hexen-1-yl propanoate (9.63×10^4), and (*Z*)-3-hexenyl butanoate (1.43×10^5) had significantly ($P < 0.05$) lower contents in OT than in ODT (3.85×10^5, 1.15×10^4, and 1.86×10^5, respectively). Therefore, OT treatment was conducive to the accumulation of HAEs, while ODT treatment was conducive to the accumulation of HEs.

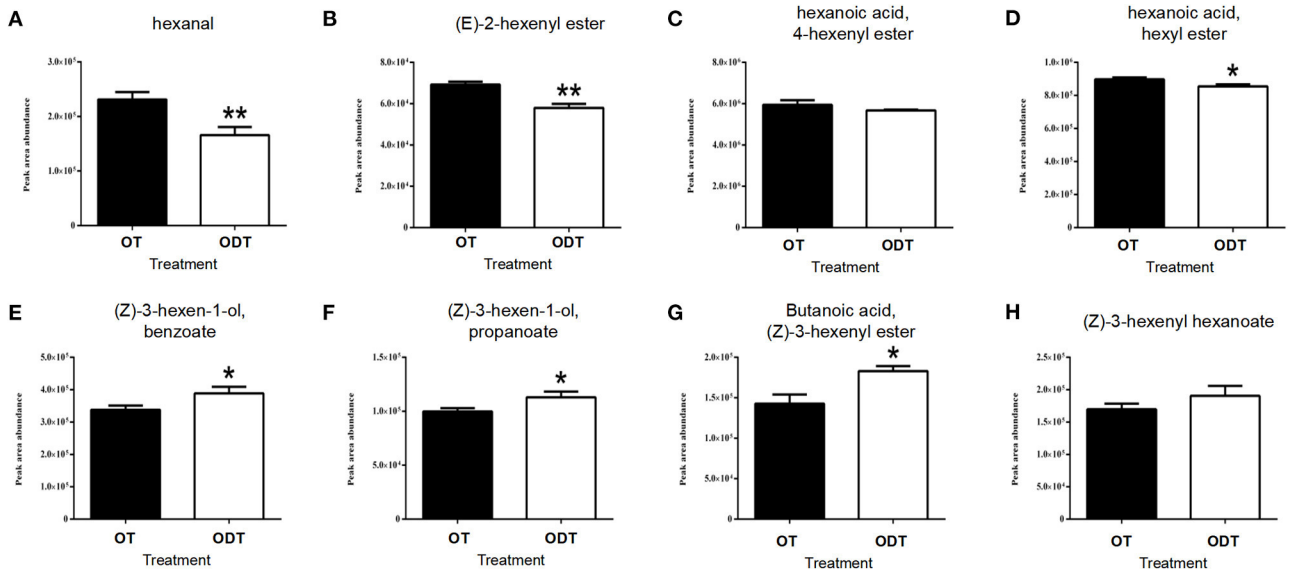

FIGURE 6 | Contents of volatile fatty acid derivatives in raw tea under normoxic and hypoxic conditions during the turnover process of oolong tea. **(A)** Hexanal, **(B)** (*E*)-2-hexenyl ester, **(C)** 4-hexenyl hexanoate, **(D)** hexyl hexanoate, **(E)** (*Z*)-3-hexen-1-yl benzoate, **(F)** (*Z*)-3-hexen-1-yl propanoate, **(G)** (*Z*)-3-hexenyl butanoate, and **(H)** (*Z*)-3-hexenyl hexanoate. Asterisks denote statistically significant differences (*$p < 0.05$; **$p < 0.01$) between relative amounts of OT and ODT. Error bars indicate the standard error (SE) of the mean.

Screening and Analysis of *CsHIP* Genes and Their Expression Patterns Under Normoxic and Hypoxic Conditions During Turnover

Hypoxia-induced protein is a common signal protein responding to hypoxic stress in higher eukaryotes. Current research on the stable expression of hypoxia-induced factor (HIF)-related genes depends on oxygen deficiency in mammals. HIF-α, a subclass of HIF, is hydroxylated with sufficient oxygen and ubiquitinated by von Hippel–Lindau disease and degradation (Kaelin, 2017). HIF-α is not degraded with increasing oxygen concentration in the atmosphere, promoting the expression of a hypoxia target gene and enhancing cell adaptability (Gregg et al., 2013). To further demonstrate the response degree of manufactured tea leaves to oxygen factors in normoxic and hypoxic microenvironments, whole-genome identification was conducted for the *CsHIG* gene family, and the potential key transcripts of *CsHIG* genes were discovered.

Information on the candidate *CsHIG* gene and its main physical and chemical properties are shown in **Supplementary Table 2**. The results showed that 8 *CsHIG* gene family members were scattered on the chromosomes. The length of the gene coding sequence (CDS) was 297–303 bp, except for the CsHIG7 member. The number of amino acids in the encoded protein was 98–100 and the molecular weight range was 11,013.71–11,084.74 Da, with CsHIG3 protein having the largest number of amino acids and highest molecular weight. The isoelectric point (pI) distribution range of the protein sequences encoded by the eight *CsHIG* gene family members was 9.07–10.21, and the pI value of CsHIF5 was the largest (10.21). The aliphatic index ranged from 86.00 to 100.71.

To understand the genetic relationship and evolutionary distance between *CsHIG* gene family members and *HIG* genes of other species, BLASTn homology comparison analysis was performed on the amino acid sequences of the eight tea HIG gene-encoded proteins obtained from the National Center for Biotechnology Information (NCBI) screening. The HIG protein amino acid sequences of cotton, poppy, turnip, peanut, and other species were obtained, and a phylogenetic tree was constructed, as shown in **Figure 7**. BLASTn analysis indicated that *CsHIG5* was clustered with HIG1 (D7SHV8.1) and HIG1 (D7TWS7.1) from grape (*Vitis vinifera*); *CsHIG7* showed high homology with HIG1 from grape (*Vitis vinifera*) and cotton (*Gossypium hirsutum*, *Gossypium raimondii*, and *Gossypium arboreum*). Furthermore, CsHIG2, CsHIG3, CsHIG4, and CsHIG8 showed high sequence homology among the members and were genetically similar to peanuts (*Arachis hypogaea*) and grapes (*Vitis vinifera, Vitis riparia*), while CsHIG1 and CsHIG6 showed high homology with HIG from cotton (*Gossypium hirsutum*, *Gossypium raimondii*, and *Gossypium arboreum*), poppy (*Papaver somniferum*), and turnip (*Brassica rapa*).

Based on the transcript coding region sequence cds.fa database during the postharvest processing of oolong tea, the results of local BLAST of eight *CsHIG* gene family members indicated that the *CsHIG1* and *CsHIG6* scores compared with the transcript Unigene1790_All were 571 and 595, with the similarity reaching 99% and 100%, respectively. Meanwhile, the comparison scores of *CsHIG1* and *CsHIG6* with the transcript CL10755.Contig2_All were 577 and 585, respectively, with similarities for both of

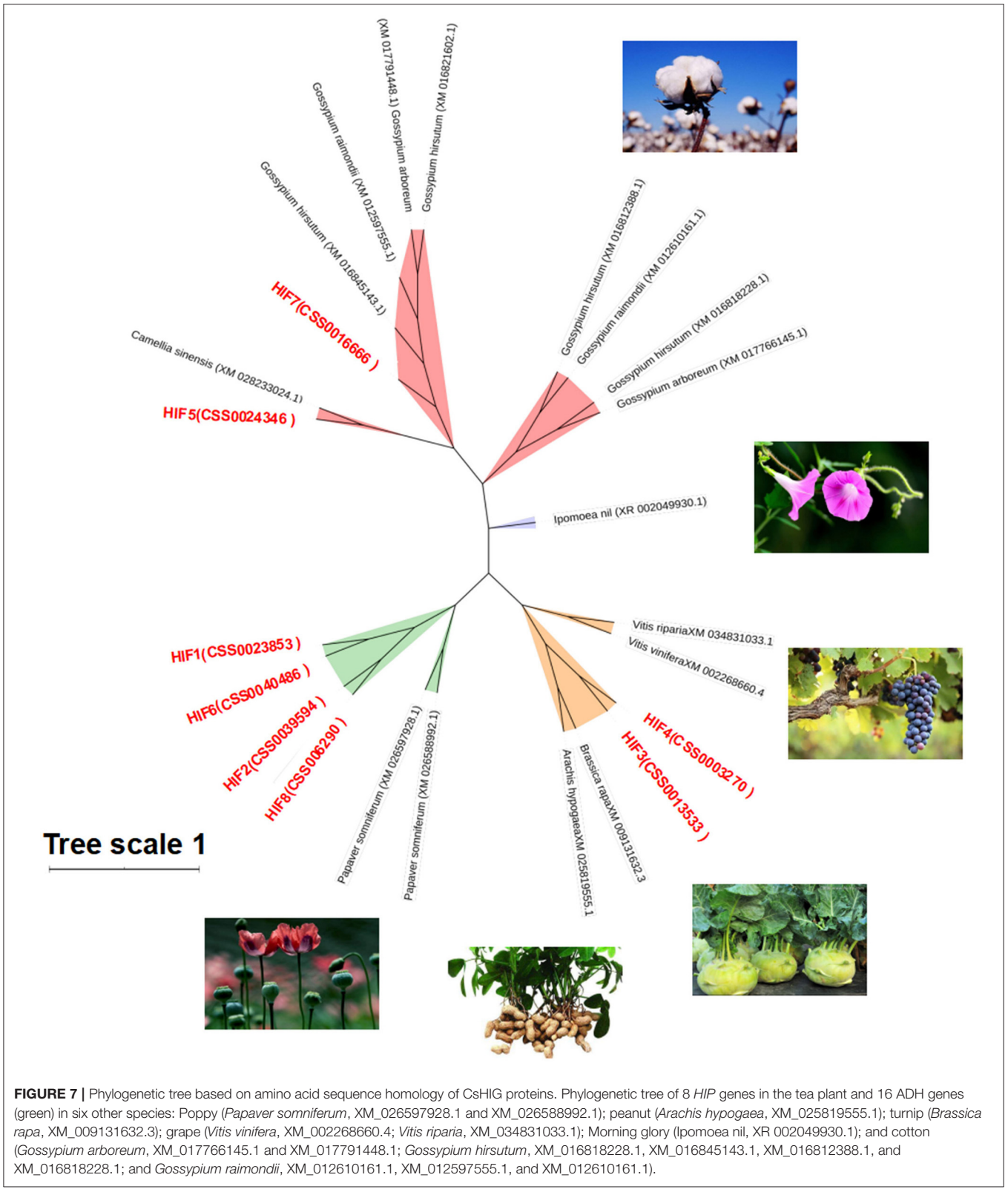

FIGURE 7 | Phylogenetic tree based on amino acid sequence homology of CsHIG proteins. Phylogenetic tree of 8 *HIP* genes in the tea plant and 16 ADH genes (green) in six other species: Poppy (*Papaver somniferum*, XM_026597928.1 and XM_026588992.1); peanut (*Arachis hypogaea*, XM_025819555.1); turnip (*Brassica rapa*, XM_009131632.3); grape (*Vitis vinifera*, XM_002268660.4; *Vitis riparia*, XM_034831033.1); Morning glory (Ipomoea nil, XR 002049930.1); and cotton (*Gossypium arboreum*, XM_017766145.1 and XM_017791448.1; *Gossypium hirsutum*, XM_016818228.1, XM_016845143.1, XM_016812388.1, and XM_016818228.1; and *Gossypium raimondii*, XM_012610161.1, XM_012597555.1, and XM_012610161.1).

99%. According to the principle that a greater matrix score results in a smaller expected value (E_value), greater identities, and a greater degree of matching, CL10755.Contig2_All and Unigene1790_All were screened as key transcripts of *CsHIG6* and *CsHIG4* genes, respectively (**Supplementary Table 3**). The RNA-Seq results showed that peak expression levels of the

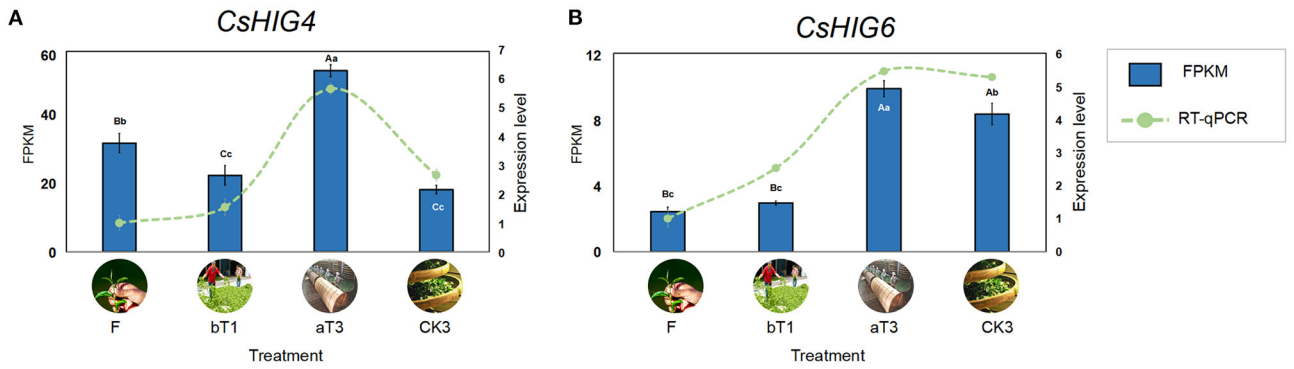

FIGURE 8 | FPKM values and RT-qPCR test verification of key *CsHIG* gene transcripts during postharvest processing of oolong tea. FPKM values and expression levels of **(A)** *CsHIG4* and **(B)** *CsHIG6*. F, Fresh tea leaves; bT1, tea leaves before first turnover treatment; aT3, tea leaves after third turnover treatment; CK3, control of aT3 without turnover treatment. Different uppercase letters ($P < 0.01$) and lowercase letters ($P < 0.05$) indicate significant differences among different treatments from Tukey's test. Error bars indicate the standard error (SE) of the mean.

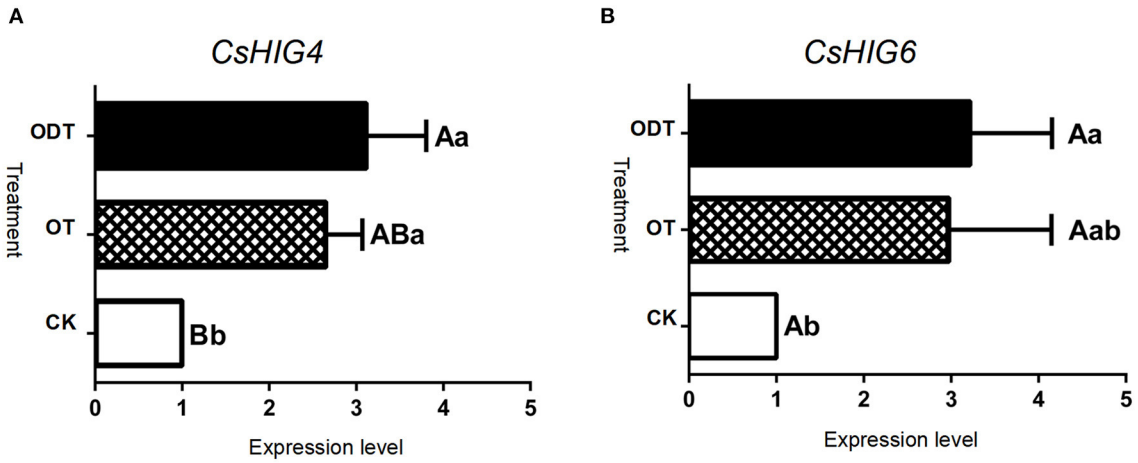

FIGURE 9 | Relative expression level of key *CsHIG* gene transcripts under normoxic and hypoxic conditions during the turnover process of oolong tea. FPKM values and expression levels of **(A)** *CsHIG4* and **(B)** *CsHIG6*. F (control group) represents fresh tea leaves without any treatment. ODT (oxygen-deficient leaves) represents fresh tea leaves turned over under hypoxic conditions. OT (normal leaves) represents fresh tea leaves turned over under normoxic conditions. Different uppercase letters ($P < 0.01$) and lowercase letters ($P < 0.05$) indicate significant differences among different treatments from Tukey's test. Error bars indicate the standard error (SE) of the mean.

two key transcripts all appeared in turnover leaves (T3). The FPKM of CL10755.Contig2_All in T3 was 1.66, 2.37, and 2.91 times those of the fresh leaves (F), withered leaves (W), and non-turnover leaves (CK3), respectively, with an extremely significant difference between each other ($P < 0.01$). Similarly, the FPKM of Unigene1790_All in T3 was 4.07, 3.45, and 1.18 times those of F, W, and CK3, respectively, with an extremely significant difference between each other ($P < 0.01$). The results of FPKM verification using RT-qPCR technology showed that the relative expression levels of CL10755.Contig2_All and Unigene1790_All tended to be consistent with FPKM during the postharvest processing of oolong tea ($r = 0.743^{**}$, $r = 0.959^{**}$. **Indicates that there was an extremely significant correlation between FPKM and relative expression level) (**Figure 8**). Therefore, the key transcripts screened, CL10755.Contig2_All and Unigene1790_All of the *CsHIG* gene showed a hypoxic stress response during the turnover process of oolong tea.

To further demonstrate the influence of the turnover microenvironment on *CsHIG* gene expression, fresh tea leaves (CK), hypoxic-turnover leaves (ODT), and normoxic-turnover tea leaves (OT) were used as materials. The results showed that, compared with CK, key transcript CL10755.Contig2_All of the *CsHIG4* gene was increased 2.65- and 3.12-fold in ODT and OT, respectively. The CL10755.Contig2_All expression levels of ODT and OT were extremely significantly ($P < 0.01$) and significantly higher ($P < 0.05$) than those

of CK, respectively, but no significant difference was observed between ODT and OT ($P > 0.05$). Similar to CL10755.Contig2_All, key transcript Unigene1790_All of the *CsHIG6* gene was increased 2.98- and 3.22-fold in ODT and OT compared with CK, respectively. The Unigene1790_All expression level in ODT was significantly higher than that in fresh leaves ($P > 0.05$) (**Figure 9**). Therefore, we have further clarified the hypoxic microenvironment created by turnover treatment, and we have screened and obtained key transcripts of *CsHIG4* and *CsHIG6* genes that responded to turnover treatment during the postharvest processing of oolong tea.

CONCLUSION

Based on the conversion law of the compound, we concluded that the C6 aldehydes of the LOX-HPL pathway might undergo oxidation reactions to form C6 acids and their derivative esters, such as hexanoic acid, (E)-2-hexenyl ester, hexanoic acid, 4-hexenyl ester, and hexanoic acid in a micro-environment with abundant oxygen supply through non-enzymatic reactions during the postharvest process of oolong tea; while, when the micro-environmental oxygen was insufficient, hypoxia-induced protein (HIP) genes would be transcribed, and ADH enzyme activity and related gene expression were up-regulated, promoting the conversion of C6 aldehydes to C6 alcohols and their derivative esters, such as (Z)-3-hexen-1-ol, benzoate, (Z)-3-hexen-1-ol, propanoate, Butanoic acid, (Z)-3-hexenyl ester, and (Z)-3-hexenyl hexanoate through enzymatic reduction reactions through non-enzymatic reactions during the postharvest process of oolong tea. In summary, the difference in oxygen factors in the micro-environment might mediate the metabolic flow of C6 aldehydes in the LOX-HPL pathway and then affect the formation and proportion of fatty acid esters of oolong tea.

DATA AVAILABILITY STATEMENT

The original contributions presented in the study are included in the article/**Supplementary Materials**, further inquiries can be directed to the corresponding author/s.

AUTHOR CONTRIBUTIONS

Z-wZ and YS conceived and designed the experiments. Z-wZ, Q-yW, Q-cH, YY, and H-lD performed the experiments. Z-xN, Z-xL, YS, and N-xY analyzed the data. Z-wZ, W-jB, Q-yW, and H-lD interpreted the results. Z-wZ, Q-yW, and Z-xL wrote the manuscript. All authors discussed the results and reviewed the final manuscript.

FUNDING

This research was supported by China Agriculture Research System of MOF and MARA (CARS-19), and the Fujian Agriculture and Forestry University Science and Technology Innovation Fund (CXZX2017178). The funders played no role in the study design, data collection, and analysis, the decision to publish, or manuscript preparation.

ACKNOWLEDGMENTS

We thank Simon Partridge, Ph.D., from Liwen Bianji (Edanz) (www.liwenbianji.cn/) for editing the English text of a draft of this manuscript.

SUPPLEMENTARY MATERIAL

The Supplementary Material for this article can be found online at: https://www.frontiersin.org/articles/10.3389/fpls.2021.738445/full#supplementary-material

REFERENCES

Chen, M. J., Guo, L., Zhou, H. W., Guo, Y. L., Zhang, Y., Lin, Z., Sun, M., et al. (2021). Absolute quantitative volatile measurement from fresh tea leaves and the derived teas revealed contributions of postharvest synthesis of endogenous volatiles for the aroma quality of made teas. *Appl. Sci.* 11:20613. doi: 10.3390/app11020613

Chen, S., Liu, H. H., Zhao, X. M., Li, X. L., Shan, W. N., Wang, X. X., et al. (2020). Non-targeted metabolomics analysis reveals dynamic changes of volatile and non-volatile metabolites during oolong tea manufacture. *Food Res. Int.* 128, 1873–7145. doi: 10.1016/j.foodres.2019.108778

Chen, S. S., Jin, X. Y., You, F. N., Zhou, Z. W., Lin, X. L., Hao, Z. L., et al. (2018). Influence of multi intermittence radiation by LED on flavor components in Tieguanyin tea. *Trans. of the Chinese Soc. of Agric. Eng.* 34, 308–314. doi: 10.11975/j.issn.1002-6819.2018.02.042

Cirilli, M., Bellincontro, A., De, S. D., Botondi, R., Colao, M. C., Muleo, R., et al. (2012). Temperature and water loss affect ADH activity and gene expression in grape berry during postharvest dehydration. *Food Chem.* 132, 447–454. doi: 10.1016/j.foodchem.2011.11.020

Eddy, S. R. and Pearson, W. R. (2011). Accelerated profile hmm searches. *PLoS Comput. Biol.* 7:e1002195. doi: 10.1371/journal.pcbi.1002195

Fu, X., Chen, Y., Mei, X., Katsuno, T., Kobayashi, E., Dong, F., et al. (2017). Regulation of formation of volatile compounds of tea (*Camellia sinensis*) leaves by single light wavelength. *Sci. Rep.* 5, 2046–2322. doi: 10.1038/srep16858

Gregg, L. S., Maimon, E. H., and Annalisa, M. V. (2013). Science signaling podcast: 12 February 2013. *Sci. Signal.* 6:5. doi: 10.1126/scisignal.2004007

Guo, L., Du, Z. H., Yao, L. H., Zhang, X, B., Zhang, Y., Lin, Z., et al. (2021). Chemical characterization of the aroma of tieguanyin oolong tea and black tea. *Food Sci.* 42, 255–261. doi: 10.7506/spkx1002-6630-20200428-361

Hao, C., Cao, S., Jin, Y., Tang, Y., and Qi, H. (2016). The relationship between CmADHs and the diversity of volatile organic compounds of three aroma types of melon (cucumis melo). *Front. Physiol.* 7:254. doi: 10.3389/fphys.2016.00254

Hu, C. J., Da, L.i., Ma, Y. X., Wei, Z., Chen, L., Zheng, X. Q., et al. (2018). Formation mechanism of the oolong tea characteristic aroma during bruising and withering treatment. *Food Chem.* 269, 202–211. doi: 10.1016/j.foodchem.2018.07.016

Kaelin, W. G. (2017). The VHL Tumor suppressor gene: insights into oxygen sensing and cancer. *Trans. Am. Clin. Climatol. Assoc.* 128, 298–307.

Kawakami, M., and Yamanishi, T. (1999). Formation of aroma components in roasted or pan-fired green tea by roasting or pan-firing treatment. *Nippon Nogeikagaku Kaishi* 73, 893–906. doi: 10.1271/nogeikagaku1924.73.893

Liu, P. P., Yin, J. F., Chen, G. S., Wang, F., and Xu, Y. Q. (2018). Flavor characteristics and chemical compositions of oolong tea processed using

different semi-fermentation times. *J. of Food Sci. Tech* 55, 1185–1195. doi: 10.1007/s13197-018-3034-0

Livak, K. J., and Schmittgen, T. D. (2001). Analysis of relative gene expression data using real-time quantitative PCR and the 2 $^{\Delta\Delta ct}$ method. *Methods* 25, 402–481. doi: 10.1006/meth.2001.1262

Matsui, K., Toyota, H., Kajiwara, T., Kakuno, T., and Hatanaka, A. (1991). Fatty acid hydroperoxide cleaving enzyme, hydroperoxide lyase, from tea leaves. *Phytochemistry* 30, 2109–2113. doi: 10.1016/0031-9422(91)83596-D

Ng, K. W., Cao, Z. J., Chen, H. B., Zhao, Z. Z., and Yi, T. (2017). Oolong tea: a critical review of processing methods, chemical composition, health effects and risk. *Crit. Rev.Food Sci. Nutr.* 58, 2957–2980. doi: 10.1080/10408398.2017.1347556

Ono, E., Handa, T., Koeduka, T., Toyonaga, H., Tawfik, M. M., Shiraishi, A., et al. (2016). CYP74B24 is the 13-hydroperoxide lyase involved in biosynthesis of green leaf volatiles in tea (*Camellia sinensis*). *Plant Physiol. Biochem.* 98, 112–118. doi: 10.1016/j.plaphy.2015.11.016

Persson, B., Hedlund, J., and Jornvall, H. (2008).The MDR superfamily. *Cell. Molecul. Life Sci.* 65, 3879–3894. doi: 10.1007/s00018-008-8587-z

Qian, X., Sun, L., Xu, X. Q., Zhu, B. Q., and Xu, H. Y. (2016). Differential expression of VvLOXA diversifies C6 volatile profiles in some vitis vinifera table grape cultivars. *Int. J. Mol. Sci.* 18:2705. doi: 10.3390/ijms18122705

Sekiya, J., Kajiwara, T., and Hatanaka, A. (1984). Seasonal changes in activities of enzymes responsible for the formation of C6-aldehydes and C6-alcohols in tea leaves, and the effects of environmental temperatures on the enzyme activities. *Plant and Cell Physiol.* 25, 269–280.

Shi, Y., Di, T., Yang, S., Wu, L., Chen, Y., Xia, T., et al. (2018). Changes in aroma components in the processing of flowery black tea. *Food Sci.* 39, 167–175. doi: 10.7506/spkx1002-6630-201808027

Xia, E., Tong, W., Hou, Y., An, Y., Chen L., Wu Q., et al. (2020). The reference genome of tea plant and resequencing of 81 diverse accessions provide insights into genome evolution and adaptation of tea plants. *Mol. Plant.* 13, 1013–1026. doi: 10.1016/j.molp.2020.04.010

Yang, Z., Baldermann, S., and Watanabe, N. (2013). Recent studies of the volatile compounds in tea. *Food Res. Int.* 53, 585–599. doi: 10.1016/j.foodres.2013.02.011

Zeng, L. T., Zhou, Y., Gui, J. D., Fu, X. M., Mei, X., Zhen, Y. P., et al. (2016). Formation of volatile tea constituent indole during the oolong tea manufacturing process. *J. Agric. Food Chem.* 64, 5011–5019. doi: 10.1021/acs.jafc.6b01742

Zhou, Z. W., Deng, H. L., Wu, Q. Y., Liu, B. B., Yue, C., Deng, T. T., et al. (2019a). Validation of reference genes for gene expression studies in post-harvest leaves of tea plant (*Camellia sinensis*). *PeerJ.* 7:6385. doi: 10.7717/peerj.6385

Zhou, Z. W., Wu, Q. Y., Yao, Z. L., Deng, H. L., Liu, B. B., Yue, C., et al. (2020). Dynamics of ADH and related genes responsible for the transformation of C6-aldehydes to C6-alcohols during the postharvest process of oolong tea. *Food Sci. Nutr.* 8, 104–113. doi: 10.1002/fsn3.1272

Zhou, Z. W., You, F. N., Liu, B. B., Deng, T. T., Lai, Z. X., and Sun, Y. (2019b). Effect of Mechanical Force during turning-over on the formation of aliphatic aroma in oolong tea. *Food Sci*. 40, 52–59.

Conflict of Interest: The authors declare that the research was conducted in the absence of any commercial or financial relationships that could be construed as a potential conflict of interest.

Publisher's Note: All claims expressed in this article are solely those of the authors and do not necessarily represent those of their affiliated organizations, or those of the publisher, the editors and the reviewers. Any product that may be evaluated in this article, or claim that may be made by its manufacturer, is not guaranteed or endorsed by the publisher.

frontiers in Plant Science

ORIGINAL RESEARCH
published: 02 December 2021
doi: 10.3389/fpls.2021.779819

Mechanism Underlying the Shading-Induced Chlorophyll Accumulation in Tea Leaves

Jiaming Chen[1,2†], Shuhua Wu[1,2†], Fang Dong[3], Jianlong Li[4], Lanting Zeng[1], Jinchi Tang[4] and Dachuan Gu[1]*

[1]Guangdong Provincial Key Laboratory of Applied Botany & Key Laboratory of South China Agricultural Plant Molecular Analysis and Genetic Improvement, South China Botanical Garden, Chinese Academy of Sciences, Guangzhou, China, [2]College of Life Sciences, University of Chinese Academy of Sciences, Beijing, China, [3]Guangdong Food and Drug Vocational College, Guangzhou, China, [4]Laboratory of Tea Plant Resources Innovation and Utilization, Tea Research Institute, Guangdong Academy of Agricultural Sciences & Guangdong Provincial Key, Guangzhou, China

Besides aroma and taste, the color of dry tea leaves, tea infusion, and infused tea leaves is also an important index for tea quality. Shading can significantly increase the chlorophyll content of tea leaves, leading to enhanced tea leaf coloration. However, the underlying regulatory mechanism remains unclear. In this study, we revealed that the expressions of chlorophyll synthesis genes were significantly induced by shading, specially, the gene encoding protochlorophyllide oxidoreductase (*CsPOR*). Indoor control experiment showed that decreased light intensity could significantly induce the expression of *CsPOR*, and thus cause the increase of chlorophyll content. Subsequently, we explored the light signaling pathway transcription factors regulating chlorophyll synthesis, including CsPIFs and CsHY5. Through expression level and subcellular localization analysis, we found that CsPIF3-2, CsPIF7-1, and CsHY5 may be candidate transcriptional regulators. Transcriptional activation experiments proved that CsHY5 inhibits *CsPORL-2* transcription. In summary, we concluded that shading might promote the expression of *CsPORL-2* by inhibiting the expression of *CsHY5*, leading to high accumulation of chlorophyll in tea leaves. The results of this study provide insights into the mechanism regulating the improvements to tea plant quality caused by shading.

Keywords: shading, light intensity, chlorophyll accumulation, *Camellia sinensis*, transcription regulation

OPEN ACCESS

Edited by:
Marco Landi,
University of Pisa, Italy

Reviewed by:
Ruohe Yin,
Shanghai Jiao Tong University, China
Kang Wei,
Chinese Academy of Agricultural Sciences (CAAS), China

***Correspondence:**
Dachuan Gu
gudachuan@scbg.ac.cn

†These authors have contributed equally to this work

Specialty section:
This article was submitted to Plant Metabolism and Chemodiversity, a section of the journal Frontiers in Plant Science

Received: *19 September 2021*
Accepted: *11 November 2021*
Published: *02 December 2021*

Citation:
Chen J, Wu S, Dong F, Li J, Zeng L, Tang J and Gu D (2021) Mechanism Underlying the Shading-Induced Chlorophyll Accumulation in Tea Leaves. Front. Plant Sci. 12:779819. doi: 10.3389/fpls.2021.779819

INTRODUCTION

Tea plants, which are cultivated worldwide, are an important cash crop. Tea, which is made from their fresh shoots, is the most popular non-alcoholic beverage (Tang et al., 2019). The economic benefits of tea are closely related to its quality. In addition to the aroma and taste, color is a key trait used for measuring tea quality. The color of the dry tea leaves and the resulting liquid influences consumer preferences and purchasing decisions (Yu et al., 2019). The pigments that contribute to tea colors generally include chlorophyll, carotenoids, and anthocyanins, of which chlorophyll is the most important pigment for determining green tea quality (Suzuki and Shioi, 2003). As a traditional agronomic practice, shading is widely used in tea-producing countries, such as China and Japan. Considerable practical experience and

scientific research have confirmed that shading can increase the overall quality of tea plants, both internally and externally (Chen et al., 2021). Moreover, shading enhances the taste and aroma of tea by affecting the synthesis of free amino acids, flavonoids, and aromatic compounds, while also affecting the appearance of tea by influencing the abundance of chlorophyll and other plant pigments as well as structural components (e.g., lignin; Ku et al., 2010; Liu et al., 2017; Zeng et al., 2020; Chen et al., 2021; Teng et al., 2021; Zhao et al., 2021). During tea plant cultivation, providing plants with sufficient shade can significantly improve tea color quality. To produce Japanese matcha, tea plants are often shaded by 60–98% for 10–30 days (Yamashita et al., 2020). The chlorophyll content of tea leaves increases significantly after shading treatment. Compared with the dry leaves of tea plants grown without shading, the dry tea leaves of plants grown in the shade are greener, which increases their economic value (Sano et al., 2018). To date, considerable research has been conducted on the phenomenon that shading improves tea quality. However, the research has focused primarily on the mechanism underlying the changes in the chemical components that affect sensory quality, including the regulation of flavonoid and free amino acid contents (Lee et al., 2013; Chen et al., 2017; Liu et al., 2018). There have been relatively few studies on the molecular basis of shading-induced chlorophyll accumulation.

Previous studies revealed that significant increases in the chlorophyll content of fresh leaves due to shading are unaffected by leaf age, shading season, and number of shading treatments but are related to the duration and degree of shading (Lee et al., 2013; Sano et al., 2018; Yamashita et al., 2020). Using an electron microscope, Liu observed that shading induces the development of tea leaf plastids, leading to an increase in the number of chloroplasts and in thylakoid compactness (Liu et al., 2020). Chlorophyll is the main pigment for photosynthesis in plants, so the synthesis of chlorophyll is a basic metabolic process (Garrone et al., 2015). In all oxygen-producing photosynthetic organisms, the light-dependent protochlorophyllide oxidoreductase (POR) enzyme is the key regulatory enzyme in the chlorophyll synthesis pathway (Lebedev and Timko, 1998; Masuda and Takamiya, 2004; Heyes and Hunter, 2005; Reinbothe et al., 2010; Scrutton et al., 2012). In one of the final steps, POR catalyzes the light-driven reduction of protochlorophyllide (PChlide) to chlorophyllide, from which chlorophyll is eventually derived (Garrone et al., 2015). For example, light-grown *Arabidopsis porB*/*porC* double mutants develop a seedling-lethal and chlorophyll-deficient phenotype (Frick et al., 2003). Additionally, rice *fgl* mutant (*OsporB* mutant) etiolated seedlings contained smaller prolamellar bodies in etioplasts, and lower levels of total and photoactive Pchlide (Sakuraba et al., 2013). However, how shading affects the chlorophyll synthesis pathway and how to regulate *POR* in tea leaves is not yet known.

Two types of shading are used during the cultivation of tea plants, namely, ecological shading and cover shading. Ecological shading involves the planting of trees in tea gardens or intercropping with economically valuable forest trees or tall and suitable tree species to provide shade. Cover shade is mainly provided by plastic greenhouse covers and sunshade net covers made from diverse materials, including straw, wheat straw, and artificial materials (Chen et al., 2021). Although there are various ways of shading plants, they generally alter environmental factors similarly. For example, they usually decrease the temperature and light intensity, change the light quality, and increase the environmental humidity (Fiorucci and Fankhauser, 2017). Among them, the change of light environment caused by shading is an important environmental factor that affects the synthesis of plant chlorophyll. In plants, light is required for photosynthesis and normal growth and development. Shading decreases the light intensity and the red (R) light: far-red (FR) light ratio, which affects plant growth and development (Fiorucci and Fankhauser, 2017). During long-term evolution, plants developed a variety of photoreceptors that perceive changes in the external light environment, including phytochromes that perceive R and FR light, cryptochromes and phototropins that perceive blue and ultraviolet A light, and UVR8, which perceives UVB light (Jiao et al., 2007; Rizzini et al., 2011). After the light signal is sensed by these photoreceptors in the plant, the downstream transcription cascade involving transcription factors is then initiated to regulate the growth and development of the plant (Jiao et al., 2007). Among these transcription factors, phytochrome-interacting factors (PIFs) and HY5 are critical for multiple pathways that integrate light signals and phytohormone signaling pathways, with key roles related to plant growth and development (Paik et al., 2017). Earlier research proved that PIFs and HY5 have the opposite regulatory effects on chlorophyll biosynthesis (Chen et al., 2004). More specifically, PIFs accumulate in seedlings grown in darkness and negatively regulate the expression of chlorophyll biosynthesis genes to inhibit the greening of seedlings (Moon et al., 2008). In contrast, HY5 regulates nuclear gene transcription and promotes seedling photomorphogenesis (Kindgren et al., 2012). Although chlorophyll synthesis has been thoroughly analyzed in model plants, the molecular regulation of chlorophyll biosynthesis in woody plants is poorly understood. For example, it is unclear how shading induces the accumulation of chlorophyll in tea plants. In recent years, the development of omics technology has further deepened our understanding of plant growth and developmental events. By applying transcriptomics technology, Liu determined that shading alters *PIF* and *HY5* expression patterns in tea plants (Liu et al., 2018). Accordingly, PIFs and HY5 may have regulatory functions, but the precise roles of these transcription factors in developing tea plants will need to be elucidated.

Because of a lack of an established genetic transformation system applicable for tea plants, there has been limited research on the molecular mechanism underlying the shade-induced regulation of chlorophyll synthesis. Therefore, the objective of this study was to clarify the regulatory effects of shading on the chlorophyll synthesis of tea plants. The effects of shading on tea plants were investigated under tea garden conditions and under simulating shading indoors conditions by decreasing the light intensity. We explored whether the decreased light intensity caused by shading is the main cause of the accumulation of chlorophyll in tea leaves. Additionally, the expression of

genes encoding key rate-limiting enzymes of the chlorophyll synthesis pathway and the transcription factors involved in the light signaling pathway were analyzed. Finally, the regulatory mechanism was analyzed *via* subcellular localization and transcriptional activation experiments. The results of this study provide insights into the regulation of tea secondary metabolism and may be useful for the breeding and selection of high-chlorophyll tea varieties.

MATERIALS AND METHODS

Sample Processing

Tea plants "Jinxuan" (containing almost 400 branches), which were 15 years old and grew consistently in tea garden, were selected to perform 2 weeks shading treatment. The shading treatment was carried on the Tea Research Institute, Guangdong Academy of Agricultural Sciences (Yingde, Guangdong, China) and started on August 2020 and March 2021. The tea plants in the treatment group (T) were covered by black shading nets for 2 weeks, the shading rate was 90%, and the light intensity was about 130 $\mu mol\, m^{-2}\, s^{-1}$. The control group (CK) was not shaded, and the light intensity was about 1,300 $\mu mol\, m^{-2}\, s^{-1}$. The branches with one bud and three leaves were collected 1st day, 7th day, and 14th day after treatment. Every five branches were randomly collected from the 400 branches combined into a group as one replicate. Three replicates were randomly collected from each treatment. The collected branches were immediately frozen in liquid nitrogen and stored at −80°C for subsequent RNA extraction and chlorophyll analysis.

The annual "Jinxuan" cutting seedlings with consistent growth were selected for the indoor control experiment, which started in May 2021. The tea seedlings were cultured in a light incubator at 25°C and the photoperiod was 16 h/8 h. The light source is the incubator's own light source. The light intensity in the control group (CK) was higher than that in the tea garden treatment group (T), which was 252 $\mu mol\, m^{-2}\, s^{-1}$. The light intensity in the experimental group was lower than that in the tea garden treatment group (T), which was 16.8 $\mu mol\, m^{-2}\, s^{-1}$. After the treatment for 21 days, the branches with one bud and three leaves were collected. Every five branches were combined into a group as one replicate. Three replicates were randomly collected from each treatment. The collected branches were immediately frozen in liquid nitrogen and stored at −80°C for subsequent RNA extraction and chlorophyll analysis.

The indoor isolated branch control experiment was carried out in November 2020, and the branches used in the experiment were provided by the Tea Research Institute of Guangdong Academy of Agricultural Sciences. The branches pruned into one bud and three leaves and cultivated in a constant temperature and humidity environment. The cultivation temperature was 25°C and the photoperiod was 16 h/8 h. Light intensity was controlled by adjusting the number of white light tubes. Light quality was regulated by two external red or far-red LED tubes (Shenzhen FHT Electronics Technology Co., Ltd., Guangdong, China). The light intensity group experiment followed the principle of changing light intensity (light radiation) and unchanged light quality (the ration of R: FR). The light intensity for high, medium, and low-light intensity treatment was 252, 84, and 3.36 $\mu mol\, m^{-2}\, s^{-1}$, respectively. The R: FR of all treatments was 1.5. The experiment of light quality group followed the principle of light quality (the ration of R: FR) change and light intensity (light radiation) unchanged. R: FR was 0.1 in high far-red light treatment and 7 in high red light treatment. The light intensity of all treatments was 252 $\mu mol\, m^{-2}\, s^{-1}$. The light intensity of the control group was 252 $\mu mol\, m^{-2}\, s^{-1}$, and the R: FR was 1.5. Taking into account that the isolated branches cannot survive for a long time, tea sample was collected after the treatment for 6 days. Every five branches were combined into a group as one replicate. Three replicates were randomly collected from each treatment. The collected branches were immediately placed in liquid nitrogen and stored at −80°C for subsequent RNA extraction and chlorophyll analysis.

Chlorophyll Extraction and Content Determination

The extraction method of chlorophyll referred to the previous research method (Fu et al., 2018). The samples were ground into fine powder in liquid nitrogen, and chlorophyll of fresh sample powder (about 100 mg) was extracted with 5 ml of 80% acetone precooled at 4°C. After shaking and mixing, the powder was placed at 4°C for 12 h in a dark environment. After centrifugation at 10000 *g* for 10 min, the supernatant was taken to measure the absorbance (A_{663} and A_{645}) and the chlorophyll content was determined.

The formula for calculating chlorophyll content was as follows (Arnon, 1949):

$$\text{Chlorophyll a} = 12.7 \times A_{663} - 2.69 \times A_{645};$$

$$\text{Chlorophyll b} = 22.9 \times A_{645} - 4.68 \times A_{663};$$

$$\text{Total chlorophyll} = 20.2 \times A_{645} + 8.02 \times A_{663}.$$

Analysis of Transcript Expression Levels of Related Genes

The fresh tea leaf sample was ground into a fine powder in liquid nitrogen, and the RNA was reverse transcribed into cDNA using PrimeScript® RT Reagent Kit (Takara) according to the instructions. The target genes were detected using quantitative real-time polymerase chain reaction (qRT-PCR), and the primers required for qRT-PCR were designed by the Web site.[1] The tested primers are shown in **Supplementary Table S1**. The qRT-PCR reaction system was as follows: 5 µl of iTaqTM Universal SYBR® Green Supermix (Bio-Rad, Hercules, CA, United States), 2.5 µl of template cDNA (80 ng/µl), and 1 µm gene-specific primers (**Supplementary Table S1**) 2.5 µl. The qRT-PCR experiment was performed on Roche LightCycle 480 (Roche Applied Science, Mannheim, Germany). The specific

[1]https://bioinfo.ut.ee/primer3-0.4.0/

procedure was as follows: 95°C for 30 s, 95°C for 5 s, and 60°C for 30 s, a total of 40 cycles. *CsEF1-α* (GeneBank no. KA280301.1) was used as the internal reference gene. The melting point curve was tested to verify the specificity of PCR products. Three biological replicates for each sample were performed qRT-PCR analysis and each biological replicate had three technical repetitions. The $2^{-\triangle\triangle CT}$ method was used to calculate the relative expression, and the gene expression results were normalized.

Cloning of CsPIF3-2/7–1 and CsHY5

CsPIF3-2/7–1 and *CsHY5* gene sequence primers were designed (**Supplementary Table S1**) in reference to the NCBI database,[2] and cDNA was used as a template. The PCR system was 20 μl. The PCR reaction program was as follows: denaturation at 98°C for 10 s, annealing at 56°C for 15 s, and extension at 72°C for 120 s, 30 cycles. The PCR product was detected and recovered, and the recovered product was ligated with the pHB-FLAG cloning vector and transformed into *E. coli* DH5α competent cells. Positive clones were selected for plasmid extraction and sequencing.

Subcellular Location Assay

The CDS of *CsPIF3-2/7–1/7–2* and *CsHY5* without stop codon was cloned into pSAT6-EYFP vector. The *Arabidopsis* protoplast isolation method is as described before (Zhou et al., 2019). Leaf cells of *Arabidopsis* were enzymolyzed with cellulase and pectase at room temperature, filtered and washed with W5, and resuspended in ice bath for 30 min, and the constructed vector was transformed into protoplasts with PEG and incubated overnight with W5. The yellow fluorescence of CsPIF3-2/7–1/7-2-YFP and CsHY5-YFP was observed by confocal laser scanning microscopy (Zeiss LSM 510, Carl Zeiss, Jena, Germany). The primers used for subcellular vector construction were shown in **Supplementary Table S1**.

Dual-Luciferase Reporter Assay

In order to detect the transcriptional activity of CsPIF3-2/7–1 and CsHY5 on *CsPORL-2*, we designed primers with reference to the promoter sequence of *CsPORL-2* (XM_028200153.1) in the NCBI database. The primers used for vector construction were shown in **Supplementary Table S1**. The promoter was cloned into pGreenII 0800-LUC dual-reporter vector (Hellens et al., 2005), and the constructed CsPIF3-2/7-1-FLAG and CsHY5-FLAG plasmids were used as effectors to infect tobacco leaves through *Agrobacterium* strain GV3101. After 2 d of co-transformation, the activities of LUC and REN luciferase were measured using a dual-luciferase reporting kit (Promega) and a microplate analyzer (Tecan Infinite F50, Tecan Aust-RIA GmbH). Due to the sequence of dual-reporter vector, when the effector has a transcription activity, the ratio of LUC to REN will change. The ratio of LUC to REN was to reflect the final transcription activity. Specifically, compared with the control group (co-transfection of the reporter with the empty vector), higher ratio indicates that effector has a role of transcription activation. Otherwise, lower ratio means the role of transcription inhibition. If there is no significant difference in LUC/REN, it indicates the effector may not transcription activity. At least three biological replicates were performed for each combination, which mean every combination were co-transformed into three tobaccos at least.

Significance Analysis

The significant between two groups was determined based on paired and independent samples *t*-tests. One-way ANOVA combined with Duncan's multiple range test was applied to figure out the differences among three groups. $p \leq 0.05$ was considered a significant difference, and $p \leq 0.01$ was a very significant difference. All statistical analyses were performed on an SPSS statistical package (Ver. 23.0).

RESULTS

Shading Treatments-Induced Chlorophyll Accumulation and the Related Gene Expression in Tea Leaves

To explore the effect of shading on the chlorophyll content of tea leaves, 15-year-old mature tea plants underwent a shading treatment in August 2020. Considering that current tea plant production methods often involve a 60–98% shading treatment and the fact that tea quality can increase substantially when plants are grown under 85% shade (Sano et al., 2018), the experimental group (T group) was grown under 90% shade. This shading treatment altered the tea plant phenotype. Specifically, the leaves were softer, larger (i.e., in terms of area), and were more intensely colored than the control leaves (**Figure 1A**). The leaf pigments were extracted with 80% acetone and the chlorophyll content was measured, which revealed the leaves of the shaded plants were greener than the control leaves (**Figure 1B**) because of a significant increase in the chlorophyll content. This shade-induced accumulation of chlorophyll was stable and increased as the number of shading treatment days increased. Additionally, this accumulation was reflected by the total chlorophyll content as well as the chlorophyll a and b contents. Interestingly, after plants were shaded for 14 days, the ratio of chlorophyll a: chlorophyll b decreased significantly, which may help plants capture light energy in a shaded environment (Chen et al., 2021; **Figure 1C**). Because the chlorophyll level is closely related to the expression of chlorophyll synthesis genes, we analyzed the shade-induced changes in the expression of genes associated with chlorophyll synthesis. The qRT-PCR analysis (**Figure 1D**) revealed that the shading treatment upregulated the expression of genes encoding key rate-limiting enzymes of chlorophyll synthesis, including *CsHEMA1*, *CsCHLH*, *CsCHLI1*, *CsCHLD*, *CsDVR1*, *CsDVR2*, *CsCAO*, *CsCHLG*, and especially *CsPOR* genes. Three *CsPOR* genes were identified in tea plants, namely, *CsPOR*, *CsPORL-1* (*CsPOR-like 1*), and *CsPORL-2* (*CsPOR-like 2*). The *CsPORL-2* transcription level in particular was significantly upregulated. Moreover, the results

[2]https://blast.ncbi.nlm.nih.gov/

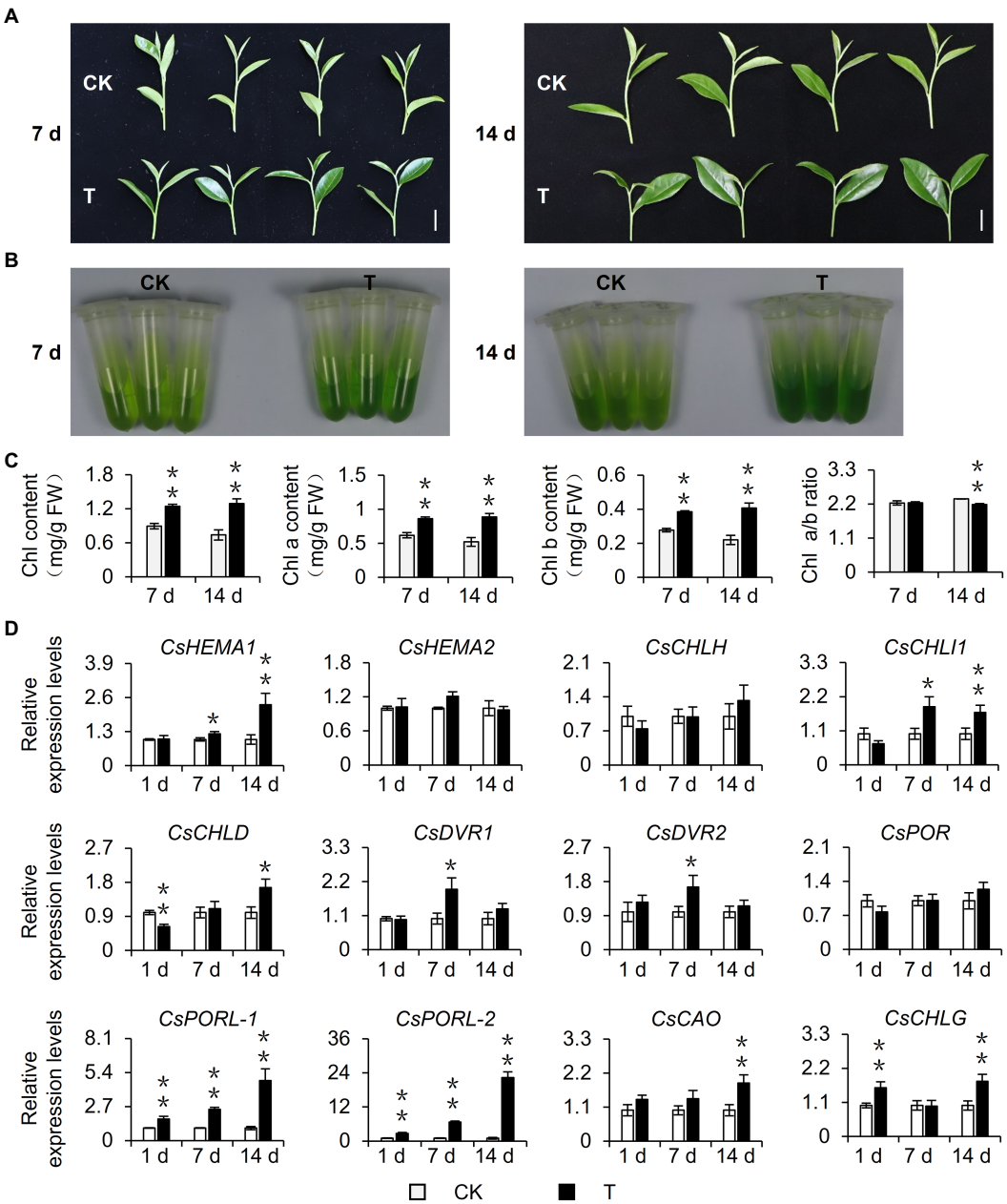

FIGURE 1 | Effect of shading treatment on the chlorophyll content of tea leaves and the expression of related genes. **(A)** The phenotype of new shoots after 7 day and 14 day shading treatment. Bar = 2 cm. **(B)** The comparison of leaf pigments after 7 day and 14 day shading treatment. **(C)** The change of chlorophyll content after shading treatment. Chl: total chlorophyll; Chl a: chlorophyll a; Chl b: chlorophyll b; and FW: fresh weight. **(D)** The changes in the gene expression of chlorophyll synthesis pathway after shading treatment. CK: no shading treatment group (about 1,300 μmol m^{-2} s^{-1}); T: 90% shading treatment group (about 130 μmol m^{-2} s^{-1}). *CsEF1-α* was used as an internal reference to normalized the changes. Data are expressed as mean ± SD ($n = 3$). *$p \leq 0.05$; **$p \leq 0.01$; and difference from CK treatment at the same time point.

of leaves phenotype, chlorophyll contents, and *CsPORL-2* expression showed the same trends in the shade samples of March 2021 (**Supplementary Figures S1A–C**). Collectively, these findings indicate shading promotes chlorophyll synthesis in tea plants and regulates the chlorophyll content of new shoots, resulting in an increase in the intensity of the green coloration of the leaves.

Decreased Light Intensity-Induced Chlorophyll Accumulation and the Related Gene Expression in Tea Leaves

Shading can alter various environmental factors, including light intensity, light quality, temperature, and humidity, of which light intensity is closely related to the photosynthesis rate of plants and influences the accumulation of organic matter. In

this study, the shading treatment caused the light intensity to decrease to only 10% of the light intensity of the control group. Therefore, we speculated that the decrease in light intensity caused by shading may be one of the environmental factors responsible for the phenotypic changes in tea plants. To eliminate the interference by multiple factors in the tea garden, we used annually cut seedlings to conduct indoor experiments, during which we simulated shading by decreasing the light intensity. After 21 days, we observed that the leaves were significantly greener than the control leaves (**Figure 2A**). This result was supported by analyses of the extracted leaf pigments (**Figure 2B**) and the chlorophyll content (**Figure 2C**). Additionally, the changes of the ratio of chlorophyll a: chlorophyll b were consistent with the results of the tea garden-shading experiments. Accordingly, the decrease in light intensity may be a key environmental factor inducing the accumulation of chlorophyll in tea leaves. We subsequently analyzed the differential expression of chlorophyll synthesis-related genes in the samples used for the indoor experiments. The decreased light intensity significantly upregulated the expression of *CsDVR2*, *CsPOR*, *CsPORL-1*, and *CsPORL-2*, which was consistent with the gene expression data for the tea garden-treated samples. Notably, the *CsPOR* transcription levels increased more stably and significantly in response to shading than the transcription levels of the other genes. In particular, *CsPORL-2* was very sensitive to shading and decreased light intensity, suggesting it may be a target gene that should be analyzed further.

Previous studies demonstrated that shading modulates light intensity but affects light quality (e.g., R: FR; Fiorucci and Fankhauser, 2017). To verify our results, we also explored the effects of changes in light intensity and light quality on the chlorophyll synthesis in detached branches. Our analysis indicated that decreasing light intensity can induce the accumulation of chlorophyll in new shoots (**Figure 3A**). Moreover, the change in light quality also affected the chlorophyll content. For example, the chlorophyll level decreased significantly under high-FR light conditions (R: FR = 0.1; **Figure 3B**). Thus, the decrease in light intensity caused by shading was the main environmental factor that induced the accumulation of chlorophyll in tea leaves, but the change in light quality also affected the chlorophyll content to some extent.

Shading and Reduced Light Intensity Regulated the Expression of Genes Related to the Light Signaling Pathway in Tea Plants

Previous studies identified PIFs and HY5 as important regulators of the light signaling pathway and confirmed their importance to chlorophyll synthesis (Chen et al., 2004; Paik et al., 2017). To further screen the potential target transcription factors affected by shading, we examined the transcription levels of *CsPIFs* and *CsHY5* homologs in the shaded samples in the tea garden. The shading treatment significantly induced the expression of *CsPIF3-2*, *CsPIF7-1*, *CsPIF7-2*, and *CsPIF8-1* in tea plants, whereas it had the opposite effect on *CsHY5* expression (**Figure 4A, Supplementary Figure S1D**). A similar gene expression analysis of the indoor cut seedling samples confirmed that *CsPIF3-2*, *CsPIF7-1*, *CsPIF7-2*, and *CsHY5* expression levels were affected by the changes in light intensity, with expression trends that were consistent with those observed for the shaded samples in the tea garden (**Figure 4B**). Moreover, the transcription factor gene expression levels were changed as the light intensity decreased, implying that shading may influence the expression of *CsPIF3-2*, *CsPIF7-1*, *CsPIF7-2*, and *CsHY5* in tea plants because of the associated decrease in light intensity, thereby regulating the transcription of the downstream chlorophyll synthesis genes.

Subcellular Localization of CsPIF3-2/7–1/7–2 and CsHY5

The tea garden-shading experiments and the indoor experiments involving decreased light intensity revealed the transcription factor genes *CsPIF3-2*, *CsPIF7-1*, *CsPIF7-2*, and *CsHY5* may encode key regulators of chlorophyll accumulation in shaded plants. These transcription factors may modulate chlorophyll synthesis by regulating the expression of genes related to chlorophyll synthesis. To further characterize the functions of these transcription factors, we first analyzed their subcellular localization using *Arabidopsis thaliana* protoplasts. The results indicated that CsPIF3-2, CsPIF7-1, and CsHY5 were located in the nucleus (**Figure 5**), suggesting they may contribute to the regulation of *CsPOR* expression. However, CsPIF7-2 was not detected in the nucleus, indicating it may not have a direct regulatory role related to *CsPOR* transcription (**Figure 5**).

CsPIF7-1 and CsHY5 Regulated the Transcription of Chlorophyll Synthesis Genes

On the basis of analyses of metabolites, gene expression, and subcellular localization, we determined the effects of shading and decreased light intensity on the light signaling pathway transcription factor genes *CsPIF3-2*, *CsPIF7-1,* and *CsHY5* and the gene encoding the chlorophyll synthesis rate-limiting enzyme CsPORL-2. To further explore the regulatory effects of CsPIF3-2, CsPIF7-1, and CsHY5 on *CsPORL-2* expression, we first searched the tea plant reference genome and cloned the *CsPORL-2* promoter sequence. The detection of G-box and E-box promoter elements (**Figure 6A**) suggests that *CsPORL-2* expression may be directly regulated by CsPIF3-2, CsPIF7-1, and CsHY5. To clarify the regulatory mechanism, we examined the effects of CsPIF3-2, CsPIF7-1, and CsHY5 on the *CsPORL-2* promoter by conducting the dual-luciferase reporter assays. The dual-luciferase reporter plasmid harbor the *CsPORL-2* promoter fused to LUC, and the REN driven by the CaMV35S promoter as an internal control, while the plasmids expressing CsPIF3-2, CsPIF7-1, and CsHY5 as the effector (**Figure 6B**). As shown in **Figure 6C**, compared with the control, the LUC/REN ratio was remarkably decreased when CsPIF7-1 and CsHY5 were expressed, respectively. Moreover, no significant change in the LUC/REN ratio was found when CsPIF3-2 was expressed (**Figure 6C**). Collectively, these results revealed that CsPIF3-2

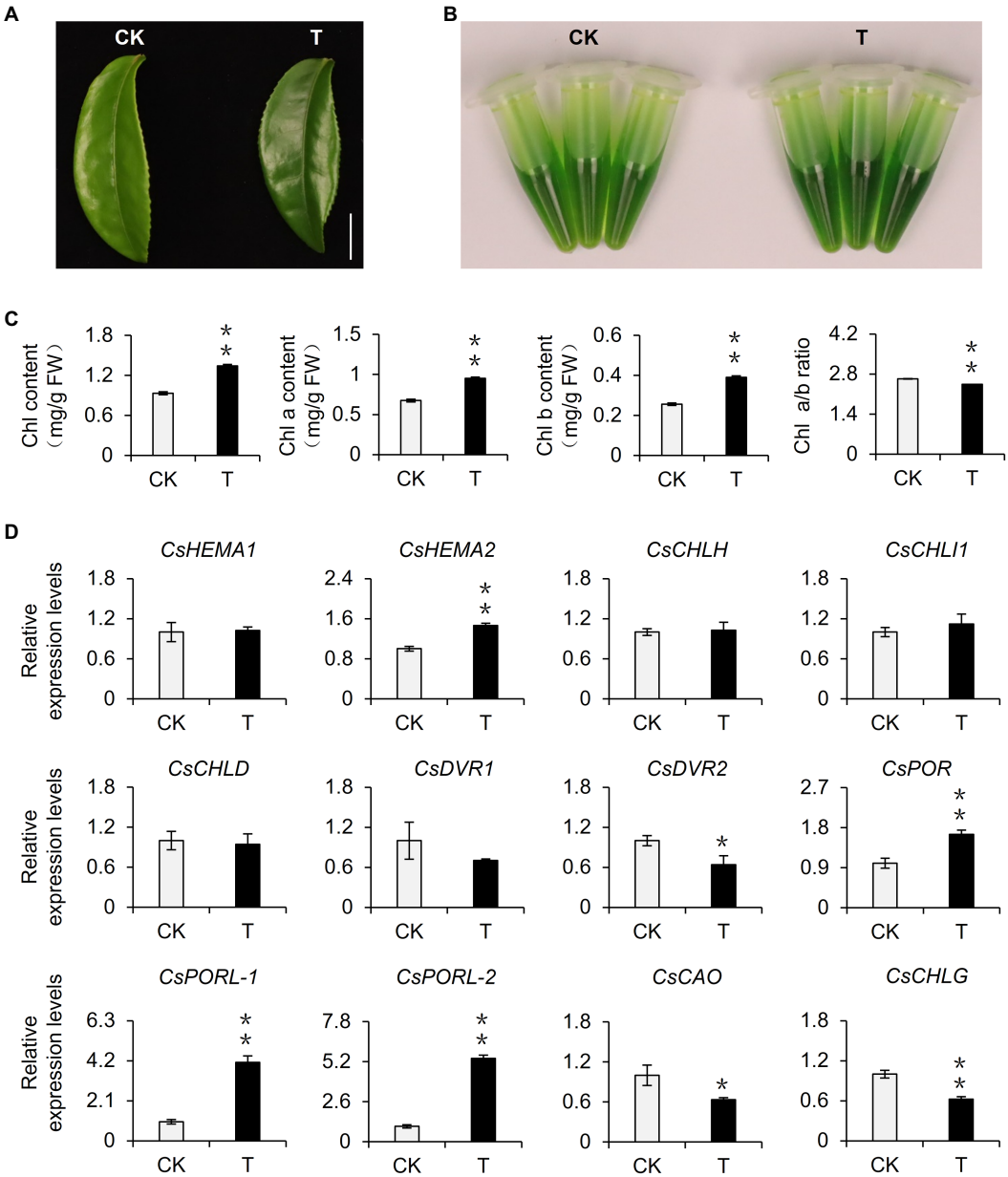

FIGURE 2 | Effect of reduced light intensity on the chlorophyll content of tea leaves and the expression of related genes. **(A)** The phenotype of third leaf after different light intensity treatments. Bar = 1 cm. **(B)** The comparison of leaf pigments after different light intensity treatments. **(C)** The change of chlorophyll content after different light intensity treatments. Chl: total chlorophyll; Chl a: chlorophyll a; Chl b: chlorophyll b; and FW: fresh weight. **(D)** The changes in the gene expression of chlorophyll synthesis pathway after different light intensity treatments. CK: 252 μmol m^{-2} s^{-1}; T: 16.8 μmol m^{-2} s^{-1}. *CsEF1-α* was used as an internal reference to normalized the changes. Data are expressed as mean ± SD ($n = 3$). Mean denoted by different sign indicates significant differences between the treatments in the same time (*mean $p < 0.05$; **mean $p < 0.01$).

did not regulate *CsPORL-2* expression, both CsPIF7-1 and CsHY5 significantly inhibited *CsPORL-2* transcription.

DISCUSSION

Among the many quality-related traits improved by shading, pigmentation, including by chlorophyll, directly affects consumer preferences regarding tea leaves. In this study, we simulated shading in indoor experiments by decreasing the light intensity. The resulting chlorophyll accumulation was similar to that observed for plants shaded in the tea garden (**Figure 2**). Hence, decreasing light intensity may be one of the main factors associated with shading that promotes chlorophyll accumulation in tea leaves. Shading would cause changes in the micro-environment of tea tree growth, including changes in

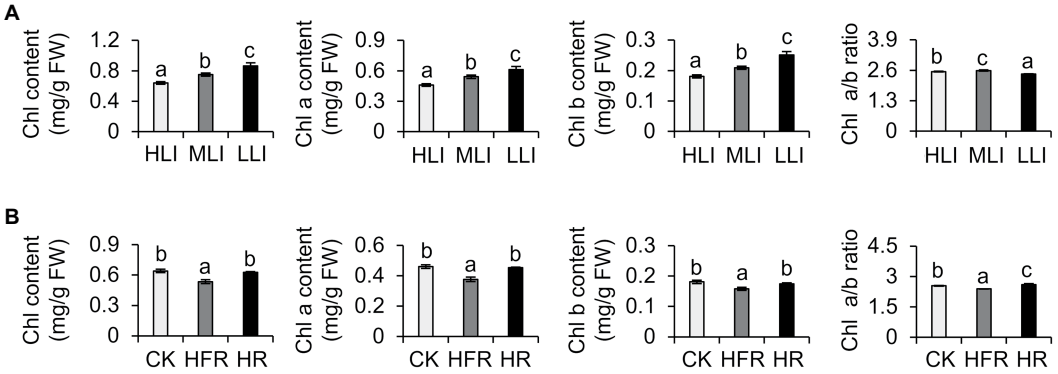

FIGURE 3 | Effect of decreased light intensity and changes in light quality on the chlorophyll level of cut tea branches. **(A)** Changes in the chlorophyll levels of cut tea branches under decreased light intensity treatment. HLI: high light intensity treatment group (252 μmol m^{-2} s^{-1}); MLI: medium light intensity treatment group (84 μmol m^{-2} s^{-1}); LLI: low-light intensity treatment group (3.36 μmol m^{-2} s^{-1}), and R: FR for all three groups were 1.5. **(B)** Changes in chlorophyll levels of cut tea branches after light quality changes. CK: R: FR was 1.5; HFR: high far-red group, R: FR was 0.1; HR: high red group, R: FR was 7, and the light intensity of the three groups was 252 μmol m^{-2} s^{-1}. Chl: total chlorophyll; Chl a: chlorophyll a; Chl b: chlorophyll b; and FW: fresh weight. Data are expressed as mean ± SD ($n = 3$). Different letters represent significant differences between groups ($p \leq 0.05$) at the same time point.

environmental factors, such as light intensity, light quality, temperature, and humidity (Fiorucci and Fankhauser, 2017). Studies on multiple species proved that temperature, light quality, and humidity affect plant chlorophyll contents (Bourque and Naylor, 1971; López-Figueroa and Niell, 1990; Huang et al., 2017). Investigations regarding celery indicated that heat and cold stresses can lead to decreased chlorophyll contents (Huang et al., 2017). An exposure to R light induces chlorophyll accumulation in seaweed (López-Figueroa and Niell, 1990). Although we did not prove that R light treatment of detached tea branches can induce chlorophyll accumulation, we determined that FR light treatment can significantly decrease chlorophyll levels (**Figure 3**). This suggests that light quality changes modulate tea plant chlorophyll synthesis, but changes in the light quality in a shaded environment may not be the main contributing factor. Additionally, highly humid environment reportedly promotes the accumulation of chlorophyll in Jack Bean (Bourque and Naylor, 1971), which is consistent with the effects of increasing environmental humidity due to the shading of tea plants. Therefore, the chlorophyll accumulation induced by the shading of tea plants may be the result of multiple factors associated with the improved micro-environment. Future investigations should focus on clarifying the effects of other environmental factors on chlorophyll accumulation in shaded tea plants. Moreover, the extent of shading influences the coloration of tea leaves. Tea plants generally grow normally in a shaded environment, with green leaves even at a 98% shading rate (Yang et al., 2012). In this study, we used 90% shading rate for the 2-week shading treatment of tea plants. The observed green coloration of the tea leaves (**Figure 1**) was consistent with the results of previous studies (Liu et al., 2020). However, if the degree of shading continues to increase, tea plants exposed to long-term shading (100% shading rate) will start to exhibit a yellowing phenotype, similar to model plants, such as *A. thaliana*. Chen et al. treated tea plants with 2 weeks of shading (100% shading rate) and revealed the degradation of chlorophyll in tea leaves, which resulted in yellow leaves (Chen et al., 2017). Increasing the shading rate by as little as 2% can alter the tea leaf phenotype. Thus, the mechanism mediating the effects of different shading rates in the later periods should be explored.

Earlier research regarding the albino tea cultivar "Baijiguan" demonstrated that shading treatment causes leaves to turn green, increases the chlorophyll content, and facilitates the normal development of chloroplasts (Wu et al., 2016). Subsequent studies on the normal tea variety "Shuchazao" indicated that shading can increase the accumulation of chlorophyll, leading to the increased green coloration of leaves (Liu et al., 2018, 2020). In this study, we obtained similar phenotypic results during our outdoor shading treatment and indoor simulated shading treatment (i.e., decreased light intensity) of "Jinxuan" tea plants, which are widely cultivated in South China (**Figures 1, 2**). These findings prove that shading induces the accumulation of chlorophyll in tea leaves, including the leaves of albino varieties, implying tea plant responses to shading are conserved among varieties. This phenomenon may reflect an adaptive mechanism of tea plants, which are generally believed to be shade-tolerant species, to low-light environments. Omics-based analyses revealed that the expression of *CsPOR* genes, which encode protochlorophyllide oxidoreductases, is significantly induced in response to shading (Wu et al., 2016; Liu et al., 2020), whereas the expression of *CsHY5*, which is an important transcription factor gene in the upstream light signaling pathway, is inhibited (Wu et al., 2016; Liu et al., 2018, 2020). The results of the current study are in accordance with these earlier findings (**Figures 1D, 4A**). However, the relationship between *CsHY5* and *CsPOR* expression and chlorophyll accumulation has not been elucidated. In this study, we observed that shading adversely affects CsHY5 to prevent it from inhibiting the expression of the downstream *CsPOR* genes, thereby promoting

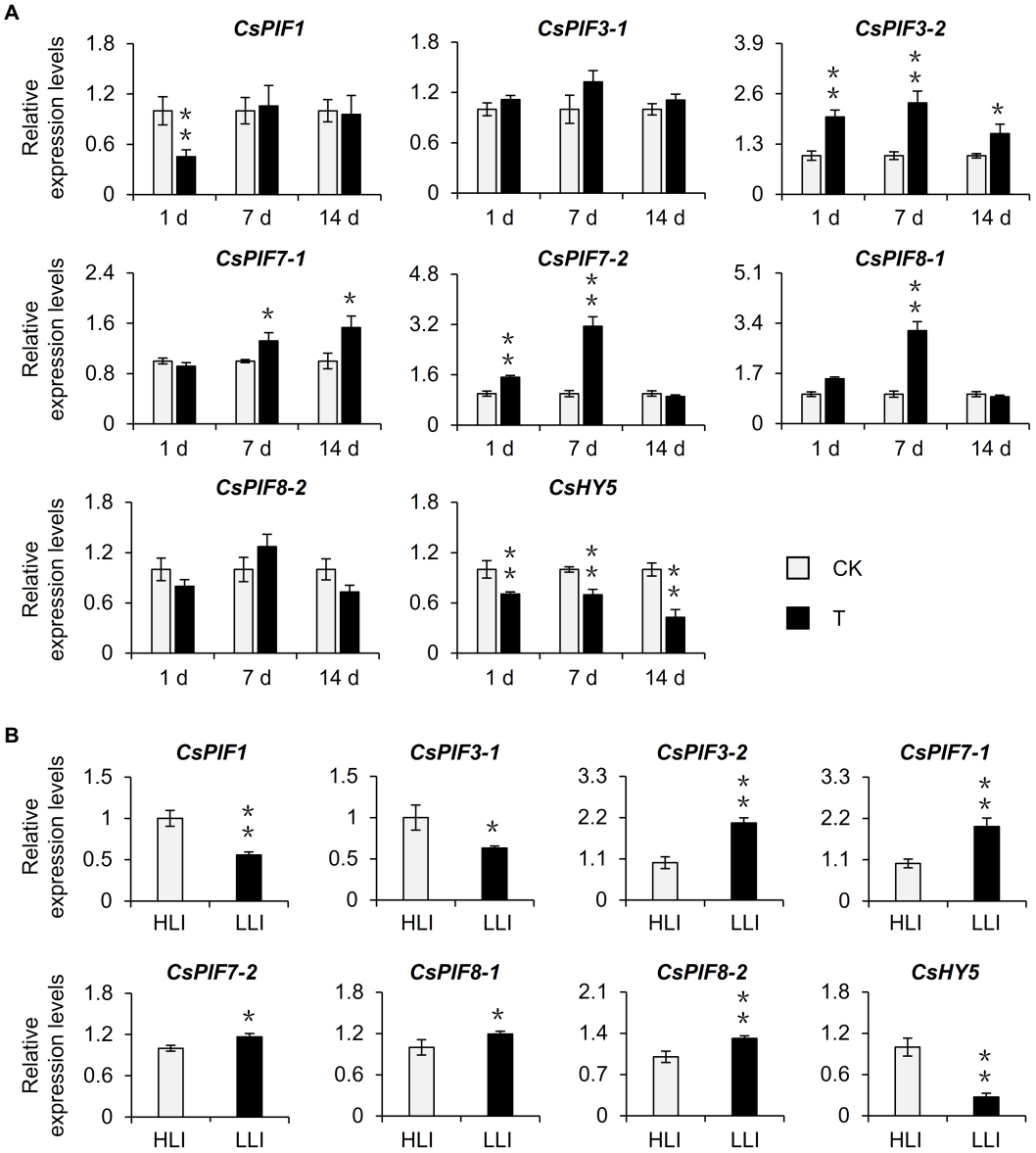

FIGURE 4 | Effects of shading and reduced light intensity on the expression of genes related to the light signal pathway in tea plants. **(A)** Changes in the expression of genes related to light signal in tea plants under shading treatment. CK: no shading treatment group (about 1,300 μmol m^{-2} s^{-1}); T: 90% shading treatment group (about 130 μmol m^{-2} s^{-1}). **(B)** Changes in the expression of light signal-related genes in tea plants under reduced light intensity. HLI: high-light intensity treatment group (252 μmol m^{-2} s^{-1}); LLI: low-light intensity treatment group (16.8 μmol m^{-2} s^{-1}), and R: FR for two groups were 1.5. *CsEF1-α* was used as an internal reference to normalized the changes. Data are expressed as mean ± SD ($n = 3$). *$p \leq 0.05$; **$p \leq 0.01$; and difference from CK treatment at the same time point.

the accumulation of chlorophyll (**Figures 4A, 6C**). A previous study on *A. thaliana* indicated that HY5 may negatively regulate the expression of *POR* genes (Lee et al., 2007). This earlier result combined with the data generated in this study indicate that *POR* expression may be regulated by HY5 in multiple species. In addition to HY5, PIFs are important transcription factors in the light signaling pathway and they also regulate the expression of chlorophyll biosynthesis genes (Moon et al., 2008). In *A. thaliana*, both PIF1 and PIF3 help regulate *POR* expression. Additionally, PIF1 can bind directly to the *PORC* promoter to modulate expression (Cheminant et al., 2011). In the current study, we determined that CsPIF3-2 has no regulatory effects on *POR* expression, which is in contrast to the inhibited *POR* transcription mediated by PIF7-1 (**Figure 6C**). Accordingly, the transcriptional regulation of *POR* genes by PIFs appears to be conserved in multiple species, but the specific regulators may differ among species. Interestingly, CsPIF7-1 negatively regulated the expression of *CsPORL-2*, which seemed were not consistent with the results of accumulation of chlorophyll

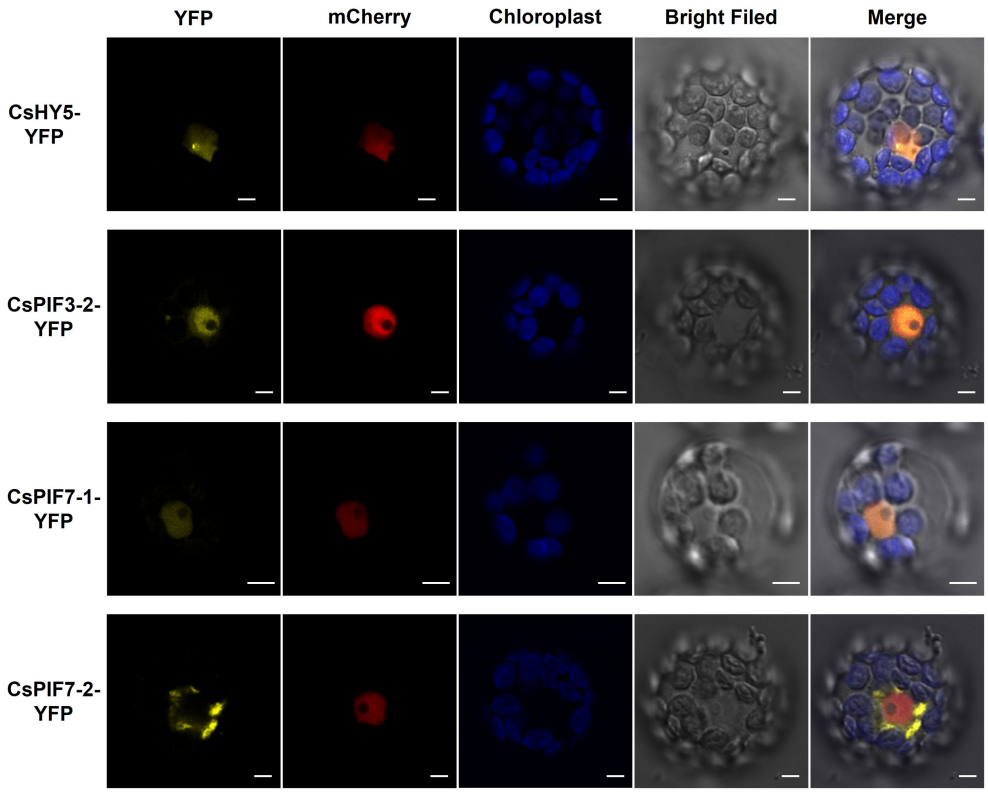

FIGURE 5 | Subcellular localization of CsPIF3/7 and CsHY5. The YFP fusion protein of CsPIF3/7 and CsHY5 was transiently expressed in *Arabidopsis* protoplasts. Yellow fluorescence represented YFP fusion protein of CsPIF3/7 and CsHY5. Red fluorescence represented mCherry protein marker for cell nucleus. Blue fluorescence was the chlorophyll autofluorescence. CsHY5-YFP, CsPIF3-2-YFP, and CsPIF7-1-YFP fusion protein were visible in nucleoplasm structures in the *Arabidopsis* leaf cell. CsPIF7-2-YFP fusion protein may be not in nucleoplasm structures. Bar = 5 μm.

and the expression of *CsPIF7-1* under shading treatment. However, recent study showed that shade-tolerant *Cardamine hirsuta* had higher HFR1 activity, which inhibited more effectively PIF action than *Arabidopsis thaliana* (Paulišić et al., 2021). As a result, a reduced PIF activity and attenuating other PIF-mediated responses were observed under shading. Since tea is also shade-tolerant plant, there may be other regulators, such as HFR1, that inhibit the activity of PIF and the regulation of downstream genes by PIF under shading. Therefore, further work needs to find upstream regulators of PIF7-1. In addition, PIF abundance is attenuated in *C. hirsute* (Paulišić et al., 2021). CsPIF7-1 as a transcription factor to regulate downstream gene expression depends on its protein stability, the protein enrichment of CsPIF7-1 under long time shading treatment was still unclear and needed further investigation. In addition, there may indeed be other regulatory mechanisms between *CsPIF7-1* and *CsPORL-2* that we do not yet know. Collectively, the regulatory roles of these transcription factors will need to be more precisely characterized.

Previous research confirmed that shading decreases the light intensity and the ratio of R: FR, which will affect plant growth and development (Fiorucci and Fankhauser, 2017). All higher plants perceive R: FR changes through members of the phytochrome photoreceptor family; this is often regarded as an indicator of the presence of nearby competitors. On the basis of their responses to shading, plants can be categorized as shade-sensitive plants that exhibit shade-avoidance responses and shade-tolerant plants (Fiorucci and Fankhauser, 2017). Shade-avoidance responses include the elongation of stems or petioles rather than branching, the increased vertical positioning of leaves (i.e., to the top of the canopy), and earlier blooming. These changes are collectively known as the shade-avoidance syndrome. In contrast, shade-avoidance responses are absent in shade-tolerant plants, which thrive on the forest floor and do not grow taller than the surrounding trees (Gommers et al., 2017). *A. thaliana* is considered to be a shade-sensitive plant species, whereas tea plants are generally considered to be shade-tolerant species. Furthermore, previous research proved that shading increases the chlorophyll a and b contents of tea plants, but the ratio of chlorophyll a: chlorophyll b was decreased and the expression levels of the corresponding photosynthesis-related genes were upregulated (Liu et al., 2020). Similar results were obtained in this study (**Figure 1C**). These changes reflect the typical shade tolerance response. However, compared with the extensive research on the shade-avoidance responses of plants, there have been relatively few investigations regarding the mechanism

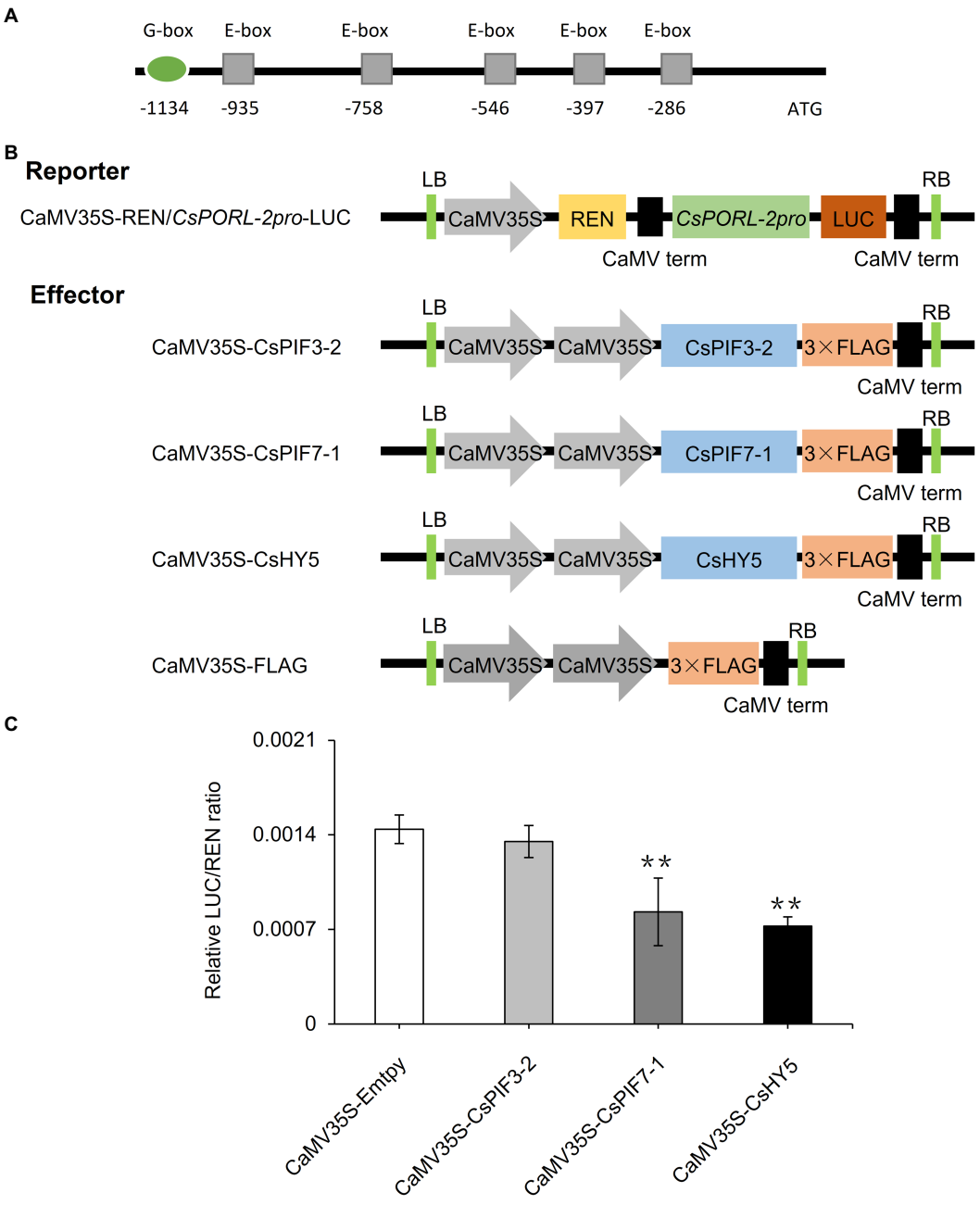

FIGURE 6 | Involvement of CsPIF3-2/7–1 and CsHY5 in regulating the expression of genes related to chlorophyll synthesis. **(A)** *CsPORL-2* promoter element analysis. **(B)** Schematic representation of the double reporter and effector plasmids used in the dual-luciferase reporter assay. **(C)** CsPIF3-2, CsPIF7-1, and CsHY5 have transcriptional regulatory activity on *CsPORL-2* promoter. The regulation of *CsPORL-2* promoter by CsPIF3-2, CsPIF7-1, and CsHY5 was showed by the ratio of LUC to REN. Data are expressed as mean ± SD ($n = 3$). $^{**}p \leq 0.01$; and difference from empty-vector control group.

underlying plant shade tolerance. Studies involving several shade-tolerant species demonstrated that specialized epidermal chloroplasts, altered gene expression patterns, and the increased efficiency of phyA-dependent pathways may enable shade-tolerant plants to adapt to low R: FR light environmental conditions (Cheminant et al., 2011; Jacobs et al., 2016; Gommers et al., 2017). Future analyses of the shade tolerance of tea plants will clarify the effects of shading on tea plants, while also elucidating the adaptive mechanism underlying the shade tolerance of plants.

This study explored the molecular basis of the shade-induced regulation of chlorophyll accumulation in tea leaves. The results were used to develop the following model (**Figure 7**). Shading significantly decreases the light intensity, which is the key environmental factor that promotes the accumulation of chlorophyll in tea leaves. Moreover, the decreased light intensity

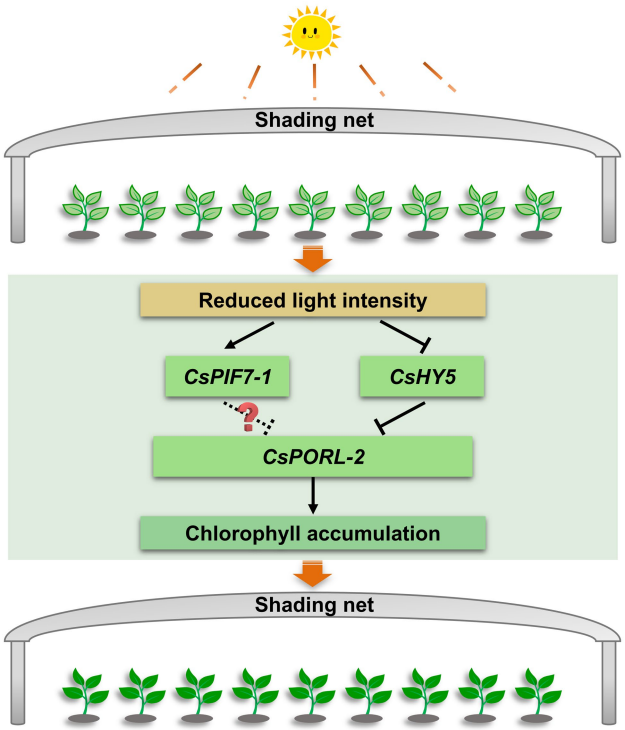

FIGURE 7 | The regulation mechanism model of chlorophyll accumulation under shade treatment of tea plants. After shading, the decrease of light intensity affects the transcription level of *CsHY5* and *CsPIF7-1*, which in turn regulates the expression of the chlorophyll synthesis gene *CsPORL-2*, and causes the accumulation of chlorophyll in tea leaves. Arrows and bars indicate positive regulation and negative regulation, respectively. The solid line indicates the regulatory mechanism in this study, while dashed line and question mark indicate unknown mechanisms.

significantly downregulates and upregulates the expression of *CsHY5* and *CsPIF7-1*, respectively. The decreased abundance of CsHY5 leads to the enhanced expression of *CsPORL-2*, which encodes a key rate-limiting enzyme involved in chlorophyll synthesis, ultimately resulting in chlorophyll accumulation. While CsPIF7-1 may also be involved in regulating the expression of *CsPORL-2* through an unknown mechanism, thereby affecting the formation of chlorophyll, but the specific regulatory mechanism needs to be further studied. These results advance our understanding of the molecular regulatory mechanism of chlorophyll accumulation in tea plant under shade treatment and provide reference for the analysis of stress tolerance of tea plant. In addition, this information will contribute to the breeding of tea varieties with high chlorophyll.

DATA AVAILABILITY STATEMENT

The datasets presented in this study can be found in online repositories. The names of the repository/repositories and accession number(s) can be found in the article/ **Supplementary Material**.

AUTHOR CONTRIBUTIONS

DG conceived and designed the experiments. JC, SW, JL, and LZ conducted the experiments. FD, JL, LZ, JT, and DG analyzed the results. JC, SW, and DG wrote the manuscript. All authors reviewed the manuscript.

FUNDING

This study was supported by the Guangdong Basic and Applied Basic Research Foundation (2020A1515010539), the Medical Science and Technology Research Foundation of Guangdong Province, China (A2019046), the Basic Frontier Science Research Program of Chinese Academy of Sciences (ZDBS-LY-SM032), and the Guangdong Provincial Special Fund for Modern Agriculture Industry Technology Innovation Teams (2020KJ120).

ACKNOWLEDGMENTS

We thank Tea Research Institute of Guangdong Academy of Agricultural Sciences for providing the tea materials.

SUPPLEMENTARY MATERIAL

The Supplementary Material for this article can be found online at: https://www.frontiersin.org/articles/10.3389/fpls.2021.779819/full#supplementary-material

Supplementary Figure S1 | Effect of shading treatment on the chlorophyll content of tea leaves and the expression of related genes. **(A)** The phenotype of new shoots after shading treatment. Bar = 2 cm. **(B)** The change of chlorophyll content after shading treatment. Chl: total chlorophyll; Chl a: chlorophyll a; Chl b: chlorophyll b; and FW: fresh weight. **(C)** The changes in the gene expression of *CsPORL-2* after shading treatment. **(D)** Changes in the expression of genes related to light signal in tea plants under shading treatment. CK: no shading treatment group (about 1,300 μmol·m^{-2}·s^{-1}); T: 90% shading treatment group (about 130 μmol·m^{-2}·s^{-1}). *CsEF1-α* was used as an internal reference to normalized the changes. Data are expressed as mean ± SD ($n = 3$). $^{*}p \leq 0.05$; $^{**}p \leq 0.01$; and difference from CK treatment at the same time point.

REFERENCES

Arnon, D. I. (1949). Copper enzymes in isolated chloroplasts polyphenoloxidase in *Beta vulgaris*. *Plant Physiol.* 24, 1–15. doi: 10.1104/pp.24.1.1

Bourque, D. P., and Naylor, A. W. (1971). Large effects of small water deficits on chlorophyll accumulation and ribonucleic acid synthesis in etiolated leaves of jack bean (*Canavalia ensiformis* [L.] DC.). *Plant Physiol.* 47, 591–594. doi: 10.1104/pp.47.4.591

Cheminant, S., Wild, M., Bouvier, F., Pelletier, S., Renou, J. P., Erhardt, M., et al. (2011). DELLAs regulate chlorophyll and carotenoid biosynthesis to prevent photooxidative damage during seedling deetiolation in *Arabidopsis*. *Plant Cell* 23, 1849–1860. doi: 10.1105/tpc.111.085233

Chen, M., Chory, J., and Fankhauser, C. (2004). Light signal transduction in higher plants. *Annu. Rev. Genet.* 38, 87–117. doi: 10.1146/annurev.genet.38.072902.092259

Chen, Y. Y., Fu, X. M., Mei, X., Zhou, Y., Cheng, S. H., Zeng, L. T., et al. (2017). Proteolysis of chloroplast proteins is responsible for accumulation of free amino acids in dark-treated tea (*Camellia sinensis*) leaves. *J. Proteome* 157, 10–17. doi: 10.1016/j.jprot.2017.01.017

Chen, J. M., Wu, S. H., Zeng, L. T., Dong, F., and Gu, D. C. (2021). Research progress on the influence of shading on tea (*Camellia sinensis*) quality and yield (*in Chinese*). *China Tea* 5, 1–10. doi: 10.3969/j.issn.1000-3150.2021.05.001

Fiorucci, A. S., and Fankhauser, C. (2017). Plant strategies for enhancing access to sunlight. *Curr. Biol.* 27, R931–R940. doi: 10.1016/j.cub.2017.05.085

Frick, G., Su, Q., Apel, K., and Armstrong, G. A. (2003). An *Arabidopsis porB porC* double mutant lacking light-dependent NADPH: protochlorophyllide oxidoreductases B and C is highly chlorophyll-deficient and developmentally arrested. *Plant J.* 35, 141–153. doi: 10.1046/j.1365-313x.2003.01798.x

Fu, X. M., Cheng, S. H., Liao, Y. Y., Huang, B. Z., Du, B., Zeng, W., et al. (2018). Comparative analysis of pigments in red and yellow banana fruit. *Food Chem.* 239, 1009–1018. doi: 10.1016/j.foodchem.2017.07.046

Garrone, A., Archipowa, N., Zipfel, P. F., Hermann, G., and Dietzek, B. (2015). Plant protochlorophyllide oxidoreductases A and B: catalytic efficiency and initial reaction steps. *J. Biol. Chem.* 290, 28530–28539. doi: 10.1074/jbc.M115.663161

Gommers, C. M., Keuskamp, D. H., Buti, S., van Veen, H., Koevoets, I. T., Reinen, E., et al. (2017). Molecular profiles of contrasting shade response strategies in wild plants: differential control of immunity and shoot elongation. *Plant Cell* 29, 331–344. doi: 10.1105/tpc.16.00790

Hellens, R. P., Allan, A. C., Friel, E. N., Bolitho, K., Grafton, K., Templeton, M. D., et al. (2005). Transient expression vectors for functional genomics, quantification of promoter activity and RNA silencing in plants. *Plant Methods* 1, 1–14. doi: 10.1186/1746-4811-1-13

Heyes, D. J., and Hunter, C. N. (2005). Making light work of enzyme catalysis: protochlorophyllide oxidoreductase. *Trends Biochem. Sci.* 30, 642–649. doi: 10.1016/j.tibs.2005.09.001

Huang, W., Ma, H. Y., Huang, Y., Li, Y., Wang, G. L., Jiang, Q., et al. (2017). Comparative proteomic analysis provides novel insights into chlorophyll biosynthesis in celery under temperature stress. *Physiol. Plant.* 161, 468–485. doi: 10.1111/ppl.12609

Jacobs, M., Lopez-Garcia, M., Phrathep, O. P., Lawson, T., Oulton, R., and Whitney, H. M. (2016). Photonic multilayer structure of begonia chloroplasts enhances photosynthetic efficiency. *Nat. Plants* 2, 16162–16166. doi: 10.1038/nplants.2016.162

Jiao, Y. L., Lau, O. S., and Deng, X. W. (2007). Light-regulated transcriptional networks in higher plants. *Nat. Rev. Genet.* 8, 217–230. doi: 10.1038/nrg2049

Kindgren, P., Noren, L., Lopez Jde, D., Shaikhali, J., and Strand, A. (2012). Interplay between HEAT SHOCK PROTEIN 90 and HY5 controls *PhANG* expression in response to the GUN5 plastid signal. *Mol. Plant* 5, 901–913. doi: 10.1093/mp/ssr112

Ku, K. M., Choi, J. N., Kim, J., Kim, J. K., Yoo, L. G., Lee, S. J., et al. (2010). Metabolomics analysis reveals the compositional differences of shade grown tea (*Camellia sinensis* L.). *J. Agric. Food Chem.* 58, 418–426. doi: 10.1021/jf902929h

Lebedev, N., and Timko, M. P. (1998). Protochlorophyllide photoreduction. *Photosynth. Res.* 58, 5–23. doi: 10.1023/A:1006082119102

Lee, L. S., Choi, J. H., Son, N., Kim, S. H., Park, J. D., Jang, D. J., et al. (2013). Metabolomic analysis of the effect of shade treatment on the nutritional and sensory qualities of green tea. *J. Agric. Food Chem.* 61, 332–338. doi: 10.1021/jf304161y

Lee, J., He, K., Stolc, V., Lee, H., Figueroa, P., Gao, Y., et al. (2007). Analysis of transcription factor HY5 genomic binding sites revealed its hierarchical role in light regulation of development. *Plant Cell* 19, 731–749. doi: 10.1105/tpc.106.047688

Liu, L. L., Li, Y. Y., She, G. B., Zhang, X. C., Jordan, B., Chen, Q., et al. (2018). Metabolite profiling and transcriptomic analyses reveal an essential role of UVR8-mediated signal transduction pathway in regulating flavonoid biosynthesis in tea plants (*Camellia sinensis*) in response to shading. *BMC Plant Biol.* 18:233. doi: 10.1186/s12870-018-1440-0

Liu, Z. W., Li, H., Wang, W. L., Wu, Z. J., Cui, X., and Zhuang, J. (2017). CsGOGAT is important in dynamic changes of theanine content in postharvest tea plant leaves under different temperature and shading spreadings. *J. Agric. Food Chem.* 65, 9693–9702. doi: 10.1021/acs.jafc.7b04552

Liu, L. L., Lin, N., Liu, X. Y., Yang, S., Wang, W., and Wan, X. C. (2020). From chloroplast biogenesis to chlorophyll accumulation: the interplay of light and hormones on gene expression in *Camellia sinensis* cv Shuchazao leaves. *Front. Plant Sci.* 11:256. doi: 10.3389/fpls.2020.00256

López-Figueroa, F., and Niell, F. (1990). Effects of light quality on chlorophyll and biliprotein accumulation in seaweeds. *Mar. Biol.* 104, 321–327. doi: 10.1007/BF01313274

Masuda, T., and Takamiya, K. (2004). Novel insights into enzymology, regulation and physiological functions of light-dependent protochlorophyllide oxidoreductase in angiosperms. *Photosynth. Res.* 81, 1–29. doi: 10.1023/B:PRES.0000028392.80354.7c

Moon, J., Zhu, L., Shen, H., and Huq, E. (2008). PIF1 directly and indirectly regulates chlorophyll biosynthesis to optimize the greening process in *Arabidopsis*. *Proc. Natl. Acad. Sci. U. S. A.* 105, 9433–9438. doi: 10.1073/pnas.0803611105

Paik, I., Kathare, P. K., Kim, J. I., and Huq, E. (2017). Expanding roles of PIFs in signal integration from multiple processes. *Mol. Plant* 10, 1035–1046. doi: 10.1016/j.molp.2017.07.002

Paulišić, S., Qin, W. T., Arora Verasztó, H., Then, C., Alary, B., Nogue, F., et al. (2021). Adjustment of the PIF7-HFR1 transcriptional module activity controls plant shade adaptation. *EMBO J.* 40:e104273. doi: 10.15252/embj.2019104273

Reinbothe, C., El Bakkouri, M., Buhr, F., Muraki, N., Nomata, J., Kurisu, G., et al. (2010). Chlorophyll biosynthesis: spotlight on protochlorophyllide reduction. *Trends Plant Sci.* 15, 614–624. doi: 10.1016/j.tplants.2010.07.002

Rizzini, L., Favory, J. J., Cloix, C., Faggionato, D., O'Hara, A., Kaiserli, E., et al. (2011). Perception of UV-B by the *Arabidopsis* UVR8 protein. *Science* 332, 103–106. doi: 10.1126/science.1200660

Sakuraba, Y., Rahman, M. L., Cho, S. H., Kim, Y. S., Koh, H. J., Yoo, S. C., et al. (2013). The rice *faded green leaf* locus encodes protochlorophyllide oxidoreductase B and is essential for chlorophyll synthesis under high light conditions. *Plant J.* 74, 122–133. doi: 10.1111/tpj.12110

Sano, T., Horie, H., Matsunaga, A., and Hirono, Y. (2018). Effect of shading intensity on morphological and color traits and on chemical components of new tea (*Camellia sinensis* L.) shoots under direct covering cultivation. *J. Sci. Food Agric.* 98, 5666–5676. doi: 10.1002/jsfa.9112

Scrutton, N. S., Groot, L. M., and Heyes, D. J. (2012). Excited state dynamics and catalytic mechanism of the light-driven enzyme protochlorophyllide oxidoreductase. *Phys. Chem. Chem. Phys.* 14, 8818–8824. doi: 10.1039/c2cp23789j

Suzuki, Y., and Shioi, Y. (2003). Identification of chlorophylls and carotenoids in major teas by high-performance liquid chromatography with photodiode array detection. *J. Agric. Food Chem.* 51, 5307–5314. doi: 10.1021/jf030158d

Tang, G. Y., Meng, X., Gan, R. Y., Zhao, C. N., Liu, Q., Feng, Y. B., et al. (2019). Health functions and related molecular mechanisms of tea components: an update review. *Int. J. Mol. Sci.* 20:6196. doi: 10.3390/ijms20246196

Teng, R. M., Wang, Y. X., Li, H., Lin, S. J., Liu, H., and Zhuang, J. (2021). Effects of shading on lignin biosynthesis in the leaf of tea plant (*Camellia sinensis* (L.) O. Kuntze). *Mol. Gen. Genomics.* 296, 165–177. doi: 10.1007/s00438-020-01737-y

Wu, Q. J., Chen, Z. A., Sun, W. J., Deng, T. T., and Chen, M. J. (2016). De novo sequencing of the leaf transcriptome reveals complex light-responsive regulatory networks in *Camellia sinensis* cv Baijiguan. *Front. Plant Sci.* 7:332. doi: 10.3389/fpls.2016.00332

Yamashita, H., Tanaka, Y., Umetsu, K., Morita, S., Ono, Y., Suzuki, T., et al. (2020). Phenotypic markers reflecting the status of overstressed tea plants subjected to repeated shade cultivation. *Front. Plant Sci.* 11:556476. doi: 10.3389/fpls.2020.556476

Yang, Z., Kobayashi, E., Katsuno, T., Asanuma, T., Fujimori, T., Ishikawa, T., et al. (2012). Characterisation of volatile and non-volatile metabolites in etiolated leaves of tea (*Camellia sinensis*) plants in the dark. *Food Chem.* 135, 2268–2276. doi: 10.1016/j.foodchem.2012.07.066

Yu, X. L., Hu, S., He, C., Zhou, J. T., Qu, F. F., Ai, Z. Y., et al. (2019). Chlorophyll metabolism in postharvest tea (*Camellia sinensis* L.) leaves: variations in color values, chlorophyll derivatives, and gene expression levels under different withering treatments. *J. Agric. Food Chem.* 67, 10624–10636. doi: 10.1021/acs.jafc.9b03477

Zeng, L., Zhou, X., Su, X., and Yang, Z. (2020). Chinese oolong tea: An aromatic beverage produced under multiple stresses. *Trends Food Sci. Technol.* 106, 242–253. doi: 10.1016/j.tifs.2020.10.001

Zhao, X. C., Zeng, X. S., Lin, N., Yu, S. W., Fernie, A. R., and Zhao, J. (2021). CsbZIP1-CsMYB12 mediates the production of bitter-tasting flavonols in tea plants (*Camellia sinensis*) through a coordinated activator-repressor network. *Hortic. Res.* 8:110. doi: 10.1038/s41438-021-00545-8

Zhou, Y., Peng, Q. Y., Zhang, L., Cheng, S. H., Zeng, L. T., Dong, F., et al. (2019). Characterization of enzymes specifically producing chiral flavor compounds (*R*)- and (*S*)-1-phenylethanol from tea (*Camellia sinensis*) flowers. *Food Chem.* 280, 27–33. doi: 10.1016/j.foodchem.2018.12.035

Conflict of Interest: The authors declare that the research was conducted in the absence of any commercial or financial relationships that could be construed as a potential conflict of interest.

Publisher's Note: All claims expressed in this article are solely those of the authors and do not necessarily represent those of their affiliated organizations, or those of the publisher, the editors and the reviewers. Any product that may be evaluated in this article, or claim that may be made by its manufacturer, is not guaranteed or endorsed by the publisher.

frontiers in Plant Science

ORIGINAL RESEARCH
published: 17 December 2021
doi: 10.3389/fpls.2021.797854

Tonoplast-Localized Theanine Transporter CsCAT2 May Mediate Theanine Storage in the Root of Tea Plants (*Camellia sinensis* L.)

Lin Feng[1,2†], Yongchao Yu[1†], Shijia Lin[1], Tianyuan Yang[1], Qi Chen[1], Linlin Liu[1], Jun Sun[1], Pengcheng Zheng[1,2], Zhaoliang Zhang[1] and Xiaochun Wan[1*]*

[1] State Key Laboratory of Tea Biology and Resource Utilization, School of Tea and Food science and Technology, Anhui Agricutural University, Hefei, China, [2] Institute of Fruit and Tea, Hubei Academy of Agricultural Sciences, Wuhan, China

OPEN ACCESS

Edited by:
Wenyan Han,
Tea Research Institute, Chinese Academy of Agricultural Sciences (CAAS), China

Reviewed by:
Mingjie Chen,
Xinyang Normal University, China
Yuhua Wang,
Nanjing Agricultural University, China

***Correspondence:**
Zhaoliang Zhang
zhlzhang@ahau.edu.cn
Xiaochun Wan
xcwan@ahau.edu.cn

[†]These authors have contributed equally to this work

Specialty section:
This article was submitted to Plant Metabolism and Chemodiversity, a section of the journal Frontiers in Plant Science

Received: 19 October 2021
Accepted: 22 November 2021
Published: 17 December 2021

Citation:
Feng L, Yu Y, Lin S, Yang T, Chen Q, Liu L, Sun J, Zheng P, Zhang Z and Wan X (2021) Tonoplast-Localized Theanine Transporter CsCAT2 May Mediate Theanine Storage in the Root of Tea Plants (Camellia sinensis L.). Front. Plant Sci. 12:797854. doi: 10.3389/fpls.2021.797854

Theanine is the component endowing tea infusion with "umami" taste and antidepression benefits. Theanine is primarily synthesized and stored in root in winter and is transported *via* vascular tissues to the new shoot in spring. However, the mechanism underlying theanine storage in the root of tea plants remains largely unknown. Cationic amino acid transporter 2 (CsCAT2) in tea plants is homologous to glutamine permease 1 (GNP1), the specific glutamine transporter in yeast. In this study, we identified CsCAT2 as an H^+-dependent theanine transporter with medium affinity for theanine. The result of subcellular localization showed that CsCAT2 was a tonoplast-localized transporter. Importantly, *CsCAT2* highly expressed in the root in winter during theanine storage and reduced its expression in the root during theanine transport from root-to-shoot in spring. In addition, *CsCAT2* expression in the roots of 5 varieties at four time points during December and April was significant negatively correlated with the capacity of theanine root-to-shoot movement. Taken together, these results suggested that CsCAT2 may mediate theanine storage in the vacuole of root cells and may negatively modulate theanine transport from root to shoot.

Keywords: ***Camellia sinensis*** **(L.) O. Kuntze, amino acid transporter, theanine storage, root-to-shoot transport, amino acid**

INTRODUCTION

Tea plant (*Camellia sinensis* L.) is a perennial and commercially valuable crop; its buds and one or two leaves below the bud are harvested for green tea manufacturing. The composition and content of amino acids in the tender shoot leaves are the critical components that endow tea with its flavor and health benefits (Wan, 2003; Hunt et al., 2010; Wan and Xia, 2015). Most amino acids contribute to the umami taste and alleviate the bitterness and astringency of tea infusions. The ratio of amino acids to polyphenols determines the quality and suitability of tea (Wan, 2003).

In the tender tea leaves, theanine accounts for more than 50% of the free amino acid content, which significantly correlates with the quality and price of green teas (Yamaguchi and Ninomiya, 2000; Wan, 2003; Feng et al., 2014). Theanine-derived metabolites produced during manufacturing contribute a roasted peanut flavor to oolong teas (Guo et al., 2018) and a roasted and caramel flavor to yellow tea (Guo et al., 2019). Theanine also contributes to the colors of tea infusion

(Yao et al., 2006), given that the colored compounds containing theanine-carbohydrate conjugates (Tanaka et al., 2005). Theanine also has many health benefits including promoting relaxation, concentration, and learning efficiency (Sharma et al., 2018).

Theanine is mainly synthesized, stored in the roots in late autumn and winter, and transported to the new shoots in spring (Ruan et al., 2012; Ashihara, 2015). However, theanine metabolism and transport processes are weak in summer and fall (Gong et al., 2020). Therefore, generally, green teas produced in spring contain higher level of theanine than those produced summer and fall (Xu et al., 2012; Jiang et al., 2018). That is the main reason why green teas produced in spring are of high quality and price (Xu et al., 2012).

In tea plant roots, theanine is mainly synthesized from ethylamine and glutamate by theanine synthetase (CsTSI) (Wei et al., 2018; Fu et al., 2021; Zhu et al., 2021). *CsTSI* is highly and specifically expressed in roots and encodes an enzyme localized in cytoplasm, suggesting that theanine is synthesized in cytoplasm of root cells (Fu et al., 2021). Fu et al. (2021) examined the subcellular distribution of theanine and found almost all the theanine (∼99%) was in the cytoplasm of root cells in March. However, in shoot, theanine was shown to be distributed in chloroplast, vacuole, cytoplasm, and mitochondria; the distribution was also dynamically changed within March, May, and November, and in response to shading treatment. Given that theanine is stored in root cells in winter and is transported to new shoots in spring, its subcellular distribution in root cells is also supposed to be dynamic. However, the dynamic subcellular distribution of theanine in roots in winter and spring has not been revealed.

Amino acid transporters (AATs) are membrane-localized proteins that mediate intercellular, intracellular, and long-distance amino acid transport (Tegeder et al., 2007; Dinkeloo et al., 2018). Recently, we identified amino acid permease (AAP) family members as theanine transporters in tea plants (Dong et al., 2020). Our results revealed that six CsAAPs exhibited theanine transport activity and are mainly expressed in the leaves, vascular bundles, and roots. Furthermore, *CsAAP1* is crucial in mediating the long-distance root-to-shoot transport of theanine (Dong et al., 2020). However, there is no clue implying that CsAAPs play a role in theanine storage in root.

In the abovementioned study, we found that glutamine permease 1 (GNP1) in yeast can also transport theanine. We searched for GNP1 homolog in tea plant by high sequence similarity. But there was no highly conserved GNP1 homolog found. The most closed protein in tea plant is CsCAT2 (Tea025016.1), which has 26.2% sequence identity to GNP1. Interestingly, in another study, we found *CsCAT2* expression in roots of tea plants was significantly induced by theanine feeding and was also induced by cold stress (Feng et al., 2018). These clues led us to ask whether CsCAT2 has theanine transport activity and plays a role in theanine transport in tea plants.

In this study, the substrate specificity and pH-dependence of CsCAT2 theanine transport were analyzed in yeast mutant 22Δ10α. The seasonal regulation of CsCAT2 expression in tea plants was analyzed, and correlation analysis was also conducted to elucidate whether CsCAT2 is involved in theanine storage and long-distance transport. Our findings indicated that CsCAT2 is a tonoplast-localized theanine transporter and its expression in the root was highly and negatively correlated with theanine accumulation in the leaf buds. These results elucidate CsCAT2's putative function in theanine storage in the root of in tea plants.

MATERIALS AND METHODS

Transient Expression in Protoplasts

The full cDNA sequence of *CsCAT2* without the stop codon was cloned into a pK7WGF 7.0 vector carrying the 35S promoter and green fluorescent protein. The plasmids encoding the fusion protein CsCAT2 were transiently transformed using chemical shock into protoplasts derived from an *Arabidopsis* cell suspension culture. Two days after the polyethylene glycol-mediated plasmid transformation, these protoplasts were analyzed using confocal microscopy (FV1000, Olympus, Japan).

Total RNA Extraction and Quantitative RT-PCR

Tea plants used were planted in Guohe Tea Plantation (Lujiang, Anhui, China). For season-dependent *CsCAT2* expression analysis, total RNA was extracted from the roots of five tea plant varieties (Zhenong 113, Yingshuang, Zhonghuang 302, Longjing 43, and Shuchazao) collected on December 12, 2017 and March 1, March 23, and April 13, 2018. The real-time reverse transcription quantitative PCR procedures and analysis were conducted following the method of Feng et al. (2018). Gene-specific primers were designed using Primer Premier 5 and was listed in **Supplementary Table 1**. Glyceraldehyde 3-phosphate dehydrogenase (*GAPDH*) gene (Song et al., 2016) was used as an internal control. Data were analyzed following the threshold cycle (Ct), and relative expression was quantified using $2^{-\Delta Ct}$ (Schmittgen and Zakrajsek, 2000).

Cloning of CsCAT2 and Yeast Complementation Assay

The sequences of CsCAT2 were amplified using the polymerase chain reaction (PCR) from Shuchazao leaves cDNA libraries and cloned with XbaI in a pYES2 yeast expression vector. The primers used in the study were presented in **Supplementary Table 1**. Recombinant plasmid or pYES2 were transferred into the 22Δ10α yeast strain (this yeast strain does not have 10 AATs and cannot grow on medium with amino acid as the sole nitrogen, except arginine) (Besnard et al., 2016), generating strains designated as 22Δ10α-*CsCAT2* and 22Δ10α-pYES2. Recombinant strains were selected on the yeast nitrogen base lacking uracil and were supplied with 2 mM ammonium sulfate. After the PCR verification, positive colonies were selected for further transport analysis.

Growth Assays of CsCAT2 on Amino Acid as the Sole Nitrogen Source

Growth assays were conducted in uracil-free YNB medium containing 2 mM of theanine, glutamine, aspartic acid, asparagine, glutamic acid, proline, γ-aminobutyric acid, or citrulline as sole nitrogen source and 2% d-galactose as the

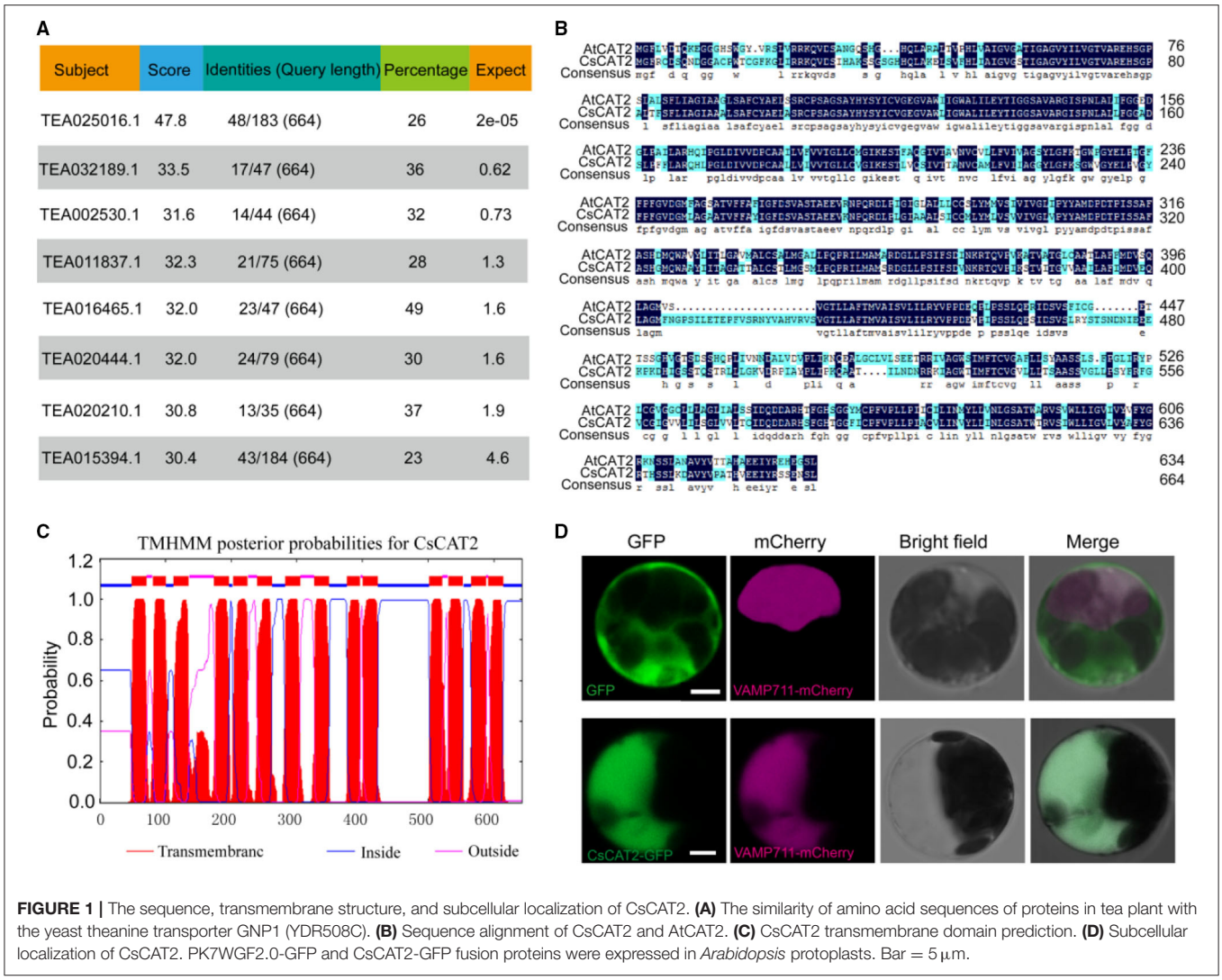

FIGURE 1 | The sequence, transmembrane structure, and subcellular localization of CsCAT2. **(A)** The similarity of amino acid sequences of proteins in tea plant with the yeast theanine transporter GNP1 (YDR508C). **(B)** Sequence alignment of CsCAT2 and AtCAT2. **(C)** CsCAT2 transmembrane domain prediction. **(D)** Subcellular localization of CsCAT2. PK7WGF2.0-GFP and CsCAT2-GFP fusion proteins were expressed in *Arabidopsis* protoplasts. Bar = 5 μm.

carbon source. Yeast cultured to an OD_{600} of 0.6 was diluted to 10^0, 10^{-1}, 10^{-2}, 10^{-3}, or 10^{-4} solutions. However, 2 μl diluted solutions were spotted onto the YNB media. The yeast growth was observed after 3 days of incubation at 30°C and was photographed with a digital camera. All experiments were performed for three independent replicates.

For growth assays in a liquid medium, 0.2 and 2 mM of theanine were used to analyze the growth of yeast, and the OD_{600} values were measured daily over 7 days.

Measurement of Theanine Transport

For kinetic analysis, cells of the wild-type yeast strains 23344c, 22Δ10α-pYES2, and 22Δ10α-CsCAT2 were grown on the YNB and 2 mM ammonium sulfate medium to OD_{600} = 0.8. Yeast cells were collected, washed three times, and then cultured in the YNB medium without nitrogen for 2 h of starvation. Theanine was added to varied concentrations of 0.09375, 0.1875, 0.375, 0.75, 2.25, and 8 mM. Yeast cells were centrifuged and collected at 0, 2, 5, 10, and 20 min after theanine was added. For the substrate specificity analysis, 200 μM of theanine was added to the respective solutions along with 2 mM of the each of the following competitors: valine, aspartic acid, alanine, glutamate (Glu), and glutamine (Gln). Yeast cells were collected and centrifuged for 10 min. To analyze the pH-dependence of theanine uptake after the nitrogen starvation treatment, the pH of the medium was adjusted to 4, 5, 6, 7, and 8 using hydrochloric acid or sodium hydroxide before the addition of 200 μM. Yeast cells were collected and centrifuged for 10 min. The pretreatment procedures for the H^+ pump inhibitor treatment before and after theanine feeding were identical to those of the kinetic analysis; 200 μM of theanine was added along with 0.01 mM carbonylcyanide m-chlorophenylhydrazone (CCCP), 0.1 mM 2, 4-dinitrophenol (DNP), and 1 mM diethylpyrocarbonate (DEPC). Yeast cells were collected and centrifuged for 10 min.

The yeast cultivation and sample processing procedures of (a), (b), (c), and (d) were identical. Following the collection of the sediment, (a), (b), (c), and (d) were each collected and washed four times with pH 4.5 buffer, containing 0.6 M sorbitol

and 50 mM potassium phosphate. After the addition of 1 ml of deionized water to the resuspended cells, the mix was bathed in 98°C water for 1 h for theanine extract.

Theanine was detected with a Waters HPLC system, equipped with a 2489 ultraviolet (UV)-visible detector and a reverse-phase C18 column (5 μm, 250 mm × 4.6 mm, Phenomenex, Los Angeles, USA). The column temperature and the detection wavelength were set to 28°C and 210 nm, respectively. The mobile phase consisted of HPLC H_2O (A), acetonitrile (B), and the gradient elution was as follows: B 0% (v/v) to 80% at 12 min, to 0% at 22 min. The flow rate is 1 ml/min, and the injection volume is 10 μl. Then, theanine concertation was calculated according to the theanine standard.

Statistical Analysis

Data were presented as mean ± standard deviation (SD) of three independent biological replicates. Statistical significance was evaluated through the one-way analysis of variance, followed by a Tukey's test using SPSS Statistics 19.0 (IBM, Chicago, USA). The correlation coefficient analysis was elucidated using the Pearson's correlation coefficient, with $p < 0.05$ was considered as statistical significance.

RESULTS

CsCAT2 Localizes in the Tonoplast

Our previous study characterized that GNP1 in yeast has theanine transport activity (Dong et al., 2020). We tried to identify GNP1 homolog in tea plants, but we failed to find highly conserved homolog in tea plants. However, we found that a protein (TEA025016.1) in tea plant has weak conservation with GNP1 (**Figure 1A**). TEA025016.1 is highly homologous to AtCAT2 (**Figure 1B**), a tonoplast-localized AAT in *Arabidopsis*. Therefore, we named TEA025016.1 as CsCAT2. CsCAT2 is conserved in plants including *Arabidopsis thaliana*, *Vitis vinifera*, *Theobroma cacao*, *Actinidia* spp., *Populus tremula*, and *Coffea canephora* (Feng et al., 2018). CsCAT2 has also classic transmembrane domains based on the prediction using TMHMM online program (**Figure 1C**).

To verify the subcellular localization of CsCAT2, cauliflower mosaic virus 35S promoter-driven *CsCAT2-GFP* and *VAMP711-mCherry* were cotransferred into *Arabidopsis* protoplast. VAMP711 is a tonoplast-localized protein (Bassil et al., 2011) and was used as the tonoplast marker in this study. The fluorescence of CsCAT2-GFP overlapped with that of VAMP711-mCherry (**Figure 1D**), indicating that CsCAT2 also localized in the tonoplast.

CsCAT2 Expression Is Seasonally Regulated

Theanine is mainly synthesized and stored in roots in winter and is then transported to new shoots in early spring (Ruan et al., 2012; Ashihara, 2015). To explore the role of CsCAT2 in theanine storage and root-to-shoot transport, we examined *CsCAT2* expression in roots at four time points including December 12, March 1, March 23, and April 13. *CsCAT2* expression was high at the December 12 time point, continuously decreased from December 12 to March 1 and March 23, and subsequently increased at April 13 (**Figure 2**). In contrast, theanine contents in new shoots continuously increased from December 1 to March 1 and March 23 and subsequently increased at April 13 (Dong et al., 2020). Additionally, theanine transport is strongest in March and then decreases in April (Fang et al., 2017; Dong et al., 2020). The consistency of *CsCAT2* expression with theanine storage in the roots suggested a role of CsCAT2 in theanine storage; the opposite change patterns between *CsCAT2* expression and theanine root-to-shoot transport suggested that CsCAT2 may negatively modulate theanine root-to-shoot transport.

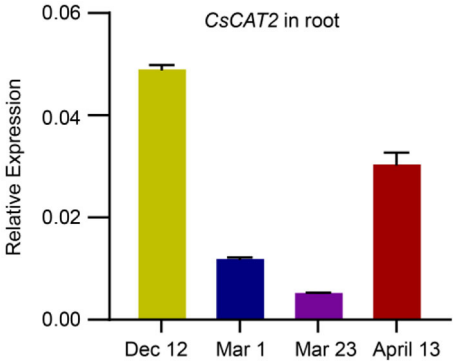

FIGURE 2 | Seasonal expression of CsCAT2 in the root of tea plant cultivar "Shuchazao" tea cultivar. The expression of CsCAT2 in the root at four time points, December 12 (Dec 12), March 1 (Mar 1), March 23 (Mar 23), and April 13, was examined by qRT-PCR. The data were calculated using the $2^{-\Delta ct}$ method and represented as mean ± SD ($n = 3$) with *CsGAPDH* as the internal control.

CsCAT2 Transports Theanine and Has a Medium Affinity for Theanine

To explore the possibility that CsCAT2 regulates theanine storage and root-to-shoot transport, we asked whether CsCAT2 can directly transport theanine. We cloned the *CsCAT2* into a pYES2 vector and transformed it into a yeast mutant strain 22Δ10α. This mutant carries mutations of 10 genes encoding AATs and cannot grow on the medium with amino acid (except arginine) as the sole nitrogen source (Besnard et al., 2016). As shown in **Figure 3**, the wild-type strain 23344c grew well on the medium supplied with 5 mM theanine as the sole nitrogen source, whereas 22Δ10α strain and 22Δ10α that transferred with vector pYES2 could not grow. However, the expression of CsCAT2 in 22Δ10α conferred the growth of this mutant (**Figure 3A**). We further cultured these yeast strain 22Δ10α/pYES2 in liquid medium with 2 mM theanine, and 22Δ10α/CsCAT2 in liquid medium with 0.2 or 2 mM of theanine as the sole nitrogen source, to observe the growth. In this assay, we also observed 22Δ10α/CsCAT2 gradually grew during 10 days culture. But 22Δ10α/pYES2 did not grow (**Figure 3B**). These results indicated that CsCAT2 transported theanine into the yeast cells.

To further assess the affinity of CsCAT2 for theanine, we next analyzed the transport kinetics of CsCAT2. The kinetic parameters calculated through theanine transport

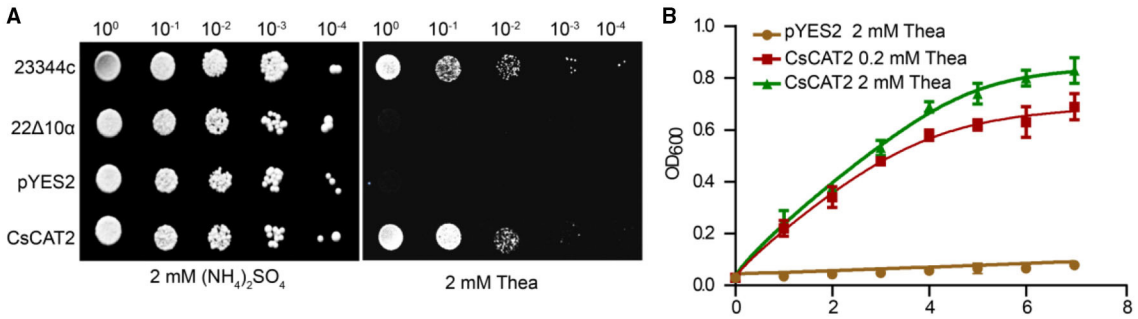

FIGURE 3 | CsCAT2-mediated theanine uptake into yeast cells. **(A)** Dot assays showed the growth phenotype of yeast lines 23344c (wild-type line), mutants 22Δ10α, 22Δ10α/pYES2 (pYES2), and 22Δ10α/pYES2-*CsCAT2* (CsCAT2), on medium with 2 mM $(NH_4)_2SO_4$ or 2 mM theanine (Thea) as nitrogen source. **(B)** The growth curve of yeast in liquid medium at different theanine concentrations as nitrogen source. The OD_{600} value was identified as a parameter for measuring yeast growth. 23344c and the empty vector pYES2 were the positive and negative controls, respectively. The result was expressed as mean ± SD ($n = 3$).

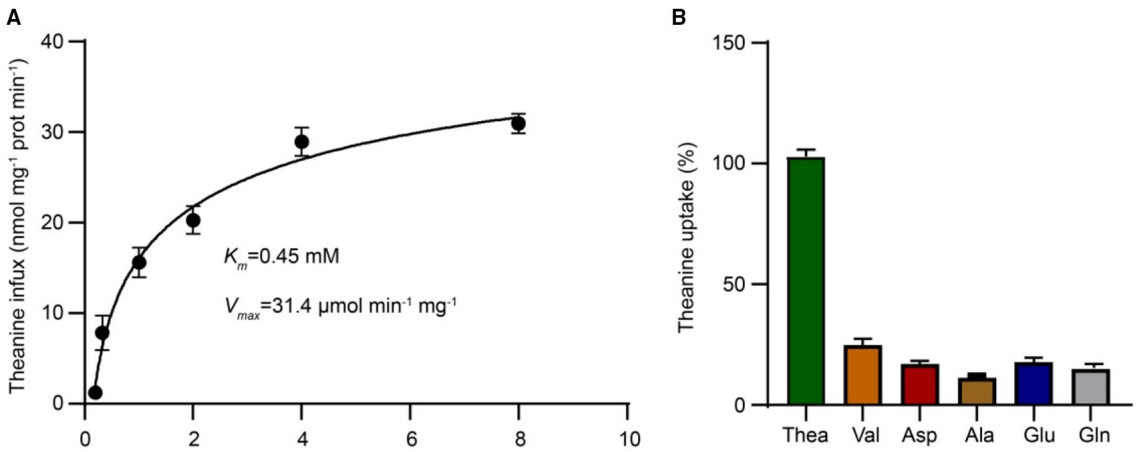

FIGURE 4 | The uptake kinetic properties and substrate selectivity analysis of theanine transport by CsCAT2. **(A)** Measurement of K_m and V_{max} values of CsCAT2 for theanine in yeast. The ordinate represents the amount of theanine absorbed by per milligram protein per minute. Prot represents protein. **(B)** Substrate specificity of CsCAT2. Theanine uptake was determined with 10-dose excess glutamine (Gln), asparate (Asp), glutamate (Glu), alanine (Ala), and valine (Val), as the competitor, respectively. The group of uptake without competitive amino acid was served as 100%. The result was expressed as mean ± SD ($n = 3$).

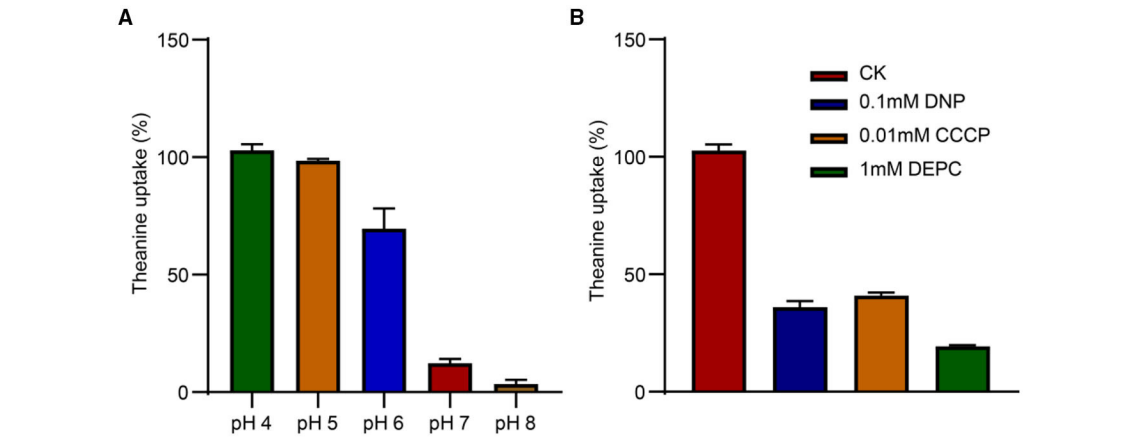

FIGURE 5 | The pH dependence of CsCAT2 uptake of theanine in 22Δ10α. **(A)** Theanine uptake by CsCAT2 at different pH values; uptake at pH 4 serve as 100%. **(B)** Theanine uptake by CsCAT2 in the presence of CCCP, DNP, and DEPC. The result was expressed as mean ± SD ($n = 3$).

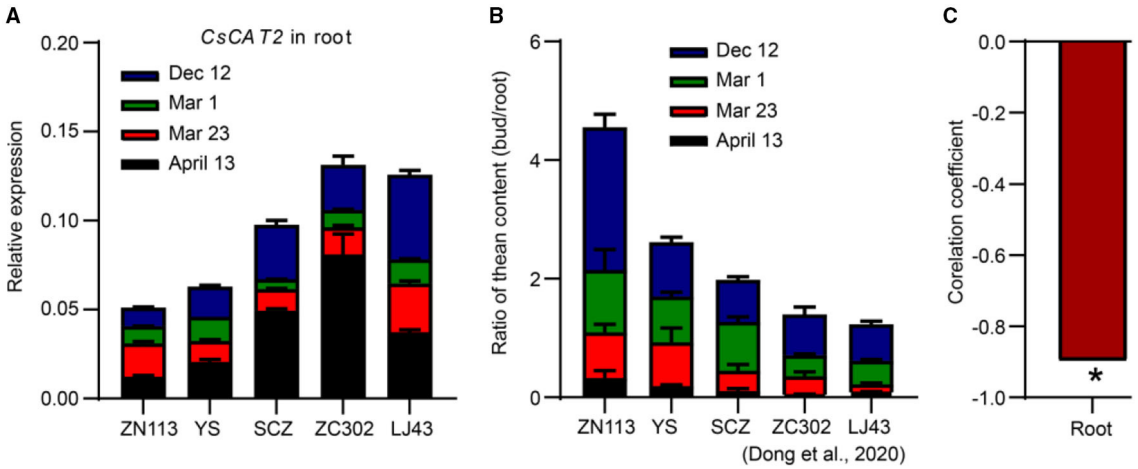

FIGURE 6 | Correlation between *CsCAT2* expression in the roots and the efficiency of theanine root-to-shoot transport. **(A)** *CsCAT2* expression in the roots of 5 tea plant cultivars at the four time points. *CsGAPDH* was used as an internal control. **(B)** The ratios of theanine in the bud to that in the root in different tea plant cultivars. The data are from Dong et al. (2020). **(C)** Correlation between the summation of *CsCAT2* expression **(B)** and the ratios **(C)** was analyzed using Pearson's correlation. ZN113, Zhenong 113; YS, Yingshuang; SCZ, Shuchazao; ZC302, Zhongcha 302; LJ43, Longjing 43. Data were analyzed using one-way ANOVA, * $p < 0.05$.

assays indicated that the *K*m and V_{max} for CsCAT2 were 0.45 mM and 31.43 μmol min^{-1} mg^{-1}, respectively (**Figure 4A**). This suggested that CsCAT2 was a medium-affinity theanine transporter.

CsCAT2 Has Broad Substrate Specificity

We next asked whether CsCAT2 can transport other amino acids. We cultured the above yeast strains in medium with Glu, glutamine (Gln), γ-aminobutyric acid (GABA), valine (Val), alanine (Ala), or aspartate (Asp), at a concentration of 2 mM, respectively, as the sole nitrogen source. The result demonstrated that CsCAT2 can also transport these amino acids (**Supplementary Figure 1**) and also demonstrated that CsCAT2 had broad substrate specificity, which was consistent with other AATs (Dong et al., 2020; Li et al., 2020, 2021).

To further investigate the substrate specificity of CsCAT2, a 10-fold dose of Val, Ala, Gln, Asp, and Glu, the dominant amino acids being transported in vascular system of tea plants (Ruan et al., 2012), was added to the medium to compete with theanine for transport. The results showed that CsCAT2's capacity to transport theanine was significantly suppressed by these amino acids (**Figure 4B**), further demonstrating that CsCAT2 can transport Glu, Gln, Ala, Asp, and Val. These results are consistent with other reports that CATs have broad substrate specificities and affinities for Glu, Ala, Gln, Asp, and Val in *Arabidopsis* (Su et al., 2004; Hammes et al., 2006; Yang et al., 2010, 2015).

CsCAT2 Transports Theanine in a pH-Dependent Manner

The transport capacity of theanine greatly decreased when the value of pH was increased from 4 to 8 in the medium (**Figure 5A**). At pH 7.0 and pH 8.0, theanine transport by CsCAT2 was almost completely inhibited. To further verify the pH or H^+-dependant CsCAT2 activity, we added protonophores 2, 4-dinitrophenol (DNP) and carbonylcyanide m-chlorophenylhydrazone (CCCP), and an H^+-coupled amino acid transport system inhibitor (DEPC), to the theanine transport system. The result showed that theanine transport activity of CsCAT2 was essentially inhibited by these reagents (**Figure 5B**). Therefore, CsCAT2 transport theanine is pH-dependant and functions as an H^+-coupled theanine transport system.

CsCAT2 Expression in the Roots Probably Correlates With the Efficiency of Theanine Root-to-Shoot Transport

The efficiency of transport of theanine from root to shoot is critical for theanine accumulation in new shoots which are the materials for tea processing. As described (**Figure 2**), *CsCAT2* expression in the root showed an opposite trend with the process of theanine transport from root to shoot, at four time points (December 1, March 1, March 23, and April 13), in a tea plant cultivar "Shuchazao." To further illustrate that CsCAT2 plays a role in theanine transport from root to shoot seasonally, we examined *CsCAT2* expression in the roots of five cultivars and analyzed the correlation between *CsCAT2* expression and the efficiency of theanine root-to-shoot transport.

Because theanine is primarily synthesized in the root in winter and then transported to the shoot, the ratio of theanine contents in the shoot and that in the root was used as a parameter for illustrating the efficiency of theanine transport from root to shoot (Dong et al., 2020). Moreover, theanine contents in the different tissues of shoot vary greatly and are highest in the leaf bud. Therefore, we used the sum of ratios of theanine contents in the roots and in the leaf buds at the four time points to quantify the efficiency of theanine root-to-shoot transport (Dong et al., 2020).

Here, the sum of *CsCAT2* expression level in the root at different time points was calculated (**Figure 6A**). We observed that the sum was lowest in cultivar Zhenong 113 (ZN113) and

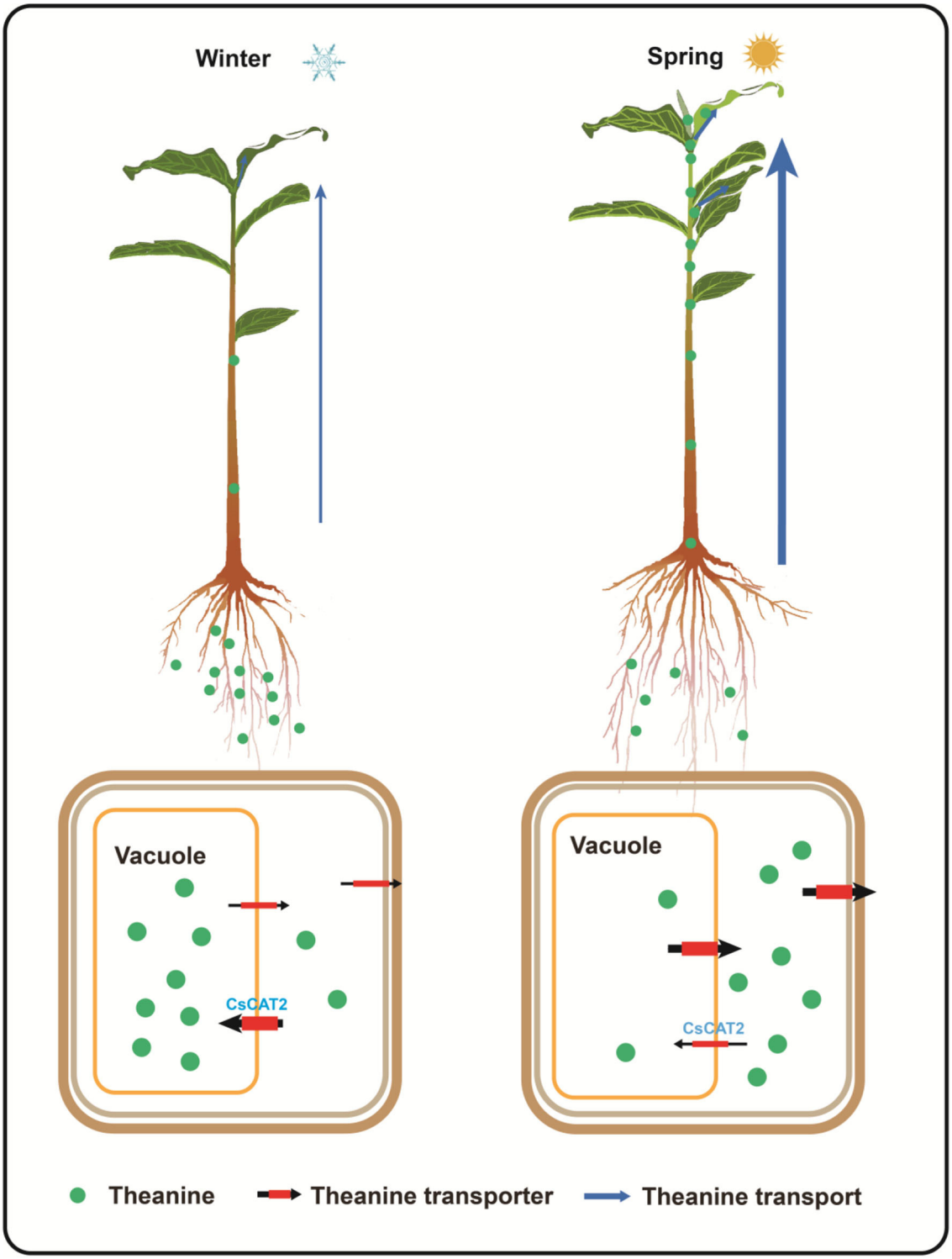

FIGURE 7 | Proposed model for theanine storage and root-to-shoot transport in tea plants. In winter, theanine is transported into vacuole for storage; in spring, theanine is exported from vacuole into cytoplasm and is then transported out of the storage cells for root-to-shoot transport. CsCAT2 likely mediates theanine transport into the vacuole. High expression of *CsCAT2* in winter confers efficient transport of theanine into vacuole; however, high expression of *CsCAT2* in spring reduces the efficiency of theanine root-to-shoot transport.

gradually increased in Yingshuang (YS), Zhongcha 302 (ZC302), and Longjing 43 (LJ43). In contrast, the efficiency of theanine root-to-shoot transport was highest in ZN113 and gradually decreased in YS, ZC302, and LJ43 (**Figure 6B**) (Dong et al., 2020). More importantly, the sum of *CsCAT2* expression in the root was significant negatively correlated with the efficiency of theanine root-to-shoot transport, with a correlation coefficient of −0.897 ($p < 0.05$; **Figure 6C**). These results further supported the notion that CsCAT2 plays a negative role in theanine root-to-shoot transport.

DISCUSSION

CsCAT2 Is a Tonoplast-Localized Theanine Transporter

In tea plants, theanine is primarily synthesized and stored in root cells, in late autumn and winter, and is transported to the new shoot, in spring (Gong et al., 2020). However, the molecular mechanism of theanine storage in root cells is still unknown. We hypothesized that theanine is stored in the vacuole and the storage is mediated and seasonally regulated by tonoplast-localized theanine transporters (**Figure 7**).

Several CAT families of AATs in plants have been shown to localize in the tonoplast and play important roles in amino acid homeostasis (Yang et al., 2013, 2014; Snowden et al., 2014). In *Arabidopsis*, AtCAT2 was shown to localize in the tonoplast and regulate amino acid levels in the leaves (Yang et al., 2014). SlCAT2, the homolog of CAT2 in tomato, was demonstrated to localize in the tonoplast of stamen cells and play a significant role in tomato flower and fruit development (Yang et al., 2013). SlCAT9, a relatively specific Glu/Asp/GABA transporter, regulates the accumulation of amino acids during fruit development and the flavor profile of the tomato fruit and has also been demonstrated to localize in the tonoplast (Snowden et al., 2014). In this study, we showed that CsCAT2 is a tonoplast-localized AAT (**Figure 1**).

Generally, CATs display board substrate specificity for neutral and acidic amino acids in plants (Su et al., 2004; Hammes et al., 2006; Yang et al., 2010, 2013, 2014, 2015; Snowden et al., 2014; Yoneda, 2017). In this study, we revealed that CsCAT2 is a theanine transporter and also has affinities for Glu, Gln, GABA, and Ala (**Figures 3**, **4**). It is noteworthy that theanine contents in root cells are very high and could reach 60 mg/g dry weight (Li et al., 2019), whereas the contents of Glu, Gln, GABA, and Ala are much lower in root cells of tea plants (Yang et al., 2020). Therefore, CsCAT2 may mainly transport theanine even though it has affinities for other amino acids.

Interestingly, *CsCAT2* expression is high in winter, decreases in early spring, and then increases in late spring (**Figure 6**). This expression pattern is consistent with theanine storage and is opposite to theanine root-to-shoot transport. We further showed that *CsCAT2* expression was significantly correlated with the efficiency of theanine root-to-shoot transport (**Figure 7**). These findings supported the notion that CsCAT2 mediates theanine storage in vacuole in the root cells. In addition, theanine was shown to mainly distribute in the cytoplasm in March (Fu et al., 2021), which is possibly caused by greatly reduced level of CsCAT2 in the tonoplast (**Figure 7**). The cytoplasm distributed theanine in root cells is probably ready for root-to-shoot transport (**Figure 7**).

CsCAT2 May Coordinate Seasonal Theanine Allocation Between Root and Shoot

Amino acids seasonally store in the roots and transport to shoots are economically efficient for adjusting plant growth according to the environment and nutrition requirement (Zeng et al., 2020; Fu et al., 2021). In early spring, the soil temperature is low, so that the absorption capacity of nitrogen from the soil is weak and insufficient to meet the nitrogen demand for the growth of new shoots. The transport of amino acids stored in root cells to the new shoot could be the effective safeguard of nitrogen requirement for the growth of new shoots (Zeng et al., 2020). Theanine is the dominant form of nitrogen storage in roots of tea plants (Ruan et al., 2012). Seasonally regulated *CsCAT2* expression likely contributes to theanine allocation between root and shoot to support new shoot growth.

In most tea plant-growing area, the shoots of tea plants have several rounds of growth-dormancy cycles, except the winter dormancy, in a year (Hao et al., 2017). We speculated that the downregulation of *CsCAT2* in the early spring might contribute to theanine transport to shoots to support the first round of shoot growth, whereas the upregulation at the late spring is conducive to reduce theanine transport to the shoots and promote bud dormancy, thereby store nitrogen sources for the next round of shoot growth in summer. Given that high-quality green teas are generally processed from the first round of new shoot of tea plants, the new shoots grown in summer are rarely harvested for green tea processing, which causes a great waste of tea resources. It will be intriguing to breed tea plant cultivars with strong growth in spring and weak growth in summer, using *CsCAT2* as a molecular marker.

DATA AVAILABILITY STATEMENT

The original contributions presented in the study are included in the article/**Supplementary Materials**, further inquiries can be directed to the corresponding authors.

AUTHOR CONTRIBUTIONS

LF, XW, and ZZ conceived the study and designed the experiments. LF, YY, and SL performed the experiments. TY, QC, LL, JS, and PZ supervised the project and participated in processing the data. LF and ZZ wrote the manuscript. XW and ZZ finalized the manuscript. All authors read and approved the final version of the manuscript.

FUNDING

This work was supported by grants from the China Postdoctoral Science Foundation (2018M632821), the Hubei Provincial

Natural Science Foundation (2019CFB178), Collaborative Innovation Project of Universities in Anhui Province (GXXT-2020-080), the Hubei Innovative Postdoctoral Position (20192344), Natural Science Foundation of Hubei Academy of Agricultural Sciences (2021NKYJJ13), and the Earmarked Fund for China Agriculture Research System (CARS-23).

ACKNOWLEDGMENTS

We thank members in XW's and ZZ's laboratories for their assistance with the experiments and data analyses. We also thank Prof. Guohua Xu in College of Resources and Environmental Sciences, Nanjing Agricultural University, for providing the yeast strains.

SUPPLEMENTARY MATERIAL

The Supplementary Material for this article can be found online at: https://www.frontiersin.org/articles/10.3389/fpls.2021.797854/full#supplementary-material

Supplementary Figure 1 | Growth of yeast strains on medium with amino acid as sole nitrogen source, with 0 nitrogen (-N) and 2 mM $(NH_4)_2SO_4$ as negative and positive controls.

Supplementary Table 1 | Primers used in the experiments.

REFERENCES

Ashihara, H. (2015). Occurrence, biosynthesis and metabolism of theanine (γ-glutamyl-L-ethylamide) in plants: a comprehensive review. *Nat. Prod. Commun*. 10, 803–810. doi: 10.1177/1934578X1501000525

Bassil, E., Tajima, H., Liang, Y. C., Ohto, M. A., Ushijima, K., Nakano, R., et al. (2011). The Arabidopsis Na+/H+ antiporters NHX1 and NHX2 control vacuolar pH and K+ homeostasis to regulate growth, flower development, and reproduction. *Plant Cell*. 23, 3482–3497. doi: 10.1105/tpc.111.089581

Besnard, J., Pratelli, R., Zhao, C., Sonawala, U., Collakova, E., Pilot, G., et al. (2016). UMAMIT14 is an amino acid exporter involved in phloem unloading in Arabidopsis roots. *J. Exp. Bot*. 67, 6385–6397. doi: 10.1093/jxb/erw412

Dinkeloo, K., Boyd, S., and Pilot, G. (2018). Update on amino acid transporter functions and on possible amino acid sensing mechanisms in plants. *Semin. Cell Dev. Biol*. 74, 105–113. doi: 10.1016/j.semcdb.2017.07.010

Dong, C., Li, F., Yang, T., Feng, L., Zhang, S., Li, F., et al. (2020). Theanine transporters identified in tea plants (*Camellia sinensis* L.). *Plant J*. 101, 57–70. doi: 10.1111/tpj.14517

Fang, R., Redfern, S. P., Kirkup, D., Porter, E. A., Kite, G. C., Terry, L. A., et al. (2017). Variation of theanine, phenolic, and methylxanthine compounds in 21 cultivars of *Camellia sinensis* harvested in different seasons. *Food Chem*. 220, 517–526. doi: 10.1016/j.foodchem.2016.09.047

Feng, L., Gao, M. J., Hou, R. Y., Hu, X. Y., Zhang, L., Wan, X. C., et al. (2014). Determination of quality constituents in the young leaves of albino tea cultivars. *Food Chem*. 155, 98–104. doi: 10.1016/j.foodchem.2014.01.044

Feng, L., Yang, T., Zhang, Z., Li, F., Chen, Q., Sun, J., et al. (2018). Identification and characterization of cationic amino acid transporters (CATs) in tea plant (Camellia sinensis). *Plant Growth Regul*. 84, 57–69. doi: 10.1007/s10725-017-0321-0

Fu, X., Liao, Y., Cheng, S., Xu, X., Grierson, D., and Yang, Z. (2021). Nonaqueous fractionation and overexpression of fluorescent tagged enzymes reveals the subcellular sites of L-theanine biosynthesis in tea. *Plant Biotechnol J*. 19, 98–108. doi: 10.1111/pbi.13445

Gong, A. D., Lian, S. B., Wu, N. N., Zhou, Y. J., Zhao, S. Q., Zhang, L. M., et al. (2020). Integrated transcriptomics and metabolomics analysis of catechins, caffeine and theanine biosynthesis in tea plant (*Camellia sinensis*) over the course of seasons. *BMC Plant Biol*. 20:294. doi: 10.1186/s12870-020-02443-y

Guo, X., Ho, C., Schwab, W., Song, C., and Wan, X. (2019). Aroma compositions of large-leaf yellow tea and potential effect of theanine on volatile formation in tea. *Food Chem*. 280, 73–82. doi: 10.1016/j.foodchem.2018.12.066

Guo, X., Song, C., Ho, C., and Wan, X. (2018). Contribution of L-theanine to the formation of 2, 5-dimethylpyrazine, a key roasted peanutty flavor in Oolong tea during manufacturing processes. *Food Chem*. 263, 18–28. doi: 10.1016/j.foodchem.2018.04.117

Hammes, U. Z., Nielsen, E., Honaas, L. A., Taylor, C. G., and Schachtman, D. P. (2006). AtCAT6, a sink- tissue-localized transporter for essential amino acids in Arabidopsis. *Plant J*. 48, 414–426. doi: 10.1111/j.1365-313X.2006.02880.x

Hao, X., Yang, Y., Yue, C., Wang, L., Horvath, D. P., and Wang, X. (2017). Comprehensive transcriptome analyses reveal differential gene expression profiles of Camellia sinensis axillary buds para-, endo-, ecodormancy, and bud flush stages. *Front. Plant Sci*. 8:553. doi: 10.3389/fpls.2017.00553

Hunt, K. J., Hung, S. K., and Ernst, E. (2010). Botanical extracts as anti-aging preparations for the skin: a systematic review. *Drugs Aging* 27, 973–985. doi: 10.2165/11584420-000000000-00000

Jiang, Y., Hua, J., Wang, B., Yuan, H., and Ma, H. (2018). Effects of variety, season, and region on theaflavins content of fermented Chinese congou black tea. *J. Food Qual*. 2018, 1–9. doi: 10.1155/2018/5427302

Li, F., Dong, C., X., Yang, T., Ma, J., Zhang, S., et al. (2019). Seasonal theanine accumulation and related gene expression in the roots and leaf buds of tea plants (*Camellia sinensis* L.). *Front. Plant Sci*. 10:1397. doi: 10.3389/fpls.2019.01397

Li, F., Dong, C., Yang, T., Bao, S., Fang, W., Lucas, W. J., et al. (2021). The tea plant CsLHT1 and CsLHT6 transporters take up amino acids, as a nitrogen source, from the soil of organic tea plantations. *Hortic. Res*. 8:178. doi: 10.1038/s41438-021-00615-x

Li, F., Li, H., Dong, C., Yang, T., Zhang, S., Bao, S., et al. (2020). Theanine transporters are involved in nitrogen deficiency response in tea plant (Camellia sinensis L.). *Plant Signal Behav*. 15:1728109. doi: 10.1080/15592324.2020.1728109

Ruan, J., Ma, L., and Yang,Y. (2012). Magnesium nutrition on accumulation and transport of amino acids in tea plants. *J. Sci. Food Agric*. 92, 1375–1383. doi: 10.1002/jsfa.4709

Schmittgen, T. D., and Zakrajsek, B. A. (2000). Effect of experimental treatment on housekeeping gene expression: validation by real-time, quantitative RT-PCR. *J. Biochem. Biophys. Methods* 46, 69–81. doi: 10.1016/S0165-022X(00)00129-9

Sharma, E., Joshi, R., and Gulati, A. (2018). L-Theanine: An astounding sui generis integrant in tea. *Food Chem*. 242:601. doi: 10.1016/j.foodchem.2017.09.046

Snowden, C. J., Thomas, B., Baxter, C. J., Smith, A. C., and Sweetlove, L. J. (2014). A tonoplast Glu/Asp/GABA exchanger that affects tomato fruit amino acid composition. *Plant J*. 81, 651–660. doi: 10.1111/tpj.12766

Song, H., Zhang, X., Shi, C., Wang, S., Wu, A., and Wei, C. L. (2016). Selection and verification of candidate reference genes for mature microRNA expression by quantitative RT-PCR in the tea plant (*Camellia sinensis*). *Genes* 7:25. doi: 10.3390/genes7060025

Su, Y. H., Frommer, W. B., and Ludewig, U. (2004). Molecular and functional characterization of a family of amino acid transporters from Arabidopsis. *Plant Physiol*. 136, 3104–3131. doi: 10.1104/pp.104.045278

Tanaka, T., Watarumi, S., Fujieda, M., and Kouno, I. (2005). New black tea polyphenol having N-ethyl-2-pyrrolidinone moiety derived from tea amino acid theanine: Isolation, characterization and partial synthesis. *Food Chem*. 93, 81–87. doi: 10.1016/j.foodchem.2004.09.013

Tegeder, M., Tan, Q., Grennan, A. K., and Patrick, J. W. (2007). Amino acid transporter expression and localisation studies in pea (*Pisum sativum*). *Funct. Plant Biol*. 34, 1019–10128. doi: 10.1071/FP07107

Wan, X. (2003). *Tea Biochemistry, 3rd edition*. Beijing, China: China Agriculture Press (in Chinese).

Wan, X., and Xia, T. (2015). *Secondary Metabolism of Tea Plant, 1st edition*. Beijing, China: Science Press (in Chinese).

Wei, C., Yang, H., Wang, S., Zhao, J., Liu, C., Gao, L., et al. (2018). Draft genome sequence of Camellia sinensis var. sinensis provides insights into the evolution of the tea genome and tea quality. *Proc. Natl. Acad. Sci. USA*. 115, E4151–E4158. doi: 10.1073/pnas.1719622115

Xu, W., Song, Q., Li, D., and Wan, X. (2012). Discrimination of the production season of Chinese green tea by chemical analysis in combination with supervised pattern recognition. *J. Agric. Food Chem*. 60, 7064–7070. doi: 10.1021/jf301340z

Yamaguchi, S., and Ninomiya, K. (2000). Umami and food palatability. *J. Nutr*. 130, 921s−926s. doi: 10.1093/jn/130.4.921S

Yang, H., Bogner, M., Stierhof, Y. D., and Ludewig, U. (2010). H+-independent glutamine transport in plant root tips. *PLoS ONE*. 5:e8917. doi: 10.1371/journal.pone.0008917

Yang, H., Krebs, M., Stierhof, Y. D., and Ludewig, U. (2014). Characterization of the putative amino acid transporter genes AtCAT2, 3 and 4: the tonoplast localized AtCAT2 regulates soluble leaf amino acids. *J Plant Physiol*. 171, 594–601. doi: 10.1016/j.jplph.2013.11.012

Yang, H., Stierhof, Y. D., and Ludewig, U. (2015). The putative cationic amino acid transporter 9 is targeted to vesicles and may be involved in plant amino acid homeostasis. *Front. Plant Sci*. 6:212. doi: 10.3389/fpls.2015.00212

Yang, T., Li, H., Tai, Y., Dong, C., Cheng, X., Xia, E., et al. (2020). Transcriptional regulation of amino acid metabolism in response to nitrogen deficiency and nitrogen forms in tea plant root (*Camellia sinensis* L.). *Sci. Rep*. 10:6868. doi: 10.1038/s41598-020-63835-6

Yang, Y., Yang, L., and Li, Z. (2013). Molecular cloning and identification of a putative tomato cationic amino acid transporter-2 gene that is highly expressed in stamens. *Plant Cell Tiss. Organ*. 112, 55–63. doi: 10.1007/s11240-012-0215-9

Yao, L., Liu, X., Jiang, Y., Caffin, N., Arcy, B. D., Singanusong, R., et al. (2006). Compositional analysis of teas from Australian supermarkets. *Food Chem*. 94, 115–122. doi: 10.1016/j.foodchem.2004.11.009

Yoneda, Y. (2017). An L-glutamine transporter isoform for neurogenesis facilitated by L-theanine. *Neurocheml Res*. 42, 2686–2697. doi: 10.1007/s11064-017-2317-6

Zeng, L., Zhou, X., Liao, Y., and Yang, Z. (2020). Roles of specialized metabolites in biological function and environmental adaptability of tea plant (*Camellia sinensis*) as a metabolite studying model. *J. Adv. Res*. 21:65. doi: 10.1016/j.jare.2020.11.004

Zhu, B. Y., Guo, J. Y., Dong, C. X., Li, F., Qiao, S. M., Lin, S. J., et al. (2021). CsAlaDC and CsTSI work coordinately to determine theanine biosynthesis in tea plants (*Camellia sinensis* L.) and confer high levels of L-theanine accumulation in a non-tea plant. *Plant Biotechnol. J*. doi: 10.1111/pbi.13722

Conflict of Interest: The authors declare that the research was conducted in the absence of any commercial or financial relationships that could be construed as a potential conflict of interest.

Publisher's Note: All claims expressed in this article are solely those of the authors and do not necessarily represent those of their affiliated organizations, or those of the publisher, the editors and the reviewers. Any product that may be evaluated in this article, or claim that may be made by its manufacturer, is not guaranteed or endorsed by the publisher.

frontiers in Plant Science

ORIGINAL RESEARCH
published: 03 January 2022
doi: 10.3389/fpls.2021.782220

Systematic Analysis of the R2R3-MYB Family in *Camellia sinensis*: Evidence for Galloylated Catechins Biosynthesis Regulation

Jingyi Li†, Shaoqun Liu†, Peifen Chen, Jiarong Cai, Song Tang, Wei Yang, Fanrong Cao, Peng Zheng and Binmei Sun**

Key Laboratory of Biology and Germplasm Enhancement of Horticultural Crops in South China, Ministry of Agriculture and Rural Areas, College of Horticulture, South China Agricultural University, Guangzhou, China

OPEN ACCESS

Edited by:
Enhua Xia,
Anhui Agricultural University, China

Reviewed by:
Yasuyuki Yamada,
Kobe Pharmaceutical University, Japan
Ding Huang,
Guangxi University of Chinese Medicine, China

***Correspondence:**
Peng Zheng
zhengp@scau.edu.cn
Binmei Sun
binmei@scau.edu.cn

†These authors have contributed equally to this work

Specialty section:
This article was submitted to Plant Metabolism and Chemodiversity, a section of the journal Frontiers in Plant Science

Received: *24 September 2021*
Accepted: *15 November 2021*
Published: *03 January 2022*

Citation:
Li J, Liu S, Chen P, Cai J, Tang S, Yang W, Cao F, Zheng P and Sun B (2022) Systematic Analysis of the R2R3-MYB Family in Camellia sinensis: Evidence for Galloylated Catechins Biosynthesis Regulation. Front. Plant Sci. 12:782220. doi: 10.3389/fpls.2021.782220

The R2R3-MYB transcription factor (TF) family regulates metabolism of phenylpropanoids in various plant lineages. Species-expanded or specific MYB TFs may regulate species-specific metabolite biosynthesis including phenylpropanoid-derived bioactive products. *Camellia sinensis* produces an abundance of specialized metabolites, which makes it an excellent model for digging into the genetic regulation of plant-specific metabolite biosynthesis. The most abundant health-promoting metabolites in tea are galloylated catechins, and the most bioactive of the galloylated catechins, epigallocatechin gallate (EGCG), is specifically relative abundant in *C. sinensis*. However, the transcriptional regulation of galloylated catechin biosynthesis remains elusive. This study mined the R2R3-MYB TFs associated with galloylated catechin biosynthesis in *C. sinensis*. A total of 118 R2R3-MYB proteins, classified into 38 subgroups, were identified. R2R3-MYB subgroups specific to or expanded in *C. sinensis* were hypothesized to be essential to evolutionary diversification of tea-specialized metabolites. Notably, nine of these *R2R3-MYB* genes were expressed preferentially in apical buds (ABs) and young leaves, exactly where galloylated catechins accumulate. Three putative *R2R3-MYB* genes displayed strong correlation with key galloylated catechin biosynthesis genes, suggesting a role in regulating biosynthesis of epicatechin gallate (ECG) and EGCG. Overall, this study paves the way to reveal the transcriptional regulation of galloylated catechins in *C. sinensis*.

Keywords: *Camellia sinensis*, galloylated catechins, R2R3-MYB, transcriptional regulation, catechin biosynthesis

Abbreviations: C, catechin; EC, epicatechin; GC, gallocatechin; EGC, epigallocatechin; CG, catechin gallate; ECG, epigallocatechin gallate; GCG, gallocatechin gallate; EGCG, epigallocatechin gallate; qRT-PCR, quantitative reverse transcription polymerase chain reaction; PAL, phenylalanine ammonia lyase; C4H, cinnamate 4-hydroxylase; 4CL, 4-coumarate: coenzyme A ligase; CHS, chalcone synthase; CHI, chalcone isomerase; F3H, flavanone-3-hydroxylase; F3′H, flavonoid 3′-hydroxylase; F3′5′H, flavonoid 3′5′-hydroxylase; FLS, flavonol synthase; DFR, dihydroflavonol 4-reductase; ANS, anthocyanidin synthase; ANR, anthocyanidin reductase; LAR, leucoanthocyanidin 4-reductase; SCPL1A, subclade 1A of serine carboxypeptidase-like acyltransferases; TFs, transcription factors; TES, tea expanded subgroup; HPLC, high-performance liquid chromatography; Trp/W, tryptophan.

INTRODUCTION

Tea from *Camellia sinensis*, along with coffee and cocoa, is one of the world's three major non-alcoholic beverages. Worldwide, approximately two billion cups of tea are consumed daily (Drew, 2019; Yamashita et al., 2020). Tea production has amplified at an average annual rate of 3.35% in the last 5 years; by 2019, worldwide tea production reached 6.49 million tons on 5.07 million hectares (Food and Agriculture Organization of the United Nations statistics[1]). Tea was used first as a food in ancient China, then it served as a medicine to prevent and cure common diseases before developing into a popular beverage (Mondal et al., 2004; Abbas et al., 2017). Nowadays, tea exhibits great commercial potential and has become a vital industry due to its health promoting properties and attractive distinct flavors (Chen et al., 2009).

The tea plant (*C. sinensis*) is rich in characteristic metabolites, such as polyphenols, amino acids, caffeine, and terpenes, that significantly contribute to its pleasant flavors and industrial and medical value (Wei et al., 2018). Catechins are the principal health-promoting bioactive compounds of tea. Catechins constitute 12–24% of the dry weight of young leaves, and account for more than 70% of the total polyphenols (Yang et al., 2012). Catechins in tea consist of a mixture of catechin (C), epicatechin (EC), gallocatechin (GC), epigallocatechin (EGC), catechin gallate (CG), epicatechin gallate (ECG), gallocatechin gallate (GCG), and epigallocatechin gallate (EGCG) (Asakawa et al., 2013). Among them, galloylated catechins ECG and EGCG are relatively abundant in tea plants and account for more than 80% of total catechins (Kim et al., 2004; Liu et al., 2012). EGCG, the most specific accumulated metabolite that quantitatively differentiated from the other plants, is the major bioactive component conferring the many health benefits of tea – it is anti-carcinogenic (Ahmad et al., 2000), anti-oxidative (Heim et al., 2002), anti-bacterial and anti-inflammatory (Taguri et al., 2004), and it prevents cardiovascular and cerebrovascular diseases (Yu X. et al., 2020). In addition, EGCG is widely used in food production on account of its strong antioxidative capacity (Nikoo et al., 2018).

To date, based on biochemical, physiological, and genetic research, the biosynthesis pathway of catechins has become clear (Yang et al., 2012; Wei et al., 2018; Yu et al., 2021). Catechins are derived from the phenylpropanoid pathway and principally accumulate in apical shoots and young leaves. Galloylated catechin content is mainly regulated at the transcriptional level by catechin biosynthesis genes *dihydroflavonol reductase* (*DFR*), *anthocyanidin reductase* (*ANR*), *leucoanthocyanidin reductase* (*LAR*), and *serine carboxypeptidase-like acyltransferases* (*SCPLs*) (Punyasiri et al., 2004; Singh et al., 2008; Eungwanichayapant and Popluechai, 2009; Ashihara et al., 2010; Wei et al., 2018). However, few studies have focused on the network(s) that regulate catechin biosynthesis, especially galloylated catechins.

R2R3-MYB transcription factors (TFs) comprise the largest family of TFs in advanced plants (Ambawat et al., 2013). In addition to possessing two imperfect MYB repeats (R2 and R3), the R2R3-MYB TFs maintain a highly conserved N-terminal MYB DNA-binding domain and an activated or repressed C-terminal domain (Lipsick, 1996; Martin and Paz-Ares, 1997; Kranz et al., 1998; Jin and Martin, 1999; Jiang et al., 2004; Dubos et al., 2010). The R2R3-MYB family is widely involved in plant growth and development, primary and secondary metabolism, hormone signal transduction, cellular proliferation, and apoptosis, as well as disease and abiotic stress response (Martin and Paz-Ares, 1997; Li M. et al., 2017). Notably, the R2R3-MYB family plays an important role in positively or negatively regulating the biosynthesis of specialized metabolites, such as flavonoids (Mehrtens et al., 2005; Hichri et al., 2011), anthocyanin (Li W. et al., 2017; Li et al., 2020; Yu M. et al., 2020), and lignin (Goicoechea et al., 2005; Bedon et al., 2007). Studies have found that new R2R3-MYB TFs emerged through species-specific duplication events (Soler et al., 2015). Species-specific evolved or expanded R2R3-MYB membership seems to confer functional diversification to organisms (Zhang et al., 2000). For example, the ancestral R2R3-MYB anthocyanin master regulator expanded into several homologous clusters within the grape (*Vitis* spp.) and maize (*Zea mays*) genomes, and differential expression of duplicated genes resulted in control of anthocyanin biosynthesis in different tissues (Zhang et al., 2000; Jiu et al., 2021). Some species-specific and expanded *R2R3-MYB* TFs govern specialized metabolite biosynthesis within lineages (Zhu et al., 2019). In *Capsicum*, five Solanaceae-specific MYB TF tandem genes duplicated in the *Cap1/Pun3* locus. *Capsicum* species have evolved placenta-specific expression of *MYB31*, which directly activates expression of capsaicinoid biosynthetic genes and results in production of genus-specialized metabolites.

In *C. sinensis*, some R2R3-MYB TFs have a demonstrated role in regulation of phenylpropanoid biosynthesis in *C. sinensis*, such as *CsAN1*, *CsMYB5a*, *CsMYB6A*, and *CsMYB75* that regulate anthocyanin pigments and *CsMYB5e* and *CsMYB5b* that involve in proanthocyanidin biosynthesis in *C. sinensis* tissues (Sun et al., 2016; He et al., 2018; Jiang et al., 2018; Wei et al., 2019; Wang et al., 2019, 2020). Recently, Chen et al. (2021) analyzed the genome-wide R2R3-MYB superfamily and found that some *CsR2R3-MYB* genes in response to drought, cold, gibberellic acid (GA), and abscisic acid (ABA) treatments and a key *CsR2R3-MYB* gene regulated some main anthocyanin components. However, the *C. sinensis* specific and expanded R2R3-MYB TFs that are potential candidate regulators of galloylated catechins biosynthesis have still not been identified.

Because of the importance of galloylated catechins in *C. sinensis*, this study focused on the specifically expanded *CsR2R3-MYB* genes and the high content of EGCG in *C. sinensis*. Differentiating from previous works, we adapted a more general genome-wide analysis method of the R2R3-MYB superfamily according to *Arabidopsis thaliana*, which greatly help to find out the specifically expanded *CsR2R3-MYB* genes and the high content of EGCG in *C. sinensis* (Soler et al., 2015; Li M. et al., 2017; Chen et al., 2021). The gene structure, conserved motifs and transcript patterns were also analyzed. Notably, three putative *R2R3-MYB* genes specifically expanded in tea plants exhibited strong correlation with key galloylated catechin biosynthesis genes and galloylated catechins content, suggesting a possible role in the regulating network of the biosynthesis of ECG and EGCG. This study proposed a new perspective of the possible

[1]https://www.fao.org/faostat/

transcriptional regulation mechanism with regard to the high accumulation of galloylated catechins in *C. sinensis*.

MATERIALS AND METHODS

Plant Materials

The "Lingtoudancong" variety of *C. sinensis* was grown at South Agricultural University in Guangzhou, China. Apical buds (ABs), first leaves, second leaves, mature leaves, old leaves, stems, and roots of three plants were sampled as one biological replicates in spring of 2021. Three biological replicates of different tissues were immediately frozen in liquid nitrogen and stored at −80°C.

Phylogenetic Analysis

Camellia sinensis MYB protein sequences were retrieved from the Tea Plant Information Archive database.[2] In total, 222 MYBs and MYB-related genes were predicted in the "Shuchazao" genome, and they were all submitted to Pfam website[3] to search for the two consecutive and conserved repeats of the MYB domain. However, only 118 of the MYBs TFs fit this characteristic, which were different from previous studies (Chen et al., 2021). The R2R3-MYB protein sequences of *A. thaliana* were obtained from the Arabidopsis Information Resource Archive database.[4] The number of R2R3-MYB gene models identified by our methodology in the genome of *A. thaliana* (126) was the same as described in the literature (Dubos et al., 2010). The homologous genes of kiwifruit, coffee, cacao and grape were retrieved from the Plant Transcription Factor Database[5] by performing a reverse BLAST search. All the R2R3-MYB sequences were aligned using ClustalX, and a neighbor-joining phylogenetic tree was constructed with 1,000 bootstrap replicates utilizing MEGAX (Kumar et al., 2016). A pairwise deletion method was chosen to dispose of the positions containing gaps or missing data in the sequences, and the delay divergent cut-off value was set to 30.

Synteny Analysis

Toolkits of TBtools software were used to carry out the synteny analysis and K_a/K_s value calculation (Chen et al., 2020). Syntenic blocks and distinct duplication events were identified by One Step MCScanX and the synteny relationships of the orthologous *R2R3-MYB* genes between the *C. sinensis* and the other selected four representative plant species were displayed by Dual Synteny Plot. Besides, the K_a and K_s values of each duplicated *MYB* gene pair were counted by Simple K_a/K_s Calculator.

Conserved Motif and Myb-Binding Sites Analysis

Functional motifs and conserved domains were identified with The MEME Suite tool[6] using the following parameters: site distribution, zero-or-one-site-per-sequence (ZOOPS) model; maximum number of motifs: 20; minimum motif width: 6; maximum motif width: 50; minimum number of sites per motif: 2; and maximum number of sites per motif: 118 (Bailey et al., 2009; Chen et al., 2021). The sequence logos of R2 and R3 repeats of the R2R3-MYB proteins were based on multiple sequence alignments and were visualized with WebLogo Version 2.8.2.[7] All obtained motifs were constructed and visualized using the Gene Structure View (Advanced) of the TBtools software. The Myb-binding sites were predicted in the 2000-bp upstream regions of the catechin biosynthesis downstream genes with PlantCARE online website[8].

RNA-Seq Expression Analysis

The RNA-seq data were downloaded from TPIA for transcript abundance analyses. The expression levels of the candidate *R2R3-MYB* TFs and catechin biosynthesis genes from different tissues of *C. sinensis* were used to generate a heatmap with TBtools software using the normalized method.

RNA Extraction and Quantitative Real-Time Polymerase Chain Reaction

Total RNA of different tissues of "Lingtoudancong" was extracted utilizing a Magen HiPure Plant RNA Mini kit B (R4151, Magen, China) according the manufacturer's instructions. First-strand cDNA was synthesized using a HiScript III RT 1st Strand cDNA Synthesis kit (R323-01, Vazyme, China) in a reaction volume of 20 μL. Quantitative real-time polymerase chain reaction (qRT-PCR) was performed in a Bio-Rad CFX384 Touch^{TM} system. Each 10 μL reaction mixture was comprised of 4.4 μL qPCR SYBR Green Master Mix (Yeasen, China), 4.4 μL double distilled water, 0.2 μL of each primer (10 μmol/μL) and 1 μL of cDNA template. The reaction program was as follows: 95°C for 5 min; then 39 cycles at 95°C for 5 s and 60°C for 30 s. A melting-curve analysis was carried out at 95°C for 5 s, which was followed by a temperature increase from 60 to 95°C. All qRT-PCR reactions were carried out in independent triplicate and *Actin* (*TEA019484.1)* was used as the housekeeping gene (Guo et al., 2019; Zhou et al., 2019). The relative expression of each gene was calculated with the $2^{-\Delta\Delta Ct}$ method as introduced in the previous research and the values were the means ± SDs (Livak and Schmittgen, 2001). The qRT-PCR primers were designed with the qPrimerDB-qPCR Primer Database.[9] Sequences of the primers are listed in **Supplementary Table 1**.

Quantification of Catechin Contents

Reference standards of C, EC, EGC, ECG, and EGCG were purchased from Shanghai Yuanye Bio-Technology Co., Ltd. (Shanghai, China). ABs, first leaves, second leaves, mature leaves, old leaves, stems and roots of "Lingtoudancong" were ground into fine powders and freeze-dried. Approximately 0.2 g of each sample powder was extracted with 8 mL of 70% methyl alcohol (diluted with ultrapure water). After ultrasonic extraction for 30 min, the supernatant was collected by centrifugation.

[2]http://tpia.teaplant.org/

[3]http://pfam.xfam.org/search/sequence

[4]https://www.arabidopsis.org/

[5]http://planttfdb.gao-lab.org/

[6]https://meme-suite.org/meme/

[7]http://weblogo.berkeley.edu/logo.cgi

[8]http://bioinformatics.psb.ugent.be/webtools/plantcare/html/

[9]https://biodb.swu.edu.cn/qprimerdb/

One milliliter of the liquid supernatant was filtered through a 0.22 μm Millipore membrane. The extracts of each sample were independently injected into three XSelect HSS C18 SB columns (4.6 × 250 mm, 5 μm, Waters Technologies, United States) for three independent replicates. The catechin monomers were separated using 0.1% aqueous formic acid (A) and 100% acetonitrile (B) as mobile phases on a Waters Alliance Series HPLC system (Waters Technologies, United States). Detection was performed at 280 nm. The data were presented as the mean ± SD ($n = 3$).

Correlation Analysis of Gene Expression and Metabolite Accumulation

The correlation analysis among TFs, catechin biosynthesis genes, and catechin monomer contents was performed *via* Pearson's correlation coefficients. The R software was adopted to visualize the relationship directly. A correlation coefficient of >0.5 was considered to be a positively associated pair, and $R < -0.5$ was thought of as a negative correlation. In the diagram, blue represents a positive correlation, and red represents a negative correlation.

RESULTS

Comparative Phylogenetic Analysis of the R2R3-MYB Families in *Camellia sinensis* and *Arabidopsis thaliana*

A total of 118 *R2R3-MYB* genes were identified in the *C. sinensis* genome after manual curation and exclusion of alternative transcripts. All identified *R2R3-MYB* genes from *C. sinensis* (118) were aligned with those of *A. thaliana* (126), and their evolutionary history was inferred by constructing a neighbor-joining phylogenetic tree (**Figure 1**). The 118 *R2R3-MYB* genes of *C. sinensis* were named in light of the systematic naming rules of *A. thaliana*, except for *CsMYB1*, *CsMYB4a*, and *CsAN1*, which had been functionally characterized previously (**Supplementary Table 3**; Yang et al., 2012; Sun et al., 2016; Li M. et al., 2017). In addition, as it is believed that genes which clustered together were considered to be in the same subgroup, and *A. thaliana* is, by far, the species for which the *R2R3-MYB* genes have been most extensively investigated, the 38 subgroups were classified by taking into account the topology of the tree and the bootstrap values (**Figure 1** and **Supplementary Table 3**) and were named according to the classification of *A. thaliana*. For new subgroups not previously proposed in *A. thaliana*, the subgroup was named after the known functionally characterized *A. thaliana* member.

The majority of subgroups contained members from both species. However, S12 was an *Arabidopsis*-specific subgroup, containing only *R2R3-MYB* members from *A. thaliana*. The members of subgroup S12, *AtMYB28*, *AtMYB29*, *AtMYB76*, *AtMYB34*, and *AtMYB5*1 regulate glucosinolate biosynthesis, a metabolite exclusive to the Brassicaceae family (Gigolashvili et al., 2007; Matus et al., 2008). In contrast, three subgroups contained *R2R3-MYB* TFs that were present only in *C. sinensis* without any homologs in *A. thaliana*. Therefore, their names we designated as Tea Expanded Subgroup A (TESA), Tea Expanded Subgroup B (TESB), and Tea Expanded Subgroup C (TESC). Remarkably, SMYB5 and S5 subgroups were comprised of more tea plant *R2R3-MYB* members than *A. thaliana* members. For example, subgroup S5 had three *C. sinensis* members (*CsMYB31*, *CsMYB32*, and *CsMYB34*), while *A. thaliana* contributed only one member, *AtMYB123/TT2*. Similarly, the SMYB5 subgroup had four members from *C. sinensis* (*CsMYB37*, *CsMYB39*, *CsMYB42*, and *CsMYB43*), but just one member (*AtMYB5*) from *A. thaliana*. In *Arabidopsis*, the members of SMYB5 and S5 subgroups are involved in the phenylpropanoid pathway. *AtMYB123* controls the biosynthesis of proanthocyanidins (PAs) in the seed coat and *AtMYB5* was partially redundant with *AtMYB123* (Gonzalez et al., 2009). The expansion of SMYB5 and S5 subgroups in *C. sinensis* suggests that diversified regulation of polyphenols emerged during the speciation of *C. sinensis*.

Overall, the phylogenetic analysis results highlighted five special subgroups TESA, TESB, TESC, S5, and SMYB5, which expanded in or were exclusively present in *C. sinensis*. Among these subgroups, a total of 21 R2R3-MYB TFs [TESA (6), TESB (4), TESC (4), S5 (3) and SMYB5 (4)] attracted our attention and were selected for further analysis as potential candidates involved metabolic processes specific to *C. sinensis*.

Functions Inferred Through Phylogenetic Analysis of the Candidate Subgroups in Six Plant Species

To evaluate the 21 *R2R3-MYB* genes of the five tea specifically expanded subgroups TESA, TESB, TESC, S5, and SMYB5, the homologous *R2R3-MYB* genes from kiwifruit, coffee, cacao, and grape were used to construct phylogenetic tree (**Supplementary Figure 1**). The number of *R2R3-MYB* TFs presented a trend of expansion in *C. sinensis* (21) similar to coffee (20), but greater than cocoa (11), kiwifruit (11), and grape (18). We surmised that the *C. sinensis* expanded *R2R3-MYB* function may have occurred through divergent evolution during speciation. For example, subgroup TESA was expanded in tea (6) relative to coffee (3), cocoa (5), kiwifruit (5), and grape (1). In the TESB subgroup, coffee (4), grape (4), and kiwifruit (3) had comparable numbers of members with *C. sinensis* (4), but only two homologous genes were found in cocoa. Subgroup TESC contained homologous genes in all species except for kiwifruit. Remarkably, no isogenous genes of TESA, TESB, or TESC subgroups were present in *A. thaliana*, indicating that these *R2R3-MYB*s evolved only in tea plant and probably have novel functions.

To uncover the roles these *R2R3-MYB* genes serve, we searched for the functional characteristics of the selected *R2R3-MYB* genes from four close relative species. Only a few homologous genes (*GSVIVT01026868001*, *Achn38246*, and *Achn172901* from the TESA subgroup; *Achn143561*, *Achn322351*, and *GSVIVT0103866001* from the TESB subgroup; and *Thecc1EG029126t1*, *GSVIVT01016765001*, and *GSVIVT01035467001* from TESC subgroup) have been experimentally verified. In the TESA subgroup, *GSVIVT01026868001* played an inhibitory role in flower development (Velasco et al., 2007), while both *Achn38246*

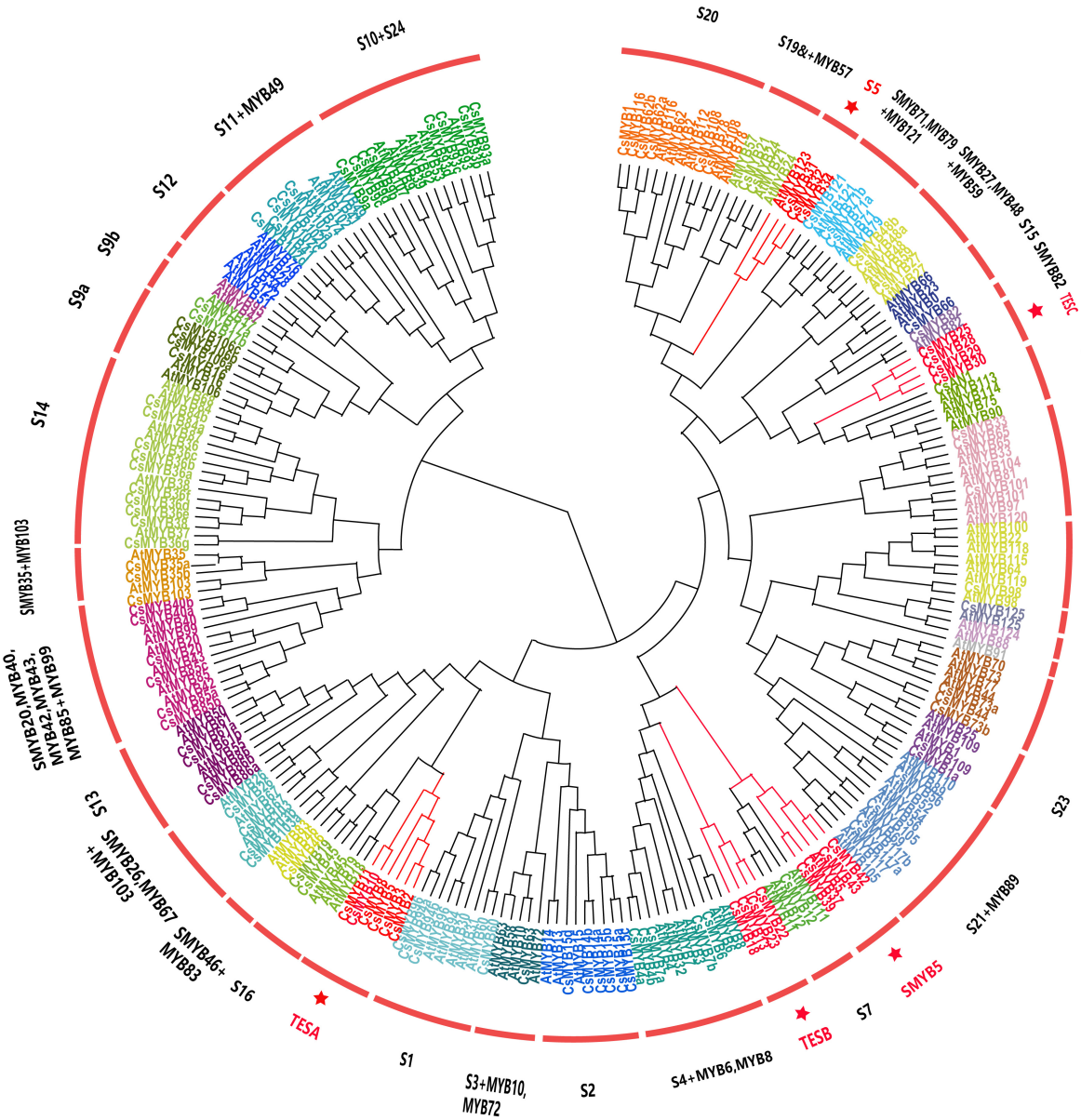

FIGURE 1 | Phylogenetic analysis of the R2R3-MYB families in *C. sinensis* and *A. thaliana*. A neighbor-joining phylogenetic tree was constructed from 244 protein sequences including all R2R3-MYB proteins from *C. sinensis* (118) and *A. thaliana* (126). Subgroups within each clade were given a different color; meanwhile, the same color indicates the genes are in the same subgroup. Subgroup short names are included next to each clade to simplify nomenclature. Subgroups that evolved and expanded exclusively in the *C. sinensis* genome are highlighted in red and marked with a red star. TESA, tea expanded subgroup A; TESB, tea expanded subgroup B; TESC, tea expanded subgroup C; SMYB5, subgroup MYB5; S5, subgroup 5.

and *Achn172901* acted as transcriptional activators involved in cold stress response (Park et al., 2010; Savage et al., 2013). Homologous genes in the TESB subgroup, *Achn143561*, *Achn322351*, and *GSVIVT0103866001*, performed a similar role in regulating plant protection against UV stress (Schenke et al., 2014). The paralogous genes of subgroup TESC (*Thecc1EG029126t1*, *GSVIVT01016765001*, and *GSVIVT01035467001*) mainly regulated plant epidermal cell fate (Savage et al., 2013; Cheng et al., 2014). Above all, we ventured that the function of the TESA, TESB, and TESC subgroups in *C. sinensis* might associate with responses to biotic and abiotic stress along with influencing certain developmental processes.

For detecting the driving force for evolution of the *C. sinensis R2R3-MYB* gene family, non-synonymous and synonymous substitution ratio (K_a and K_s) analyses were performed among the whole *CsR2R3-MYB* genes (**Supplementary Table 4**). Additionally, collinearity analysis among *C. sinensis* and the four selected plant lineages was carried out to explore the evolutionary mechanisms of the *C. sinensis* 2R-MYB family (**Supplementary Figure 2** and **Supplementary Tables 5–8**).

Conserved Motif Analysis of *R2R3-MYB*s

The R2 and R3 MYB domains of the 118 *C. sinensis R2R3-MYB* TFs were analyzed (**Supplementary Figure 3**). The R2 and R3 domains contain a set of characteristic amino acids, which include the highly conserved and evenly distributed tryptophan residues (Trp, W) known to be critical for sequence-specific binding of DNA (Stracke et al., 2001; Cao et al., 2013), demonstrating that the R2 and R3 MYB repeats of the MYB DNA-binding domain are highly conserved in *C. sinensis*, consistent with previous findings of the counterpart genes in other plant lineages (Wilkins et al., 2009; Du et al., 2012; Li et al., 2016). Most of the conserved residues were situated between the second and third conserved W residues in each MYB repeat, elucidating that the first area of them was less conserved than the other two.

Conserved amino acid motifs represent functional areas that are maintained during evolution. The conserved motifs within the 118 R2R3-MYB sequences were analyzed and aligned using MEME Suite. A total of 20 conserved motifs were identified in the R2R3-MYB family (**Supplementary Figure 4**). Six of these, motifs 1–6, were present in all R2R3-MYB members except for CsMYB1a and thus were designated as "general motifs"; the rest of the motifs (motifs 7–20) were considered to be "specific motifs," since they were present in only one or several R2R3-MYB members. For instance, motifs 16 and 9 were unique to CsMYB1a and CsMYB117a; meanwhile, motifs 15 and 19 were contained only in three genes. Overall, the members clustering to the same clade harbored similar motif patterns.

Expression Patterns of the R2R3-MYB Family

The expression patterns of 118 genes encoding *R2R3-MYB* TFs were analyzed in different tissues. No transcripts were detected for *CsMYB101* (*TEA028392.1*) and *CsMYB117b* (*TEA002233.1*), suggesting they are pseudogenes in *C. sinensis*. The genes were classified into seven expression clusters, based on their distinct transcript patterns in various tissues and organs (**Figure 2**). The 21 genes in RNA-seq-based cluster 1 were expressed mainly in flowers; genes in cluster 2 (14) were predominantly expressed in fruits; genes in cluster 3 (29) were mainly expressed in tender roots; genes in cluster 4 (8) were expressed at comparable levels in both ABs and tender roots; cluster 5 genes (18) were mainly present in apical shoots and young leaves; while cluster 6 genes (21) were mainly expressed in stems and finally, cluster 7 genes (5) were equally expressed in mature leaves, old leaves, and stems. Normally, genes within the same phylogenetic subgroup exhibit distinct transcript profiles (Dubos et al., 2010). Such was the case for subgroup S14: the members in this subgroup were detected in RNA-seq-based clusters 1, 3, and 6. In *A. thaliana*, members of S14 were generally related to axillary bud formation and cell differentiation. In some cases, however, genes belonging to the same subgroups might also have similar transcription profiles in the same tissue, organ or cell type. Such was the case with the TESA subgroup; all were present in RNA-seq-based cluster 3. Likewise, all members of subgroup S5 gathered in cluster 5.

Previous reports have pointed out that most of the genes involved in flavonoid formation and catechin biosynthesis were preferentially expressed in ABs and young leaves, where most galloylated catechins accumulate (Wei et al., 2018). Accordingly, *R2R3-MYB*s in RNA-seq-based cluster 5, whose expression level was highest in these two tender tissues, are the most likely candidates regulating catechin biosynthesis. As is shown in **Figure 2**, almost half of the genes found in cluster 5 (9) belonged to the subgroups that specifically evolved in or expanded in *C. sinensis,* subgroups S5, SMYB5, TESB, and TESC. It is worth noting that genes of subgroup S5 and SMYB5 were confirmed to be involved in flavonoid formation in *A. thaliana* (Nesi et al., 2001; Stracke et al., 2001), whereas subgroup TESB was inferred to be relevant to UV protection and subgroup TESC to control plant epidermal cell fate specification.

In silico Analysis of R2R3-MYB Expression and Catechin Accumulation

Catechins are the major type of polyphenols in the tea plant, comprising up to 70% of the polyphenols deriving from the phenylpropanoid pathway (**Figure 3A**). **Figure 3B** shows that catechin contents, especially the contents of the galloylated catechins EGCG and ECG, are significantly higher in ABs and young leaves than in other tissues. Therefore, for understanding the possible correlation between the galloylated catechins and the *CsR2R3-MYB*s that specifically evolved or expanded in *C. sinensis*, we focused on the nine *R2R3-MYB*s grouped in cluster 5 (*CsMYB22*, *CsMYB29*, *CsMYB30*, *CsMYB31*, *CsMYB32*, *CsMYB34*, *CsMYB37*, *CsMYB39*, and *CsMYB42*) because they were preferentially expressed in ABs and young leaves.

Further, the transcript abundance of the nine potential *R2R3-MYB* TFs and the catechin biosynthesis genes were investigated in different tissues. The results clearly showed that the genes in the catechin biosynthesis pathway display tissue-specific expression patterns. The genes downstream of catechin biosynthesis (*CsSCPL1A7*, *CsANR*, *CsLAR, CsDFR, CsFLS*, *CsF3H*, and *CsF3′5′H)* were highly expressed in ABs and young leaves, whereas the upstream genes (*CsPAL*, *Cs4CL,* and *CsC4H*) were highly expressed in root and flower (**Figure 3C**). The promotors of the catechin biosynthesis downstream genes (*CsSCPL1A7*, *CsANR*, *CsLAR, CsDFR, CsF3H*, and *CsF3′5′H*) have several Myb-binding domains (**Supplementary Figure 5**). Interestingly, the nine candidate *R2R3-MYB* TFs showed preferential expression in ABs and young leaves, which was consistent with the expression pattern of the downstream catechin biosynthetic genes, indicating that those *R2R3-MYB*s have relevance to catechin biosynthesis.

To identify the relationship between transcript abundance and catechin contents, a comprehensive gene-to-metabolite correlation analysis was conducted. As shown in **Figure 3D**, the three genes in the catechin biosynthesis pathway (*CsPAL*, *CsC4H*, and *Cs4CL*) that were not tender parts-specific indeed showed a low correlation or negatively correlated to catechin content. Comparatively, the expression level of the nine candidate *R2R3-MYB* TFs was positively correlated to the transcript abundance patterns of the catechin biosynthesis pathway downstream

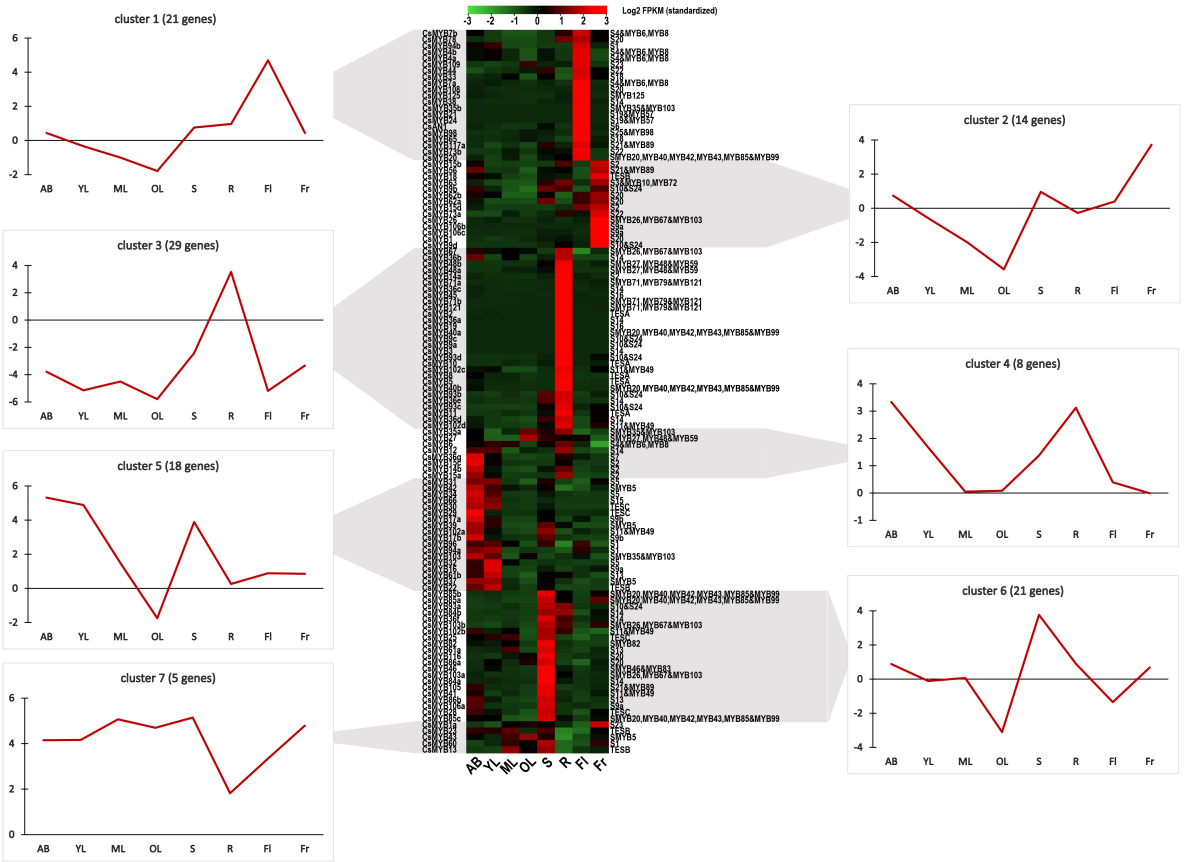

FIGURE 2 | Heatmap of the 118 *CsR2R3-MYB* genes transcribed in the tissues of *C. sinensis*. The 118 *CsR2R3-MYB* genes clustered into seven expression groups, based on their tissue-specific expression. The gene name is indicated on the left of the heatmap, and the short name of the phylogenetic subgroup is on the right. Transcript abundance is expressed in standardized log2 fragments per kilobase of exon per million fragments mapped (FPKM) values. Next to each RNA-seq-based cluster, there is a graph with the mean transcript abundance for the entire cluster in each tissue. AB, apical bud; YL, young leaf; ML, mature leaf; OL, old leaf; S, stem; R, root; Fl, flower; Fr, fruit. Data were obtained from the Tea Plant Information Archive (http://tpia.teaplant.org/).

genes (*CsSCPL1A7*, *CsANR*, *CsLAR*, *CsDFR*, *CsFLS*, *CsF3H*, and *CsF3′5′H)* and correlated with the contents of EGCG and ECG, with inter-gene-to-metabolite Pearson's correlation coefficients over 0.55. *CsMYB30*, *CsMYB34*, *CsMYB37*, and *CsMYB42* exhibited good performance compared with the others, each having a correlation coefficient exceeding 0.75, indicating an extremely strong correlation. Notably, *CsMYB34* had the strongest correlation with the catechin biosynthesis pathway downstream genes (>0.9), especially with *CsSCPL1A7* (0.99). Besides that, the coefficients between *CsMYB34* and EGCG and ECG contents were 0.89 and 0.86, respectively.

Validation of the Correlation Between *R2R3-MYB* Transcription Factors and Catechins

To validate the relationship between *R2R3-MYB* TFs and catechins, HPLC and qRT-PCR assays were carried out. Different tissues of the tea plant were tested for the contents of different catechin monomers *via* HPLC (**Figure 4A** and **Supplementary Table 9**). As shown in **Figure 4A**, there was a high level of EGCG in all tested tissues compared with the other catechin monomers, reaching the highest level in ABs and young leaves (FL and SL). Additionally, the expression patterns of the nine specially evolved and expanded candidate *CsR2R3-MYB*s and catechin biosynthesis genes in different tissues were verified by qRT-PCR. According to the relative expression patterns, there were four distinct clusters (clusters A–D) (**Figure 4B**). The genes upstream of catechin biosynthesis (*CsPAL*, *CsC4H*, and *Cs4CL*) grouped in cluster A and were highly expressed in roots, consistent with the absence of catechins in roots (**Figure 3C**). *CsMYB22*, *CsMYB31* and *CsMYB42* (cluster B) had distinctly high expression in old leaves, and were not AB- or young leaf-specific. Remarkably, *CsMYB30*, *CsMYB32*, *CsMYB34*, and *CsMYB37*, which clustered with critical genes downstream of catechins biosynthesis (cluster D) were highly expressed in ABs and first leaves, where EGCG and ECG accumulated (**Figure 4A**), preliminarily validating the intimate correlation between *CsMYB30*, *CsMYB32*, *CsMYB34*, *CsMYB37*, and catechin biosynthesis.

For further confirmation, gene-to-metabolite correlation analysis of *CsMYB30*, *CsMYB32*, *CsMYB34*, *CsMYB37*, key genes of the catechin biosynthesis pathway, and the accumulation of

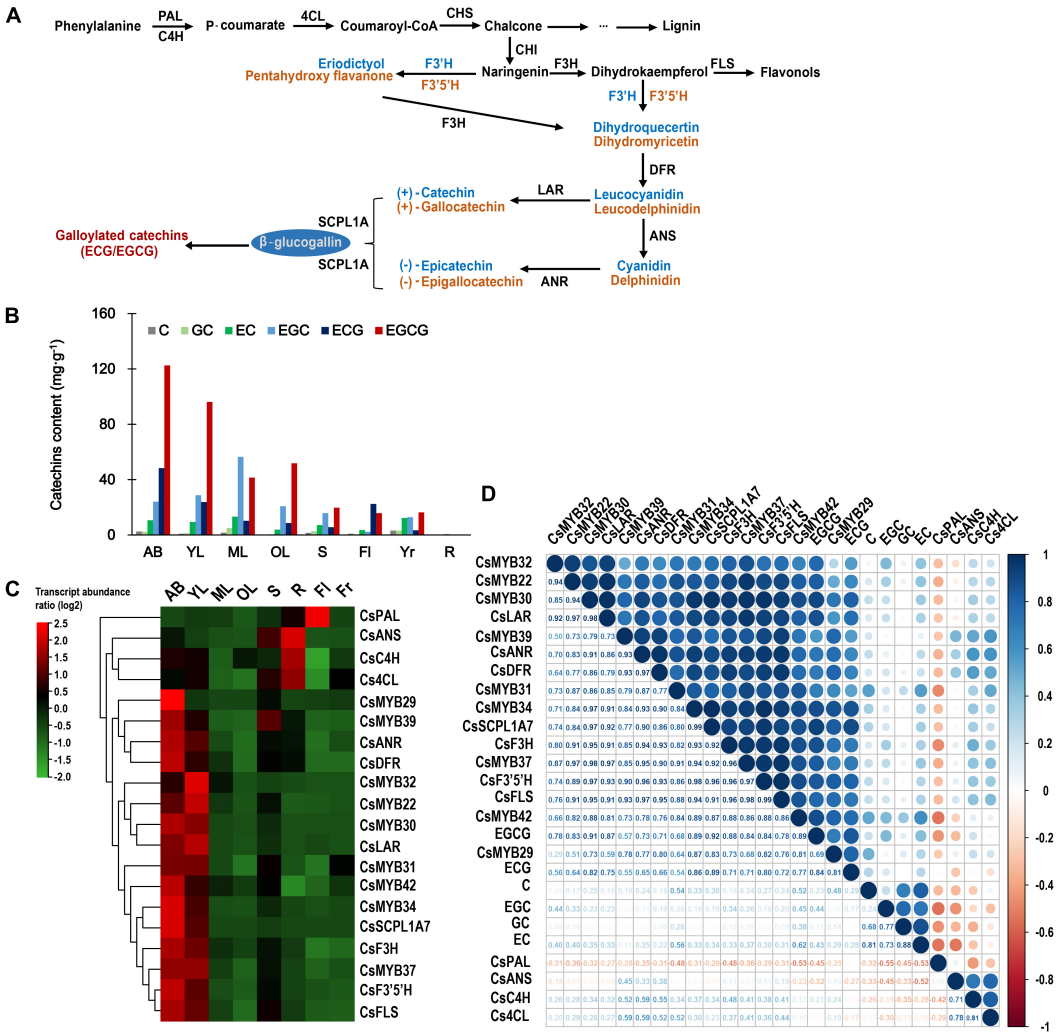

FIGURE 3 | Expression pattern analysis and correlation analysis of tea-specific or tea-expanded *CsR2R3-MYB*s. **(A)** The biosynthetic pathway of catechins. *CHS*, *CHI*, *F3H*, *F3′H*, *F3′5′H*, *DFR*, *ANS*, *LAR*, *ANR*, and *SCPL1A* represent genes encoding chalcone synthase, chalcone isomerase, flavanone 3-hydroxylase, flavonoid 3′-hydroxylase, flavonoid 3′,5′-hydroxylase, dihydroflavonol 4-reductase, anthocyanidin synthase, leucoanthocyanidin reductase, anthocyanidin reductase, and type 1A serine carboxypeptidase-like acyltransferases, respectively. **(B)** The contents of six catechin monomers in eight tissues. **(C)** Heatmap of RNA-seq transcript abundance patterns of the 20 *CsR2R3-MYB* genes from the *C. sinensis* genome in eight different tissues. AB, apical bud; YL, young leaf; ML, mature leaf; OL, old leaf; S, stem; R, root; Fl, flower; Fr, fruit. **(D)** Correlative analysis of *CsR2R3-MYB* genes, structural genes, and catechins accumulation patterns in eight representative tissues of *C. sinensis* plants. $R > 0.5$ indicates a positive correlation; $R < -0.5$ indicates a negative correlation. Data were obtained from the Tea Plant Information Archive (http://tpia.teaplant.org/).

catechins was conducted (**Figure 4C**). The results confirmed the extremely low correlation between four of the candidate TFs and the genes upstream of catechin biosynthesis *CsPAL*, *CsC4H*, and *Cs4CL*. In contrast, *CsMYB30*, *CsMYB34*, and *CsMYB37* were strongly associated with most of the major genes downstream of the galloylated catechin biosynthesis pathway (*CsSCPL1A7*, *CsANR*, *CsLAR*, and *CsDFR*) as well as ECG and EGCG contents (>0.7). Particularly, *CsMYB37* showed the highest correlation level with the highest inter-correlation coefficients within the four major functional genes *CsSCPL1A7*, *CsANR*, *CsLAR, CsDFR* and the contents of EGCG and ECG reaching to 0.79, 0.78, 0.88, 0.85, 0.87 and 0.8, respectively. However, *CsMYB30*, *CsMYB34*, and *CsMYB37* were less related to the other downstream catechin biosynthesis genes (*CsFLS*, *CsF3H*, and *CsF3′5′H*) according to their lower Pearson's correlation coefficients. Consistent with the *in silico* results in **Figure 3D**, the correlation among *CsMYB32*, the galloylated catechin contents and the biosynthesis genes was weaker than the other three *R2R3-MYB*s. In more detail, it had a relatively low correlation coefficient with ECG (0.52) and EGCG (0.67), and a relatively low correlation coefficient with genes *CsSCPL1A*, *CsANR*, *CsLAR*, and *CsDFR* (0.5, 0.36, 0.74 and 0.37, respectively).

The results provide convincing clues that *CsMYB30*, *CsMYB34*, and *CsMYB37* might be the key TFs regulating galloylated catechins biosynthesis for the abundance of EGCG in *C. sinensis*.

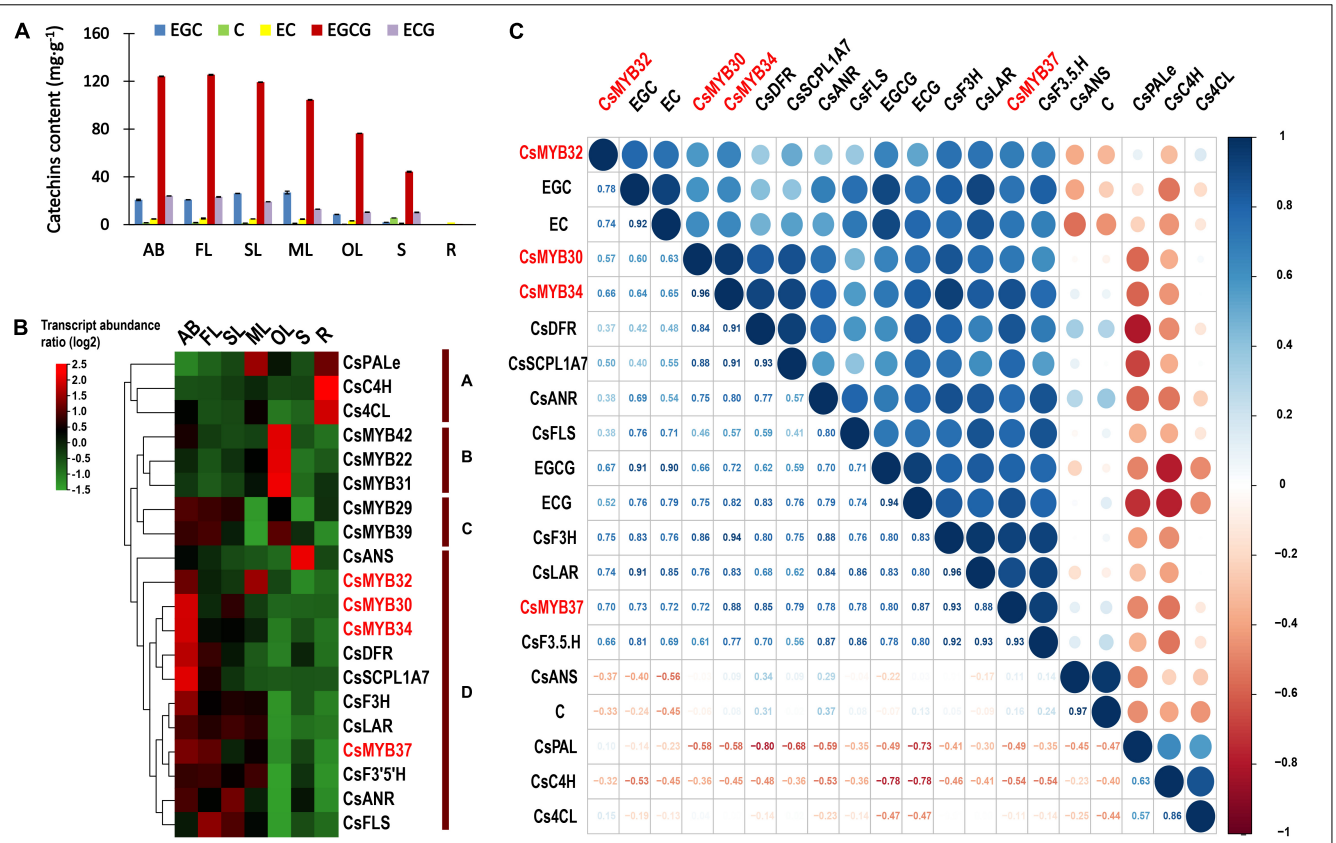

FIGURE 4 | Expression profiling validation and correlation analysis. **(A)** The contents of six catechin monomers in seven tissues as measured with an HPLC system. **(B)** Heatmap of qRT-PCR transcript abundance patterns in seven different tissues. **(C)** Correlative analysis of four potential *CsR2R3-MYB* TFs, catechin biosynthesis genes and catechin accumulation patterns in different tissues of tea plants. $R > 0.5$, positive correlation; $R < -0.5$, negative correlation. AB, apical bud; YL, young leaf; SL, second leaf; ML, mature leaf; OL, old leaf; S, stem; R, root.

DISCUSSION

Plants are rich in metabolites that allow them to adapt to the environment and resist biotic and abiotic stress (Howe and Jander, 2008). These metabolites are widely used as natural products for treating human diseases and are valuable raw materials for modern industry (Plomion et al., 2001; Howe and Jander, 2008; Guo et al., 2018; Fang et al., 2019). *C. sinensis* is an advantageous model system to dig into plant-specific metabolite biosynthesis and genetic regulation with rich and differential metabolite profiles. Its metabolites, such as flavonoids, caffeine, and volatile terpenes, accumulate in abundance and share characteristics with the same metabolites in other plant lineages (Yu M. et al., 2020).

Galloylated catechins are specialized secondary metabolites relatively abundantly present in *C. sinensis* (Wei et al., 2018). Contrary to the small amount of galloylated catechins present in the form of ECG generally in other plants (Bontpart et al., 2018), they are abundant in *C. sinensis*, and EGCG, only massively accumulated in tea plants, is the predominant form (Kim et al., 2004; Steinmann et al., 2013). It is the most bioactive component among the catechin enantiomers, and is derived from the flavonoid branch of the phenylpropanoid metabolite pathway. The acyltransferase family, belonging to subclade 1A of serine carboxypeptidase-like (SCPL) acyltransferases, acts as the most critical downstream gene family involved in the production of EGCG and ECG (Wei et al., 2018). This family extensively expanded to 22 members in the *C. sinensis* genome, while the *Vitis vinifera* genome contains half that number (11) (Wei et al., 2018). Two key enzymes Epicatechin:1-*O*-galloyl-b-*D*-glucose *O*-galloyltransferase (ECGT) and UDP-glucose: galloyl-1-*O*-b-*D*-glucosyltransferase (UGGT) are recruited to catalyze the last two reactions in this bioprocess (Liu et al., 2012). The biosynthesis of galloylated catechins in *C. sinensis* has been comprehensively investigated with regard to the biosynthesis genes of the pathway. However, the transcriptional regulation of these pathways remains to be illuminated.

Genes responsible for plant secondary metabolite biosynthesis are coordinately regulated by TFs, a regulatory superfamily that dynamically drives the evolution of plant metabolic pathways for special compounds (Shoji et al., 2021). The regulatory network of this gene superfamily is highly conserved both in angiosperms and gymnosperms (Zhang et al., 2014). The *R2R3-MYB* TFs confer tissue-specific or development stage-specific

patterns for metabolites in the same biosynthesis pathway; often, multiple paralogs coexist in one species (Zhang et al., 2014). Lignin, flavonoids, anthocyanins, and capsaicinoids are four different types of secondary metabolites synthesized from the phenylpropanoid pathway that are regulated by *R2R3-MYB* TFs (Soler et al., 2015; Sun et al., 2016; Zhu et al., 2019). Remarkably, the great expansion of this transcription-regulatory superfamily in plant lineages appears to account for the diversity of regulatory functions that the *R2R3-MYB* TFs undertake in plant-specific metabolic bioprocesses (Millard et al., 2019). As demonstrated in detail by the analysis of Soler et.al, the R2R3-MYB subgroups in *Eucalyptus grandis*, *V. vinifera* and *Populus trichocarpa*, which were equipped with expanded members, greatly determined the diversification of specific functions in lignin biosynthesis (Soler et al., 2015).

Based on the consideration of the massive accumulation of galloylated catechins (ECG and EGCG) in tea plant and tea-specific *R2R3-MYB* TFs identified in this work, we hypothesize that the biosynthesis of the peculiar galloylated catechins is absolutely influenced at the transcription regulation level. Different from the result that concentrates on the involvement of some *CsR2R3-MYB* genes in response to drought, cold, GA, and ABA treatments and proposing a key C*sR2R3-MYB* gene that regulate some main anthocyanin components, which are revealed in the recent genome-wide report of this family (Chen et al., 2021), we firstly emphasize on confirming the putative *R2R3-MYB* candidates that directly function in the production of *Camellia*-abundantly accumulated compounds (EGCG) among the tea-specific *R2R3-MYB* TFs.

The comprehensive and comparative phylogenetic analysis of *CsR2R3-MYB* TFs, backed by multiple sequence alignment among *C. sinensis* and *A. thaliana,* suggests that most of the members in this family are conserved. Most *R2R3-MYB*s share similar functions to the homologous counterparts studied in *A. thaliana*. Some of the *R2R3-MYB* TFs that clustered in TESA, TESB, and TESC subgroups evolved exclusively in *C. sinensis*, but have isogenous genes in *Actinidia chinensis*, *V. vinifera*, *Theobroma cacao*, and *Coffea canephora* genomes. Thus, we speculated that TESA, TESB, and TESC are either obtained in *C. sinensis* or lost in *A. thaliana* lineages after divergence from their most recent common ancestor during two whole-genome duplication (WGD) events. In addition, members of SMYB5 and S5 subgroups, regulating flavonoids biosynthesis in *A. thaliana*, are greatly expanded in *C. sinensis*, which suggests that they might be either functionally redundant genes or genes that undertake some novel functions in the tea plant.

Considering that galloylated catechins highly accumulate in ABs and young leaves, we speculated that the *CsR2R3-MYB* TFs that were preferentially expressed in these tender tissues along with the major catechin-biosynthesis genes were the most promising candidates putatively regulating the biosynthesis of galloylated catechins. Consistent with previous results (Wei et al., 2018), our study observed high expression levels of key galloylated catechin biosynthesis genes *SCPL1A, ANR, LAR*, and *DFR* in tender tissues, while the expression of upstream genes (*PAL*, *C4H*, and *4CL*) in the phenylpropanoid pathway that are mainly relevant to the generation of condensed polymer PAs, was in fruits, flowers and roots. However, *CsMYB42* was preferentially expressed in tender tissues and had a strong correlation with catechin biosynthesis genes and the contents of ECG and EGCG in the "Shuchazao" variety (**Figure 3D**), while it was preferentially expressed in old leaves in the "Lingtoudancong" variety (**Figure 4C**). Thus, differences can be observed in different *C. sinensis* varieties. Eventually, through systematic analyses, *CsMYB30* (TESC subgroup), *CsMYB34* (S5 subgroup), and *CsMYB37* (SMYB5 subgroup) were confirmed as the potential *R2R3-MYB* TFs relevant to the extensive accumulation of ECG and EGCG in *C. sinensis*, however, further investigation is needed. This study has laid a theoretical framework and valuable foundation for the future work, as we have provided a preliminarily evidence for illuminating that the high accumulation of galloylated catechins in *C. sinensis* are likely to be caused by the expanded R2R3-MYB TFs. Nevertheless, it is still necessary to further exploration and validate these results.

CONCLUSION

A total of 118 *R2R3-MYB* gene members, classified into 38 subgroups, were identified in the *C. sinensis* genome. Notably, five subgroups (TESA, TESB, TESC, S5, and SMYB5) containing 21 *R2R3-MYB* TFs were identified to be remarkably expanded in or completely unique to *C. sinensis*. Furthermore, gene structure predictions, expression profile validation, and correlation analyses were subsequently conducted to screen out candidate *R2R3-MYB* TFs regulating galloylated catechin biosynthesis. *CsMYB30*, *CsMYB34*, and *CsMYB37* were specifically expanded and their expression level were strongly correlated with galloylated catechin contents, suggesting the probable function in galloylated catechin biosynthesis. The present study firstly revealed the *C. sinensis* specific and expanded R2R3-MYB TFs that are potential regulators of galloylated catechins biosynthesis, which underpinned a basic understanding of the uniquely massive accumulation of galloylated catechins in *C. sinensis.*

DATA AVAILABILITY STATEMENT

The original contributions presented in the study are included in the article/**Supplementary Material**, further inquiries can be directed to the corresponding authors.

AUTHOR CONTRIBUTIONS

JL performed the qRT-PCR, analyzed and interpreted the data, made the data charts, and wrote the manuscript. SL conceived the project and supervised the research. PC carried out the HPLC test. JC, ST, and WY collected the materials for the experiments and provided useful suggestions. FC reviewed and edited the manuscript. PZ funded the research and reviewed the manuscript. BS designed the project, supervised the research, interpreted the data, and edited the manuscript. All authors contributed to the article and approved the submitted version.

FUNDING

This work was supported by the Natural Science Foundation of Guangdong Province (2021A1515012091) and the Science and Technology Projects of Guangzhou (202102020290).

SUPPLEMENTARY MATERIAL

The Supplementary Material for this article can be found online at: https://www.frontiersin.org/articles/10.3389/fpls.2021.782220/full#supplementary-material

REFERENCES

Abbas, M., Saeed, F., Anjum, F. M., Afzaal, M., Tufail, T., Bashir, M. S., et al. (2017). Natural polyphenols: an overview. *Int. J. Food Prop.* 20, 1689–1699. doi: 10.1080/10942912.2016.1220393

Ahmad, N., Gupta, S., and Mukhtar, H. (2000). Green tea polyphenol epigallocatechin-3-gallate differentially modulates nuclear factor κB in cancer cells versus normal cells. *Arch. Biochem. Biophys.* 376, 338–346. doi: 10.1006/abbi.2000.1742

Ambawat, S., Sharma, P., Yadav, N. R., and Yadav, R. C. (2013). MYB transcription factor genes as regulators for plant responses: an overview. *Physiol. Mol. Biol. Plants* 19, 307–321. doi: 10.1007/s12298-013-0179-1

Asakawa, T., Hamashima, Y., and Kan, T. (2013). Chemical synthesis of tea polyphenols and related compounds. *Curr. Pharm. Des.* 19, 6207–6217. doi: 10.2174/1381612811319340012

Ashihara, H., Deng, W.-W., Mullen, W., and Crozier, A. (2010). Distribution and biosynthesis of flavan-3-ols in Camellia sinensis seedlings and expression of genes encoding biosynthetic enzymes. *Phytochemistry* 71, 559–566. doi: 10.1016/j.phytochem.2010.01.010

Bailey, T. L., Boden, M., Buske, F. A., Frith, M., Grant, C. E., Clementi, L., et al. (2009). MEME Suite: tools for motif discovery and searching. *Nucleic Acids Res.* 37, 202–208. doi: 10.1093/nar/gkp335

Bedon, F., Grima-Pettenati, J., and Mackay, J. (2007). Conifer R2R3-MYB transcription factors: sequence analyses and gene expression in wood-forming tissues of white spruce (Picea glauca). *BMC Plant Biol.* 7:17. doi: 10.1186/1471-2229-7-17

Bontpart, T., Ferrero, M., Khater, F., Marlin, T., Vialet, S., Vallverdù-Queralt, A., et al. (2018). Focus on putative serine carboxypeptidase-like acyltransferases in grapevine. *Plant Physiol. Biochem.* 130, 356–366. doi: 10.1016/j.plaphy.2018.07.023

Cao, Z.-H., Zhang, S.-Z., Wang, R.-K., Zhang, R.-F., and Hao, Y.-J. (2013). Genome wide analysis of the apple MYB transcription factor family allows the identification of MdoMYB121 gene confering abiotic stress tolerance in plants. *PLoS One* 8:e69955. doi: 10.1371/journal.pone.0069955

Chen, C., Chen, H., Zhang, Y., Thomas, H. R., Frank, M. H., He, Y., et al. (2020). TBtools: an integrative toolkit developed for interactive analyses of big biological data. *Mol. Plant* 13, 1194–1202. doi: 10.1016/j.molp.2020.06.009

Chen, X., Wang, P., Gu, M., Lin, X., Hou, B., Zheng, Y., et al. (2021). R2R3-MYB transcription factor family in tea plant (*Camellia sinensis*): genome-wide characterization, phylogeny, chromosome location, structure and expression patterns. *Genomics* 113, 1565–1578. doi: 10.1016/j.ygeno.2021.03.033

Chen, Y., Yu, M., Xu, J., Chen, X., and Shi, J. (2009). Differentiation of eight tea (*Camellia sinensis*) cultivars in China by elemental fingerprint of their leaves. *J. Sci. Food Agric.* 89, 2350–2355. doi: 10.1002/jsfa.3716

Cheng, Y., Zhu, W., Chen, Y., Ito, S., Asami, T., and Wang, X. (2014). Brassinosteroids control root epidermal cell fate via direct regulation of a MYB-bHLH-WD40 complex by GSK3-like kinases. *Elife* 3:e02525. doi: 10.7554/eLife.02525

Drew, B. (2019). The growth of tea. *Nature* 566, S2–S4. doi: 10.1038/d41586-019-00395-4

Du, H., Yang, S.-S., Liang, Z., Feng, B.-R., Liu, L., Huang, Y.-B., et al. (2012). Genome-wide analysis of the MYB transcription factor superfamily in soybean. *BMC Plant Biol.* 12:106. doi: 10.1186/1471-2229-12-106

Dubos, C., Stracke, R., Grotewold, E., Weisshaar, B., Martin, C., and Lepiniec, L. (2010). MYB transcription factors in Arabidopsis. *Trends Plant Sci.* 15, 573–581. doi: 10.1016/j.tplants.2010.06.005

Eungwanichayapant, P. D., and Popluechai, S. (2009). Accumulation of catechins in tea in relation to accumulation of mRNA from genes involved in catechin biosynthesis. *Plant Physiol. Biochem.* 47, 94–97. doi: 10.1016/j.plaphy.2008.11.002

Fang, C., Fernie, A. R., and Luo, J. (2019). Exploring the Diversity of Plant Metabolism. *Trends Plant Sci.* 24, 83–98. doi: 10.1016/j.tplants.2018.09.006

Gigolashvili, T., Yatusevich, R., Berger, B., Müller, C., and Flügge, U.-I. (2007). The R2R3-MYB transcription factor HAG1/MYB28 is a regulator of methionine-derived glucosinolate biosynthesis in Arabidopsis thaliana. *Plant J.* 51, 247–261. doi: 10.1111/j.1365-313X.2007.03133.x

Goicoechea, M., Lacombe, E., Legay, S., Mihaljevic, S., Rech, P., Jauneau, A., et al. (2005). EgMYB2, a new transcriptional activator from Eucalyptus xylem, regulates secondary cell wall formation and lignin biosynthesis. *Plant J.* 43, 553–567. doi: 10.1111/j.1365-313X.2005.02480.x

Gonzalez, A., Mendenhall, J., Huo, Y., and Lloyd, A. (2009). TTG1 complex MYBs, MYB5 and TT2, control outer seed coat differentiation. *Dev. Biol.* 325, 412–421. doi: 10.1016/j.ydbio.2008.10.005

Guo, L., Winzer, T., Yang, X., Li, Y., Ning, Z., He, Z., et al. (2018). The opium poppy genome and morphinan production. *Science* 362, 343–347. doi: 10.1126/science.aat4096

Guo, Y., Chang, X., Zhu, C., Zhang, S., Li, X., Fu, H., et al. (2019). De novo transcriptome combined with spectrophotometry and gas chromatography-mass spectrometer (GC-MS) reveals differentially expressed genes during accumulation of secondary metabolites in purple-leaf tea (Camellia sinensis cv Hongyafoshou). *J. Hortic. Sci. Biotechnol.* 94, 349–367. doi: 10.1080/14620316.2018.1521708

He, X., Zhao, X., Gao, L., Shi, X., Dai, X., Liu, Y., et al. (2018). Isolation and characterization of key genes that promote flavonoid accumulation in purple-leaf tea (*Camellia sinensis L.*). *Sci. Rep.* 8:130. doi: 10.1038/s41598-017-18133-z

Heim, K. E., Tagliaferro, A. R., and Bobilya, D. J. (2002). Flavonoid antioxidants: chemistry, metabolism and structure-activity relationships. *J. Nutr. Biochem.* 13, 572–584. doi: 10.1016/s0955-2863(02)00208-5

Hichri, I., Barrieu, F., Bogs, J., Kappel, C., Delrot, S., and Lauvergeat, V. (2011). Recent advances in the transcriptional regulation of the flavonoid biosynthetic pathway. *J. Exp. Bot.* 62, 2465–2483. doi: 10.1093/jxb/erq442

Howe, G. A., and Jander, G. (2008). Plant immunity to insect herbivores. *Annu. Rev. Plant Biol.* 59, 41–66. doi: 10.1146/annurev.arplant.59.032607.092825

Jiang, C., Gu, X., and Peterson, T. (2004). Identification of conserved gene structures and carboxy-terminal motifs in the Myb gene family of *Arabidopsis* and *Oryza sativa L.* ssp. indica. *Genome Biol.* 5:R46. doi: 10.1186/gb-2004-5-7-r46

Jiang, X., Huang, K., Zheng, G., Hou, H., Wang, P., Jiang, H., et al. (2018). *CsMYB5a* and *CsMYB5e* from *Camellia sinensis* differentially regulate anthocyanin and proanthocyanidin biosynthesis. *Plant Sci.* 270, 209–220. doi: 10.1016/j.plantsci.2018.02.009

Jin, H., and Martin, C. (1999). Multifunctionality and diversity within the plant *MYB*-gene family. *Plant Mol. Biol.* 41, 577–585. doi: 10.1023/a:1006319732410

Jiu, S., Guan, L., Leng, X., Zhang, K., Haider, M. S., Yu, X., et al. (2021). The role of VvMYBA2r and VvMYBA2w alleles of the MYBA2 locus in the regulation of anthocyanin biosynthesis for molecular breeding of grape (*Vitis* spp.) skin coloration. *Plant Biotechnol. J.* 19, 1216–1239. doi: 10.1111/pbi.13543

Kim, S. Y., Ahn, B. H., Min, K. J., Lee, Y. H., Joe, E. H., and Min, D. S. (2004). Phospholipase D isozymes mediate epigallocatechin gallate-induced cyclooxygenase-2 expression in astrocyte cells. *J. Biol. Chem.* 279:38125. doi: 10.1074/jbc.M402085200

Kranz, H. D., Denekamp, M., Greco, R., Jin, H., Leyva, A., Meissner, R. C., et al. (1998). Towards functional characterisation of the members of the *R2R3-MYB* gene family from *Arabidopsis thaliana*. *Plant J.* 16, 263–276. doi: 10.1046/j.1365-313x.1998.00278.x

Kumar, S., Stecher, G., and Tamura, K. (2016). MEGA7: molecular evolutionary genetics analysis version 7.0 for bigger datasets. *Mol. Biol. Evol.* 33, 1870–1874. doi: 10.1093/molbev/msw054

Li, M., Li, Y., Guo, L., Gong, N., Pang, Y., Jiang, W., et al. (2017). Functional characterization of tea (*Camellia sinensis*) MYB4a transcription factor using an integrative approach. *Front. Plant Sci.* 8:943. doi: 10.3389/fpls.2017.00943

Li, W., Ding, Z., Ruan, M., Yu, X., Peng, M., and Liu, Y. (2017). Kiwifruit R2R3-MYB transcription factors and contribution of the novel *AcMYB75* to red kiwifruit anthocyanin biosynthesis. *Sci. Rep.* 7:16861. doi: 10.1038/s41598-017-16905-1

Li, S., Sun, L., Fan, X., Zhang, Y., Jiang, J., and Liu, C. (2020). Functional analysis of *Vitis davidii* R2R3-MYB transcription factor *Vd- MYB14* in the regulation of flavonoid biosynthesis. *J. Fruit Sci.* 37, 783–792. doi: 10.13925/j.cnki.gsxb.20190577

Li, X., Xue, C., Li, J., Qiao, X., Li, L., Yu, L., et al. (2016). Genome-wide identification, evolution and functional divergence of MYB transcription factors in Chinese White Pear (*Pyrus bretschneideri*). *Plant Cell Physiol.* 57, 824–847. doi: 10.1093/pcp/pcw029

Lipsick, J. S. (1996). One billion years of Myb. *Oncogene* 13, 223–235.

Liu, Y., Gao, L., Liu, L., Yang, Q., Lu, Z., Nie, Z., et al. (2012). Purification and characterization of a novel galloyltransferase involved in catechin galloylation in the tea plant (*Camellia sinensis*)*. *J. Biol. Chem.* 287, 44406–44417. doi: 10.1074/jbc.M112.403071

Livak, K. J., and Schmittgen, T. D. (2001). Analysis of relative gene expression data using real-time quantitative PCR and the 2(-Delta Delta C(T)) Method. *Methods* 25, 402–408. doi: 10.1006/meth.2001.1262

Martin, C., and Paz-Ares, J. (1997). MYB transcription factors in plants. *Trends Genet.* 13, 67–73. doi: 10.1016/S0168-9525(96)10049-4

Matus, J. T., Aquea, F., and Arce-Johnson, P. (2008). Analysis of the grape MYB R2R3 subfamily reveals expanded wine quality-related clades and conserved gene structure organization across Vitis and Arabidopsis genomes. *BMC Plant Biol.* 8:83. doi: 10.1186/1471-2229-8-83

Mehrtens, F., Kranz, H., Bednarek, P., and Weisshaar, B. (2005). The Arabidopsis transcription factor MYB12 is a flavonol-specific regulator of phenylpropanoid biosynthesis. *Plant Physiol.* 138, 1083–1096. doi: 10.1104/pp.104.058032

Millard, P. S., Kragelund, B. B., and Burow, M. (2019). R2R3 MYB Transcription Factors – Functions outside the DNA-Binding Domain. *Trends Plant Sci.* 24, 934–946. doi: 10.1016/j.tplants.2019.07.003

Mondal, T. K., Bhattacharya, A., Laxmikumaran, M., and Ahuja, P. S. (2004). Recent advances of tea (*Camellia sinensis*) biotechnology. *Plant Cell. Tissue Organ Cult.* 76, 195–254. doi: 10.1023/B:TICU.0000009254.87882.71

Nesi, N., Jond, C., Debeaujon, I., Caboche, M., and Lepiniec, L. (2001). The *Arabidopsis TT2* gene encodes an R2R3-MYB domain protein that acts as a key determinant for proanthocyanidin accumulation in developing seed. *Plant Cell* 13, 2099–2114. doi: 10.1105/tpc.010098

Nikoo, M., Regenstein, J. M., and Ahmadi Gavlighi, H. (2018). Antioxidant and antimicrobial activities of (-)-Epigallocatechin-3-gallate (EGCG) and its potential to preserve the quality and safety of foods. *Compr. Rev. Food Sci. Food Saf.* 17, 732–753. doi: 10.1111/1541-4337.12346

Park, M.-R., Yun, K.-Y., Mohanty, B., Herath, V., Xu, F., Wijaya, E., et al. (2010). Supra-optimal expression of the cold-regulated OsMyb4 transcription factor in transgenic rice changes the complexity of transcriptional network with major effects on stress tolerance and panicle development. *Plant. Cell Environ.* 33, 2209–2230. doi: 10.1111/j.1365-3040.2010.02221.x

Plomion, C., Leprovost, G., and Stokes, A. (2001). Wood formation in trees. *Plant Physiol.* 127, 1513–1523. doi: 10.1104/pp.010816

Punyasiri, P. A. N., Abeysinghe, I. S. B., Kumar, V., Treutter, D., Duy, D., Gosch, C., et al. (2004). Flavonoid biosynthesis in the tea plant *Camellia sinensis*: properties of enzymes of the prominent epicatechin and catechin pathways. *Arch. Biochem. Biophys.* 431, 22–30. doi: 10.1016/j.abb.2004.08.003

Savage, N., Yang, T. J. W., Chen, C. Y., Lin, K.-L., Monk, N. A. M., and Schmidt, W. (2013). Positional signaling and expression of ENHANCER OF TRY AND CPC1 are tuned to increase root hair density in response to phosphate deficiency in *Arabidopsis thaliana*. *PLoS One* 8:e75452. doi: 10.1371/journal.pone.0075452

Schenke, D., Cai, D., and Scheel, D. (2014). Suppression of UV-B stress responses by flg22 is regulated at the chromatin level via histone modification. *Plant. Cell Environ.* 37, 1716–1721. doi: 10.1111/pce.12283

Shoji, T., Umemoto, N., and Saito, K. (2021). Genetic divergence in transcriptional regulators of defense metabolism: insight into plant domestication and improvement. *Plant Mol. Biol.* [Online ahead of print] doi: 10.1007/s11103-021-01159-3

Singh, K., Rani, A., Kumar, S., Sood, P., Mahajan, M., Yadav, S. K., et al. (2008). An early gene of the flavonoid pathway, flavanone 3-hydroxylase, exhibits a positive relationship with the concentration of catechins in tea (*Camellia sinensis*). *Tree Physiol.* 28, 1349–1356. doi: 10.1093/treephys/28.9.1349

Soler, M., Camargo, E. L. O., Carocha, V., Cassan-Wang, H., San Clemente, H., Savelli, B., et al. (2015). The Eucalyptus grandis R2R3-MYB transcription factor family: evidence for woody growth-related evolution and function. *New Phytol.* 206, 1364–1377. doi: 10.1111/nph.13039

Steinmann, J., Buer, J., Pietschmann, T., and Steinmann, E. (2013). Anti-infective properties of epigallocatechin-3-gallate (EGCG), a component of green tea. *Br. J. Pharmacol.* 168, 1059–1073. doi: 10.1111/bph.12009

Stracke, R., Werber, M., and Weisshaar, B. (2001). The *R2R3-MYB* gene family in *Arabidopsis thaliana*. *Curr. Opin. Plant Biol.* 4, 447–456. doi: 10.1016/s1369-5266(00)00199-0

Sun, B., Zhu, Z., Cao, P., Chen, H., Chen, C., Zhou, X., et al. (2016). Purple foliage coloration in tea (*Camellia sinensis L.*) arises from activation of the R2R3-MYB transcription factor *CsAN1*. *Sci. Rep.* 6:32534. doi: 10.1038/srep32534

Taguri, T., Tanaka, T., and Kouno, I. (2004). Antimicrobial activity of 10 different plant polyphenols against bacteria causing food-borne disease. *Biol. Pharm. Bull.* 27, 1965–1969. doi: 10.1248/bpb.27.1965

Velasco, R., Zharkikh, A., Troggio, M., Cartwright, D. A., Cestaro, A., Pruss, D., et al. (2007). A high quality draft consensus sequence of the genome of a heterozygous grapevine variety. *PLoS One* 2:e1326. doi: 10.1371/journal.pone.0001326

Wang, P., Liu, Y., Zhang, L., Wang, W., Hou, H., Zhao, Y., et al. (2020). Functional demonstration of plant flavonoid carbocations proposed to be involved in the biosynthesis of proanthocyanidins. *Plant J.* 101, 18–36. doi: 10.1111/tpj.14515

Wang, P., Ma, G., Zhang, L., Li, Y., Fu, Z., Kan, X., et al. (2019). A Sucrose-Induced MYB (SIMYB) transcription factor promoting proanthocyanidin accumulation in the tea plant (*Camellia sinensis*). *J. Agric. Food Chem.* 67, 1418–1428. doi: 10.1021/acs.jafc.8b06207

Wei, C., Yang, H., Wang, S., Zhao, J., Liu, C., Gao, L., et al. (2018). Draft genome sequence of *Camellia sinensis var. sinensis* provides insights into the evolution of the tea genome and tea quality. *Proc. Natl. Acad. Sci. U. S. A.* 115, E4151–E4158. doi: 10.1073/pnas.1719622115

Wei, K., Wang, L., Zhang, Y., Ruan, L., Li, H., Wu, L., et al. (2019). A coupled role for *CsMYB75* and *CsGSTF1* in anthocyanin hyperaccumulation in purple tea. *Plant J.* 97, 825–840. doi: 10.1111/tpj.14161

Wilkins, O., Nahal, H., Foong, J., Provart, N. J., and Campbell, M. M. (2009). Expansion and diversification of the *Populus* R2R3-MYB family of transcription factors. *Plant Physiol.* 149, 981–993. doi: 10.1104/pp.108.132795

Yamashita, H., Uchida, T., Tanaka, Y., Katai, H., Nagano, A. J., Morita, A., et al. (2020). Genomic predictions and genome-wide association studies based on RAD-seq of quality-related metabolites for the genomics-assisted breeding of tea plants. *Sci. Rep.* 10:17480. doi: 10.1038/s41598-020-74623-7

Yang, D., Liu, Y., Sun, M., Zhao, L., Wang, Y., Chen, X., et al. (2012). Differential gene expression in tea (*Camellia sinensis L.*) calli with different morphologies and catechin contents. *J. Plant Physiol.* 169, 163–175. doi: 10.1016/j.jplph.2011.08.015

Yu, M., Man, Y., Lei, R., Lu, X., and Wang, Y. (2020). Metabolomics study of flavonoids and anthocyanin-related gene analysis in Kiwifruit (*Actinidia chinensis*) and Kiwiberry (*Actinidia arguta*). *Plant Mol. Biol. Rep.* 38, 353–369. doi: 10.1007/s11105-020-01200-7

Yu, X., Xiao, J., Chen, S., Yu, Y., Ma, J., Lin, Y., et al. (2020). Metabolite signatures of diverse Camellia sinensis tea populations. *Nat. Commun.* 11:5586. doi: 10.1038/s41467-020-19441-1

Yu, S., Li, P., Zhao, X., Tan, M., Ahmad, M. Z., Xu, Y., et al. (2021). *CsTCP*s regulate shoot tip development and catechin biosynthesis in tea

plant (*Camellia sinensis*). *Hortic. Res.* 8:104. doi: 10.1038/s41438-021-00538-7

Zhang, P., Chopra, S., and Peterson, T. (2000). A segmental gene duplication generated differentially expressed myb-homologous genes in *Maize*. *Plant Cell* 12:2311. doi: 10.2307/3871231

Zhang, Y., Butelli, E., and Martin, C. (2014). Engineering anthocyanin biosynthesis in plants. *Curr. Opin. Plant Biol.* 19, 81–90. doi: 10.1016/j.pbi.2014.05.011

Zhou, C., Zhu, C., Fu, H., Li, X., Chen, L., Lin, Y., et al. (2019). Genome-wide investigation of superoxide dismutase (SOD) gene family and their regulatory miRNAs reveal the involvement in abiotic stress and hormone response in tea plant (*Camellia sinensis*). *PLoS One* 14:e0223609. doi: 10.1371/journal.pone.0223609

Zhu, Z., Sun, B., Cai, W., Zhou, X., Mao, Y., Chen, C., et al. (2019). Natural variations in the MYB transcription factor MYB31 determine the evolution of extremely pungent peppers. *New Phytol.* 223, 922–938. doi: 10.1111/nph.15853

Conflict of Interest: The authors declare that the research was conducted in the absence of any commercial or financial relationships that could be construed as a potential conflict of interest.

frontiers in Plant Science

ORIGINAL RESEARCH
published: 08 February 2022
doi: 10.3389/fpls.2022.833489

Exogenous Application of Gallic Acid Induces the Direct Defense of Tea Plant Against *Ectropis obliqua* Caterpillars

*Xin Zhang[1,2], Wei Ran[1,2], Xiwang Li[1,2], Jin Zhang[1,2], Meng Ye[1,2], Songbo Lin[1,2], Miaomiao Liu[1,2] and Xiaoling Sun[1,2]**

[1] Tea Research Institute, Chinese Academy of Agricultural Sciences, Hangzhou, China, [2] Key Laboratory of Tea Biology and Resources Utilization, Ministry of Agriculture, Hangzhou, China

OPEN ACCESS

Edited by:
Lanting Zeng,
South China Botanical Garden, Chinese Academy of Sciences (CAS), China

Reviewed by:
Yunqiu Yang,
Anhui Agricultural University, China
Guoxin Zhou,
Zhejiang A&F University, China

***Correspondence:**
Xiaoling Sun
xlsun@tricaas.com;
xlsun1974@163.com

Specialty section:
This article was submitted to Plant Metabolism and Chemodiversity, a section of the journal Frontiers in Plant Science

Received: 11 December 2021
Accepted: 05 January 2022
Published: 08 February 2022

Citation:
Zhang X, Ran W, Li X, Zhang J, Ye M, Lin S, Liu M and Sun X (2022) Exogenous Application of Gallic Acid Induces the Direct Defense of Tea Plant Against Ectropis obliqua Caterpillars. Front. Plant Sci. 13:833489. doi: 10.3389/fpls.2022.833489

Gallic acid (GA), an important polyphenolic compound in the plant, is a well-known antioxidant, antihyperglycemic, and anti-lipid peroxidative agent. Recently, GA treatment exhibited ameliorative effects on plants in response to some abiotic stresses. However, the elicitation effect of GA on plant defense against herbivorous insects has not yet been reported. In this study, we found that the exogenous application of GA induced the direct defense of tea plant (*Camellia sinensis*) against tea geometrid (*Ectropis obliqua*) larvae, through activating jasmonic acid (JA) signaling and phenylpropanoid pathways. These signaling cascades resulted in the efficient induction of several defensive compounds. Among them, astragalin, naringenin, and epigallocatechin-3-gallate were the three of the most active anti-feeding compounds. However, the exogenous GA treatment did not affect the preference of *E. obliqua* female moths and larval parasitoid *Apanteles* sp. Our study suggests that GA may serve as an elicitor that triggers a direct defense response against tea geometrid larvae in tea plants. This study will help to deepen the understanding of the interaction between plants and phytophagous insects and also provide theoretical and technical guidance for the development of plant defense elicitors.

Keywords: induced defense, gallic acid, jasmonic acid, flavonoids, tea geometrid larvae

INTRODUCTION

During the long course of co-evolution with insect herbivores, plants have evolved a series of induced defense mechanisms to cope with herbivore attacks (Howe and Jander, 2008; Wu and Baldwin, 2010). Induced defense responses are first activated by the damage- and herbivore-associated molecular patterns and then regulated by a complex signaling network, including Ca^{2+} influxes, kinase cascades, reactive oxygen species, jasmonic acid (JA), salicylic acid (SA), ethylene (ET), and hydrogen peroxide (H_2O_2). The network finally reshapes the transcriptomes, proteomes, and metabolomes, resulting in the production of defensive compounds, such as secondary metabolites, protein inhibitors, and herbivore-induced plant volatiles (HIPVs), which in turn increase the direct or indirect resistance of plants to herbivores (Wu and Baldwin, 2010;

Schuman and Baldwin, 2016; Wang et al., 2020). A growing number of studies have shown that chemical elicitors can also trigger plant-induced defenses against herbivores, including naturally occurring phytohormones, plant volatiles, and synthetic substances (Moreira et al., 2012; Zhou et al., 2018; Chen et al., 2020). The mechanisms underlying the action of different kinds of elicitors are also different. For example, many active elicitors trigger defense responses by boosting hormonal signaling pathways, thereby regulating plant resistance against herbivores (Li et al., 2018; Xin et al., 2019; Chen et al., 2020), while a newly reported chemical elicitor 4-fluorophenoxyacetic acid was found to increase plant resistance by modulating the production of peroxidases, H_2O_2, and flavonoids, and directly triggering the formation of flavonoid polymers without affecting the canonical hormonal pathways (Wang et al., 2020). Thus, it is still necessary to identify new chemical elicitors that induce plant defenses against herbivores and reveal the underlying mechanisms, which would be beneficial for not only insights into the precise mechanisms of induced defense but also developing new pest control strategies.

Polyphenols are secondary metabolites widely distributed in plants, and many of them are known to play important biological roles, such as resistance factors against either microbes or herbivores (Chen, 2008; War et al., 2012; Schuman and Baldwin, 2016). Furthermore, certain polyphenol compounds have been found to act as stimulators of plant stress responses in addition to their direct antibiosis action (Gozzo and Faoro, 2013; Kamatham et al., 2016; Qiu et al., 2017). Gallic acid (GA) is an important polyphenol compound in many plants, such as the tea plant (*Camellia sinensis*). GA not only has antimicrobial and insecticidal activities but also acts as a critical contributor to tea taste (Zeng et al., 2020; Zhou et al., 2020). Recently, several researchers reported that GA exhibited its regulatory role in inducing abiotic stress tolerance of plants. For example, GA was found to enhance the defense state of the rice (*Oryza sativa*) plant by promoting the expression of genes and accumulation of phenols, flavonoids, and callose (Singh et al., 2017). GA was found to increase antioxidant activities in soybean (*Glycine max*) under cold stress *via* enhancing activities of catalase and peroxidase, but declining total ascorbate and glutathione (Ozfidan-Konakci et al., 2019), while a contrary phenomenon was reported in tomato (*Solanum lycopersicum*) that GA application protected tomato callus cells from excessive boron stress by increasing the content of ascorbate and flavonoids (Farghaly et al., 2021). The exogenous application of GA in maize (*Zea mays*) seedlings was reported to have positive effects on stress parameters and lowered the impact of oxidative stress caused by copper exposure (Yetissin and Kurt, 2020). Moreover, GA derivatives also showed plant immunity inducer properties in tobacco (*Nicotiana tabacum*) by regulating the signaling pathway leading to defense reactions (Goupil et al., 2017, 2020). However, the steered effect of GA on the resistance of plants against herbivores remains largely unknown.

The tea plant is an economically important woody species, as its young leaves are the raw material for tea processing (Zeng et al., 2020). However, the tea geometrid (*Ectropis obliqua*), one of the most common herbivores in tea plantations, always causes serious damage to tea production, reducing the quality of tea (Jiang et al., 2019; Zhang J. et al., 2020). Chemical insecticides are commonly used for controlling tea geometrid, but they are harmful to both the environment and human health (Xin et al., 2016). Although the chemical ecology investigations of the tea plant lag far behind rice, maize, and other herbaceous plants, the current development still revealed that JA, ET, auxin, and other signaling pathways were involved in induced defense response in tea plants against tea geometrid (Wang et al., 2015, 2016; Xin et al., 2017; Zhang J. et al., 2020; Zhang X. et al., 2020; Li et al., 2021). Therefore, exploiting chemical elicitors, especially natural molecules, is an efficient and feasible strategy to increase the defense resistance of tea plants to herbivores. In this study, we found that the exogenous application of GA enhanced the direct defense of tea plants to tea geometrid caterpillars, upregulated the expression levels of defensive genes related to JA singling and phenylpropanoid pathways, and finally resulted in an efficient induction of defensive compounds, which will provide theoretical and technical guidance for the development of plant defense elicitors.

MATERIALS AND METHODS

Plant and Insects

Camellia sinensis cv. Longjing 43 was used in this study. Two-year-old seedlings were planted individually in plastic pots (14 cm diameter × 15 cm high) and kept in a greenhouse (26 ± 2°C, 12/12 h photoperiod, 65 ± 5% relative humidity). Each plant was irrigated once every other day and fertilized monthly with compound fertilizer. The tea plants used for the experiment were in a uniform appearance.

Ectropis obliqua larvae were originally obtained from the tea plantation of Tea Research Institute, Chinese Academy of Agricultural Sciences, Hangzhou, China, and reared with fresh tea shoots of Longjing 43 in net cages (75 cm × 75 cm × 75 cm). All the larvae were kept in insectary with 26 ± 2°C, 12/12 h photoperiod, and 70–80% RH. After one generation, caterpillars were used for the experiments. Pupae were distinguished according to their morphological characteristics (Miller et al., 1982) and kept in different cages separately. After eclosion, one newly emerged female moth and two male moths were paired in plastic containers (12 cm high × 7 cm diameter) for 1 day to obtain fully mated female moths. A diluted honey aqueous solution (10%) was provided as a food source. Virgin female moths 1 day after eclosion and mated female moths that never laid eggs were used for Y-tube olfactometer bioassay.

The cocoons of *Apanteles* sp., an important larval parasitoid of tea geometrid, were collected from the tea plantation of Tea Research Institute, Chinese Academy of Agricultural Sciences, Hangzhou, China, and reared on *E. obliqua* larvae. Wasps were used for the experiments over one generation. A diluted honey aqueous solution (10%) was provided as a food source. Wasps were separated by sex according to morphological characteristics, 0.5-day-old male and female wasps were paired for 24 h, and only mated female wasps were used for the bioassay.

Gallic Acid Treatment

Gallic acid (Sigma, United States) was made up to 500 mg/L with being dissolved in double-distilled water (ddH_2O), which is physiologically correlated with the concentration of it in tea plants (Ran et al., 2018). Treated plants were uniformly sprayed with 10 ml GA solution. Control plants were sprayed with the equivalent amount of ddH_2O. Samples for RNA extraction were harvested at 3, 12, and 48 h post-treatment; samples for catechins and caffeine analysis were harvested at 12 h post-treatment; and samples for flavonoids analysis were harvested at 24 h post-treatment. Six independent replicates were performed for each treatment and pooled into three samples for analysis.

RNA Extraction and Real-Time Quantitative PCR Analysis

Total RNA was extracted *via* TRIzol™ kit according to the instructions of the manufacturer (TIANGEN, Beijing, China). Primer Script™ RT Reagent Kit (TaKaRa, Dalian, China) was used for synthesizing the first-strand cDNA from the total RNA. The real-time quantitative PCR (qRT-PCR) was performed on LightCycler 480 with the SYBR Green I Master (Roche Diagnostics, Mannheim, Germany). The relative expressions were calculated using the $2^{-\Delta\Delta Ct}$ method. *CsGAPDH* was used as the reference gene. Primers of all the measured genes were listed in **Supplementary Table 1**.

Catechins and Caffeine Analysis

The analysis of catechins and caffeine was performed following the International Standards Organization (ISO) ISO 14502-2-2005 (E) procedure with minor modifications (International Organization for Standardization [ISO], 2005); 100 mg tea leaf powders were extracted by 1 ml 70% methanol. Samples were analyzed by high-performance liquid chromatography (HPLC). The separations were carried out using a Waters e2695 series HPLC system (Waters Co., Milford, MA, United States) equipped with a reversed-phase C12 column (4 μm, 250 mm × 4.6 mm i.d., Phenomenex) and a C12 guard column, and the eluate was monitored by UV spectroscopy using a diode array detector at 280 nm. Compounds were confirmed by comparison of retention time with internal standards, and the content of individual compounds was calculated by the external standard method, *via* comparing the chromatographic peaks with that of the internal standard. Standard chemicals were purchased from Sigma Chemical Company (St. Louis, MO, United States).

Flavonoids Analysis

According to the method described by Lin et al. (2020), 200 mg leaf powders were extracted with 1 ml 80% methanol for analyzing flavonoids, and then, the mixture was vortexed for 10 min and sonicated for 5 min, for a total of three times. After centrifugation at 12,000 rpm for 30 min, the supernatant was filtered through a 0.22 μm nylon membrane filter into autosampler vials. The samples were measured by the UPLC/MS/MS analysis with the Waters ACQUITY UPLC H-Class System (Milford, MA, United States) coupled to Waters Xevo TQ-S Micro Triple-Quadrupole Mass Spectrometer. A total of 11 flavonoids, namely, astragalin, naringenin, apigenin-5-*O*-glucoside, cosmosiin, isovitexin, prunin, luteolin-7-*O*-glucoside, isoorientin, rutin, eriodictyol-7-*O*-glucoside, and isoquercitrin, were detected. The content of flavonoids was quantified using the calibration curves of corresponding standard solutions.

Herbivore Performance Bioassay

The most apical unfolded, but not yet expanded, the leaf was designated as leaf position one, and the other leaves were numbered sequentially down the stem. The second leaves of control and GA-treated tea plants were covered by a fine-mesh sleeve and introduced with one 2-day-old caterpillar which has been starved for 8 h (n = 50). During feeding, if the leaf were almost half exhausted, the caterpillar would be transferred to nearby intact leaves in the same branch. Larval mass was measured 5, 9, and 13 days after the inoculation.

Diet Assay

According to the method described by Yang et al. (2013), an artificial diet supplemented with GA, naringenin, or prunin was used for herbivore performance bioassay. Different gradients based on the physiological concentration in plants (GA with 0 and 500 mg/L; naringenin with 0, 3, and 6 μg/L; prunin with 0, 100, and 500 μg/L) were set for each treatment. Each concentration was replicated 40–50 times. At 7 and 10 days after the start of feeding, the larval mass was weighted.

Preference Bioassay

The preference behavior of *Apanteles* sp. wasps and virgin or mated *E. obliqua* female moths were tested in a Y-tube olfactometer. *Apanteles* sp. wasps were allowed to choose between GA-treated plant and control plant. The behavioral responses of virgin or mated *E. obliqua* female moths to a pair of odors (caterpillars feeding treatment vs. GA plus caterpillars feeding treatment) were tested. The potted tea plant infested with 30 s-instar caterpillars (starved for 8 h before being used) for 24 h and then removed was regarded as caterpillars feeding treatment. The potted tea plant was pre-treated with GA for 24 h and then treated as the above was regarded as GA plus caterpillars feeding treatment. The parasitoids or moths that did not choose within 5 min will be defined as a non-responding individual and recorded as "no choice." The position of tubes attached to sample jars was reversed after each replication to remove directional bias. After testing four wasps or moths, the olfactometer tube was replaced. The bioassay was conducted between 15:00 pm and 18:00 pm and replicated at least thirty-two times.

Statistical Analysis

All the statistical analyses were performed by the Statistica (Institute Inc., Cary, NC, United States). The Student's t-test was used for comparing differences between the treatment and control. Effects of metabolites at different concentrations on the growth of larvae were analyzed *via* one-way ANOVA with Turkey's honest significant difference (HSD) *post hoc* test for multiple comparisons, and the correlation between the parameters was performed by Pearson's correlation coefficient

analysis. The differences in the number of *Apanteles* sp. female adults entering each arm of the olfactometer were analyzed by Kruskal–Wallis test (χ^2 approximation).

RESULTS

Gallic Acid Treatment Enhances the Direct Resistance of Tea Plants to Tea Geometrid Larvae

To explore the potential effect of exogenous application of GA on the direct resistance of tea plants, we compared the weight gain of tea geometrid fed with GA-treated and control plants. The results showed that the exogenous application of GA to tea plants significantly reduced the weight gain of larvae by 14.8 and 26.8% at 9 and 13 days, respectively, compared with control (**Figure 1**). Furthermore, we found that an artificial diet supplemented with GA in a similar concentration to the exogenous application did not affect the weight gain of caterpillars (**Supplementary Figure 1**). The data demonstrate the anti-feeding effect of GA treatment probably *via* triggering the defense responses in tea plants. However, GA treatment did not influence the preference behavior of *Apanteles* sp. (**Figure 2A**) and the behavioral responses of virgin or mated *E. obliqua* female moths (**Figure 2B**).

Gallic Acid Treatment Upregulates the Expression Levels of Key Defensive Genes in Tea Plants

CsOPR3 and *CsJAZ1* are key component genes of the JA signaling pathway, and *CsPAL1/2* and *CsSDH1* are vital synthetic genes of the phenylpropanoid pathway. GA treatment promoted the transcription of *CsOPR3*, and the level was induced to 1.9 times that in control; the level of *CsJAZ1* was induced to 12.2 and 7.9 times that in control at 3 and 12 h, respectively (**Figure 3**). In addition, the expression of *CsPAL1*, *CsPAL2*, and *CsSDH1* was also significantly upregulated by GA treatment, and the levels were induced to 2.1, 4.5, and 3.6 times, respectively, of that in control (**Figure 3**). The results suggested that the exogenous application of GA steered the synthesis and transduction of the JA and phenylpropanoid pathways.

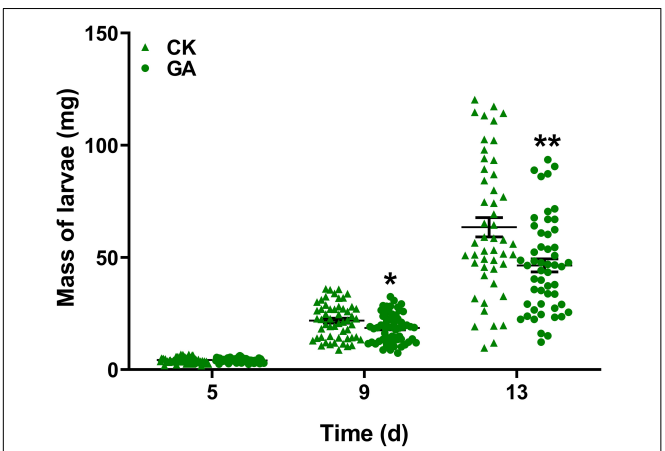

FIGURE 1 | Effect of gallic acid (GA)-treated tea plants on *Ectropis obliqua* larval weight gain. Data are presented as means ± SE (n = 50), and asterisk indicates significant differences between GA treatment and control (*P < 0.05, **P < 0.01, Student's t-test).

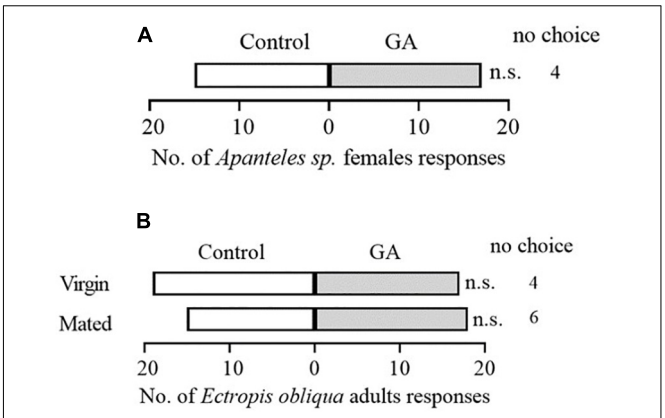

FIGURE 2 | Behavioral responses of mated *Apanteles* sp. female wasps to volatiles emitted from GA-treated vs. control plant **(A)**, and mated or virgin *Ectropis obliqua* female moths to volatiles emitted from GA-treated plus caterpillars feeding vs. caterpillars feeding plants **(B)**. Numbers refer to the number of each tested insect choosing an odor source. n > 32 per treatment. *n.s.*, P > 0.05, χ^2 test.

Gallic Acid Treatment Alters the Metabolic Profile of Tea Plants

Astragalin, prunin, and naringenin (3 out of the 10 detected flavonoids) accumulated significantly in the GA treatment, which was increased by 2.4, 2.2, and 4.5-folds higher than those in control (**Figure 4A** and **Supplementary Figure 2**). In addition, significant induction in the content of caffeine and galloylated catechins was also noticed in the GA-treated plants. The concentration of caffeine was significantly increased by 43%; epicatechin-3-gallate (ECG) and epigallocatechin-3-gallate (EGCG) were significantly increased by 22 and 27%, respectively (**Figure 4B**). Thus, the exogenous application of GA altered the metabolic profile of tea plants by regulating the synthesis of metabolic compounds related to flavonoids, caffeine, and catechins. Moreover, the effects of prunin and naringenin were selected for further verification.

Effects of Prunin and Naringenin on the Performance of Tea Geometrid

The results of this study showed that the addition of naringenin significantly decreased the larval weight, with a reduction of about 30% compared with control, except the 7 days at the concentration of 6 μg/L. In addition, there was a negative correlation between larval weight and naringenin concentration at 10 days (r = −0.280, P = 0.005). Compared with control, the addition of prunin slightly, but not significantly, affected the growth ratio of tea geometrid (**Figure 5**).

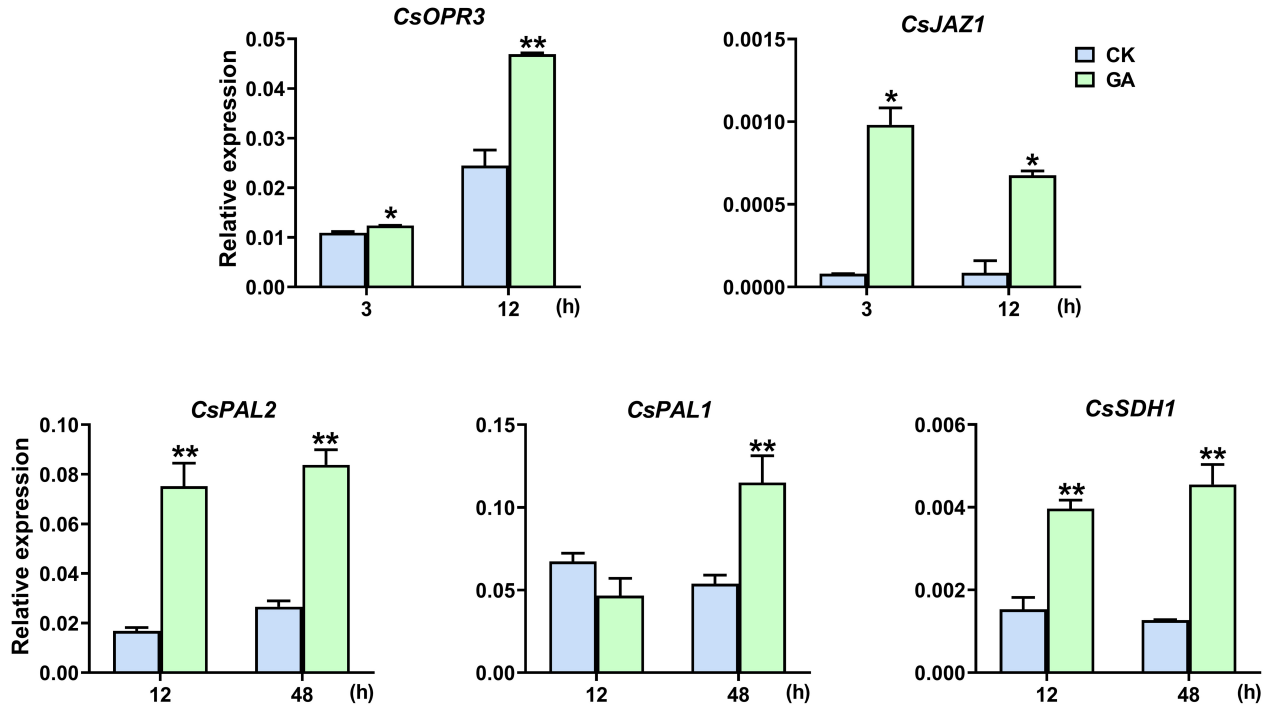

FIGURE 3 | GA treatment upregulated the expression levels of genes. Data are presented as means + SE (n = 3), and the asterisk indicates significant differences between GA treatment and CK (*P < 0.05, **P < 0.01, Student's t-test).

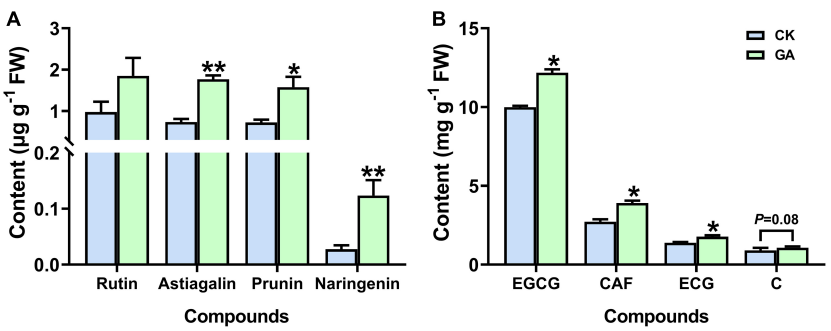

FIGURE 4 | GA treatment enhanced the accumulation of metabolites. **(A)** Flavonoids. **(B)** Caffeine and catechins. Data are presented as means + SE (n = 3), and the asterisk indicates significant differences between GA-treated and control plant (*P < 0.05, **P < 0.01, Student's t-test).

DISCUSSION

Plant-induced defense against herbivore attacks can be deployed as an important strategy in pest management. So far, a large number of studies have shown that chemical elicitors and small molecular compounds can increase the resistance of plants against insects by inducing defensive responses (Xin et al., 2016; Lin et al., 2020; Wang et al., 2020). In this study, we found that the exogenous application of GA induced the direct resistance of tea plants to tea geometrid larvae. The expression levels of genes related to JA and phenylpropanoid pathways were upregulated, and the accumulation of caffeine, galloylated catechins, astragalin, prunin, and naringenin was enhanced. Furthermore, astragalin, naringenin, and EGCG were proved to be the three most active anti-feeding compounds. However, GA treatment did not affect the preference of *E. obliqua* female moths and parasitoid *Apanteles* sp. These results provide shreds of evidence for GA, a natural compound in the plant, acting as an elicitor that increases plant resistance to herbivore larvae but did not affect volatile organic compounds-mediated defenses to the insect and its natural enemies.

Jasmonic acid and phenylpropanoid pathways play key roles in induced defensive responses and have been reported in several plants (Howe and Jander, 2008; Lou et al., 2015; Schuman and Baldwin, 2016). Transcriptome analysis revealed that genes related to JA signaling and phenylpropanoid biosynthesis are involved in inducible defenses responses in tea plants against tea geometrid (Wang et al., 2015, 2016). Previously, 12-oxophytodienoate reductase 3 (OPR3) was reported to act as a key enzyme in the biosynthesis of JA and its mutant plant

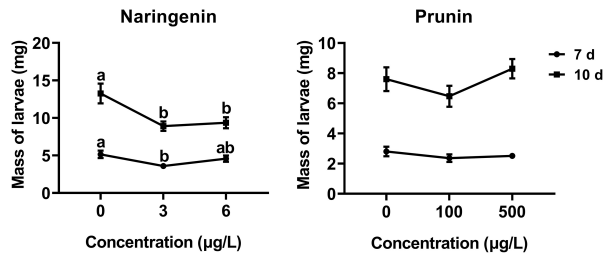

FIGURE 5 | Effects of naringenin and prunin on the weight gain of tea geometrid larvae. Data are presented as means ± SE (n = 40), and different letters indicate significant differences among treatments [$P < 0.05$, Turkey's honest significant difference (HSD) *post hoc* test].

changed JA-induced resistance to insects (Browse, 2009), while JAZ1 is an important component of JA signaling transduction, which has been identified as an early JA-responsive gene (Staswick, 2008; Oh et al., 2012). Our previous works have demonstrated that both *CsOPR3* and *CsJAZ1* in tea plants were responsive to JA and tea geometrid attacks (Xin et al., 2017; Zhang X. et al., 2020). In this study, we found that the expression levels of JA pathway-related genes, *CsOPR3* and *CsJAZ1*, and phenylpropanoid pathway genes, *CsPAL1/2* and *CsSDH*, were upregulated by GA treatment. In line with that GA has been reported to activate the expression of phenylpropanoid pathway genes, *OsPAL* and *OsCHS*, and methyl jasmonate-regulated gene, *OsWRKY71*, in rice (Singh et al., 2017). Moreover, the upregulation of transcription levels of genes related to JA signaling and phenylpropanoid pathways in GA-treated plants may be correlated with the accumulation of defensive compounds, which in turn regulate antioxidants and alleviate reactive oxygen generation in rice (Singh et al., 2017). The exogenous application of GA in tea plants also elicited subsequent responses with the production of defensive secondary metabolites. Our results suggested that GA may activate JA signaling and phenylpropanoid pathways to modulate tea plant resistance.

Plants develop a strategy to accumulate a variety of metabolites against herbivorous insects, including flavonoids, caffeine, and nitrogen and sulfur-containing compounds (Treutter, 2006; Chen, 2008; Mazid et al., 2011). Hitherto, the defensive role of secondary metabolites in plant-insect interactions has been widely elucidated (Mazid et al., 2011; Gols, 2014). They may act as feeding deterrents, digestibility reducers, and toxins of herbivores, and their accumulation is often enhanced by insect infestation (Mazid et al., 2011). For example, naringenin was reported to inhibit the larval growth and development of the common cutworm *Spodoptera litura* (Stec et al., 2020). Transgenic tobacco with higher content of caffeine exhibited a relatively high resistance to herbivores (Ashihara et al., 2008). In tea plants, caffeine was found to inhibit the oviposition of *Xyleborus fornicatus* and protect tender tissues from the damage of beetles (Hewavitharanage et al., 1999). Our group also found that astragalin negatively affected the growth rate of tea geometrid, and the anti-feeding effect was intensified by feeding time (Lin et al., 2022, accepted). JA was involved in the induction of EGCG, and there was a negative correlation between the level of EGCG in the diet and tea geometrid larval mass (Li et al., 2021). In this study, significant induction of flavonoid compounds by GA treatment was noticed, especially naringenin, astragalin, and EGCG. In addition, an artificial diet supplemented with naringenin significantly reduced the larval growth rate of tea geometrid. Consistent with previous results in rice and tomato plants, the exogenous treatment of GA promoted the total flavonoids content (Singh et al., 2017; Farghaly et al., 2021). Our study provided further evidence on which flavonoids were regulated by GA. Thus, the induction of naringenin, astragalin, EGCG, and caffeine might be the reason for the larval growth reduction in GA-treated plants. Although the increment of caffeine and flavonoids in GA-treated plants may attribute to the enhanced resistance of tea plants, other metabolites may also function as defense compounds against tea geometrid, and the underlying mechanisms still need deeper investigation in the future.

CONCLUSION

The exogenous application of GA induced the direct defense of tea plants against tea geometrid larvae, through activating the JA signaling and phenylpropanoid pathways. Astragalin, naringenin, and EGCG were the three most active anti-feeding compounds, whose accumulation was enhanced by the exogenous application of GA in tea plants. However, the exogenous GA treatment did not affect the preference of *E. obliqua* female moths and larval parasitoid *Apanteles* sp. Our study suggests that GA may serve as an elicitor that triggers the direct defense response of tea plants against tea geometrid larvae.

DATA AVAILABILITY STATEMENT

The raw data supporting the conclusions of this article will be made available by the authors, without undue reservation.

AUTHOR CONTRIBUTIONS

XZ, WR, and XS: conceptualization. XZ, SL, and ML: experiments and data analysis. XZ and XL: materials. XZ: writing – original draft preparation. JZ, MY, and XS: writing – review and suggestion. All authors read and agreed to the published version of the manuscript.

FUNDING

This research was funded by the Zhejiang Provincial Natural Science Foundation of China (LQ20C140006), National Natural Science Foundation of China (31972280), and Central Public-interest Scientific Institution Basal Research Fund (1610212019001).

SUPPLEMENTARY MATERIAL

The Supplementary Material for this article can be found online at: https://www.frontiersin.org/articles/10.3389/fpls.2022.833489/full#supplementary-material

REFERENCES

Ashihara, H., Sano, H., and Crozier, A. (2008). Caffeine and related purine alkaloids: biosynthesis, catabolism, function and genetic engineering. *Phytochemistry* 69, 841–856. doi: 10.1016/j.phytochem.2007.10.029

Browse, J. (2009). Jasmonate passes muster: a receptor and targets for the defense hormone. *Annu. Rev. Plant. Biol.* 60, 183–205. doi: 10.1146/annurev.arplant.043008.092007

Chen, M. S. (2008). Inducible direct plant defense against insect herbivores: a review. *Insect. Sci.* 15, 101–114. doi: 10.1111/j.1744-7917.2008.00190.x

Chen, S. L., Zhang, L. P., Cai, X. M., Li, X., Bian, L., Luo, Z. X., et al. (2020). (E)-Nerolidol is a volatile signal that induces defenses against insects and pathogens in tea plants. *Hortic. Res.* 7:52. doi: 10.1038/s41438-020-0275-7

Farghaly, F. A., Salam, H. K., Hamada, A. M., and Radi, A. A. (2021). The role of benzoic acid, gallic acid and salicylic acid in protecting tomato callus cells from excessive boron stress. *Sci. Hortic.* 278:109867. doi: 10.1016/j.scienta.2020.109867

Gols, R. (2014). Direct and indirect chemical defences against insects in a multitrophic framework. *Plant Cell Environ.* 37, 1741–1752. doi: 10.1111/pce.12318

Goupil, P., Benouaret, R., and Richard, C. (2017). Ethyl gallate displays elicitor activities in tobacco plants. *J. Agric. Food Chem.* 65, 9006–9012. doi: 10.1021/acs.jafc.7b03051

Goupil, P., Peghaire, E., Benouaret, R., Richard, C., Sleiman, M., and Alaoui, H. (2020). Relationships between plant defense inducer activities and molecular structure of gallomolecules. *J. Agric. Food Chem.* 68, 15409–15417. doi: 10.1021/acs.jafc.0c05719

Gozzo, F., and Faoro, F. (2013). Systemic acquired resistance (50 years after discovery): moving from the lab to the field. *J. Agric. Food Chem.* 61, 12473–12491. doi: 10.1021/jf404156x

Hewavitharanage, P., Karunaratne, S., and Kumar, N. S. (1999). Effect of caffeine on shot-hole borer beetle (*Xyleborus fornicatus*) of tea (*Camellia sinensis*). *Phytochemistry* 51, 35–41. doi: 10.1016/S0031-9422(98)00610-4

Howe, G. A., and Jander, G. (2008). Plant immunity to insect herbivores. *Annu. Rev. Plant Biol.* 59, 41–66. doi: 10.1146/annurev.arplant.59.032607.092825

International Organization for Standardization [ISO] (2005). *Determination of Substances Characteristic of Green and Black Tea. Part 1: Content of Total Polyphenols in Tea. Colorimetric Method Using Folin-Ciocalteu Reagent*. Geneva: International Organization for Standardization.

Jiang, C. K., Ma, J. Q., Apostolides, Z., and Chen, L. (2019). Metabolomics for a millenniums-old crop: tea plant (*Camellia sinensis*). *J. Agric. Food Chem.* 67, 6445–6457. doi: 10.1021/acs.jafc.9b01356

Kamatham, S., Neela, K. B., Pasupulati, A. K., Pallu, R., Singh, S. S., and Gudipalli, P. (2016). Benzoylsalicylic acid isolated from seed coats of *Givotia rottleriformis* induces systemic acquired resistance in tobacco and Arabidopsis. *Phytochemistry* 126, 11–22. doi: 10.1016/j.phytochem.2016.03.002

Li, H., Yu, Y., Li, Z., Arkorful, E., Yang, Y., Liu, X., et al. (2018). Benzothiadiazole and b-aminobutyricacid induce resistance to Ectropis obliqua in tea plants (*Camellia sinensis* (L.) *O. Kuntz*). *Molecules* 23:1290. doi: 10.3390/molecules23061290

Li, X. W., Zhang, J., Lin, S. B., Xing, Y. X., Zhang, X., Ye, M., et al. (2021). (+)-catechin, epicatechin and epigallocatechin gallate are important inducible defensive compounds against *ectropis grisescens* in tea plants. *Plant Cell Environ.* [Epub online ahead of print] doi: 10.1111/pce.14216

Lin, S. B., Dong, Y. N., Li, X. W., Xing, Y. X., Liu, M. M., and Sun, X. L. (2020). JA-Ile-macrolactone 5b induces tea plant (*Camellia sinensis*) resistance to both herbivore *Ectropis obliqua* and pathogen *Colletotrichum camelliae*. *Int. J. Mol. Sci.* 21:1828. doi: 10.3390/ijms21051828

Lin, S. B., Ye, M., Li, X. W., Xing, Y. X., Liu, M. M., and Zhang, J. (2022). A novel inhibitor of the JA signaling pathway represses herbivore resistance in tea plants. *Hortic. Res.* uhab038. doi: 10.1093/hr/uhab038

Lou, Y. G., Hu, L. F., and Li, J. C. (2015). *Herbivore-Induced Defenses in Rice and Their Potential Application in Rice Planthopper Management*. Netherlands: Springer Press.

Mazid, M., Khan, T., and Mohammad, F. (2011). Role of secondary metabolites in defense mechanisms of plants. *Biol. Med.* 3, 232–249.

Miller, T. A., Highfill, J. W., and Cooper, W. J. (1982). Relationships between pupal size and sex in giant silkworm moths (Saturniidae). *J. Lepid Soc*. 36, 207–216.

Moreira, X., Zas, R., and Sampedro, L. (2012). "Methyl jasmonate as chemical elicitor of induced responses and anti-herbivory resistance in young conifer trees," in *Plant Defence: Biological Control*, eds M. J. Mérillon and M. K. Ramawat (Netherlands: Springer Press), 345–362. doi: 10.1007/978-94-007-1933-0_15

Oh, Y., Baldwin, I. T., and Galis, I. (2012). NaJAZh regulates a subset of defense responses against herbivores and spontaneous leaf necrosis in *Nicotiana attenuata* plants. *Plant Physiol.* 159, 769–788. doi: 10.1104/pp.112.193771

Ozfidan-Konakci, C., Yildiztugay, E., Yildiztugay, A., and Kucukoduk, M. (2019). Cold stress in soybean (*Glycine max* L.) roots: exogenous gallic acid promotes water status and increases antioxidant activities. *Bot. Serb.* 43, 59–71. doi: 10.2298/BOTSERB1901059O

Qiu, D. W., Dong, Y. J., Zhang, Y., Li, S. P., and Shi, F. C. (2017). Plant immunity inducer development and application. *Mol. Plant Microbe Interact.* 30, 355–360. doi: 10.1094/MPMI-11-16-0231-CR

Ran, W., Zhang, J., Zhang, X., Lin, S. B., and Sun, X. L. (2018). Infestation of *Ectropis obliqua* affects the catechin metabolism in tea plants. *J. Tea Sci.* 38, 24–30.

Schuman, M. C., and Baldwin, I. T. (2016). The layers of plant responses to insect herbivores. *Ann. Rev. Entomol.* 61, 373–394. doi: 10.1146/annurev-ento-010715-023851

Singh, A., Gupta, R., and Pandey, R. (2017). Exogenous application of rutin and gallic acid regulate antioxidants and alleviate reactive oxygen generation in *Oryza sativa L. Physiol. Mol. Biol. Plants.* 23, 301–309. doi: 10.1007/s12298-017-0430-2

Staswick, P. E. (2008). JAZing up jasmonate signaling. *Trends Plant Sci.* 13, 66–71. doi: 10.1016/j.tplants.2007.11.011

Stec, K., Kozlowska, J., Wroblewska-Kurdyk, A., Kordan, B., Aniol, M., and Gabrys, B. (2020). Effect of naringenin and its derivatives on the probing behavior of *Myzus persicae* (Sulz.). *Molecules* 25:3185. doi: 10.3390/molecules25143185

Treutter, D. (2006). Significance of flavonoids in plant resistance: a review. *Extreme. Mech. Lett.* 4, 147–157. doi: 10.1007/s10311-006-0068-8

Wang, D., Li, C. F., Ma, C. L., and Chen, L. (2015). Novel insights into the molecular mechanisms underlying the resistance of *Camellia sinensis* to *Ectropis oblique* provided by strategic transcriptomic comparisons. *Sci. Hortic.* 192, 429–440. doi: 10.1016/j.scienta.2015.06.005

Wang, W. W., Zhou, P. Y., Mo, X. C., Hu, L. F., Jin, N., Chen, X., et al. (2020). Induction of defense in cereals by 4-fluorophenoxyacetic acid suppresses insect pest populations and increases crop yields in the field. *Proc. Natl. Acad. Sci. U.S.A.* 117, 12017–12028. doi: 10.1073/pnas.2003742117

Wang, Y. N., Tang, L., Hou, Y., Wang, P., Yang, H., and Wei, C. L. (2016). Differential transcriptome analysis of leaves of tea plant (*Camellia sinensis*) provides comprehensive insights into the defense responses to *Ectropis oblique* attack using RNA-Seq. *Funct. Integr. Genom.* 16, 383–398. doi: 10.1007/s10142-016-0491-2

War, A. R., Paulraj, M. G., Ahmad, T., Buhroo, A. A., Hussain, B., Ignacimuthu, S., et al. (2012). Mechanisms of plant defense against insect herbivores. *Plant Signal. Behav.* 7, 1306–1320. doi: 10.4161/psb.21663

Wu, J. Q., and Baldwin, I. T. (2010). New insights into plant responses to the attack from insect herbivores. *Ann. Rev. Genet.* 44, 1–24. doi: 10.1146/annurev-genet-102209-163500

Xin, Z. J., Cai, X. M., Chen, S. L., Luo, Z. X., Bian, L., Li, Z. Q., et al. (2019). A disease resistance elicitor laminarin enhances tea defense against a piercing herbivore *Empoasca* (*Matsumurasca*) *onukii* Matsuda. *Sci. Rep.* 9:814. doi: 10.1038/s41598-018-37424-7

Xin, Z. J., Li, X. W., Li, J. C., Chen, Z. M., and Sun, X. L. (2016). Application of chemical elicitor (Z)-3-hexenol enhances direct and indirect plant defenses against tea geometrid *Ectropis obliqua*. *Biocontrology* 61, 1–12. doi: 10.1007/s10526-015-9692-1

Xin, Z. J., Zhang, J., Ge, L. G., Lei, S., Han, J. J., Zhang, X., et al. (2017). A putative 12-oxophytodienoate reductase gene *CsOPR3* from *Camellia sinensis*, is involved in wound and herbivore infestation responses. *Gene* 615, 18–24. doi: 10.1016/j.gene.2017.03.013

Yang, Z. W., Duan, X. N., Jin, S., Li, X. W., Chen, Z. M., Ren, B. Z., et al. (2013). Regurgitant derived from the tea geometrid *Ectropis obliqua* suppresses wound-induced polyphenol oxidases activity in tea plants. *J. Chem. Ecol.* 39, 744–751. doi: 10.1007/s10886-013-0296-x

Yetissin, F., and Kurt, F. (2020). Gallic acid (GA) alleviating copper (Cu) toxicity in maize (*Zea mays L.*) seedlings. *Int. J. Phytoremediation* 22, 420–426. doi: 10.1080/15226514.2019.1667953

Zeng, L. T., Zhou, X. C., Liao, Y. Y., and Yang, Z. Y. (2020). Roles of specialized metabolites in biological function and environmental adaptability of tea plant (*Camellia sinensis*) as a metabolite studying model. *J. Adv. Res.* 34, 159–171. doi: 10.1016/j.jare.2020.11.004

Zhang, J., Zhang, X., Ye, M., Li, X. W., Lin, S. B., and Sun, X. L. (2020). The jasmonic acid pathway positively regulates the polyphenol oxidase-based defense against tea geometrid caterpillars in the tea plant (*Camellia sinensis*). *J. Chem. Ecol.* 46, 308–316. doi: 10.1007/s10886-020-01158-6

Zhang, X., Ran, W., Zhang, J., Ye, M., Lin, S. B., Li, X. W., et al. (2020). Genome-wide identification of the tify gene family and their expression profiles in response to biotic and abiotic stresses in tea plants (*Camellia sinensis*). *Int. J. Mol. Sci.* 21:8316. doi: 10.3390/ijms21218316

Zhou, P. Y., Mo, X. C., Wang, W. W., Chen, X., and Lou, Y. G. (2018). The commonly used bactericide bismerthiazol promotes rice defenses against herbivores. *Int. J. Mol. Sci.* 19:1271. doi: 10.3390/ijms19051271

Zhou, X. C., Zeng, L. T., Chen, Y. J., Wang, X. W., Liao, Y. Y., Xiao, Y. Y., et al. (2020). Metabolism of gallic acid and its distributions in tea (*Camellia sinensis*) plants at the tissue and subcellular levels. *Int. J. Mol. Sci.* 21:5684. doi: 10.3390/ijms21165684

Conflict of Interest: The authors declare that the research was conducted in the absence of any commercial or financial relationships that could be construed as a potential conflict of interest.

Publisher's Note: All claims expressed in this article are solely those of the authors and do not necessarily represent those of their affiliated organizations, or those of the publisher, the editors and the reviewers. Any product that may be evaluated in this article, or claim that may be made by its manufacturer, is not guaranteed or endorsed by the publisher.

frontiers | Frontiers in Plant Science

ORIGINAL RESEARCH
published: 15 April 2022
doi: 10.3389/fpls.2022.894840

Carbon and Nitrogen Metabolism Are Jointly Regulated During Shading in Roots and Leaves of *Camellia Sinensis*

Chenyu Shao[1,2,3†], *Haizhen Jiao*[1,2,3†], *Jiahao Chen*[1,2,3†], *Chenyu Zhang*[1,2,3,4], *Jie Liu*[1,2,3], *Jianjiao Chen*[1,2,3], *Yunfei Li*[1,2,3], *Jing Huang*[1,2,3], *Biao Yang*[1,2,3], *Zhonghua Liu*[1,2,3*] and *Chengwen Shen*[1,2,3*]

[1] Key Laboratory of Tea Science of Ministry of Education, Hunan Agricultural University, Changsha, China, [2] National Research Center of Engineering and Technology for Utilization of Botanical Functional Ingredients, Hunan Agricultural University, Changsha, China, [3] Co-innovation Center of Education Ministry for Utilization of Botanical Functional Ingredients, Hunan Agricultural University, Changsha, China, [4] Tea Research Institution, Chinese Academy of Agricultural Sciences, Hangzhou, China

Numerous studies have shown that plant shading can promote the quality of green tea. However, the association of shading with metabolic regulation in tea leaves and roots remains unelucidated. Here, the metabolic profiling of two tea cultivars ("Xiangfeicui" and "Jinxuan") in response to shading and relighting periods during the summer season was performed using non-targeted metabolomics methods. The metabolic pathway analyses revealed that long-term shading remarkably inhibit the sugar metabolism such as glycolysis, galactose metabolism, and pentose phosphate pathway in the leaves and roots of "Xiangfeicui," and "Jinxuan" were more sensitive to light recovery changes. The lipid metabolism in the leaves and roots of "Xiangfeicui" was promoted by short-term shading, while it was inhibited by long-term shading. In addition, the intensity of the flavonoid metabolites in the leaves and roots of "Jinxuan" were upregulated with a trend of rising first and then decreasing under shading, and five flavonoid synthesis genes showed the same trend (F3H, F3′5′H, DFR, ANS, and ANR). Simultaneously, the amino acids of the nitrogen metabolism in the leaves and roots of the two cultivars were significantly promoted by long-term shading, while the purine and caffeine metabolism was inhibited in the leaves of "Xiangfeicui." Interestingly, CsGS1.1 and CsTSI, amino acid synthase genes was upregulated in the leaves and roots of two cultivars. These results indicated that shading could participate in carbon and nitrogen metabolic regulation of both leaf and root, and root metabolism could have a positive association with leaf metabolism to promote the shaded tea quality.

Keywords: ***Camellia sinensis*, leaves, roots, shading, metabolism, carbon, nitrogen**

OPEN ACCESS

Edited by:
Vagner A. Benedito,
West Virginia University, United States

Reviewed by:
Xinghui Li,
Nanjing Agricultural University, China
Muhammad Saeed,
Northwest A&F University, China

***Correspondence:**
Chengwen Shen
scw69@163.com
Zhonghua Liu
larkin-liu@163.com

† *These authors contributed equally to this work*

Specialty section:
This article was submitted to Plant Metabolism and Chemodiversity, a section of the journal Frontiers in Plant Science

Received: *12 March 2022*
Accepted: *25 March 2022*
Published: *15 April 2022*

Citation:
Shao C, Jiao H, Chen J, Zhang C, Liu J, Chen J, Li Y, Huang J, Yang B, Liu Z and Shen C (2022) Carbon and Nitrogen Metabolism Are Jointly Regulated During Shading in Roots and Leaves of Camellia Sinensis. Front. Plant Sci. 13:894840. doi: 10.3389/fpls.2022.894840

INTRODUCTION

Green tea, a type of unfermented tea rich in secondary metabolites, is valued for its "umami" flavor and sweet taste and is known for its antibacterial, anti-obesity, antioxidant, and anticancer activity (Prasanth et al., 2019). The annual tea sales exceed $43 billion globally, more than $11 billion of which is accounted for by green tea (Hu et al., 2018). High-quality green tea is primarily dependent on the contents of the initial metabolite, which differs markedly among cultivars and is strongly influenced by external environmental factors (Pongsuwan et al., 2008; Tang et al., 2021). Secondary metabolites including amino acids, flavonoids, lipids, and terpenoids vary significantly in fresh leaves of different tea cultivars (Maritim et al., 2021). In the same cultivar, the quality and value of tea vary considerably with the harvest season (Dai et al., 2015). Due to the distinct variations in the day length, rainfall, sunlight, and/or temperature between spring, summer and autumn, the chemical composition of tea is dramatically different in different seasons (Nowogrodzki, 2019; Wang et al., 2021). The polyphenol/amino acid ratio is inversely correlated with green tea quality, where a lower ratio makes tea more brisk but less bitter (Guo et al., 2021). Therefore, as summer and autumn tea, which are harvested in warm months (between June and October), possess a high ratio, comparatively few fresh leaves are collected because of the resultant bitterness (Zhang Q. et al., 2020). Therefore, it is necessary to develop strategies for improving the quality of summer and autumn tea.

High light intensity and temperature are essential ecological factors that accelerate flavonoid biosynthesis, tricarboxylic acid (TCA) cycle, and photorespiration in summer tea (Liu et al., 2016). Shading treatment is an effective measure for controlling the amount of sunlight to modify major quality-related metabolites in tea leaves and improve tea flavor (Ku et al., 2010; Ji et al., 2018; Li et al., 2020). In this traditional cultivation method, tea plants are covered with shading nets when new shoots emerge until they are harvested after 14 and 30 days (Sano et al., 2018). During this shading period, the contents of chlorophylls and free amino acids such as theanine are increased, and that of catechins is decreased (Ji et al., 2018). Certain studies have showed that most enzymes controlling amino acid biosynthesis are downregulated in response to shading and the proteolysis of chloroplast proteins results in the accumulation of free amino acids (Chen et al., 2017). Shading improves tea quality by inhibiting the expression of genes regulating flavonoid biosynthesis such as *PAL*, *4CL*, and *CHS* (Liu et al., 2018). Shading also influences metabolism in tea roots. Alterations in exogenous nitrogen modulated the genes encoding amino acid biosynthesis in the roots including CsGDH, CsAlaDC, CsAspAT, and others (Yang et al., 2020). However, few studies have investigated the metabolic changes in shaded leaves and roots. Shading may negatively impact tea yield as it forces the plants to grow under low light for extended periods. Recurring artificial shading affects leaf photosynthesis and stomatal transpiration (Yamashita et al., 2020). The sudden onset of intense light after prolonged shading may induce oxidative stress in tea plants (Sano et al., 2020). Hence, the optimal time to pick fresh high-quality tea leaves under shading has not yet been established.

Metabolomic analysis, widely used on tea plants, is a technology used extensively for the comprehensive profiling and comparison of metabolites. Metabolomic approaches including ^{1}H NMR, gas chromatography-mass spectrometry (GC-MS), and ultra-performance liquid chromatography combined with time of flight mass spectrometry (UPLC-TOF-MS/MS) have been widely used to explore metabolite accumulation in tea plants (Zhang et al., 2014; Ji et al., 2018; Li et al., 2020). However, the changes in metabolites relating to the carbon and nitrogen metabolism in the leaves and roots of different tea cultivars over different shading periods are unclear. Therefore, in the present study, "Xiangfeicui" and "Jinxuan" were selected for shading (0, 4, and 12 days) and light recovery (4 days). UHPLC-Q-TOF-MS/MS was used to explore the dynamic changes that occur in shaded tea leaves and roots. The aim of this study is not only to provide a framework for better understanding the regulation of leaf and root metabolites in tea cultivars under different shading conditions, but also propose strategies for shade adaptability of different tea cultivars to effectively improve the quality of green tea in the summer and autumn.

MATERIALS AND METHODS

Plant Materials and Experimental Design

The tea plant [*Camellia sinensis* (L.) O. Kuntze cv. "Xiangfeicui" (XFC) and "Jinxuan" (JX)] were cultivated at the experimental tea farm of the Hunan Tea Research Institute in Changsha, China (113.21°E, 28.28°N). They grew for 12 days under 95% shade created by covering the plants with black high-density polyethylene netting, and the net was removed to allow light recovery for 4 days. In 2020, one bud and two leaves were plucked on August 10, 14, 22, and 26, respectively. Light intensity, air temperature and relative humidity, and soil temperature and humidity were measured at 14:00 daily. The samples were washed with ultrapure water and divided into three parts. The first lot comprised fresh leaves used to measure chlorophyll and carotenoid content. The second lot consisted of leaves that were quickly fixed with liquid nitrogen and stored in a −80°C refrigerator for evaluating biochemical composition. The third lot was processed into green tea.

A pot experiment was conducted on the same shading treatment. Each pot contained three healthy 1-year tea plants and 4.5 kg yellow-red soil, and there were six pots per treatment. The dimensions of each pot were top outer diameter: 26.5 cm, top inner diameter: 23 cm, base diameter: 18 cm, and height: 25 cm. There were four drainage holes in the base, and trays were placed under the pots. New shoots could be used for shading when they reached the one terminal bud/two young leaf stage. In 2020, one bud and two leaves and the white absorption roots (**Supplementary Figure 1**) were collected on September 1, 5, 13, and 17, respectively. The main root lengths and numbers of lateral roots were measured at four sampling points. The samples were washed with ultrapure water and divided into two parts. The first was quickly fixed with liquid

nitrogen and stored in a −80°C refrigerator until metabolic analyses (six biological replicates). The second was examined under transmission electron microscopy (fresh leaves).

Sensory Evaluation

Green tea was processed by one professional tea processor (**Supplementary Figure 2**). Fresh tea samples were first fixed in an electric frying pot (6CST-70; Xiangfeng Machinery Ltd., Changsha, China) maintained at 320°C using an infrared thermometer (TASI-8601; Suzhou TASI Electronics Ltd., Suzhou, China). After 2 min, they were removed and set on a bamboo plate to cool for 10 min and mechanically rolled for 10 min with a rolling machine (6CD-280; Xiangfeng Machinery Ltd., Changsha, China). The leaves were dried at 220°C in the pot until their moisture content was ∼50% and mechanically rolled for 10 min. The leaves were dried in the pot again at 120°C until their moisture content was ∼20%. The leaves were then machine-dried at 80°C in a tea dryer (6CHBZ-20; Xiangfeng Machinery Ltd., Changsha, China) until their moisture content was ∼5%.

Sensory evaluation was scored independently by 5 professional tea tasters on a 100-point scale, with the appearance of dry tea accounting for 25%, brew color for 10%, aroma for 25%, taste for 30%, and infused leaf for 10% of the scale. All members of the tea assessment group are professional teachers from Hunan Agricultural University. Dry tea (3 g) was brewed with boiling water (150 mL) for 4 min. After brewing, brew color, aroma, taste, and infused leaves were evaluated (**Supplementary Figure 3**). Scoring rules (**Supplementary Table 1**) were established according to the National Standard of China (GB/T23776-2018) (Zhou et al., 2020).

Catechin, Caffeine, and Theanine Content

Catechin, caffeine, and theanine contents were determined using a high-performance liquid chromatography (HPLC) system (Waters 590; Waters Corp., Milford, MA) equipped with a Hypersil ODS 2 C18 column (5 mL, 4.6 × 250 mm, 35 μm) at 280 nm, by referring to the national standards (GB/T 8313–2018, GB/T 8314–2013). Solvents A (2% acetic acid) and B (acetonitrile) were run in a linear gradient from 93 to 55% for 20 min, after which the flow rate was maintained at 1.4 mL/min for 5 min. They were quantitatively determined by comparing the peak areas of samples with a known standard (Sigma-Aldrich, USA). The amino acid content was determined following the methods described previously (Li Z. X. et al., 2016). The amino acid composition was measured by HPLC using an AccQ Tag column (3.9 × 150 mm) (Waters 600; Waters Corp., Milford, MA, USA) and a fluorescence detector, after derivatization with AccQ Fluor Reagent Kit following the manufacturer's protocol.

Photosynthetic Pigments and Biochemical Components

A digital lux meter (TES 1332; Olympus Imaging 95 Corp., Tokyo, Japan) measured light intensity. A SPAD chlorophyll meter (Konica Minolta Inc., Osaka, Japan) measured leaf SPAD indicating the relative chlorophyll content. The ethanol method was used to determine chlorophyll A and B and carotenoid content in fresh leaves (Zhang C. et al., 2020). State Standards of China Nos. GB/T8313-2008 and GB/T8314-2013 were used to analyze tea leaf polyphenolic and free amino acid content. The foregoing measurements were made within 1 week after sampling.

Transmission Electron Microscopy Analysis (TEM)

Samples were prepared for TEM as follows (Li N. et al., 2016). Briefly, fresh leaves were sliced into 1-mm^2 sections, fixed with 2.5% (v/v) glutaraldehyde at 20°C for 2 h, and rinsed thrice with phosphate-buffered solution (pH 7.4) for 15 min each time. The leaf cells were post-fixed with 1% (v/v) OsO_4 at 20°C for 5 h and dehydrated in an ethanol concentration gradient series [30, 50, 70, 80, 90, 95, and 100% (v/v) for 1 h at each concentration]. The samples were then embedded in 100% Epon-812 and polymerized in an oven at 60°C for 48 h. The embedded samples were cut into ultrathin sections (60–80 nm) with an ultramicrotome (EM UC7; Leica Microsystems Inc., Mannheim, Germany) and stained with uranyl acetate and lead citrate for 30 min. Images were acquired and analyses were made using TEM (HT7700; Hitachi Ltd., Tokyo, Japan).

UHPLC-Q-TOF MS for Metabolomics

Extraction Procedure

Tea samples (80 mg) were quickly frozen in liquid nitrogen and pulverized with a mortar and pestle. One thousand microliters methanol/acetonitrile/H_2O (2:2:1, v/v/v) mixture were added for metabolite extraction. The mixture was centrifuged at 14,000 × g and 4°C for 15 min, and the supernatant was dried in a vacuum centrifuge. For the LC-MS analysis, the samples were re-dissolved in 100 μL acetonitrile/water (1:1, v/v).

LC-MS/MS Analysis

The analyses were performed in the UHPLC (1290 Infinity LC; Agilent Technologies, Santa Clara, CA, USA) coupled to a quadrupole time-of-flight (AB Sciex TripleTOF 6600; AB Sciex, Framingham, MA, USA) at Shanghai Applied Protein Technology Co. Ltd., Shanghai, China.

For hydrophilic interaction liquid chromatography separation, the samples were analyzed with a 2.1 × 100 mm ACQUITY UPLC BEH 1.7 μm column (Waters Corp., Dublin, Ireland). In ESI positive and ESI negative modes, mobile phase A consisted of 25 mM ammonium acetate and 25 mM ammonium hydroxide in water while mobile phase B consisted of acetonitrile. The gradient was 85% B for 1 min, linear reduction to 65% over 11 min, reduction to 40% in 0.1 min, holding for 4 min, and increasing to 85% in 0.1 min. There was a 5-min re-equilibration period.

For reverse-phase liquid chromatography separation, a 2.1 × 100 mm ACQUITY UPLC HSS T3 1.8 μm column (Waters Corp., Dublin, Ireland) was used. In ESI positive mode, mobile phase A was water plus 0.1% (v/v) formic acid while mobile phase B was acetonitrile plus 0.1% (v/v) formic acid. In ESI negative mode, mobile phase A was 0.5 mM ammonium fluoride in water while mobile phase B was acetonitrile. The gradient was 1% B for 1.5 min, linear increase to 99% over 11.5 min, holding for

3.5 min, and reduction to 1% in 0.1 min. There was a 3.4-min re-equilibration period. The flow rate was 0.3 mL/min, the column temperature was maintained at 25°C, and the aliquot injection volume was 2 μL.

The ESI source conditions were as follows: Ion Source Gas1 (Gas1), 60; Ion Source Gas2 (Gas2), 60; curtain gas (Vinocur and Altman, 2005), 30; source temperature, 600°C; and IonSpray Voltage Floating, ±5,500 V. In MS-only acquisition, the instrument was set to acquire over the m/z range 60–1,000 Da and the TOF MS scan accumulation time was set to 0.20 s/spectrum. In auto-MS/MS acquisition, the instrument was set to acquire over the m/z range 25–1,000 Da and the product ion scan accumulation time was set to 0.05 s/spectrum. The product ion scan was performed using information-dependent acquisition in high-sensitivity mode. The parameters were as follows: collision energy, 35 ± 15 eV; declustering potential, 60 V (+) and −60 V (–); exclusion of isotopes within 4 Da; and 10 candidate ions to monitor per cycle.

Data Processing and Analysis

Raw MS data (wiff.scan files) were converted to MzXML files with Proteo Wizard MS Convert before being imported into XCMS software. Peaks were selected using the following parameters: centWave m/z = 25 ppm; peakwidth = c (10, 60); and prefilter = c (10, 100). Peaks were grouped using the following parameters: bw = 5; mzwid = 0.025; and minfrac = 0.5. Collection of Algorithms of MEtabolite pRofile Annotation (CAMERA) was used to annotate isotopes and adducts. For the extracted ions, only variables with >50% non-zero measurements values in ≥1 group were conserved. Metabolites were identified by comparing m/z accuracy (<25 ppm) and using MS/MS spectra with an in-house database built using available authentic standards.

After normalization to total peak intensity, the processed data were analyzed in the R package ropls (R Core Team, Vienna, Austria) and subjected to multivariate Pareto-scaled principal component analysis (PCA) and orthogonal partial least-squares discriminant analysis (OPLS-DA). Seven-fold cross-validation and response permutation tests were run to evaluate model robustness. The variable importance in the projection (VIP) value of each variable in the OPLS-DA model was calculated to evaluate its contribution to the classification. Metabolites with VIP >1 were subjected to a univariate-level Student's *t*-test to establish the significance of each metabolite.

Quantitative Real-Time Polymerase Chain Reaction

Total RNA was extracted from the leaves and roots with the RNA extraction kit (Tiangen, Beijing, China), and complementary DNA (cDNA) was synthesized with a PrimeScript^{TM} RT Reagent kit (Takara, Dalian, China). **Supplementary Table 2** lists the primer pairs used for qRT-PCR; glyceraldehyde 3-phosphate dehydrogenase (GAPDH, GenBank accession No. GE651107) was the reference gene. The thermal cycling protocol followed the manufacturer's instructions. Three independent biological replicates of each reaction were conducted, and the relative transcript levels of target genes were calculated against those of GAPDH by the $2^{-\Delta\Delta CT}$ method.

Statistical Analyses

Least significant difference (LSD), Duncan's multiple range, and Student's *t*-tests were performed in SPSS v. 25.0 (SPSS Inc., Chicago, IL, USA) to evaluate differences among treatment means. $P < 0.05$ was considered statistically significant. All data are presented as mean ± standard deviation (SD) based on three independent biological replicates. Figures were plotted in GraphPad Prism v. 8.0.1 (GraphPad Software, La Jolla, CA, USA) and TBtool (Chen et al., 2020a).

RESULTS

Changes in Light Intensity, Temperature, and Humidity

As shown in **Figure 1A**, the light radiation levels at canopy level for the unshaded controls and shaded plants were 13,040–92,530 lx and 650–5,870 lx, respectively. Thus, 95.12% of solar irradiation was blocked by shading. The average canopy air temperature and soil temperature under shading were 2.82 and 5.19°C lower than that in the control conditions, respectively. The average canopy air humidity and soil humidity under shading were 9.14 and 12.77% higher than that in the control conditions, respectively (**Figure 1C**). These indicate that shading significantly improves the growth environment of tea plants in summer and autumn.

Changes in Photosynthetic Pigments and Ultrastructures

As shown in **Figure 1D**, the chlorophyll A and B levels were higher in JX leaves (JXL) than in XFC leaves (XFL). For both cultivars, the leaf chlorophyll A and B contents significantly increased under shading ($p < 0.05$). The total chlorophyll content and the chlorophyll A/B ratios increased with shading duration ($p < 0.05$). In both XFL and JXL, the carotenoid content did not changed but reached its maximum by the 12th day of shading ($p < 0.05$). After 4 days of light recovery, the chlorophyll A and B and total chlorophyll content decreased in both tea varieties ($p < 0.05$). These indicate that shading significantly enhances the degree of green in tea leaves.

In pot experiment (**Figure 2A**), XFC and JX did not differ markedly in terms of their main root lengths (**Figure 2E**). However, the numbers of lateral roots in JX had significantly increased during shading ($p < 0.05$). In addition, we measured the SPAD value in XFL and JXL, and the trend was consistent with previous chlorophyll contents (**Figure 2D**). TEM was used to assess the effects of shading on leaf chloroplast ultrastructure (**Figures 2B,C**). Starch granules (SG), osmiophilic granules (OG), thylakoids (Th), and tightly stacked grana (Gr) were observed in both XFC and JX leaf chloroplasts. Grana stacking and thylakoids were enriched in both XFL and JXL during shading. The volume of chloroplasts increased remarkably, and the structure became more compact. These findings were consistent with the measured changes in chlorophyll content. However, the number of SG decreased after 4 days of shading and OG quantity and volume declined with shading duration.

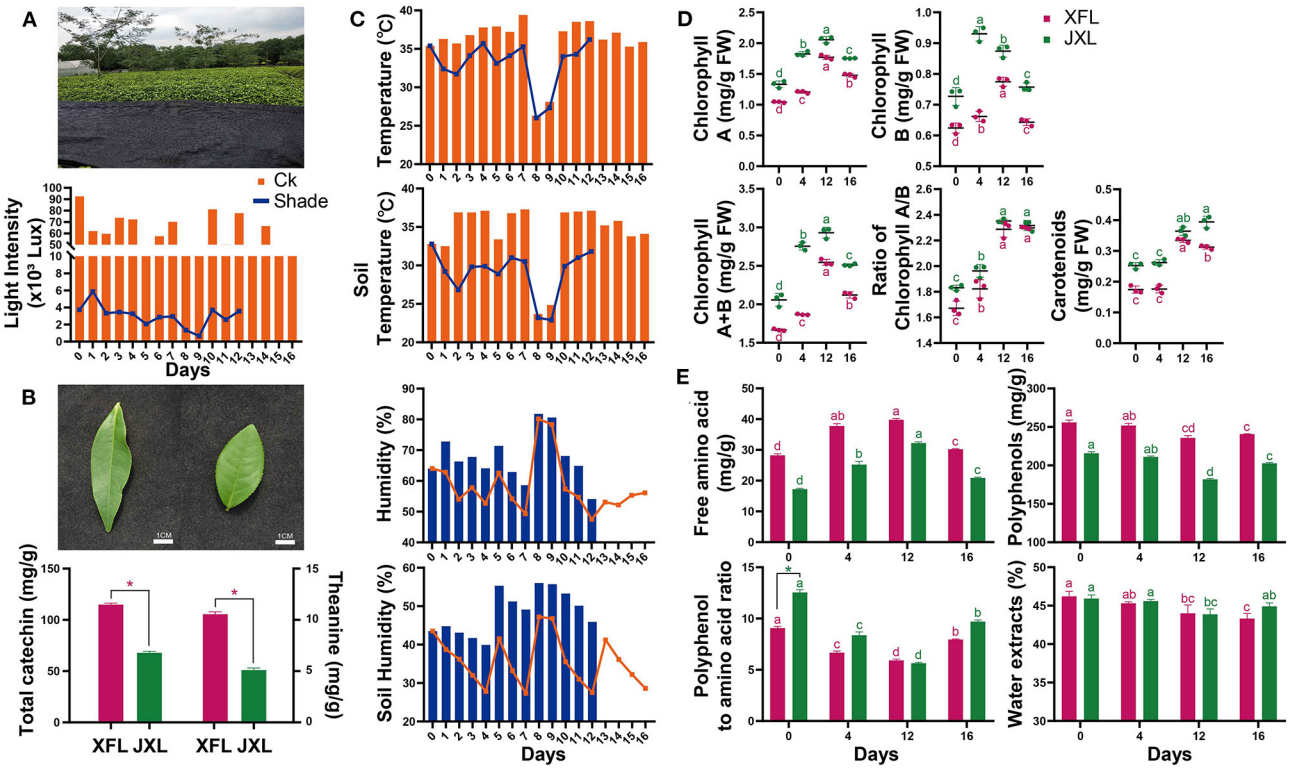

FIGURE 1 | Shading photograph, light intensity **(A)**, leaf shape, the total catechin and theanine content of two tea cultivars **(B)**, air temperature and humidity, and soil temperature and humidity **(C)** were measured of tea plants. The contents of chlorophyll A, chlorophyll B, chlorophyll A/B, total chlorophyll, carotenoids **(D)** and free amino acids, tea polyphenols, polyphenol:amino acid ratio, and water extract **(E)** in the leaves of "Xiangfeicui" and "Jinxuan" (mean ± SD, three biological replicates per treatment groups) under shading treatments. Data were assessed by one-way ANOVA followed by Duncan's multiple range test. *$p < 0.05$. Ck, control check; Shade, shading treatment; XFL, leaf of "Xiangfeicui" cultivar; JXL, leaf of "Jinxuan" cultivar. Different letters in same color represent $p < 0.05$.

Changes in Polyphenols, Amino Acids, and Sensory Quality

As shown in **Figure 1B**, the total catechin and theanine contents in XFL were 1.69 and 2.07 times higher than in JXL ($p < 0.05$). At the same time, the polyphenol/amino acid ratios of XFL and JXL were 9.07 ± 0.18 and 12.54 ± 0.26 in the 0th day of shading, respectively (**Figure 1E**). The free amino acid content significantly increased while the polyphenol content significantly decreased after 12-day shading ($p < 0.05$). In both varieties, the polyphenol/amino acid ratios significantly decreased during shading ($p < 0.05$), and the lowest ratios of XFL and JXL were 5.92 ± 0.12 and 5.64 ± 0.09, respectively. After light recovery, the polyphenol, free amino acid content, and the polyphenol/amino acid ratio significantly increased to control levels ($p < 0.05$). The polyphenol/amino acid ratio is mainly responsible for umami taste and overall quality of the tea. Compared with XFL, JXL contain lower catechin and theanine contents, and higher polyphenol/amino acid ratio. However, shading promotes tea quality and affects the two varieties to different degrees. This is contrary to our results and needs to be further explored.

Shading treatments had a greater impact on the appearance, aroma, taste, and infused leaf quality of tea, but with less impact on the infusion color (**Supplementary Table 3**). Compared with unshaded tea, the leaves after 12 days of shading (12XFL and 12JXL) got the highest score: 90.7 ± 0.2 and 92.4 ± 0.2, respectively ($p < 0.05$). They had a strong aroma as well as a fresh and umami taste, in contrast to the control's slight aroma and pure and slightly astringent taste. These indicate that shading can significantly reduce the bitterness and astringency of tea, thus improving the taste and quality of summer and autumn green tea.

Changes in Catechins, Caffeine, and Theanine Contents

To explore the differences in the biochemical components of unshaded and shaded leaves, the contents of catechins (C, EC, ECG, GCG, EGC, and EGCG), caffeine (CAF) and theanine in the tested tea leaf samples were determined. **Table 1** shows that the concentration of theanine and caffeine in XFL and JXL increased significantly after 4- and 12-day shading ($p < 0.05$). Catechin contents in XFL and JXL at the 4th and 12th day were lower than in the unshaded leaves, while C, EC, ECG, EGCG content in two varieties had no significant change until the 12th day. Among them, non-galloylated catechins (C, EC, and EGC) contents in unshaded XFL and JXL were 1.58-, 1.71-, 3.82-, 1.33-, 1.49-, and 1.58-fold higher than in shaded leaves, respectively ($p < 0.05$,

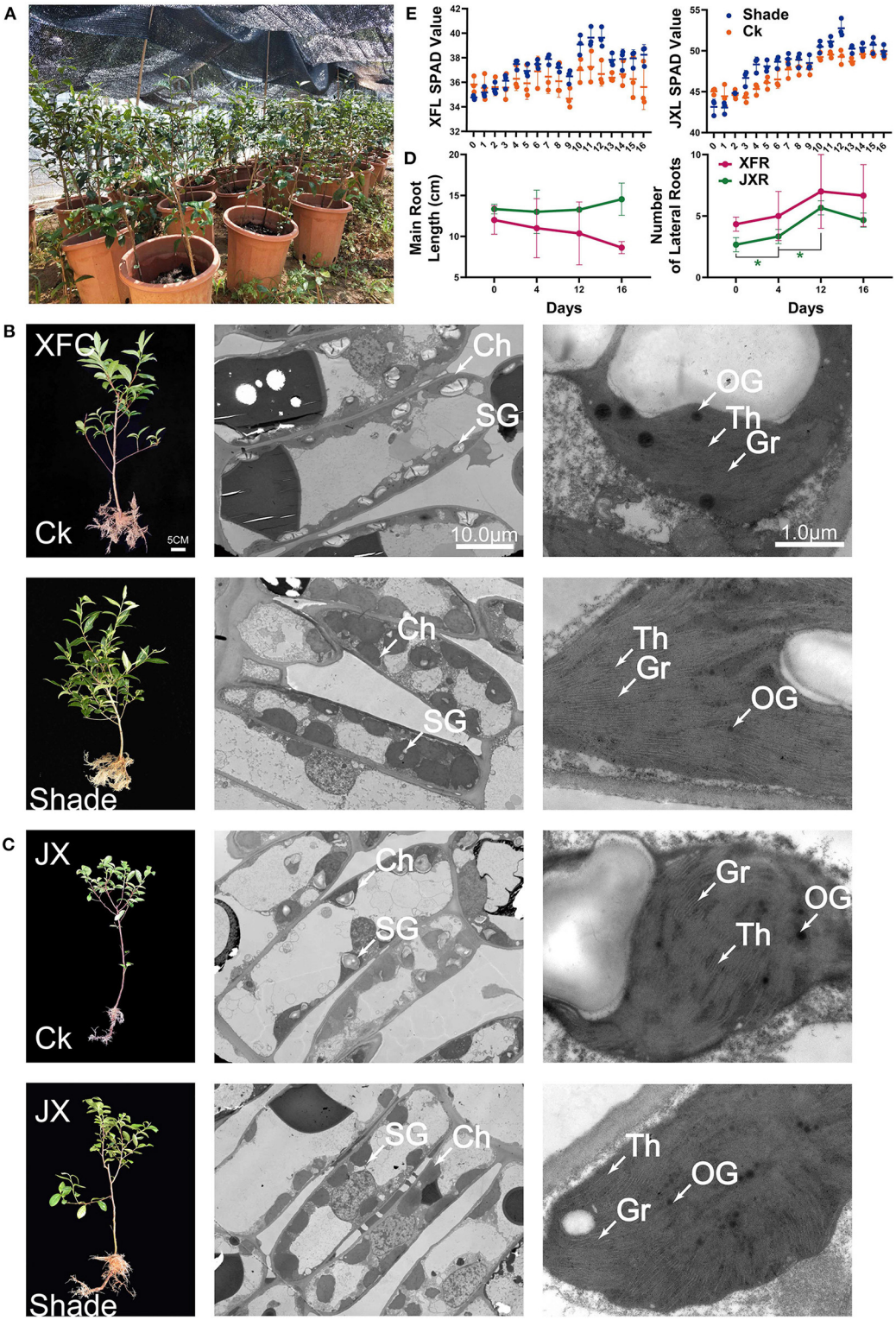

FIGURE 2 | Schematic of pot experiment **(A)**. Whole plant phenotype; effect of shading on the ultrastructure of cell organelles in leaves of two tea cultivars **(B,C)**. The values of main root length, lateral root number **(D)**, and SPAD **(E)** of two tea cultivars (means ± SD, three biological replicates per treatment group) under shaded and unshaded conditions. Data were assessed by one-way ANOVA followed by Duncan's multiple range test. *$p < 0.05$. Ck, control check; Shade, shading treatment; XFC, "Xiangfeicui" cultivar; JX, "Jinxuan" cultivar; Ch, chloroplast; SG, starch granule; OG, osmiophilic granule; Gr, grana; Th, thylakoid; SPAD, soil and plant analyzer development, measuring relative chlorophyll content; XFL, leaf of "Xiangfeicui" cultivar; JXL, leaf of "Jinxuan" cultivar; XFR, root of "Xiangfeicui" cultivar; JXR, root of "Jinxuan" cultivar.

TABLE 1 | Biochemical compositions of leaves in two tea cultivars under different shading periods.

Cultivar	Shading periods (day)	Theanine	Caffeine	DL-C	EC	ECG	GCG	EGC	EGCG
XFL	0	10.55 ± 0.23^{bc}	35.58 ± 1.92^{c}	6.48 ± 0.38^{a}	7.32 ± 0.03^{a}	11.21 ± 0.21^{b}	6.82 ± 0.65^{b}	32.52 ± 0.72^{a}	50.50 ± 1.04^{b}
	4	11.89 ± 0.09^{a}	42.57 ± 0.47^{b}	6.80 ± 0.06^{a}	7.72 ± 0.47^{a}	11.82 ± 0.75^{b}	9.17 ± 0.96^{a}	24.87 ± 0.64^{b}	49.74 ± 0.31^{b}
	12	10.90 ± 0.11^{b}	51.83 ± 1.79^{a}	4.09 ± 0.96^{b}	4.29 ± 0.13^{c}	9.16 ± 0.73^{c}	5.38 ± 0.53^{b}	8.51 ± 1.02^{d}	31.36 ± 0.84^{c}
	16	10.08 ± 0.48^{c}	44.55 ± 0.99^{b}	5.87 ± 0.28^{a}	6.36 ± 0.44^{b}	14.45 ± 0.26^{a}	5.49 ± 0.82^{b}	23.51 ± 0.33^{c}	59.49 ± 1.17^{a}
JXL	0	5.10 ± 0.20^{b}	27.29 ± 1.29^{c}	3.90 ± 0.57^{a}	6.49 ± 0.47^{a}	6.47 ± 0.37^{bc}	3.57 ± 0.25^{a}	19.51 ± 0.64^{a}	27.86 ± 0.12^{b}
	4	7.28 ± 0.23^{a}	30.61 ± 1.64^{b}	4.16 ± 0.31^{a}	6.01 ± 0.68^{a}	7.54 ± 1.10^{b}	3.02 ± 0.09^{b}	13.00 ± 0.33^{c}	27.28 ± 0.54^{b}
	12	7.74 ± 0.01^{a}	34.73 ± 1.25^{a}	2.93 ± 0.30^{b}	4.35 ± 0.32^{b}	5.90 ± 0.23^{c}	2.90 ± 0.31^{bc}	12.35 ± 0.22^{c}	22.87 ± 1.20^{c}
	16	5.07 ± 0.05^{b}	31.75 ± 0.29^{b}	4.35 ± 0.56^{a}	6.16 ± 0.54^{a}	11.75 ± 0.32^{a}	2.58 ± 0.19^{c}	16.05 ± 0.14^{b}	39.26 ± 2.38^{a}

Concentrations (dry weight, mg/g). Data were presented as mean ± SD (standard deviation) and were assessed by one-way ANOVA followed by Duncan's multiple range test. DL-C, Catechin; EC, (–)-Epicatechin; ECG, (–)-Epicatechin gallate; GCG, (–)-Gallocatechin gallate; EGC, (–)-Epigallocatechin; EGCG, (–)-Epigallocatechin gallate; XFL, leaf of "Xiangfeicui"; JXL, leaf of "Jinxuan". ^{a,b,c}Different letters of same cultivar in row represent $p < 0.05$.

each). After light recovery, the contents of eight biochemical components tended to the original level ($p < 0.05$), while GCG showed a opposite trend. Catechins are mainly responsible for the bitter and astringent taste of the tea. Compared with unshaded tea, shaded tea of XFL and JXL usually contain lower levels of catechins, and provide a fresh flavor.

Metabolomics Analysis

Identification of Metabolites

In total, 185 differential metabolites in leaves and 165 differential metabolites in roots, were obtained for subsequent analysis (**Supplementary Table 4**). As shown in **Figures 3A,B**, leaf metabolites were divided into 15 categories, mainly including "carbohydrates and carbohydrate conjugates," "amino acids, peptides, and analogs," "nucleosides, nucleotides, and analogs," "lipids and lipid-like molecules," "organic acids and derivatives," "benzenoids," "organoheterocyclic compounds," and "flavonoids"; root metabolites were divided into 17 categories, mainly including "amino acids, peptides, and analogs," "carbohydrates and carbohydrate conjugates," "lipids and lipid-like molecules," "organonitrogen compounds," "nucleosides, nucleotides, and analogs," and "organic acids and derivatives."

Multivariate Analysis of Extracts From the Leaves and Roots

PCA and OPLS-DA were performed to visualize general clustering patterns and reveal differences between tea cultivars in terms of their leaf and root metabolomes over various shading durations. The PCA model was based on the secondary metabolites detected by UHPLC-Q-TOF MS and showed a separation trend in the leaves and roots of the tea cultivars. **Figures 3C,D** shows that XFL and XFC roots (XFR) were separated to the right side of the PC1 axis while JXL and JX roots (JXR) were separated to the left side of the PC1 axis. Thus, PC1 was separated by tea variety and accounted for 27.5 and 30.4% of the difference, respectively. Moreover, the samples classified by shading treatment were separated in the PC2 axis and 12JXL and 12XFL were further from their unshaded controls than 4JXL and 4XFL were. The light recovery samples (16JXL and 16XFL) were relatively closer to the unshaded controls (0JXL and 0XFL). Thus, PC2 was separated by shading duration and accounted for 15.2 and 16% of the difference, respectively. Multivariate analysis indicate that shading modulates metabolite levels in tea leaves and roots. Therefore, we conducted a further analysis of the metabolomics around metabolite pathways.

Analysis of Differentially Expressed Metabolites (DEMs)

To study the effects of shading on tea cultivar leaf and root metabolic profiling, we selected various metabolites based on VIP >1 and Fold change ≥1.5 or ≤0.67 between samples (**Supplementary Table 4**). We divided the screening samples into two parts: one is the comparison between XFC and JX, and the other is the comparison of different shade stages. In total, 111 leaf DEMs and 112 root DEMs between varieties, and 173 leaf DEMs and 144 root DEMs with different shade stage were identified, respectively. As shown in **Figures 4A,B**, we organized and visualized all DEMs through hierarchical clustering analysis (HCA) using the Euclidean distance coefficient and the complete linkage method. Based on the relative differences in metabolites between cultivars and among shading treatments, the compounds in the leaves and roots were grouped into four clusters (I, II, III, and IV). In **Figure 4A**, cluster I metabolites under shading (days 4 and 12) were more concentrated than those under light exposure, and the metabolite levels in XFL were higher than in JXL, such as Theanine, L-Aspartate, and L-Glutamine. Cluster II, included Kaempferol, Theaflavin, and Gallic acid, occurred at higher levels in the JXL than in the XFL, and the metabolites in 0XFL were the highest level of XFL. Cluster III comprised catechins, α-Farnesene, 4-Aminobutyric acid, and Sucrose, were detected at higher levels in the XFL than in the JXL in all stages, and decreased their contents during the shading period. In cluster IV, the metabolite levels significantly increased under shading and reached the highest expression at the 12th day

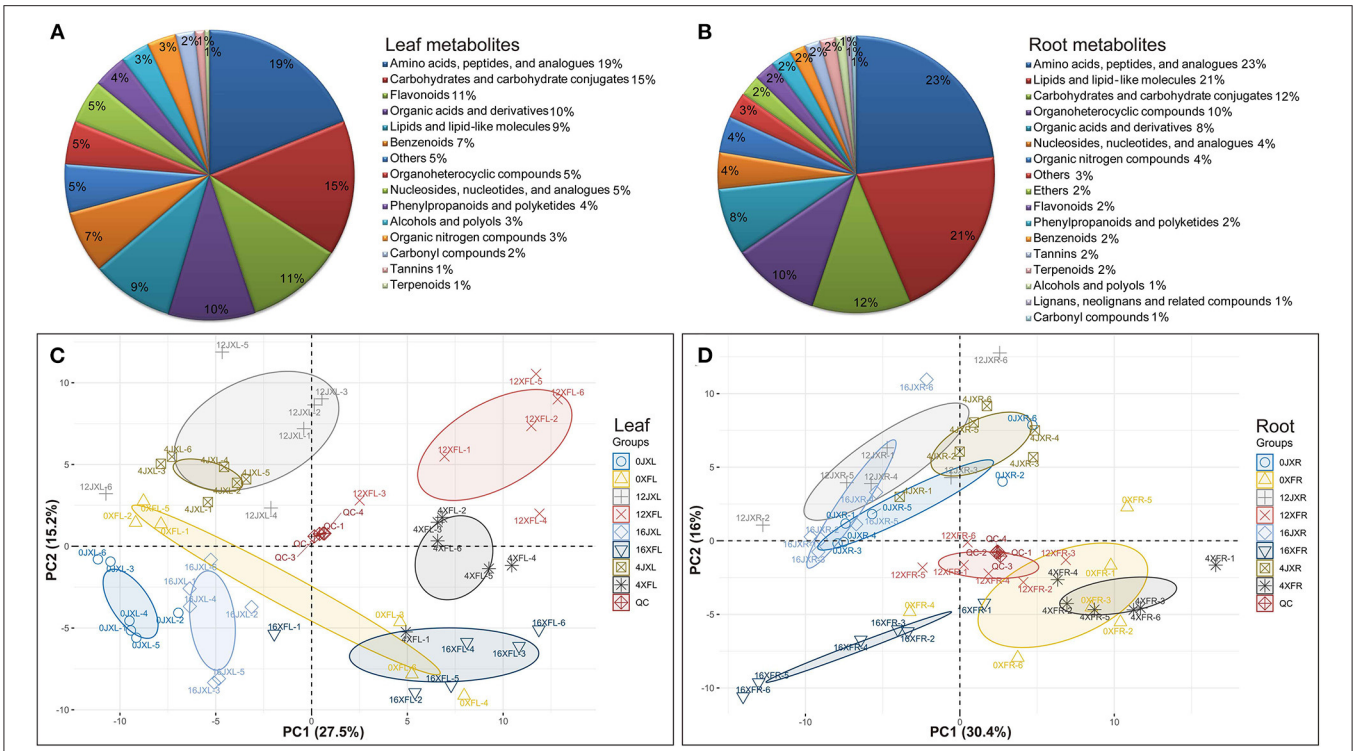

FIGURE 3 | The classification of 185 differential metabolites in leaves **(A)** and 165 differential metabolites in roots **(B)**. PCA score plot of tea samples based on the relative variation of the leaf metabolites **(C)** and root metabolites **(D)** detected by UHPLC-Q TOF MS using the leaves and roots harvested from two cultivars under shading. The legend (Group) describes the abbreviations for the unshaded "Xiangfeicui" leaves (0XFL), XFC leaves after 4 days of shading (4XFL), XFC leaves after 12 days of shading (12XFL), XFC leaves after 4 days of regaining light (16XFL), unshaded "Jinxuan" leaves (0JXL), JX leaves after 4 days of shading (4JXL), JX leaves after 12 days of shading (12JXL), JX leaves after 4 days of regaining light (16JXL); XFC roots when the plants were unshaded (0XFR), XFC roots after 4 days of shading (4XFR), XFC roots after 12 days of shading (12XFR), XFC roots after 4 days of regaining light (16XFR), JX roots when the plants were unshaded (0JXR), JX roots after 4 days of shading (4JXR), JX roots after 12 days of shading (12JXR), and JX roots after 4 days of regaining light (16JXR). Each sample has six biological replicates (1–6). QC represents quality control.

(12XFL and 12JXL), such as L-Asparagine, L-Glutamate, and L-Phenylalanine; these metabolites had higher level in XFL than in JXL.

Figure 4B shows that cluster I included (+)-Catechin, L-Phenylalanine and Jasmine lactone, and they occurred at higher levels in JXR than in XFR. Cluster II, included Sucrose, D-Mannose, and Myo-inositol, occurred at higher levels in XFR than in JXR, and the metabolite levels were decreased after the 12-day shading. Cluster III comprised Betaine, 4-Aminobutyric acid, Theanine, and L-Aspartate, were detected at higher levels in XFR than in JXR in the 0th and 4th day, and reached their highest contents after the 4-day shading. In cluster IV, the metabolites were detected at higher levels in 4XFR than in 4JXR, such Linoleic acid, Oleic acid, Oleanolic acid, L-Asparagine, and L-Glutamine. These results showed the changes of metabolites in tea leaves and roots to possibly be due to the difference in variety and shading duration.

Venn Analysis of DEMs in Leaves and Roots

DEMs Exposed to Shading at Various Durations

We conducted upset plot analysis of DEMs involved in leaves and roots. As shown in **Figure 5A**, the light recovery stage in leaves (16XFL vs. 16JXL) had the highest number of total DEMs and unique DEMs (68 and 16, respectively). There were 15 common DEMs to all stages in leaves, such as (+)-Catechin, (−)-Epicatechin, Epigallocatechin gallate, and Procyanidin B2. A total of 27 DEMs were caused by shading and relight treatments (14 unique DEMs in 0XFL vs. 0JXL and 13 common in other three stages), including L-Arginine, Sucrose, Kaempferol, Rutin, Urea, and Theaflavin. Sixteen unique DEMs under shading (day 4 and 12) included L-Leucine, D-Proline, and L-Asparagine, and 10 unique DEMs with non-shaded treatment (day 0 and 16) included Theanine, Indole-3-pyruvic acid, and D-Mannose. As shown in **Figure 5B**, the number of up-regulated DEMs were more in XFR than in JXR at all stages except the 16th day. There were 26 DEMs (15 unique DEMs in 16XFR vs. 16JXR and 11 common in other three stages) in roots during the light recovery stage, such as myo-Inositol, Oleic acid, Stachyose, L-Pyroglutamic acid, and D-Proline. Fourteen DEMs included Linoleoyl ethanolamide, Linoleic acid, and Nicotinamide, were present at all stages. The shading and relight treatment caused 18 unique DEMs, including D-Allose, Indoleacetic acid, 4-Aminobutyric acid, and Procyanidin B2. A total of 26 DEMs were caused by shading

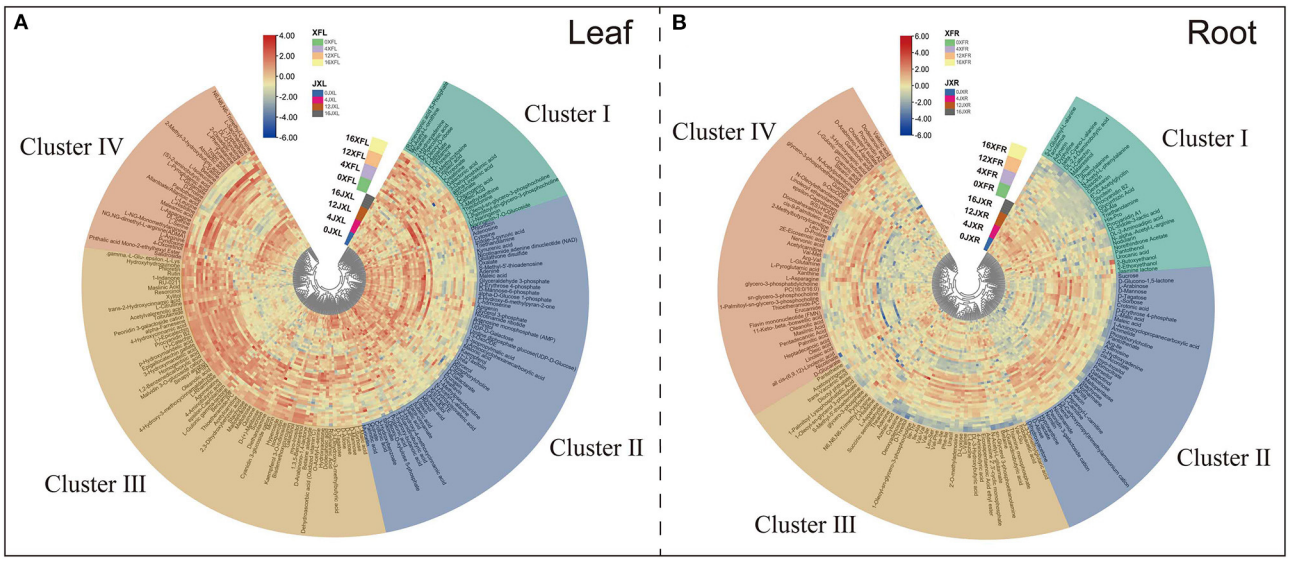

FIGURE 4 | Hierarchical clustering of 185 leaf differential metabolites **(A)** and 165 differential root metabolites **(B)** identified from two tea cultivars with different shading periods. From center to edge, unshaded "Jinxuan" leaves (0JXL), JX leaves after 4 days of shading (4JXL), JX leaves after 12 days of shading (12JXL), JX leaves after 4 days of regaining light (16JXL), the unshaded "Xiangfeicui" leaves (0XFL), XFC leaves after 4 days of shading (4XFL), XFC leaves after 12 days of shading (12XFL), XFC leaves after 4 days of regaining light (16XFL); JX roots when unshaded (0JXR), JX roots after 4 days of shading (4JXR), JX roots after 12 days of shading (12JXR), and JX roots after 4 days of regaining light (16JXR), XFC roots when unshaded (0XFR), XFC roots after 4 days of shading (4XFR), XFC roots after 12 days of shading (12XFR), XFC roots after 4 days of regaining light (16XFR). Each sample has six biological replicates (1–6). The metabolite levels changed, and they could be organized into four clusters named clusters I, II, III, and IV. Blue indicates relatively low intensity, while red indicates relatively high intensity.

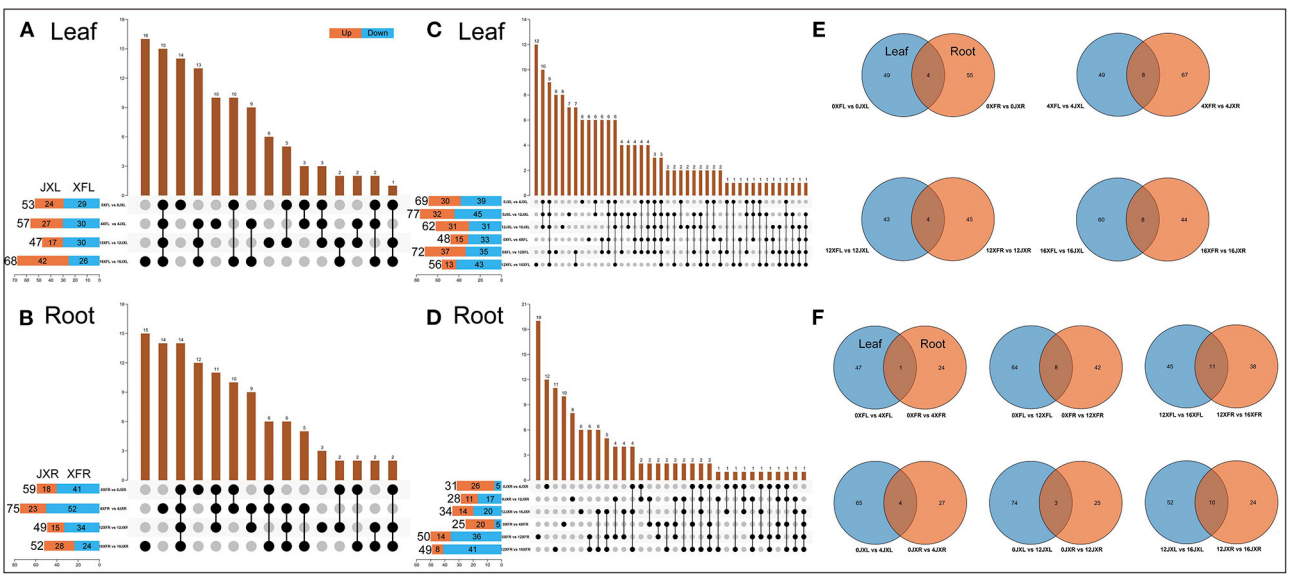

FIGURE 5 | The Venn analysis of differential metabolites involved in leaves and roots of two tea cultivars. The value of the row represents the total number of differential metabolites and "vs." means that the latter value to the previous value. Orange means the latter value is larger, while blue means the previous is larger. The value of the columns indicates the number of metabolites that are common to several sets of comparisons. **(A)** Comparison of leaf differential metabolites among cultivars in different shading periods. **(B)** Comparison of root differential metabolites among cultivars in different shading periods. **(C)** Comparison of leaf differential metabolites between different shading periods within the same cultivar. **(D)** Comparison of root differential metabolites between different shading periods within the same cultivar. **(E)** Differential metabolites shared in leaves and roots among two cultivars during the same shading period. **(F)** Differential metabolites shared in leaves and roots with the different shading duration. XFL, the leaf of "Xiangfeicui" cultivar; JXL, the leaf of "Jinxuan" cultivar; XFR, the root of "Xiangfeicui" cultivar; JXR, the root of "Jinxuan" cultivar.

(day 4 and 12), such as four dipeptides (Leu-Thr, Arg-Val, Arg-Ile, Leu-Ser), Theanine, DL-Indole-3-lactic acid, and L-Glutamine.

As shown in **Figure 5C**, the amount of leaf DEMs in two varieties with different shading durations both showed a trend of first increase (day 4 to day 12) and then decrease (light recovery). The 12-day shading treatment promoted the more up-regulated DEMs in 0XFL vs. 12XFL. There were 12 unigue DEMs in 12XFL vs. 16XFL, such as DL-Serine, L-Glutamine and 4-Aminobutyric acid. Ten common DEMs included Sucrose, Isoquercitin, D-Tagatose, Kaempferol, and Indole-3-pyruvic acid, were caused by shading and relight treatment in JXL. Twelve common DEMs were present at all durations in XFL and JXL, including Tyramine, L-Leucine, L-Phenylalanine, Betaine, L-Histidine, L-Isoleucine, and D-Fructose. The 12-day shading treatment caused 8 and 7 unigue DEMs in XFL and JXL, respectively; the 4-day shading treatment caused both 4 unigue DEMs in XFL and JXL. There were both 6 common DEMs at the 4th and 12th day in XFL [such as Theaflavin, (−)-Epicatechin and 7-Methylxanthine] and JXL (such as Kaempferol 3-O-rutinoside and Apigenin). As shown in **Figure 5D**, the amount of down-regulated DEMs in XFR and JXR increased after the 12-day shading and relight treatment. The 12-day shading caused the highest amount of unigue DEMs in 0XFR vs. 12XFR, including Stearic acid, D-Mannose, L-Asparagine, Indoleacetic acid, Adenosine, and D-Tagatose; 8 unigue DEMs in JXR, such as Theanine. There were 12 unigue DEMs in 0JXR vs. 4JXR at the 4th day of shading, such as 4-Guanidinobutyric acid, N-Acetyl-L-glutamate, and Procyanidin B2; 10 unigue DEMs in 0XFR vs. 4XFR, including Val-Met, Nicotinate, and DL-Indole-3-lactic acid. A total 6 common DEMs were present during the relight stage between XFR and JXR, such as L-Leucine, D-Proline, and L-Aspartate. These results indicated that changes of tea plant metabolites under shading were remarkably associated with cultivar and shade duration.

Common DEMs in Leaves and Roots

As shown in **Figure 5E**, we obtained the common DEMs in leaves and roots by comparing the two varieties at various shading durations. In the 0th day of shading, D-Allose, D-Tagatose, and (+)-Catechin were the common DEMs. There were 8 common DEMs in the 4th day, including Sucrose, Stachyose, Procyanidin B2, (+)-Catechin, and D-Proline. In addition, Procyanidin B2 was present at all stages except the 0th day, and expressed higher level in XFL than in JXL but lower level in XFR than in JXR. As shown in **Figure 5F**, (+)-Catechin was relatively more abundant both in two varieties at the 4th day. Betaine was relatively more abundant in JXL and JXR after 4- and 12-shading treatments, and 8 common DEMs included L-Asparagine, L-Histidine, and L-Sorbose in XFL and XFR under 12-day shading. The light recovery stage induced the most common DEMs in XFL-XFR and JXL-JXR (11 and 10, respectively), such as L-Leucine, L-Aspartate, and D-Proline. These results showed the shading mediated the joint metabolic regulation of tea leaves and roots.

Gene Expression of Main Tea Quality-Metabolites

qRT-PCR was used for verification of the key genes, which regulated important tea quality-metabolites, including 13 genes related to flavonoid biosynthesis and 3 amino acid biosynthesis related genes. As presented in **Figures 6A–M**, all genes except FLS involved in flavonoid metabolism in XFL and JXL, including phenylalanine ammonia lyase (*PAL*), 4-coumarate: CoA ligase (*4CL*) gene, chalcone synthase (*CHS*) gene, flavonoid 3′-monooxygenase (*F3′H*) gene and leucoanthocyanidin reductase (*LAR*) gene, were downregulated under 12-day shading. The shading treatment downregulated flavonoid related genes, indicating that the significant decrease in catechin contents was mainly attributed to the reduction in bitterness of the tea. In addition, the biosynthetic genes, including flavanone 3-hydroxylase (*F3H*) gene, flavonoid 3′,5′-hydroxylase (*F3′5′H*) gene, dihydroflavonol-4-reductase (*DFR*) gene, anthocyanidin synthase (*ANS*) gene, and anthocyanidin reductase (*ANR)* gene, were upregulated in JXL, and cinnamate 4-hydroxylase (*C4H*) gene, chalcone isomerase (*CHI*) gene, and *DFR* were upregulated in XFL at the 4th day, which might be due to the stress response to shading of tea plants. As shown in **Figures 6N–P**, Glutamine synthetase 2 (*CsGS2*) gene that mediated the theanine biosynthesis in XFL and JXL were downregulated under shading, while glutamine synthetase 1.1 (*CsGS1.1*) expression increased remarkably in JXL under shading. Interestingly, our results showed that theanine synthetase I (*CsTSI*) gene was significantly up-regulated in XFR under shading. This suggested that shading could lead to increased expression of specific amino acid synthesis genes in tea leaves and roots but different in various cultivars. These results indicated that expression pattern of these genes was consistent with related metabolites.

DISCUSSION

Shading Periods Dramatically Improved Green Tea Quality by Affecting the Photosynthesis, Biochemical Composition, and Gene Expression

Hot and dry weather tends to make green tea bitter and astringent (Li X. et al., 2016). However, the present study demonstrated that shading helped optimize the light intensity, temperature, and humidity of the environment in which the tea was grown. The level of chlorophyll and carotenoids, which are the major pigments that influence the tea leaf color, are participated in light harvesting and essential for photoprotection against excessive illumination (Chen et al., 2021). In tea plants, reduced light intensity caused by shading induces genes, transcription factors, and phytohormones involved in chlorophyll biosynthesis (Liu et al., 2020). In the present study, shading significantly increased the chlorophyll and carotenoid contents of both XFL and JXL in the field trial. However, the carotenoid content was only decreased in XFL after relight treatment, indicating that the light recovery treatment might differentially regulate

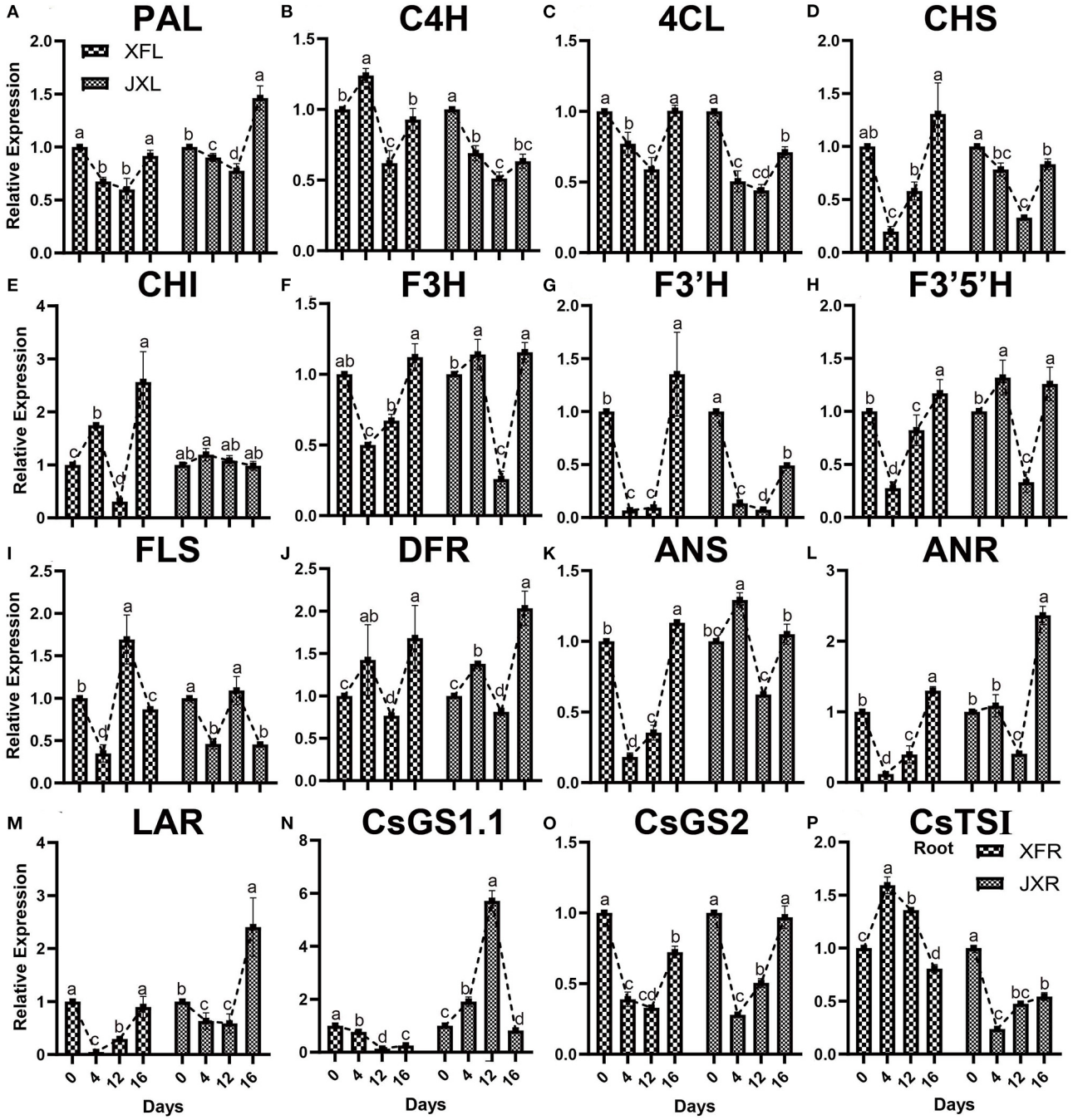

FIGURE 6 | Expression of a selected set of genes in the leaves and roots of two cultivars ("Xiangfeicui" and "Jinxuan") exposed to different shading treatments. The expression of each gene was calculated relative to GAPDH gene. **(A)** *PAL*, phenylalanine ammonia lyase; **(B)** *C4H*, cinnamate 4-hydroxylase; **(C)** *4CL*, 4-coumarate–CoA ligase; **(D)** *CHS*, chalcone synthase; **(E)** *CHI*, chalcone isomerase; **(F)** *F3H*, flavanone 3-hydroxylase; **(G)** *F3′H*, flavonoid 3′-monooxygenase; **(H)** *F3′5′H*, flavonoid 3′,5′-hydroxylase; **(I)** *FLS*, flavonol synthase; **(J)** *DFR*, dihydroflavonol-4-reductase; **(K)** *ANS*, anthocyanidin synthase; **(L)** *ANR*, anthocyanidin reductase; **(M)** *LAR*, leucoanthocyanidin reductase; **(N)** *CsGS1.1*, glutamine synthetase 1.1; **(O)** *CsGS2*, glutamine synthetase 2; **(P)** *CsTSI,* theanine synthetase I (in root). Data were assessed by one-way ANOVA followed by Duncan's multiple range test. XFL, the leaf of "Xiangfeicui" cultivar; JXL, the leaf of "Jinxuan" cultivar; XFR, the root of "Xiangfeicui" cultivar; JXR, the root of "Jinxuan" cultivar.

the accumulation of carotenoid pigments in the JX cultivar, which consisted of low polyphenol and amino acid levels (Song et al., 2017). Simultaneously, TEM analysis showed that shading markedly increased the volume of chloroplasts in the mesophyll cells and made the grana and thylakoids compact, indicating that shading promoted chloroplast development and led to an

increase in photosynthetic pigments (Chen et al., 2017; Gao et al., 2021).

The polyphenols and amino acids are important components of tea taste composition (Zhu et al., 2017). Our results showed that the polyphenol contents were significantly decreased in 12-day shaded XFL and JXL than in 4-day shaded leaves, and the amino acid contents increased with shading duration. Simultaneously, in the sensory evaluation, we observed that shaded green tea had a higher overall quality score than unshaded green tea and JX scored higher than XFC after 12 days of shading, indicating that the shading treatment might improve the tea quality and differentially regulate the content of carbon and nitrogen compounds for metabolic regulation (Li et al., 2020). The polyphenol/amino acid ratio is an important indicator to measure the quality of tea (Zhang Q. et al., 2021). XFC was a high polyphenol and amino acid contents variety with lower polyphenol/amino acid ratio, while JX was a low polyphenol and amino acid contents variety with higher polyphenol/amino acid ratio. In this study, the polyphenol/amino acid ratios were both decreased in XFL and JXL under shading, while the greater decline of the ratio was observed in 12-day JXL. Interestingly, JX is also suitable for black and oolong tea production. The results of the present study underscore the fact that high-quality green tea can be prepared from non-green tea varieties (Zhang G. et al., 2020). Altogether, these findings showed significant differences between the two cultivars, suggesting that the shading treatment might play important roles in JX cultivar because it had low polyphenol and amino acid contents (Li et al., 2020).

Shading improved the types and proportions of the secondary metabolites conducive to high tea quality, and promoted nitrogen metabolism in tea leaves possibly by increasing proteolysis (Yu and Yang, 2020). However, in this study, the levels of biosynthesized non-protein amino acids (Theanine) significantly increased in shaded XFL and JXL except the 12-day shaded XFL, indicating that long-time shading treatment might inhibit the increase of theanine level in XFL, which had high polyphenol and amino acid contents (Yang et al., 2021). In addition, it might have been an increase in protein hydrolysis that explained the measured amino acid distributions and levels (Chen et al., 2017). However, we found that *CsGS1.1* and *CsTSI* were upregulated in shaded JXL and XFR, respectively, which was consistent with previous results (Fu et al., 2021). Thus, shading may, in fact, have induced certain amino acid synthase genes in the leaves and roots (Liu et al., 2017). Caffeine contributes to the intensity of tea flavor, which increased under different shading periods. Extensive study has showed that high light intensity increases the expression of the structural genes and the activity of several important enzymes associated with the biosynthesis of flavonoids, which lead to high contents of catechins (Ye et al., 2021). Recently, some study found that shading tea plants remarkably decreased the catechin contents in tea buds (Zhang et al., 2022). Certain studies suggested that low light intensity downregulates the signal transduction pathways mediated by UVR8 and HY5 and suppresses transcription factors such as MYB (Liu et al., 2018; Zhao et al., 2021). However, we found that the 4-day shading treatment only lowered the EGC in XFL and JXL, while the 12-day shading treatment significantly decreased most catechin contents, including C, EC, ECG, GCG, EGC, and EGCG, indicating that shading treatment significantly reduced the bitterness and astringency by decreasing catechin contents and short-time shading might have slight effect on catechins of tea plants (Lin et al., 2021). In addition, our study measured the expression of 13 flavonoid biosynthesis genes, and they were differentially downregulated in the leaves of both cultivars under shading. However, some gene expression showed a significant upward trend in 4-day shaded leaves, including *C4H*, *CHI*, and *DFR* in XFL and *F3H*, *F3′5′H*, *DFR*, and *ANS* in JXL, respectively, which was consistent with the result that catechins only declined after 12-day shading. These results revealed that the observed decline in flavonoid content might be the result of regulatory gene downregulation under shading (Yu et al., 2021). Thus, the findings indicated that the control of the light intensity regulates the composition of tea quality-compounds in different tea plant varieties.

The Differences in Metabolic Pathways of Two Tea Varieties Under Different Shading Periods

Shading affects both the aerial and belowground environments. However, researchers seldom link the metabolic changes that occur in leaves and roots with shading. In this study, we identified and measured carbon and nitrogen metabolites in both organs. Carbon-based compounds include soluble sugars and starch that serve as substrates for tea polyphenol biosynthesis via the shikimic acid and phenylpropane pathways (Li X. et al., 2019). Amino acids and caffeine are major nitrogen-based compounds; amino acids are synthesized via glycolysis, TCA cycle, and the oxidative pentose phosphate pathway, and caffeine is produced by purine and pentose phosphate pathway (Chen et al., 2020b; Yang et al., 2020). In addition, lipid metabolism associated with tea aroma, synthesized via glycolysis and amino acid pathways (Gai et al., 2020). Thus, the carbon and nitrogen metabolisms are closely integrated. To analyze the different metabolites between the two tea varieties, we proposed different metabolic pathways with reference to the KEGG database and other literatures.

Sugar Metabolism

Sugars furnish metabolic energy for plants and serve as substrates and signaling molecules in various metabolic pathways, and could supply carbon skeletons for the synthesis of amino acids and nucleotides (Ruan, 2014). The glycolysis, tricarboxylic acid (TCA) cycle, galactose metabolism, pentose phosphate pathway, and fructose and mannose metabolism are the main pathways in the carbohydrate metabolism (**Figure 7**). Interestingly, we found that there were obvious differences of leaves and roots between XFC and JX under different shading periods. Glucose is an initial substrate for glycolysis, and other metabolites are known as intermediate product (Liu X. et al., 2016). We found that most metabolites of XFL in glycolysis and pentose phosphate pathway, including UDP-glucose, α-D-Glucose-1P, D-Glyceraldehyde-3P, and D-Erythrose-4P, had lower intensities under shading treatments. Concordantly, we found that the root metabolites in XFR such as Sucrose, L-Sorbose, D-Mannose,

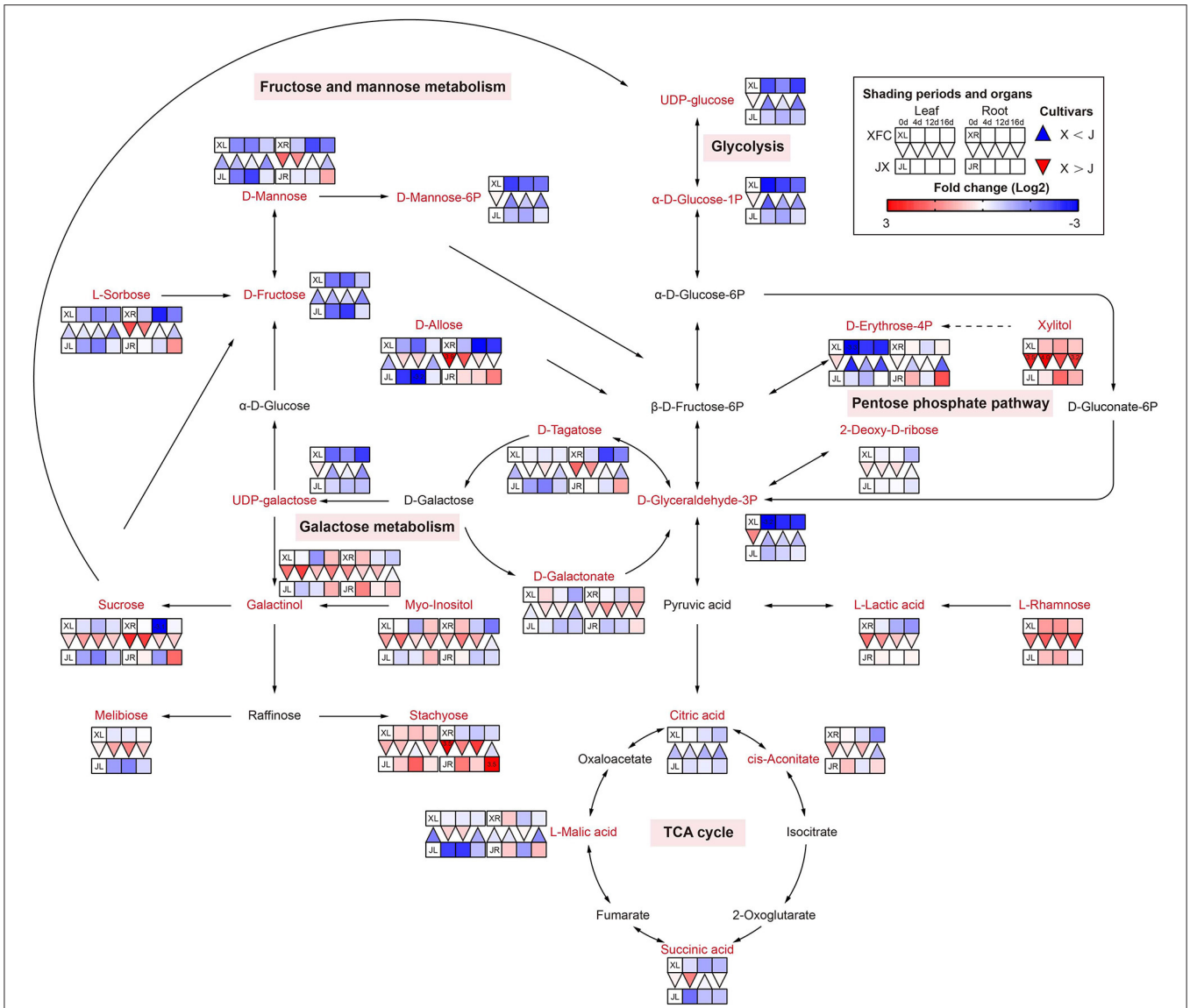

FIGURE 7 | The metabolite differences during sugar metabolism in the two tea cultivars under different shading periods. The identified metabolites are marked with a red color. In the legend, the squares at two lines express the different cultivars, "Xiangfeicui" (XFC) and "Jinxuan" (JX). The squares at eight columns express the different shading periods. The squares in the left part represent the leaves and the right part represents the roots. Blue indicates relatively low and red indicates relatively high intensity. The red triangle indicates relatively higher intensity of metabolites in XFC (X) than in JX (J), and the inverted blue triangle indicates relatively lower intensity of metabolites in XFC (X) than in JX (J). The degree of change was described with the depth of color, and the depth of the colors is based on the log2-fold change value between the samples. XL, leaf of "Xiangfeicui"; XR, root of "Xiangfeicui"; JL, leaf of "Jinxuan"; JR, root of "Jinxuan".

D-Tagatose, and D-Allose, showed decline to a greater extent than in the JXR under 12-day shading. In addition, the XFL had higher levels on intermediate production than the JXL, including Stachyose, L-Rhamnose, and Xylitol. Interestingly, we found significant increasing trends of JXR after relight treatment in sugar pathways and TCA cycle, such as Sucrose, Stachyose, D-Erythrose-4P, D-Allose, L-Sorbose, D-Mannose, L-Malic acid, and cis-Aconitate. Under natural conditions, the tea plants were shown to have higher contents of sugar, such as glucose and fructose derived from the hydrolysis of sucrose, which generally act as osmoprotectants and are involved in the glycolytic pathway (Dumont and Rivoal, 2019). To supplement their carbon skeletons during shading, the plants hydrolyzed large amounts of polysaccharides into soluble sugars and decreased their overall sucrose content (Du et al., 2020). Our results indicated that the shading treatment showed remarkably negative effect on sugar contents but varied significantly among the varieties. Under shade conditions, the need for energy by XFC is lower than JX and downstream products wound be enhanced, while JX were more sensitive to light recovery changes. The reduction in the synthesis of glucose might cause a feedback mechanism by shifting stored glucose to amino acid metabolism instead of

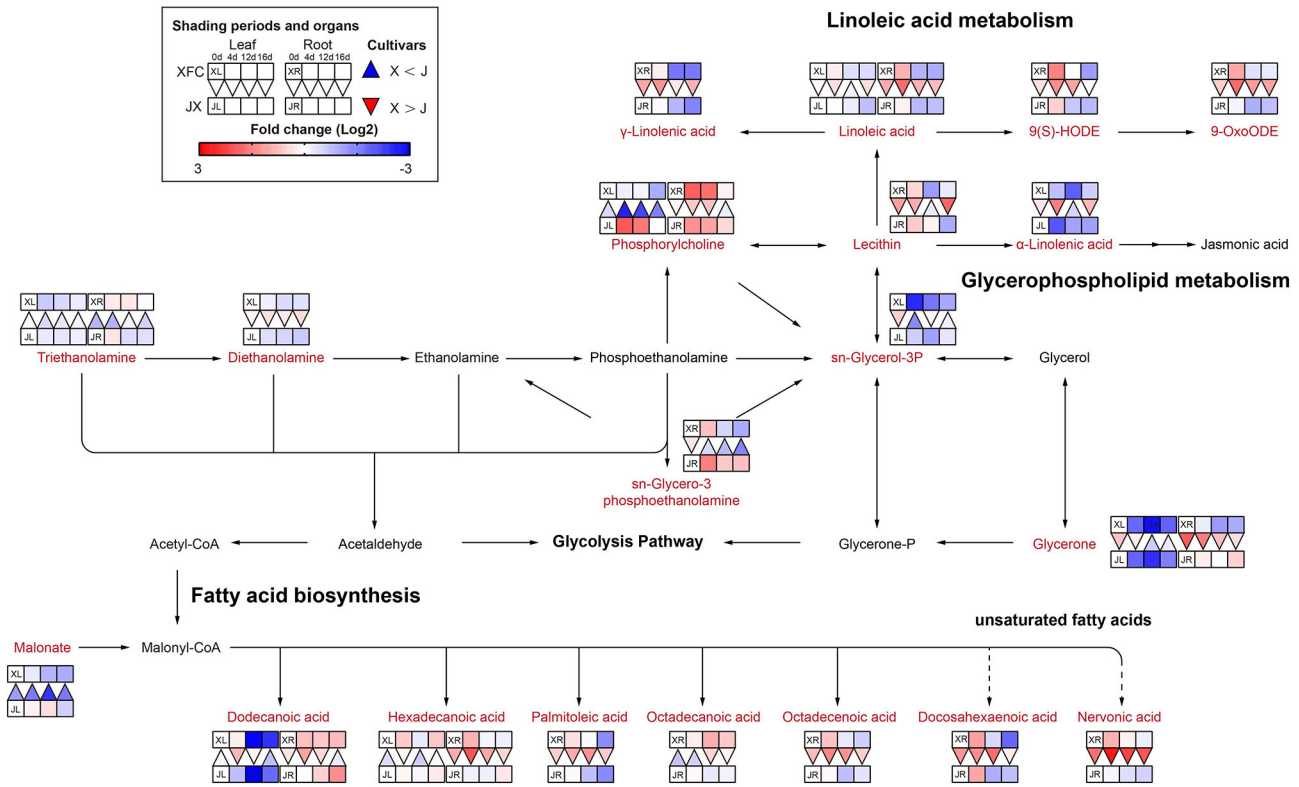

FIGURE 8 | The metabolite differences during lipid metabolism in the two tea cultivars under different shading periods. The identified metabolites are marked with a red color. In the legend, the squares at two lines express the different cultivars, "Xiangfeicui" (XFC) and "Jinxuan" (JX). The squares at eight columns express the different shading periods. The squares in the left part represent the leaves and the right part represents the roots. Blue indicates relatively low and red indicates relatively high intensity. The red triangle indicates relatively higher intensity of metabolites in XFC (X) than in JX (J), and the inverted blue triangle indicates relatively lower intensity of metabolites in XFC (X) than in JX (J). The degree of change was described with the depth of color, and the depth of the colors is based on the log2-fold change value between the samples. XL, leaf of "Xiangfeicui"; XR, root of "Xiangfeicui"; JL, leaf of "Jinxuan"; JR, root of "Jinxuan".

normal carbon metabolism, which leads to the accumulation of amino acids (Li et al., 2020).

Lipid Metabolism

The lipids are the primary precursor of aromatic volatiles compounds and have an important cold-tolerance role in tea plants (Wang et al., 2020). They can generate other aroma compounds after oxidative degradation, among which α-linolenic acid, linoleic acid, oleic acid, and palmitic acid are the precursors of six to ten carbon aroma compounds (Liu M. Y. et al., 2017). Lipid metabolism is comprised of several pathways, including linoleic acid metabolism, glycerophospholipid metabolism and fatty acid biosynthesis (**Figure 8**). Most lipids only were detected in the root and had a higher levels after 4-day shading treatment in XFR than in JXR, including γ-Linolenic acid, Linoleic acid, 9(S)-HODE, 9-OxoODE and all fatty acids (except the Octadecanoic acid), and the same occurred in the leaves of XFC. However, the longer shading treatment could significantly reduce the lipid levels in the leaves and roots of XFC and JX. Linoleic acid is an important precursor of aroma compounds (Guo et al., 2020). In **Figure 8**, the Linoleic acid intensities of XFC in leaves and roots under 4-day shading treatments displayed a upward trend compared to those of the control, but the intensities showed a clear downregulation under 12-day shading treatments. These results indicated that XRC leaves and roots under 4 days of shading treatment had a more active metabolism, which might promote the content of aroma compounds in tea plants (Li J. et al., 2019). In summary, it could be inferred that 4-day shading treatment seems to be advantageous for the aroma of XFC.

Flavonoid Metabolism

It is generally known that flavonoids are carbon-based secondary metabolites, and flavonoids play an important role in the taste of tea (Lin et al., 2021). Catechins are proven antioxidants and can improve stress resistance in plants (Chobot et al., 2009). Proanthocyanidins are formed by combining multiple catechins and also have strong antioxidant capacity (Ma et al., 2019). As shown in **Figure 9**, the levels of (+)-catechin, procyanidin B2, and procyanidin A1 in the leaves and roots of JX, significantly increased after 4-day shading treatment, and then decreased under 12-day shading, indicating that the tea plants might exhibit a stress response in the early stages of shading, which was different from other plant studies (Hussain

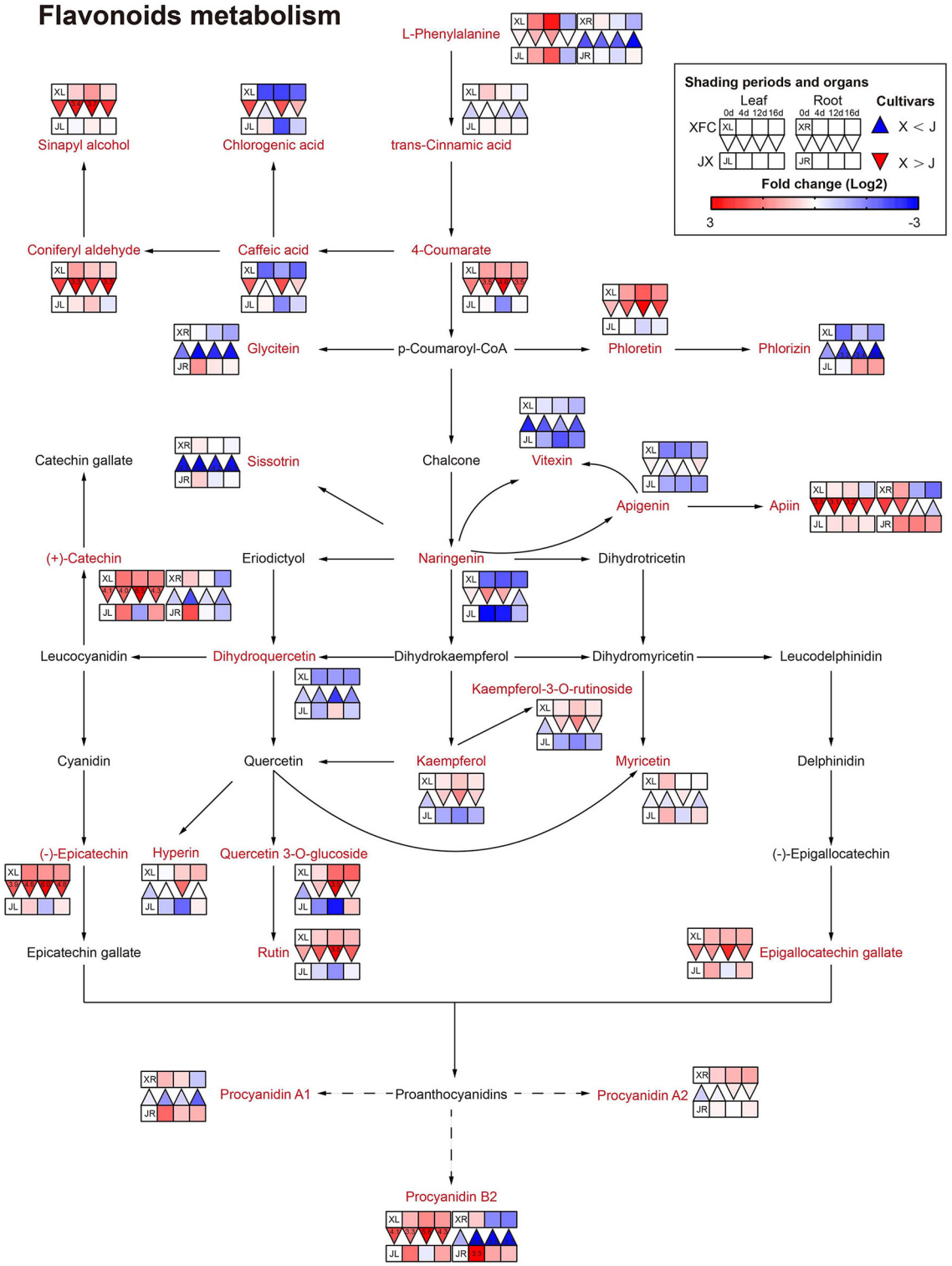

FIGURE 9 | The metabolite differences during flavonoids metabolism in the two tea cultivars under different shading periods. The identified metabolites are marked with a red color. In the legend, the squares at two lines express the different cultivars, "Xiangfeicui" (XFC) and "Jinxuan" (JX). The squares at eight columns express the different shading periods. The squares in the left part represent the leaves and the right part represents the roots. Blue indicates relatively low and red indicates relatively high intensity. The red triangle indicates relatively higher intensity of metabolites in XFC (X) than in JX (J), and the inverted blue triangle indicates relatively lower intensity of metabolites in XFC (X) than in JX (J). The degree of change was described with the depth of color, and the depth of the colors is based on the log2-fold change value between the samples. XL, leaf of "Xiangfeicui"; XR, root of "Xiangfeicui"; JL, leaf of "Jinxuan"; JR, root of "Jinxuan".

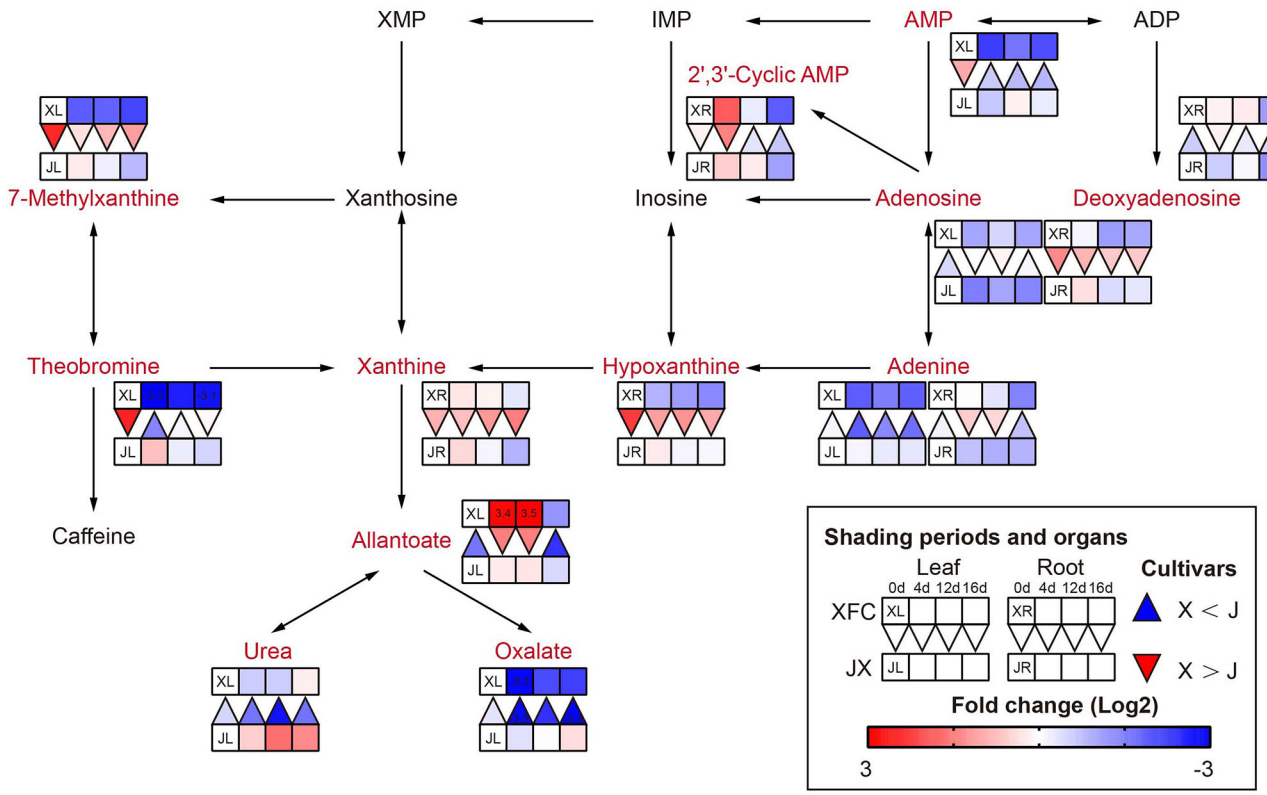

FIGURE 10 | The metabolite differences during purine and caffeine metabolism in the two tea cultivars under different shading periods. The identified metabolites are marked with a red color. In the legend, the squares at two lines express the different cultivars, "Xiangfeicui" (XFC) and "Jinxuan" (JX). The squares at eight columns express the different shading periods. The squares in the left part represent the leaves and the right part represents the roots. Blue indicates relatively low and red indicates relatively high intensity. The red triangle indicates relatively higher intensity of metabolites in XFC (X) than in JX (J), and the inverted blue triangle indicates relatively lower intensity of metabolites in XFC (X) than in JX (J). The degree of change was described with the depth of color, and the depth of the colors is based on the log2-fold change value between the samples. XL, leaf of "Xiangfeicui"; XR, root of "Xiangfeicui"; JL, leaf of "Jinxuan"; JR, root of "Jinxuan".

et al., 2020). In addition, the 12-day shading treatment reduced the concentrations of most flavonoids in JXL, including 4-Coumarate, Naringenin, Vitexin, Apigenin, (+)-catechin, (−)-Epicatechin, Epigallocatechin gallate, Kaempferol, Rutin, and some flavonols, while these compounds had upward trends and higher levels in XFL under shading. This result revealed that the response of the flavonoid contents between varieties to shading was different. In contrast to the varieties with relatively high catechin contents, JX with relatively low catechin contents, was more susceptible to down-regulation caused by shading. The flavonoid metabolism is reportedly influenced by the TCA cycle and the biosynthesis of carbohydrates and amino acids (Araújo et al., 2014). Thus, the flavonoid metabolism is controlled in many ways, and the shading treatments could differentially regulate the intensity of flavonoid metabolism in tea plants.

Nitrogen Metabolism

Amino acids are main nitrogen-based metabolites that affect tea quality. The biosynthesis of amino acids occurs primarily in glycolysis, the TCA cycle and the oxidative pentose phosphate pathway (Fernie et al., 2004). The purine alkaloids were synthesized by the pentose phosphate pathway (Li Y. et al., 2016). As shown in **Figure 10**, purine and alkaloid compounds showed a significant decline under shading treatments in XFL, such as Adenine, 7-Methylxanthine, and Theobromine, while most metabolites were increased in shaded JXL, indicating that the shading was different for nitrogen allocation in different tea varieties (Li et al., 2020). It is possible that a small quantity of one substance at upstream results in a larger quantity accumulation of another downstream. As shown in **Figure 11**, there were nine pathways observed, which were associated with amino acids, such as alanine, aspartate and glutamate metabolism, phenylalanine metabolism and tyrosine metabolism. Nearly all the amino acids have a similar rule of change under shading treatments; the 4-day shading treatments increased the concentrations of amino acids in the tea leaves and roots, and the 12-day shading treatments led their concentrations to the highest levels, including L-Asparagine, L-Glutamate, L-Histidine, L-Phenylalanine, L-Arginine, L-Serine, L-Valine,

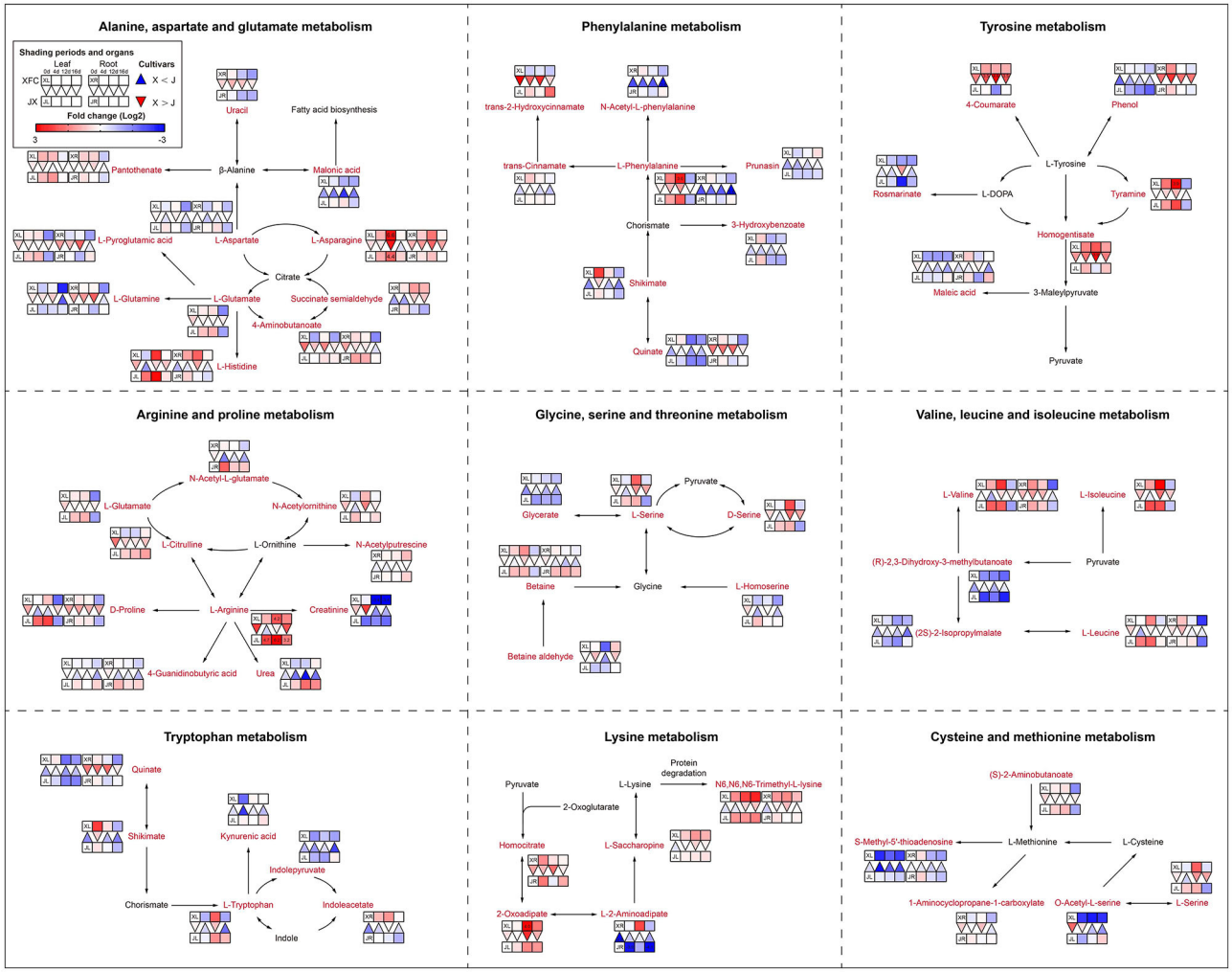

FIGURE 11 | The metabolite differences during amino acid metabolism in the two tea cultivars under different shading periods. The identified metabolites are marked with a red color. In the legend, the squares at two lines express the different cultivars, "Xiangfeicui" (XFC) and "Jinxuan" (JX). The squares at eight columns express the different shading periods. The squares in the left part represent the leaves and the right part represents the roots. Blue indicates relatively low and red indicates relatively high intensity. The red triangle indicates relatively higher intensity of metabolites in XFC (X) than in JX (J), and the inverted blue triangle indicates relatively lower intensity of metabolites in XFC (X) than in JX (J). The degree of change was described with the depth of color, and the depth of the colors is based on the log2-fold change value between the samples. XL, leaf of "Xiangfeicui"; XR, root of "Xiangfeicui"; JL, leaf of "Jinxuan"; JR, root of "Jinxuan".

and Betaine (Lee et al., 2013). However, the level of L-Glutamine, L-Aspartate, 4-Aminobutanoate, and L-Tryptophan were no significant change in 4-day shaded leaves. Meanwhile, our results displayed a significant decrease on the amino acid content after the relight treatment. Shading promotes nitrogen metabolism in tea leaves possibly by increasing proteolysis, and in the present study, we found that this increase occurred in both leaves and roots (Yu and Yang, 2020; Yang et al., 2021). These findings suggested that the longer shading treatments was more conductive to N metabolism both in the tea leaves and roots, which was the primary reason that why shaded green tea was fresher than the regular tea (Zhang Y. et al., 2021). This was inconsistent with the conclusion of some previous studies (Li et al., 2020). In general, the N provision for sustaining growth is contributed by the translocation of soil N from new uptake by the root and the remobilization of the N reserves stored within the plants (Yang et al., 2020). In the present study, the increased content of nitrogen-based metabolites in roots might indicate that shading seems to promote nitrogen uptake from the soil in tea plants (Li et al., 2021).

CONCLUSION

Through physiological and biochemical analysis, phenotypic analysis, untargeted metabolomics methods, combined with the expression analysis of selected genes, we have found that long-term shading can improve the quality of summer and autumn green tea compared with short-term shading.

Short-term shading may have caused stress on tea plants. By using metabolomics analysis of leaves and roots, we found that carbon and nitrogen metabolism jointly promoted tea quality, including sugar metabolism, lipid metabolism, flavonoid metabolism, amino acid metabolism, and purine alkaloid metabolism. Our work shows that metabolites in different tea varieties, including green tea quality-related compounds like amino acid and catechins, are affected differently during different shading periods. A limitation of this study is that we did not explore the effect of shading on the tea processing. Hence, considerably more work will need to be done to determine which metabolites and genes regulate the quality of shaded tea during processing.

DATA AVAILABILITY STATEMENT

The original contributions presented in the study are included in the article/**Supplementary Material**, further inquiries can be directed to the corresponding author/s.

AUTHOR CONTRIBUTIONS

CSha: conceptualization, writing—original draft, writing—review, editing, and mapping. HJ and JiahC: investigation, resources, and supervision. CZ and JL: validation. JianC: formal analysis. YL: data curation. JH and BY: visualization. ZL: project administration. CShe: project administration and funding acquisition. All authors contributed to the article and approved the submitted version.

FUNDING

This work was supported by Joint Funds of National Natural Science Foundation of China (Grant No. U19A2030); the National Natural Science Foundation of China (Grant No. 31271789); Central Committee Guides Local Science and Technology Development Program (Grant No. 2019XF5041); and the Special Project for the Construction of Modern Agricultural Industrial Technology Systems in Hunan Province (Xiang Nongfa) (Grant No. 2020112).

ACKNOWLEDGMENTS

We appreciate the help of Yankai Kang in the field experiment.

SUPPLEMENTARY MATERIAL

The Supplementary Material for this article can be found online at: https://www.frontiersin.org/articles/10.3389/fpls.2022.894840/full#supplementary-material

REFERENCES

Araújo, W. L., Martins, A. O., Fernie, A. R., and Tohge, T. (2014). 2-oxoglutarate: linking TCA cycle function with amino acid, glucosinolate, flavonoid, alkaloid, and gibberellin biosynthesis. *Front. Plant Sci.* 5:552. doi: 10.3389/fpls.2014.00552

Chen, C., Chen, H., Zhang, Y., Thomas, H. R., Frank, M. H., He, Y., et al. (2020a). TBtools: an integrative toolkit developed for interactive analyses of big biological data. *Mol. Plant*. 13, 1194–1202. doi: 10.1016/j.molp.2020.06.009

Chen, J., Wu, S., Dong, F., Li, J., Zeng, L., Tang, J., et al. (2021). Mechanism underlying the shading-induced chlorophyll accumulation in tea leaves. *Front. Plant Sci.* 12:779819. doi: 10.3389/fpls.2021.779819

Chen, Y., Fu, X., Mei, X., Zhou, Y., Cheng, S., Zeng, L., et al. (2017). Proteolysis of chloroplast proteins is responsible for accumulation of free amino acids in dark-treated tea (*Camellia sinensis*) leaves. *J. Proteomics*. 157, 10–17. doi: 10.1016/j.jprot.2017.01.017

Chen, Y., Zeng, L., Liao, Y., Li, J., Zhou, B., Yang, Z., et al. (2020b). Enzymatic reaction-related protein degradation and proteinaceous amino acid metabolism during the black tea (*Camellia sinensis*) manufacturing process. *Foods* 9:66. doi: 10.3390/foods9010066

Chobot, V., Huber, C., Trettenhahn, G., and Hadacek, F. (2009). (+/-)-catechin: chemical weapon, antioxidant, or stress regulator? *J. Chem. Ecol.* 35, 980–996. doi: 10.1007/s10886-009-9681-x

Dai, W., Qi, D., Yang, T., Lv, H., Guo, L., Zhang, Y., et al. (2015). Nontargeted analysis using ultraperformance liquid chromatography-quadrupole time-of-flight mass spectrometry uncovers the effects of harvest season on the metabolites and taste quality of tea (*Camellia sinensis* L.). *J. Agric. Food Chem.* 63, 9869–9878. doi: 10.1021/acs.jafc.5b03967

Du, Y., Zhao, Q., Chen, L., Yao, X., Zhang, W., Zhang, B., et al. (2020). Effect of drought stress on sugar metabolism in leaves and roots of soybean seedlings. *Plant Physiol. Biochem.* 146, 1–12. doi: 10.1016/j.plaphy.2019.11.003

Dumont, S., and Rivoal, J. (2019). Consequences of oxidative stress on plant glycolytic and respiratory metabolism. *Front. Plant Sci.* 10:166. doi: 10.3389/fpls.2019.00166

Fernie, A. R., Carrari, F., and Sweetlove, L. J. (2004). Respiratory metabolism: glycolysis, the TCA cycle and mitochondrial electron transport. *Curr. Opin. Plant Biol.* 7, 254–261. doi: 10.1016/j.pbi.2004.03.007

Fu, X., Liao, Y., Cheng, S., Xu, X., Grierson, D., and Yang, Z. (2021). Nonaqueous fractionation and overexpression of fluorescent-tagged enzymes reveals the subcellular sites of L-theanine biosynthesis in tea. *Plant Biotechnol. J.* 19, 98–108. doi: 10.1111/pbi.13445

Gai, Z., Wang, Y., Ding, Y., Qian, W., Qiu, C., Xie, H., et al. (2020). Exogenous abscisic acid induces the lipid and flavonoid metabolism of tea plants under drought stress. *Sci. Rep.* 10:12275. doi: 10.1038/s41598-020-69080-1

Gao, X., Zhang, C., Lu, C., Wang, M., Xie, N., Chen, J., et al. (2021). Disruption of photomorphogenesis leads to abnormal chloroplast development and leaf variegation in *Camellia sinensis*. *Front. Plant Sci.* 12:720800. doi: 10.3389/fpls.2021.720800

Guo, L., Du, Z. H., Wang, Z., Lin, Z., Guo, Y. L., and Chen, M. J. (2020). Location affects fatty acid composition in *Camellia sinensis* cv. Tieguanyin fresh leaves. *J. Food Sci. Technol.* 57, 96–101. doi: 10.1007/s13197-019-04034-8

Guo, Z., Barimah, A. O., Yin, L., Chen, Q., Shi, J., El-Seedi, H. R., et al. (2021). Intelligent evaluation of taste constituents and polyphenols-to-amino acids ratio in matcha tea powder using near infrared spectroscopy. *Food Chem.* 353:129372. doi: 10.1016/j.foodchem.2021.129372

Hu, J., Webster, D., Cao, J., and Shao, A. (2018). The safety of green tea and green tea extract consumption in adults - results of a systematic review. *Regul. Toxicol. Pharmacol.* 95:412–433. doi: 10.1016/j.yrtph.2018.03.019

Hussain, S., Pang, T., Iqbal, N., Shafiq, I., Skalicky, M., Brestic, M., et al. (2020). Acclimation strategy and plasticity of different soybean genotypes in intercropping. *Funct. Plant Biol.* 47, 592–610. doi: 10.1071/FP19161

Ji, H. G., Lee, Y. R., Lee, M. S., Hwang, K. H., Park, C. Y., Kim, E. H., et al. (2018). Diverse metabolite variations in tea (*Camellia sinensis* L.) leaves grown under various shade conditions revisited: a metabolomics study. *J. Agric. Food Chem.* 66, 1889–1897. doi: 10.1021/acs.jafc.7b04768

Ku, K. M., Choi, J. N., Kim, J., Kim, J. K., Yoo, L. G., Lee, S. J., et al. (2010). Metabolomics analysis reveals the compositional differences of shade grown tea (*Camellia sinensis* L.). *J. Agric. Food Chem.* 58, 418–426. doi: 10.1021/jf902929h

Lee, L. S., Choi, J. H., Son, N., Kim, S. H., Park, J. D., Jang, D. J., et al. (2013). Metabolomic analysis of the effect of shade treatment on the nutritional and sensory qualities of green tea. *J. Agric. Food Chem*. 61, 332–338. doi: 10.1021/jf304161y

Li, F., Dong, C., Yang, T., Bao, S., Fang, W., Lucas, W. J., et al. (2021). The tea plant CsLHT1 and CsLHT6 transporters take up amino acids, as a nitrogen source, from the soil of organic tea plantations. *Hortic. Res*. 8:178. doi: 10.1038/s41438-021-00615-x

Li, J., Zeng, L., Liao, Y., Gu, D., Tang, J., and Yang, Z. (2019). Influence of chloroplast defects on formation of jasmonic acid and characteristic aroma compounds in tea (*Camellia sinensis*) leaves exposed to postharvest stresses. *Int. J. Mol. Sci*. 20:1044. doi: 10.3390/ijms20051044

Li, N., Yang, Y., Ye, J., Lu, J., Zheng, X., and Liang, Y. (2016). Effects of sunlight on gene expression and chemical composition of light-sensitive albino tea plant. *Plant Growth Regul*. 78, 253–262. doi: 10.1007/s10725-015-0090-6

Li, X., Ahammed, G. J., Li, Z. X., Zhang, L., Wei, J. P., Shen, C., et al. (2016). Brassinosteroids improve quality of summer tea (*Camellia sinensis* L.) by balancing biosynthesis of polyphenols and amino acids. *Front. Plant Sci*. 7:1304. doi: 10.3389/fpls.2016.01304

Li, X., Zhang, L. P., Zhang, L., Yan, P., Ahammed, G. J., and Han, W. Y. (2019). Methyl salicylate enhances flavonoid biosynthesis in tea leaves by stimulating the phenylpropanoid pathway. *Molecules* 24:362. doi: 10.3390/molecules24020362

Li, Y., Chen, C., Li, Y., Ding, Z., Shen, J., Wang, Y., et al. (2016). The identification and evaluation of two different color variations of tea. *J. Sci. Food Agric*. 96, 4951–4961. doi: 10.1002/jsfa.7897

Li, Y., Jeyaraj, A., Yu, H., Wang, Y., Ma, Q., Chen, X., et al. (2020). Metabolic regulation profiling of carbon and nitrogen in tea plants [*Camellia sinensis* (L.) O. Kuntze] in response to shading. *J. Agric. Food Chem*. 68, 961–974. doi: 10.1021/acs.jafc.9b05858

Li, Z. X., Yang, W. J., Ahammed, G. J., Shen, C., Yan, P., Li, X., et al. (2016). Developmental changes in carbon and nitrogen metabolism affect tea quality in different leaf position. *Plant Physiol. Biochem*. 106, 327–335. doi: 10.1016/j.plaphy.2016.06.02

Lin, N., Liu, X., Zhu, W., Cheng, X., Wang, X., Wan, X., et al. (2021). Ambient ultraviolet B signal modulates tea flavor characteristics via shifting a metabolic flux in flavonoid biosynthesis. *J. Agric. Food Chem*. 69, 3401–3414. doi: 10.1021/acs.jafc.0c07009

Liu, G. F., Han, Z. X., Feng, L., Gao, L. P., Gao, M. J., Gruber, M. Y., et al. (2017). Metabolic flux redirection and transcriptomic reprogramming in the albino tea cultivar 'Yu-Jin-Xiang' with an emphasis on catechin production. *Sci. Rep*. 7:45062. doi: 10.1038/srep45062

Liu, J., Zhang, Q., Liu, M., Ma, L., Shi, Y., and Ruan, J. (2016). Metabolomic analyses reveal distinct change of metabolites and quality of green tea during the short duration of a single spring season. *J. Agric. Food Chem*. 64, 3302–3309. doi: 10.1021/acs.jafc.6b00404

Liu, L., Li, Y., She, G., Zhang, X., Jordan, B., Chen, Q., et al. (2018). Metabolite profiling and transcriptomic analyses reveal an essential role of UVR8-mediated signal transduction pathway in regulating flavonoid biosynthesis in tea plants (*Camellia sinensis*) in response to shading. *BMC Plant Biol*. 18:233. doi: 10.1186/s12870-018-1440-0

Liu, L., Lin, N., Liu, X., Yang, S., Wang, W., and Wan, X. (2020). From chloroplast biogenesis to chlorophyll accumulation: the interplay of light and hormones on gene expression in *Camellia sinensis* cv. Shuchazao leaves. *Front. Plant Sci*. 11:256. doi: 10.3389/fpls.2020.00256

Liu, M. Y., Burgos, A., Ma, L., Zhang, Q., Tang, D., and Ruan, J. (2017). Lipidomics analysis unravels the effect of nitrogen fertilization on lipid metabolism in tea plant (*Camellia sinensis* L.). *BMC Plant Biol*. 17:165. doi: 10.1186/s12870-017-1111-6

Liu, X., Zhang, Y., Yang, C., Tian, Z., and Li, J. (2016). AtSWEET4, a hexose facilitator, mediates sugar transport to axial sinks and affects plant development. *Sci. Rep*. 6:24563. doi: 10.1038/srep24563

Ma, Z., Huang, Y., Huang, W., Feng, X., Yang, F., and Li, D. (2019). Separation, identification, and antioxidant activity of polyphenols from lotus seed epicarp. *Molecules* 24:4007. doi: 10.3390/molecules24214007

Maritim, T. K., Seth, R., Parmar, R., and Sharma, R. K. (2021). Multiple-genotypes transcriptional analysis revealed candidates genes and nucleotide variants for improvement of quality characteristics in tea (*Camellia sinensis* (L.) O. Kuntze). *Genomics* 113(1 Pt 1), 305–316. doi: 10.1016/j.ygeno.2020.12.020

Nowogrodzki, A. (2019). How climate change might affect tea. *Nature* 566, S10–S11. doi: 10.1038/d41586-019-00399-0

Pongsuwan, W., Bamba, T., Harada, K., Yonetani, T., Kobayashi, A., and Fukusaki, E. (2008). High-throughput technique for comprehensive analysis of Japanese green tea quality assessment using ultra-performance liquid chromatography with time-of-flight mass spectrometry (UPLC/TOF MS). *J. Agric. Food Chem*. 56, 10705–10708. doi: 10.1021/jf8018003

Prasanth, M. I., Sivamaruthi, B. S., Chaiyasut, C., and Tencomnao, T. (2019). A review of the role of green tea (*Camellia sinensis*) in antiphotoaging, stress resistance, neuroprotection, and autophagy. *Nutrients* 11:474. doi: 10.3390/nu11020474

Ruan, Y. L. (2014). Sucrose metabolism: gateway to diverse carbon use and sugar signaling. *Annu. Rev. Plant Biol*. 65, 33–67. doi: 10.1146/annurev-arplant-050213-040251

Sano, S., Takemoto, T., Ogihara, A., Suzuki, K., Masumura, T., Satoh, S., et al. (2020). Stress responses of shade-treated tea leaves to high light exposure after removal of shading. *Plants* 9:302. doi: 10.3390/plants9030302

Sano, T., Horie, H., Matsunaga, A., and Hirono, Y. (2018). Effect of shading intensity on morphological and color traits and on chemical components of new tea (*Camellia sinensis* L.) shoots under direct covering cultivation. *J. Sci. Food Agric*. 98, 5666–5676. doi: 10.1002/jsfa.9112

Song, L., Ma, Q., Zou, Z., Sun, K., Yao, Y., Tao, J., et al. (2017). Molecular link between leaf coloration and gene expression of flavonoid and carotenoid biosynthesis in *Camellia sinensis* cultivar 'Huangjinya'. *Front. Plant Sci*. 8:803. doi: 10.3389/fpls.2017.00803

Tang, S., Zheng, N., Ma, Q., Zhou, J., and Wu, L. (2021). Applying nutrient expert system for rational fertilisation to tea (*Camellia sinensis*) reduces environmental risks and increases economic benefits. *J. Clean. Prod*. 305:127197. doi: 10.1016/j.jclepro.2021.127197

Vinocur, B., and Altman, A. (2005). Recent advances in engineering plant tolerance to abiotic stress: achievements and limitations. *Curr. Opin. Biotechnol*. 16, 123–132. doi: 10.1016/j.copbio.2005.02.001

Wang, H., Cao, X., Yuan, Z., and Guo, G. (2021). Untargeted metabolomics coupled with chemometrics approach for Xinyang Maojian green tea with cultivar, elevation and processing variations. *Food Chem*. 352:129359. doi: 10.1016/j.foodchem.2021.129359

Wang, P., Chen, S., Gu, M., Chen, X., Chen, X., Yang, J., et al. (2020). Exploration of the effects of different blue LED light intensities on flavonoid and lipid metabolism in tea plants via transcriptomics and metabolomics. *Int. J. Mol. Sci*. 21:4606. doi: 10.3390/ijms21134606

Yamashita, H., Tanaka, Y., Umetsu, K., Morita, S., Ono, Y., Suzuki, T., et al. (2020). Phenotypic markers reflecting the status of overstressed tea plants subjected to repeated shade cultivation. *Front. Plant Sci*. 11:556476. doi: 10.3389/fpls.2020.556476

Yang, T., Li, H., Tai, Y., Dong, C., Cheng, X., Xia, E., et al. (2020). Transcriptional regulation of amino acid metabolism in response to nitrogen deficiency and nitrogen forms in tea plant root (*Camellia sinensis* L.). *Sci. Rep*. 10:6868. doi: 10.1038/s41598-020-63835-6

Yang, T., Xie, Y., Lu, X., Yan, X., Wang, Y., Ma, J., et al. (2021). Shading promoted theanine biosynthesis in the roots and allocation in the shoots of the tea plant (*Camellia sinensis* L.) cultivar shuchazao. *J. Agric. Food Chem*. 69, 4795–4803. doi: 10.1021/acs.jafc.1c00641

Ye, J. H., Lv, Y. Q., Liu, S. R., Jin, J., Wang, Y. F., Wei, C. L., et al. (2021). Effects of light intensity and spectral composition on the transcriptome profiles of leaves in shade grown tea plants (*Camellia sinensis* L.) and regulatory network of flavonoid biosynthesis. *Molecules* 26:5836. doi: 10.3390/molecules26195836

Yu, S., Li, P., Zhao, X., Tan, M., Ahmad, M. Z., Xu, Y., et al. (2021). CsTCPs regulate shoot tip development and catechin biosynthesis in tea plant (*Camellia sinensis*). *Hortic. Res*. 8:104. doi: 10.1038/s41438-021-00538-7

Yu, Z., and Yang, Z. (2020). Understanding different regulatory mechanisms of proteinaceous and non-proteinaceous amino acid formation in tea (*Camellia sinensis*) provides new insights into the safe and effective alteration of tea flavor and function. *Crit. Rev. Food Sci. Nutr*. 60, 844–858. doi: 10.1080/10408398.2018.1552245

Zhang, C., Yi, X., Gao, X., Wang, M., Shao, C., Lv, Z., et al. (2020). Physiological and biochemical responses of tea seedlings (*Camellia sinensis*)

to simulated acid rain conditions. *Ecotoxicol. Environ. Saf.* 192:110315. doi: 10.1016/j.ecoenv.2020.110315

Zhang, G., Yang, J., Cui, D., Zhao, D., Li, Y., Wan, X., et al. (2020). Transcriptome and metabolic profiling unveiled roles of peroxidases in theaflavin production in black tea processing and determination of tea processing suitability. *J. Agric. Food Chem.* 68, 3528–3538. doi: 10.1021/acs.jafc.9b07737

Zhang, Q., Bi, G., Li, T., Wang, Q., Xing, Z., LeCompte, J., et al. (2022). Color shade nets affect plant growth and seasonal leaf quality of *Camellia sinensis* grown in Mississippi, the United States. *Front Nutr.* 9:786421. doi: 10.3389/fnut.2022.786421

Zhang, Q., Hu, J., Liu, M., Shi, Y., De Vos, R., and Ruan, J. (2020). Stimulated biosynthesis of delphinidin-related anthocyanins in tea shoots reducing the quality of green tea in summer. *J. Sci. Food Agric.* 100, 1505–1514. doi: 10.1002/jsfa.10158

Zhang, Q., Liu, M., Mumm, R., Vos, R., and Ruan, J. (2021). Metabolomics reveals the within-plant spatial effects of shading on tea plants. *Tree Physiol.* 41, 317–330. doi: 10.1093/treephys/tpaa127

Zhang, Q., Shi, Y., Ma, L., Yi, X., and Ruan, J. (2014). Metabolomic analysis using ultra-performance liquid chromatography-quadrupole-time of flight mass spectrometry (UPLC-Q-TOF MS) uncovers the effects of light intensity and temperature under shading treatments on the metabolites in tea. *PLoS ONE* 9:e112572. doi: 10.1371/journal.pone.0112572

Zhang, Y., Li, P., She, G., Xu, Y., Peng, A., Wan, X., et al. (2021). Molecular basis of the distinct metabolic features in shoot tips and roots of tea plants (*Camellia sinensis*): characterization of MYB regulator for root theanine synthesis. *J. Agric. Food Chem.* 69, 3415–3429. doi: 10.1021/acs.jafc.0c07572

Zhao, X., Zeng, X., Lin, N., Yu, S., Fernie, A. R., and Zhao, J. (2021). CsbZIP1-CsMYB12 mediates the production of bitter-tasting flavonols in tea plants (*Camellia sinensis*) through a coordinated activator-repressor network. *Hortic. Res.* 8:110. doi: 10.1038/s41438-021-00545-8

Zhou, J., Yu, X., He, C., Qiu, A., and Ni, D. (2020). Withering degree affects flavor and biological activity of black tea: a non-targeted metabolomics approach. *LWT* 130:109535. doi: 10.1016/j.lwt.2020.109535

Zhu, M., Li, N., Zhao, M., Yu, W., and Wu, J. L. (2017). Metabolomic profiling delineate taste qualities of tea leaf pubescence. *Food Res. Int.* 94, 36–44. doi: 10.1016/j.foodres.2017.01.026

Conflict of Interest: The authors declare that the research was conducted in the absence of any commercial or financial relationships that could be construed as a potential conflict of interest.

Publisher's Note: All claims expressed in this article are solely those of the authors and do not necessarily represent those of their affiliated organizations, or those of the publisher, the editors and the reviewers. Any product that may be evaluated in this article, or claim that may be made by its manufacturer, is not guaranteed or endorsed by the publisher.

frontiers | Frontiers in Plant Science

ORIGINAL RESEARCH
published: 11 May 2022
doi: 10.3389/fpls.2022.833682

Cytosolic *Nudix Hydrolase 1* Is Involved in Geranyl β-Primeveroside Production in Tea

Hanchen Zhou[1,2†], Shijie Wang[1†], Hao-Fen Xie[1], Guofeng Liu[1,3], Lubobi Ferdinand Shamala[1], Jingyi Pang[1], Zhengzhu Zhang[1], Tie-Jun Ling[1] and Shu Wei[1*]*

[1]State Key Laboratory of Tea Plant Biology and Utilization, Anhui Agricultural University, Hefei, China, [2]Tea Research Institute, Anhui Academy of Agricultural Sciences, Huangshan, China, [3]Henan Provincial Key Laboratory of Tea Plant Biology, Xinyang Normal University, Xinyang, China

OPEN ACCESS

Edited by:
Weiwei Wen,
Huazhong Agricultural University, China

Reviewed by:
Ziyin Yang,
South China Botanical Garden (CAS), China
Yuhua Wang,
Nanjing Agricultural University, China

***Correspondence:**
Shu Wei
weishu@ahau.edu.cn
Tie-Jun Ling
lingtj@ahau.edu.cn

[†]These authors have contributed equally to this work

Specialty section:
This article was submitted to Plant Metabolism and Chemodiversity, a section of the journal Frontiers in Plant Science

Received: 12 December 2021
Accepted: 19 April 2022
Published: 11 May 2022

Citation:
Zhou H, Wang S, Xie H-F, Liu G, Shamala LF, Pang J, Zhang Z, Ling T-J and Wei S (2022) Cytosolic Nudix Hydrolase 1 Is Involved in Geranyl β-Primeveroside Production in Tea. Front. Plant Sci. 13:833682. doi: 10.3389/fpls.2022.833682

Geraniol is a potent tea odorant and exists mainly as geranyl glycoside in *Camellia sinensis*. Understanding the mechanisms of geraniol biosynthesis at molecular levels in tea plants is of great importance for practical improvement of tea aroma. In this study, geraniol and its glycosides from tea plants were examined using liquid chromatography coupled with mass spectrometry. Two candidate geraniol synthase (*GES*) genes (*CsTPS*) and two Nudix hydrolase genes (*CsNUDX1-cyto* and *CsNUDX1-chlo*) from the tea genome were functionally investigated through gene transcription manipulation and gene chemical product analyses. Our data showed that in tea leaves, levels of geranyl β-primeveroside were dramatically higher than those of geranyl β-glucoside, while free geraniol was undetectable in this study. A tempo-spatial variation of geranyl β-primeveroside abundance in tea plants existed, with high levels in young and green tissues and low levels in mature or non-green tissues. Cytosolic CsNUDX1-cyto showed higher hydrolysis activity of geranyl-pyrophosphate to geranyl-monophosphate (GP) *in vitro* than did chloroplastidial CsNUDX1-chlo. A transgenic study revealed that expression of *CsNUDX1-cyto* resulted in significantly more geranyl β-primeveroside in transgenic *Nicotiana benthamiana* compared with non-transgenic wild-type, whereas expression of *CsNUDX1-chlo* had no effect. An antisense oligo-deoxynucleotide study confirmed that suppression of *CsNUDX1-cyto* transcription in tea shoots led to a significant decrease in geranyl β-primeveroside abundance. Additionally, *CsNUDX1-cyto* transcript levels and geranyl β-primeveroside abundances shared the same tempo-spatial patterns in different organs in the tea cultivar "Shucha Zao," indicating that *CsNUDX1-cyto* is important for geranyl β-primeveroside formation in tea plants. Results also suggested that neither of the two candidate GES genes in tea plants did not function as GES in transgenic *N. benthamiana*. All our data indicated that *CsNUDX1-cyto* is involved in geranyl β-primeveroside production in tea plants. Our speculation about possible conversion from the chemical product of CsNUDX1-cyto to geranyl β-primeveroside in plants was also discussed.

Keywords: *Camellia sinensis*, geraniol biosynthesis, geranyl β-primeveroside, Nudix hydrolase 1, tea aroma

INTRODUCTION

Geraniol is an acyclic monoterpene alcohol produced by many plant species, including rose (Baydar and Baydar, 2005) and ginger grass (*Cymbopogon martinii*; Dubey and Luthra, 2001). It is a signaling molecule which plays key roles in plant-environment interactions, such as pest repelling (Wei et al., 2004b), antimicrobial activity (Inouye et al., 2001), pollinator attraction (Magnard et al., 2015), and priming cold tolerance in adjacent plants to enhance plant resistance to cold stress (Zhao et al., 2020). Geraniol possesses a pleasant and sweet rose odor with perception threshold values ranging from 4 to 75 ppb (parts per billion; Burdock, 2001), and also exhibits various biochemical and pharmacological properties. It has been widely used for household, cosmetic and pharmaceutical products (Chen and Viljoen, 2010). Moreover, like some other plant aroma compounds, geraniol also affects human food acquisition, and aroma is a consumer preference determinant of tea products (*Camellia sinensis*). Geraniol is one of the most abundant volatiles in tea (Ho et al., 2015), and imparts its unique floral scent to different tea varieties (Wang et al., 1993; Ubota, 2002; Gui et al., 2015; Han et al., 2016; Kang et al., 2019).

Unlike the floral scent produced from intact flowers, vegetative scents are often generated after vegetative tissue damage (Dong et al., 2016). Fresh and intact tea leaves emit very few volatile odorants and possess no smell, but they may contain a substantial amount of glycosidically conjugated geraniol, which is thought to be involved in detoxification of lipophilic and membrane-toxic terpenols (Stahl-Biskup et al., 1993) and regulation of signal transduction in plants (Bock, 2015). The conjugated volatile terpenoids can be released upon tissue disruption (Takeo, 1981) and contribute to tea aroma through the processing procedure (Ho et al., 2015). In many cultivars of *Camellia sinensis*, the main glycoside of geraniol is geranyl β-primeveroside (Wang et al., 2000). It has been recently suggested that formation of geranyl β-primeveroside in tea shoots results from sequential glycosylation reactions driven by uridine diphosphate glycosyltransferases CsGT1 and CsGT2 (Ohgami et al., 2015). Biosynthesis of geraniol or its precursor is considered to be the starting point for geranyl β-primeveroside formation and accumulation in tea plants. However, no geraniol synthase (*GES*) genes have been identified in tea plants, while many *GES* genes have been found in other plant species (Degenhardt et al., 2009). Interestingly, it was once suggested that a leafhopper geraniol synthase was likely contributing to tea geraniol production and the characteristic aroma of "Oriental Beauty" tea (Zhou et al., 2019).

In plants, geraniol and other monoterpenes are usually produced by corresponding terpene synthases (TPS) through the terpenoid biosynthesis pathway. This knowledge has been applied towards enhancement of crop product aroma. For example, sweet basil geraniol synthase (*ObGES*; Iijima et al., 2004) has been successfully employed to enrich geraniol and its derivatives (Davidovich-rikanati et al., 2007) in tomato fruit for flavor improvement. Recently, a noncanonical pathway for geraniol production has been revealed in a rose hybrid, in which a cytosolic Nudix hydrolase (RhNUDX1) was found to catalyze phosphohydrolysis of geranyl pyrophosphate (GPP) into geranyl monophosphate (GP), followed by dephosphorylation with an endogenous phosphatase to produce geraniol (Magnard et al., 2015). It is of interest to find out whether the crucial genes in the canonical and/or noncanonical pathways shown in **Figure 1** are functional in tea plants for geraniol and geranyl β-primeveroside biosynthesis.

In this study, the crucial genes in the putative canonical and noncanonical pathways for biosynthesis of geraniol and its β-primeveroside in tea plants were investigated for the ultimate purpose to improve geraniol-specific tea aromas. Our data indicated that the noncanonical pathway through *CsNUDX1-cyto* is involved in tea geranyl β-primeveroside production. These findings will promote a further elucidation of tea geraniol and its glycoside production at molecular levels, and may have the potential to improve tea geraniol-related aroma through targeted molecular breeding approaches.

MATERIALS AND METHODS

Materials

The following 10 cultivars of *C. sinensis* var. *sinensis* maintained in the Guo-He Tea Germplasm Collection of this university

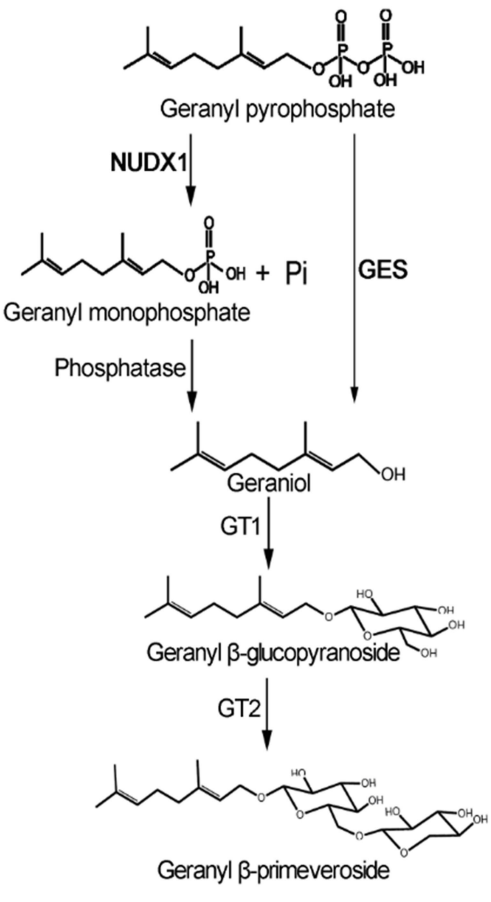

FIGURE 1 | Possible pathways for geraniol and its glycoside production in tea plants. GES, geraniol synthase; NUDX1, Nudix hydrolase1; GT1, UDP-glycosyltransferases; GT2, UDP-xylosyltransferase.

(Hefei, China) were used in this study: "Shucha Zao" ("SCZ"), "Echa NO.1" ("EC1"), "Echa NO.5" ("EC5"), "Fuding Dabai" ("FDDB"), "Mingshan Baihao" ("MSBH"), "Mingxuan 213" ("MX213"), "Wancha 91" ("WC91"), "Zhongcha 108" ("ZC108"), "Zhongcha 102" ("ZC102"), and "Zhenong 117" ("ZN117"). Tea plant samples were all excised from tea cultivars, immediately deep frozen in dry ice and then brought to the lab for storage at −80°C for further use. For transgenic studies, plants of *Nicotiana tabacum* cv. "Yunyan 85" and *Nicotiana benthamiana* were grown in pots containing a peat and vermiculite mixture (1:3, *v*/*v*) and kept in a growth chamber with a 16 h photoperiod of 150 μM m^{-2} s^{-1}, at temperatures of 22°C/25°C (night/day) and 60% relative humidity. Plants were regularly fertilized and watered.

For chemical analysis, geranyl *β*-primeveroside and linalyl *β*-primeveroside were synthesized by Na-Fu Biotech (Shanghai, China)[1] and further verified with nuclear magnetic resonance spectroscopy (**Supplementary Table S1**). Geranyl *β*-D-glucopyranoside was synthesized by Prof Zhengzhu Zhang's group at Anhui Agricultural University. Geraniol, citral, linalool, geranyl diphosphate, and geranyl monophosphate were purchased from Sigma (Shanghai, China).

Volatile Collection From Tea Infusion and Plant Tissues and GC-MS Analysis

For geraniol quantitative analysis of tea infusion, black teas were made according to a local black tea processing protocol (DB34/T1086-2009) using the four widely-grown tea cultivars ("WC91," "ZC108," "ZN117," and "SCZ") in Qimen county in the Tea Research Institution, Anhui Academy of Agricultural Sciences. Briefly, one or two leaves with one bud were plucked from Qimen, Anhui Province, China and spread indoors for 4–6 h. Subsequently, a hot wind blower was used for withering the tea leaves (for 6 h at 30°C), followed by rolling for 60 min and then fermented for 120 min at 26°C. The tea leaves were further dried and then stored at −40°C for aroma analysis. Head-space abundances of geraniol emitted from tea infusions of different black teas were analyzed together with other volatiles using gas chromatography–mass spectrometry (GC-MS) and were performed in triplicate. The tea infusion volatile collection and analysis were conducted according to Han et al. (2016) with a slight modification. Each tea sample (0.5 g) was placed into a 20 ml vial with 5 ml boiling distilled water and kept for 5 min in a water bath at 70°C. An SPME fiber (65 μM PDMS/DVB Stable Flex, Supelco Inc., Bellefonte, PA, United States) was used to collect the volatiles for 30 min, then 5 μl ethyl decanoate (0.01%) was added to the samples as the internal standard. An Agilent 7697A GC coupled to an Agilent 7890A MS system was used to conduct the volatile analysis. Linalool and geraniol identification and quantification were performed using authentic standards according to a previously published protocol running for 45.0 min (Han et al., 2016). For better resolution of volatiles collected from tea infusions, the GC program was modified to run for 59.6 min with a slow increase in temperature.

Enzymatically released geraniol analysis was conducted according to Wei et al. (2004a) with some minor modifications: 200 mg fresh samples were homogenized in liquid nitrogen and 20 U almond *β*-glucosidase (Aldrich-Sigma, Shanghai, China) was added to the homogenized leaf sample, followed by 30 min incubation at 37°C prior to headspace SPME collection and GC–MS analysis as previously described.

Database Search for Tea Candidate Genes for Geraniol Biosynthesis

RhNUDX1 (GenBank accession number JQ820249; Magnard et al., 2015) and functional geraniol synthase genes in sweet basil and another six plant species, were used as query sequences to retrieve their corresponding homologues from the tea genome (Wei et al., 2018; Xia et al., 2019) by BLASTX. Prediction of protein subcellular localization was performed using the online software ChloroP1.1.[2] Protein sequences of the two tea *NUDX1* genes obtained by BLASTX, *RhNUDX1*, and the Arabidopsis homologue (AT1G68760) were compared using ClustalW2.[3]

Prokaryotic Expression and Enzymatic Analysis

Coding sequences for the two tea C*sNUDX1* genes were subcloned into the *Nde* I/*Xho* I sites of pET15b and the functional Arabidopsis homologue AtNUDX1 was used as a positive control (Liu et al., 2018b). The resulting chimeric genes were separately introduced into the *Escherichia coli* BL21 (DE3) Rosetta strain. Prokaryotic protein expression, His-tag removal, protein purification, and *in vitro* enzymatic activity determination were carried out as previously described (Liu et al., 2018b). The reaction products were then analyzed exactly as previously described on a Shimadzu 20 AD UFLC system coupled with a Qtrap 5500 (AB Sciex, United States; Liu et al., 2018b). Five microliters of reaction product from each assay was used for product analysis using authentic standards as controls. The mass spectrometer was operated in the negative ionization mode using multiple reaction monitoring (MRM) for the transitions of *m*/*z* 313.10 to 78.9 and 233.10 to 78.9 (corresponding to GPP and GP, respectively) with the previously optimized parameters (Liu et al., 2018b).

Subcellular Localization Analysis

The two tea CsNUDIX1s were fused at their C-termini with green fluorescent protein mGFP5 (GenBank U87973.1) through recombinant polymerase chain reaction (PCR) using gene specific primers (**Supplementary Table S3**) and then subcloned into pBP121 between the *Xba* I and *Sac* I sites. The plant expression vectors containing the GFP fusion constructs were then separately introduced into *Agrobacterium tumefaciens* strain GV3101, and these were used for transient expression in *N. benthamiana* as conducted earlier (Liu et al., 2018a). GFP fluorescent signal was observed 3 days after the infiltration using an Olympus FV1000 confocal laser scanning microscope

[1]www.chemhui.cn

[2]www.cbs.dtu.dk/services/ChloroP/

[3]www.ebi.ac.uk/Tools/msa/clustalw2/

(Olympus Corporation, Beijing, China) with excitation and emission wavelengths of 484 and 507 nm, respectively.

Functional Characterization in Transgenic Tobacco Plants

Each of the coding sequences of the four candidate genes was subcloned into the *Xba* I and blunted *Sal I* sites of pCAMBIA2300 downstream of the Cauliflower mosaic virus 35S (CaMV 35S) promoter (Cambia, Canberra, Australia) and introduced into *A. tumefaciens* (GV3101) for *N. benthamiana* leaf transient expression according to Sparkes et al. (2006). The geraniol synthase gene (*ObGES*; AAR11765.1) from sweet basil (*Ocimum basilicum* L. cv. Sweet Dani; Iijima et al., 2004) was used as a positive control, and the non-transgenic wild type was used as a negative control. Transformed and control leaves were then excised for chemical analysis.

Suppression of *CsNUDX1* Expression in Tea Plants

To suppress plant endogenous target gene expression, the approach using antisense oligonucleotides (asODN) was employed, and the 10 top candidate asODNs were obtained using tea NUDX1 sequences as inputs into Soligo software (Ding and Lawrence, 2003; Dinç et al., 2011). These asODNs-CsNUDX1-cyto were synthesized by Invitrogen (Shanghai, China), and each asODN was prepared at 20 μM. "SCZ," an elite cultivar of *Camellia sinensis* var. *sinensis* with publicized genome sequence data and abundant geraniol and its glycoside, was selected for *CsNUDX1* suppression study. Field-grown tender tea shoots, each with three unfolded leaves, were excised and inserted into Eppendorf tubes containing 1 ml of 20 μM AsODN-CsNUDX1-cyto. These tea shoots were maintained in a growth chamber in which temperatures was set at 22°C/25°C (night/day), with a 16 h photoperiod at 60 $\mu M\, m^{-2}\, s^{-1}$ and 60% relative humidity. The asODN solution was added into each tube daily in amounts needed to maintain the solution volume. As a control, a 17-mer random nonsense oligonucleotide 5′-GGCGGCTAACGCTTCGA-3′ was applied according to (Dinç et al., 2011). The shoots were then sampled at different time intervals for gene expression and metabolic profiling. Biological triplicates were performed for each treatment.

Quantitative Analysis of *CsNUDX1* Transcripts

For gene transcript quantification, total RNA from different organs such as shoot stems and leaves at three different developmental stages of field-grown plants were obtained using the Takara RNAzol kit and then treated with DNaseI (Takara, Dalian, China) to remove contaminating genomic DNA. The cDNA samples were obtained by reverse transcription using the PrimerScript™ RT kit (Takara, Dalian, China). Transcript levels were quantified using quantitative real-time PCR with gene-specific primers (**Supplementary Table S3**). The reaction system was prepared using TransStart Top Green qPCR Mix Kit (TransGen, Beijing, China) following the manufacturer's instructions. The reaction volume was 25 μl, and contained 12.5 μl 2× reaction solution, 10 μM primers, 1 μl template and water. The amplification efficiencies of the test were all above 85%. The transcript data were normalized using the internal reference gene 18S rRNA. The gene transcript level was calculated using the $2^{-\Delta\Delta Ct}$ method (Livak and Schmittgen, 2001).

Chemical Analysis of Plant Extracts

The elite cultivar "SCZ" was used for tempo-spatial abundance analysis of geranyl glycosides in tea plants. Basipetally the first, second, and third leaves, and tender stems were excised from the currently growing shoots and flowers at four different developmental stages and tender roots were also excised from tea plants as shown in **Figure 2**. Moreover, variation analysis of geranyl primeveroside abundances among all the above-mentioned 10 cultivars were also performed. For chemical analysis, plant extracts were prepared and analyzed according to a previously published method (Flamini et al., 2014) with minor modifications. Briefly, homogenized plant samples (0.100 g each) were weighed to a precision of four decimal places, and were added to ice-cold methanol that was pre-acidified with 0.1% (*v*/*v*) formic acid based on the ratio of 300 μl/100 mg fresh sample weight. Supernatants were obtained after vortexing, sonication at 36 KHz (KQ-500DE, Kunshan, China) and centrifugation at 4500 RPM for 10 min (D3024, Scilogex, Marietta, GA 30062, United States). The extracts were filtered through 0.22 μm syringe filters (QFC06-SF022N13, Qingfeng, China). Plant extracts were analyzed with ultra-high performance-liquid chromatography-quadrupole time-of-flight mass spectrometry (UHPLC-Q-TOF-MS). Five microliters of the filtered extract were injected into an Agilent UHPLC 1290 Infinity II coupled to an Agilent 6545 Q-TOF-MS with an ESI source (Agilent Technologies, Santa Clara, CA) in the positive or negative ionization mode. Chromatographic separation was performed using a Zorbax reverse-phase column (RRHD SB-C18, 3×150 mm, 1.8 μM; Agilent Technologies, Santa Clara, CA) using the gradient elution program and Q-TOF conditions as per Flamini et al. (2014). Compounds were identified based on the comparison of accurate retention times and MS data between samples and authentic standards. The intensity of the identified compound in the samples was represented using the corresponding peak area normalized to the amount of fresh plant tissues.

Statistical Analysis

All quantitative analyses were performed with at least three biological replicates, and statistical differences among the means were analyzed using ANOVA followed by the Bonferroni test (SPSS statistics 19.0 software). A correlation analysis between the expression levels of *CsNUDX1*, *CsGT1*, and *CsGT2* genes and the abundance values of geranyl *β*-primeveroside was also performed using the Pearson method in SPSS software.

RESULTS

Free Geraniol in Tea Infusion and Tempo-Spatial Patterns of Geranyl Glycosides in Tea Plants

Black tea infusions made from tea cultivars "WC91," "ZC108," "ZN117," and "SCZ" released high levels of geraniol into the

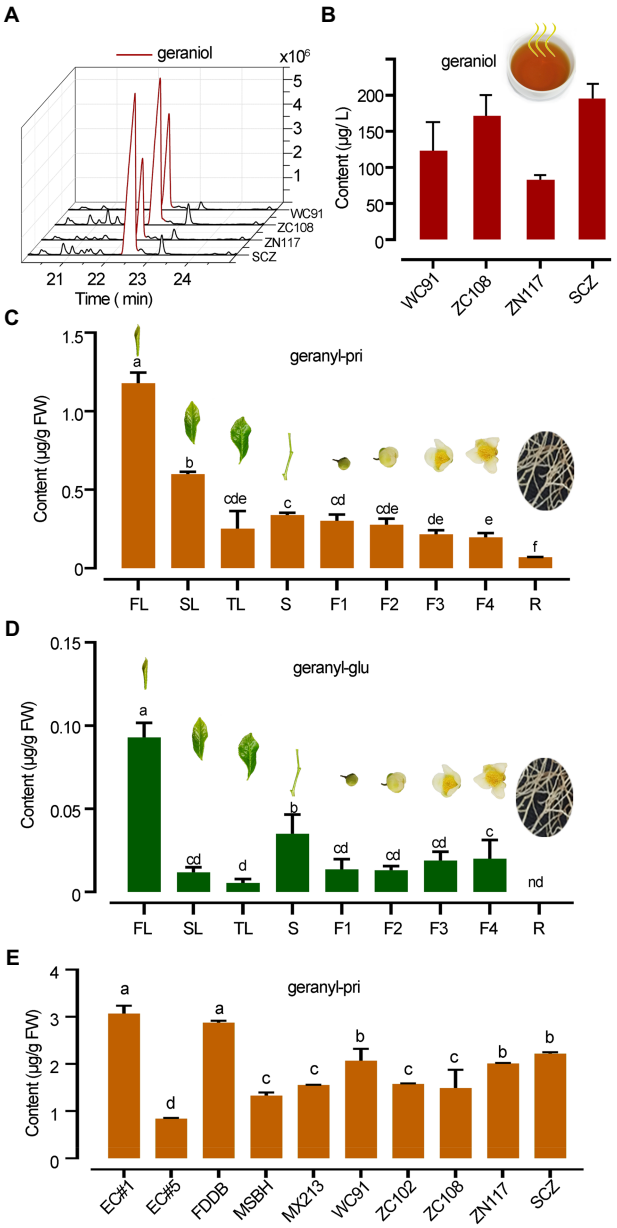

FIGURE 2 | Distinct abundance difference in geraniol and its glycosides in tea. **(A,B)** GC chromatography and quantitative column presentation of geraniol SPME collected in tea infusion headspace of different teas. **(C,D)** The abundances of geranyl primeveroside (geranyl-pri) and geranyl glucoside (geranyl-glu) in different organs of "SCZ" tea plants. FL, SL, and TL, first, second and third leaves; S, tender shoot stem; F1–F4, flowers at different developmental stages; R, tender roots. **(E)** Quantification of geranyl primeveroside in different tea cultivars. Columns with different letters had significant differences in the abundances of the same compound ($p < 0.05$) using the statistical method described in text. EC1, "Echa NO.1"; EC5, "Echa NO.5"; FDDB, "Fuding Dabai"; MSBH, "Mingshan Baihao"; MX213, "Mingxuan 213"; WC91, "Wancha 91"; ZC102, "Zhongcha 102"; ZC108, "Zhongcha 108"; ZN117, "Zhenong 117"; SCZ, "Shucha Zao."

headspace, ranging from 73.0 to 195.0 $\mu g\,L^{-1}$ (**Figures 2A,B**). Qualitative analysis identified geraniol from the infusion of black teas, geranyl glucoside and primeveroside in freshly excised tea leaves by comparing the chromatography and mass spectrometry data obtained from plant samples and authentic standards (**Supplementary Table S1**; **Supplementary Figures S1, S2**). However, in this study, geraniol was not detected in the methanol extracts of plant tissues despite having over 90% recovery rate using methanol as a geraniol solvent. A quantitative analysis further revealed that the mean abundance of geranyl β-primeveroside in tea plants was much greater than that of geranyl β-glucoside, which was only 7.89% of primeveroside in first leaf of tea plants. Young leaves contained the highest levels of geranyl β-primeveroside, while tender roots contained the lowest levels and those in the stem and fully opened flowers were in between, indicating a tempo-spatial pattern of geranyl glycosides in tea plants (**Figure 2C**). Significantly less amounts of geranyl β-glucoside were also noted in different tea organs (**Figure 2D**). Moreover, the abundances of geranyl β-glucoside in the 10 tea cultivars were quantified, and all were at quite high levels with an average of 1.88 $\mu g\,g^{-1}$ FW (Fresh weight); however, the abundances among these cultivars varied significantly (p, 0.05), and ranged from 0.84 $\mu g\,g^{-1}$ FW to 3.07 $\mu g\,g^{-1}$ FW (**Figure 2E**). Our data indicated that for many tea cultivars, geranyl β-glucoside accumulated in a tempo-spatial pattern and was the main glycoside of geraniol, whereas free geraniol was undetectable.

Functional Characterization of Crucial Genes in Canonical and Noncanonical Geraniol Biosynthetic Pathways

Two tea homologues (TEA006189 and TEA000568) of rose RhNUDX1 (GenBank: AFW17224.1), a critical enzyme for geraniol production in rose flowers through a noncanonical pathway (Magnard et al., 2015), were retrieved from the tea genome through a BLASTP search. Both tea genes possessed the conserved Nudix box (GX5EX7REUXEEXGU, where U is a bulky hydrophobic residue and X is any residue; Liu et al., 2018b), indicating that both were members of Nudix hydrolase family. The online prediction indicated that TEA000568 contained a putative 70 amino acid chloroplast transit peptide, while TEA006189 contained no transit peptide; thus, these are presumably being targeted to the chloroplast and the cytoplasm, respectively. A *GFP* reporter gene was fused in-frame at the 3′ end of both *CsNUDX1* genes and then introduced into plant leaves along with cytoplasm control of GFP and putatively plastidial but truncated *CsNUDX1* with removed transit peptide (**Figure 3A**). GFP fused with putatively cytoplasmic CsNUDX1 exhibited green signals surrounding the cytoplasm, similar as the green signals of cytosolic GFP (35S-GFP). Interestingly, green signals of GFP fused with truncated CsNUDX1 without the putative transit peptide (CsNUDX1-Δ70chlo-GFP) displayed a similar cytosolic pattern of green signals in the merged view. On the contrary, GFP fused with putatively plastidial CsNUDX1 displayed its green signals with distinct subcellular location, well overlapped with red signals of chloroplasts, suggesting that it was a true chloroplastidial protein with a transit peptide containing 70 amino acid residues. Our data confirmed the predicted subcellular localizations of the two NUDX1 proteins.

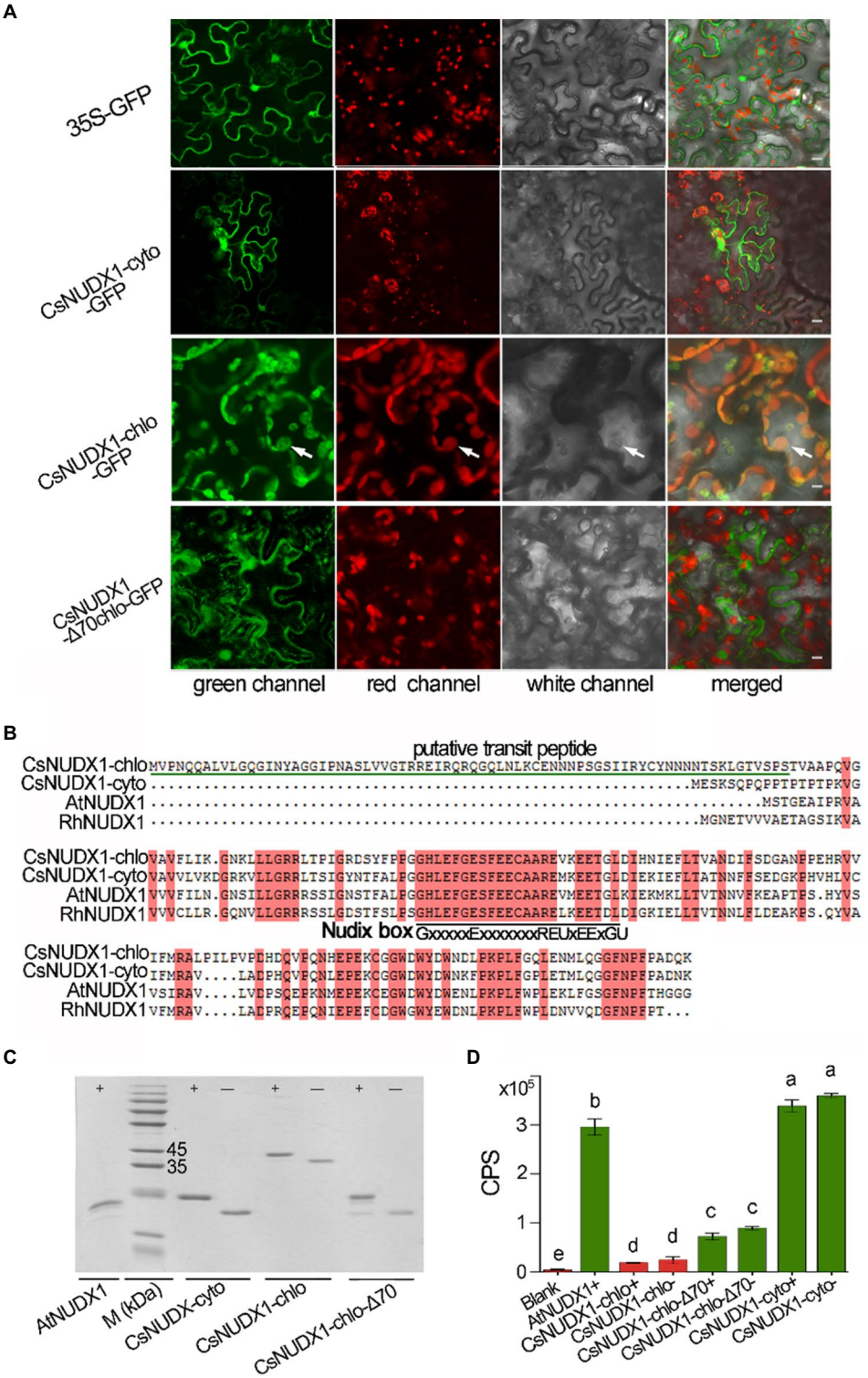

FIGURE 3 | Characterization of *CsNUDX1-cyto* and *CsNUDX1-chlo*. **(A)** Subcellular localization analyses using CsNUDX1 fused with green fluorescent protein mGFP5 (GenBank U87973.1). White arrows indicate chloroplasts. All constructs were expressed in abaxial leaf surface except CsNUDX1-chlo-GFP expressed in adaxial surface. 35S-GFP, GFP gene alone driven by 35S promoter; CsNUDX1-Δ70chlo-GFP, GFP fused CsNUDX1-chlo without putative transit peptides. Scale, 10 μm. **(B)** Tea proteins aligned with the homologues of Arabidopsis (NP_177044.1) and rose (AFW17224.1). **(C)** SDS- polyacrylamide gel electrophoresis of *Escherichia coli* expressed *CsNUDX1* with/without His-tag and Arabidopsis *AtNUDX1* with His-tag as control. M (kDa), a protein marker (kilo Dalton); CsNUDX1-chlo-Δ70, CsNUDX1-chlo with deleted the putative transit peptide containing 70 amino acid residues at its N-terminus. **(D)** The levels of *in vitro* product geranyl

FIGURE 3 | monophosphate (GP) produced by CsNUDIX1-cyto and CsNUDX-chlo and their recombinant variants. Columns with different letters had significant differences in the abundances of product GP ($p < 0.05$). CPS, count per second of the product ion detected. Blank, without any protein added in the reaction mixture; Protein variant plus "+" or "−" denotes protein with or without the His-tag.

Thus, the two genes were thereafter named as *CsNUDX1-chlo* for *TEA000568* and *CsNUDX1-cyto* for *TEA006189*. The respective CsNUDX1-cyto and CsNUDX1-chlo proteins contain 156 and 220 amino acid residues and share high similarities to the functional homologues in Arabidopsis and rose (**Figure 3B**). CsNUDX1-cyto and CsNUDX1-chlo had 78 and 64% similarity with the RhNUDX1 protein, respectively. For the *in vitro* functional assay, *CsNUDX1-cyto* and *CsNUDX1-chlo* were expressed in *E. coli* and corresponding recombinant proteins with or without an N-terminally linked His-tag were obtained (**Figure 3C**). The Arabidopsis AtNUDX1 protein with a His-tag was also obtained as positive control. Results showed that CsNUDX1-cyto possessed a stronger GPP to GP hydrolysis activity than the Arabidopsis AtNUDX1 ($p < 0.05$; **Figure 3D**). Nevertheless, the hydrolysis activity of CsNUDX1-chlo with/without the His-tag was barely detectable (**Figure 3D**). CsNUDX1-chlo-Δ70 (with the putative transit peptide removed) exhibited an increased activity compared to the full length CsNUDX1-chlo, but its activity was still weak compared to CsNUDX1-cyto (**Figure 3D**).

We also made further effort to identify tea *GES* genes. *ObGES*, together with other seven functional geraniol synthase genes, were applied as query sequences to search for homologous candidate *GES* genes in the tea genome. The highest similarities were found for *CSA008212* (49% with the *Cinnamomum tenuipilum* homologue) and *TEA014987* (44% with that of *Catharanthus roseus*; **Supplementary Table S2**). The two candidate genes were cloned, sequenced, and transiently expressed in *N. benthamiana*, which has proved an effective approach for examination of GES activities *in planta* (Dong et al., 2013). However, compared to the buffer control, no significantly increased amounts of geraniol or its primeveroside were detected in the transgenic leaves (**Supplementary Figure S3**), suggesting that neither of the two possessed detectable catalytic activities for production of geraniol or its primeveroside.

Transgenic Study on the Function of *CsNUDX1-cyto* and *CsNUDX1-chlo in Planta*

For further functional investigation of the two *CsNUDX1* genes in plants, *CsNUDX1-cyto* and *CsNUDX1-chlo* were each transiently expressed under control of the CaMV 35S promoter in *N. benthamiana* (*CsNUDX1-cyto*$^+$ or *CsNUDX1-chlo*$^+$), while *ObGES* was also expressed in the same transgenic system (*ObGES*$^+$) as a positive control and non-transgenic wild type (WT) as negative control. Geranyl *β*-primeveroside and geranyl *β*-glucoside were identified in the transgenic and non-transgenic leaves of *N. benthamiana* (**Figure 4A**). Quantitative analysis indicated that both transgenic leaves *CsNUDX1-cyto*$^+$ and *ObGES*$^+$ contained significantly higher levels of geranyl *β*-primeveroside and geranyl *β*-glucoside than WT, whereas there were no differences in the levels of two geranyl glycosides between *CsNUDX1-chlo*$^+$ and wildtype (**Figure 4B**). Furthermore, compared to the wild type and *CsNUDX1-chlo*$^+$ samples, significantly higher levels of released geraniol were detected from both *CsNUDX1-cyto*$^+$ and *ObGES*$^+$ leaf samples following glycoside hydrolysis with exogenous glucosidase (**Figures 4C,D**). Moreover, increased levels of geraniol derivatives citral and neral, as well as some other volatiles were also detected from both *CsNUDX1-cyto*$^+$ and *ObGES*$^+$ leaf samples, but not from *CsNUDX1-chlo*$^+$ samples. Without glycoside hydrolysis, free geraniol (as a fragment ion with *m/z* 137.133 in positive mode) was undetectable in any tested plant tissue extracts, even in *ObGES*$^+$ extracts in which the chemical product of *ObGES* has been demonstrated to be geraniol (Iijima et al., 2004). The precursor ion of GP (*m/z* 233.093), which is the *in vitro* product of CsNUDX1 found in this study, was not detected either. These results revealed that expression of *CsNUDX1-cyto* in transgenic leaves of *N. benthamiana* significantly increased levels of geranyl primeveroside, whereas expression of *CsNUDX1-chlo* did not lead to an increase. After CsNUDX1-cyto mediates the first step, production of geranyl primeveroside most likely results from chemical conversion *via* other endogenous enzymes.

Functional Characterization of *CsNUDX1-cyto* in Tea Plants

Since tea plants are recalcitrant to *Agrobacterium*-mediated genetic transformation and *CsNUDX1-chlo* had a minor effect on geranyl *β*-primeveroside accumulation *in planta*, only *CsNUDX1-cyto* was functionally validated in tea plants using an improved gene suppression method with gene-specific asODNs. A mixture of 10 asODNs, all specifically complementary to the fragments (139–165 bp or 180–200 bp) near the 5′ end of *CsNUDX1-cyto*, was used to treat excised tender shoots of "SCZ" (**Figure 5A**). Quantitative real time PCR (qPCR) results showed that a 24 h treatment with asODN-CsNUDX1-cyto resulted in a significant transcript reduction ($p < 0.01$) of the target *CsNUDX1-cyto* compared to treating with the random nonsense oligo (CK; **Figure 5B**). Abundance of geranyl *β*-primeveroside in the treated tea leaves was significantly reduced ($p < 0.01$; **Figure 5C**). Notably, the abundance of linalyl *β*-primeveroside was unchanged ($p > 0.05$; **Figure 5D**), indicating these AsODNs specifically suppressed the target gene. Our data demonstrated that CsNUDX1-cyto functions as a key catalyst for production of geraniol and its primeveroside in tea shoots, as revealed in the transgenic tobacco plants.

In addition, a tempo-spatial transcriptional pattern of *CsNUDX1-cyto* in leaves, stem, flowers and roots in "SCZ' plants was noted (**Figure 5E**). The highest transcript level was found in buds, followed by those in the other green tissues (young and mature leaves, and stems), whereas the lowest levels were in non-green tissues: fully opened flowers and

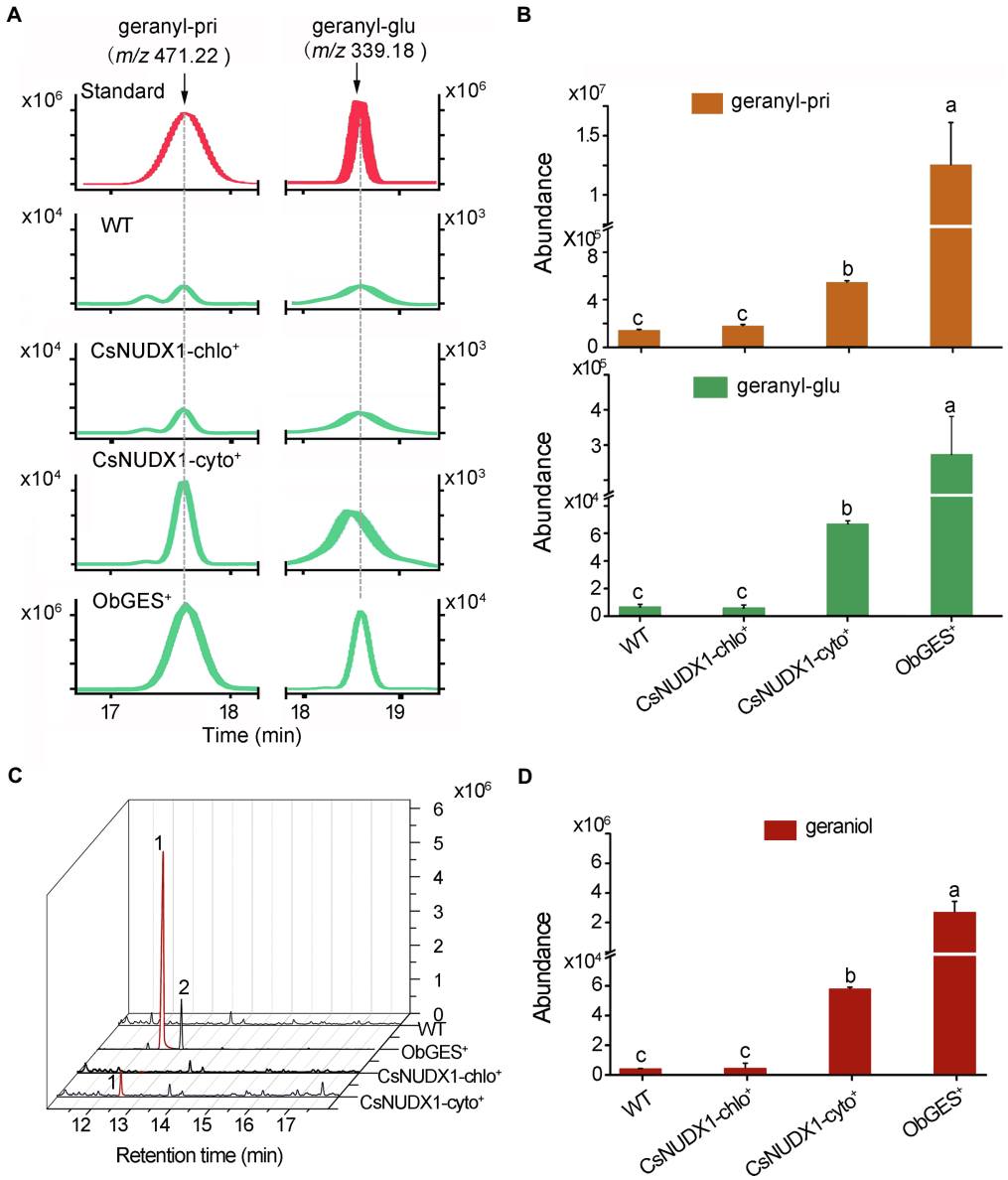

FIGURE 4 | Functional characterization of the two tea *CsNUDX1s*. **(A)** Liquid chromatographs of geranyl glucoside, primeveroside found in the transgenic *Nicotiana benthamiana* leaves transiently overexpressing *CsNUDX1-cyto*, *CsNUDX1-chlo*, *ObGES* respectively, compared to non-transgenic wild-type (WT). The compounds were identified by comparing their corresponding unique ions (*m/z*) and retention times to those of the authentic standards. **(B)** Quantitative analysis of geranyl glucoside and primeveroside in different transgenic leaves. Columns with the same letters had no significant difference ($p > 0.05$). **(C)** Gas chromatograph of geraniol headspace-SPME collected from different transgenic and non-transgenic leaves after hydrolysis of glycosides with exogenous addition of glucosidase. Peaks 1 and 2, represent geraniol and citral, respectively; Geranyl-pri, geranyl *β*-primeveroside; geranyl-glu, geranyl *β*-glucoside; *ObGES*$^+$, *CsNUDX1-cyto*$^+$, and *CsNUDX1-chlo*$^+$, the transgenics overexpressing corresponding genes; WT, non-transgenic wild-type. **(D)** Quantitative column presentation of geraniol abundances with the data obtained from **(C)**.

tender roots. Interestingly, a similar pattern of differential geranyl primeveroside abundances were found for the above organs of "SCZ" (**Figures 2C**, **5E**). The amounts of geranyl-primeveroside and transcript levels of *CsNUDX1-cyto* in the tested organs of "SCZ" were highly correlated in a tempo-spatial manner, as indicated by the Pearson correlation coefficient of 0.864.

DISCUSSION

Geraniol is a potent odorant of many tea products and is present as glycosidic conjugates in tea plants. In this study, we found that the levels of geraniol released from tea infusion are well above its perception threshold of 75 ppb (Burdock, 2001), and the finding that geranyl *β*-primeveroside was the

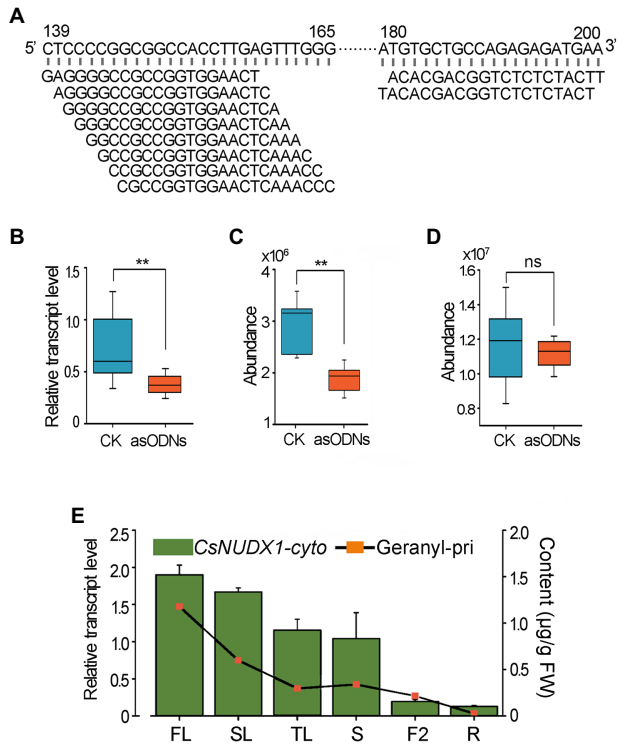

FIGURE 5 | Functional characterization of *CsNUDX1-cyto* in tea plants using AsODNs approach. **(A)** Top 10 asODNs retrieved using Soligo software (Ding and Lawrence, 2003) for *CsNUDX1-cyto* suppression experiments. **(B)** A significant reduction (**$p < 0.01$) in the transcript level of *CsNUDX1-cyto* after asODNs treatment. **(C)** A significant reduction (**$p < 0.01$) in the abundance of geranyl β-primeveroside in the treated tea tender shoots ($p < 0.01$). **(D)** No significant change (ns) in the abundance of linalyl β-primeveroside in treated tea shoots compared to control ($p > 0.05$). **(E)** Highly correlated tempo-spatial transcript levels of *CsNUDX1-cyto* and the abundances of geranyl β-primeveroside in tea plants (correlation coefficient of 0.864). FL, SL, and TL, first, second, and third leaves; S, tender shoot stem; F2, flowers at stage 2, slightly opened; R, tender roots. *CsNUDX1-cyto*, Transcript levels of *CsNUDX1-cyto* in different organs of "SCZ" plants; Geranyl-pri, Abundances of geranyl primeveroside in different organs of "SCZ" plants.

main geranyl glycoside present in tea leaves agreed with previous findings (Wang et al., 2000). Our combined evidence from *in vitro* enzymatic assays, gene manipulation as well as gene chemical product analysis further revealed that geranyl β-primeveroside was enhanced due to the action of CsNUDX1-cyto, and the downstream steps likely occurred through endogenous chemical conversion by other enzymes, starting from GP-derived geraniol to geranyl β-primeveroside.

In tea plants, two tea homologous variants of *RhNUDX1*, a critical gene in the noncanonical pathway for geraniol biosynthesis in rose (Magnard et al., 2015), were identified in this study. Our *in vitro* assays revealed that cytosolic CsNUDX1-cyto was capable of hydrolyzing GPP to GP, while chloroplastidial CsNUDX1-chlo exhibited limited GPP hydrolysis activity even after removal of its putative transit peptide (70 amino acid residues), which is common to many other nucleus-encoded chloroplast proteins in plants (Archer and Keegstra, 1990). Protein sequence alignment further revealed that CsNUDX1-cyto shared the same amino acid residues at positions L38 and P129 as the Arabidopsis AtNUDX1 (NP_177044.1). However, CsNUDX1-chlo possessed different amino acid residues at these positions; the L38P and P129Q substitutions in CsNUDX1-chlo were most likely the reason for the significant reduction in activity of CsNUDX1-chlo, as mutations of these two positions in the Arabidopsis AtNUDIX1 almost completely abolishes the activity (Liu et al., 2018b). Thus, it may be possible that the significant difference in hydrolytic activity between the two tea NUDX1 proteins results from their protein sequences. However, a more recent finding indicated that a plastidial Nudix1 from *Tanacetum cinerariifolium* has high specificity for chrysanthemyl pyrophosphate, rather than GPP (Li et al., 2020); thus, tea CsNUDX1-chlo may be able to hydrolyze a different substrate other than GPP.

In this study, transgenic leaves of *N. benthamiana* expressing *CsNUDX1-cyto* produced significantly more geranyl primeveroside than the non-transgenic wild type, whereas that expressing *CsNUDX1-chlo* had the same geranyl primeveroside levels as wild type. This indicates that the distinct *in vitro* hydrolytic activities of the two CsNUDX1s would be the consequence of their sequence-dependent functions rather than their varying subcellular locations in plant cells, as there are GPP pools in both the cytoplasm and chloroplasts (Dong et al., 2013; Ueoka et al., 2020). Moreover, transgenic data also suggested that the chemical conversion of the *CsNUDX1-cyto* product GP occurred in the transgenic plants. Compared to non-transgenic wild type, expression of *ObGES* in transgenic *N. benthamiana* leaves, whose chemical product is geraniol (Iijima et al., 2004), resulted in a significant increase in geranyl β-primeveroside instead of geraniol. This indicated that the geraniol produced from *ObGES* overexpression was effectively converted into geranyl β-primeveroside in the transgenic *ObGES*$^+$ *N. benthamiana* leaves due to endogenous glycosylation by the host plant. Expression of *CsNUDX1-cyto* also enhanced geranyl β-primeveroside production in transgenic *N. benthamiana* leaves, suggesting that the same chemical conversion from geraniol to the primeveroside would also occur in *CsNUDX1-cyto* expressing transgenics. Meanwhile, GP was verified *in vitro* as the direct chemical product of CsNUDX1-cyto, and was most likely converted to geraniol due to the action of unknown endogenous phosphatases as suggested in a rose hybrid (Magnard et al., 2015). Interestingly, *CsNUDX1-cyto* enhancement of geranyl β-primeveroside was comparatively less than that produced in *ObGES* expressed transgenics ($p < 0.05$), and this was probably because *CsNUDX1-cyto* is less effective than *ObGES*. Our data also showed that expression of *CsNUDX1-chlo*, which was unable to convert GPP to GP *in vitro*, did not result in an increase in either geraniol or geranyl primeveroside in transgenic *CsNUDX1-chlo*$^+$; this confirms in an opposite way that chemical conversion from geraniol to its primeveroside did not occur when GP production was not enhanced. Furthermore, after addition of exogeneous glycosidase to release glycosidically bound volatiles, there was increased emission of geraniol and its derivative citral in both transgenics *CsNUDX1-cyto*$^+$ and *ObGES*$^+$ relative to the non-transgenic control. This not only confirms the occurrence

of the endogenous glycosylation of geraniol in both transgenics, but also suggests that in addition to chemical conversion from GP to geraniol and to geranyl primeveroside, other geraniol chemical modifications such as geraniol oxidation would also be occurring. All our transgenic study results clearly demonstrated that *CsNUDX1-cyto* is involved in geranyl primeveroside formation through the intermediate metabolites GP, geraniol and subsequent geraniol glycosylation, although the endogenous enzymes catalyzing these reactions have yet to be identified.

Furthermore, functional validation of *CsNUDX1-cyto* in tea plants was conducted in this study using an improved gene suppression method with gene-specific asODNs (Liu et al., 2018a) to overcome the recalcitrance of tea plants to *Agrobacterium*-mediated genetic transformation. Our data confirmed that geranyl *β*-primeveroside is the chemical product of *CsNUDX1-cyto* in tea plants, as it was in transgenics *CsNUDX1-cyto*$^{+}$ or *ObGES*$^{+}$. Additionally, similar tempo-spatial patterns of *CsNUDX1-cyto* expression and geranyl primeveroside abundance in the plants of the tea cultivar "SCZ" were found with high levels in young and green tissues and low levels in fully opened flowers and roots. The gene expression levels and geranyl *β*-primeveroside abundances among different tissues were well correlated. These data suggested that in tea plants, *CsNUDX1-cyto* could be involved in geraniol and its primeveroside biosynthesis in a noncanonical pathway.

More recently, geraniol has been reported to be sequentially glycosylated into glucoside and primeveroside due to the high substrate selectivity of the endogenous glycosyl transferases GT1 (to geraniol) and GT2 (to geranyl glucoside), respectively (Ohgami et al., 2015). We quantified transcript levels of *CsGT1*, and *CsGT2* and abundances of geranyl primeveroside in young and mature leaves as well as in tender roots in the plants of tea cultivars "Zijuan" and "WC91," and found that their transcript levels were well correlated with the primeveroside abundance in "Zijuan" (correlation coefficients were 0.976 and 0.997 for *CsGT1* and *CsGT2*, respectively) and in "WC91" (0.866 and 0.930 for *CsGT1* and *CsGT2*, respectively); thus, our data support the observation of Ohgami et al. (2015). In the genome of *N. benthamiana*,[4] multiple homologous genes of *CsGT1* and *CsGT2* were found. Four genes *NbS00016902g0104.1*, *NbS00057453g0005.1*, *NbS00044548g0005.1*, and *NbS00057453g0006.1* are homologues of *GT1* and *NbS00006161g0001.1* and *NbS00007621g0001.1* are those of *GT2*. All shared high identities in protein sequences (>60%). These are likely involved in biosynthesis of geranyl primeveroside in *N. benthamiana*. Further investigations through gene manipulation are required to validate the roles of the two sugar moiety transferase genes in geranyl *β*-primeveroside production in tea plants.

So far, no functional geraniol synthase (*GES*) genes acting in the canonical pathway in tea plants have been reported. In the current work, two of the tea *GES* candidates found through homology searches did not result in any increase in geraniol and its glycoside abundances in the transient transgenic study. Functional characterization of all annotated monoterpene synthase genes (Zhou et al., 2020) is underway to search for tea geraniol synthase, since the chemical function of a terpene synthase cannot be predicted because subtle changes in protein sequence could result in distinct product (Bohlmann et al., 1999). However, no *GES* gene has been reported in *Arabidopsis* thus far (Chen et al., 2011), though *Arabidopsis* possesses detectable geranyl glycoside (Sugimoto et al., 2015); thus, one cannot exclude the possibility that the canonical terpene pathway for geraniol biosynthesis *via* GES may not exist in some plants.

[4]solgenomics.net/organism/Nicotiana_benthamiana/genome

DATA AVAILABILITY STATEMENT

The original contributions presented in the study are included in the article/**Supplementary Material**, further inquiries can be directed to the corresponding authors.

AUTHOR CONTRIBUTIONS

SW, T-JL, GL, and HZ conceived the project. HZ and SW did most of the experiments. T-JL and JP did the prokaryotic expression and *in vitro* assays. H-FX and T-JL verified authentic standards using nuclear magnetic resonance spectroscopy. ZZ completed geranyl glucoside synthesis. LS completed the manuscript draft. T-JL and SW finalized the manuscript. All authors contributed to the article and approved the submitted version.

FUNDING

The research described here was funded by the National Natural Science Foundation of China (Grant Number 31370687) to SW and (Grant Number 32002096) to HZ.

ACKNOWLEDGMENTS

Prof. Ping Yin, Drs. Jian Liu, and Delin Zhang at Huazhong Agricultural University helped with the prokaryotic expression and *in vitro* assays. Jie Yu and Kun Liu at Anhui Agricultural University have made a great contribution with geranyl glucoside synthesis. We thank Margaret Y. Gruber and Min-Jun Gao at Agriculture and Agri-Food Canada for their critical review of this manuscript.

SUPPLEMENTARY MATERIAL

The Supplementary Material for this article can be found online at: https://www.frontiersin.org/articles/10.3389/fpls.2022.833682/full#supplementary-material

REFERENCES

Archer, E. K., and Keegstra, K. (1990). Current views on chloroplast protein import and hypotheses on the origin of the transport mechanism. *J. Bioenerg. Biomembr.* 22, 789–810.

Baydar, H., and Baydar, N. G. (2005). The effects of harvest date, fermentation duration and tween 20 treatment on essential oil content and composition of industrial oil rose (*Rosa damascena* Mill.). *Ind. Crop. Prod.* 21, 251–255. doi: 10.1016/j.indcrop.2004.04.004

Bock, K. W. (2015). The UDP-glycosyltransferase (UGT) superfamily expressed in humans, insects and plants: animal-plant arms-race and co-evolution. *Biochem. Pharmacol.* 99, 11–17. doi: 10.1016/j.bcp.2015.10.001

Bohlmann, J., Phillips, M., Ramachandiran, V., Katoh, S., and Croteau, R. (1999). cDNA cloning, characterization, and functional expression of four new monoterpene synthase members of the Tpsd gene family from grand fir (*Abies grandis*). *Arch. Biochem. Biophys.* 368, 232–243. doi: 10.1006/abbi.1999.1332

Burdock, G. (2001). *Fenaroli's Handbook of Flavor Ingredients. 4th Edn*. Boca Raton, FL: CRC Press.

Chen, F., Tholl, D., Bohlmann, J., and Pichersky, E. (2011). The family of terpene synthases in plants: a mid-size family of genes for specialized metabolism that is highly diversified throughout the kingdom. *Plant J.* 66, 212–229. doi: 10.1111/j.1365-313X.2011.04520.x

Chen, W., and Viljoen, A. M. (2010). Geraniol – a review of a commercially important fragrance material. *S. Afr. J. Bot.* 76, 643–651. doi: 10.1016/j.sajb.2010.05.008

Davidovich-rikanati, R., Sitrit, Y., Tadmor, Y., Iijima, Y., Bilenko, N., Bar, E., et al. (2007). Enrichment of tomato flavor by diversion of the early plastidial terpenoid pathway. *Nat. Biotechnol.* 25, 899–901. doi: 10.1038/nbt1312

Degenhardt, J., Köllner, T. G., and Gershenzon, J. (2009). Monoterpene and sesquiterpene synthases and the origin of terpene skeletal diversity in plants. *Phytochemistry* 70, 1621–1637. doi: 10.1016/j.phytochem.2009.07.030

Dinç, E., Tóth, S. Z., Schansker, G., Ayaydin, F., Kovács, L., Dudits, D., et al. (2011). Synthetic antisense oligodeoxynucleotides to transiently suppress different nucleus- and chloroplast-encoded proteins of higher plant chloroplasts. *Plant Physiol.* 157, 1628–1641. doi: 10.1104/pp.111.185462

Ding, Y., and Lawrence, C. E. (2003). A statistical sampling algorithm for RNA secondary structure prediction. *Nucleic Acids Res.* 31, 7280–7301. doi: 10.1093/nar/gkg938

Dong, F., Fu, X., Watanabe, N., Su, X., and Yang, Z. (2016). Recent advances in the emission and functions of plant vegetative volatiles. *Molecules* 21:124. doi: 10.3390/molecules21020124

Dong, L., Miettinen, K., Goedbloed, M., Verstappen, F. W. A., Voster, A., Jongsma, M. A., et al. (2013). Characterization of two geraniol synthases from *Valeriana officinalis* and *Lippia dulcis*: similar activity but difference in subcellular localization. *Metab. Eng.* 20, 198–211. doi: 10.1016/j.ymben.2013.09.002

Dubey, V. S., and Luthra, R. (2001). Biotransformation of geranyl acetate to geraniol during palmarosa (*Cymbopogon martinii*, Roxb. wats. var. *motia*) inflorescence development. *Phytochemistry* 57, 675–680. doi: 10.1016/S0031-9422(01)00122-4

Flamini, R., De Rosso, M., Panighel, A., Dalla Vedova, A., De Marchi, F., and Bavaresco, L. (2014). Profiling of grape monoterpene glycosides (aroma precursors) by ultra-high performanceliquid chromatography-high resolution mass spectrometry (UHPLC/QTOF). *J. Mass Spectrom.* 49, 1214–1222. doi: 10.1002/jms.3441

Gui, J., Fu, X., Zhou, Y., Katsuno, T., Mei, X., and Deng, R. (2015). Does enzymatic hydrolysis of glycosidically bound volatile compounds really contribute to the formation of volatile compounds during the Oolong tea manufacturing process? *J. Agric. Food Chem.* 63, 6905–6914. doi: 10.1021/acs.jafc.5b02741

Han, Z. X., Rana, M. M., Liu, G. F., Gao, M. J., Li, D. X., Wu, F. G., et al. (2016). Green tea flavour determinants and their changes over manufacturing processes. *Food Chem.* 212, 739–748. doi: 10.1016/j.foodchem.2016.06.049

Ho, C., Zheng, X., and Li, S. (2015). Tea aroma formation. *Food Sci. Hum. Wellness* 4, 9–27. doi: 10.1016/j.fshw.2015.04.001

Iijima, Y., Gang, D. R., Fridman, E., Lewinsohn, E., and Pichersky, E. (2004). Characterization of geraniol synthase from the peltate glands of sweet basil. *Plant Physiol.* 134, 370–379. doi: 10.1104/pp.103.032946

Inouye, S., Takizawa, T., and Yamaguchi, H. (2001). Antibacterial activity of essential oils and their major constituents against respiratory tract pathogens by gaseous contact. *J. Antimicrob. Chemother.* 47, 565–573. doi: 10.1093/jac/47.5.565

Kang, S., Yan, H., Zhu, Y., Liu, X., Lv, H. P., Zhang, Y., et al. (2019). Identification and quantification of key odorants in the world's four most famous black teas. *Food Res. Int.* 121, 73–83. doi: 10.1016/j.foodres.2019.03.009

Li, W., Lybrand, D. B., Xu, H., Zhou, F., Last, R. L., and Pichersky, E. (2020). A trichome-specific, plastid-localized Tanacetum cinerariifolium Nudix protein hydrolyzes the natural pyrethrin pesticide biosynthetic intermediate *trans*-chrysanthemyl diphosphate. *Front. Plant Sci.* 11:482. doi: 10.3389/fpls.2020.00482

Liu, J., Guan, Z., Liu, H., Qi, L., Zhang, D., Zou, T., et al. (2018b). Structural insights into the substrate recognition mechanism of *Arabidopsis thaliana* GPP-bound NUDX1 for noncanonical monoterpene biosynthesis. *Mol. Plant* 11, 218–221. doi: 10.1016/j.molp.2017.10.006

Liu, G. F., Liu, J. J., He, Z. R., Wang, F. M., Yang, H., Yan, Y. F., et al. (2018a). Implementation of CsLIS/NES in linalool biosynthesis involves transcript splicing regulation in *Camellia sinensis*. *Plant Cell Environ.* 41, 176–186. doi: 10.1111/pce.13080

Livak, K. J., and Schmittgen, T. D. (2001). Analysis of relative gene expression data using real-time quantitative PCR and the 2-CT method. *Methods* 25, 402–408. doi: 10.1006/meth.2001.1262

Magnard, J., Roccia, A., Caissard, J., Vergne, P., Sun, P., Hecquet, R., et al. (2015). Biosynthesis of monoterpene scent compounds in roses. *Science* 349, 81–83. doi: 10.1126/science.aab0696

Ohgami, S., Ono, E., Horikawa, M., Murata, J., Totsuka, K., Toyonaga, H., et al. (2015). Volatile glycosylation in tea plants: sequential glycosylations for the biosynthesis of aroma b-primeverosides are catalyzed by two *Camellia sinensis* glycosyltransferases. *Plant Physiol.* 168, 464–477. doi: 10.1104/pp.15.00403

Sparkes, I. A., Runions, J., Kearns, A., and Hawes, C. (2006). Rapid, transient expression of fluorescent fusion proteins in tobacco plants and generation of stably transformed plants. *Nat. Protoc.* 1, 2019–2025. doi: 10.1038/nprot.2006.286

Stahl-Biskup, E., Holthuijzen, F. I. J., Stengele, M., and Schulz, G. (1993). Glycosidically bound volatiles—a review 1986–1991. *Flavour Fragr. J.* 8, 61–80. doi: 10.1002/ffj.2730080202

Sugimoto, K., Matsui, K., and Takabayashi, J. (2015). Conversion of volatile alcohols into their glucosides in Arabidopsis. *Commun. Integr. Biol.* 8:e992731. doi: 10.4161/19420889.2014.992731

Takeo, T. (1981). Production of linalool and geraniol by hydrolytic breakdown of bound forms in disrupted tea shoots. *Phytochemistry* 20, 2145–2147. doi: 10.1016/0031-9422(81)80103-3

Ueoka, H., Sasaki, K., Miyawaki, T., Ichino, T., Tatsumi, K., Suzuki, S., et al. (2020). A Cytosol-localized geranyl diphosphate synthase from *Lithospermum erythrorhizon* and its molecular evolution. *Plant Physiol.* 182, 1933–945. doi: 10.1104/pp.19.00999

Ubota, K. I. K. (2002). Identification of potent odorants in Chinese jasmine green tea scented with flowers of *Jasminum sambac*. *J. Agric. Food Chem.* 50, 4878–4884. doi: 10.1021/jf020282h

Wang, H., Takeo, T., Ina, K., and Li, M. (1993). Characteristic aroma components of Qimen black tea (in Chinese). *J. Tea Sci.* 13, 61–68.

Wang, D., Yoshimura, T., Kubota, K., and Kobayashi, A. (2000). Analysis of glycosidically bound aroma precursors in tea leaves. 1. Qualitative and quantitative analyses of glycosides with aglycons as aroma compounds. *J. Agric. Food Chem.* 48, 5411–5418. doi: 10.1021/jf000443m

Wei, S., Marton, I., Dekel, M., Shalitin, D., Lewinsohn, E., Bravdo, B. A., et al. (2004a). Manipulating volatile emission in tobacco leaves by expressing *Aspergillus niger* β-glucosidase in different subcellular compartments. *Plant Biotechnol. J.* 2, 341–350. doi: 10.1111/j.1467-7652.2004.00077.x

Wei, S., Reuveny, H., Bravdo, B. A., and Shoseyov, O. (2004b). Hydrolysis of glycosidically bound volatiles from apple leaves (cv. Anna) by *Aspergillus niger* β-glucosidase affects the behavior of codling moth (*Cydia pomonella* L.). *J. Agric. Food Chem.* 52, 6212–6216. doi: 10.1021/jf0495789

Wei, C., Yang, H., Wang, S., Zhao, J., Liu, C., Gao, L., et al. (2018). Draft genome sequence of *Camellia sinensis* var. *sinensis* provides insights into

the evolution of the tea genome and tea quality. *Proc. Natl. Acad. Sci. U. S. A.* 115, E4151–E4158. doi: 10.1073/pnas.1719622115

Xia, E., Li, F., Tong, W., Li, P., Wu, Q., Zhao, H., et al. (2019). Tea plant information archive (TPIA): a comprehensive genomics and bioinformatics platform for tea plant. *Plant Biotechnol. J.* 17, 1938–1953. doi: 10.1111/pbi.13111

Zhao, M., Wang, L., Wang, J., Jin, J., Zhang, N., Lei, L., et al. (2020). Induction of priming by cold stress via inducible volatile cues in neighboring tea plants. *J. Integr. Plant Biol.* 62, 1461–1468. doi: 10.1111/jipb.12937

Zhou, Y., Liu, X., and Yang, Z. (2019). Characterization of terpene synthase from tea green leafhopper being involved in formation of geraniol in tea (*Camellia sinensisii*) leaves and potential effect of geraniol on insect-derived endobacteria. *Biomol. Ther.* 9:808. doi: 10.3390/biom9120808

Zhou, H. C., Shamala, L. F., Yi, X. K., Yan, Z., and Wei, S. (2020). Analysis of terpene synthase family genes in *Camellia sinensis* with an emphasis on abiotic stress conditions. *Sci. Rep.* 10:933. doi: 10.1038/s41598-020-57805-1

Conflict of Interest: The authors declare that the research was conducted in the absence of any commercial or financial relationships that could be construed as a potential conflict of interest.

Publisher's Note: All claims expressed in this article are solely those of the authors and do not necessarily represent those of their affiliated organizations, or those of the publisher, the editors and the reviewers. Any product that may be evaluated in this article, or claim that may be made by its manufacturer, is not guaranteed or endorsed by the publisher.

frontiers | Frontiers in Plant Science

ORIGINAL RESEARCH
published: 19 May 2022
doi: 10.3389/fpls.2022.880227

An Integrated Metabolome and Transcriptome Analysis Reveal the Regulation Mechanisms of Flavonoid Biosynthesis in a Purple Tea Plant Cultivar

SaSa Song[1†], Yu Tao[1†], LongHan Gao[1], HuiLing Liang[1], DeSong Tang[1], Jie Lin[1], YuChun Wang[1], Frederick G. Gmitter Jr.[2] and ChunFang Li[1]**

[1] College of Tea Science and Tea Culture, Zhejiang A&F University, Hangzhou, China, [2] Institute of Food and Agricultural Sciences, Citrus Research and Education Center, University of Florida, Lake Alfred, FL, United States

OPEN ACCESS

Edited by:
Chuankui Song,
Anhui Agricultural University, China

Reviewed by:
Shiqi Zhao,
Zhejiang University, China
Xiaozhen Huang,
Guizhou University, China

***Correspondence:**
Frederick G. Gmitter Jr.
fgmitter@ufl.edu
Chunfang Li
lichunfang@zafu.edu.cn

† These authors have contributed equally to this work and share first authorship

Specialty section:
This article was submitted to Plant Metabolism and Chemodiversity, a section of the journal Frontiers in Plant Science

Received: 21 February 2022
Accepted: 15 April 2022
Published: 19 May 2022

Citation:
Song S, Tao Y, Gao L, Liang H, Tang D, Lin J, Wang Y, Gmitter FG Jr and Li C (2022) An Integrated Metabolome and Transcriptome Analysis Reveal the Regulation Mechanisms of Flavonoid Biosynthesis in a Purple Tea Plant Cultivar. Front. Plant Sci. 13:880227. doi: 10.3389/fpls.2022.880227

Purple tea plant cultivars, enrich with flavonoids and anthocyanins, are valuable materials for manufacturing tea with unique color and flavor. Researchers found that 'Zijuan' leaves changed from purple to green mainly caused by the decreased flavonoids and anthocyanins concentrations. The mechanism of flavonoids and anthocyanin biosynthesis has been studied in many purple tea plant cultivars and the key genes which regulated the biosynthesis of flavonoid and anthocyanins in different purple tea plant cultivars were quite different. Also, the molecular regulation mechanism underlying the flavonoids and anthocyanins biosynthesis during leaves development and color changes is less-thoroughly understood. In this study, an integrative analysis of transcriptome and metabolome was performed on the purple leaves and green leaves of 'Zijuan' tea plant to reveal the regulatory networks correlated to flavonoid biosynthesis and to identify key regulatory genes. Our results indicated that the 'Zijuan' new shoots leaves were purple might be due to the copigmentation of quercetin and kaempferol derivatives. In 'Zijuan' tea plant cultivar, flavonoids metabolites concentrations in purple leaves and green leaves were significantly influenced by the genes involved in flavonoid biosynthesis, transcriptional regulation, transport, and hormone response. Transcription factors including NAC008, MYB23, and bHLH96 and transporters such as ABC transporter I might be responsible for the flavonoid and anthocyanins accumulation in purple leaves. This study provides a new insight into the metabolism and molecular mechanisms underlying flavonoid and anthocyanin biosynthesis in tea plant.

Keywords: flavonoid, Zijuan, RNA-seq, metabolomics, UPLC-Q-TOF/MS, anthocyanins, quercetin, kaempferol

INTRODUCTION

'Zijuan' [*Camellia sinensis* var. *asssamica* (Masters) kitamura] is a special broad-leaf variety of tea plant that produces new shoots that are purple-colored and mature leaves that are green-colored. A decreased concentration in the flavonoids and anthocyanins causes the leaf color change from purple to green (Wang et al., 2017). The purple tea plant leaves were found to have a significantly

higher concentration of total phenolic compounds, flavonoids, and anthocyanins, whereas the green leaves were found to have a higher concentration of porphyrin, chlorophyll, and carotenoids (Kerio et al., 2013; Kilel et al., 2013; Shen et al., 2018). Anthocyanins not only play various human health-correlated biological functions, such as acting as antimicrobial agents and antioxidants, lowering blood lipids, and preventing colorectal cancer, but also protect plants against various biotic and abiotic stresses, including low phosphate stresses and cold/freezing (Hsu et al., 2012). Therefore, the high concentration of flavonoids and anthocyanins has been employed as one of the tea plant breeding objects.

The combination analysis of high-throughput functional genomics large-scale datasets has been used on the analysis the functions of genes which might involve in plant metabolism regulating (Zhang et al., 2018). The integration of transcriptome and metabolome datasets by correlation and clustering analyses has been shown to be a useful approach to connect genes with metabolites in many plants, including crops (Kovinich et al., 2011), trees (Hamanishi et al., 2015; Shen et al., 2018; Zhang et al., 2018), fruits (Savoi et al., 2016), and potatoes (Cho et al., 2016). In tea plants, using metabolites and transcriptional profiling analysis found that glycosyl might determine the stable accumulation of anthocyanins in purple tea plant cultivar and anthocyanidin synthase, anthocyanidin 3-*O*-glucoside 6″-*O*-acyltransferase, anthocyanidin 3-*O*-glucosyltransferase, as well as transcriptional factors such as WRKY, and MYB were take part in transforming anthocyanins and increasing anthocyanins concentrations (Mei et al., 2020). Anthocyanin is biosynthesized through the phenylpropanoid and flavonoid pathways. Phenylalanine ammonia lyase (PAL) deaminates phenylalanine into cinnamic acid and involved in the biosynthesis of plant phenolics. In tea plants, the PAL activity in the purple leaves was shown to be two times higher than that of the green leaves (Li et al., 2017). A R2R3-MYB transcription factor CsMYB6A were found could activate the expression of flavonoid biosynthesis pathway genes and resulted the increasing of anthocyanins concentrations in purple tea plant leaves (He et al., 2018). Although a great effort has been focused on the genes implicated in flavonoids biosynthesis, with several key genes being identified (Li et al., 2017; Wei et al., 2019), insights into the molecular regulation mechanism of flavonoid and anthocyanin biosynthesis and transportation remain to be less-thoroughly uncovered.

Researchers have found that the vital genes which involved in regulating the biosynthesis of anthocyanins in different purple tea plant cultivars were quite different. The expression levels of *4-coumarate CoA ligase* (*4CL*), *chalcone synthase* (*CHS*), *flavonoid 3′-monooxygenase* (*F3′H*), and *flavonol synthase* (*FLS*) were in accordance with the dynamic concentration of delphinidin and cyanidin in 'Zijuan' (Mei et al., 2020). In 'ZiYan,' the expression levels of *4CL*, *chalcone isomerase* (*CHI*), *flavanone 3-hydroxylase* (*F3H*), *F3′H*, and *flavonoid 3′,5′-hydroxylase* (*F3′5′H*) were consistent with the dynamic concentration of delphinidin and cyanidin (Mei et al., 2020). This study focused on the representative purple tea plant cultivar 'Zijuan.' Combined analysis of the metabolome and transcriptome was performed in the purple and green leaves to discover the regulatory networks correlated to flavonoid and anthocyanin biosynthesis and to identify the pivotal regulatory genes. Transcriptional and metabolic changes were analyzed statistically using metabolite-gene correlated networks. Transcriptional profiles and metabolite profiles were obtained using high-throughput RNA-sequencing and liquid chromatography-tandem mass spectrometry (LC-MS/MS), respectively. Flavonoids and anthocyanins were identified and quantified using molecular formula-based masses and MS2 spectra. Correlation analysis of differential flavonoids concentrations and differentially expressed genes (DEGs) showed the strong correlations between flavonoid compounds and DEGs, which were involved in flavonoid biosynthesis, transcriptional regulation, transport and hormone response. The network of differential flavonoids and DEGs discovered a regulatory system in the purple leaves of 'Zijuan,' provides a novel insight into the molecular mechanisms underlying flavonoid and anthocyanin biosynthesis in tea plant.

MATERIALS AND METHODS

Plant Materials

'Zijuan' tea plants were grown on the tea plantation of the Zhejiang A&F University, Zhejiang province, China. The 2nd and 3rd leaves with a purple color and the 4th and 5th leaves with a green color were collected from at least ten tea plants on April 10, 2017 (**Figure 1A**). Six biological replicates were used for each chemical assay, and three biological replicates were applied for the transcriptome analysis. All the tea plant leaf samples were immediately frozen in liquid nitrogen and then stored at -80°C before analysis.

Anthocyanin Analysis

The concentration of total anthocyanin in purple leaves and green leaves of 'Zijuan' were quantified using a spectrophotometer (UV-160 Shimadzu, Japan) (Proctor, 1974). With intermittent shaking (10 s on a vortex mixer), 10 ml of 0.1 M HCl in ethanol was used to extract 0.1 g of leaf sample at 60°C for 30 min. After that, the extract solution was filtered, and the absorbance was measured at 530, 620, and 650 nm, respectively. The concentration of anthocyanin was determined according to the following formula: $\Delta A = (A^{530} - A^{620}) - 0.1(A^{650} - A^{620})$. The concentration of anthocyanin were measured by the following formula: total anthocyanin (μmol/g) = $(\Delta A \times 100)/(4.62 \times$ sample weight). The concentration of anthocyanin is presented as the mean $\pm$ standard deviation (SD) ($n = 6$). Significance was determined using Student's *t*-test ($p < 0.05$) for differences between the purple leaves and the green leaves.

Metabolomic Data Acquisition by UPLC-Q-TOF/MS

A total of 50 mg per leaf sample was added to 1 ml of 70% methanol with 20 μl of internal standard (0.03 mg ml^{-1} L-2-Cl-phenylalanine), and then ground at 60 Hz for 2 min. Total metabolites in the leaves were extracted in an ultrasonic bath

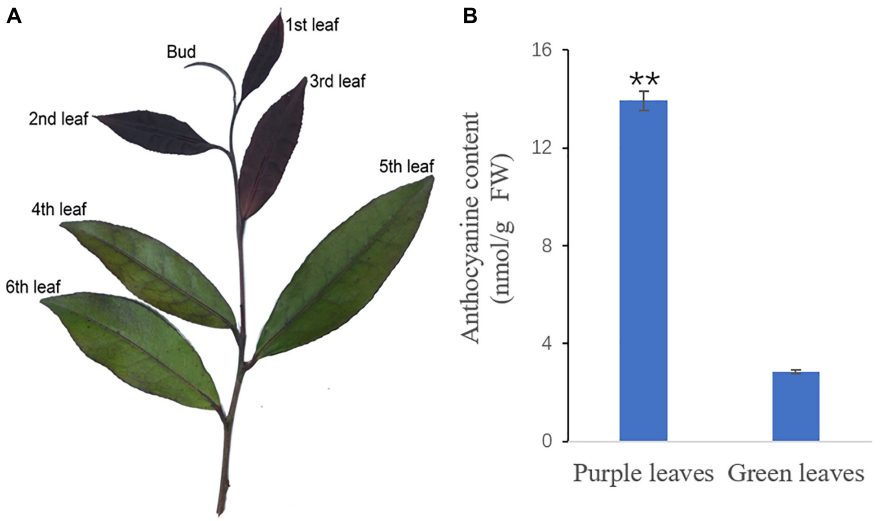

FIGURE 1 | The new shoot of 'Zijuan' and the total anthocyanin concentrations in the purple and green tea plant leaves. **(A)** The purple leaves (2nd leaf and 3rd leaf) and the green leaves (4th leaf and 5th leaf) from 'Zijuan' tea plant new shoots were analyzed in this study. **(B)** The total anthocyanin concentrations in the purple and green leaves. **represents a significant difference between the purple leaves and the green leaves in the tea plant ($p < 0.01$).

for 30 min and then centrifuged at 15,000 *g* for 10 min. The upper phase of the aqueous methanol extract was filtered through a 0.22 μm PTFE filter. A total of 3 μL of the extract was injected into an Agilent 1290 Infinity UHPLC. The metabolites were separated on a Waters ACQUITY UPLC BEH Amide Column (1.71 μm, 100 mm × 2.1 mm). The Mobile phase A was 25 mM ammonium acetate in water and 25 mM ammonium hydroxide, and mobile phase B was acetonitrile. The flow rate was 0.5 ml/min, and the gradient profile was 5% A from 0 to 0.5 min, 35% A from 0.5 to 7 min, 60% A from 7 to 8 min, 60% A from 8 to 9 min, and 5% A from 9.1 to 12 min. The metabolomic data were acquired in both electrospray ionization negative (ESI-) and positive (ESI+) modes. Ion spray voltage was –4.0 kV in ESI- and 5.0 kV in ESI+, the nebulizer gas was 60 psi, the heater gas was 60 psi, the curtain gas was 35 psi, and the turbo spray temperature was 650°C.

Data Processing and Differential Metabolites Identification

UPLC-Q-TOF/MS raw data files were imported into XCMS[1] to produce a peak table that included information on the retention time, MS intensity, and mass-to-charge ratio (m/z) for each metabolite. The intensities of mass peaks for each sample were normalized by inputting the datasets of UPLC-Q-TOF/MS into the SIMCA-P+ 14.0 software package (Umetrics, Umea, Sweden). Principal component analysis (PCA) was conducted to detect the intrinsic variation between the purple leaves and the green leaves. Orthogonal partial least squares discriminant analysis (OPLS-DA) was used to discriminate and characterize the purple and the green leaves. Differential metabolites were identified as those with a variable influence on projection (VIP) value greater than 1 and with a *p* value less than 0.05. Differential metabolites were annotated with METLIN.[2] The identified differential metabolites were enriched into distinct metabolic pathways according to the Kyoto Encyclopedia of Genes and Genomes (KEGG) database to analyze the metabolic differences in purple leaves and green leaves in 'Zijuan.'

Transcriptome Library Construction and RNA-Sequencing

Total RNA was isolated from three purple leaf samples and three green leaf samples in 'Zijuan' tea plant, using RNeasy Plus Mini Kit (Qiagen, Valencia, CA, United States). The libraries were constructed, and paired-end sequencing was performed on the Illumina HiSeq^{TM} 2000 platform, according to the manufacturer's instructions. Fluorescent image analysis, base calling, and quality value calculations were performed using the Illumina Pipeline with default settings. HISAT2 first aligned the reads with the tea plant (*C. sinensis* var. *sinensis*) genome sequence, and then StringTie (v2.0.6) assembled the reads into unigenes (Daehwan et al., 2015; Mihaela et al., 2015; Wei et al., 2018; Xia et al., 2020). Unannotated transcriptional regions were identified by comparing with the original genome annotation (Wei et al., 2018; Xia et al., 2020) and were named as Camellia_sinensis.newGene.

Unigene Functional Annotation and Expression Analysis

Using the BLASTp algorithm, all unigenes were annotated by searching against the Swiss-Prot protein sequence database (Swiss-Prot), and proteins with the highest sequence similarity to given unigenes were retrieved. In the same way as outlined above, the unigenes were blast with the Kyoto Encyclopedia of

[1]http://metlin.scripps.edu

[2]https://metlin.scripps.edu/

Genes and Genomes database (KEGG), and the unigenes that enriched with KEGG database were retained for detailed pathway analysis. The expression levels of each unigene were calculated based on fragments per kilobase of exon per million mapped reads (FPKM) values using StringTie (Mihaela et al., 2015). The significance of each gene expression level difference between the purple and the green leaves was assessed using the DEseq (Wang et al., 2010) on the FPKM values from three cDNA libraries from the purple leaves and three cDNA libraries from the green leaves. To identify the DEGs between the purple leaves and green leaves, a false discovery rate (FDR) ≤ 0.01 and Fold Change ≥ 4 was used to judge the gene expression differences significance between the purple leaves and green leaves. The DEGs annotated as involved in flavonoids pathway were clustered hierarchically according to their log FPKM values. Using KOBAS (Mao et al., 2005), the statistical enrichment of DEGs in KEGG pathways were tested.

Quantitative Real-Time PCR Analysis

Total RNA of the purple leaves and green leaves in the 'Zijuan' tea plant was isolated using the RNeasy Plus Mini Kit (Qiagen). To remove DNA prior to cDNA synthesis, the samples were treated with TURBO DNase (Ambion, Austin, TX, United States). The quantitative Real-Time PCR (qRT-PCR) reaction mixture included 2 μL template cDNA, 5 μM each of the forward and reverse primers, and 10 μL SsoFast EvaGreen Supermix. PCR amplification was conducted at 60°C as annealing temperature using ABI 7500 real-time PCR system (Applied Biosystems). Each analyzed unigene was tested with three biological replicates and three technical replicates. The quantitative data were analyzed using the $2^{-\Delta\Delta CT}$ method, with the GAPDH gene as an internal standard. The primer pairs used for the qRT-PCR are listed in **Supplementary Table 5**.

Correlation Analysis of the Transcriptome and the Metabolome

To obtain key genes involved in flavonoid biosynthesis, DEGs and differentially accumulated flavonoids between the purple leaves and the green leaves were selected for integrative analysis. Pearson correlation coefficients (PCC) between differential metabolites and DEGs, and *p* value of PCC (PCCP) were calculated. The Pearson correlation coefficients (PCC) ≥ 0.90 or $\leq$-0.90 and the PCCP < 0.05 were selected. The coexpression network was exhibited using Cytoscape (version 2.8.2) (Shannon et al., 2003).

RESULTS

Comparison of Total Anthocyanin Concentration Between Purple and Green Leaves in 'Zijuan' Tea Plant

The new shoots of 'Zijuan' were dark purple, but as they developed, they became completely green. The purple leaves (2nd and 3rd leaves), green leaves (4th and 5th leaves), and total anthocyanin concentration in these leaves are presented in **Figure 1**. The total anthocyanin content in the green leaves was 2.85 nmol/g, while that in the purple leaves was significantly greater, 13.93 nmol/g (**Figure 1B**).

Metabolic Differences Between the Purple Leaves and the Green Leaves

Principal component analysis was used to compare the metabolite composition differences between the purple leaves and the green leaves, based on the metabolic database got from UPLC-Q-TOF/MS in the ESI+ and ESI- mode. The purple and green leaves were obviously separated in the PC1 × PC2 × PC3 score plots (**Figures 2A,B**). The first principal components (PC1) in ESI+ mode (71.9% of the total variables) and in ESI- mode (74.1% of the total variables) was clearly separated between the purple and green leaves. Furthermore, OPLS-DA was used for modeling the differences between the purple leaves and the green leaves in 'Zijuan.' A total of 64 differential metabolites were identified, 27 of which were upregulated and 37 of which were downregulated when comparing the purple with the green leaves (**Figure 2C**).

Based on the mass ion peaks detected in the UPLC-Q-TOF/MS analysis, the metabolites in the flavonoid biosynthesis pathway were selected. These selected flavonoids and anthocyanins, and correlated metabolites were arranged to their corresponding positions in the flavonoid biosynthesis pathway that was constructed according to KEGG and literature references (**Figure 3**). The concentrations of the metabolites in the flavonoids biosynthesis pathways were significantly different between the purple leaves and the green leaves. Procyanidin B3, kaempferol 7-galactoside 3-rutinoside, kaempferol 3-(2″-rhamnosyl-6″-acetylgalactoside) 7-rhamnoside, quercetin 7-glucuronide 3-Rham, quercetin 3-glucoside 7-xyloside, and quercetin 3-(4″-acetylrhamnoside) 7-rhamnoside were more abundant in the purple leaves, whereas phenylalanine, naringin, quercetin, quercetin 3-(3-p-coumaroylglucoside), isoquercitin, leucodelphinidin, procyanidin B2, cyanidin 3-*O*-(2-*O*-β-D-glucuronosyl)- β-D-glucoside, and epigallocatechin gallate were abundant in the green leaves (**Figure 3A**). 3′-*O*-methyl-(-)-epicatechin 7-*O*-glucuronide, (-)-epigallocatechin 3-p-coumaroate, and (-)-epicatechin-3-*O*-gallate were found at significantly higher concentrations in the purple leaves than in the green leaves (**Figure 3A**).

Differential Expression Genes Between the Purple Leaves and the Green Leaves

Transcriptome analysis showed that 4,729 transcripts were differentially expressed in the purple and green leaves. Compared with the green leaves, there were 1,671 upregulated and 3,058 downregulated transcripts in the purple leaves (**Supplementary Table 1**). To further determine the functions of the DEGs, KOBAS (Mao et al., 2005) was applied to analyze the statistical enrichment of DEGs in KEGG pathways, and the phenylpropanoid biosynthesis, starch and sucrose metabolism and flavonoid biosynthesis were the three most prominent pathways identified (**Figures 4A,B**). DEGs involved in flavonoid biosynthesis, such as *CHS*, *FLS*, *flavonoid 3′5′ hydroxylase* (*F3′5′H*), and *anthocyanidin reductase* (*ANR*), were enriched

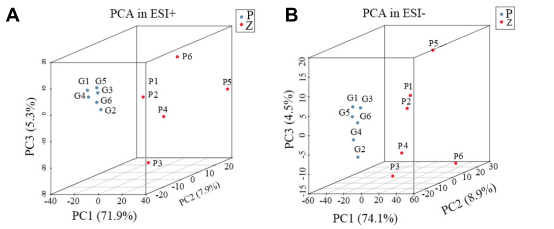

C

Metabolite ID	Name	Mzmed	Fold_change	log_2FC (P vs G)
Amino acides				
meta_11	L-Norleucine	132.1011208	0.342777305	-1.544656504
meta_12	L-Leucine	132.1010946	0.173028041	-2.530922233
meta_13	D-Aspartic acid	134.044067	1.962198704	0.972471145
meta_22	L-Glutamate	148.0599541	1.493690974	0.578881703
meta_31	DL-Homoserine	161.0911114	1.808132534	0.85450043
meta_44	Theanine	175.1068134	2.07795378	1.055163564
meta_103	L-Valine	235.1671231	0.271371378	-1.881659527
meta_190	γ-L-Glutamyl-L-Valine	288.1540849	2.153785967	1.106874889
meta_272	α-N-Phenylacetyl-L-glutamine	325.1382389	0.415133938	-1.268351216
meta_39	L-Phenylalanine	166.0853126	0.358944898	-1.478165702
Alkaloids				
meta_24	Xanthine	153.0396529	0.253941599	-1.977431348
meta_40	7-Methylxanthine	167.0555023	5.582790934	2.480986531
meta_66	Caffeine	195.0863356	3.032629899	1.600569443
meta_174	1-Methyladenosine	282.1184559	1.473443314	0.559191559
meta_182	Xanthosine	285.0815393	0.315372089	-1.66487311
meta_239	Thymidine	309.0392483	0.191944595	-2.38123816
Organic acids				
meta_742	Chlorophyllide b	629.2219326	0.507447632	-0.978669149
meta_1009	Pheophytin a	871.5693004	0.151689952	-2.720802569
meta_290	Chlorogenic acid	337.088533	0.51512561	-0.957003828
meta_11	L-Malic acid	133.0145455	2.542607626	1.346308843
meta_46	Quinate	191.0561182	6.21803334	2.636458352
meta_238	Chlorogenic acid	354.1041105	0.491694373	-1.02416625
Carbohydrates				
meta_300	D-Maltose	342.1144154	0.256865416	-1.960915433
meta_557	Raffinose	522.2009016	0.351442052	-1.508641265
meta_663	UDP-D-Galactose	584.0862802	3.477665134	1.798119021
meta_77	L-Fucose	206.1008734	1.548712422	0.631069277
meta_20	Coumarin	147.0429725	7.849308583	2.972565578
meta_38	D-(+)-Galactose	179.0560448	2.772904679	1.471398023
meta_39	D-Sorbitol	181.0713867	0.307640541	-1.700682461
meta_59	D-Lyxose	209.0661685	4.482596077	2.164334505
meta_67	L-Fucose	223.0818074	0.144717594	-2.788687771
Flavonols, flavones, and their glycosides				
meta_111	2'-Hydroxychalcone	242.1221011	0.199564881	-2.325070233
meta_595	Naringin	579.1618624	0.230382973	-2.117894
meta_189	Flavanone	288.1043228	0.506060342	-0.982618675
meta_117	Isoflavanone	247.0776553	0.476117616	-1.070610087
meta_223	Quercetin	303.0488436	0.218269317	-2.195818758
meta_253	Quercetin 3'-methyl ether	317.064374	0.277518135	-1.849346046
meta_687	Quercetin 3-glucoside 7-xyloside	597.4855369	3.467135606	1.793744264
meta_751	Quercetin 7-(rhamnosylglucoside)	633.1399927	0.402686006	-1.312272759
meta_797	Quercetin 4',7-diglucoside	665.1085163	0.382107354	-1.387950071
meta_661	Quercetin 7-glucuronide 3-rhamnoside	623.1244953	1.675921716	0.744954761
meta_639	Quercetin 3-(3-p-coumaroylglucoside)	609.125425	0.279460798	-1.839282175
meta_684	Quercetin 3-(4"-acetylrhamnoside) 7-rhamnc	635.1838134	3.901861016	1.96416239
meta_421	Isoquercitin	463.0870879	0.442512651	-1.176209393
meta_268	Leucodelphinidin	323.0730541	0.460777344	-1.117858311
meta_371	Kaempferol 3-*O*-beta-D-xyloside	383.0757039	0.358377233	-1.480449105
meta_683	Kaempferol 3-*O*-rutinoside	595.1634898	0.398676288	-1.326710292
meta_909	Kaempferol 7-galactoside 3-rutinoside	757.2156613	1.936035215	0.953105194
meta_937	Kaempferol 3-(2"-rhamnosyl-6"-acetylgalactoside) 7-rhamnoside;	783.2432337	0.099988695	-3.322091197
meta_950	Kaempferol 3-gentiobioside 7-rhamnoside	795.172027	2.064719595	1.045945866
meta_959	Kaempferol 3-(2"-rhamnosyl-6"-acetylgalactoside) 7-rhamnoside	805.213724	9.43222948	3.237598819
meta_976	Kaempferol 7-galactoside 3-rutinoside	833.1273236	2.829205488	1.500396965
meta_1025	Kaempferol 3-[2"-(6"'-coumaroylglucosyl)-rhamnoside] 7-glucoside	903.2526273	0.376626046	-1.408795319
meta_480	Peonidin 3-galactoside cation	463.1223438	0.39931527	-1.324399851
meta_735	Myricetin 3,3'-digalactoside;	625.1524061	12.86884883	3.685811099
meta_798	Myricetin 3,3'-digalactoside;	665.5126214	0.512207123	-0.96520078
meta_935	Luteolin 7-*O*-[β-D-glucuronosyl-(1->2)-β-D-glucuronide]-4'-*O*-β-D-glucuronide	779.5953366	0.17327731	-2.528845342
meta_589	Procyanidin B2	577.134703	0.534730788	-0.90311535
meta_691	Procyanidin B3	601.1294525	2.391884562	1.258147763
meta_665	Cyanidin 3-*O*-(2-*O*-β-D-glucuronosyl)-β-D-glucoside	624.1371535	0.22757267	-2.135600786
meta_401	(-)-Epigallocatechin 3-p-coumaroate	451.4141009	4.656789422	2.219335645
meta_384	(-)-Epicatechin 3-*O*-gallate	441.0815429	1.342355926	0.424767253
meta_455	Epigallocatechin gallate	441.0810301	0.211518756	-2.241142498
meta_498	3'-*O*-Methyl-(-)-epicatechin 7-*O*-glucuronide	481.4236289	2.107306284	1.075400016

FIGURE 2 | Principal component analysis score plot and differential metabolites of the purple leaves and the green leaves in 'Zijuan' tea plant. **(A)** PCA score plots derived from metabolite ions obtained from ESI+ modes. **(B)** PCA score plots derived from metabolite ions obtained from ESI- modes. P1–P6 represented six purple leave samples and G1–G6 represented six green leave samples. **(C)** Relative fold change of differential metabolites in the purple-leaf and green-leaf in 'Zijuan' according to UPLC-Q-TOF-MS analysis.

in the phenylpropanoid biosynthesis and flavonoid biosynthesis pathways (**Supplementary Table 2**).

Differentially expressed genes involved in flavonoid and phenylpropanoid pathways were clustered by the Pearson correlation based on the expressional level of each DEG in the purple or green leaves (**Figure 3B** and **Supplementary Table 3**). The expression level of *PAL* (TEA014166.1, TEA023243.1, TEA034008.1, TEA003137.1, TEA003374.1) and *4CL* (Camellia_sinensis_newGene_17148, Camellia_sinensis_newGene_32935, TEA009431.1, TEA018887.1, TEA019187.1, TEA019224.1, TEA019275.1, TEA024967.1, TEA002100.1, TEA027829.1, TEA028833.1, TEA031627.1, TEA034012.1) in the purple leaves were significantly higher than in the green leaves (**Figure 3B**). The expression level of *CHI* (TEA007049.1, TEA013101.1, TEA014874.1, TEA022023.1_CHI, TEA034003.1) in the purple leaves were also significantly higher than in the purple leaves. All the DEGs encoding F3H (Camellia_sinensis_newGene_21655, TEA006643.1, TEA009737.1, TEA010326.1, TEA010328.1_F3H, TEA014951.1_F3H, TEA016601.1_F3H, TEA023946.1_F3H, TEA028622.1_F3H, TEA034025.1_F3H) were expressed at a higher level in the purple leaves than in the green leaves. The transcription levels of *FLS* (Camellia_sinensis_newGene_21655, TEA006643.1_gene, TEA010328.1_gene, TEA016601.1_gene) in the purple leaves were significantly higher than those in the green leaves. The differential gene expression levels between purple and green leaves were validated using quantitative real-time PCR (qRT-PCR) (**Figure 5**) with gene-specific primers (**Supplementary Table 5**). From the RNA isolated from the purple leaves and the green leaves, the genes involved in flavonoid biosynthesis and regulation, including *NAC008*, *PAL*, *4CL*, *F3H*, *leucoanthocyanidin reductase* (*LAR*), *FLS*, and *CHS* were found to be highly expressed in the purple leaves, whereas *NAC86* was highly expressed in the green leaves.

Correlation Analysis Between Differentially Expressed Genes and Differential Metabolites in the Flavonoid Biosynthesis Pathway

To gain insight into the regulatory network of flavonoids and anthocyanins biosynthesis in purple and green leaves in tea plant, a correlation analysis was carried out between the concentration changes in the differential metabolites and the expression level changes of DEGs. For this analysis, DEGs annotated as involved in flavonoid metabolism, transcription regulation, transport, and hormone response, and differential metabolites including naringin, procyanidin, epigallocatechin gallate (EGCG), epigallocatechin (EGC), and derivatives of kaempferol, quercetin, and cyanidin, were selected (**Figure 6** and **Supplementary Table 4**). The upregulation of the genes encoding MYB23 and bHLH96 in the purple leaves were highly correlated with the accumulation of flavonoids, including kaempferol 3-(2″-rhamnosyl-6″-acetylgalactoside) 7-rhamnoside, kaempferol 3-*O*-rutinoside, and quercetin 3-glucoside 7-xyloside. Two NAC transcription factors genes, *NAC008* and *NAC090*, were strongly correlated to procyanidin B3, kaempferol 3-*O*-rutinoside,

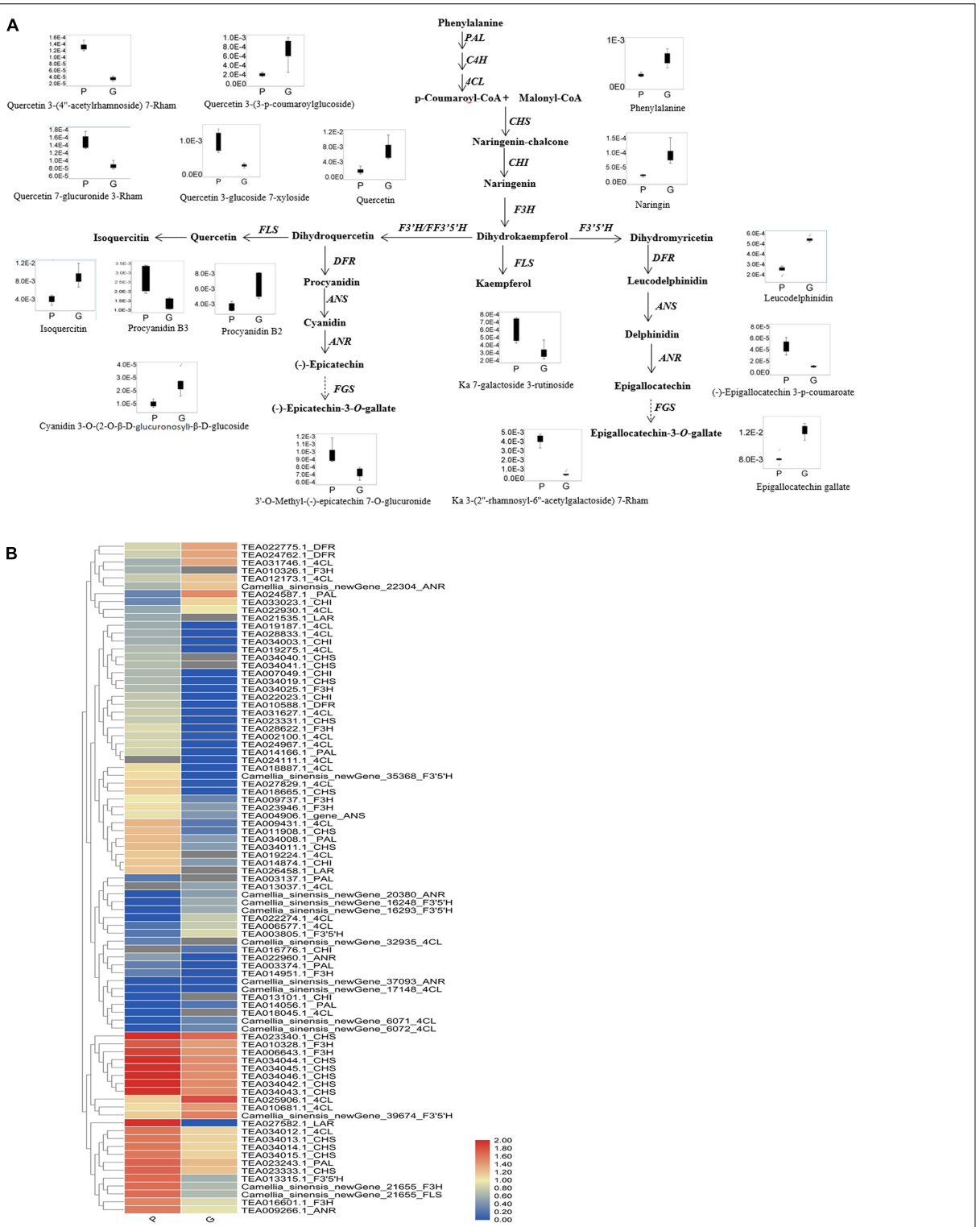

FIGURE 3 | Flavonoid biosynthetic pathway and the expression level of DEGs. **(A)** Flavonoid and anthocyanin biosynthetic pathway. This pathway was constructed based on the KEGG pathway and literature references. Ka, kaempferol; Rham, rhamnose; Box-and-whisker plots are shown for the concentration changes in the phenylprophanoids, flavone glycosides, flavonol glycosides, dihydroflavonol glycosides, and anthocyanins in the purple leaves (P) and the green leaves (G). The maximum and minimum values of each metabolite concentration among the six biological replicates are represented at the upper and lower ends of the whisker, respectively. **(B)** Heat map of the expression levels of the flavonoid biosynthetic unigenes in the purple leaves and the green leaves. The annotations are displayed on the right side of each unigene. The scale represents the logarithms of the FPKM (fragments per kilobase of exon model per million reads mapped) values of each unigene. The unigenes were clustered by the Pearson correlation.

A

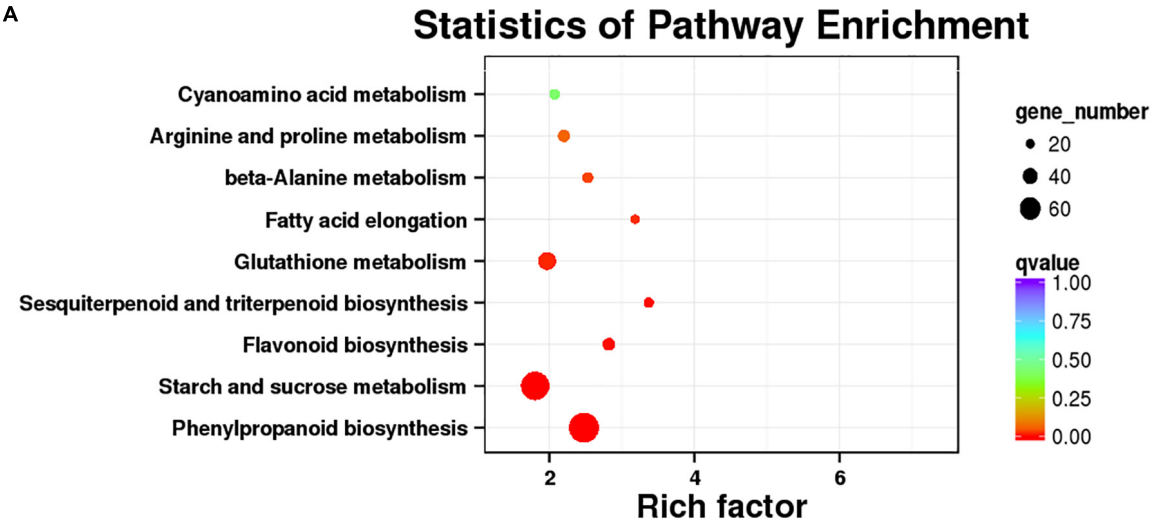

B

KEGG Pathway	KEGG _ID	DEG Number	Gene Number
Cyanoamino acid metabolism	ko00460	16	85
Arginine and proline metabolism	ko00330	20	100
beta-Alanine metabolism	ko00410	17	74
Fatty acid elongation	ko00062	13	45
Glutathione metabolism	ko00480	34	190
Sesquiterpenoid and triterpenoid biosynthesis	ko00909	15	49
Flavonoid biosynthesis	ko00941	21	82
Starch and sucrose metabolism	ko00500	60	366
Phenylpropanoid biosynthesis	ko00940	63	280

FIGURE 4 | Kyoto Encyclopedia of Genes and Genomes database enrichment analysis of DEGs in the purple-leaf and green-leaf in 'Zijuan'. **(A)** The KEGG enrichment analysis of the DEGs showed the pathways with the significant enrichment. **(B)** List of the DEGs number which were enriched in the KEGG pathways.

quercetin, quercetin 4′,7-diglucoside, respectively, and EGCG. The expression of DEGs implicated in the hormone response, such as ethylene-responsive transcription factor (ERF), were closely correlated to the concentration of EGCG, quercetin, flavanone, kaempferol derivatives, myricetin 3,3′-digalactoside, and procyanidin B3 (**Supplementary Table 4**). The expression levels of five DEGs annotated as ABC transporter I family members were strongly correlated to the concentration of quercetin, EGCG, procyanidin B3, myricetin 3,3′-digalactoside, kaempferol 7-sophoroside, kaempferol 7-galactoside 3-rutinoside, quercetin 3-glucoside 7-xyloside, and quercetin 4′,7-diglucoside (**Figure 6**).

DISCUSSION

'Zijuan' is a special tea plant cultivar that produces purple-colored new shoots and green-colored mature leaves. The concentration of total anthocyanin in the purple leaves was significantly greater than in the green leaves (**Figure 1B**). This result is the same with the previous studies which suggest that the color difference between the purple leaves and the green leaves correlated mainly with anthocyanin accumulation (Li et al., 2017). Three major pigment classes, including chlorophylls, carotenoids, and flavonoids contribute to the color of the plant (Iwashina, 2015). A decreased concentration in the flavonoids and anthocyanins causes the leaf color change from purple to green. The purple tea plant leaves were found to have a significantly higher concentration of total phenolic compounds, flavonoids, and anthocyanins, whereas the green leaves were found to have a higher concentration of porphyrin, chlorophyll, and carotenoids (Kerio et al., 2013; Kilel et al., 2013; Shen et al., 2018). In our study, the compositions of the flavonoids downstream including quercetin 3-glucoside 7-xyloside, quercetin 7-glucuronide 3-rhamnoside, quercetin 3-(4″-acetylrhamnoside) 7-rhamnoside, kaempferol 3-gentiobioside 7-rhamnoside, kaempferol 3-(2″-rhamnosyl-6″-acetylgalactoside) 7-rhamnoside, and kaempferol

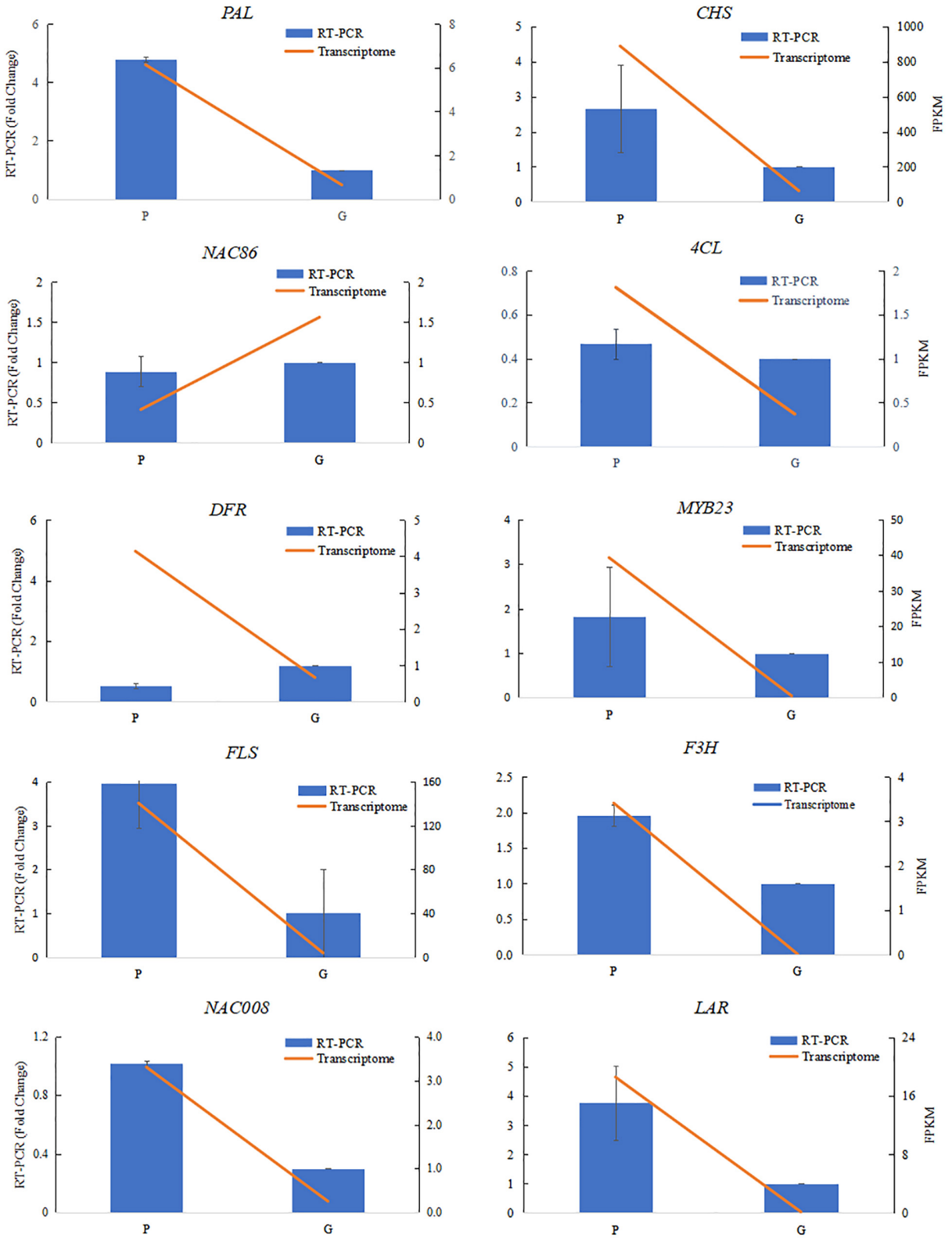

FIGURE 5 | Verification of RNA-sequencing results using qRT-PCR assays. Ten differentially expressed genes were selected from the flavonoid biosynthesis pathway and transcriptional factors involved in flavonoid biosynthesis. The qRT-PCR data were normalized using the "housekeeping" gene GAPDH. The fold change in normalized GAPDH levels in the purple-leaf (P) and green-leaf (G) in 'Zijuan' was calculated. The qRT-PCR primers are listed in **Supplementary Table 5**.

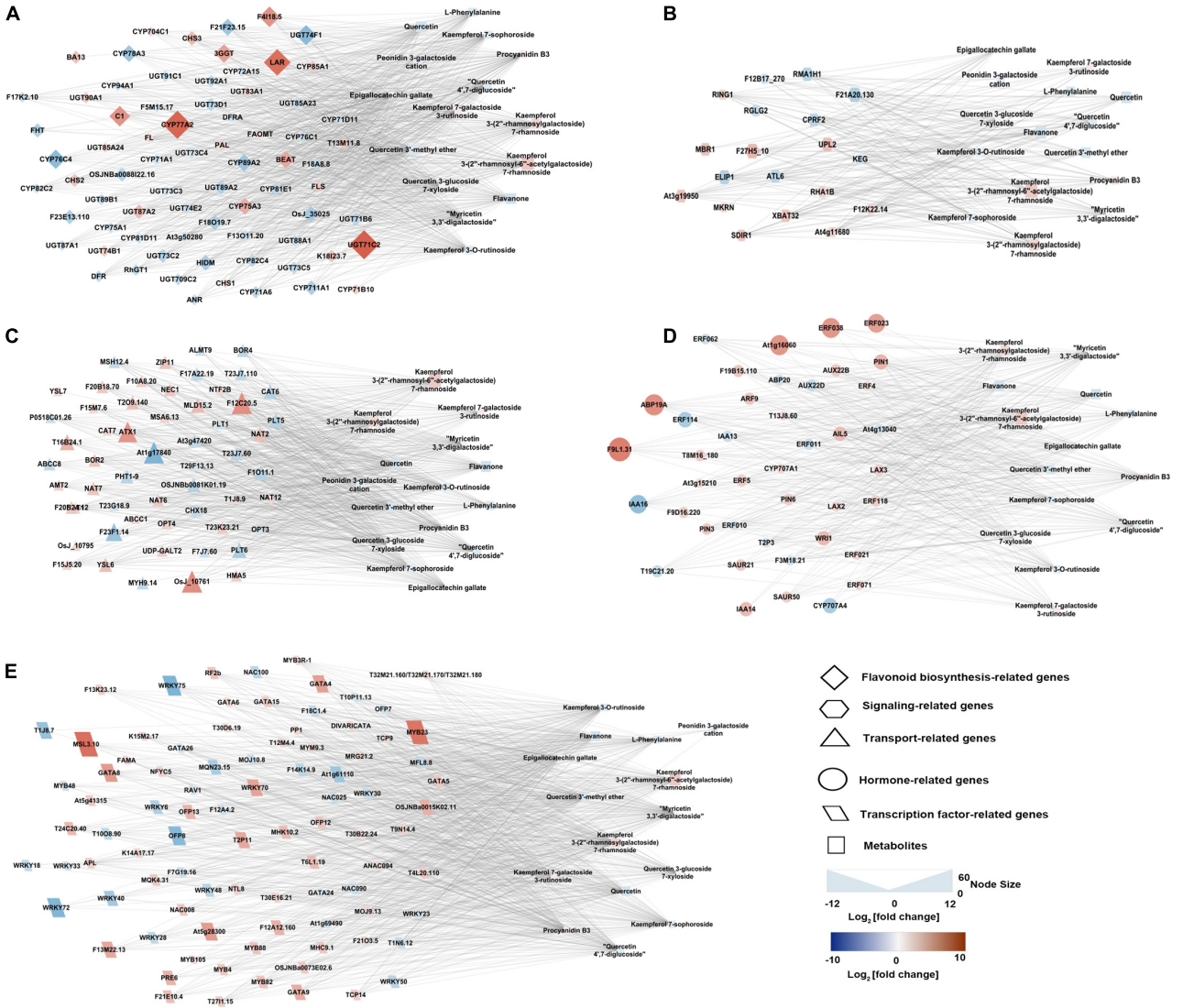

FIGURE 6 | Connection network between genes (regulatory and structural) and flavonoid- and anthocyanin-correlated metabolites. **(A)** Flavonoid biosynthesis structural genes and metabolites network. **(B)** Signaling-related genes and metabolites network. **(C)** Transport related genes and metabolites network. **(D)** Hormone-related genes and metabolites network. **(E)** Transcription factor related genes and metabolites network. The network was visualized with the Cytoscape software (version 2.8.2).

7-galactoside 3-rutinoside were quite different between the purple and green leaves, suggesting that these metabolites likely play an important role in determining the leaf color in 'Zijuan.' Some of the flavonoids and anthocyanins in plants are responsible for the purple, red and blue colors; when their contents are very high, they cover the green color of the chlorophylls (Iwashina, 2015). The purple flower color may be caused by copigmentation with flavonol glycosides such as quercetin and kaempferol (Williams et al., 2002). In our study, several kaempferol and quercetin derivatives including kaempferol 7-galactoside 3-rutinoside, kaempferol 3-gentiobioside 7-rhamnoside, kaempferol 3-(2″-rhamnosyl-6″-acetylgalactoside) 7-rhamnoside, quercetin 7-glucuronide 3-rhamnoside, quercetin 3-glucoside 7-xyloside, and quercetin 3-(4″-acetylrhamnoside) 7-rhamnoside were more abundant in the purple leaves than in the green leaves. The purple leaves of 'Zijuan' might be expressed by copigmentation between kaempferol and quercetin derivatives.

Flavonoids are biosynthesized from the phenylpropanoid pathway. The higher expression level of *PAL* and *4CL* in the purple leaves resulted the production of p-coumaroyl-CoA and provided adequate precursor metabolites for flavonoid biosynthesis in the purple leaves (**Figure 3** and **Supplementary Table 3**), which might be the key reasons for the higher concentrations of anthocyanin, flavonol and flavone in the purple leaves. Chalcone isomerase (CHI) catalyzes the transformation of chalcone to naringenin. The higher expression level of *CHI* in the purple leaves could biosynthesize a large

amount of naringenin in the purple leaves and provided the intermediates for the downstream biosynthesis of flavones, flavonols, and anthocyanins. F3H, F3′5′H, and F3′H are three vital enzymes in the flavonoid biosynthesis pathway, catalyzing the formation of hydroxylated derivatives such as dihydroquercetin and dihydromyricetin (Wang et al., 2014). A high expression level of *F3H* in the purple leaves facilitated the biosynthesis of flavones, flavonols, and anthocyanins (**Figures 3A,B**). All the DEGs which encoding F3H were expressed at a higher level in the purple leaves than in the green leaves. Compared to the green leaves, the purple leaves had a higher concentration of procyanidin B3, quercetin derivatives, including quercetin 7-glucuronide 3-Rham, quercetin 3-glucoside 7-xyloside, and quercetin 3-(4″-acetylrhamnoside) 7-rhamnoside, and kaempferol derivatives, including kaempferol 7-galactoside 3-rutinoside and kaempferol 3-(2″-rhamnosyl-6″-acetylgalactoside) 7-rhamnoside (**Figures 2C**, **3A**), indicating that F3H was the main hydroxylase in the tea plant and plays key roles in flavonoid biosynthesis by regulating the flux through procyanidin and quercetin. FLS catalyzes the transformation of dihydroquercetin and dihydrokaempferol into quercetin and kaempferol, respectively (Tian et al., 2015). The transcription levels of *FLS* in the purple leaves were significantly higher than those in the green leaves, and the concentration of quercetin derivatives in the purple leaves, such as quercetin 7-glucuronide 3-rhamnoside, quercetin 3-glucoside 7-xyloside, and quercetin 3-(4″-acetylrhamnoside) 7-rhamnoside were significantly higher than that in the green leaves (**Figures 2C**, **3A**), suggesting that FLS might play key roles in production of quercetin by dihydroquercetin in the tea plant.

Transcription factors, including GATA, bHLH48, NAC008, MYB, and WRKY, which were strongly correlated with differential metabolites, were demonstrated to be strongly upregulated in the purple leaves compared with the green leaves (**Supplementary Table 4**). Studies on the regulation of flavonoid biosynthesis in diverse plant species have demonstrated that MYB/bHLH complexes are involved in the regulation of flavonoid biosynthesis in a conservative manner across species (Nesi et al., 2001). Researchers have found that a WD40-repeat protein, a R2R3-MYB transcription factor and a bHLH-type regulation factor can form a WD40/R2R3-MYB/bHLH complex, which is involved in the control of flavonoid pathways in different plants (Jaakola, 2013). R2R3-MYB transcription factors in the tea plant are take part in flavonoid biosynthesis by activating the expression of flavonoid-correlated structural genes (He et al., 2018; Wang et al., 2018). In this study, the upregulation of the genes encoding MYB23 and bHLH96 in the purple leaves highly correlated with the accumulation of epigallocatechin gallate, quercetin 3-glucoside 7-xyloside, procyanidin B3, quercetin 3′-methyl ether, and quercetin 4′,7-diglucoside, which might be regulated by the WD40/bHLH/R2R3-MYB-mediated pathway. The NAC transcription factor can induce the transcription of the R2R3-MYB gene and lead to anthocyanin accumulation in the peach (Zhou et al., 2015). In Arabidopsis under high-light stress, researchers have found that the NAC transcription factor was involved in the induction of genes correlated to flavonoid biosynthesis, resulting in anthocyanin accumulation (Morishita et al., 2009). In our research, we found two NAC transcription factors gene *NAC008* was strongly correlated to EGCG and quercetin 3-glucoside 7-xyloside, respectively. This might indicate that the NAC transcription factor could also regulate flavonoid biosynthesis in the tea plant.

During fruit ripening, the color changes is accompanied by anthocyanin accumulation and rapid ethylene production (Faragher and Brohier, 1984). Previous research has showed that exogenous treatment with an ethylene-releasing compound could enhance the expression of the flavonoid biosynthesis pathway genes such as *CHS*, *F3H*, *ANS*, and *UDPG flavonoid glucosyl transferase* (*UFGT)* and the anthocyanin was accumulated in grape skins (He and Giusti, 2010). Among the DEGs correlated to the flavonoid biosynthesis pathway, homologs for *CHS*, *F3′5′H*, *FLS*, and *LAR* were more strongly upregulated in the purple leaves than in the green leaves (**Figure 3B**). The concentration of total polyphenol, flavonoids, and anthocyanins were higher after treatment with ethylene precursor 1-aminocyclopropane-1-carboxylicacid (ACC) (Ke et al., 2018). These results indicated that ethylene might promote the biosynthesis of flavonoids in the tea plant leaves.

Flavonoids are transported into the vacuole after synthesized in the cytosol (Zhao, 2015). To avoid toxicity, flavonoids, which are biosynthesized in the cytoplasm, are transported into vacuoles *via* transporters for isolation or storage. In plants, the ATP-binding cassette (ABC) transporter protein is one of the most important class of transporters. ZmMRP3 (multidrug resistance-associated protein 3), which is an ABC-type transporter protein, has been identified to be taken part in the flavonoids transport in *Zea mays* (Goodman et al., 2004). The expression levels of DEGs annotated as ABC transporter I family members were strongly correlated to the concentration of epigallocatechin gallate, flavanone, kaempferol 3-(2″-rhamnosylgalactoside) 7-rhamnoside, kaempferol 3-(2″-rhamnosyl-6″-acetylgalactoside) 7-rhamnoside, and these transporter genes might take part in the transmembrane transport of anthocyanins and flavonoids in the tea plant (**Figure 6**).

In conclusion, this study performed an integrated metabolome and transcriptome analysis of the purple leaves and the green leaves of the 'Zijuan' tea plant. Due to the higher expression levels of genes involved in the phenylpropanoid and flavonoid biosynthesis pathways in the purple leaves, there were significantly higher concentrations of flavonoids (especially kaempferol and quercetin derivatives) in the purple leaves compared with the green leaves. By correlation analysis, DEGs, which showed expression levels that strongly correlated with the concentrations of flavonoid, were identified, including transporters and transcription factors such as *NAC008*, *MYB23*, *bHLH96,* and *ABC transporter I*, which might be involved in flavonoid biosynthesis or transport. In conclusion, this study provides a new insight into the mechanism of the biosynthesis and accumulation of flavonoids and anthocyanins in the tea plant, and also constructed a correlation network of transcriptional expression levels and metabolite concentrations which could be

used to apply genetic approaches to clarify the mechanism of flavonoids and anthocyanins regulation.

DATA AVAILABILITY STATEMENT

The datasets presented in this study can be found in online repositories. The names of the repository/repositories and accession number(s) can be found below: National Center for Biotechnology Information (NCBI) BioProject database under accession number PRJNA661139.

AUTHOR CONTRIBUTIONS

CL and HL designed the experiments and coordinated the project. SS and YT collected all the samples and performed the transcriptomic and metabolomic analyses. LG and DT performed the data analysis and qRT-PCR experiments. JL and YW performed the anthocyanin analysis. CL and FG wrote and edited the manuscript. All authors have read and approved the final manuscript.

FUNDING

This work was financially supported by the Zhejiang Provincial Natural Science Foundation of China (No. LY19C160003), the National Natural Science Foundation of China (No. 31800582), the Scientific Research Project of Zhejiang Education Department (No. Y202147613), and the program of China Scholarship Council (No. 201908330115).

SUPPLEMENTARY MATERIAL

The Supplementary Material for this article can be found online at: https://www.frontiersin.org/articles/10.3389/fpls.2022.880227/full#supplementary-material

REFERENCES

Cho, K., Cho, K. S., Sohn, H. B., Ha, I. J., Hong, S. Y., Lee, H., et al. (2016). Network analysis of the metabolome and transcriptome reveals novel regulation of potato pigmentation. *J. Exp. Bot.* 67, 1519–1533. doi: 10.1093/jxb/erv549

Daehwan, K., Ben, L., and Salzberg, S. L. (2015). HISAT: a fast spliced aligner with low memory requirements. *Nat. Methods* 12, 357–360. doi: 10.1038/nmeth.3317

Faragher, J. D., and Brohier, R. L. (1984). Anthocyanin accumulation in apple skin during ripening: regulation by ethylene and phenylalanine ammonia-lyase. *Sci. Hortic.* 22, 89–96. doi: 10.1016/0304-4238(84)90087-6

Goodman, C. D., Casati, P., and Walbot, V. (2004). A multidrug resistance-associated protein involved in anthocyanin transport in Zea mays. *Plant Cell.* 16:1812. doi: 10.1105/tpc.022574

Hamanishi, E. T., Barchet, G. L. H., Rebecca, D., Mansfield, S. D., and Campbell, M. M. (2015). Poplar trees reconfigure the transcriptome and metabolome in response to drought in a genotype- and time-of-day-dependent manner. *BMC. Genom.* 16:329. doi: 10.1186/s12864-015-1535-z

He, J., and Giusti, M. M. (2010). Anthocyanins: natural colorants with health-promoting properties. *Annu. Rev. Food Sci. Technol.* 1:163. doi: 10.1146/annurev.food.080708.100754

He, X., Zhao, X., Gao, L., Shi, X., Dai, X., Liu, Y., et al. (2018). Isolation and characterization of key genes that promote flavonoid accumulation in purple-leaf tea (*Camellia sinensis* L.). *Sci. Rep*. 8:130. doi: 10.1038/s41598-017-18133-z

Hsu, C. P., Shih, Y. T., Lin, B. R., Chiu, C. F., and Lin, C. C. (2012). Inhibitory effect and mechanisms of an anthocyanins- and anthocyanidins-rich extract from purple-shoot tea on colorectal carcinoma cell proliferation. *J. Agric. Food Chem.* 60, 3686–3692. doi: 10.1021/jf204619n

Iwashina, T. (2015). Contribution to flower colors of flavonoids including anthocyanins: a Review. *Nat. Prod. Commun.* 10, 529–544. doi: 10.1177/1934578x1501000335

Jaakola, L. (2013). New insights into the regulation of anthocyanin biosynthesis in fruits. *Trends Plant Sci.* 18, 477–483. doi: 10.1016/j.tplants.2013.06.003

Ke, S. W., Chen, G. H., Chen, C. T., Tzen, J. T. C., and Yang, C. Y. (2018). Ethylene signaling modulates contents of catechin and ability of antioxidant in *Camellia sinensis*. *Bot. Stud.* 59:11. doi: 10.1186/s40529-018-0226-x

Kerio, L. C., Wachira, F. N., Wanyoko, J. K., and Rotich, M. K. (2013). Total polyphenols, catechin profiles and antioxidant activity of tea products from purple leaf coloured tea cultivars. *Food Chem.* 136, 1405–1413. doi: 10.1016/j.foodchem.2012.09.066

Kilel, E. C., Faraj, A. K., Wanyoko, J. K., Wachira, F. N., and Mwingirwa, V. (2013). Green tea from purple leaf coloured tea clones in Kenya- their quality characteristics. *Food Chem.* 141, 769–775. doi: 10.1016/j.foodchem.2013.03.051

Kovinich, N., Saleem, A., Arnason, J. T., and Miki, B. (2011). Combined analysis of transcriptome and metabolite data reveals extensive differences between black and brown nearly-isogenic soybean (*Glycine max*) seed coats enabling the identification of pigment isogenes. *BMC Genom.* 12:381. doi: 10.1186/1471-2164-12-381

Li, J., Lv, X. J., Wang, L. X., Qiu, Z. M., Song, X. M., Lin, J. K., et al. (2017). Transcriptome analysis reveals the accumulation mechanism of anthocyanins in 'Zijuan' tea (*Camellia sinensis* var. asssamica (Masters) kitamura) leaves. *Plant Growth Regul.* 81, 51–61. doi: 10.1007/s10725-016-0183-x

Mao, X., Tao, C., Olyarchuk, J. G., and Wei, L. (2005). Automated genome annotation and pathway identification using the KEGG Orthology (KO) as a controlled vocabulary. *Bioinformation* 21, 3787–3793. doi: 10.1093/bioinformatics/bti430

Mei, Y., Xie, H., Liu, S., Zhu, J., and Wei, C. (2020). Metabolites and transcriptional profiling analysis reveal the molecular mechanisms of the anthocyanin metabolism in the "Zijuan" Tea Plant (*Camellia sinensis* var. *assamica*). *J. Agric. Food Chem.* 69, 414–427. doi: 10.1021/acs.jafc.0c06439

Mihaela, P., Pertea, G. M., Antonescu, C. M., Tsung-Cheng, C., Mendell, J. T., and Salzberg, S. L. (2015). StringTie enables improved reconstruction of a transcriptome from RNA-seq reads. *Nat. Biotechnol.* 33, 290–295. doi: 10.1038/nbt.3122

Morishita, T., Kojima, Y., Maruta, T., Nishizawa-Yokoi, A., Yabuta, Y., and Shigeoka, S. (2009). Arabidopsis NAC Transcription Factor, ANAC078, regulates flavonoid biosynthesis under high-light. *Plant Cell Physiol.* 50, 2210–2222. doi: 10.1093/pcp/pcp159

Nesi, N., Jond, C., Debeaujon, I., Caboche, M., and Lepiniec, L. (2001). The Arabidopsis TT2 gene encodes an R2R3 MYB domain protein that acts as a key determinant for proanthocyanidin accumulation in developing seed. *Plant Cell.* 13, 2099–2114. doi: 10.1105/tpc.010098

Proctor, J. T. A. (1974). Color stimulation in attached apples with supplementary light. *Can. J. Plant Sci.* 54, 499–503. doi: 10.4141/cjps74-084

Savoi, S., Wong, D. C. J., Arapitsas, P., Miculan, M., Bucchetti, B., Peterlunger, E., et al. (2016). Transcriptome and metabolite profiling reveals that prolonged drought modulates the phenylpropanoid and terpenoid pathway in white grapes (*Vitis vinifera* L.). *BMC Plant Biol.* 16:67. doi: 10.1186/s12870-016-0760-1

Shannon, P., Markeil, A., Ozier, O., Baliga, N. S., Wang, J. T., Ramage, D., et al. (2003). Cytoscape: a software environment for integrated models of biomolecular interaction networks. *Genome. Res.* 13, 2498–2504. doi: 10.1101/gr.1239303

Shen, J. Z., Zou, Z. W., Zhang, X. Z., Zhou, L., Wang, Y. H., Fang, W. P., et al. (2018). Metabolic analyses reveal different mechanisms of leaf color change in two purple-leaf tea plant (*Camellia sinensis* L.) cultivars. *Hortic. Res.* 5:7. doi: 10.1038/s41438-017-0010-1

Tian, J., Han, Z. Y., Zhang, J., Hu, Y., Song, T., and Yao, Y. (2015). The balance of expression of dihydroflavonol 4-reductase and flavonol synthase regulates flavonoid biosynthesis and red foliage coloration in Crabapples. *Sci. Rep.* 5:12228. doi: 10.1038/srep12228

Wang, L. K., Feng, Z. X., Wang, X. W., and Zhang, X. G. (2010). DEGseq: an R package for identifying differentially expressed genes from RNA-seq data. *Bioinformation* 26, 136–138. doi: 10.1093/bioinformatics/btp612

Wang, L. X., Pan, D. Z., Meng, L., Abubakar, Y. S., Li, J., Lin, J. K., et al. (2017). Regulation of anthocyanin biosynthesis in purple leaves of Zijuan tea (*Camellia sinensis* var. kitamura). *Int. J. Mol. Sci.* 18:833. doi: 10.3390/ijms18040833

Wang, W. L., Wang, Y. X., Li, H., Liu, Z. W., Cui, X., and Zhuang, J. (2018). Two MYB transcription factors (CsMYB2 and CsMYB26) are involved in flavonoid biosynthesis in tea plant [*Camellia sinensis (L.)* O. Kuntze]. *BMC Plant Biol.* 18:288. doi: 10.1186/s12870-018-1502-3

Wang, Y. S., Xu, Y. J., Gao, L. P., Yu, O., Wang, X. Z., He, X. J., et al. (2014). Functional analysis of flavonoid 3',5'-hydroxylase from tea plant (*Camellia sinensis*): critical role in the accumulation of catechins. *BMC Plant Biol.* 14:347. doi: 10.1186/s12870-014-0347-7

Wei, C., Yang, H., Wang, S., Zhao, J., Liu, C., Gao, L., et al. (2018). Draft genome sequence of *Camellia sinensis* var. sinensis provides insights into the evolution of the tea genome and tea quality. *Proc. Natl. Acad. Sci. U S A.* 115:201719622. doi: 10.1073/pnas.1719622115

Wei, K., Wang, L., Zhang, Y., Ruan, L., Li, H., Wu, L., et al. (2019). A coupled role for CsMYB75 and CsGSTF1 in anthocyanin hyperaccumulation in purple tea. *Plant J.* 97, 825–840. doi: 10.1111/tpj.14161

Williams, C. A., Greenham, J., Harborne, J. B., Kong, J. M., and Tatsuzawa, F. (2002). Acylated anthocyanins and flavonols from purple flowers of Dendrobium cv. 'Pompadour'. *Biochem. Syst. Ecol.* 30, 667–675. doi: 10.1016/S0305-1978(01)00147-8

Xia, E., Tong, W., Hou, Y., An, Y., and Wan, X. (2020). The reference genome of tea plant and resequencing of 81 diverse accessions provide insights into genome evolution and adaptation of tea plants. *Mol. Plant* 13, 1013–1026. doi: 10.1016/j.molp.2020.04.010

Zhang, S., Zhang, L., Tai, Y., Wang, X., Ho, C. T., and Wan, X. (2018). Gene discovery of characteristic metabolic pathways in the tea plant (*Camellia sinensis*) using 'Omics'-based network approaches: a Future Perspective. *Front. Plant Sci.* 9:480. doi: 10.3389/fpls.2018.00480

Zhao, J. (2015). Flavonoid transport mechanisms: how to go, and with whom. *Trends Plant Sci.* 20, 576–585. doi: 10.1016/j.tplants.2015.06.007

Zhou, H., Lin-Wang, K., Wang, H., Gu, C., Dare, A. P., Espley, R. V., et al. (2015). Molecular genetics of blood-fleshed peach reveals activation of anthocyanin biosynthesis by NAC transcription factors. *Plant J.* 82, 105–121. doi: 10.1111/tpj.12792

Conflict of Interest: The authors declare that the research was conducted in the absence of any commercial or financial relationships that could be construed as a potential conflict of interest.

Publisher's Note: All claims expressed in this article are solely those of the authors and do not necessarily represent those of their affiliated organizations, or those of the publisher, the editors and the reviewers. Any product that may be evaluated in this article, or claim that may be made by its manufacturer, is not guaranteed or endorsed by the publisher.

frontiers | Frontiers in Plant Science

ORIGINAL RESEARCH
published: 27 May 2022
doi: 10.3389/fpls.2022.910768

Identification and Expression Analysis of *CAMTA* Genes in Tea Plant Reveal Their Complex Regulatory Role in Stress Responses

Qiying Zhou[1,2,3], Mingwei Zhao[1,2,3], Feng Xing[1,2,3], Guangzhi Mao[1,2,3], Yijia Wang[1,2,3], Yafeng Dai[1,2,3], Minghui Niu[1,2,3] and Hongyu Yuan[1,2,3]**

[1]Henan Key Laboratory of Tea Plant Biology, Xinyang Normal University, Xinyang, China, [2]Henan Engineering Research Center of Tea Deep-Processing, Xinyang Normal University, Xinyang, China, [3]Institute for Conservation and Utilization of Agro-Bioresources in Dabie Mountains, Xinyang Normal University, Xinyang, China

OPEN ACCESS

Edited by:
Enhua Xia,
Anhui Agriculture University, China

Reviewed by:
Xujun Zhu,
Nanjing Agricultural University, China
Fei Guo,
Huazhong Agricultural University, China

***Correspondence:**
Qiying Zhou
zhouqy@xynu.edu.cn
Hongyu Yuan
yhongyu92@163.com

Specialty section:
This article was submitted to Plant Metabolism and Chemodiversity, a section of the journal Frontiers in Plant Science

Received: 01 April 2022
Accepted: 03 May 2022
Published: 27 May 2022

Citation:
Zhou Q, Zhao M, Xing F, Mao G, Wang Y, Dai Y, Niu M and Yuan H (2022) Identification and Expression Analysis of CAMTA Genes in Tea Plant Reveal Their Complex Regulatory Role in Stress Responses. Front. Plant Sci. 13:910768. doi: 10.3389/fpls.2022.910768

Calmodulin-binding transcription activators (CAMTAs) are evolutionarily conserved transcription factors and have multi-functions in plant development and stress response. However, identification and functional analysis of tea plant (*Camellia sinensis*) *CAMTA* genes (*CsCAMTAs*) are still lacking. Here, five *CsCAMTAs* were identified from tea plant genomic database. Their gene structures were similar except *CsCAMTA2*, and protein domains were conserved. Phylogenetic relationship classified the CsCAMTAs into three groups, CsCAMTA2 was in group I, and CsCAMTA1, 3 and CsCAMTA4, 5 were, respectively, in groups II and III. Analysis showed that stress and phytohormone response-related *cis*-elements were distributed in the promoters of *CsCAMTA* genes. Expression analysis showed that *CsCAMTAs* were differentially expressed in different organs and under various stress treatments of tea plants. Three-hundred and four hundred-one positive co-expressed genes of *CsCAMTAs* were identified under cold and drought, respectively. *CsCAMTAs* and their co-expressed genes constituted five independent co-expression networks. KEGG enrichment analysis of *CsCAMTAs* and the co-expressed genes revealed that hormone regulation, transcriptional regulation, and protein processing-related pathways were enriched under cold treatment, while pathways like hormone metabolism, lipid metabolism, and carbon metabolism were enriched under drought treatment. Protein interaction network analysis suggested that CsCAMTAs could bind (G/A/C)CGCG(C/G/T) or (A/C)CGTGT *cis* element in the target gene promoters, and transcriptional regulation might be the main way of *CsCAMTA*-mediated functional regulation. The study establishes a foundation for further function studies of *CsCAMTA* genes in stress response.

Keywords: tea plant, genome-wide, expression analysis, *CAMTA*, gene family

INTRODUCTION

Calcium (Ca^{2+}) is a well-known second messenger that can be activated by various exogenous and endogenous signals (Zhang et al., 2014; Furio et al., 2020). Then, the signals are relayed by downstream proteins, including calmodulins/calmodulin-like proteins (CaMs/CMLs), calcium-dependent protein kinases (CDPKs), and calcineurin B-like proteins (CBLs), to regulate gene expression and different biochemical processes (Rahman et al., 2016; Wei et al., 2017). Calmodulin-binding transcription activators (CAMTAs) are a kind of novel and well-studied CaM-interacting transcription factors and are evolutionarily conserved in almost all eukaryotes (Yang et al., 2015; Kakar et al., 2018). After being identified in tobacco, genome-wide identification and analysis of *CAMTA* genes have been done in many plant species, including Arabidopsis (*Arabidopsis thaliana*; Bouché et al., 2002), rice (*Oryza sativa*; Choi et al., 2005), maize (*Zea mays*; Yue et al., 2015), soybean (*Glycine max*; Wang et al., 2015), grape (*Vitis vinifera*; Shangguan et al., 2014), cotton (*Gossypium* spp.; Pant et al., 2018), medicago (*Medicago truncatula*; Yang et al., 2015), citrus (*Citrus sinensis* and *Citrus clementina*; Zhang et al., 2019a), and poplar (*Populus trichocarpa*; Wei et al., 2017).

CAMTA proteins are characterized by containing several conserved functional domains from the N terminus to the C terminus, including CG-1 domain, TIG/IPT (transcription-associated immunoglobulin domain/immunoglobulin-like fold shared by plexins and transcription factors) domain, ankyrin repeat (ANK) domain, IQ domain (IQXXXRGXXXR), and calmodulin-binding domain (CaMBD). The CG-1 domain is a specific DNA binding domain, usually with nuclear localization signal (NLS) at N terminus. The TIG/IPT domain is responsible for non-specific DNA-binding. The ANK domain is evolved to mediate protein–protein interactions. The IQ domain is Ca^{2+}-independent CaM interacting domain, while the CaMBD domain is Ca^{2+}-dependent CaM binding domain (Yang et al., 2012; Rahman et al., 2016; Büyük et al., 2019). By binding with the (G/A/C)CGCG(C/G/T) or (A/C)CGTGT *cis* element in the promoter region, CAMTA proteins thus can interact and regulate the transcription of target genes (Yue et al., 2015; Noman et al., 2019; Sun et al., 2020).

CAMTA protein is a pivotal component of the Ca^{2+} signal transduction pathway and plays important roles in plant growth and development, as well as in an array of stress responses (Yang et al., 2012; Shangguan et al., 2014; Zhang et al., 2019a). Tobacco (*Nicotiana tabacum*) *NtER1*, the first *CAMTA* gene identified in plant, was a trigger for senescence and death, with high expression in senescing tissues (Yang et al., 2015). AtCAMTA1 and AtCAMTA5 were important regulators in *Arabidopsis* pollen development by affecting the expression of *AVP1* gene, which functioned in the vacuolar pH maintenance (Zhang et al., 2019a). Recent research showed that AtCAMTA6/SR3 was important for seed germination under salt stress environment (Shkolnik et al., 2019). *CAMTA* genes also exhibited dynamic expression patterns in different organs and development stages and was related to fruit ripen (Yang et al., 2012; Ouyang et al., 2019). *AtCAMTA1*, *AtCAMTA2,* and *AtCAMTA3* could regulate plant cold tolerance together by inducing the expression of *CBF* genes (Doherty et al., 2009; Kim et al., 2013; Novikova et al., 2020). *CAMTA* gene was also contributed to plant drought resistance (Pandey et al., 2013; Meer et al., 2019; Saeidi et al., 2019). Expression of *citrus CAMTA* gene was upregulated under salt stress, indicating a role of *CAMTA* gene in salt stress (Ouyang et al., 2019). AtCAMTA3 was proved to regulate glucose metabolism and ethylene-induced senescence and also important for plant defense against insect herbivores (Qiu et al., 2012; Yang et al., 2015). Recently, *AtCAMTA1*, *AtCAMTA2,* and *AtCAMTA3* were reported to participate in plant immune reactions (Kim et al., 2020; Sun et al., 2020). In addition, *CAMTA* gene could respond to plant hormone signals and display a close relationship with ethylene (ET), SA (salicylic acid) and JA (jasmonic acid; Yang et al., 2015; Yue et al., 2015; Wei et al., 2017).

Tea is one of the three most popular non-alcoholic beverages in the world and is made from leaves of tea plant (*Camellia sinensis*). In recent years, gene function studies and role of transcription factors have been focused in tea plant science (Wei et al., 2018; Zhang et al., 2020). As a kind of sessile organism, tea plant is vulnerable to external environmental stresses, such as cold, drought, salt, and pest attack (Zhang et al., 2017; Li et al., 2019; Zhou et al., 2019a). CAMTAs, one kind of important regulator in plant growth, development, and stress response, have not been identified and studied in tea plant to date. In this study, tea plant *CAMTA* (*CsCAMTA*) genes were identified from the reported genomic database (Wei et al., 2018). The phylogenetic relationship, gene structure, promoter *cis* elements of *CsCAMTA* genes, and conserved CsCAMTA protein domains were analyzed. *CsCAMTA* gene expression profiles in different organs and under different stress treatments, co-expression networks of *CsCAMTA* genes under cold and drought stresses, and KEGG enrichment analysis of *CsCAMTA*s and their co-expressed genes were done. Also, interaction network of CsCAMTA proteins in tea plant was built, and the putative binding sites in the target genes were identified. This work provides the first survey of *CsCAMTA* genes in tea plant and is important for further function studies of *CsCAMTA* genes and tea plant resistance improvement.

MATERIALS AND METHODS

Identification and Analysis of Putative *CsCAMTA* Genes in Tea Plant

The whole genomic sequence data of tea plant were downloaded from the State Key Laboratory of Tea Plant Biology and Utilization[1] according to Wei et al. (2018). The hidden Markov models (HMMs) of CAMTA family (Pfam03859, CG-1 domain; Pfam01833, TIG domain; Pfam12796, Ank domain; Pfam00612, IQ domain) were used to identify *CsCAMTA* genes from the tea plant genomic database by HMMER (V3.3) software. Then, a BLASTp program was used to search the tea plant protein database by employing the amino acid sequences of *Arabidopsis*

[1]http://pcsb.ahau.edu.cn:8080/CSS/

CAMTAs as a query. At last, the putative CsCAMTAs identified by the HMMER and BLASTp programs were put together. Redundant CsCAMTAs were removed, and the remaining putative CsCAMTAs were further confirmed by domain analysis using the CDD (Conserved Domain Database[2]) and SMART[3] programs. Those containing CG-1 domain, TIG domain, Ank domain, and IQ domain were recognized as *CsCAMTA* gene family members.

Molecular weights (MW) and isoelectric points (pI) of the recognized CsCAMTA proteins were computed by the Compute pI/Mw tool of ExPASy.[4] The physicochemical properties of CsCAMTA proteins were computed by ProtParam Tool.[5] The most similar homolog of each *CsCAMTA* gene was analyzed by search against the Araport11 transcripts (DNA) database using BLASTN program, and the expect value (E-value) was given after the alignment. Subcellular locations of the identified CsCAMTA proteins were predicted using the CELLO v.2.5[6] online tool.

Phylogenetic Relationship Analysis

CAMTA protein sequences of *Arabidopsis*, *Oryza sativa* (ssp. Japonica), *Vitis vinifera*, *Populus trichocarpa*, and *Citrus clementina* were downloaded from the PlantTFDB v5.0 database.[7] CAMTA proteins in *Arabidopsis* and *Populus trichocarpa* were named according to Doherty et al. (2009) and Wei et al. (2017), respectively. Multiple sequence alignment was done by using the Clustalw program. The phylogenetic tree construction was accomplished by the MEGA 6.0 software with the neighbor joining method, and the bootstrap was set as 1,000 replications (Tamura et al., 2013).

Gene Structure and Sequence Analysis

The transcript sequences, DNA sequences, and protein sequences of *CsCAMTA* genes were obtained from the tea plant genomic database. The conserved domains of CsCAMTA proteins were identified in Pfam database. NLS of the CsCAMTA proteins was analyzed by Motif scan.[8] The calmodulin binding domain (CaMBD) sequences of CsCAMTA proteins were identified manually according to the conserved motif sequence (WXVX(2) LXKX(2)[LF]RWRX[KR]X(3)[FL]RX) of CAMTA protein in *Arabidopsis* (Pant et al., 2018). Conserved domains, gene structures, and the CaMBD sequence logo of the CsCAMTAs were visualized by the TBtools toolkit (Chen et al., 2020).

Promoter *cis*-Elements Analysis of *CsCAMTA* Genes

To investigate the promoter *cis*-elements of *CsCAMTA* genes, 2.0 kb genomic DNA sequences upstream of the initiation codon (ATG) were retrieved from the Tea Plant Information Archive (TPIA; Xia et al., 2019). Stress response and hormone regulation related *cis*-elements were predicted by PlantCARE.[9]

Analysis of *CsCAMTA* Gene Expression by RNA-seq Data

The RNA-seq data of tea plant different tissues (Wei et al., 2018) and those of tea plants under cold acclimation treatments (Li et al., 2019), under NaCl treatment and drought stress treatment (Zhang et al., 2017) and under MeJA treatment (Shi et al., 2015), were, respectively, downloaded from the public database according to the cited literature. Gene expression level was represented by the FPKM (Fragments per kilobase of transcript sequence per millions fragments mapped) value using the Tophat and Cufflink softwares (Trapnell et al., 2010). The expression heatmaps were generated and visualized by the TBtools toolkit (Chen et al., 2020).

Gene Co-expression Network and KEGG Analysis

To understand the co-expression network of *CsCAMTA* genes under cold and drought stresses, positive co-expressed genes of *CsCAMTAs* were retrieved from the Tea Plant Information Archive according to the Pearson's correlation based on the TPM (Transcripts per million) value of the transcriptomic data (TPIA; Xia et al., 2019). For the co-expression network of *CsCAMTA* genes under cold stress, the threshold of Pearson's correlation was $\geq$0.98, with *value of* $p \leq 0.05$. Under PEG-simulated drought stress, the threshold of Pearson's correlation was $\geq$0.98, *value of p* was $\leq$0.001. Then, Cytoscape (version 3.7.2) software was employed to visualize the co-expression networks.

Protein sequences of *CsCAMTAs* and their co-expressed genes were extracted from the tea genomic database (Wei et al., 2018). The KO IDs of CsCAMTAs and their co-expressed gene-coding proteins were acquired by mapping the protein sequences to the KEGG database *via* KAAS. The significantly enriched pathways were analyzed by the KOBAS software with value of $p \leq 0.05$.

Protein Interaction Network Analysis

For protein interaction network analysis, CsCAMTA protein orthologs in *Arabidopsis* were used and analyzed by employing the online STRING tools.[10]

Tea plant homologs of the *Arabidopsis* proteins displayed in the interaction network were identified by BLASTp program. Then, 2.0 kb genomic DNA sequences upstream of the initiation codon (ATG) of the identified tea plant homologous genes were retrieved from the Tea Plant Information Archive (TPIA; Xia et al., 2019). The conserved CAMTA binding *cis* elements (G/A/C)CGCG(C/G/T) and (A/C)CGTGT were examined in the 2.0 kb upstream genomic region of the identified tea plant homologous genes.

[2]http://www.ncbi.nlm.nih.gov/cdd
[3]http://smart.embl-heidelberg.de/
[4]http://web.expasy.org/compute_pi/
[5]http://web.expasy.org/protparam/
[6]http://cello.life.nctu.edu.tw/
[7]http://planttfdb.gao-lab.org/
[8]http://myhits.isb-sib.ch/cgi-bin/motif_scan
[9]http://bioinformatics.psb.ugent.be/webtools/plantcare/html/
[10]https://string-db.org/cgi/input.pl?sessionId=3MKiLYehXbcT&input_page_show_search=on

Plant Materials and Treatments

Xinyang "Quntizhong" were cultivated in the Experimental Tea Garden of Xinyang Normal University. For tissue expression pattern analysis, apical buds, the first and the second leaves downward from the apical bud (young leaves), mature leaves, old leaves, stems, flowers, fruits, and roots were collected from the same Xinyang "Quntizhong." Tender branches (about 15 cm long) from the same "Quntizhong" tea plant were collected and then used for treatments. For cold treatment, the branches were inserted into the tissue culture bottles with 0.3 cm depth of water and placed in 4°C culture chamber, 70% relative humidity, and 12-h photoperiod with 100 μmol m^{-2} s^{-1} light intensity, while the controls were placed at the tissue culture room at 25°C, 70% relative humidity, and 12-h photoperiod with 100 μmol m^{-2} s^{-1} light intensity. For NaCl treatment, the tea plant branches were inserted into the tissue culture bottles with 300 mM NaCl. For PEG-simulated drought treatment, the tea plant branches were inserted into the tissue culture bottles with 10% PEG6000. For MeJA treatment, the tea plant branches were inserted into the tissue culture bottles with 1 mM MeJA solution which was dissolved in ethanol. The final concentration of ethanol in 1 mM MeJA was 0.5%. For the NaCl and PEG-simulated drought treatments, tea plant branches inserted into the tissue culture bottles with deionized water were used as controls. For the MeJA treatment, tea plant branches inserted into the tissue culture bottles with 0.5% ethanol were used as controls. Both the treatments and controls were placed in the tissue culture room at 25°C, 70% relative humidity, and 12-h photoperiod with 200 μmol m^{-2} s^{-1} light intensity. One to three leaves downward from the apical bud were, respectively, collected after 0, 3, 6, 12, 24, and 48 h of each treatment. For different tea plant tissues and each treatment, materials of three independent biological repeats were collected. The collected plant materials were frozen in liquid nitrogen quickly and stored in −80°C for RNA extraction.

qRT-PCR Analysis

Total RNAs of the collected tea plant materials were, respectively, isolated by the modified CTAB method (Zhou et al., 2019a). Then, cDNA of each sample was synthesized from the total RNA by using the PrimeScript™ RT Reagent Kit (Takara) following the manufacturer's instructions. qRT-PCR analysis was carried out on the LightCycler 96 real-time PCR instrument (Roche) using BrightGreen 2 × qRT-PCR MasterMixes (ABM, Canada). qRT-PCR amplification was as follows: 95.0°C 3 min, followed by 40 cycles of 95.0°C 15 s, 20 s at the primer-specific annealing temperature, and 72.0°C 30 s. Melting curve was generated by heating from 65°C to 95°C in 0.5°C increments to check the primer specificity. The glyceraldehyde-3-phosphate dehydrogenase gene of tea plant (*CsGAPDH*) was used as the internal reference gene, and the relative gene expression was calculated according to the $2^{-\Delta\Delta Ct}$ method (Zhou et al., 2019a). Specific primers of *CsCAMTA* genes and the *CsGAPDH* gene were designed by primer 3.0 and listed in **Supplementary Table S1**.

RESULTS

Genome-Wide Identification of *CAMTA* Gene in Tea Plant

By BLASTp and hidden Markov models (HMMs) search of the tea plant genomic database, the returned CsCAMTAs were checked again by the CDD (Conserved Domain Database) and the SMART programs for identifying the conserved domains of CAMTA protein. In total, five *CsCAMTA* genes containing the CG-1 domain, TIG domain, Ank domain, and IQ domain were identified, which were named *CsCAMTA1-5*, respectively. Details of the identified *CsCAMTA* genes, such as gene ID, amino acid number, molecular weight, isoelectric point (pI), instability index, grand average of hydropathicity (GRAVY), aliphatic index, the *Arabidopsis* homolog, E-value of each *CsCAMTA* gene compared with its corresponding *Arabidopsis* homolog, and subcellular localization of CsCAMTAs, are summarized in **Table 1**. The deduced CsCAMTA protein lengths were varied from 864 to 1,419 amino acids, with the molecular weights ranged from 97.26 to 157.99 kDa, and the predicted isoelectric points were ranged from 5.83 to 6.55. As shown in **Table 1**, the GRAVY values of all the identified CsCAMTA proteins were negative, indicating they were hydrophilic proteins. The instability index value above 40 was predicted as unstable. Results showed that the instability index value of CsCAMTA2 was below 40 while those of the other CsCAMTA proteins were above 40 (**Table 1**), indicating the instability of CsCAMTAs except CsCAMTA2. The predicted aliphatic indexes suggested high thermal stability of CsCAMTA proteins, with CsCAMTA2 having the highest aliphatic index of 82.76 and CsCAMTA3 having the lowest aliphatic index of 74.16. When the *AtCAMTA* homologs were identified, it showed that *AtCAMTA4* was the homolog of *CsCAMTA1* and *CsCAMTA3* genes, *AtCAMTA3* was the homolog of *CsCAMTA2* gene, and *AtCAMTA5* was the homolog of *CsCAMTA4* and *CsCAMTA5* genes, with the smallest E-value. Subcellular localization prediction showed that all CsCAMTA proteins were located in cell nucleus, and CsCAMTA2 and CsCAMTA5 also had a cytoplasmic localization (**Table 1**).

CsCAMTA Gene Structure and Conserved Domains Analysis

The exon–intron structure of *CsCAMTA* genes was analyzed by mapping the transcript sequences to the corresponding genomic sequences. Results showed that most of the *CsCAMTA* genes had similar gene structures, with 10–12 introns. Except that *CsCAMTA2* gene contained 19 introns, and *CsCAMTA4* gene contained 13 introns, among which, one located in the 5′ untranslated region (**Figure 1A**). To better understand the potential functions of CsCAMTAs, conserved domains and NLS of the CsCAMTAs were analyzed. Results displayed that all CsCAMTA proteins contained one CG-1 and one TIG/IPT domain, while more than one ANK and IQ domains were contained in most of the CsCAMTA proteins. The NLS was identified in most of the CsCAMTA proteins except

TABLE 1 | The *CAMTA* genes in tea plant and properties of the deduced proteins.

Name	Gene ID	Amino acids size (aa)	MW (kDa)	pI	GRAVY	Instability index	Aliphatic index	*Arabidopsis* homolog	*E*-value	Subcellular location
CsCAMTA1	*TEA025813.1*	1,028	114.8	6.08	−0.516	46.14	79.14	*AtCAMTA4*	2.00E-151	Nuclear
CsCAMTA2	*TEA012477.1*	1,419	157.99	6.41	−0.345	39.39	82.76	*AtCAMTA3*	2.00E-88	Nuclear, Cytoplasmic
CsCAMTA3	*TEA006574.1*	984	109.83	5.93	−0.516	45.8	74.16	*AtCAMTA4*	0	Nuclear
CsCAMTA4	*TEA011186.1*	953	107.62	6.55	−0.468	44.04	75.14	*AtCAMTA5*	7.00E-106	Nuclear
CsCAMTA5	*TEA011490.1*	864	97.26	5.83	−0.39	43.38	77.27	*AtCAMTA5*	7.00E-105	Nuclear, Cytoplasmic

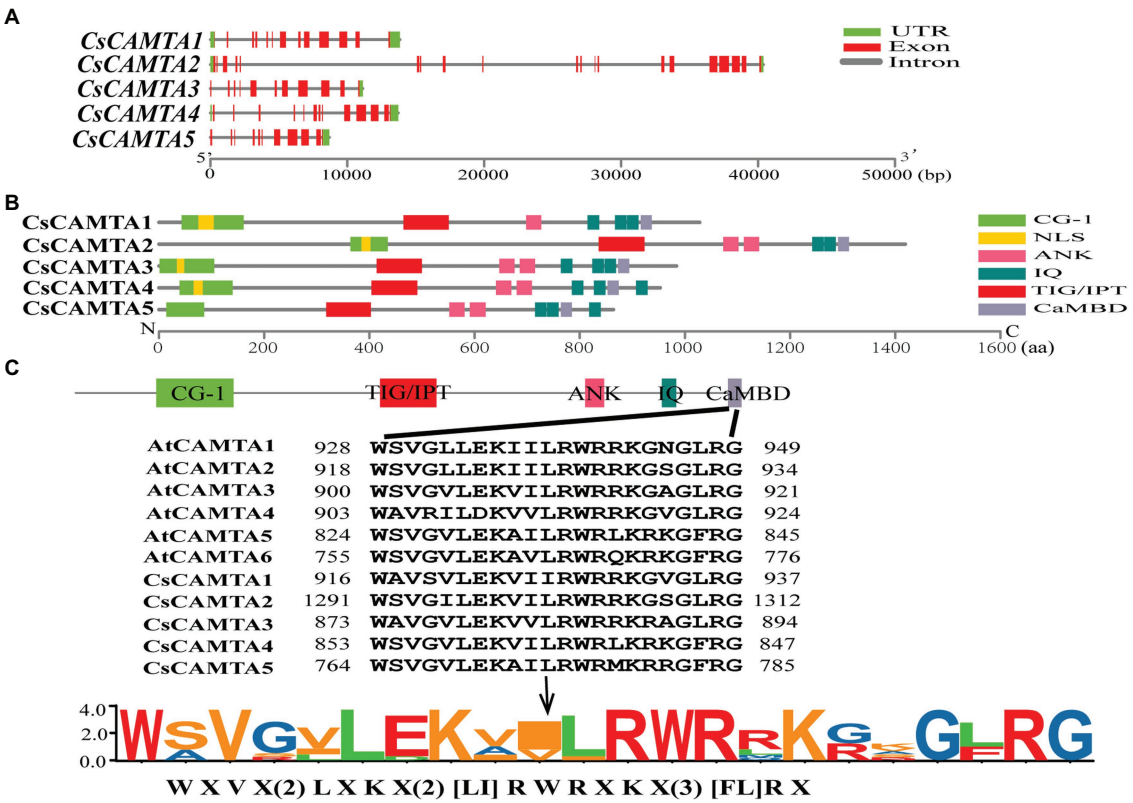

FIGURE 1 | Gene structure, protein functional domains, and CaMBD domain conservation analysis of CsCAMTA family. **(A)** The exon–intron organization of *CsCAMTA* genes. Exons and introns are, respectively, represented by red boxes and gray lines. The untranslated region (UTR) is indicated by green boxes. **(B)** Schematic representation of functional domains of CsCAMTA proteins. CG-1, DNA binding domain; NLS, nuclear localization signal; ANK, ankyrin repeats; IQ, Ca^{2+}-independent CaM-interacting domain; TIG/IPT, non-specific DNA binding domain; CaMBD, Ca^{2+}-dependent CaM binding domain. **(C)** CaMBD sequence alignment and the CaMBD sequence logo of CsCAMTA and AtCAMTA proteins. "[]" suggests the amino acids allowed in this position of the CaMBD motif; "X" denotes any amino acid, and "()" indicates the number of amino acids.

CsCAMTA5, and it was laid inside the CG-1 domain (**Figure 1B**). The CaMBD was identified in all of the five CsCAMTAs (**Figure 1B**), it had a consensus sequence of WXVX(2)LXKX(2)[LI]RWRXKX(3)[FL]RX (**Figure 1C**), which was very similar to that in *Arabidopsis* and tomato (Bouché et al., 2002; Pant et al., 2018).

Phylogenetic Analysis of *CsCAMTA* Genes

To investigate the phylogenetic relationship of *CsCAMTA* genes with those in other plants, a phylogenetic tree containing 33 CAMTA proteins from tea plant, arabidopsis, rice, grape, poplar, and citrus was built. Information of the CAMTA proteins from the six plant species was provided in **Supplementary Table S2**. Results showed that the CAMTA proteins could be clustered into three groups (I, II, and III); each group had the CsCAMTA protein member (**Figure 2**). Group I was the largest one, with 15 members from six plant species, including CsCAMTA2, AtCAMTA1, AtCAMTA2, and AtCAMTA3. There were 9 members in both group II and III, respectively. CsCAMTA1, CsCAMTA3, and AtCAMTA4, together with two CAMTAs in rice (OsCAMTA1 and OsCAMTA2), two CAMTAs in poplar

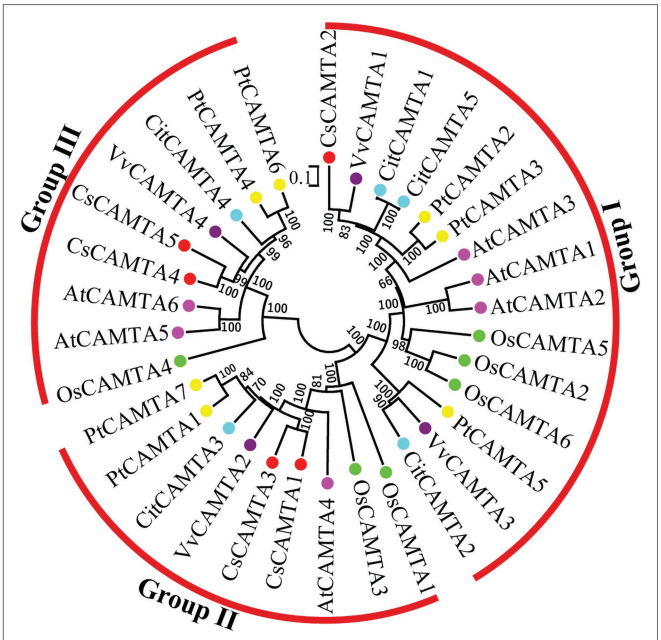

FIGURE 2 | The phylogenetic tree of CAMTA proteins from *Camellia sinensis* (CsCAMTA), *Arabidopsis* (AtCAMTA), *Oryza sativa* (OsCAMTA), *Vitis vinifera* (VvCAMTA), *Populus trichocarpa* (PtCAMTA), and *Citrus clementine* (CitCAMTA) was built by MEGA 6.0 software. Bootstrap values are displayed beside the branches. Dots with different colors represented CAMTA proteins of different plant species (Red, *Camellia sinensis*; Purple, *Vitis vinifera*; Blue, *Citrus clementine*; Yellow, *Populus trichocarpa*; Pink, *Arabidopsis*; Green, *Oryza sativa*).

(PtCAMTA1 and PtCAMTA7), VvCAMTA2 in grape, and CitCAMTA3 in citrus were belonged to group II. CsCAMTA4, CsCAMTA5, along with AtCAMTA5, AtCAMTA6, grape VvCAMTA4, citrus CitCAMTA4, poplar PtCAMTA4 and PtCAMTA6, and rice OsCAMTA4 were presented in group III (**Figure 2**).

Cis Elements in the Promoters of *CsCAMTA* Genes

To understand the putative function of *CsCAMTA* genes in tea plant, the promoter *cis*-elements of *CsCAMTA* genes were investigated. Results revealed that *cis*-elements related to stress and hormone response were found in the promoter of *CsCAMTA* genes (**Figure 3**; **Supplementary Table S3**). *CsCAMTA5* gene had the most number of stress and hormone response-related *cis*-elements in its promoter, whereas *CsCAMTA4* gene had the least. The LTR (low-temperature responsiveness) and the MBS (MYB binding site involved in drought-inducibility) *cis*-elements were existed in all *CsCAMTA* gene promoters except those of *CsCAMTA2* and *CsCAMTA4*. The TC-rich repeat (involved in defense and stress responsiveness) was identified in the promoters of *CsCAMTA4* and *CsCAMTA5*. The CGTCA-motif (involved in the MeJA-responsiveness) was found in all *CsCAMTA* gene promoters except that of *CsCAMTA4*. The TCA element (involved in salicylic acid responsiveness) was found in the promoters of *CsCAMTA3* and *CsCAMTA5*. The ABRE element was found in all of the identified *CsCAMTA* gene promoters except that of *CsCAMTA3*. The O_2-site (involved in zein metabolism regulation), TATC element (involved in gibberellin-responsiveness), and AuxRR core element (involved in auxin responsiveness) were specifically found in the *CsCAMTA2* gene promoter (**Figure 3**; **Supplementary Table S3**).

Expression Profiles of *CsCAMTA* Genes in Different Organs and Under Different Abiotic Stresses

Tissue-specific expression analysis would help us to understand the roles of *CsCAMTA* genes. By employing the publicly available RNA-seq data, tissue-specific expression patterns of *CsCAMTA* genes were displayed with heatmap according to the FPKM values (**Figure 4A**). Results showed that *CsCAMTA2* and *CsCAMTA4* genes relatively had higher expression level in almost all tissues, and *CsCAMTA2* had the highest expression level in fruit, *CsCAMTA4* had the highest expression level in mature leaf. *CsCAMTA3* displayed the highest expression level in old leaf, and its expression was relatively lower in flower and root. *CsCAMTA1* and *CsCAMTA5* genes displayed higher expression in root, stem, and fruit and lower expression level in flower and different developmental stages of leaf tissues (Apical bud, Yong leaf, Old leaf; **Figure 4A**). Further qRT-PCR analysis showed that *CsCAMTA2* and *CsCAMTA4* genes had relative higher expression level in almost all the vegetative tissues examined; the *CsCAMTA2* gene also showed higher expression level in fruits, when compared with the expression level in roots (**Figure 5A**). *CsCAMTA3* gene displayed higher expression in stems, young leaves, and old leaves and lower expression in flowers and fruits, compared with its expression in roots (**Figure 5A**). Except higher expression of *CsCAMTA1* gene was shown in buds and old leaves, the expression levels of *CsCAMTA1* and *CsCAMTA5* genes were lower in the measured tissues, when compared with that in the roots (**Figure 5A**).

To understand functions of *CsCAMTA* genes in stress response, expression profiles of *CsCAMTA* genes were analyzed using the public RNA-seq data first. After cold acclimation (CA) treatment, results showed that expression levels of *CsCAMTA2*, *CsCAMTA3*, and *CsCAMTA5* were upregulated, while those of *CsCAMTA1* and *CsCAMTA4* were downregulated, when compared with that of control (CK). *CsCAMTA4* and *CsCAMTA5* displayed the highest expression level in tea plant after the de-acclimation treatment (DA; **Figure 4B**). qRT-PCR analysis showed that the expression of *CsCAMTA2* gene was upregulated after cold treatment. *CsCAMTA3* and *CsCAMTA4* genes also displayed upregulation after 6 h of the cold treatment, but their expression was downregulated after 12 and 24 h of the cold treatment (**Figure 5B**). The expression levels of *CsCAMTA1* and *CsCAMTA5* genes were significantly downregulated after cold treatment (**Figure 5B**). Under NaCl treatment, RNA-seq data analysis showed that expression levels of all the *CsCAMTA* genes were downregulated after 24 and 48 h of the treatment,

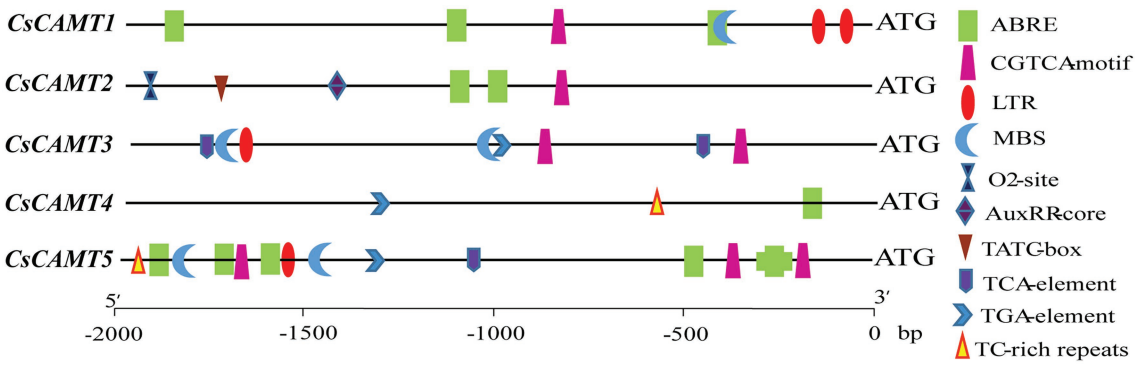

FIGURE 3 | Stress and phytohormone-response related *cis* elements in the promoter of *CsCAMTA* genes.

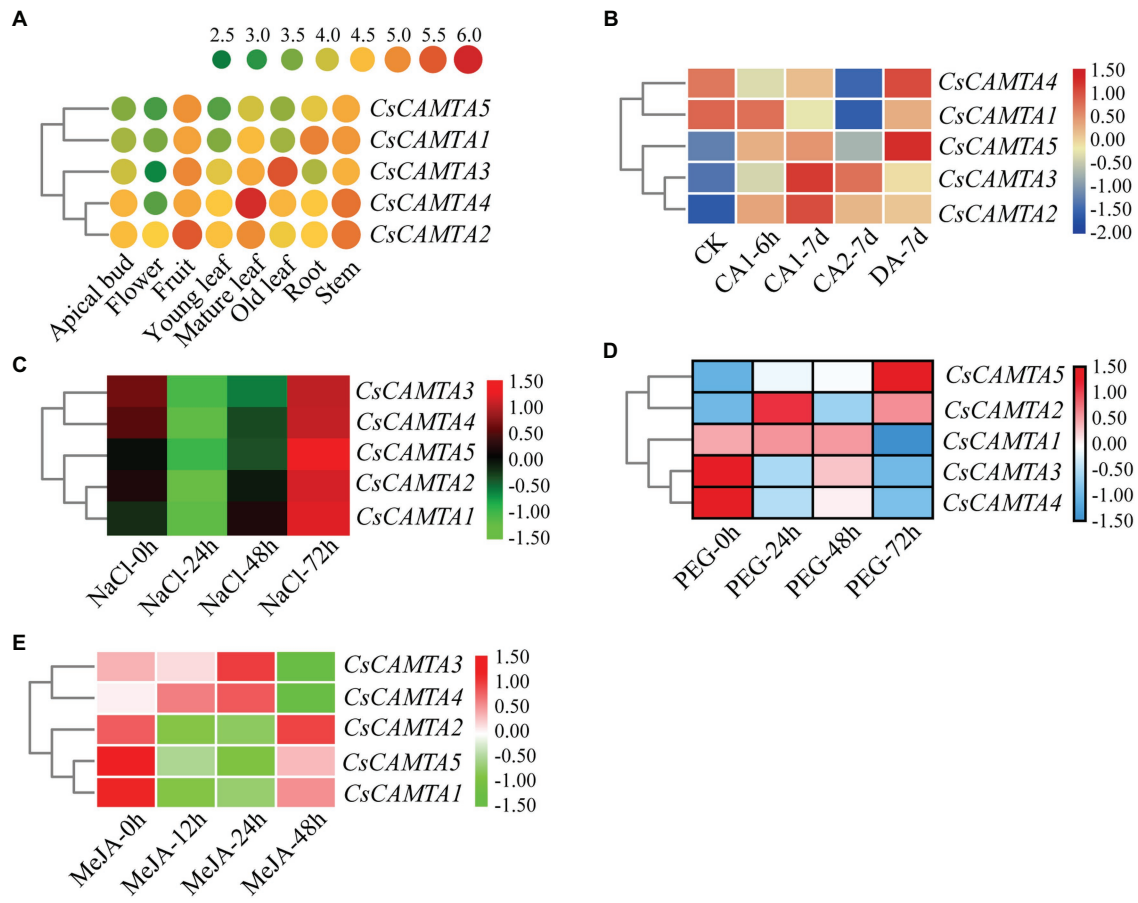

FIGURE 4 | *CsCAMTA* gene expression pattern analysis by publicly available RNA-seq data. **(A–E)** Respectively, denote the expression pattern of *CsCAMTA* genes in different tea plant tissues, under cold acclimation, under salt stress, under PEG-simulated drought stress, and after MeJA treatments. CK, control conditions (Day/night, 25°C 12 h/20°C 12 h); CA1, cold acclimation (Day/night, 10°C 12 h/4°C 12 h); CA2, cold acclimation (Day/night, 4°C 12 h/0°C 12 h); DA, de-acclimation (Day/night, 25°C 12 h/20°C 12 h); NaCl, 200 mM sodium chloride; PEG, 25% polyethylene glycol; MeJA, 0.25% (v/v) methyl jasmonate.

except that the expression of *CsCAMTA1* gene was increased after 48 h of the treatment, when compared with the expression level at 0 h. However, expression levels of all the *CsCAMTA* genes were upregulated after 72 h of the NaCl treatment (**Figure 4C**). By qRT-PCR analysis, results showed that the expression of *CsCAMTA1*, *3*, and *5* genes was downregulated after both the 24 and 48 h of NaCl treatment (**Figure 5C**). The expression of *CsCAMTA4* gene was upregulated after 24 h and had no obvious change after 48 h of NaCl treatment, while the expression of *CsCAMTA4* gene was upregulated

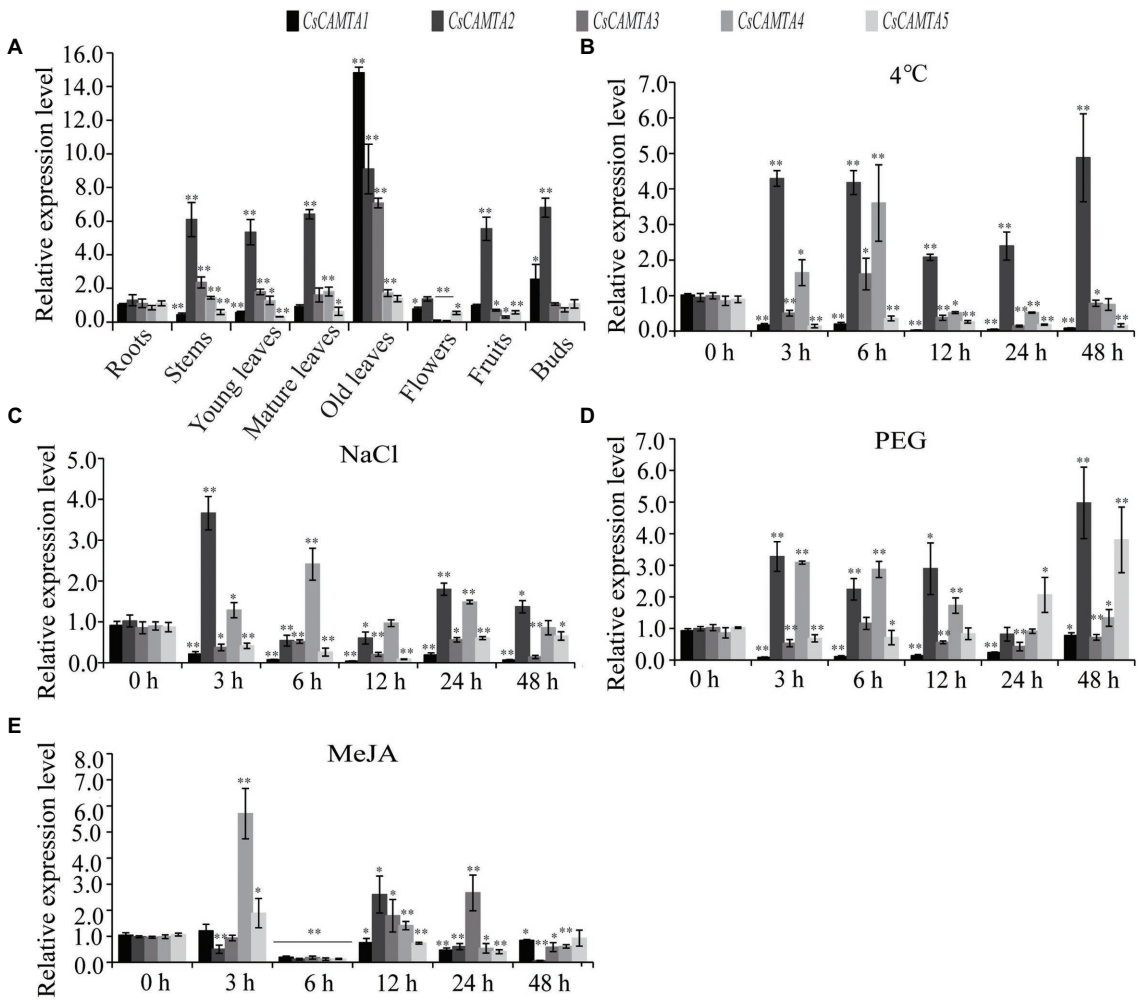

FIGURE 5 | *CsCAMTA* gene expression pattern by qRT-PCR analysis. **(A–E)** Respectively, denote the expression pattern of *CsCAMTA* genes in different tea plant tissues, under cold treatment, under NaCl treatment, under PEG treatment, and under MeJA treatment. The relative expression level was normalized using that of *CsGAPDH* gene. Values are the mean and SD of three biological replicates. Statistical analysis was the Student's *t*-test, $^{*}p < 0.05$ and $^{**}p < 0.01$.

after 24 and 48 h of NaCl treatment (**Figure 5C**). After PEG-simulated drought treatment, RNA-seq data analysis showed that the expression levels of *CsCAMTA3* and *CsCAMTA4* were downregulated, and that of *CsCAMTA1* showed no obvious change after 24 and 48 h, but was downregulated after 72 h of the PEG treatment (**Figure 4D**), while those of *CsCAMTA2* and *CsCAMTA5* were upregulated. Expression of *CsCAMTA2* and *CsCAMTA5* was upregulated after 24 h of the PEG treatment. The expression of *CsCAMTA5* gene exhibited a continuous increase, and it displayed the highest expression level at 72 h of the treatment (**Figure 4D**). qRT-PCR analysis showed that the expression of *CsCAMTA1* and *CsCAMTA3* genes was downregulated, while that of *CsCAMTA2* and *CsCAMTA4* genes was upregulated, after PEG treatment (**Figure 5D**). The expression of *CsCAMTA5* gene was downregulated after 3 and 6 h and was upregulated after 24 and 48 h after PEG treatment (**Figure 5D**). Expression of *CsCAMTA* genes under MeJA treatment was also investigated, RNA-seq data analysis showed that expression levels of *CsCAMTA1*, *CsCAMTA2,* and *CsCAMTA5* were downregulated, and that of *CsCAMTA4* was upregulated after 12 and 24 h of the treatment. Expression level of *CsCAMTA3* gene was downregulated after 12 and upregulated after 24 h of the MeJA treatment. After 48 h of the treatment, expression of all the *CsCAMTA* genes was decreased, except that of *CsCAMTA2* showed a little increment, when compared with the expression level at 0 h (**Figure 4E**). After MeJA treatment, qRT-PCR analysis showed that the expression of *CsCAMTA1* and *5* was downregulated after 12 and 24 h, and that of *CsCAMTA2* and *4* was upregulated after 12 h and downregulated after 24 h (**Figure 5E**). The expression of *CsCAMTA3* was upregulated after both 12 and 24 h of MeJA treatment (**Figure 5E**). After 48 h of MeJA treatment, except the expression of *CsCAMTA5* gene showed no obvious change, that of the other *CsCAMTA* genes was downregulated (**Figure 5E**).

Functional Annotation and Co-expression Network of *CsCAMTA* Genes Under Cold and Drought Treatments

To understand the putative functions of *CsCAMTA* genes in tea plant, functional annotation of *CsCAMTA* genes was investigated in GO, KEGG, TrEMBL, Swissprot, and Nr database, respectively. Results showed that the five identified *CsCAMTA* genes were annotated as calmodulin-binding transcription activators in TrEMBL, Swissprot, and Nr databases. According to GO and KEGG annotation, *CsCAMTA1* and *CsCAMTA3* were annotated as proteins related to lipase, ester hydrolase, LPA acyltransferase, and signal recognition; *CsCAMTA4* and *CsCAMTA5* were related to transcription regulation, motor protein, and mitosis, and *CsCAMTA4* was also involved in lipid metabolism; *CsCAMTA2* was annotated as MLO family protein (**Supplementary Table S4**).

To further understand the function of *CsCAMTA* genes under cold and drought stresses, gene co-expression networks of *CsCAMTAs* were analyzed (**Figures 6A,B**; **Supplementary Table S5**). Our results showed that *CsCAMTA* genes had 300 and 401 positive co-expressed genes under cold and drought stress treatments, respectively. Under cold stress, the *CsCAMTA* gene co-expression network was constituted by 305 nodes and 300 edges. *CsCAMTA3* had the most number (156) of co-expressed genes, while *CsCAMTA2* had the least number (21) of co-expressed genes (**Figure 6A**; **Supplementary Table S5**). Under PEG-simulated drought treatment, there were 406 nodes and 401 edges in the *CsCAMTA* gene co-expression network. *CsCAMTA4* had the most number (223) of co-expressed genes, while *CsCAMTA2* had the least number (6) of co-expressed genes. In total, five co-expression networks were formed between *CsCAMTAs* and their co-expressed genes under both cold and drought stress treatments. No co-expression was seen between the five identified *CsCAMTA* genes (**Figure 6B**; **Supplementary Table S5**).

CsCAMTAs and their positive co-expressed genes were subjected to KEGG analysis to identify the enrichment of functional categories. Results showed that *CsCAMTAs* and their positive co-expressed genes were enriched in 10 metabolic pathways under cold treatment, including RNA transport, ubiquitin-mediated proteolysis, mRNA surveillance pathway, linoleic acid metabolism, steroid biosynthesis, arachidonic acid metabolism, etc. (**Figure 6C**; **Supplementary Table S6**). Under PEG-simulated drought stress, 15 metabolic pathways including starch and sucrose metabolism, ubiquinone, and other terpenoid-quinone biosynthesis, glycosphingolipid biosynthesis, arachidonic acid metabolism, biosynthesis of secondary metabolites, linoleic acid metabolism, lysine degradation, etc., were enriched by

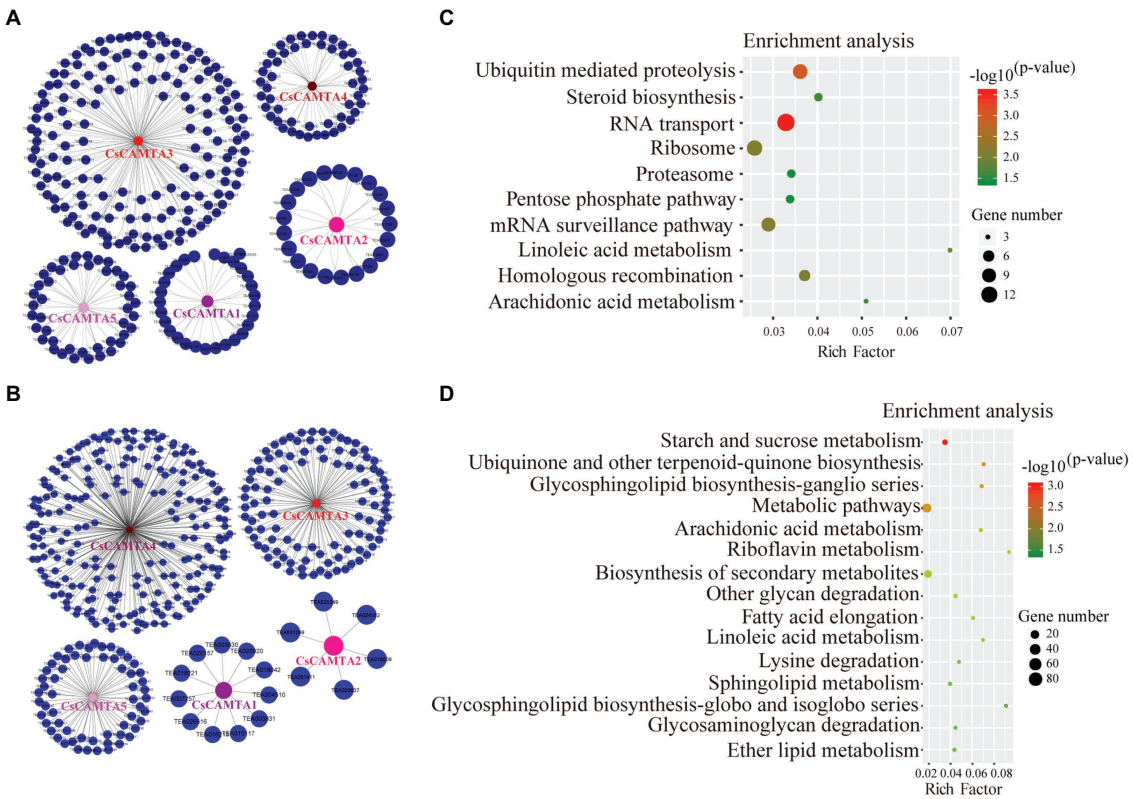

FIGURE 6 | *CsCAMTA* gene co-expression network and the KEGG enrichment analysis of *CsCAMTAs* and their co-expressed genes under cold and PEG-simulated drought stress, respectively. **(A)** *CsCAMTA* gene co-expression network under cold stress; **(B)** *CsCAMTA* gene co-expression network under PEG-simulated drought stress; **(C)** KEGG enrichment analysis of *CsCAMTAs* and their positive co-expressed genes under cold stress; **(D)** KEGG enrichment analysis of *CsCAMTAs* and their positive co-expressed genes under PEG-simulated drought stress.

CsCAMTAs and the positive co-expressed genes (**Figure 6D**; **Supplementary Table S6**).

Interaction Network of CsCAMTA Proteins in Tea Plant

To understand the functional mechanisms of CsCAMTA proteins, protein interaction network analysis was done by using STRING software. Results showed that the five CsCAMTA proteins corresponded to three *Arabidopsis* homologs and had 25 potential interacting proteins (**Figure 7**). CsCAMTA2 corresponded to CMTA3, CsCAMTA4, and CsCAMTA5 corresponded to AT4G16150, CsCAMTA1, and CsCAMTA3 corresponded to AT1G67310 (**Figure 7**; **Supplementary Table S7**). Further analysis demonstrated that CMTA3 (CsCAMTA2) and AT4G16150 (CsCAMTA4 and CsCAMTA5), respectively, had the most (19) and the least (4) number of interacting proteins, while AT1G67310 (CsCAMTA1 and CsCAMTA3) had six interacting proteins. The CMTA3 (CsCAMTA2) interacting proteins including 11 transcription factors (such as CBF, CBP60G, RHL41, MYB15, ICE1, etc.), two calcium-related protein kinases (CIPK14, CRLK1), and 6 functional proteins (such as EDS1, CM2, XLG2, etc.). As to AT1G67310 (CsCAMTA1 and CsCAMTA3) and AT4G16150 (CsCAMTA4 and CsCAMTA5), two of their interacting proteins were transcription factors. AT4G16150 (CsCAMTA4, CsCAMTA5) and AT1G67310 (CsCAMTA1, CsCAMTA3) could also interact with CIPK14. It was also seen that AT3G62140, coding a NEFA-interacting nuclear protein, could interact with AT4G16150 (CsCAMTA4, CsCAMTA5), AT1G67310 (CsCAMTA1, CsCAMTA3), and CAMT3 (CsCAMTA2; **Figure 7**; **Supplementary Table S7**).

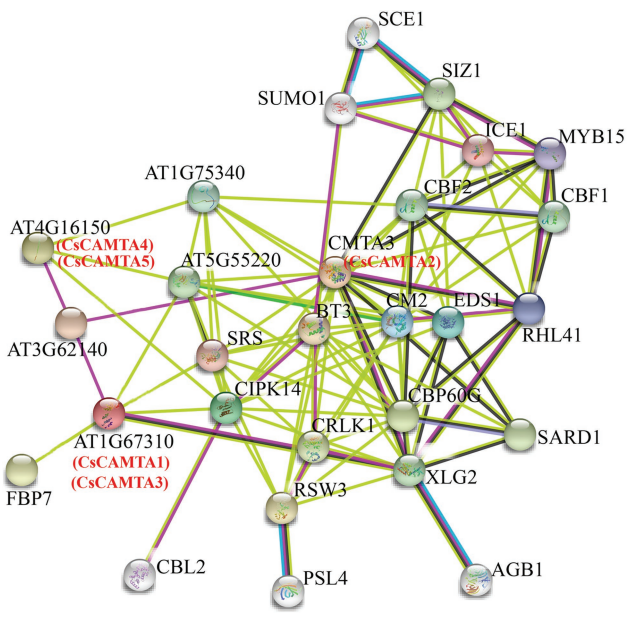

FIGURE 7 | Putative interaction networks of CsCAMTA proteins in tea plant according to their orthologs in *Arabidopsis*. The Arabidopsis proteins and the homologous proteins in tea plant are displayed in black and red characters, respectively.

Studies have demonstrated that CAMTA transcription factor bound with the (G/A/C)CGCG(C/G/T) or (A/C)CGTGT *cis* element in the target gene promoter to regulate their expression (Noman et al., 2019; Sun et al., 2020). To further investigate the interaction network of CsCAMTA proteins in tea plant, promoter sequences of the 25 potential interacting protein homolog-coding genes in tea plant and those of the *CsCAMTA* genes were analyzed. Results revealed that the (G/A/C)CGCG(C/G/T) *cis* element was existed in the promoters of nine tea plant genes which coding proteins were homologous to AT1G67310.1, CBL2, SUMO1, CBF2, SARD1, MYB15, RHL41, AT4G16150.1, and XLG2 in the protein interaction network (**Figure 7**; **Supplementary Table S8**). The (A/C)CGTGT *cis* element was identified in the promoters of seven tea plant genes homologous to those coding CRLK1, CBF1, AT1G75340, CMTA3, SARD1, SCE1, and AT4G16150.1 (**Supplementary Table S8**). (A/C)CGTGT and (G/A/C)CGCG(C/G/T) were also, respectively, found in the promoter of *CsCAMTA2* and *CsCAMTA3*, and both were identified in the promoter of *CsCAMTA5* (**Supplementary Table S8**).

DISCUSSION

Tea plant is a kind of leafy economic crop and is vulnerable to external stresses (Zhang et al., 2017; Wu et al., 2018; Li et al., 2019; Zhou et al., 2019a). To do investigation on genes those function in leaf development regulation and stress resistance will be very important for quantity increment and quality improvement of tea. CAMTAs are important players in plant stress response as well as in plant development (Zhang et al., 2014; Yang et al., 2015; Furio et al., 2020). Although studies on CAMTA have been reported in many plant species, identification of CAMTA in tea plant lags behind. Here, genome-wide identification of *CAMTA* gene was first done, and five *CsCAMTA* genes were identified from the tea plant genome (**Table 1**). The number of *CAMTA* genes in tea plant was similar to that in *Arabidopsis* (6), *Oryza sativa* (6), *Zea mays* (7), *Medicago truncatula* (7), *citrus clementina* (4), and *Vitis vinifera* (4), but smaller than that in *Glycine max* (14) and *Brassica rapa* (9). It was consistent with the 4–8 *CAMTA* gene number identified in higher flowering plant species, although the tea plant genome size was, respectively, more than nine-fold and three-fold larger than that of *Brassica rapa* and *Glycine max* (Rahman et al., 2016; Wei et al., 2018; Xia et al., 2019). The result may reflect the evolutionary conservation of *CAMTA* gene in higher plants and a high ratio of repetitive sequences in tea plant genome.

CsCAMTA proteins displayed conserved characters in tea plant. The amino acid size of CsCAMTA proteins was ranged from 864 to 1,419, and all of the CsCAMTAs were predicted as nuclear localization proteins, which were similar to those reported in other plants (**Table 1**; Yang et al., 2015; Yue et al., 2015; Pant et al., 2018; Büyük et al., 2019; Meer et al., 2019). The typical CAMTA protein contains CG-1, TIG/IPT, ANK, IQ, and CaMBD domains. It was also reported that non-TIG/IPT domain CAMTA protein appeared in newly evolved flowering land plants (Rahman et al., 2016; Pant et al., 2018; Büyük

et al., 2019). In our study, all the identified CsCAMTA proteins own the TIG/IPT domain (**Figure 1B**), indicating CsCAMTA proteins emerged before the divergence of flowering plants and non-flowering plants. IQ and CaMBD domains can interact with calmodulin in Ca^{2+}-independent and Ca^{2+}-dependent pathway, respectively; typical CAMTA protein always has two IQ domains, and the quantity of IQ domain is reported to affect CAMTA protein clustering in phylogenetic tree (Rahman et al., 2016; Pant et al., 2018). The five identified CsCAMTA proteins have both IQ and CaMBD domains (**Figure 1B**), suggesting that they can interact with calmodulin either there is Ca^{2+} or not. Phylogenetic analysis showed that CsCAMTA proteins were clustered in three different groups, which may be related to the IQ domain number and/or the relative position of IQ domain to CaMBD domain (**Figure 1B**). Gene structure analysis showed that most of the *CsCAMTA* genes had 10–13 introns, which was consistent with 12 introns found in most of the vascular plants (**Figure 1A**; Rahman et al., 2016; Kakar et al., 2018; Saeidi et al., 2019). *CsCAMTA2* had 19 introns, which was more than the most intron number (15) identified in other vascular plants (**Figure 1A**; Rahman et al., 2016; Pant et al., 2018). Intron, existing in eukaryotic genome, is believed important for gene expression regulation and for new functional protein generation (Chorev and Carmel, 2012; Wu et al., 2019). The high intron number may be related to the multifunction of *CsCAMTA2* in tea plant, although function study of *CsCAMTA2* is lacking. *AtCAMTA3*, the homologous gene of *CsCAMTA2* in *Arabidopsis*, was displayed important roles in freezing tolerance, SA mediated immune response, insect feeding response, hypersensitive response, etc. (Doherty et al., 2009; Laluk et al., 2012; Yue et al., 2015).

CAMTAs are important regulators of plant growth and development. AtCAMTA1 and 5 can regulate pollen development; tobacco NtER1 and Arabidopsis AtCAMTA3 were involved in ethylene-induced senescence process (Yang et al., 2015; Zhang et al., 2019a). Homologous phylogenetic analysis showed that CsCAMTA2, AtCAMTA1, and AtCAMTA3 were in group I, CsCAMTA4, CsCAMTA5, and AtCAMTA5 were in group III (**Figure 2**), which suggested that CsCAMTA2 might function in both senescence process and pollen development, and CsCAMTA4, 5 might function in regulating pollen development. Considering high expression of *CsCAMTA2* and lower expression of *CsCAMTA4* and *CsCAMTA5* in flower (**Figures 4A, 5A**), *CsCAMTA2*, *CsCAMTA4,* and *CsCAMTA5* may involve in pollen development by different regulating mechanisms. Expression analysis also showed that most of the *CsCAMTAs* had higher expression level in leaf tissues, and *CsCAMTA1* and *5* displayed relative lower expression in young and mature leaves and higher expression in old leaves (**Figures 4A, 5A**). Whether *CsCAMTA1* and *5* have function in regulating leaf senescence is worth investigating. Because tea plant is a kind of leaf-type economic crop, keeping leaf tender and delaying senescence of leaf is important for tea flavor and economic value improvement (Wu et al., 2018).

Studies also demonstrated that CAMTAs were crucial for stress response (Kim et al., 2013, 2020; Kakar et al., 2018). Our results showed that *CsCAMTA2* gene was responsive to cold, salt, and PEG-simulated drought treatments, as well as MeJA treatment (**Figures 4, 5**). Phylogenetic analysis showed that CsCAMTA2 was in group I, together with AtCAMTA1, AtCAMTA2, and AtCAMTA3 (**Figure 2**). In *Arabidopsis*, research showed that AtCAMTA1 played an important role in drought resistance; AtCAMTA3 was involved in cold response, pathogen defense response, resistance to insect herbivory, etc. (Yang et al., 2015; Pant et al., 2018). AtCAMTA2 was reported to function in metal stress detoxification and osmotic stress responses (Shen et al., 2015). These results suggested that the *CsCAMTA2* gene might be important for both biotic and abiotic stress responses of tea plant. According to the phylogenetic analysis, CsCAMTA1 and 3 were clustered together with AtCAMTA4 in group II (**Figure 2**). Gene expression analysis showed that the transcriptional levels of *CsCAMTA1* and *3* were obviously changed after cold, salt, or PEG-simulated drought treatments, suggesting that *CsCAMTA1* and *3* were involved in the response to these stresses. Although function of *AtCAMTA4* was not clear at present, research showed that expression of the *AtCAMTA4* homologs such as *CitCAMTA3* in *citrus* (*Ciclev10030636m*; Zhang et al., 2019a), *PtCAMTA1* and *7* in *Populus* (Wei et al., 2017), and *Pvul-CAMTA3* and *8* in *Phaseolus vulgaris* (Büyük et al., 2019), was significantly affected by salt and dehydration, cold, and salt stress, respectively. Recent study also showed that the *AtCAMTA4* homolog *TaCAMTA4* negatively regulated the basic resistance to leaf rust fungus in wheat (Wang et al., 2019). OsCAMTA1 (LOC_Os01g69910), clustered in group II with AtCAMTA4, CsCAMTA1 and 3, was reported important for cold resistance (Kim et al., 2013; Yue et al., 2015). CsCAMTA4 and 5 were clustered with AtCAMTA5 and 6 in group III (**Figure 2**). Our study showed that expression of *CsCAMTA4* and *5* was response to cold, salt, PEG-simulated drought, and MeJA treatments (**Figures 4, 5**), although *AtCAMTA5* and *6* were reported to function in plant development regulation (Shkolnik et al., 2019; Zhang et al., 2019a). *Citrus* CitCAMTA4 (Ciclev10004273m) and poplar PtCAMTA4 and 6 were clustered with AtCAMTA5 and 6 by phylogenetic analysis (**Figure 2**). The expression of *CitCAMTA4* (Ciclev10004273m) and *PtCAMTA4* and *6* was, respectively, regulated by salt and dehydration, cold, and salt stress (Wei et al., 2017; Büyük et al., 2019; Zhang et al., 2019a), suggesting that *CsCAMTA4* and *5* may also involve in stress response. Further analysis demonstrated that various stress-responsive *cis* elements were laid out in the promoters of *CsCAMTA* genes (**Figure 3**; **Supplementary Table S3**), supporting the role of *CsCAMTAs* in stress response.

Function annotation supports conserved function of CsCAMTAs in tea plant. By homologous annotation using TrEMBL, Swissprot, and Nr databases, all of the five *CsCAMTA* genes were annotated as calmodulin-binding transcription activators (**Supplementary Table S4**). GO and KEGG analysis showed that *CsCAMTA1*, *3* and *4* were annotated as lipase, ester hydrolase, LPA acyltransferase, and signal recognition and involved in transcription process (**Supplementary Table S4**). It has reported that CAMTA is important Ca^{2+} signal transducer, and can regulate the lipase-coding gene *EDS1* and *PAD4* expression, which are important for cold resistance and

SA-mediated immune response (Yue et al., 2015; Kim et al., 2020). LPA acyltransferase was ABA responsive and induced by salt and drought stresses, and it was important for female gametophyte development in *Arabidopsis* (Kim et al., 2005; Aboagla and Hong, 2017). CsCAMTA5 was involved in transcription regulation and annotated as abnormal spindle-like microcephaly-associated protein, or myosin by GO and KEGG (**Supplementary Table S4**), suggesting that CsCAMTA5 was related to development and molecular mobility. Research demonstrated that calmodulin could regulate mobility of myosin V (Nguyen and Higuchi, 2005). CsCAMTA2 was also annotated as MLO-like protein and involved in stress response by GO and KEGG (**Supplementary Table S4**). These results indicated that CsCAMTA played important roles in signal transduction, development, and biotic and abiotic stress response in tea plant, which was the same as the function of CAMTA identified in other plants. There was no co-expression between the identified *CsCAMTA* genes (**Figures 6A,B**; **Supplementary Table S5**), indicating the *CsCAMTA* genes had different spatiotemporal expression models, or different biological functions. Cold and drought are two kinds of environmental stresses that tea plant is vulnerable to encounter during the life span (Liu et al., 2016; Li et al., 2019). The KEGG analysis suggested that *CsCAMTA* genes involved in cold response mainly by hormone regulation (such as linoleic acid metabolism, steroid biosynthesis, and arachidonic acid metabolism), transcriptional regulation (such as RNA transport and mRNA surveillance pathway), and protein processing (such as ubiquitin mediated proteolysis, ribosome, and proteasome; **Figure 6C**; **Supplementary Table S6**). Enrichment of these pathways was also shown in *Haloxylon ammodendron*, *Anthurium*, *Ricinus communis,* and other plants under cold stress (Tian et al., 2013; Eremina et al., 2016; Peng et al., 2019). Under PEG-simulated drought stress, pathways like hormone metabolism (including linoleic acid metabolism, and arachidonic acid metabolism), lipid metabolism (including sphingolipid metabolism, glycosphingolipid biosynthesis, fatty acid metabolism, ether lipid metabolism, etc.), carbon metabolism (including starch and sucrose metabolism, and glycan degradation) were enriched by *CsCAMTAs* and their co-expressed genes (**Figure 6D**; **Supplementary Table S6**). These pathways were also enriched in drought stressed *Cynanchum thesioides*, *Eruca vesicaria*, *Vicia sativa*, and *Glycine max* (Huang et al., 2019; Zhang et al., 2019b; Min et al., 2020). Under cold or drought stress, research showed that *CAMTA*-regulated genes always enriched in the similar pathways as described above (Kim et al., 2013; Pandey et al., 2013). These results suggested CsCAMTAs were involved in stress response by conserved regulating mechanism, and the transcriptome data was valuable for *CsCAMTA* gene function analysis in tea plant.

Protein interaction analysis showed that 57.9% of the CsCAMTA2-interacting proteins, 50% of the CsCAMTA4 and CsCAMTA5-interacting proteins, and 33.3% of the CsCAMTA1 and CsCAMTA3-interacting proteins were DNA binding proteins (**Figure 7**; **Supplementary Table S7**), suggesting that transcriptional regulation might be the main way of CsCAMTA mediated functional regulation. It is clear that ICE1, CBF1, and CBF2 are key regulators in cold and drought stresses (Kim et al., 2013; Zhou et al., 2019b). SARD1, EDS1, and CBP60G are involved in SA synthesis and thus important for SA mediated immunity response (Kim et al., 2013). RSW3, XLG2, and CIPK14 are important regulators in plant development and stress response (Heo et al., 2012; Ren et al., 2017; Lia et al., 2019). So, by interacting with those proteins, CsCAMTA played various roles in biotic and abiotic stresses response, as well as in growth and development. CAMTA can bind to the (G/A/C)CGCG(C/G/T) or the (A/C)CGTGT *cis* element in promoter region of the target genes (Yue et al., 2015; Sun et al., 2020). Our analysis showed that there were 16 tea plant homologous genes to those of *Arabidopsis* in the interaction network had the (G/A/C)CGCG(C/G/T) or the (A/C)CGTGT *cis* element in their promoter regions. In the promoter regions of *TEA023367.1* (*SARD1* gene homolog in tea plant) and *CsCAMTA5*, both (G/A/C)CGCG(C/G/T) and (A/C)CGTGT *cis* elements were identified (**Supplementary Table S8**). These results indicated that the interaction network in *Arabidopsis* may also exist in tea plant, and CsCAMTAs can interact with those *Arabidopsis* homologs in tea plant. It also showed that the (G/A/C)CGCG(C/G/T) or the (A/C)CGTGT *cis* element was laid in the promoter of *CsCAMTA2* and *3*, suggesting that *CsCAMTAs* may regulate a biological event by cooperation. In *Arabidopsis*, it demonstrated that *CAMTA1*, *2* and *3* were function together to suppress SA biosynthesis and to enhance freezing tolerance (Kim et al., 2013; Yang et al., 2015). In the interaction network, AT3G62140 can interact with AT4G16150 (CsCAMTA4, CsCAMTA5), AT1G67310 (CsCAMTA1, CsCAMTA3), and CAMT3 (CsCAMTA2; **Figure 7**; **Supplementary Table S7**); this result suggested that the *CsCAMTAs* can regulate some biological processes together. Further studies by using transgenic plant materials or biochemical assays will provide more evidences for *CsCAMTA* gene function identification and the interaction network of CsCAMTA proteins.

DATA AVAILABILITY STATEMENT

Publicly available datasets were analyzed in this study. This data can be found here: The cold acclimation RNA-Seq data are available in the NCBI's.Sequence Read Archive (SRA) database (accession number: SRP108833). For NaCl and PEG treatments are available from the European Nucleotide Archive database (ENA; https://www.ebi.ac.uk/ena/browser/home) under project number accession PRJEB11522. For MeJA available in the NCBI SRA (sequence read archive, http://www.ncbi.nlm.nih.gov/sra/) respository under the accession number of SRP060335. For different tissues that was accessed from pcsb.ahau.edu.cn:8080/CSS/ (data downloading with user name 20170705F16HTSCCKF2479, password rwn160912abc).

AUTHOR CONTRIBUTIONS

QZ and HY contributed to conceptualization, supervision, and funding acquisition. MZ and FX performed project administration. FX, GM, and YW performed formal analysis. GM and YW

done data curation. YW and YD contributed to methodology. YD and MN performed visualization and provided software. MZ and HY was involved in investigation. FX and MN performed validation. QZ and GM performed writing—original draft. FX and HY performed writing—review and editing. All authors contributed to the article and approved the submitted version.

FUNDING

The work was supported by the National Key Research and Development Program of China (2021YFD1601103), the National Natural Science Foundation of China (no. U1404319), Scientific and Technological Research Projects of Henan Province (202102110230, 212102110399, and 222102110238), Key Scientific Research Projects of Universities in Henan Province (22A210023), the Training Program for Young Backbone Teachers in Colleges and Universities of Henan Province (2021GGJS100), Nanhu Scholars Program for Young Scholars of XYNU (2016060), and the National Training Programs of Innovation and Entrepreneurship for Undergraduates (202110477011).

SUPPLEMENTARY MATERIAL

The Supplementary Material for this article can be found online at: https://www.frontiersin.org/articles/10.3389/fpls.2022.910768/full#supplementary-material

REFERENCES

Aboagla, A. A. A., and Hong, Y. (2017). Lysophosphatidic acid Acyltransferase2 (LPAT2) enhances abscisic acid response and plays a positive role in osmotic stress in rice. *J. Cell Sci. Ther.* 8:1 (Suppl). doi: 10.4172/2157-7013.C1.039

Bouché, N., Scharlat, A., Snedden, W., Bouchez, D., and Fromm, H. (2002). A novel family of calmodulin-binding transcription activators in multicellular organisms. *J. Biol. Chem.* 277, 21851–21861. doi: 10.1074/jbc.M200268200

Büyük, İ., İlhan, E., Şener, D., Özsoy, A. U., and Aras, S. (2019). Genome-wide identification of CAMTA gene family members in *Phaseolus vulgaris* L. and their expression profiling during salt stress. *Mol. Biol. Rep.* 46, 2721–2732. doi: 10.1007/s11033-019-04716-8

Chen, C. J., Chen, H., Zhang, Y., Thomas, H. R., Frank, M. H., He, Y., et al. (2020). TBtools: an integrative toolkit developed for interactive analyses of big biological data. *Mol. Plant* 13, 1194–1202. doi: 10.1016/j.molp.2020.06.009

Choi, M. S., Kim, M. C., Yoo, J. H., Moon, B. C., Koo, S. C., Park, B. O., et al. (2005). Isolation of a calmodulin-binding transcription factor from rice (*Oryza sativa* L.). *J. Biol. Chem.* 280, 40820–40831. doi: 10.1074/jbc.M504616200

Chorev, M., and Carmel, L. (2012). The function of introns. *Front. Genet.* 3:55. doi: 10.3389/fgene.2012.00055

Doherty, C. J., Van Buskirk, H. A., Myers, S. J., and Thomashow, M. F. (2009). Roles for *Arabidopsis* CAMTA transcription factors in cold regulated gene expression and freezing tolerance. *Plant Cell* 21, 972–984. doi: 10.1105/tpc.108.063958

Eremina, M., Rozhon, W., and Poppenberger, B. (2016). Hormonal control of cold stress responses in plants. *Cell. Mol. Life Sci.* 73, 797–810. doi: 10.1007/s00018-015-2089-6

Furio, R. N., Martínez-Zamora, G. M., Salazar, S. M., Coll, Y., Perato, S. M., Martos, G. G., et al. (2020). Role of calcium in the defense response induced by brassinosteroids in strawberry plants. *Sci. Hortic.* 261:109010. doi: 10.1016/j.scienta.2019.109010

Heo, J. B., Sung, S., and Assmann, S. M. (2012). Ca^{2+}-dependent GTPase, extra-large G protein 2 (XLG2), promotes activation of DNA-binding protein related to vernalization 1 (RTV1), leading to activation of floral integrator genes and early flowering in *Arabidopsis*. *J. Biol. Chem.* 287, 8242–8253. doi: 10.1074/jbc.m111.317412

Huang, B. L., Li, X., Liu, P., Ma, L., Wu, W., Zhang, X., et al. (2019). Transcriptomic analysis of *Eruca vesicaria* subs. Sativa lines with contrasting tolerance to polyethylene glycol-simulated drought stress. *BMC Plant Biol.* 19:419. doi: 10.1186/s12870-019-1997-2

Kakar, K. U., Nawaz, Z., Cui, Z., Cao, P., Jin, J., Shu, Q., et al. (2018). Evolutionary and expression analysis of *CAMTA* gene family in *Nicotiana tabacum* yielded insights into their origin, expansion and stress responses. *Sci. Rep.* 8, 10322–10314. doi: 10.1038/s41598-018-28148-9

Kim, Y., Gilmour, S. J., Chao, L., Park, S., and Thomashow, M. F. (2020). *Arabidopsis* CAMTA transcription factors regulate pipecolic acid biosynthesis and priming of immunity genes. *Mol. Plant* 13, 157–168. doi: 10.1016/j.molp.2019.11.001

Kim, H. U., Li, Y., and Huang, A. H. (2005). Ubiquitous and endoplasmic reticulum–located lysophosphatidyl acyltransferase, LPAT2, is essential for female but not male gametophyte development in *Arabidopsis*. *Plant Cell* 17, 1073–1089. doi: 10.1105/tpc.104.030403

Kim, Y., Park, S., Gilmour, S. J., and Thomashow, M. F. (2013). Roles of CAMTA transcription factors and salicylic acid in configuring the low-temperature transcriptome and freezing tolerance of *Arabidopsis*. *Plant J.* 75, 364–376. doi: 10.1111/tpj.12205

Laluk, K., Prasad, K. V., Savchenko, T., Celesnik, H., Dehesh, K., Levy, M., et al. (2012). The calmodulin-binding transcription factor SIGNAL RESPONSIVE1 is a novel regulator of glucosinolate metabolism and herbivory tolerance in *Arabidopsis*. *Plant Cell Physiol.* 53, 2008–2015. doi: 10.1093/pcp/pcs143

Li, Y. Y., Wang, X. W., Ban, Q. Y., Zhu, X. X., Jiang, C. J., Wei, C. L., et al. (2019). Comparative transcriptomic analysis reveals gene expression associated with cold adaptation in the tea plant *Camellia sinensis*. *BMC Genomics* 20:624. doi: 10.1186/s12864-019-5988-3

Lia, A., Gallo, A., Marti, L., Roversi, P., and Santino, A. (2019). EFR-mediated innate immune response in *Arabidopsis thaliana* is a useful tool for identification of novel ERQC modulators. *Genes* 10:15. doi: 10.3390/genes10010015

Liu, S. C., Xu, Y. X., Ma, J. Q., Wang, W. W., Chen, W., Huang, D. J., et al. (2016). Small RNA and degradome profiling reveals important roles for microRNAs and their targets in tea plant response to drought stress. *Physiol. Plant.* 158, 435–451. doi: 10.1111/ppl.12477

Meer, L., Mumtaz, S., Labbo, A. M., Khan, M. J., and Sadiq, I. (2019). Genome-wide identification and expression analysis of calmodulin-binding transcription activator genes in banana under drought stress. *Sci. Hortic.* 244, 10–14. doi: 10.1016/j.scienta.2018.09.022

Min, X., Lin, X., Ndayambaza, B., Wang, Y., and Liu, W. (2020). Coordinated mechanisms of leaves and roots in response to drought stress underlying full-length transcriptome profiling in *Vicia sativa* L. *BMC Plant Biol.* 20, 165–121. doi: 10.1186/s12870-020-02358-8

Nguyen, H., and Higuchi, H. (2005). Motility of myosin V regulated by the dissociation of single calmodulin. *Nat. Struct. Mol. Biol.* 12, 127–132. doi: 10.1038/nsmb894

Noman, M., Jameel, A., Qiang, W. D., Ahmad, N., Liu, W. C., Wang, F. W., et al. (2019). Overexpression of *GmCAMTA12* enhanced drought tolerance in *Arabidopsis* and soybean. *Int. J. Mol. Sci.* 20:4849. doi: 10.3390/ijms20194849

Novikova, D. D., Cherenkov, P. A., Sizentsova, Y. G., and Mironova, V. V. (2020). metaRE R package for meta-analysis of transcriptome data to identify the *cis*-regulatory code behind the transcriptional reprogramming. *Genes* 11:634. doi: 10.3390/genes11060634

Ouyang, Z. G., Mi, L. F., Duan, H. H., Hu, W., Chen, J. M., Peng, T., et al. (2019). Differential expressions of *citrus* CAMTAs during fruit development and responses to abiotic stresses. *Biol. Plant.* 63, 354–364. doi: 10.32615/bp.2019.041

Pandey, N., Ranjan, A., Pant, P., Tripathi, R. K., Ateek, F., Pandey, H. P., et al. (2013). CAMTA1 regulates drought responses in *Arabidopsis thaliana*. *BMC Genomics* 14:216. doi: 10.1186/1471-2164-14-216

Pant, P., Iqbal, Z., Pandey, B. K., and Sawant, S. V. (2018). Genome-wide comparative and evolutionary analysis of calmodulin-binding transcription activator (CAMTA) family in *Gossypium* species. *Sci. Rep.* 8, 1–17. doi: 10.1038/s41598-018-23846-w

Peng, M. C., Wang, Y. L., Wang, M., and Chu, G. (2019). Transcriptome profiling of *Haloxylon ammodendron* seedling at low temperature condition. *Appl. Ecol. Environ. Res.* 17, 1411–1429. doi: 10.15666/aeer/1701_14111429

Qiu, Y., Xi, J., Du, L., Suttle, J. C., and Poovaiah, B. W. (2012). Coupling calcium/calmodulin-mediated signaling and herbivore-induced plant response through calmodulin-binding transcription factor AtSR1/CAMTA3. *Plant Mol. Biol.* 79, 89–99. doi: 10.1007/s11103-012-9896-z

Rahman, H., Yang, J., Xu, Y. P., Munyampundu, J. P., and Cai, X. Z. (2016). Phylogeny of plant CAMTAs and role of AtCAMTAs in nonhost resistance to *Xanthomonas oryzae* pv. Oryzae. *Front. Plant Sci.* 7:177. doi: 10.3389/fpls.2016.00177

Ren, Y., Li, Y., Jiang, Y., Wu, B., and Miao, Y. (2017). Phosphorylation of WHIRLY1 by CIPK14 shifts its localization and dual functions in *Arabidopsis*. *Mol. Plant* 10, 749–763. doi: 10.1016/j.molp.2017.03.011

Saeidi, K., Zare, N., Baghizadeh, A., and Asghari-Zakaria, R. (2019). *Phaseolus vulgaris* genome possesses *CAMTA* genes, and *phavuCAMTA1* contributes to the drought tolerance. *J. Genet.* 98:31. doi: 10.1007/s12041-019-1069-2

Shangguan, L., Wang, X., Leng, X., Liu, D., Ren, G., Tao, R., et al. (2014). Identification and bioinformatics analysis of signal responsive/calmodulin-binding transcription activators gene models in Vitis Vinifera. *Mol. Biol. Rep.* 41, 2937–2949. doi: 10.1007/s11033-014-3150-5

Shen, C., Yang, Y., Du, L., and Wang, H. (2015). Calmodulin-binding transcription activators and perspectives for applications in biotechnology. *Appl. Microbiol. Biotechnol.* 99, 10379–10385. doi: 10.1007/s00253-015-6966-6

Shi, J., Ma, C., Qi, D., Lv, H., Yang, T., Peng, Q., et al. (2015). Transcriptional responses and flavor volatiles biosynthesis in methyl jasmonate-treated tea leaves. *BMC Plant Biol.* 15:233. doi: 10.1186/s12870-015-0609-z

Shkolnik, D., Finkler, A., Pasmanik-Chor, M., and Fromm, H. (2019). Calmodulin-binding transcription activator 6: a key regulator of Na^+ homeostasis during germination. *Plant Physiol.* 180, 1101–1118. doi: 10.1104/pp.19.00119

Sun, T., Huang, J., Xu, Y., Verma, V., Jing, B., Sun, Y., et al. (2020). Redundant CAMTA transcription factors negatively regulate the biosynthesis of salicylic acid and N-hydroxypipecolic acid by modulating the expression of *SARD1* and *CBP60g*. *Mol. Plant* 13, 144–156. doi: 10.1016/j.molp.2019.10.016

Tamura, K., Stecher, G., Peterson, D., Filipski, A., and Kumar, S. (2013). MEGA6: molecular evolutionary genetics analysis version 6.0. *Mol. Biol. Evol.* 30, 2725–2729. doi: 10.1093/molbev/mst197

Tian, D. Q., Pan, X. Y., Yu, Y. M., Wang, W. Y., Zhang, F., Ge, Y. Y., et al. (2013). *De novo* characterization of the *Anthurium* transcriptome and analysis of its digital gene expression under cold stress. *BMC Genomics* 14:827. doi: 10.1186/1471-2164-14-827

Trapnell, C., Williams, B. A., Pertea, G., Mortazavi, A., Kwan, G., Van Baren, M. J., et al. (2010). Transcript assembly and quantification by RNA-Seq reveals unannotated transcripts and isoform switching during cell differentiation. *Nat. Biotechnol.* 28, 511–515. doi: 10.1038/nbt.1621

Wang, Y., Wei, F., Zhou, H., Liu, N., Niu, X., Yan, C., et al. (2019). TaCAMTA4, a Calmodulin-interacting protein, involved in defense response of wheat to *Puccinia triticina*. *Sci. Rep.* 9, 1–8. doi: 10.1038/s41598-018-36385-1

Wang, G., Zeng, H., Hu, X., Zhu, Y., Chen, Y., Shen, C., et al. (2015). Identification and expression analyses of calmodulin-binding transcription activator genes in soybean. *Plant and Soil* 386, 205–221. doi: 10.1007/s11104-014-2267-6

Wei, C., Yang, H., Wang, S., Zhao, J., Liu, C., Gao, L., et al. (2018). Draft genome sequence of *Camellia sinensis* var. sinensis provides insights into the evolution of the tea genome and tea quality. *Proc. Natl. Acad. Sci. U. S. A.* 115, E4151–E4158. doi: 10.1073/pnas.1719622115

Wei, M., Xu, X., and Li, C. (2017). Identification and expression of CAMTA genes in *Populus trichocarpa* under biotic and abiotic stress. *Sci. Rep.* 7:17910. doi: 10.1038/s41598-017-18219-8

Wu, J., Li, A., Cai, H., Zhang, C., Lei, C., Lan, X., et al. (2019). Intron retention as an alternative splice variant of the cattle *ANGPTL6* gene. *Gene* 709, 17–24. doi: 10.1016/j.gene.2019.05.031

Wu, Z. J., Ma, H. Y., and Zhuang, J. (2018). iTRAQ-based proteomics monitors the withering dynamics in postharvest leaves of tea plant (*Camellia sinensis*). *Mol. Genet. Genomics* 293, 45–59. doi: 10.1007/s00438-017-1362-9

Xia, E. H., Li, F. D., Tong, W., Li, P. H., Wu, Q., Zhao, H. J., et al. (2019). Tea plant information archive: a comprehensive genomics and bioinformatics platform for tea plant. *Plant Biotechnol. J.* 17, 1938–1953. doi: 10.1111/pbi.13111

Yang, T., Peng, H., Whitaker, B. D., and Conway, W. S. (2012). Characterization of a calcium/calmodulin-regulated *SR/CAMTA* gene family during tomato fruit development and ripening. *BMC Plant Biol.* 12:19. doi: 10.1186/1471-2229-12-19

Yang, Y., Sun, T., Xu, L., Pi, E., Wang, S., Wang, H., et al. (2015). Genome-wide identification of *CAMTA* gene family members in *Medicago truncatula* and their expression during root nodule symbiosis and hormone treatments. *Front. Plant Sci.* 6:459. doi: 10.3389/fpls.2015.00459

Yue, R., Lu, C., Sun, T., Peng, T., Han, X., Qi, J., et al. (2015). Identification and expression profiling analysis of calmodulin-binding transcription activator genes in maize (Zea mays L.) under abiotic and biotic stresses. *Front. Plant Sci.* 6:576. doi: 10.3389/fpls.2015.00576

Zhang, Q., Cai, M. C., Yu, X. M., Wang, L. S., Guo, C. F., Ming, R., et al. (2017). Transcriptome dynamics of *Camellia sinensis* in response to continuous salinity and drought stress. *Tree Genet. Genomes* 13:78. doi: 10.1007/s11295-017-1161-9

Zhang, L., Du, L., and Poovaiah, B. W. (2014). Calcium signaling and biotic defense responses in plants. *Plant Signal. Behav.* 9:e973818. doi: 10.4161/15592324.2014.973818

Zhang, D., Han, Z., Li, J., Qin, H., Zhou, L., Wang, Y., et al. (2020). Genome-wide analysis of the SBP-box gene family transcription factors and their responses to abiotic stresses in tea (*Camellia sinensis*). *Genomics* 112, 2194–2202. doi: 10.1016/j.plaphy.2013.05.021

Zhang, J., Pan, X., Ge, T., Yi, S., Lv, Q., Zheng, Y., et al. (2019a). Genome-wide identification of *citrus CAMTA* genes and their expression analysis under stress and hormone treatments. *J. Hortic Sci. Biotech.* 94, 331–340. doi: 10.1080/14620316.2018.1504631

Zhang, X., Yang, Z., Li, Z., Zhang, F., and Hao, L. (2019b). *De novo* transcriptome assembly and co-expression network analysis of *Cynanchum thesioides*: identification of genes involved in resistance to drought stress. *Gene* 710, 375–386. doi: 10.1016/j.gene.2019.05.055

Zhou, Q. Y., Cheng, X., Wang, S. S., Liu, S. R., and Wei, C. L. (2019a). Effects of chemical insecticide imidacloprid on the release of C6 green leaf volatiles in tea plants (*Camellia sinensis*). *Sci. Rep.* 9, 1–6. doi: 10.1038/s41598-018-36556-0

Zhou, Q., Han, Y., Pan, J., Yuan, H., Li, X., Qin, M., et al. (2019b). Research progress in plant cold resistance mechanism. *J. Xinyang Normal Univ. (Natural Sci. Edn.)* 3, 511–516 (in Chinese with English Abstract). doi:10.3969/j.issn.1003-0972.2019.03.031

Conflict of Interest: The authors declare that the research was conducted in the absence of any commercial or financial relationships that could be construed as a potential conflict of interest.

Publisher's Note: All claims expressed in this article are solely those of the authors and do not necessarily represent those of their affiliated organizations, or those of the publisher, the editors and the reviewers. Any product that may be evaluated in this article, or claim that may be made by its manufacturer, is not guaranteed or endorsed by the publisher.

frontiers | Frontiers in Plant Science

ORIGINAL RESEARCH
published: 24 June 2022
doi: 10.3389/fpls.2022.909765

Effects of Different Shading Treatments on the Biomass and Transcriptome Profiles of Tea Leaves (*Camellia sinensis* L.) and the Regulatory Effect on Phytohormone Biosynthesis

Zhou-Tao Fang[1†], *Jing Jin*[2†], *Ying Ye*[1], *Wei-Zhong He*[3], *Zai-Fa Shu*[3], *Jing-Na Shao*[3], *Zhu-Sheng Fu*[4], *Jian-Liang Lu*[1*] and *Jian-Hui Ye*[1*]

[1] Tea Research Institute, Zhejiang University, Hangzhou, China, [2] Zhejiang Agricultural Technical Extension Center, Hangzhou, China, [3] Lishui Institute of Agriculture and Forestry Sciences, Lishui, China, [4] Zhejiang Minghuang Natural Products Development Co., Ltd., Hangzhou, China

Our previous study showed that colored net shading treatments had comparable effects on the reduction of bitter and astringent compounds such as flavonol glycosides in tea leaves, compared with black net shading treatment, whereas the effects on the biomass and phytohormones are still unclear. In this study, we investigated the phytohormone and transcriptome profiles of tea leaves under different shading treatments, using black, blue, and red nets with the same shade percentages. The bud density, fresh weight of 100 buds, and yield under blue net shading treatments were greatly elevated by 2.00-fold, 1.24-fold, and 2.48-fold, compared with black net shading treatment, while their effects on flavonoid composition were comparable with black net shading treatment. The transcriptome profiles of different shade net-treated samples were well resolved and discriminated from control. The KEGG result indicated that the pathways of phenylpropanoid biosynthesis, MAPK signaling pathways, and plant hormone signal transduction were differentially regulated by different shading treatments. The co-expression analysis showed that the contents of salicylic acid and melatonin were closely correlated with certain light signal perception and signaling genes ($p < 0.05$), and UVR8, PHYE, CRY1, PHYB, PHOT2, and HY5 had more close interactions with phytohormone biosynthetic genes ($p < 0.05$). Our results suggest that different shading treatments can mediate the growth of tea plants, which could be attributed to the regulatory effect on phytohormones levels, providing an instruction for the production of summer/autumn tea and matcha.

Keywords: ***Camellia sinensis*** **(L.) O. Kuntze, light intensity, light spectral composition, biomass, transcriptome, phytohormones**

OPEN ACCESS

Edited by:
Chuankui Song,
Anhui Agriculture University, China

Reviewed by:
Yuhua Wang,
Nanjing Agricultural University, China
Ma. Cristina Vazquez Hernandez,
Tecnologico Nacional de México en Roque, Mexico

***Correspondence:**
Jian-Liang Lu
jllu@zju.edu.cn
Jian-Hui Ye
jianhuiye@zju.edu.cn

[†] These authors have contributed equally to this work

Specialty section:
This article was submitted to Plant Metabolism and Chemodiversity, a section of the journal Frontiers in Plant Science

Received: *31 March 2022*
Accepted: *30 May 2022*
Published: *24 June 2022*

Citation:
Fang Z-T, Jin J, Ye Y, He W-Z, Shu Z-F, Shao J-N, Fu Z-S, Lu J-L and Ye J-H (2022) Effects of Different Shading Treatments on the Biomass and Transcriptome Profiles of Tea Leaves (Camellia sinensis L.) and the Regulatory Effect on Phytohormone Biosynthesis. Front. Plant Sci. 13:909765. doi: 10.3389/fpls.2022.909765

INTRODUCTION

Tea is a popular non-alcoholic drink over the world. The ground powder and extract of tea leaves are common raw materials and ingredients of food products, such as bakery, ready-to-drink tea, and matcha latte. Tea is produced from the leaves of the plant *Camellia sinensis* (L.) O. Kuntze, which contain abundant secondary metabolites, such as catechins, flavonol glycosides, and caffeine (Samynathan et al., 2021). Many of the metabolites are bitter and/or astringent, forming the unique flavor of tea (Ye et al., 2022). As raw materials and ingredients of food products, the bitterness and astringency of tea need reduction so as to endow foods with better flavor (Ye et al., 2022). In addition to tea breeding (Xia et al., 2020), agronomic practices are efficient to reduce the bitter and astringent taste of tea, e.g., shading treatment and fertilization (Ye et al., 2022). Black net shading treatment is effective to decrease the accumulation of bitter and astringent compounds like flavonol glycosides in tea leaves (Jin et al., 2021). However, the growth of tea plants is also attenuated or even adversely impacted due to the weak light condition. Long-time shading treatment leads to the greatly reduced biomass of young shoots per unit area or growth rate of young shoots (Sano et al., 2018; Ye et al., 2022). In many tea plantations for producing matcha, heavy fertilization of organic fertilizer is implemented to keep the good growth status of tea plants. The utilization of shade nets, high input of organic fertilizer, and the decreased production yield cause the relatively high production cost of matcha.

Light condition is an important environmental factor in the growth and metabolism of tea plants (Homma et al., 2011). UV-light (below 400 nm), visible light (400–710 nm), and infrared radiation (710–1,000 nm) comprise the sunlight, and the visible light spectrum consisted of blue light (400–495 nm), green light (495–570 nm), yellow light (570–590 nm), and red light (590–710 nm) (Zoratti et al., 2014). Plants have the perception of light, including light intensity, direction, specific wavelengths, and photoperiod. Different types of light receptors were found in plants, including blue-light receptor phototropins (PHOTs), blue light, UV-A receptor cryptochromes (CRYs), UV-B receptor, UV resistance locus 8 (UVR8), and phytochromes (PHYs) that perceive red/far-red light signals (Paik and Huq, 2019). Elongated hypocotyl5 (HY5), suppressor of PHYA (SPA), and constitutively photomorphogeni1 (COP1) are important components of light signal transduction (Yadav et al., 2020). Up to date, the regulatory effects of light intensity and light quality on tea plants mainly focus on the secondary metabolism in tea leaves (Zheng et al., 2019; Lin et al., 2021; Ye et al., 2021). It was reported that blue light elevated the expressions of *CRY2/3*, *SPAs*, *HY5*, and *R2R3-MYBs*, leading to the enhanced accumulation of anthocyanins and catechins in tea plants (Zheng et al., 2019). UV promoted the accumulation of flavonol glycosides in tea plants, which was associated with the upregulated expressions of *UVR8* and *HY5* (Lin et al., 2021; Ye et al., 2021). In addition, the biosynthesis and transportation of hormones in plants can also be affected by the light condition (Weller et al., 2009; Ding et al., 2011; Yi et al., 2020). Light regulated the biosynthesis of gibberellin in pea by mediating COP1/HY5 pathway (Weller et al., 2009). Light promoted the biosynthesis of jasmonate in *Arabidopsis* to regulate photomorphogenesis (Yi et al., 2020). The levels of hormones in plants are related to the growth rate, biomass, and resistance of plants. The information about the effect of light condition on the production yield of tea plants is scarce. In our previous study, flavonol glycosides were greatly reduced under both black and blue net shading treatments, while the production yield of tea plants under blue net shading treatment was apparently higher than that of black net shading treatment (Jin et al., 2021). The impact of light condition on the biomass of tea plants and the light-mediated regulatory effect on the biosynthesis of phytohormones in tea plants need further investigations.

In this study, the effects of different shading treatments (black, blue, and red nets with the same shade percentages) on the biomass of tea plants "Longjing 43" were investigated, in terms of bud density, weight of 100 buds, and production yield. In addition to the composition of flavonoids, the biosynthesis of phytohormones in tea leaves under different shading treatments was studied and compared using the combination of phytohormone and transcriptome analyses. Kyoto Encyclopedia of Genes and Genomes (KEGG) pathway enrichment analysis was performed to reveal the biological and metabolic changes of tea leaves under different shading treatments. Co-expression analysis was carried out to explore the correlations of light signal transduction-related gene expressions with the phytohormone levels and the transcriptional levels of phytohormone biosynthetic genes.

MATERIALS AND METHODS

Chemicals and Reagents

Individual catechins (EGCG, EGC, ECG, EC, GCG, GC, CG, C, all > 95%) and flavonol (myricetin, quercetin, kaempferol, all > 95%) were bought from Sigma-Aldrich (Shanghai, China). Acetonitrile and methanol (HPLC grade) were bought from Merck KGaA Company (Darmstadt, Germany). Ethanol was purchased from Sinopharm Chemical Reagent Co., Ltd. (Shanghai, China). The HPLC grade phytohormones including abscisic acid (ABA, ≥98%), gibberellin 1 (GA1, 95%), gibberellin 3 (GA3, 98%), indole-3-acetic acid (IAA, ≥98%), *trans*-zeatin-riboside (tZR, ≥98%), zeatin (Z, 95%), jasmonic acid (JA, 95%), melatonin (≥95%), and salicylic acid (SA, 95%) were all purchased from Shanghai Yuanye Bio-Technology Co., Ltd. (Shanghai, China).

Shading Treatment and Sampling

Camellia sinensis cv. Longjing 43 (4 years old, height 0.78 m), growing in the Songyang Tea Plantation of Lishui Academy of Agricultural Sciences (Lishui County, Zhejiang, China, 28°577′ N, 119°377′ E), was used for the study. Shortly after light pruning, the polyethylene nets, including black, blue, and red nets (4 m × 6 m, the shade percentages of 95%), were used to shade tea plants from the middle of June to the end of June 2021, at the height of 2 m above ground level. All the shade nets were bought from Taizhou Huiming Shade Net Co., Ltd. (Taizhou,

China). The shading treatments were implemented according to the method of our previous work (Jin et al., 2021; Ye et al., 2021). After shading for 15 days (29 June 2021), the tea plants were at the stage of two leaves and one bud, and the second leaves basipetal from the apical bud were randomly collected. The tea plants with edge effect were avoided. Three independent biological replicates were randomly collected, and 3–5 tea plants were used for each biological repeat. The fresh tea leaves were immediately placed in liquid nitrogen for 30 min. The tea leaves of the same biological replicate were mixed quickly and divided evenly into three portions for transcriptomic, flavonoid, and phytohormone analyses. All the samples were stored at −80°C prior to these analyses.

Illumination and Light Measurement

The parameters of light condition were measured on the same date of harvest. The light intensity at the height of tea shoots was measured by light intensity sensors of TOP Instruments (Zhejiang Top Instrument Co., Ltd., Hangzhou, China), and the UV intensity was measured by the TENMARS UVAB light meter (TENMARS Electronics Co., Ltd, Taiwan, China). The intensity of the visible spectrum was recorded by HopooColor OHSP-350C Illumination Analyzer (HopooColor Technology Co., Ltd., Hangzhou, China).

Biomass Measurements

Bud Density

The number of buds in a certain area of tea row (length 1 m, width 1.05 m) was counted. The bud density was calculated based on the number of buds per square meter. For each treatment, three different areas (length 1 m, width 1.05 m) in the same tea row were employed for the bud density measurements.

Weight of 100 Buds

The young shoots were manually plucked at the plucking standard of two leaves and one bud, and every 100 young shoots under different shading treatments were weighed.

Production Yield (g/m^2)

For each treatment, the young shoots in a certain area of tea row (length 1 m, width 1.05 m) were harvested at the standard of two leaves and one bud and weighed, and the production yield per square meter was calculated. For each treatment, three different areas (length 1 m, width 1.05 m) in the same tea row were employed for the production yield measurements.

Phytohormone Analysis

The phytohormones were extracted and analyzed by a commercial service company (Gene Denovo Biotechnology, Guangzhou, China) according to the method reported by Ye et al. (2021). After extraction and purification, the phytohormones were analyzed by the UHPLC-MS/MS system consisting of Waters Acquity UPLC and AB SCIEX 5500 QQQ-MS. A multiple reaction monitoring (MRM) mode was used for quantifying ABA, GA3, GA1, IAA, JA, SA, Z, melatonin, and tZR. Data acquisition, peak integration, and calculations were carried out using the MultiQuant software.

Determination of Flavonoids

Flavonoids were extracted and analyzed according to the method reported by Zheng et al. (2018). Fresh tea leaves were freeze-dried, ground, and sifted through a 0.45-mm sifter. The ground tea sample (0.15 g) was extracted with 25 ml of 50% (v/v) ethanol solution at 100 rpm and 70°C for 30 min. After centrifugation at 12,000 rpm and 4°C for 15 min, the supernatants were analyzed using ultra-high-performance liquid chromatography–diode array detector–tandem mass spectrometry (Waters Corporation, Milford, MA, USA, UPLC–DAD–MS) as reported by Zheng et al. (2018). Catechins were quantified by authentic standards, and flavonol glycosides were quantified by their aglycones.

Transcriptomic and Bioinformatic Analyses

The RNA isolation and sequencing were conducted by Gene Denovo Biotechnology Co., Ltd. (Guangzhou, China). The total RNA was extracted using the TRIzol reagent kit (Invitrogen, Carlsbad, CA,USA) according to the manufacturer's protocol. The eukaryotic mRNA was enriched by oligo (dT) beads and further fragmented into short fragments. The obtained short fragments were reverse-transcripted into cDNA by using NEBNext Ultra RNA Library Prep Kit for Illumina (NEB #7530,New England Biolabs, Ipswich, MA, USA). After end repaired, A base added, and ligated to Illumina sequencing adapters, the ligated products were selected by agarose gel electrophoresis, PCR amplified, and purified using the AMPure XP Beads (1.0X) to obtain the library. The cDNA library was sequenced using Illumina Novaseq6000. The raw reads were filtered by fastp (version 0.18.0) to obtain the high-quality clean reads by removing adaptor, duplication, and ambiguous sequences (reads with above 10% "N" rate), as well as low quality reads containing more than 50% of low quality (Q-value $\leq$ 20) bases. The reference tea genome of "Longjing 43" (Wang et al., 2020) was used to map clean reads using HISAT2. 2.4, with "-rna-strandness RF" and other parameters set as a default (Pertea et al., 2016; Wei et al., 2018). The mapped reads of each sample were assembled by StringTie v1.3.1. The differentially expressed genes (DEGs) in the RNA-Seq dataset were identified by DESeq2 ($|\log_2$ fold change$| > 1$, FDR < 0.05) based on the read counts.

Quantitative Real-Time Polymerase Chain Reaction Analysis

For quantitative real-time polymerase chain reaction (RT-qPCR) analysis, an RNA sample (1 μg) was converted into first-strand cDNA using PrimeScript™ RT Reagent Kit with gDNA Eraser (TaKaRa Biotechnology Co., Ltd., Dalian, China). The specific primers of selected genes in **Supplementary Table 1** were designed by NCBI Primer-BLAST according to the genome sequences of *Camellia sinensis* cv. Shuchazao (Wei et al., 2018). The qPCR cycling was carried out by Applied Biosystems™ StepOnePlus™ Real-Time PCR System (Applied Biosystems™ ABI, Carlsbad, CA, USA) based on the introduction of PowerUp™ SYBR™ Green Master Mix (Thermo Fisher Scientific Inc., Carlsbad, CA, USA): 95°C for 120 s and 40 cycles at 95°C for 3 s, annealing at 60°C for 30 s. The relative expression level of each gene was calculated by $2^{-\Delta\Delta Ct}$ method, using

TABLE 1 | The biomass parameters of tea plants under different shading treatments.

Treatment[a]	Bud density (bud/m^2)	Fresh weight of 100 buds (g)	Yield (g/m^2)
Control	383 ± 2a	15.5 ± 0.1a	67.2 ± 1.6a
Black net shading treatment	173 ± 2c	11.8 ± 0.1c	23.0 ± 0.6c
Blue net shading treatment	347 ± 9b	14.6 ± 0.5b	57.0 ± 1.4b
Red net shading treatment	344 ± 4b	14.1 ± 0.2b	54.7 ± 1.3b

[a]*The plucking standard was two leaves and one bud. Data were present as mean ± SD (n = 3). Data with different alphabetic letters (a, b, c) in the same column were significantly different at $p < 0.05$.*

β-actin as an endogenous control. Technical duplicates were employed for each biological replicate.

Data Analysis

All the tests were repeated three times, and the mean value ± SD was presented. The significant difference analysis was carried out by the SAS System for Windows version 8.1 (SAS Institute Inc., Cary, NC, USA), using a Tukey's test. The Origin 9.1 (Originlab Corporation, Northampton, MA, USA) was used for heatmap plotting and correlation analysis. Principal component analysis (PCA) was conducted using the Minitab 17 statistical software (Minitab. LLC, State College, PA, USA). The bubble diagrams of KEGG were drafted on the online platform of OmicShare tools (http://www.omicshare.com/tools). The co-expression results were visualized by Cytoscape (v3.7.2).

RESULTS

Effects of Shading Treatments on the Biomass of Tea Leaves

Different shading treatments altered the light condition underneath. The visible spectrum as well as the intensities of light and UV are shown in **Supplementary Figure 1**. The effect of shading treatments on the light condition underneath was in an agreement with our previous study (Ye et al., 2021). **Table 1** shows the biomass parameters of tea leaves under different shading treatments. Obviously, the tea plants naturally growing in the sun (CK) had the greatest biomass, in terms of bud density (383 buds/m^2), fresh weight of 100 buds (15.5 g), and production yield (67.2 g/m^2) at the plucking standard of two leaves and one bud, while the lowest biomass was achieved for black net shading treatment (bud density of 173 buds/m^2, 100 bud fresh weight of 11.8 g, and production yield of 23.0 g/m^2). The biomass of blue and red nets-treated tea plants was in between. Thus, shading treatment greatly reduced the bud density, bud weight, and the yield of young shoots. The biomass of blue and red net shading treatments was significantly higher than that of the black net shading treatment, with bud density and production yield being around two-fold and 2.5-fold of those under black net shading treatment. The fresh bud weights were increased by 23.7% and 19.5% under blue and red net shading treatments, compared with the black net shading treatment. Therefore, the biomass of tea plants was closely related to the growth light condition.

Effects of Shading Treatments on the Levels of Phytohormones in Tea Leaves

The growth of tea plants is affected by phytohormone levels, leading to different biomass. **Supplementary Table 2** shows the levels of endogenous phytohormones in tea leaves under different shading treatments, including ABA, GA1, GA3, IAA, JA, melatonin, SA, tZR, and Z. **Figure 1** shows the PCA score plot and loading plot of tea leaves under different shade treatments based on the levels of endogenous phytohormones. The first two principal components (PC) accounted for 82.1% of the total variance (PC1 = 46.8%, PC2 = 35.3%). Different shading-treated samples were clustered and well discriminated from other samples. Specifically, CK and BN were located in the positive direction of PC1, while BKN and RN were located in the negative direction of PC1 (**Figure 1A**). Besides, CK and BKN were distributed in the positive direction of PC2, while BN and RN were distributed in the negative part of PC2 (**Figure 1A**). Thus, PC2 reflected the impact of light spectral composition. The loading plot showed that CK was discriminated from the shading-treated samples due to its highest levels of IAA and JA, while BKN was distinguished from other samples due to the highest contents of tZR and Z (**Figure 1B**). BN was characterized by the relatively high level of SA, while RN was characterized by the high level of ABA (**Figure 1B**). Hence, the biosynthesis of phytohormones in tea leaves was differentially regulated under different shading treatments.

Effects of Shading Treatments on the Contents of Flavonoids in Tea Leaves

Table 2 shows the contents of catechins and flavonol glycosides in the tea leaves under different shading treatments. RN contained the highest content of total catechins (TC) at 138.6 mg/g dry weight (DW), subsequently followed by BN (135.7 mg/g DW) and BKN (133.0 mg/g DW), while CK contained the lowest content of TC at 128.4 mg/g DW. CK contained the highest level of total flavonol glycosides (TFG), followed by RN, while BN and BKN contained the lowest levels of TFG being around 3.28 mg/g. The shading treatment (95% shade percentage) slightly elevated the content of TC by 3.6–7.9% compared with CK, while it sharply reduced the content of TFG by 51.6–64.6%. The increase in TC was mainly attributed to the increase in EGCG, with the increased percentage being 15%. Thus, flavonol glycosides were more sensitive to the growth light condition than catechin compounds, which was consistent with the previous studies (Jin et al., 2021; Ye et al., 2021). The flavonoid composition of BN was

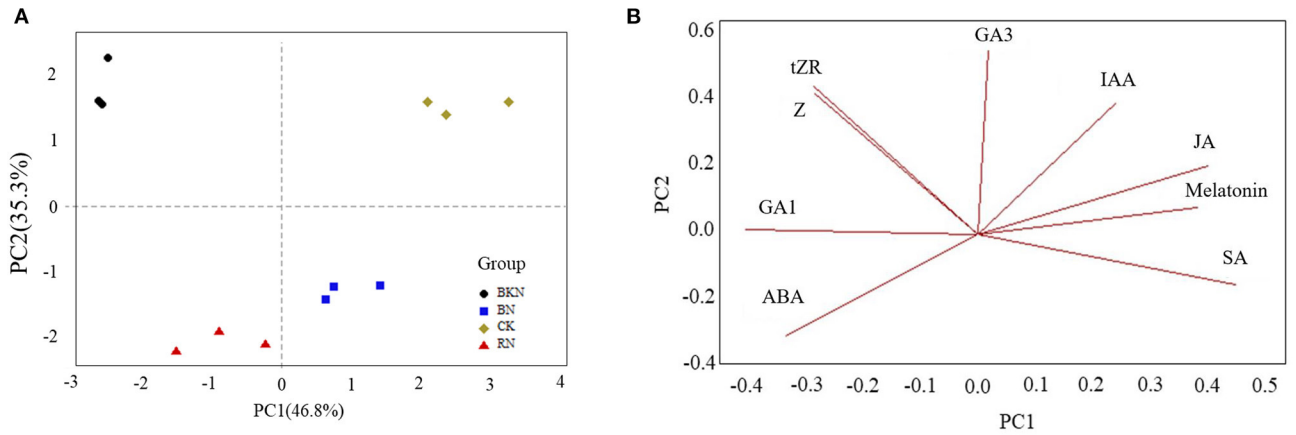

FIGURE 1 | The PCA score plot **(A)** and loading plot **(B)** of tea leaves under different shading treatments based on the levels of endogenous phytohormones.

close to that of BKN, suggesting that blue net shading treatment exerted a similar effect on flavonoid compounds in tea leaves to black net shading treatment. The comparable effects of blue and black net shading treatments on the reduction of flavonol glycosides in tea leaves have been reported (Jin et al., 2021).

Transcriptome Profiles of Different Tea Samples and KEGG Enrichment Analysis

Supplementary Table 3 shows the information of the RNA-Seq data. There were 45.0–51.4 million, 46.1–52.9 million, 36.5–48.0 million, and 43.1–49.9 million RNA-Seq clean paired-end reads, respectively, obtained for control, BKN, BN, and RN (**Supplementary Table 3**). **Figure 2A** is the PCA score plot of RNA-Seq data, and the samples under different shading treatments were clustered and well discriminated from each other. The new genes are listed in **Supplementary Table 4**. The results of gene expression obtained by RNA-Seq were validated by RT-qPCR, with R^2 being 0.823 (**Supplementary Figure 2**). This suggests that the RT-qPCR results were highly correlated with the corresponding transcriptomic data, and the transcriptomic dataset was able to represent the transcript abundances. **Figure 2B** shows the number of upregulated and downregulated DEGs in different tea samples compared in pairs. The pair of CK vs. BN had the lowest number of DEGs (168 upregulated and 139 downregulated DEGs), while the pair of CK vs. BKN had the highest number of DEGs (1,503 upregulated and 846 downregulated DEGs), subsequently followed by the pair of BKN vs. BN (397 upregulated and 1,175 downregulated DEGs). This was consistent with the result in **Figure 2A**. The DEGs of different comparison pairs were analyzed by KEGG functional enrichment. In **Figure 2C**, phenylpropanoid biosynthesis and MAPK signaling pathways were significantly enriched in the pairs of CK vs. BKN, CK vs. RN, BKN vs. BN, and BKN vs. RN, while only protein processing in the endoplasmic reticulum and brassinosteroid biosynthesis pathways was enriched in the pairs of CK vs. BN. This suggests that the least number of enriched pathways was observed for the pairs of CK vs. BN. In particular, the pathway of plant hormone signal transduction was enriched in the pairs of BKN vs. BN, CK vs. BKN, and CK vs. RN, which was in an agreement with the PCA result that BN had the shortest distance from CK based on the composition of phytohormones (**Figure 1A**). Hence, different shading treatments could differentially regulate the hormone signal transduction in tea leaves.

Phytohormone Biosynthesis Network

Figure 3 shows the biosynthetic pathways of the major phytohormones in tea leaves, with the annotation of transcriptional levels of structural genes. IAA, melatonin, and SA are originated from the same compound chorismate, and the key structural genes in the phytohormone biosynthetic pathways were affected by different light conditions. For example, the transcription levels of indole-3-pyruvate monooxygenase (YUC), the key enzyme for the biosynthesis of IAA, were downregulated by 0.61–0.83-fold in the shading-treated samples compared with CK. The expression of *YUC* in BN was higher than those of BKN and RN, which generally agreed with the levels of IAA in different samples. Great difference in gene expressions was also observed in *serotonin-N-acetyltransferase (SNAT)*, *caffeic acid-O-methyltransferase (COMT),* and *N-acetylserotonin methyltransferase (ASMT)* involved in the biosynthesis of melatonin. The lowest expression levels of *isochorismate synthase (ICS)* and *chorismate mutase (CM)* were observed in the BKN samples, which was consistent with the lowest content of SA in BKN. Only the expressions of *cytokinin hydroxylase (CYP735A)* showed a concordant change trend with the levels of Z and tRZ in different tea samples. No obvious correlation was observed in other biosynthetic genes of Z and tZR. A similar phenomenon was also observed in ABA, Gas, and JA that the levels of these three phytohormones were not apparently correlated with the transcription levels of key structural genes.

TABLE 2 | The contents of catechins and flavonol glycosides in the fresh tea leaves under different shading treatments.

Compounds[a]	CK	BKN	BN	RN
Catechins (mg/g dry weight)				
GC[b]	1.42 ± 0.08a	0.93 ± 0.05b	0.81 ± 0.04c	1.02 ± 0.05b
EGC[b]	17.58 ± 0.27c	16.91 ± 0.16d	18.47 ± 0.11b	24.16 ± 0.21a
C[b]	1.70 ± 0.08a	1.10 ± 0.09c	1.37 ± 0.15b	1.18 ± 0.19bc
EC[b]	9.22 ± 0.16a	6.55 ± 0.04c	7.03 ± 0.05b	2.32 ± 0.03d
EGCG[b]	75.47 ± 0.38b	87.13 ± 0.71a	88.31 ± 0.72a	87.78 ± 0.41a
GCG[b]	0.27 ± 0.01b	0.32 ± 0.01a	0.28 ± 0.02b	0.21 ± 0.01c
ECG[b]	22.31 ± 0.24a	19.86 ± 0.20c	19.28 ± 0.18d	20.93 ± 0.29b
CG[b]	0.42 ± 0.01b	0.19 ± 0.01c	0.14 ± 0.01d	0.97 ± 0.04a
TC[d]	128.39 ± 0.31d	132.99 ± 0.76c	135.69 ± 1.07b	138.56 ± 0.72a
	(100.0%)	(103.58%)	(105.68%)	(107.91%)
Flavonol glycosides (μg/g dry weight)				
M-gal-rha-glu[c]	200 ± 15a	146 ± 7b	146 ± 8b	158 ± 14b
M-gal[c]	2524 ± 37a	1007 ± 5d	1132 ± 41c	1450 ± 16b
M-glu[c]	1592 ± 5a	347 ± 1d	416 ± 12c	587 ± 8b
Q-gal-rha-glu[c]	1205 ± 7a	283 ± 2c	249 ± 1d	475 ± 5b
Q-glu-rha-glu[c]	1102 ± 6a	167 ± 3c	152 ± 1c	268 ± 14b
Q-glu-rha-rha[c]	564 ± 29b	621 ± 3a	504 ± 18c	572 ± 8b
Q-glu-rha[c]	228 ± 13a	45 ± 1c	50 ± 4c	76 ± 4b
Q-gal[c]	804 ± 5a	141 ± 2c	167 ± 3c	262 ± 7b
Q-glu[c]	258 ± 1a	48 ± 1c	54 ± 1c	80 ± 1b
K-glu-rha-glu[c]	533 ± 6a	335 ± 4c	281 ± 10d	380 ± 7b
K-gal[c]	125 ± 4a	94 ± 4c	75 ± 6c	108 ± 2b
K-glu-rha[c]	46 ± 2a	27 ± 2b	22 ± 3c	27 ± 1b
K-glu[c]	52 ± 4a	21 ± 0c	21 ± 1c	30 ± 1b
TFG[d]	9233 ± 91a	3281 ± 19c	3270 ± 20c	4473 ± 80b
	(100%)	(35.53%)	(35.42%)	(48.44%)

[a]EC, (–)-epicatechin; EGC, (–)-epigallocatechin; ECG, (–)-epicatechin gallate; EGCG, (–)-epigallocatechin gallate; GC, (+)-gallocatechin; C, (+)-catechin; TC, total catechins; M-gal-rha-glu, myricetin galactosyl-rhamnosyl-glucoside; M-gal, myricetin galactoside; M-glu, myricetin glucoside; K-glu-rha-gal, kaempferol glucosyl-rhamnosyl-galactoside; K-gal, kaempferol galactoside; K-glu-rha, kaempferol glucosyl-rhamnoside; K-glu, kaempferol glucoside; Q-gal-rha-glu, quercetin galactosyl-rhamnosyl-glucoside; Q-glu-rha, quercetin glucosyl-rhamnoside; Q-glu-rha-rha, quercetin glucosyl-rhamnosyl-rhamnoside; Q-glu-rha-glu, quercetin glucosyl-rhamnosyl-glucoside; Q-gal, quercetin galactoside; Q-glu, quercetin glucoside; TFG, total flavonol glycosides; CK, tea sample grown in natural light; BKN, black net shade-treated sample; BN, blue net shade-treated sample; RN, red net shade-treated sample. Data with different alphabetic letters (a, b, c, d) in the same row were significantly different at $p < 0.05$. Significant difference analysis was carried out by the SAS System for Windows version 8.1 (SAS Institute Inc., Cary, NC, USA) using Tukey's test. Data were expressed as mean ± SD (n = 3).

[b]Quantified by the corresponding authentic standards.

[c]Relatively quantified by the corresponding aglycone.

[d]Data in brackets are the percentage of TC or TFG compared with CK.

Association of Phytohormone Biosynthesis With Light Signal Transduction

Figure 4A shows the heatmap of light signal-related gene expressions under different shading treatments. Obviously, CK generally had the highest expressions of light receptors and signal transduction genes, subsequently followed by BN and RN, while BKN had the lowest expressions. This was in a general agreement with the radiation intensities under different shading treatments. Specifically, *CRY1*, *CRY2,* and *PHOT1* that perceive blue light were transcriptionally upregulated under blue net shading treatment, compared with CK. However, the transcriptional levels of light signal transduction-related genes *HY5*, *SPA1,* and *COP1* in BN were much lower than those in CK, despite the relatively high expressions of light receptors. Thus, the higher expressions of light receptor genes in CK than BN, such as *UVR 8* and *PHYE*, might be more related to the light signal transduction of *HY5*, *SPA1*, and *COP1*. The correlation network of light signal-related genes and phytohormone levels is shown in **Figure 4B**. Among these nine endogenous phytohormones, the contents of SA and melatonin were highly positively correlated with the expressions of light receptor and signal transduction genes, with Pearson's coefficients being above 0.80. The transcriptional levels of several biosynthetic genes also showed correlations with the expressions of light receptor and signal transduction genes (**Figure 4C**). *UVR8*, *PHOT2*, *PHYB*, *CRY1*, *PHYE*, and *HY5* had more close interactions than other light signal-related genes. This is generally consistent with the direct or indirect correlations in **Figure 4B**. *CM*, *YUC*, *cytochrome P450 714B2 (CYP714B2)*,

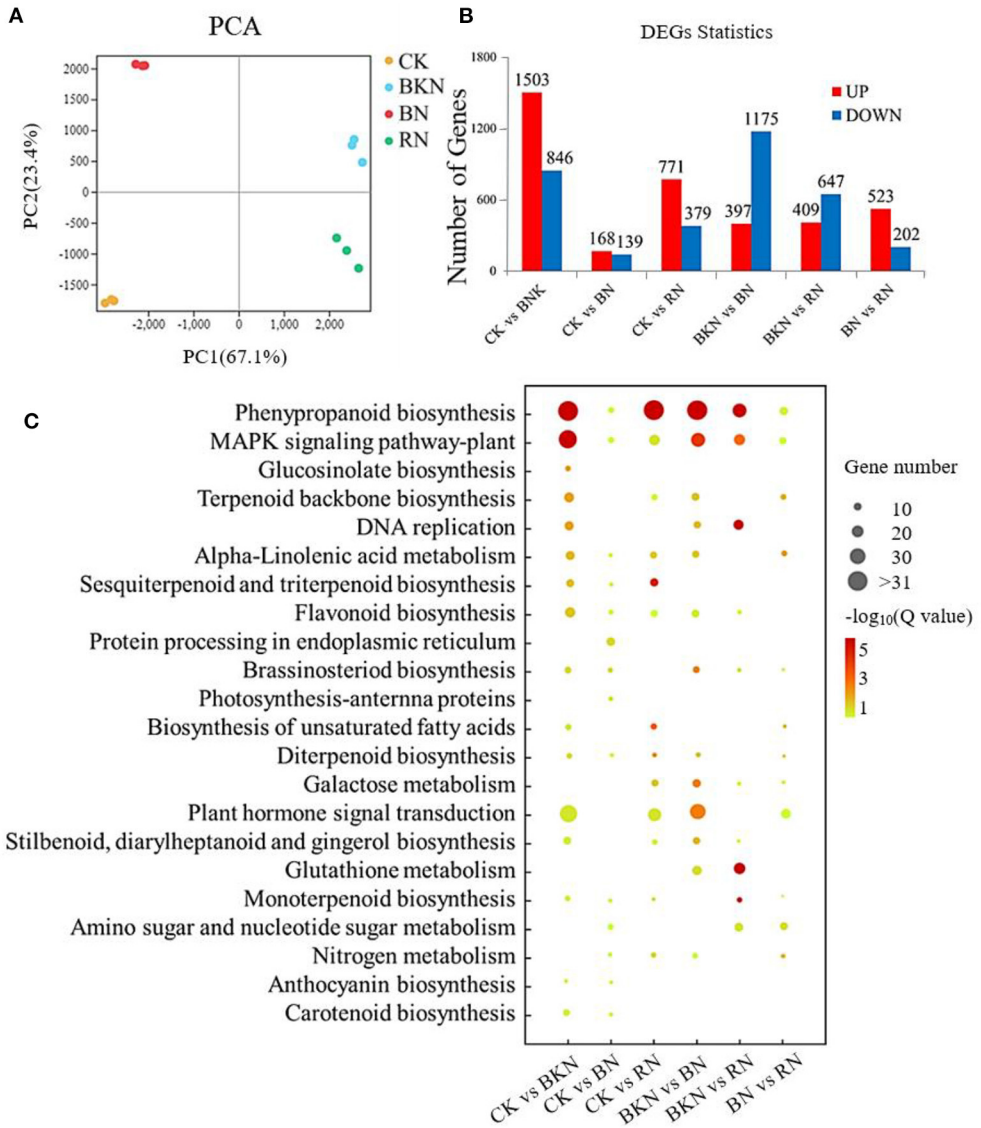

FIGURE 2 | The gene expression profiles of the 2nd tea leaves. **(A)** PCA analysis; **(B)** DEG numbers; **(C)** the enriched KEGG pathways of DEGs. The number of replicates is 3.

ASMT, *lipoxygenase (LOX),* and *CYP707A* were highly positively correlated with the expressions of the corresponding light signal-related genes, while *CYP735A*, allene oxide cyclase (*AOC*), *allene oxide synthase (AOS)*, *JAR*, *OPR*, *NCED*, and *JMT* had highly negative correlations (**Figure 4C**).

DISCUSSION

The intensity and quality of light are important factors in the biomass and metabolism of plants (Fan et al., 2013; Chang and Chang, 2014; Kaiser et al., 2019). The growth of plants is accelerated, and the biomass of crops is increased under the appropriate light condition (Fu et al., 2017). In field management, prolonging illumination duration and supplementary lighting are propitious to the production yield of plants (Bian et al., 2016; Zheng et al., 2018). Our study showed that the biomass of young shoots of "Longjing 43" was affected by different shading treatments, which was positively correlated with radiation intensity. Despite the great difference in the biomass between the black net-treated sample and the colored net-treated samples, the contents of flavonol glycosides were greatly reduced under all the shading treatments. This was consistent with our previous studies (Jin et al., 2021; Ye et al., 2021). The transcriptions of light signal-related genes were also regulated by different shading treatments. In this study (tea plants "Longjing 43"), the expressions of light signal-related genes in BN were relatively higher than those in BKN and RN, including *HY5*, *PHYE*, *PHYB*, *PHYA1*,

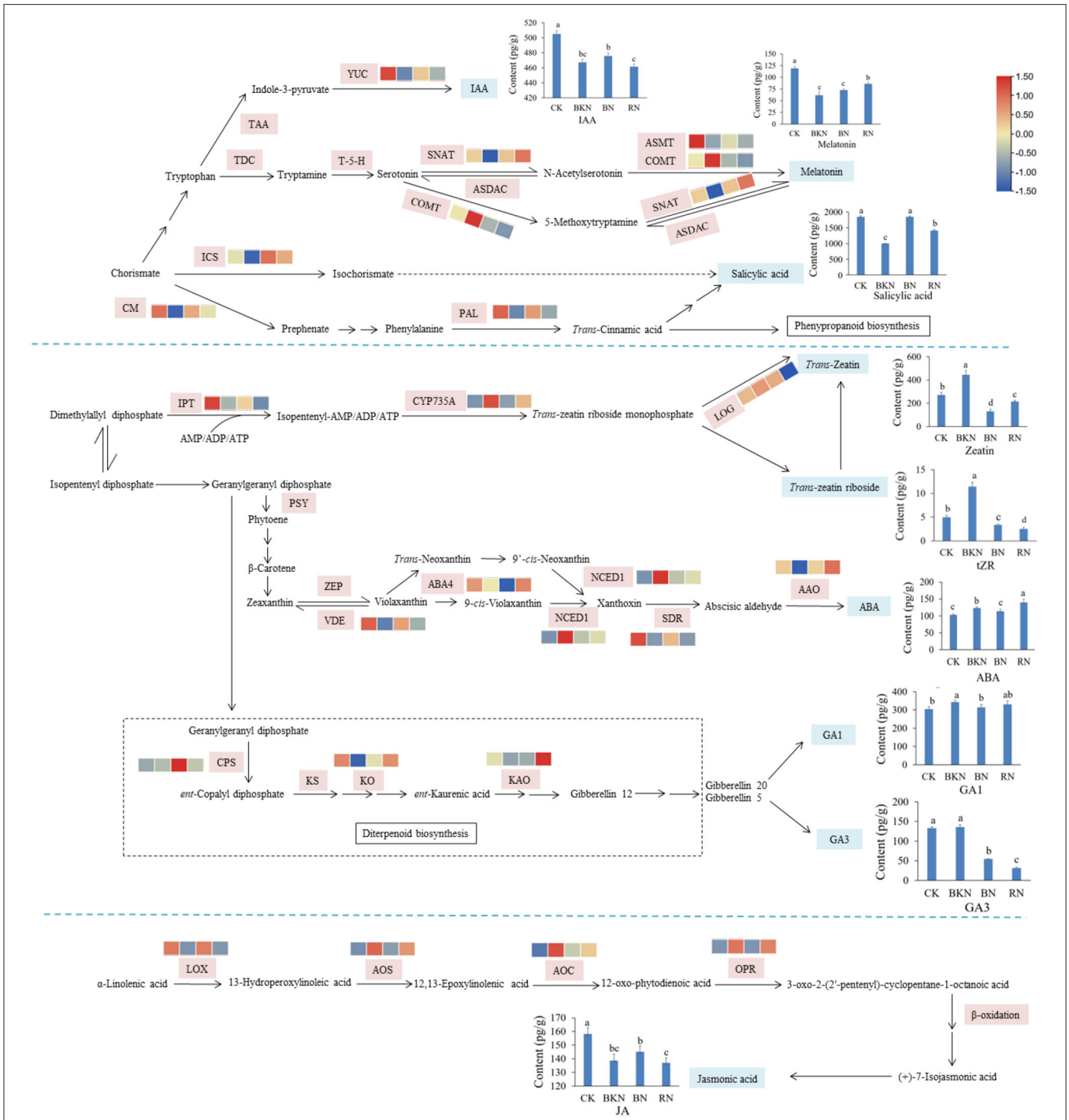

FIGURE 3 | Visualization of the expression levels of the structural genes in the biosynthetic pathway of phytohormones in tea leaves. The contents of 8 detected phytohormones annotated with their structures are shown by line charts. CK, tea sample without shade; BKN, black net shade-treated sample; BN, blue net shade-treated sample; RN, red net shade-treated sample. PAL, phenylalanine ammonia-lyase; CM, chorismate mutase; ICS, isochorismate synthase;YUC:indole-3-pyruvate monooxygenase; IPT, adenylate isopentenyltransferase; CYP735A, cytokinin hydroxylase; CYP714B2, cytochrome P450 714B2; LOG, cytokinin riboside 5′-monophosphate phosphoribohydrolase; AMP, adenosine 5′-monophosphate; NCED, 9-*cis*-epoxycarotenoid dioxygenase; SDR, short chain dehydrogenase/reductase; MoCo, molybdenum cofactor; CYP707A, abscisic acid 8′-hydroxylase CYP707A; SNAT, serotonin-N-acetyltransferase; ASMT, N-acetylserotonin methyltransferase; COMT, caffeic acid-*O*-methyltransferase; CPS, *ent*-copalyl diphosphate synthase; KO, *ent*-kaurene oxidase; KAO, *ent*-kaurenoic acid oxidase; 20ox, Gibberellin 20; LOX, lipoxygenase; AOS, allene oxide synthase; AOC, allene oxide cyclase; OPR, 12-oxophytodienoate reductase; JAR, jasmonoyl-L-amino acid synthetase; JMT, jasmonate *O*-methyltransferase.

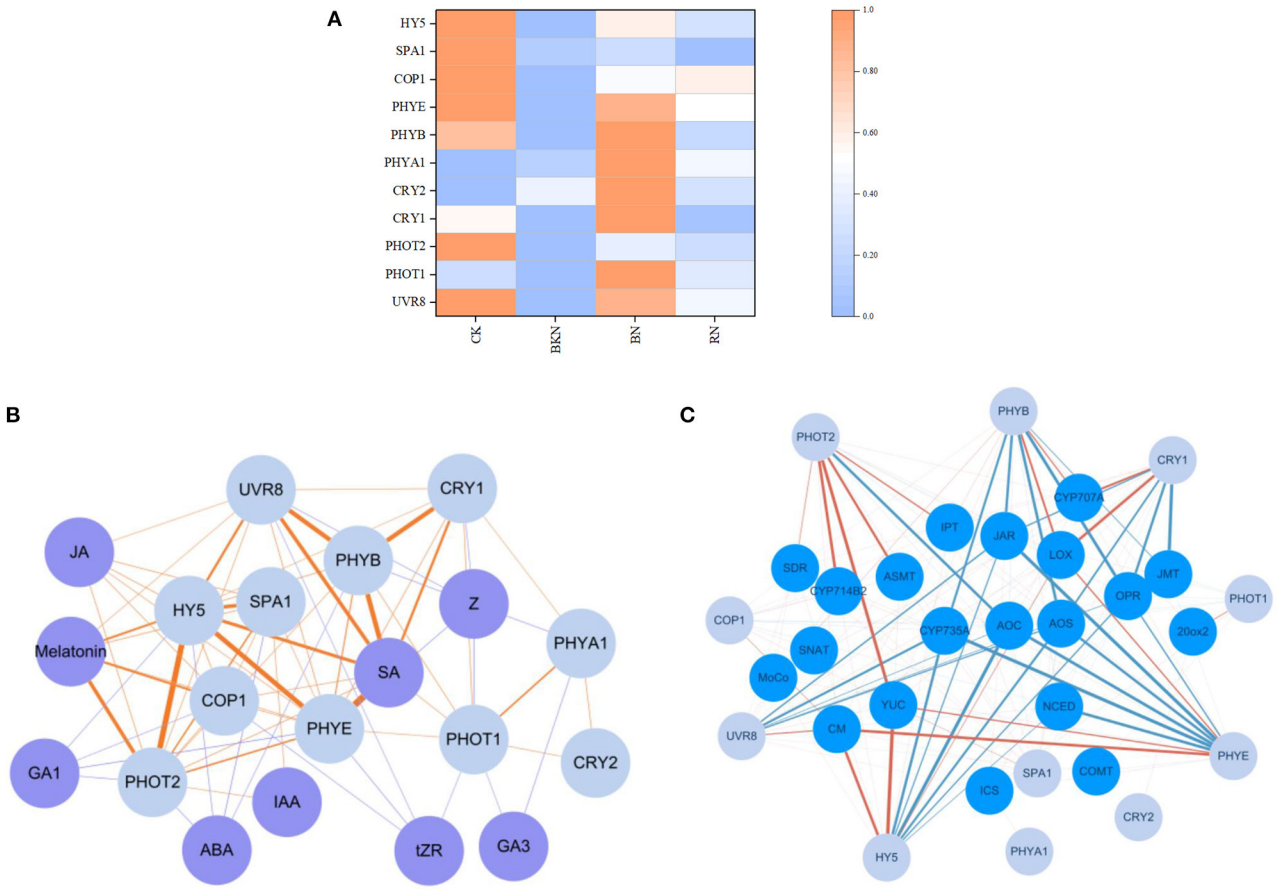

FIGURE 4 | The effects of different shading treatments on the expressions of light signal and phytohormone biosynthesis-related genes in tea leaves. **(A)** The heatmap of light signal-related genes, **(B)** the correlation network of light signal-related genes (light blue nodes) and phytohormone levels (purple nodes), and **(C)** the correlation network of light signal-related genes (light blue nodes) and phytohormone biosynthetic genes (blue nodes). The co-expression networks of the FPKM values of light signal perception and signaling genes (PHYB, PHYE, PHOT1, CRY1, CRY2, UVR8, COP1, SPA1, and HY5) and the phytohormone contents (ABA, GA1, GA3, IAA, JA, melatonin, SA, tZR, and Z), as well as the FPKM values of light signal perception and signaling genes (PHYB, PHYE, PHOT1, CRY1, CRY2, UVR8, COP1, SPA1, and HY5) and the phytohormone biosynthetic genes (CM, ICS, YUC, IPT, CYP735A, CYP714B2, NCED, SDR, MoCo, CYP707A, SNAT, ASMT, COMT, 20ox2, LOX, AOS, AOC, OPR, JAR, and JMT), were conducted using the Cytoscape software (version 3.8.0). Significant correlation was presented based on the statistical test with a robust cutoff ($p < 0.05$). The orange color lines represented positive correlation and the blue color lines represented negative correlation. The correlation coefficient increased from 0.80 to 0.99 as the line color deepened. HY5, Elongated hypocotyl 5; SPA1, suppressor of PHYA; COP1:constitutive photomorphogenesis 1; PHYs, phytochromes; CRYs, cryptochromes; UVR8, UV resistance locus 8; ABA, abscisic acid; GA1, gibberellin A1; GA3, gibberellin A3; IAA, indole-3-acetic acid; JA, jasmonic acid; SA, salicylic acid; tZR, *trans*-zeatin-riboside; Z, zeatin; CM, chorismate mutase; ICS, isochorismate synthase; YUC, indole-3-pyruvate monooxygenase; IPT, adenylate isopentenyltransferase; CYP735A, cytokinin hydroxylase; CYP714B2, cytochrome P450 714B2; NCED, 9-*cis*-epoxycarotenoid dioxygenase; SDR, short chain dehydrogenase/reductase; MoCo, molybdenum cofactor; CYP707A, abscisic acid 8′-hydroxylase CYP707A; SNAT, serotonin-N-acetyltransferase; ASMT, N-acetylserotonin methyltransferase; COMT, caffeic acid-*O*-methyltransferase; 20ox2, gibberellin 20; LOX, lipoxygenase; AOS, allene oxide synthase; AOC, allene oxide cyclase; OPR, 12-oxophytodienoate reductase; JAR, jasmonoyl-L-amino acid synthetase; JMT; jasmonate *O*-methyltransferase; CK, tea sample grown in nature light; BKN, black net shade-treated sample; BN, blue net shade-treated sample; RN, red net shade-treated sample. Each cell represents the mean value of 3 replicates.

CYR1, *CYR2*, *PHOT1*, *PHOT2*, and *UVR8*. Higher expressions of *HY5, PHYE, PHYB*, and *CRY1* were also reported in tea plants "Fudingdabaicha" under blue net-shading treatment, compared with black net and red net-shading treatments (Ye et al., 2021). The slight difference in upregulated transcriptions of light signal-related genes could be attributed to the cultivar difference. Menendez et al. (2021) associated the expression of *HY5* with the production yield of crops. Our study showed that CK had the highest production yield of young shoots, subsequently followed by BN and RN, while BKN had the lowest yield. The higher production yields of BN and RN were mainly due to the greatly increased bud density and elevated bud weight under blue and red net shading treatments, compared with BKN. Since the shading treatments were carried out shortly after light pruning, the growth stage of tea plants was normalized among different treatments. The great increase in bud density and bud weight could be attributed to the phytohormone changes under different light conditions. According to the result of phytohormone

analysis, different samples had different phytohormone profiles. The accumulation of SA and ABA might be more sensitive to light quality, compared with other phytohormones. The impact of light quality on the biomass production of rice has also been reported, which was associated with the change in net assimilation rate (Ohashi-Kaneko et al., 2006).

The biosynthesis of phytohormones in plants is regulated by light condition (Yang and Li, 2017; Yadav et al., 2020). Our study investigated the correlations between phytohormone levels and the expressions of light signal-related genes and found that SA was closely correlated with the expression levels of *UVR8, PHYB, HY5, PHYE*, and *CRY1*, while melatonin had correlations with *PHOT2, HY5*, and *COP1*. Kurepin et al. (2010) reported that the level of SA was regulated by light in the hypocotyls of *Helianthus annuus* seedlings. SA is also involved in the radiation-induced stress of plants (Uppalapati et al., 2007). PHYB was reported playing an important role in the SA-induced defenses of phyb mutant (de Wit et al., 2013). Besides, UV-B not only regulated the SA-induced signal transduction (Demkura et al., 2010) but also promoted the accumulation of melatonin in plants (Hardeland, 2016). Our result also showed that the levels of SA and melatonin in the 2nd tea leaves were more affected by the intensities of blue light and UV, compared with other phytohormones. However, no great correlation was observed between the expressions of light signal-related genes and the levels of other phytohormones, which might be associated with the leaf samples collected. Since the 2nd leaves were collected for transcriptome analysis, and the biosynthesis of IAA, GAs, Z, and tRZ may be largely attenuated in the expanding leaves. The biosynthesis of IAA, GAs, Z, and tZR is especially vigorous in the meristematic tissues, such as the growing tips or apical of stems and roots, while their biosyntheses are attenuated in the mature and developing organs. Besides, the transcriptional levels of relevant structural genes showed no obvious coordination with the levels of ABA, GAs, and JA, since the transportation and transformation of phytohormones also importantly regulate the phytohormone levels in plants in addition to biosynthesis. The effects of light condition on the transportation and transformation of phytohormones need attention in the future study.

DATA AVAILABILITY STATEMENT

The datasets presented in this study can be found in online repositories. The names of the repository/repositories and accession number(s) can be found below: https://bigd.big.ac.cn/, No. PRJCA008920.

AUTHOR CONTRIBUTIONS

JJ and J-HY designed the research. Z-TF wrote the manuscript. W-ZH, Z-FS, J-NS, and JJ conducted the field experiment. Z-FS, J-NS, and YY collected the experimental materials and did the analysis. J-LL and Z-SF did the supervision. J-HY and J-LL revised the manuscript. All authors listed here contributed and approved the manuscript.

FUNDING

This study was financially supported by the Zhejiang Science and Technology Major Program on Agricultural New Variety Breeding-Tea Plant (2021C02067-5), the Major Agricultural Technology Collaborative Extension Project of Zhejiang Province (2020XTTGCY04), and the Zhejiang Province Six Aspects of Agriculture, Rural areas and Farmers Science and Technology Cooperation Project (2021SNLF014).

SUPPLEMENTARY MATERIAL

The Supplementary Material for this article can be found online at: https://www.frontiersin.org/articles/10.3389/fpls.2022.909765/full#supplementary-material

REFERENCES

Bian, Z. H., Cheng, R. F., Yang, Q. C., Wang, J., and Lu, C. G. (2016). Continuous light from red, blue, and green light-emitting diodes reduces nitrate content and enhances phytochemical concentrations and antioxidant capacity in lettuce. *J. Am. Soc. Hortic. Sci.* 141, 186–195. doi: 10.21273/JASHS.141.2.186

Chang, C. L., and Chang, K. P. (2014). The growth response of leaf lettuce at different stages to multiple wavelength-band light-emitting diode lighting. *Sci. Hortic.* 179, 78–84. doi: 10.1016/j.scienta.2014.09.013

de Wit, M., Spoel, S. H., Sanchez-Perez, G. F., Gommers, C. M. M., Pieterse, C. M. J., Voesenek, L. A. C. J., et al. (2013). Perception of low red:far-red ratio compromises both salicylic acid- and jasmonic acid-dependent pathogen defences in *Arabidopsis*. *Plant J.* 75, 90–103. doi: 10.1111/tpj.12203

Demkura, P. V., Abdala, G., Baldwin, I. T., and Ballare, C. L. (2010). Jasmonate-dependent and -independent pathways mediate specific effects of solar ultraviolet B radiation on leaf phenolics and antiherbivore defense. *Plant Physiol.* 152, 1084–1095. doi: 10.1104/pp.109.148999

Ding, Z. J., Galvan-Ampudia, C. S., Demarsy, E., Langowski, L., Kleine-Vehn, J., Fan, Y. W., et al. (2011). Light-mediated polarization of the PIN3 auxin transporter for the phototropic response in Arabidopsis. *Nat. Cell Biol.* 13, 447–452. doi: 10.1038/ncb2208

Fan, X. X., Xu, Z. G., Liu, X. Y., Tang, C. M., Wang, L. W., and Han, X. L. (2013). Effects of light intensity on the growth and leaf development of young tomato plants grown under a combination of red and blue light. *Sci. Hortic.*153, 50–55. doi: 10.1016/j.scienta.2013.01.017

Fu, Y. M., Li, H. Y., Yu, J., Liu, H., Cao, Z. Y., Manukovsky, N. S., et al. (2017). Interaction effects of light intensity and nitrogen concentration on growth, photosynthetic characteristics and quality of lettuce (*Lactuca sativa L. Var. youmaicai). Sci. Hortic.*214, 51–57. doi: 10.1016/j.scienta.2016.11.020

Hardeland, R. (2016). Melatonin in plants - diversity of levels and multiplicity of functions. *Front. Plant Sci.* 7, 198–212. doi: 10.3389/fpls.2016.00198

Homma, T., Anzai, T., Matsuo, K., Kanemitsu, N., Satoh, H., and Hiramoto, H. (2011). Effects of continuous irradiation of LED light on growth of young tea plants. *Acta Hortic.* 907, 233–236. doi: 10.17660/ActaHortic.2011.907.35

Jin, J., Lv, Y. Q., He, W. Z., Li, D., Ye, Y., Shu, Z. F., et al. (2021). Screening the key region of sunlight regulating the flavonoid profiles of young shoots in tea plants (*Camellia sinensis* L.) based on a field experiment. *Molecules* 26, 7158–7172. doi: 10.3390/molecules26237158

Kaiser, E., Weerheim, K., Schipper, R., and Dieleman, J. A. (2019). Partial replacement of red and blue by green light increases biomass and

yield in tomato. *Sci. Hortic.* 249, 271–279. doi: 10.1016/j.scienta.2019.02.005

Kurepin, L. V., Walton, L. J., Reid, D. M., and Chinnappa, C. C. (2010). Light regulation of endogenous salicylic acid levels in hypocotyls of *Helianthus annuus* seedlings. *Botany* 88, 668–674. doi: 10.1139/B10-042

Lin, N., Liu, X. Y., Zhu, W. F., Cheng, X., Wang, X. H., Wan, X. C., et al. (2021). Ambient ultraviolet B signal modulates tea flavor characteristics via shifting a metabolic flux in flavonoid biosynthesis. *J. Agric. Food Chem.* 69, 3401–3414. doi: 10.1021/acs.jafc.0c07009

Menendez, Y. C., Sanchez, D. H., Snowdon, R., Rondanini, D. P., and Botto, J. F. (2021). Unraveling the impact on agronomic traits of the genetic architecture underlying plant-density responses in canola. *J. Exp. Bot.* 72, 5426–5441. doi: 10.1093/jxb/erab191

Ohashi-Kaneko, K., Matsuda, R., Goto, E., Fujiwara, K., and Kurata, K. (2006). Growth of rice plants under red light with or without supplemental blue light. *Soil Sci. Plant Nutr.* 52, 444–452. doi: 10.1111/j.1747-0765.2006.00063.x

Paik, I., and Huq, E. (2019). Plant photoreceptors: Multi-functional sensory proteins and their signaling networks. *Semin. Cell Dev. Biol.* 92, 114–121. doi: 10.1016/j.semcdb.2019.03.007

Pertea, M., Kim, D., Pertea, G. M., Leek, J. T., and Salzberg, S. L. (2016). Transcript-level expression analysis of RNA-seq experiments with HISAT, StringTie and Ballgown. *Nat. Protoc.* 11, 1650–1667. doi: 10.1038/nprot.2016.095

Samynathan, R., Thiruvengadam, M., Nile, S. H., Shariati, M. A., Rebezov, M., and Mishra, R. K. (2021). Recent insights on tea metabolites, their biosynthesis and chemo-preventing effects: A review. *Crit. Rev. Food Sci. Nutr.* 21, 1–20. doi: 10.1080/10408398.2021.1984871

Sano, T., Horie, H., Matsunaga, A., and Hirono, Y. (2018). Effect of shading intensity on morphological and color traits and on chemical components of new tea (*Camellia sinensis* L.) shoots under direct covering cultivation. *J. Sci. Food Agric.* 98, 5666–5676. doi: 10.1002/jsfa.9112

Uppalapati, S. R., Ishiga, Y., Wangdi, T., Kunkel, B. N., Anand, A., Mysore, K. S., et al. (2007). The phytotoxin coronatine contributes to pathogen fitness and is required for suppression of salicylic acid accumulation in tomato inoculated with *Pseudomonas syringae* pv. tomato DC3000. *J. Sci. Food Agric.* 20, 955–965. doi: 10.1094/MPMI-20-8-0955

Wang, X., Feng, H., Chang, Y., Ma, C., and Yang, Y. (2020). Population sequencing enhances understanding of tea plant evolution. *Nat. Commun.* 11, 4447–4484. doi: 10.1038/s41467-020-18228-8

Wei, C., Hua, Y., Wang, S., Jian, Z., and Wan, X. (2018). Draft genome sequence of *Camellia sinensis* var. *sinensis provides insights into the evolution of the tea genome and tea quality. Proc Natl. Acad. Sci. USA* 115, E4151–E4158. doi: 10.1073/pnas.1719622115

Weller, J. L., Hecht, V., Schoor, J. K. V., Davidson, S. E., and Ross, J. J. (2009). Light regulation of gibberellin biosynthesis in pea is mediated through the COP1/HY5 Pathway. *Plant Cell* 21, 800–813. doi: 10.1105/tpc.108.063628

Xia, E. H., Tong, W., Wu, Q., Wei, S., Zhao, J., and Zhang, Z. Z. (2020). Tea plant genomics: achievements, challenges and perspectives. *Hortic. Res.-England* 7, 7–25. doi: 10.1038/s41438-019-0225-4

Yadav, A., Singh, D., Lingwan, M., Yadukrishnan, P., Masakapalli, S. K., and Datta, S. (2020). Light signaling and UV-B-mediated plant growth regulation. *J. Integr. Plant Biol.* 62, 1270–1292. doi: 10.1111/jipb.12932

Yang, C. W., and Li, L. (2017). Hormonal Regulation in Shade Avoidance. *Front. Plant Sci.* 8, 1527–1534. doi: 10.3389/fpls.2017.01527

Ye, J. H., Lv, Y. Q., Liu, S. R., Jin, J., Wang, Y. F., Wei, C. L., et al. (2021). Effects of light intensity and spectral composition on the transcriptome profiles of leaves in shade grown tea plants (*Camellia sinensis* L.) and regulatory network of flavonoid biosynthesis. *Molecules* 26, 5836–5854. doi: 10.3390/molecules26195836

Ye, J. H., Ye, Y., Yin, J. F., Jin, J., Liang, Y. R., and Liu, R. Y. (2022). Bitterness and astringency of tea leaves and products: formation mechanism and reducing strategies. *Trends Food Sci. Technol.* 123, 130–143. doi: 10.1016/j.tifs.2022.02.031

Yi, R., Yan, J. B., and Xie, D. X. (2020). Light promotes jasmonate biosynthesis to regulate photomorphogenesis in *Arabidopsis*. *Sci. China-Life Sci.* 63, 943–952. doi: 10.1007/s11427-019-1584-4

Zheng, C., Ma, J. Q., Ma, C. L., Shen, S. Y., Liu, Y. F., and Chen, L. (2019). Regulation of growth and flavonoid formation of tea plants (Camellia sinensis) by blue and green Light. *J. Agric. Food Chem.* 67, 2408–2419. doi: 10.1021/acs.jafc.8b07050

Zheng, Y. J., Zhang, Y. T., Liu, H. C., Li, Y. M., Liu, Y. L., and Hao, Y. W. (2018). Supplemental blue light increases growth and quality of greenhouse pak choi depending on cultivar and supplemental light intensity. *J. Integr. Agric.* 17, 2245–2256. doi: 10.1016/S2095-3119(18)62064-7

Zoratti, L., Karppinen, K., Escobar, A. L., Haggman, H., and Jaakola, L. (2014). Light-controlled flavonoid biosynthesis in fruits. *Front. Plant Sci.* 5, 534–549. doi: 10.3389/fpls.2014.00534

Conflict of Interest: Z-SF is employed by the Zhejiang Minghuang Natural Products Development Co., Ltd.

The remaining authors declare that the research was conducted in the absence of any commercial or financial relationships that could be construed as a potential conflict of interest.

Publisher's Note: All claims expressed in this article are solely those of the authors and do not necessarily represent those of their affiliated organizations, or those of the publisher, the editors and the reviewers. Any product that may be evaluated in this article, or claim that may be made by its manufacturer, is not guaranteed or endorsed by the publisher.

frontiers | Frontiers in Plant Science

TYPE Original Research
PUBLISHED 02 March 2023
DOI 10.3389/fpls.2022.910895

OPEN ACCESS

EDITED BY
Chuankui Song,
Anhui Agriculture University, China

REVIEWED BY
Xinchao Wang,
Tea Research Institute (CAAS), China
Sezai Ercisli,
Atatürk University, Turkey

*CORRESPONDENCE
Shan Jin
jinshan0313@163.com

†These authors have contributed equally to this work and share first authorship

SPECIALTY SECTION
This article was submitted to Plant Metabolism and Chemodiversity, a section of the journal Frontiers in Plant Science

RECEIVED 01 April 2022
ACCEPTED 29 August 2022
PUBLISHED 02 March 2023

CITATION
Li MY, Zhang YZ, Zhang ZY, Zhang YH, Ren QQ and Jin S (2023) Differences in transcriptomic and metabolomic analyses of metabolites of shoots on tea plants of different ages and relevant regulatory network. *Front. Plant Sci.* 13:910895. doi: 10.3389/fpls.2022.910895

Differences in transcriptomic and metabolomic analyses of metabolites of shoots on tea plants of different ages and relevant regulatory network

Meng Yuan Li[1†], Yun Zhi Zhang[1†], Zi You Zhang[2], Yan Hui Zhang[3], Qian Qian Ren[1] and Shan Jin[1*]

[1]Fujian Key Laboratory of Tea Science, Fujian Agriculture and Forestry University, Fuzhou, China, [2]Yunnan National Tea Museum, Kunming, China, [3]Yunnan Bachishan Tea Co., Ltd., Kunming, China

To investigate differences in fresh leaves of tea plants at different ages in gene expression, metabolism, and dried tea quality, and to provide references to a deep exploration on metabolite differential accumulation of fresh leaves of tea plants at different ages as well as the regulation mechanism, two groups of fresh leaves from tea plants at different ages (group JP: 20-, 200-, and 1,200-year tea plants; group YX: 50-, 100-, and 400-year tea plants) were chosen as materials, and their differences in gene expression, metabolites, and metabolic regulatory network were investigated by transcriptomics and metabolomics. A total of 12,706 differentially expressed genes (DEGs) were screened from the fresh tea leaves in the JP group, of which tea-20 vs. tea-200 had the largest number of DEGs, up to 9,041 (4,459 down-regulated genes, 4,582 up-regulated genes). A total of 644 common genes in the fresh leaves of three different ages of tea plants in the JP group were differentially expressed. A total of 8,971 DEGs were screened from the fresh leaf samples of tea plants in the YX group, of which the number of DEGs obtained in the tea-50 vs. tea-400 comparison combination was the largest with a total of 3,723 (1,722 up-regulated genes and 2,001 down-regulated genes). A total of 147 common genes were differentially expressed in the fresh leaves of three different tree ages in the YX group. The pathway enrichment analysis showed that most up-regulated DEGs and their related metabolic pathways were similar in the two groups, and that the metabolic pathways of common significant enrichment included flavonoid biosynthesis, phenylpropane biosynthesis, carbon metabolism, amino acid biosynthesis, and plant pathogen interaction. The metabolomics results showed that 72 and 117 different metabolites were screened from the JP and YX groups, respectively. Most of the different metabolites in the two groups were flavonoids, phenolic acids, amino acids, and their derivatives. Among them, the number of down-regulated flavonoids in older tea plants is generally higher than the number of up-regulated flavonoids. Moreover, according to the sensory evaluation results of dried

tea of fresh leaves from tea plants of different ages, tea-1200 and tea-400 showed the highest sensory evaluation scores in their groups. With increase in plant age, the fragrance of the tea was more elegant, and it changed from a dense scent to a faint scent; the tea tasted sweet and its freshness increased, while the sense of astringency was weakened and the concentration declined. Therefore, the quality difference of tea of different tree ages is mainly related to secondary metabolic pathways such as the flavonoid biosynthesis pathway. With increase in tea age, a large number of gene expression in the flavonoid biosynthesis pathway is down-regulated, which reduces the content of bitter flavonoid substances in fresh leaves and makes tea soup more mellow.

KEYWORDS

tea plants of different ages, transcribe, metabolism, flavonoid biosynthesis, quality

Introduction

Plant metabolites are a source of countless medicinal compounds, while the diversity of multidimensional chemical structures has made them superior to treat serious diseases. Some have already been reported as promising alternative medicines and lead compounds for drug repurposing and discovery. These small molecules exert a wide range of effects on a plant and on other living organisms. They induce flowering, fruit set, and abscission in perennial plant growth or regulate the signal of deciduous behavior in the plant (Jiang et al., 2021; Saran et al., 2021; Solovyeva et al., 2021). Studies on tea metabolites have been a hot topic in recent years.

China is the origin of tea plants, and it is the first country in the world to discover, cultivate, and use tea plants (Yu, 1986). Tea has attracted wide attentions as a type of high-quality drink, especially unique tea plant resources and tea products like ancient tree tea and Dancong. The ancient tree tea refers to tea leaves that are prepared from fresh leaves of ancient tea plants according to some processing techniques. It generally includes ancient-tree Pu'er, ancient tree red tea, and ancient tree green tea (Yang et al., 2016). At present, some studies have demonstrated that the sensory quality of older tea plants is better than that of younger tea plants. This is mainly manifested by teas from older trees tasting more mellow and having higher resistance to brew (Liang et al., 2006). The fresh leave quality of tea plants is the basis of the high quality of a tea (Ye, 2010). Chen et al. (2011) carried out a comparative analysis on bud leaf macro-components between ancient tea plants and terraced tea plants and found that major chemical components (e.g., tea polyphenol, amino acids, and caffeine) in fresh leaves of ancient tea plants were significantly higher than those in fresh leaves of terraced tea plants. Zhou et al. (2010) studied the fragrance of terraced tea and ancient tree tea in different regions of Yunnan province and found a significant different in the fragrance of tea products. It can be seen from ancient tree tea that quality varies in different places of origin and that each product has unique characteristics (Qiao et al., 2018). At present, the research on the influence of tree age on the quality of tea mostly focuses on the quality analysis of dry tea, but there are few reports on reasons for the quality difference.

With technological development in recent years, omics research methods represented by metabolomics, transcriptomics, and proteomics have been widely used to study tea plants (Su et al., 2017). Among them, metabolomics separates and detects metabolites in the metabolism process through chromatography and mass spectrum technologies, and it can analyze metabolic pathways intuitively. Metabolomics has been extensively applied to study the influence of processing techniques, environment, and place of origin on tea quality (Dai and Lv, 2019). Based on high-throughput sequencing, transcriptomics investigates the gene expressions of a tissue or an organ from the RNA level, and it has been extensively applied to research studies concerning stress resistance and functional genes of tea plants as well as specific tea plant resources (Tang et al., 2018). Omics technology has become an important mean to study tea science (Zhao, 2019). However, multi-omics has not been used to analyze the metabolic changes in fresh leaves and formation of dry tea quality differences in wild tea plants of different ages.

In this study, fresh leaves from wild tea plants of different ages were collected as research materials, and their differences were analyzed by combining metabolomics and transcriptomics. Meanwhile, the quality difference of their dry tea was analyzed by sensory evaluation. Multiple omics approaches were used to study the differential genes, metabolites and related regulatory metabolic networks of fresh leaves of tea plants in different tree ages, and to analyze the reasons for the formation of differences in dry tea quality in different tree ages, so as to provide a reference for further exploring the differential accumulation of

metabolism and its regulatory mechanism of fresh leaves of tea plants in different tree ages.

Materials and methods

Experimental materials

Fresh leaves of group JP were collected on 10 May 2020 from three tea plants in the same plot of n wild tea garden in Maandi town (22°40′N, 103°34′E, elevation = 920 m), Jinping Miaoyao Dai Autonomous county, Honghezhou, Yunnan province, China. The three tea plants were about 20, 200, and 1,200 years old (marked as T-20, T-200, and T-1200, respectively), and all of them are *Camellia sinensis var. Assamica*. For the location of the three tea plants in the tea garden, T-200 was about 10 m in the downhill direction of T-1200 and about 7 m in the uphill direction of T-20.

Fresh leaves of group YX were collected on 27 May 2020 from three tea plants in the same plot of the wild tea garden in Manghuai town (24°31′N, 100°24′E, elevation = 1,440 m), Yun county, Lincang city, Yunnan province, China. The three tea plants were about 50, 100, and 400 years old (labeled T-50, T-100, and T-400, respectively); all of them were *Camellia taliensis*. The three tea plants T-50, T-100, and T-400 were like the three vertices of an isosceles triangle, and the distance between two trees was about 8 m.

Tea samples of the two groups were picked with one bud and two leaves, with three biological replicates for each year. After fresh leaves were harvested, they were wrapped in tin foil paper, quickly frozen in liquid nitrogen, transferred to a refrigerator at −80°C for storage, and used for transcriptome sequencing and metabolome detection.

The age of the wild tea plants in this study is mainly determined according to the local people and the local government, combined with the appearance characteristics of the tea plants such as breast stem, crown width, and branch level. The ages of all the tested tea plants were approximate, not accurate.

Transcriptome sequencing

Library construction

Agarose gel electrophoresis (AGE) and NanoPhotometer spectrophotometer were used to detect the quality and concentration of RNA samples, and Agilent 2100 bioanalyzer was used to detect the integrity of RNA samples. After the samples were tested and qualified, a library was built. The kit for library construction used the NEBNext® UltraTM RNA Library Prep Kit of Illumina. The built library was diluted to 1.5 ng/μl, and the library was tested with the Agilent 2100 bioanalyzer. Later, an accurate quantization of the effective concentration of library (>2 nM) was carried out by qRT-PCR. Pooling of different libraries was performed according to machine data size under the goal, and sequencing was performed with an Illumina HiSeq platform (Conesa et al., 2016).

Data quality control and analysis

The image data gained with the Illumina HiSeq high-throughput sequencing platform were transformed into a lot of high-quality original data by CASAVA basic group identification. Reads with joint and N content >10% as well as low-quality ($Q \leq 20$) reads with more than 50% basic groups were eliminated. Meanwhile, clean reads were acquired by sequencing error rate check and GC content distribution check. The indexes of reference genomes were built using HISAT2 v2.0.5. Besides, pairing terminal clean reads were compared with reference genomes[1] using HISAT2 v2.0.5. FPKMs (fragments per kilobase of transcript per million fragments mapped) quantized the gene expression level, and reads mapped onto each gene were calculated with the feature Count. Next, the FPKMs of each gene were calculated according to the length of the gene (Liao et al., 2014).

New genes were predicted with the StringTie software (Pertea et al., 2015). The differential expression between any two samples was analyzed with the DESeq2 R software. Moreover, *P*-value was adjusted with the method proposed by Benjamini and Hochberg to control the false discovery rate (FDR), | and log2 fold change| ≥1 (Tea-20, Tea-200 and Tea-1200 inter-group screening standards were 0). Moreover, FDR <0.05 was used as the threshold to screen differentially expressed genes. A gene ontology (GO) enrichment analysis and a KEGG pathway analysis of differentially expressed genes (DEGs) were performed using clusterProfiler R.

Real-time fluorescence quantification PCR verification

To further test the reliability of the RNA-Seq results, a real-time fluorescence quantification PCR (qRT-PCR) verification was performed on candidate DEGs. Among DEGs gained from sequencing, a total of 11 were screened as potential genes in the biosynthesis pathway of flavonoids. All the qRT-PCR primers are designed using the Beacon Designer7.7 software, and the primer sequences are shown in **Table 1**.

The above RNA was used as the template, and it was synthesized into cDNA according to the inverse transcription kit technique of a Takara Primer ScriptTM RT Reagent Kit with gDNA Eraser (Perfect Real Time). β-Actin was used as the internal reference gene. The quantitative analysis was carried out according to the specification of the TB Green™ Premix Ex Taq™ II (Tli RNaseH Plus, RR820A) kit, and the quantification PCR instrument used was BIO-RAD Cycler® CFX96 Real-Time PCR System (BIO-RAD, United States). The reaction program

1 http://tpdbtmp.shengxin.ren:81/analyses_search_locus.html

TABLE 1 Primer design for qRT-PCR.

Gene	Primer sequences (forward)	Primer sequences (reverse)
b-actin	TGACCAAGCACACTCCACACTATCG	TGCCCCCTTATCATCATCCACAA
TEA024897	AGAGACTCAAGAGATGATGGATGT	TGTCAGCACTAGCAATGTCAAT
TEA027576	CAGTGGACCCTACTCTAAACC	CAGTGGACCCTACTCTAAACC
TEA008320	GAGACCTTCATCGGAGAG	AGAATCGGCAGAGCAAGTATAATC
TEA030958	GGATGCTGACAAGGACAACTAC	GCTCCATTCCAGAGGGTGTT
TEA025184	GGATGCTGACAAGGACAACTAC	ACATCGGACTCTCACCTCTC
TEA001789	CCAACTATATGCTGTCTATGTC	TCCAGGCTTGCTAACTAC
TEA006847	AATGGCATCTGATAGTTGTG	CCAGGTAGGAATCGTTCT
TEA032087	GATGAGTGATGAGGACCTTCTGA	ACCTTGGTGAGGAGTACAGTAG
TEA001157	CCACCGTCTCACCTCCTAAG	TGGCATAGTTGACCTTGTTGAATC

was set at 95 C for 30 s, 95 C for 5 s, and 60 C for 30 s, for 40 cycles. The $2^{-\Delta\Delta}$CT method was used to analyze the relative changes in gene expression from real-time quantitative PCR experiments.

Metabolite extraction and detection

After vacuum freeze drying, the samples were ground (30 Hz, 1.5 min) into powder with a grinder (MM 400, Retsch). A total of 100 mg sample powders were collected and dissolved into 6 ml extracting solution. The mixture was put in a refrigerator (4 C) overnight (six times of swirling). After 10 min of centrifuging at the rate of 10,000 *g*, the supernatant was collected and filtered with a millipore filter (0.22 μm) and finally stored for UPLC-MS/MS analysis.

Liquid phase conditions: Waters ACQUITY UPLC HSS T3 C18 (1.8 μm, 2.1 mm × 100 mm) was used as the chromatographic column. Ultrapure water and acetonitrile were used as moving phases A and B (both were added with 04% acetic acid). The proportion of the B phase increased from 5 to 95% in the period of 0-10 min. This proportion was kept for 1 min and then decreased to 5% within 1 min. Later, it was balanced to 14 min. The flow rate, column temperature, and sample size were 35 ml/min, 40 C, and 4 μl, respectively. Mass spectral condition: temperature of the electrospray ionization, mass spectral voltage, and gas curtain were 550 C, 5,500 V, and 30 psi, respectively. The impact-induced ionization parameter was set to High. In triple quadrupole, each ion pair is scanned and tested according to optimized declustering potential and collision. The extensive targeted metabolomics test is accomplished by Wuhan Matwell Company. The data analysis of metabolites was accomplished with Analyst 1.6.3, MultiaQuant, and R. The intergroup differences of sample metabolites were simplified and maximized by PCA and orthogonal partial least square-discriminant analysis (OPLS-DA). Differential metabolites were screened by combining fold change with variable importance projection (VIP) in the OPLS-DA model. The standard was set fold change ≥2 or fold change ≤0.5 and VIP ≥1.

Sensory evaluation analysis of groups JP and YX

Processing of dried tea of groups JP and YX

We plucked one bud and two leaves of tea plants of different ages, and obtained dried tea samples by the process of deactivation, rolling, drying under sunlight, etc., for sensory evaluation. The processing of tea is shown in **Figure 1**.

Dried tea evaluation of groups JP and YX

Sensory evaluations of dried tea samples of groups JP and YX were performed according to Standard GB/T23776-2018 (Zhang et al., 2020). By combining scoring and comments, the total score was calculated by weighted average mode. The total score was 100, including 20% of appearance, 25% of fragrance, 15% of liquor color, 30% of taste, and 10% of leave bottom. Specifically, 5 g of representative dried tea samples (tea-water ratio = 1:50) were put in corresponding evaluation cups full of boiled water. We covered the cups for 2 min. The liquor was poured into evaluation bowls quickly according to the brewing order. After evaluating liquor color, smelling the fragrance of leaf bottom, and tasting, the second brewing was performed for 5 min. The liquor was poured into bowls to evaluate its color, fragrance, taste, and leaf bottom. The color of the liquor was mainly assessed by the first brewing, while the fragrance and taste were mainly judged by the second brewing. The sensory evaluation of two groups of tea samples in different years was set up with three repetitions.

Results and analysis

Transcriptome analysis

Sequencing quality analysis

According to the transcriptome sequencing results of fresh leave samples of group JP (Tea-20, Tea-200, and Tea-1200) (**Table 2**), the clean data of each sample were higher than

FIGURE 1
Tea processing process.

TABLE 2 Evaluation of tea transcriptome data of group JP.

Sample	Raw-reads	Clean-reads	Clean-bases	Error rate	Q20 (%)	Q30 (%)	GC_pct (%)
Tea20-1	64,769,842	63,893,584	9.58G	0.03	97.93	94.08	43.41
Tea20-2	59,268,374	58,661,094	8.8G	0.03	97.68	93.48	43.46
Tea20-3	56,519,888	55,765,676	8.36G	0.03	97.73	93.63	43.5
Tea200-1	56,807,338	561,912,60	8.43G	0.03	97.89	94.04	44.12
Tea200-2	60,247,792	59,581,844	8.94G	0.03	97.76	93.69	43.92
Tea200-3	72,251,112	71,475,114	10.72G	0.03	97.9	94.01	44.04
Tae1200-1	55,784,798	55,147,874	8.27G	0.03	97.77	93.73	44.08
Tea1200-2	51,069,328	50,576,524	7.59G	0.03	97.73	93.65	43.88
Tae1200-3	59,290,044	58,648,896	8.8G	0.03	97.77	93.78	43.54

7 Gb and the percentage of Q30 basic groups was higher than 93%. The success rate of samples matching with the reference genomes is higher than 80%, and a total of 31,540 genes were expressed. In this analysis, 12,817 new genes were identified with the StringTie software. Among them, 2,985 new genes had annotations in the GO database and 2,112 new genes were annotated onto 74 KEGG pathways. In a word, the transcriptome sequencing results were good and could provide good original data for subsequent data assembly.

According to the transcriptome sequencing results of fresh leave samples of group YX (Tea-50, Tea-100, and Tea-400) (Table 3), a total of 68.37 Gb of clean data were acquired from transcriptomic sequencing, and the clean data of each sample reached 6 Gb. The percentage of Q30 basic groups was higher than 89%. The success rate of samples matching with the reference genomes was higher than 80%, and a total of 31,540 genes were expressed. In this analysis, 30,878 new genes were identified with the StringTie software. Among them, 16,329 new genes had annotations in the GO, NR, and Tremble databases. This reflects that the transcriptome sequencing results were good and could provide good original data for subsequent data assembly.

Screening of differentially expressed genes

Gene expression levels were quantized by feature counts, and the expression level of genes was represented by FPKMs. DEGs were screened according to $|\log2\ (\text{fold change})| > 0$ and padj < 0.05 (Figure 2).

From the transcriptomic sequencing of group JP, a total of 12,706 DEGs were screened. Specifically, Tea-20 vs. Tea-200 showed the most DEGs, amounting to 9,041 (including 4,459 downregulated genes and 4,582 upregulated genes). Tea-200 vs. Tea-1200 had moderate DEGs, amounting to 7,418 (including 3,609 downregulated genes and 3,809 upregulated genes). Tea-20 vs. Tea-1200 presented the least DEGs, amounting to 4,329 (including 2,112 downregulated genes and 2,217 upregulated genes). The Venn diagram of the number of DEGs in fresh leaves of tea plants of three different ages is shown in Figure 2A. There are 644 DEGs that are differentially expressed in the fresh leaves of tea plants of three different ages.

From the transcriptomic sequencing of group YX, a total of 8,971 DEGs were screened. Tea-50 vs. Tea-400 showed the most DEGs, amounting to 3,723 (including 1,722 upregulated genes and 2,001 downregulated genes). Tea-100 vs. Tea-400 had moderate DEGs, amounting to 3,559 (including 1,780 upregulated genes and 1,779 down-regulated genes). Tea-50 vs. Tea-100 presented the least DEGs, amounting to 1,689 (including 661 up-regulated genes and 1,028 downregulated genes). The Venn diagram of the number of DEGs in fresh leaves of tea plants of three different ages is shown in Figure 2C. There are 147 DEGs in the fresh leaves of tea plants of three different ages.

Based on above analysis, groups JP and YX both presented that the number of DEGs is positively related with age gap in the comparison pair and that the number of significantly downregulated DEGs is far higher than that

TABLE 3 Evaluation of tea transcriptome data of group YX.

Sample	Raw reads	Clean reads	Clean base	Error rate	Q20 (%)	Q30 (%)	GC pet (%)
Tea50-1	45,195,862	44,465,896	6.67	0.02	96.38	90.67	43.44
Tea50-2	50,450,168	48,879,880	7.33	0.02	95.94	89.83	43.69
Tea50-3	47,998,520	47,343,828	7.1	0.02	96.17	90.28	44
Tea100-1	51,610,704	50,826,614	7.62	0.02	96.09	90.06	43.89
Tea100-2	46,947802	46,223,142	6.93	0.02	96.46	90.87	44.2
Tea100-3	55,371,554	54,321,062	8.15	0.02	96.16	90.27	44.49
Tea400-1	49,572,182	48,611,350	7.29	0.02	96.23	90.33	43.11
Tea400-2	72,416,374	69,986,928	10.5	0.02	98.23	94.3	43.78
Tea400-3	45,538,182	44,619,128	6.69	0.02	96.6	91.08	43.92

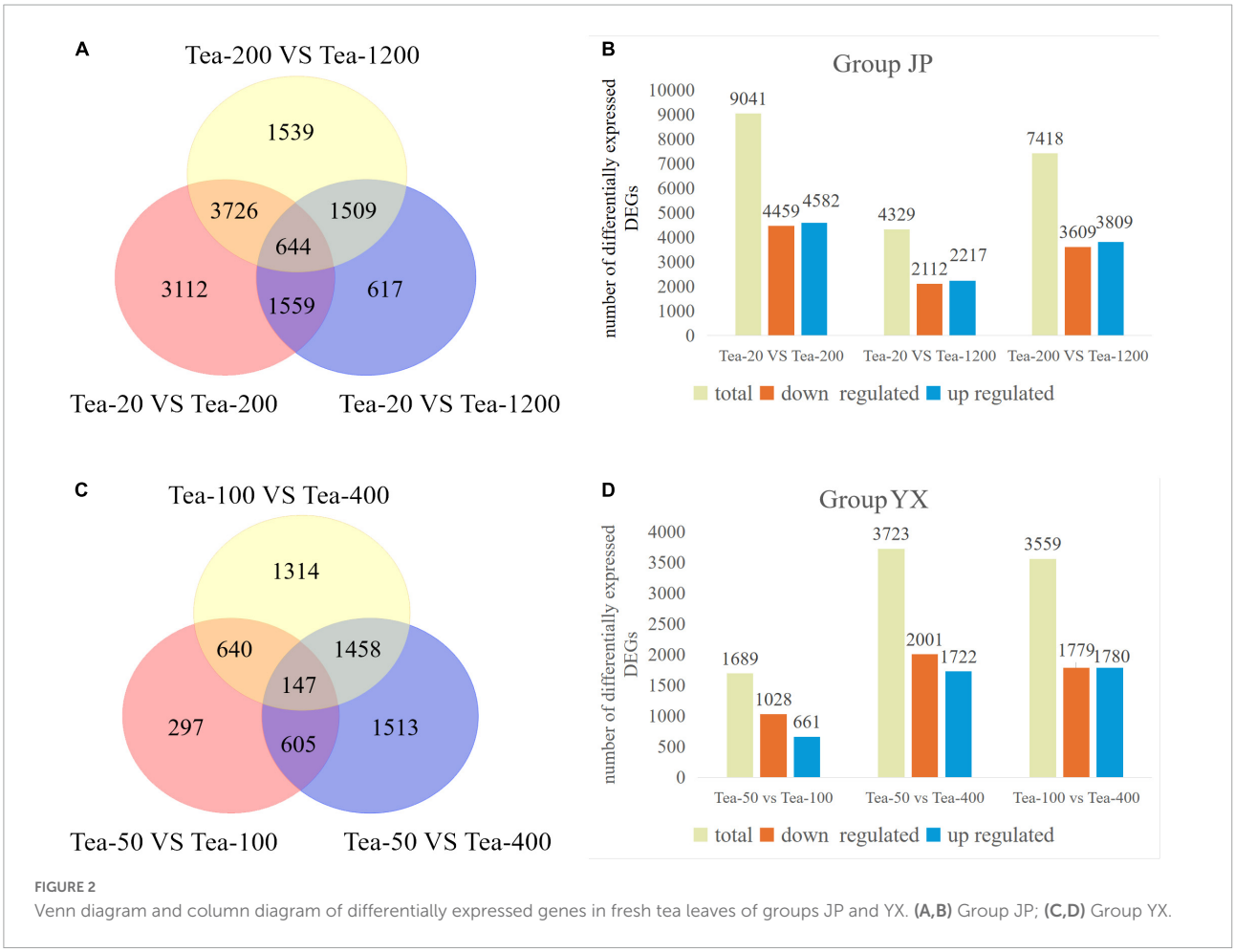

FIGURE 2
Venn diagram and column diagram of differentially expressed genes in fresh tea leaves of groups JP and YX. **(A,B)** Group JP; **(C,D)** Group YX.

of significantly upregulated DEGs. This indicates that gene expression varies significantly in fresh leaves of tea plants of different ages. In other words, the number of DEGs increases with increase in tree age.

Gene ontology enrichment analysis

Gene ontology is a comprehensive database that describes gene functions, and it can be divided into biological process, cellular component, and molecular function. Padj (corrected *P*-value) <0.05 was chosen as the threshold of significance analysis. The GO functionally significant enrichment is shown (Figure 3).

To understand changes in the gene expression levels of tea plants of different ages, GO analyses of groups JP and YX were carried out. It was found that among the three comparison pairs of group JP, DEGs were mostly enriched in molecular function and biological process, but that only

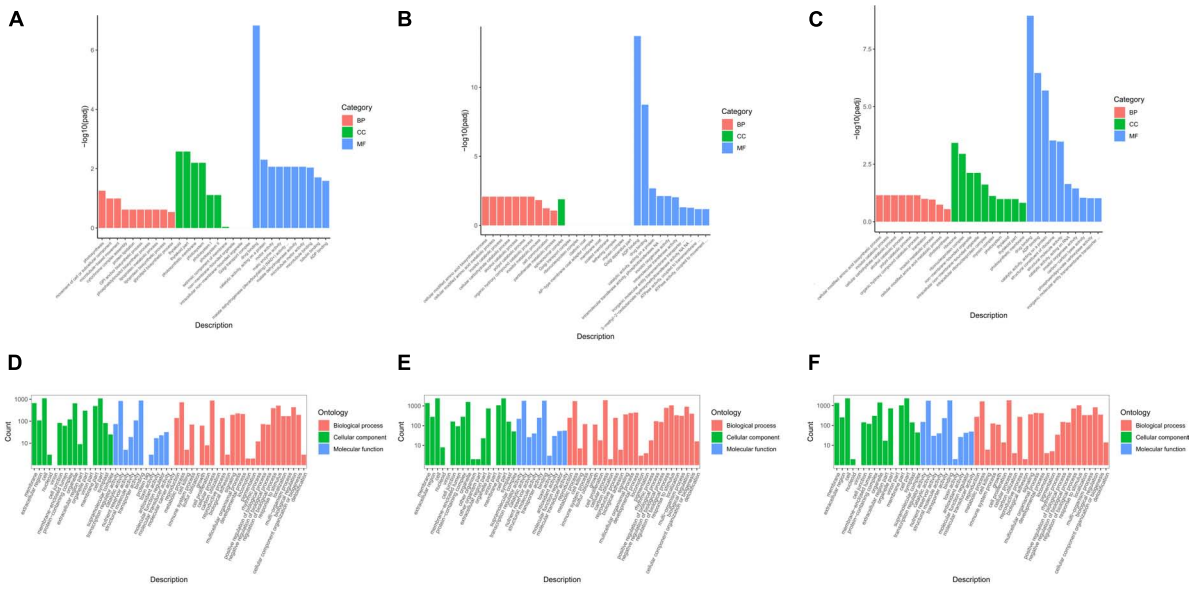

FIGURE 3
Gene ontology (GO) enrichment analysis of differentially expressed genes (DEGs) in groups JP and YX. **(A)** Tea-20 vs. Tea-200, **(B)** Tea-20 vs. Tea-1200, **(C)** Tea-200 vs. Tea-1200, **(D)** Tea-50 vs. Tea-100, **(E)** Tea-50 vs. Tea-400, and **(F)** Tea-100 vs. Tea-400.

few were enriched in cellular component. Moreover, DEGs in molecular function and biological process were significantly enriched in metabolic pathways such as photosynthesis, catalytic activity acting on proteins, ADP binding, and biosynthesis of amino acids. Therefore, gene expressions related with molecular function and biological process are significantly different among Tea-20, Tea-200, and Tea-1200. Among the three comparison pairs of group YX, DEGs of Tea-400 vs. Tea-50 and Tea-400 vs. Tea-100 were mainly enriched in cellular composition, molecular function, and biological process. Metabolic pathways with significant enrichment of DEGs include membrane and organelle, catalytic activity, and transfer activity as well as cell process, metabolic process, and biological regulation.

KEGG enrichment analysis of differentially expressed genes

To further study the differences between groups JP and YX on the molecular level, KEGG pathway enrichment was carried out on DEGs. The first 20 KEGG pathways with DEG enrichment were selected (Figure 4).

According to the KEGG enrichment analysis results of group JP, DEGs of Tea-20 vs. Tea-200 (Figure 4A) were enriched significantly in 110 KEGG pathways, including the photosynthesis pathway, glycerolipid metabolic pathway, carbon metabolism and amino acids, biosynthesis of flavonoids, biosynthesis of phenylalanine metabolism, and so on. DEGs of Tea-20 vs. Tea-1200 (Figure 4B) are mainly annotated in 100 KEGG pathways. Among them, KEGG paths with significant enrichment of DEGs include endoplasmic reticulum protein processing, carbon metabolism, biosynthesis of amino acids, and biosynthesis of phenylpropane. There are 934 DEGs of Tea-200 vs. Tea-1200 (Figure 4C) that are related with 108 pathways such as ribosome, carbon metabolism, biosynthesis of amino acids, glycerolipid metabolism, biosynthesis of flavonoids, and plant pathogen interaction.

According to the KEGG enrichment analysis results of group YX, 638 DEGs of Tea-50 vs. Tea-100 (Figure 4D) were annotated onto 126 metabolic pathways. Pathways with significant DEG enrichment include the metabolism pathway, biosynthesis of phenylpropane, plant pathogen interaction, biosynthesis of secondary metabolites, biosynthesis of flavonoidsm, etc. For Tea-50 vs. Tea-400 (Figure 4E), 1,494 DEGs were annotated by 135 KEGG pathways, which were mainly related with metabolism and genetic information processing. Significant enrichments occur in metabolic pathways, biosynthesis of secondary metabolites, and biosynthesis of flavonoids. For Tea-100 vs. Tea-400 (Figure 4F), 1,462 DEGs were related with 134 metabolic pathways, and significant enrichment occurs in plant pathogen interaction, metabolic pathway, and carbon metabolism.

To sum up, among the three comparison pairs of Tea-20, Tea-200, and Tea-1200, significant enrichment of DEGs was observed in carbon metabolism and biosynthesis of amino acids. Among the three comparison pairs of Tea-50, Tea-100, and Tea-400, significant enrichment of DEGs was observed in metabolic pathway, biosynthesis of secondary metabolites, plant pathogen interaction, biosynthesis of flavonoids, and biosynthesis of phenylpropane. Among the six comparison pairs, significant enrichment of DEGs was observed in biosynthesis of flavonoids and biosynthesis of phenylpropane.

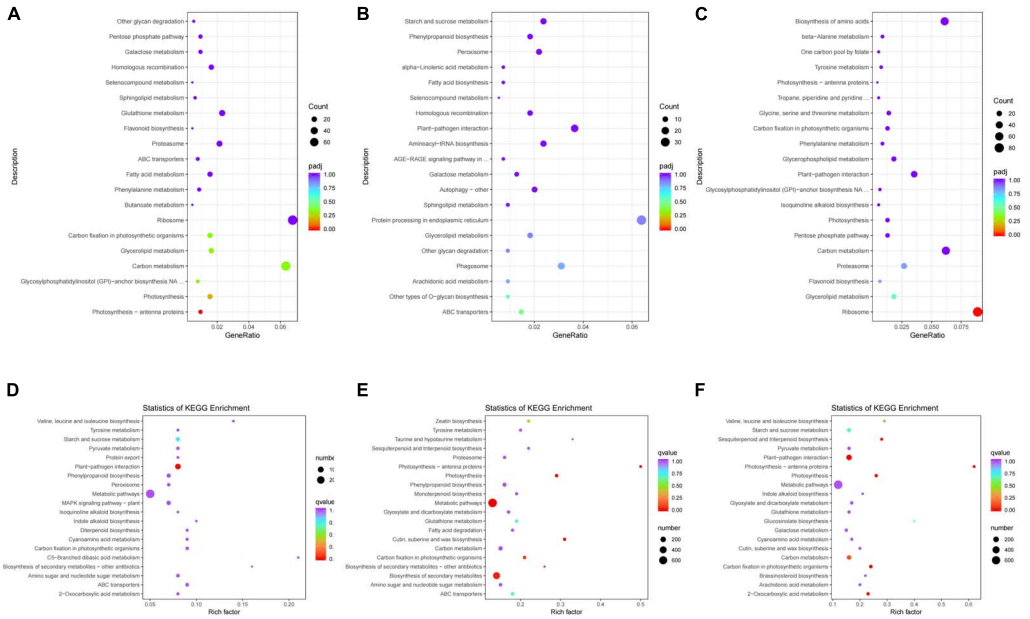

FIGURE 4
KEGG pathway enrichment analysis of differentially expressed genes (DEGs) in panels **(A–C)** group JP and **(D–F)** group XY. **(A)** Tea-20 vs. Tea-200, **(B)** Tea-20 vs. Tea-1200, **(C)** Tea-200 vs. Tea-1200, **(D)** Tea-50 vs. Tea-100, **(E)** Tea-50 vs. Tea-400, and **(F)** Tea-100 vs. Tea-400.

Analysis of related pathways of flavonoid synthesis

Flavonoids are the most important secondary metabolites of tea plants and play a decisive role in tea flavor and healthcare function. The flavonoid biosynthesis pathway starts from the phenylpropane metabolism pathway. L-Phenylalanine in the starting substrate in the pathway; the pathway of phenylpropane generates coumaroyl A and trans-coumaryl coenzyme A, which are precursor substances of the synthesis pathway of flavonoids. The results of groups JP and YX groups are as follows (**Figure 5**):

The expression levels of *CHS* (TEA018665), *C4H* (TEA034001), and *DoOMT* (TEA030958) in Group JP of tea plants did not follow certain rules with the change of tea plants age, that is, the expression of *CHS*, *C4H*, and *DoOMT* were higher in Tea-20 and Tea-1200 than that in Tea-400. However, the expression of *F3H* (TEA006847) in Group JP of tea plants gradually decreased with the decline of the tea plants age, that is, the expression of *F3H* was the highest in Tea-1200, the expression of Tea-20 was the lowest. The expression level of *CCoAOMT* (TEA000392) was the highest in Tea-20, the expression of Tea-200 was the lowest. In group YX, the expression levels of *FLS* (TEA023723, TEA010762), *HCT* (TEA003148, TEA032135), *LAR* (TEA021535), *C4H* (TEA016772), and *COMT* (TEA012735) showed an increasing trend with increase in tea plant years; that is, the expression levels of these genes were highest in Tea-400 tea plants, the expression levels of Tea-50 were the lowest. However, the expression levels of *CHS* (TEA023331), *DFR* (TEA030009), and *FLS* (TEA010328) in Group YX of tea plants were significantly higher in Tea-50 and Tea-100, and the expression of *HCT* (TEA010128) was also highest in Tea-50.

Pathway analysis of phenylpropane biosynthesis

Synthesis of polyphenol in tea plants involves the pathway of shikimic acid, pathway of phenylpropane, and pathway of flavonoids (Han, 2018). The differential gene analysis of the phenylpropane biosynthesis pathway between Groups JP and XY group found that (**Figure 6**):

In the Group JP, the expression levels of *CCoAOMT* (TEA000392), *CAD* (TEA024897), *POD* (TEA027576) in Tea-20 were significantly higher than that in Tea-200 and Tea-1200; while the expression of anthocyanidin 3-O-glucosyltransferase5 (TEA029495) was the highest in Tea-1200. The expression levels of CAD (TEA025404), *POD6* (TEA022953), *C4H* (TEA034001), *4CL* (TEA009431), and *CYP736A* (TEA032382) in Tea-20 and Tea-1200 were the significantly higher than that in Tea-200. The expression of *REF1* (TEA010889) gradually increased with the decrease of tea plant years. In Group YX, the expression levels of *POD11* (TEA024164), *F5H* (TEA000057), and *PAL* (TEA014166) increased with the age of tea plants gradually decrease; while *CAD* (TEA018278, TEA000402), *POD4* (TEA027359), *POD5* (TEA005749), *CCR* (TEA032793), and *COMT* (TEA010574) gradually increased with the increase of tea plant years, and the expression levels of *POD2* (TEA031894) and *REF1* (TEA033460) in Tea-400 and Tea-100 were significantly higher than that in Tea-50.

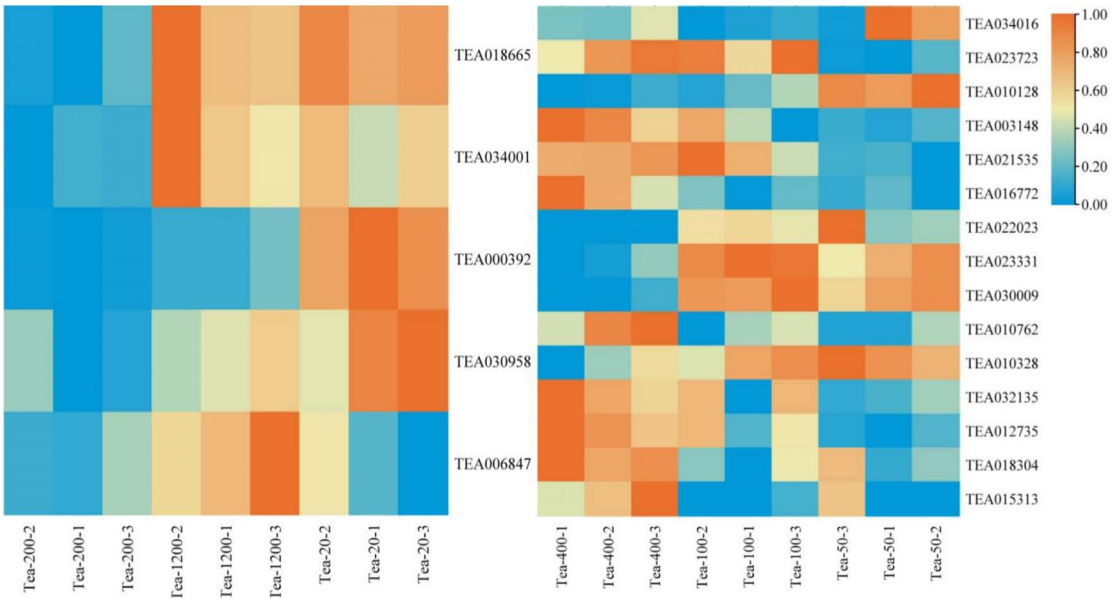

FIGURE 5
Heat map of the flavonoid synthesis pathway and related gene expression in tea shoots of different years. The left heat map for Group JP, and the right heat map for Group YX.

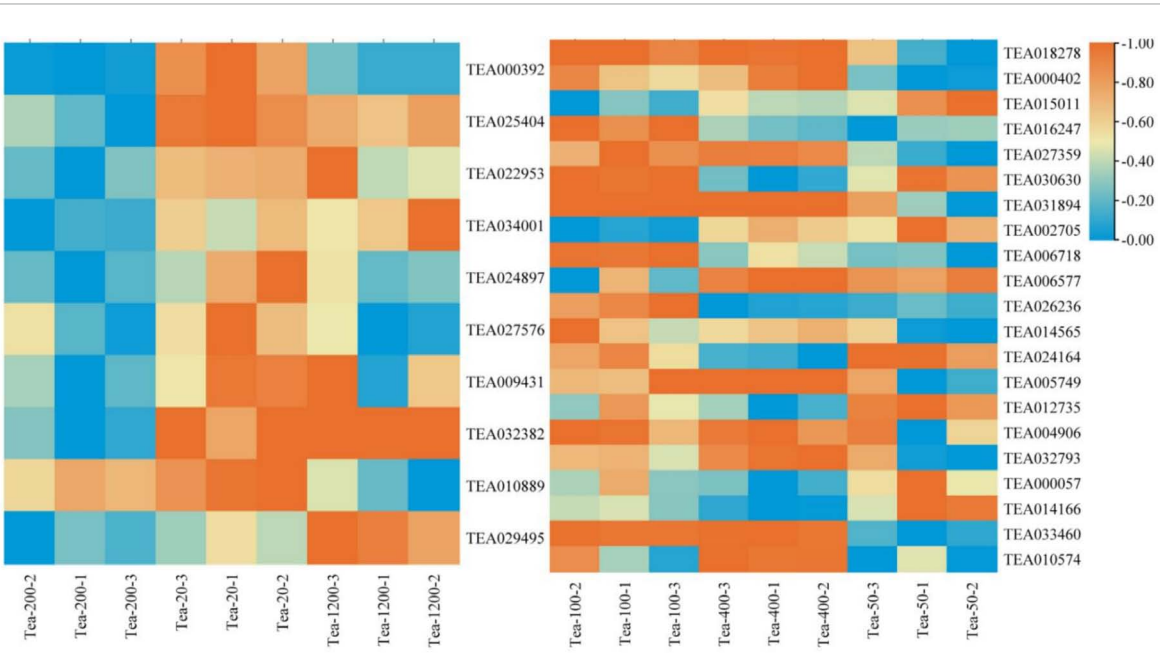

FIGURE 6
Heat map of the phenylpropane biosynthesis pathway and related gene expression in tea shoots of different years. The left heat map for Group JP, and the right heat map for Group YX.

qRT-PCR verification of transcriptomic results

To further verify the transcriptomic sequencing data, nine candidate genes were chosen for qRT-PCR test, including biosynthesis pathway of phenylpropanoids, biosynthesis pathway of flavonoids, and genes related with photosynthesis. According to the results, the expression mode of the selected genes is basically consistent with the transcriptomic sequencing results, indicating reliability and repeatability of the RNA-seq data (Figure 7). Therefore, the receipts obtained in this study can be used to study the differences in

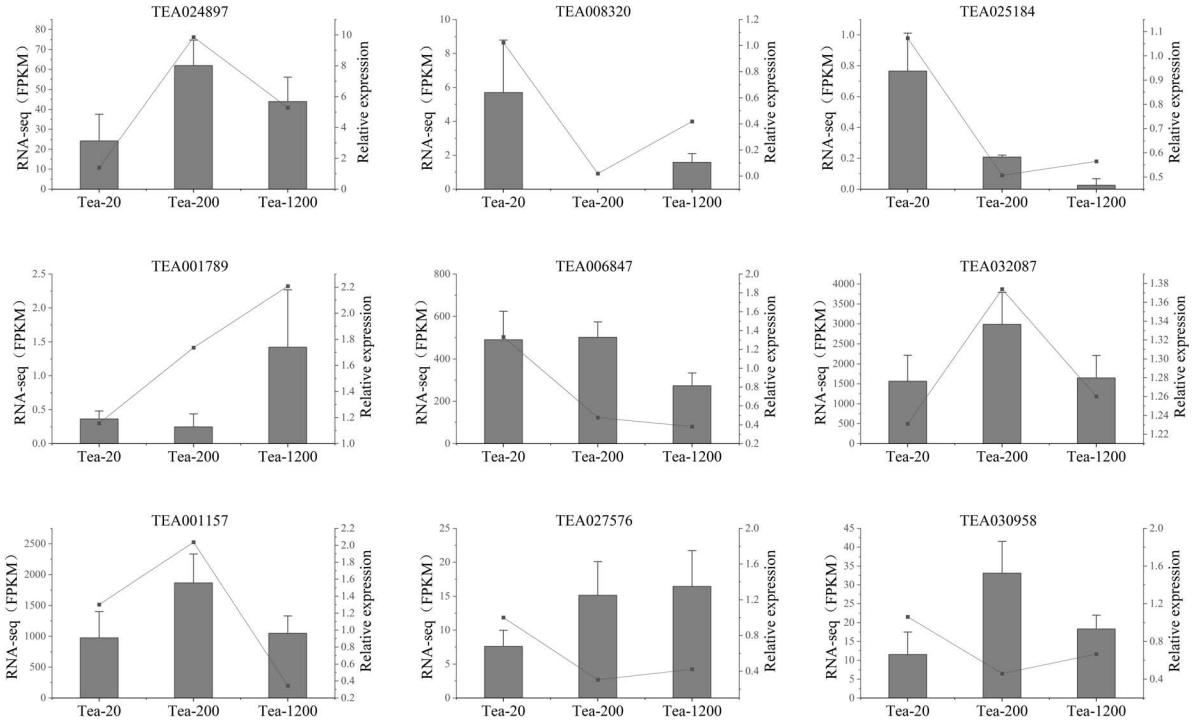

FIGURE 7
qRT-PCR verification of transcriptomic sequencing. Fragments per kilobase of transcript per million fragments mapped (FPKM) of transcriptome data (gray columns) and relative expressions of qRT-PCR test (black points) are represented.

metabolites of tea shoots of different years and their regulatory mechanisms.

Metabonmics analysis

Differential metabolite statistics

By comparing the metabolome database built by Maiwei company, 433 and 440 metabolites were tested in Groups JP and YX, mainly including flavonoids, lipids, amino acids and derivatives, nucleotides and derivatives, organic acids, and so on. Moreover, it can be found from the heat map clustering analysis based on concentration data of metabolites that all biological repetitions cluster well. This reflects that the metabolomics data are reliable (**Figures 8A,B**).

The metabolomics results of group JP (**Figures 8C,D**) showed that a total of 72 differential metabolites were screened. Thirty-six differential metabolites were screened from Tea-20 vs. Tea-200, including 20 significantly upregulated differential metabolites and 16 significantly downregulated differential metabolites. Among them, the significantly upregulated differential metabolites mainly include flavonoids such as vitexin, pufferin, citronellin, and naringenin, and the significantly downregulated differential metabolites mainly include procyanidin, catechin, 3-O-p-coumaroyl Quinic acid, etc. Similarly, 36 differential metabolites were screened from Tea-200 vs. Tea-1200, including 12 significantly upregulated differential metabolites and 24 significantly downregulated differential metabolites. Among them, the significantly upregulated differential metabolites mainly include flavonoids such as myricetin, proanthocyanidin, and (−)-epiafzelechin, and the significantly downregulated differential metabolites mainly include vitexin, mannitol, and other substances. However, Tea-20 vs. Tea-1200 had the lowest number of differential metabolites with a total of 31 (10 significantly up-regulated and 21 significantly down-regulated), and the differential metabolites were mainly flavonoids and phenolic acids. Compared with Tea-20 and Tea-200, the number of down-regulated metabolites in the fresh leaves of Tea-1200 was more than the number of the upregulated, and most of the down-regulated metabolites were flavonoids. This indicates that the content of most flavonoids is lower in the fresh leaves of the older tea plants than in those of the younger tea plants.

Similar phenomena were discovered in group XY. A total of 117 differential metabolites were screened in group XY (**Figures 8E,F**). Tea-50 vs. Tea-100 had 63 differential metabolites (25 up-regulated and 38 down-regulated). Among them, most of the differential metabolites are flavonoids and phenolic acids such as tangerine peelin, vitexin, isovitexin, coniferoside, dregnoside, and luteolin. In Tea-50 vs. Tea-400, there were 73 differential metabolites,

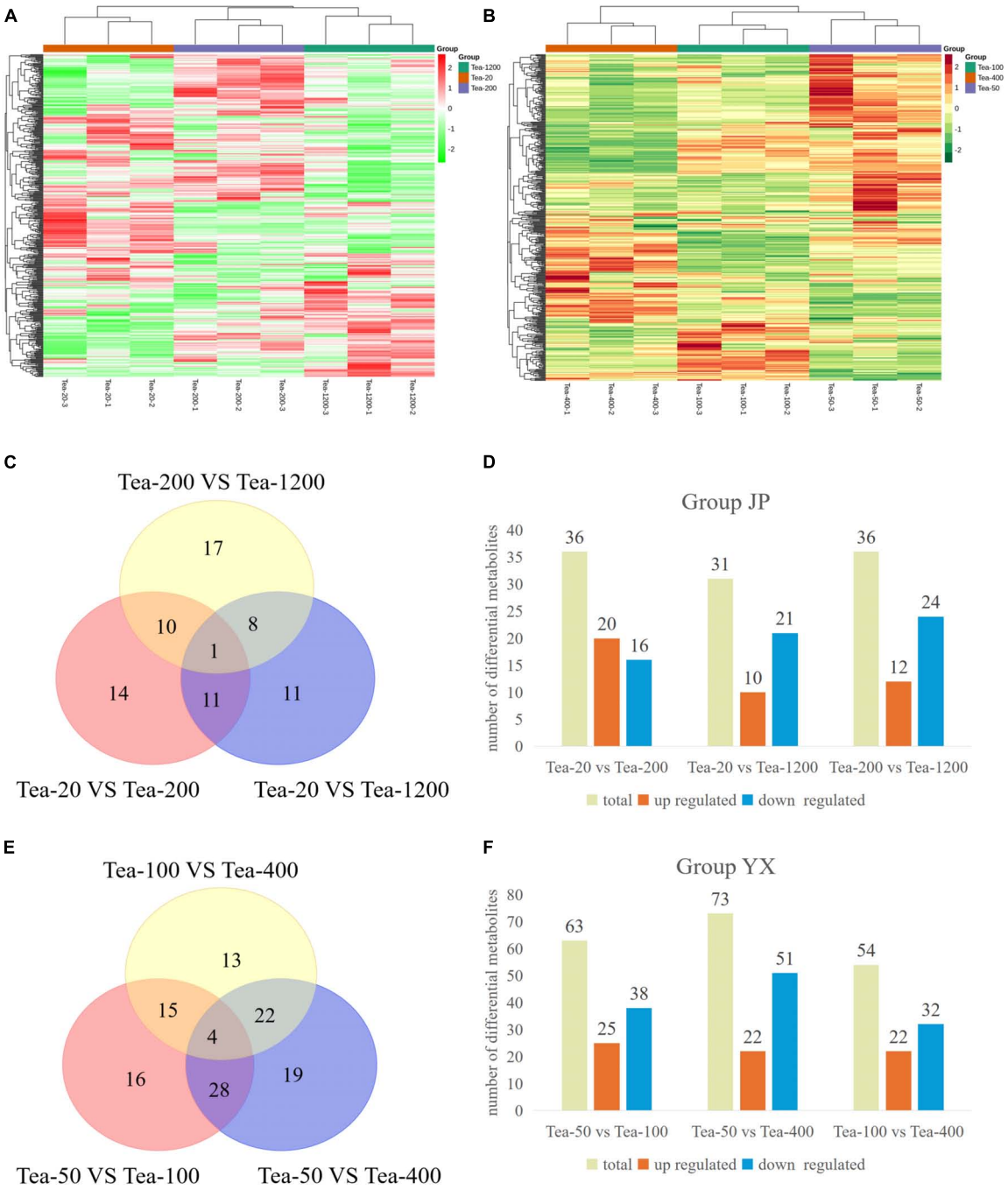

FIGURE 8
(A,B) Cluster heat map and **(C–F)** statistical map of differential metabolites of fresh leaves of trees of different ages.

including 22 significantly up-regulated ones and 51 significantly downregulated ones. Most of the differential metabolites are flavonoids such as myricetin, vitexin, and citronella. In Tea-100 vs. Tea-400, there were 54 differential metabolites, including 22 upregulated ones and 32 significantly downregulated ones. Most of which were still flavonoids and phenolic acids.

It can be seen that the different metabolites of fresh tea leaves in groups JP and YX at different years are mainly flavonoids, tannins, and phenolic acids. Compared with the younger tea plants, the number of downregulated flavonoids in the older tea plants is generally more than the number of upregulated flavonoids, which may be related to the gradual aging of the older tea plants.

Analysis of differential metabolite content

By differential metabolite content analysis of fresh tea leaves of groups JP and YX at different years, some differential metabolites show a regular change with increase in tree age, as shown in **Figure 9**.

Among the 72 differential metabolites in group JP, the contents of amino acids and their derivatives, such as D-serine, and most flavonoids, such as butin, naringenin, vitexin, pinobanksin, syringen, and dihydrokaempferol, gradually decreased with increase in tea plant age. However, the content of proanthocyanidins such as catechin, procyanidin B1, C1, and C2, and phenolic acids such as 3-o-p-coumaroyl quinic acid, methyl gallate, isochlorogenic acid A, and isochlorogenic acid C increased significantly with increase in tea age. The contents of myricetin and quercitirin in Tea-200 were highest, while those in Tea-1200 were lowest; The contents of D-sorbitol, vitexin. and apigenin 5-o-glucoside were lowest in Tea-200 and highest in Tea-20.

Among the 117 differential metabolites in group YX, the contents of flavonoids such as gallic acid, myricetin, protocatechuic acid, and dihydrokaempferol, phenolic acids such as ferulic acid, coniferyl alcohol, and chlorogenic acid methyl ester, and amino acids and their derivatives such as L-aspartic acid, L-histidine, L-leucine, and L-isoleucine decreased with increase in tea age. However, the contents of flavonoids such as gallate catechin gallate (GCG), methyl gallate, naringenin, L-epicatechin, and quercetin, phenolic acids such as methyl p-coumarate, and procyanidins B2, C1, and C2 gradually increased with increase in tea age. The content of metabolites such as flavonoids (−)–epigalactocatechin, (+)–galactocatechin, nobiletin, vitexin, and eriodictyol was highest in Tea-100 and lowest in Tea-50 trees.

KEGG enrichment analysis of differential metabolites

The KEGG database is the integrated metabolic pathway inquiry provided for researchers, and it is an important tool for metabolic network analysis of organisms. KEGG annotation and enrichment analysis were performed on the screened differential metabolites (**Figure 10**).

According to the KEGG analysis of differential metabolites in group JP, differential metabolites of Tea-20 vs. Tea-200 were mainly enriched in 44 metabolic pathways. Metabolic pathways with significant enrichment mainly include biosynthesis of flavonoids, biosynthesis of flavone and flavonol, and biosynthesis of flavones as well as metabolism of galactose, fructose, mannose, and vitamin B6. Differential metabolites of Tea-20 vs. Tea-1200 were mainly enriched in 13 metabolic pathways, and metabolic pathways of significant enrichment involve biosynthesis of anthocyanin, biosynthesis of flavonoids, flavone, and flavonol as well as metabolism of vitamin B6. Differential metabolites of Tea-200 vs. Tea-1200 were mainly enriched in 26 metabolic pathways, and metabolic pathways of significant enrichment involve biosynthesis of flavonoids, flavone and flavonol, metabolism of galactose, fructose, and mannose, oxidative phosphorylation, and thiamine metabolism. Therefore, metabolic pathways with common enrichment of differential metabolites among the three comparison pairs of group JP mainly involve biosynthesis of flavonoids, flavone, and flavonol as well as metabolism of galactose, fructose, mannose, and vitamin B6.

According to the KEGG analysis of differential metabolites of group XY, differential metabolites of Tea-50 vs. Tea-100 were mainly enriched in 33 metabolic pathways. Significant enrichment pathways involve biosynthesis of flavonoids, flavone, flavonol, and phenylpropane as well as metabolism of tyrosine and vitamin B6. Differential metabolites of Tea-50 vs. Tea-400 were mainly enriched in 48 metabolic pathways. Metabolic pathways of significant enrichment involve biosynthesis of flavonoids, flavone, and flavonol as well as metabolism of fructose, mannose, phenylalanine, tyrosine, and vitamin B6. Differential metabolites of Tea-50 vs.Tea-100 were mainly enriched in 37 metabolic pathways. Metabolic pathways of significant enrichment involve metabolism of caffeine and purine as well as biosynthesis of phenylpropane, secondary metabolites, carbapenems, arginine, flavonoids, flavone, and flavonol. Therefore, metabolic pathways of common significant enrichment of differential metabolites in three comparison pairs of group XY involve biosynthesis of flavone, flavonol, and phenylpropane as well as metabolism of vitamin B6, fructose, and mannose.

To sum up, metabolic pathways of common significant enrichment of differential metabolites of groups JP and XY mainly involve biosynthesis of flavonoids, flavone, flavonol, and phenylpropane as well as metabolism of fructose and mannose.

Differential metabolite expression analysis

By the metabolome analysis of fresh tea leaves in groups JP and YX in different years, it was found that most of the differential metabolites of fresh tea leaves in different years were flavonoids and phenolic acids, and the results are as follows (**Figure 9**).

A total of 433 metabolites were detected in fresh tea leaves of group JP. Among them, the content of amino acids and their derivatives D-serine, naringenin, vitexin, butin, pinobanksin, syringetin, and dihydrokaempferol, and most of the flavonoids gradually decreased with increase in tea plant years. Catechin-catechin-catechin, procyanidin B1, procyanidin C1, procyanidin C2, and other proanthocyanidins, and phenolic acids such as 3-O-p-coumaroyl quinic acid, isochlorogenic acid A, isochlorogenic acid C, and other phenolic acids, with increase in tea plant years, their expression levels increased significantly in the Tea-200 and Tea-1200 tea plants. The expression levels of myricetin, quercitrin, theaflavin 3,3′-digallate, (−)-epiafzelechin, and 1,2,3,6-tetragalloyl glucose are the lowest

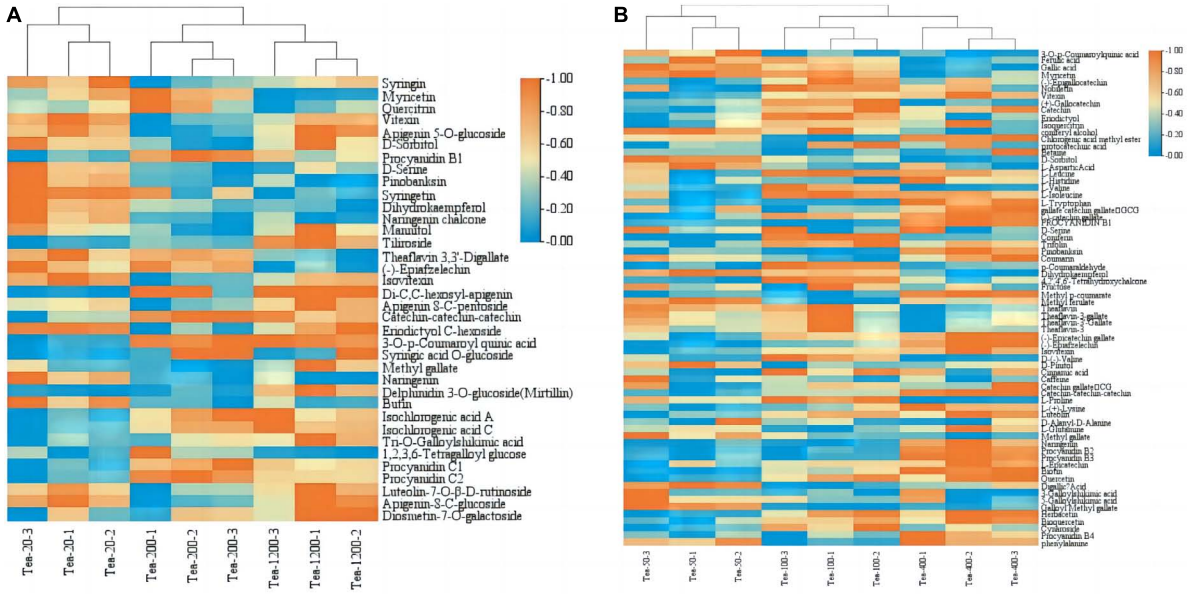

FIGURE 9
Expression analysis of different metabolites in fresh leaves of tea plants of different tree ages in groups JP **(A)** and YX **(B)**.

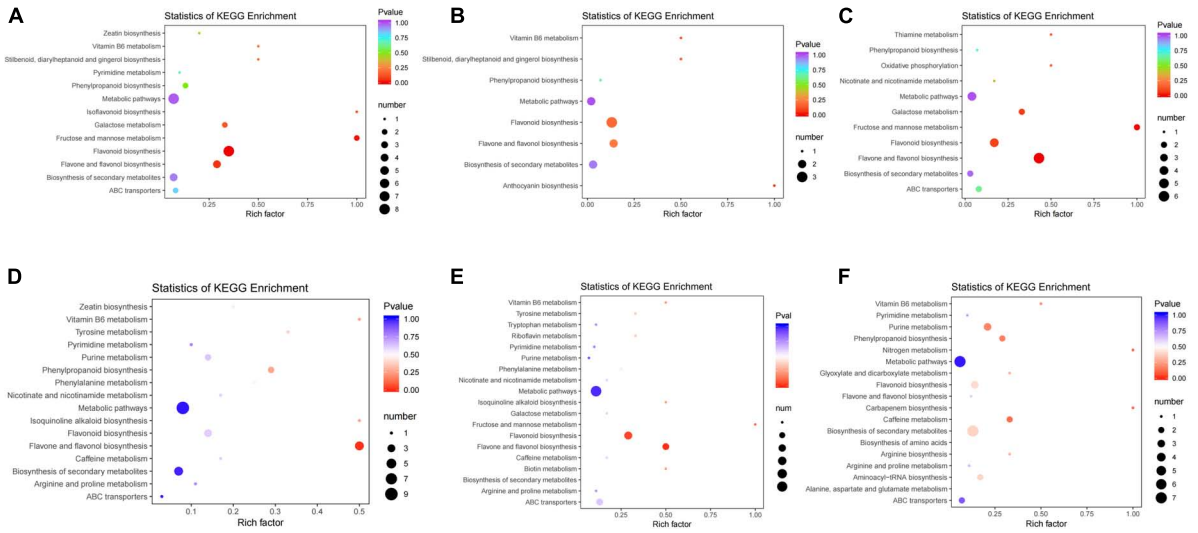

FIGURE 10
KEGG pathway enrichment analysis of differential metabolites of groups JP and YX. **(A)** Tea-20 vs. Tea-200, **(B)** Tea-20 vs. Tea-1200, **(C)** Tea-200 vs. Tea-1200, **(D)** Tea-50 vs. Tea-100, **(E)** Tea-50 vs. Tea-400, and **(F)** Tea-100 vs. Tea-400.

in the tea plant of Tea-1200. The expression levels of D-sorbitol, apigenin 5-O-glucoside, mannitol, isovitexin, apigenin 8-C-pentoside, eriodictyol C-hexoside, methyl gallate, luteolin-7-O-β-D-rutinoside, and apigenin-8-C-glucoside are the lowest in the tea plant of Tea-200.

A total of 440 metabolites were detected in fresh tea leaves of group XY; among them were flavonoids such as gallic acid, myricetin, protocatechuic acid, and dihydrokaempferol, phenolic acids such as ferulic acid, coniferyl alcohol, chlorogenic acid methyl ester, and amino acids such as L-aspartic acid, L-histidine, L-leucine, and L-isoleucine. The contents of derivative substances all showed the characteristics of gradually decreasing with increase in tea plant years. Flavonoids such as GCG, methyl gallate, naringenin, L-epicatechin, quercetin, phenolic acids such as methyl p-coumarate and the content of procyanidin B2, procyanidin C1, procyanidin C2 increased gradually

with increase in tea plant years. The expression levels of flavonoids (−)-epigallocatechin, (+)-gallocatechin, nobiletin, vitexin, eriodictyol, and other metabolites in Tea-100 tea plant is highest, and its expression level is lowest in Tea-50 tea plants.

Metabolomics and transcriptomics conjoint analysis

The results of the KEGG enrichment analysis of the differential genes and differential metabolites of fresh tea leaves in groups JP and XY showed that (**Figure 11**):

Differential metabolites of Tea-20 vs. Tea-200 have the strongest enrichment in the biosynthesis pathway of flavonoids, and that differential metabolites of Tea-200 vs. Tea-1200 have relatively stronger enrichment in metabolic pathways of fructose and mannose. Differential metabolites were mainly enriched in biosynthesis pathways of flavonoids. In group YX, differential metabolites of Tea-50 vs. Tea-100 have strong enrichment in biosynthesis pathways of flavone and flavonol, while DEGs were enriched in biosynthesis pathways of phenylpropane. In Tea-50 vs. Tea-400, DEGs have a relatively high enrichment degree in the biosynthesis pathway of metabolic pathway and secondary metabolites. This demonstrates that the fresh leaves of tea plants of different ages differ significantly in metabolic pathways and synthesis of secondary metabolites, especially in the biosynthesis pathway of flavonoids and metabolic pathways of fructose and mannose. Gene expression and metabolite synthesis are significantly different among the tea plants of different ages.

Differential gene and differential metabolite correlation network analysis

A correlation analysis was performed on differential genes and metabolites related to flavonoid biosynthesis and phenylpropane biosynthesis in tea plants in groups JP and YX, and the Pearson correlation coefficient R was calculated with R language, with $R > 0.8$ being a significant correlation. The standard of Cytoscape is used to draw the interaction network diagram, and the results are as follows (**Figure 12**).

In group JP, caffeoyl-CoA (Tea30958), *CHS* (TEA018665), naringenin (pme0376), pinobanksin (mws0914), 4,2′,4′,6′-tetrahydroxychalcone (mws1140), apigenin8-C-pentoside (pmp000116), vitexin (mws0048) and (−)-epiafzelechin (mws1422), and other flavonoids were significantly related; among which caffeoyl-CoA positive regulated naringenin, pinobanksin, 4,2′,4′,6′-tetrahydroxychalcone dihydrokaempferol (mws1094), and other substances, and *CHS* negatively regulated the content of (−)-epicatechin and positively regulated that of vitexin and apigenin-8-C-glucoside.

In group YX, caffeoyl-CoA, *CCOAOMT* (TEA012735), *LAR* (TEA021535), 2-oxoglutarate (2OG), and Fe (II)-dependent oxygenase superfamily protein (TEA023723), anthocyanin 3-O-glucosyltransferase 2 (*UF3GT*, TEA008907) and vitexin (mws0048), afzelechin (3,5,7,4′-tetrahydroxyflavan) (pme3285), luteolin (pme0088) were significantly negatively correlated. *CCOAOMT* (TEA012735) positively regulated myricetin (mws0032) and (−)-epiafzelechin (mws1422), and reversely regulated the expression of dihydrokaempferol (mws1094). Chalcone synthase (TEA023331), flavonol synthase (TEA010328), and *HCT* (TEA014150) negatively regulates myricetin (mws0032) substances. *GH1* (TEA004281) is significantly negatively correlated with coniferin (mws0906). *CCR* (TEA026236) positively regulates the content of Coniferin (mws0906). *CAD* (TEA006254) negatively regulates the content of coniferin (mws0906).

Sensory evaluation of dried tea samples of groups JP and XY

The sensory evaluation and comprehensive scores of dried tea samples of group JP are shown (**Table 4**). Group JP has the highest total score in sensory evaluation (90.55). Moreover, the taste and leaf bottom of group JP are significantly superior to those of Tea-200 and Tea-20. The dried tea of group JP is yellow green and bright, and the liquor is yellow green and bright. It tastes mellow. The total sensory score of Tea-20 (89.45) is only next to that of Tea-1200, and its score in fragrance is the highest. Tea-20 has dense scent, yellow green and clean liquor, fat and strong appearance, green and bright color with distinctive hairs, and yellow green and fat leaf bottom. It tastes similar to Tea-200. The dried tea samples of Tea-200 (87.75) have fat and strong appearances, green and bright color with distinctive hairs, faint scent, and yellow green and fat leaf bottom.

Sensory evaluation and comprehensive scores of dried tea samples of Group XY are shown (**Table 5**). Tea-400 presents the highest total score in sensory evaluation (88.75), and it tastes significantly better than the rest of the two tea samples. Moreover, Tea-400 has higher scores in liquor color and appearance than Tea-100. It has a mellow taste, is yellow green and bright liquor, and has a fat and strong appearance and a uniform color. Its scores in fragrance and leaf bottom are significantly lower than those of Tea-100 and Tea-50. The sensory evaluation score of Tea-50 (88.15) is only next to that of Tea-400, but its scores in fragrance and leaf bottom are the highest. Tea-50 has a dense scent, is a yellow green and bright liquor, and has a fat and strong appearance a uniform color, and a uniform fat yellow green leaf bottom. However, the total score in sensory evaluation of Tea-100 is the lowest (86.6). The liquor color and taste of Tea-100 are mostly similar with those of Tea-50, and the convergence is relatively strong.

To sum up, Tea-1200 and Tea-400 showed the highest sensory evaluation scores. Moreover, fragrance becomes more elegant with increase in age of tea plants, and the dense scent changed to a faint scent gradually. The liquor tastes sweeter and fresher with increase in tea plant age. Its taste changes from thick or strong to mellow, and the astringency is weakened.

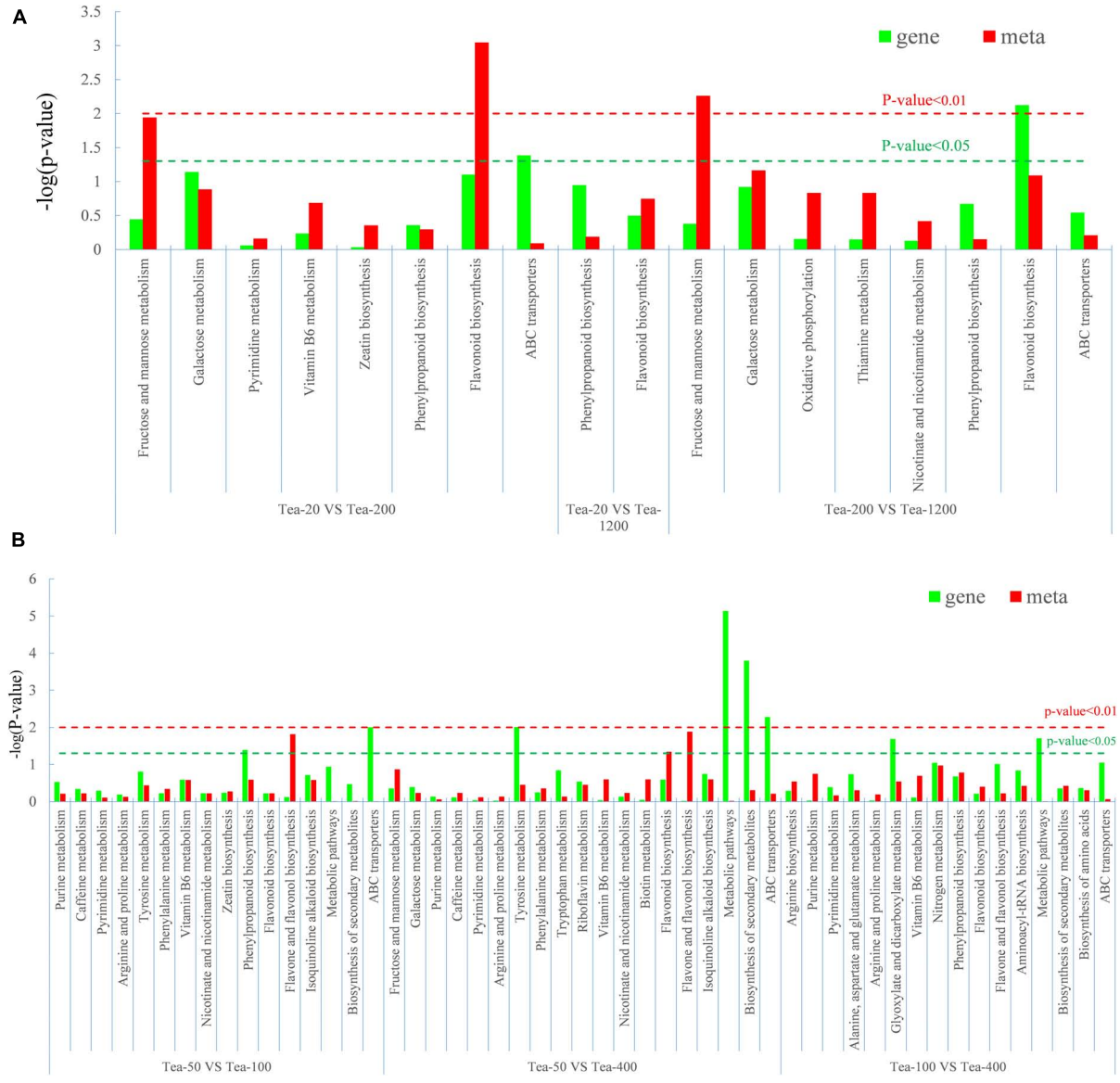

FIGURE 11
Degree of relevant pathway enrichment of differential metabolites and differentially expressed genes (DEGs). **(A)** Group JP and **(B)** Group YX.

Discussion

Differentially expressed genes of tea plants of different ages are mainly concentrated in flavonoid biosynthesis, flavonoid and flavonol biosynthesis, and phenylpropane metabolism

By network conjoint analysis of key genes and differential metabolites related with biosynthesis of flavonoids in groups JP and XY, there are six significantly correlated differential metabolites and six DEGs in group JP, as well as eight significantly correlated differential metabolites and 18 DEGs in group XY. Most flavones and key genes are positively related. This demonstrates that expressions of the structural genes related with synthesis of flavonoids are upregulated, which activates the synthesis and accumulation of flavonoids effectively (Yu et al., 2021). The coumaroyl A and trans-coumaryl coenzyme A produced by the phenylpropane pathway are precursor substances of the biosynthesis pathway of flavonoids. The phenylpropane pathway synthesizes the upstream phenylalanine deaminase (*PAL*) and cinnamate 4-hydroxylase (*C4H*). *PAL* is a multigene family that has different functions, and it participates in formation of secondary metabolites (e.g., plant flavonoids and lignins) (Mu et al., 2010;

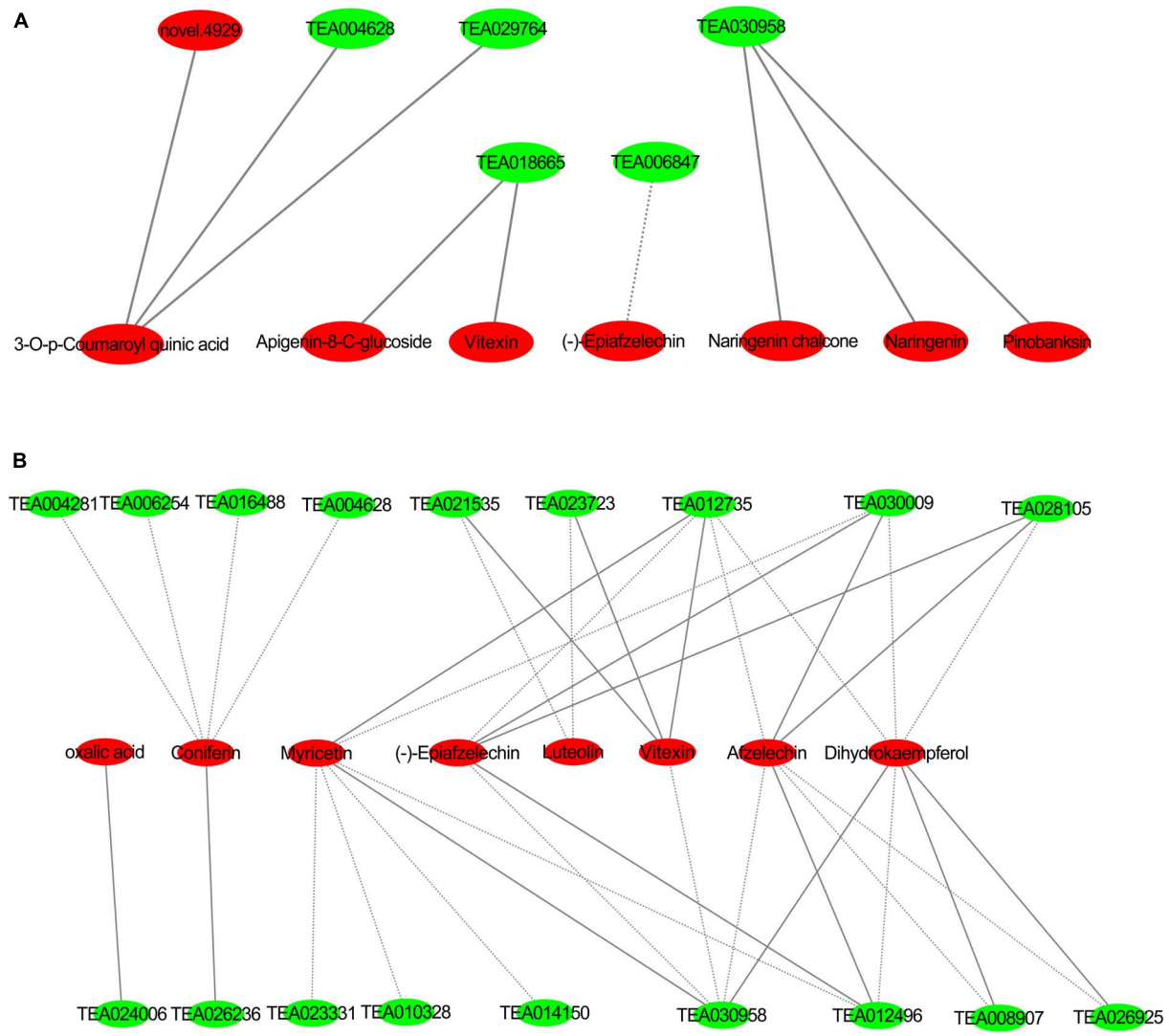

FIGURE 12
Interaction networks of differentially expressed genes and metabolites in phenylpropanoid pathway and flavonoid pathway **(A)** group JP; **(B)** group YX, red: differential metabolites, green: differentially expressed genes; solid line forward adjustment; dashed line reverse adjustment.

Lv et al., 2021). *PAL* locates at the inlet of the metabolic pathway of phenylalanine, and it is a rate-limiting enzyme in the pathway of shikimic acid. It catalyzes phenylalanine deamination to generate cinnamic acid (Lv, 2011). With increase in tea plant age, the expression of *PAL* increases gradually, and it reaches the highest level in Tea-400. However, expressions of flavones like vitexin and isovitexin in Tea-400 are the lowest. This indicates that *PAL* can regulate flavones. In other words, *PAL* can reverse-regulate vitexin and isovitexin. This agrees with the research conclusion of Zhang et al. (2009) that the total contents isoflavone in soybean leaves, contents of three aglycones, and relative expression of *PAL* in leaves have a synergistic growth and reduction trends. As the second enzyme in the phenylpyruvic acid pathway, *C4H* catalyzes the hydroxylation of trans-cinnamic acid and generates 4-cumaric acid. Transcriptional abundance may influence the synthesis pathway of lignins and flavones in plants (Jin et al., 2010). In this study, the expression level of *C4H* in the Tea-400 of group YX is significantly higher than those of Tea-100 and Tea-50. In group JP, the expression level of *C4H* in Tea-200 is significantly higher than those of Tea-20 and Tea-1200. *4CL* and *CHS* are at the downstream of the biosynthesis pathway of flavonoids. *4CL*, *CHS*, and CHI catalyze the formation of naringenin (Luo et al., 2009). Expressions of *CHS* and *4CL* in Tea-100 and Tea-200 are the highest. Expressions of differential metabolites such as naringenin, aromadendrin, and chalcone in Tea-100 and Tea-200 are significantly higher than those in the other tea plant samples. Therefore, *4CL* and *CHS* can positively regulate the

TABLE 4 Results of sensory quality evaluation of dried tea samples of different ages in group JP.

Samples	Appearance (20%)		Liquor color (15%)		Fragrance (25%)		Tastes (30%)		Leave bottom (10%)		Total score
	Comments score		Comments score		Comments score		Comments score		Comment score		
Tea-20	Fat and strong, green and bright, tippy	89 ± 1a	Yellowish green, clean and bright	90 ± 1.32a	Dense scent	93 ± 1.8a	Strong	87 ± 1.73b	Yellowish green, fat and thick	88 ± 2.65b	89.45 ± 1.06ab
Tea-200	Fat and strong, greent, tippy	88 ± 2.65a	Yellowish green, bright	89 ± 2.18a	Faint scent	86 ± 1.73b	Strong	88 ± 0.5b	Yellowish green, fat and thick	89 ± 1b	87.75 ± 1.09b
Tea-1200	Fat and strong, green, tippy	88 ± 1.73a	Yellowish green,bright	89 ± 1.32a	Faint scent	88 ± 1.5b	Mellow, refreshing and sweet	94 ± 1a	Yellowish green, fat and thick, uniform, fresh and bright	94 ± 1.32a	90.55 ± 0.89a

TABLE 5 Results of sensory quality evaluation of dried tea samples of different ages in group XY.

Samples	Appearance (20%)		Liquor color (15%)		Fragrance (25%)		Tastes (30%)		Leave bottom (10%)		Total score
	Comments scores		Comments scores		Comments scores		Comments scores		Comments scores		
Tea-50	Fat and strong, green, even	89 ± 1.32a	Yellowish green	86 ± 2.18b	dense scent	91 ± 1.32a	Thick	88 ± 1.8b	Yellowish green, soft and relatively bright	83 ± 2.6a	88.15 ± 1.00a
Tea-100	Fat and strong, green, relatively even	88 ± 1.73a	Yellowish green, relatively bright	87 ± 0.87b	faint scent	85 ± 0.5b	Thick	87 ± 1.5b	Yellowish green, soft and bright	86 ± 1.8a	86.60 ± 0.69b
Tea-400	Fat and strong, green, relatively even	88 ± 1.8a	Yellowish green and bright	91 ± 0.87a	faint scent	86 ± 2.65b	Mellow, fresh and sweet	92 ± 1.8a	Yellowish green, soft and relatively bright	84 ± 1.73a	88.75 ± 0.55a

10.3389/fpls.2022.910895

biosynthesis of substances like naringenin, aromadendrin, and chalcone. Therefore, we speculate that the differential expression of several enzyme genes such as *PAL*, *C4H*, and *CHS* may be the main reasons for the difference in metabolites of fresh leaves of different tea plant ages.

Younger tea plants have more vigorous metabolism than older tea plants

According to the analysis of transcriptional sequencing of groups JP and XY, a total of 20,788 and 8,971 DEGs were screened, respectively. For group JP, there are 10,108 upregulated genes and 10,680 downregulated genes. In group XY, there are 4,163 upregulated genes and 4,804 downregulated genes. The number of downregulated genes in both groups JP and XY is higher than that of upregulated genes. In other words, the quantity of DEGs is positively related with age of tea plants. The expression levels of differential genes between the younger and older tea plants are significantly different. Therefore, the younger tea plants have more vigorous metabolism. This agrees well with the conclusion of Liu et al. (2022) on the metabolism and transcriptional results of ginkgo trees of different ages: the metabolism of younger leaves is more vigorous than that of old leaves, and the monthly genetic expressions of young trees generally have significant differences, while age differences lead to more obvious differences in flavones and terpenes of ginkgo trees.

Difference in metabolites of fresh leaves of tea plants of different ages is the reason for difference in their dried tea quality

Tea is a kind of healthy beverage, and it is highly appreciated by consumers for its rich taste (Xu et al., 2021). Secondary metabolites like tea polyphenol (TP), caffeine, and amino acids are closely related with tastes and functions of tea (Huang et al., 2018). The TP in fresh leaves of tea plants is a major component of secondary metabolites of tea, and it influences tea quality (Tang et al., 2015). TP is mainly composed of catechinic acids, flavones and flavonols, anthocyanin and leucoanthocyanidin, phenolic acid, and depside (Yang et al., 2013). Fresh leaves of high quality are the vital foundation of forming an excellent quality of tea. Some study pointed out that the material basis of the finished quality of wild tea is better than that of terraced tea (Bai et al., 2018). However, relevant studies are not comprehensive. In this study, metabolite differences among fresh leaves from tea plants of different ages and relevant regulation mechanism were analyzed by metabolomics and transcriptomics. According to the metabolomics sequencing of groups JP and XY, differential metabolites between older tea plants and younger tea plants are mainly flavonoids, polyphenols (phenolic acids and tannin), and alkaloids. Moreover, the quantity of downregulated flavonoids in older tea plants is higher than that of upregulated ones, which might be related with senescence of old tea plants. Polyphenols are mainly related with biosynthesis of phenylpropane and flavonoids. Specifically, flavone substances exist widely in various organs of plants. They not only participate in formation of flowers, fruits, and seed colors but also protect plants from ultraviolet damage and prevent the invasion of pathogenic microorganism (Chen et al., 2011). Flavones in fresh leaves of tea plants are gentle and astringent, and can increase the bitter taste of caffeine. Flavones are one of the factors that influence liquor color and taste quality, resulting in bitter taste (Zeng, 2015). In this study, the expressions of flavones of Tea-1200 are significantly lower than those of Tea-20 and Tea-200. According to the sensory evaluation of dried tea samples of groups JP and XY, the liquor of wild tea tastes sweeter and fresher but less bitter, while liquor of the younger tea is more bitter and lasting. Zhang (2018) found that flavones are one of the influencing factors of the liquor color of tea. Wild tea has lower content of flavones than terraced tea, and it tastes fresher and less bitter. This is consistent with the conclusions of this study. Amino acids are major refreshing substance in tea, and they account for about 3% of total dry substances (Hu et al., 2017). In this study, the expressions of amino acids (e.g., DL-proline, xanthine, L-glutamine, and L-proline) and their derivatives were analyzed, and it was found that contents of amino acids decrease with increase in tea plant age. This indicates that contents of amino acids in younger tea samples are higher than that in older tea samples. This is consistent with the research conclusion of Wang (2020) when studying the formation mechanism of quality differences of Wuyi rock tea samples of different stages: contents of amino acids in fresh leaves decrease gradually with increase in tea plant age.

Data availability statement

The datasets presented in this study can be found in online repositories. The names of the repository/repositories and accession number(s) can be found below: https://www.ncbi.nlm.nih.gov/bioproject/PRJNA869892.

Author contributions

SJ conceived the study, organized, and implemented the study. SJ and YZZ conducted the experiments and evaluated the result together with MYL. MYL and YZZ wrote the manuscript. SJ revised the manuscript. ZYZ and YHZ provides experimental materials and investigated the relevant information about the

materials. QQR participated in sampling and data analysis. All authors discussed the results and content and contributed to the article and approved the submitted version.

Funding

This work was supported by the Natural Science Foundation of Fujian Province (2020J01544) and Open Project of State Key Laboratory for Ecological Prevention and Control of Crop Pests in Fujian and Taiwan (SKL20190010).

Conflict of interest

YHZ was employed by Yunnan Bachishan Tea Co., Ltd.

The remaining authors declare that the research was conducted in the absence of any commercial or financial relationships that could be construed as a potential conflict of interest.

Publisher's note

Supplementary material

The Supplementary Material for this article can be found online at: https://www.frontiersin.org/articles/10.3389/fpls.2022.910895/full#supplementary-material

References

Bai, Y., Mou, D., and Wang, J. (2018). Research progress on biosynthesis of flavonoids and their response to drought stress. *Anhui Agric. Sci.* 46, 24–26.

Chen, J., Liang, M., Wang, L., Yang, Y., and Luo, Z. (2011). A comparative study on the macrocomponents of fresh leaves and the quality of finished tea between ancient tea gardens and terraced tea gardens. *China Agric. Sci. Bull.* 27, 339–344.

Conesa, A., Madrigal, P., Tarazona, S., Gomez-Cabrero, D., Cervera, A., McPherson, A., et al. (2016). Erratum to: A survey of best practices for RNA-seq data analysis. *Genome Biol.* 17:181. doi: 10.1186/s13059-016-1047-4

Dai, Y., and Lv, Y. (2019). Research progress on the application of metabolomics technology in tea science. *Jiangsu Agric. Sci.* 47, 24–28.

Han, Y. (2018). *Coding and noncoding RNAs involved in tea plant flavonoid metabolism*. Hefei: Anhui Agricultural University.

Hu, J., Zhang, X., and Zhao, L. (2017). Teaching reform practice of tea review and inspection course under employment orientation. *Anhui Agric. Sci.* 45, 249–250.

Huang, H., Yao, Q., Xia, E., and Gao, L. (2018). Metabolomics and transcriptomics analyses reveal nitrogen influences on the accumulation of flavonoids and amino acids in young shoots of tea plant (*Camellia sinensis* L.) associated with tea flavor. *J. Agric. Food Chem.* 66, 9828–9838. doi: 10.1021/acs.jafc.8b01995

Jiang, C. K., Liu, Z. L., Li, X. Y., Ercisli, S., Ma, J. Q., and Chen, L. (2021). Non-volatile metabolic profiling andregulatory network analysis in fresh shoots of tea plant and its wild relatives. *Front. Plant Sci.* 12:746972. doi: 10.3389/fpls.2021.746972

Jin, S., Lu, M., and Gao, J. (2010). Cloning and tissue expression analysis of the gene c4h related to lignin synthesis in Phyllostachys edulis. *For. Sci. Res.* 23, 319–325.

Liang, M., Xia, L., Zhang, J., Fang, C., and Chen, J. (2006). A comparative study on the quality of old tree tea and Taiwanese tea. *J. Yunnan Agric. Univ.* 21, 493–497.

Liao, Y., Smyth, G. K., and Shi, W. (2014). FeatureCounts: An efficient general purpose program for assigning sequence reads to genomic features. *Bioinformatics (Oxf. Engl.)* 30, 923–930. doi: 10.1093/bioinformatics/btt656

Liu, Z., Gao, Q., Li, H., Jiang, M., and Chen, R. (2022). Expression analysis of key genes in Ginkgo terpenoid biosynthesis under different growth years based on metabolomics and transcriptomics. *Chin. Herb. Med.* 53, 1138–1147.

Luo, Y., Song, T., Wen, D., Tang, M., and Cai, W. (2009). Growth changes of tea tree shoots internodes and leaf extension angle and their effects on machine-picking of famous tea. *J. Zhejiang Univ.* 35, 420–424.

Lv, G. (2011). *Study on the correlation between lignin, bent neck and aphid resistance of multi-head cut chrysanthemum*. Nanjing: Nanjing Agricultural College.

Lv, S., Wu, Y., Jia, Y., He, F., Xie, X., Jiang, B., et al. (2021). Cloning and functional analysis of the PAL gene of Rhododendron yunnanensis. *Chin. J. Bioeng.* 38, 374–385.

Mu, D., Fu, J., Liu, S., and Han, B. (2010). Research progress on the regulation mechanism of plant volatiles metabolism induced by insect pests. *J. Ecol.* 30, 4221–4233. doi: 10.1093/aob/mcw284

Pertea, M., Pertea, G. M., Antonescu, C. M., Chang, T., Mendell, J. T., and Salzberg, S. L. (2015). StringTie enables improved reconstruction of a transcriptome from RNA-seq reads. *Nat. Biotechnol.* 33, 290–295. doi: 10.1038/nbt.3122

Qiao, X., Li, C., Huang, H., Wu, H., and Zuo, C. (2018). Analysis of biochemical constituents of sun-dried green tea from Baiyingshan ancient tea trees in Yunnan. *Tea Newsl.* 45, 19–22.

Saran, P. L., Singh, S., Solanki, V., Choudhary, R., and Manivel, P. (2021). Evaluation of *Asparagus adscendens* accessions for root yield and shatavarin IV content in India. *Turk. J. Agric. For.* 45, 475–483. doi: 10.3906/tar-2006-42

Solovyeva, A. E., Shelenga, T. V., Konarev, A. V., Kurina, A. B., Kornyukhin, D. L., Fateev, D. A., et al. (2021). Nutritional and biologically active compounds in Russian (VIR) Brassicaceae vegetable crops collection. *Turk. J. Agric. For.* 45, 541–556. doi: 10.3906/tar-2010-95

Su, X., Ma, Y., Yang, X., Kong, J., Zuo, X., and Zhao, M. (2017). Research progress of application of omics technology in tea science research. *Food Ind. Technol. Food Ind. Technol.* 38, 333–340. doi: 10.3389/fpls.2022.973197

Tang, Q., Tang, X., and Song, W. (2018). Transcriptomic technology and its application in tea plant research. *Nat. Prod. Res. Dev.* 30, 900–906.

Tang, Y., Fang, H., Tang, S., Li, J., Zhou, B., and Cai, J. (2015). Biochemical basis of regional differences in Fenghuang Dancong tea quality. *Food Sci.* 36, 168–173.

Wang, Q. (2020). *The mechanism of the formation of differences in the quality of Wuyi rock tea with different tree ages*. Xianyang: Northwest A&F University.

Xu, P., Gong, S., Yang, Y., and Wang, Y. (2021). Excavation and practice of ideological and political elements in the course "Tea Culture and Tea Health". *Chin. Tea* 43, 60–65.

Yang, C., Ran, L., Wang, Q., Wang, H., and Cheng, T. (2013). Seasonal variation analysis of basic biochemical components of Jianghua Kucha resources. *Southwest Agric. J.* 26, 1402–1405.

Yang, X., Yi, B., Li, Y., Duan, Z., Yang, Y., Shang, W., et al. (2016). Diversity analysis of main biochemical components in wild ancient tea resources. *China Agric. Sci. Bull.* 32, 133–139.

Ye, N. (2010). Composition and evaluation of tea quality traits. *Chin. Tea* 32, 10–11.

Yu, F. (1986). On the origin and center of origin of tea trees. *Tea Sci.* 1–8.

Yu, J., Zhang, N., Shi, J., Yang, Y., Meng, X., Xue, J. P., et al. (2021). Research progress on the regulation mechanism of plant hormones on flavonoid metabolism. *Chin. J. Trad. Chin. Med.* 46, 3806–3813. doi: 10.19540/j.cnki.cjcmm.20210522.103

Zeng, M. (2015). *Research on chemical basis of characteristic flavor of ancient Pu'er raw tea*. El Paso, TX: Southwest University.

Zhang, D., Li, W., Li, D., and Li, Y. (2009). Relationship between isoflavone content in soybean leaves and relative expression of PAL gene. *Soybean Sci.* 28, 670–673.

Zhang, H. (2018). Quickly distinguish ancient Pu'er tea from Taiwanese tea. *Mod. Agric.* 8:99.

Zhang, Y., Liu, Y., and Lu, C. (2020). A brief discussion on the generation, evolution and perfection of Chinese tea sensory evaluation terms. *Chin. Tea* 42, 20–23.

Zhao, X. (2019). *Multi-omics techniques to explore the defense response of tea plants in response to the feeding of small green leafhoppers*. Fuzhou: Agriculture and Forestry University.

Zhou, B., Ren, H., Xia, K., Zhang, J., and Zhou, J. (2010). Comparison of aroma components between Taiwanese tea and old tree tea from 9 producing areas in Yunnan. *China Agric. Sci. Bulletin* 26, 54–60.

Frontiers in Plant Science

Cultivates the science of plant biology and its applications

The most cited plant science journal, which advances our understanding of plant biology for sustainable food security, functional ecosystems and human health.

Discover the latest Research Topics

See more →

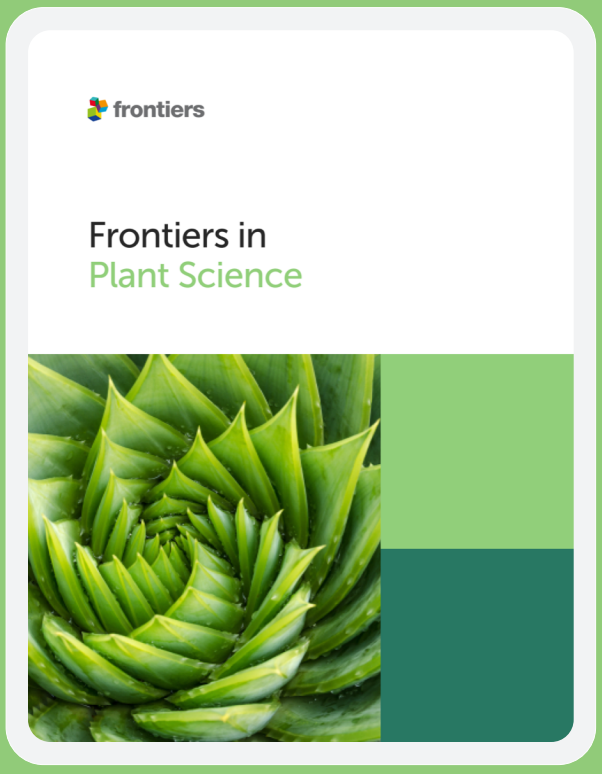

Frontiers

Avenue du Tribunal-Fédéral 34
1005 Lausanne, Switzerland
frontiersin.org

Contact us

+41 (0)21 510 17 00
frontiersin.org/about/contact